Author:
Waldron, Madelene L

Title:
Novel Methods for the Cleavage of C-N Bonds

Novel Methods for the Cleavage of C–N Bonds

Madelene Waldron

A thesis submitted to the University of Bristol in accordance with the requirements for award of the degree of PhD in the Faculty of Science

School of Chemistry, 15th June 2022

Author's Declaration

I declare that the work in this dissertation was carried out in accordance with the requirements of the University's *Regulations and Code of Practise for Research Degree Programmes* and has not been submitted for any other academic award. Except where indicated by specific reference in the text, the work is the candidate's own work. Work done in collaboration with, or with the assistance of, others, is indicated as such. Any views expressed in the dissertation are those of the author.

Signed: MADELENE WALDRON

Date: 15th June 2022

Abstract

Studies towards C–N bond activation and cleavage, involving aryl, benzyl, aziridine, and pyrrolidine systems are presented. The work aims to develop a novel method, or methods, for the cleavage of C–N bonds without the requirement of directing groups or quaternisation strategies.

Examination of secondary phosphine oxide ligands as amphoteric, transient directing groups for the cross-coupling of aryl amines has been carried out, resulting in a successful proof-of-concept reaction. Extensive optimisation studies have been undertaken, resulting in no advancement in yield, and so exploration in this area has not been advanced further at this time.

A new method for the efficient conversion of α-primary benzylamines into benzyl iodides has been developed. Advancement of this discovery has resulted in novel methods for the telescoped two-step cross-coupling of benzylamines, and the nucleophilic substitution of benzylamines, via benzyl iodide intermediates. This method does not require directing groups, and isolation of the benzyl iodide intermediate is not necessary for effective transformations.

The scope of the benzylamine cross-coupling has been expanded to include α-secondary benzylamines, with unique cross-coupling conditions developed for this procedure. This transformation is rendered challenging by competing iodide elimination reactions during the synthesis of α-secondary benzyl iodides, and competing β-hydride elimination during cross-coupling.

Additionally, the established protocol for the conversion of amines into halides has been applied to the ring opening of aziridines and pyrrolidines. An unusual mechanism was observed upon the application of the developed conditions to an aziridine substrate, though ring opening was effective. Furthermore, efficient ring opening was achieved upon application of the developed conditions to a 2-aryl pyrrolidine substrate, though competing alkene formation was also observed. Optimisation studies revealed an efficient method for the ring opening of 2-aryl pyrrolidines to give ester or bromide intermediates.

Acknowledgements

A PhD is no simple undertaking, and I know I would not be here without the help of so many people. First, I must thank Professor John Bower for his direction and encouragement throughout the last four years. This project would not look the same without his expert guidance. To Javi: working with you was an absolute delight. Your instincts inside the lab absolutely helped drive this project, but your friendship truly made the project joyful. I thoroughly enjoyed our discussions about language—both English and Spanish! Also: to Josh, Karim, and Peter, for your help progressing this project. You each brought your own instincts and truly helped take this work to new heights. I know this work is in fine hands, moving forward.

To the rest of the Bower Group. It has truly evolved over the years, and it was a pleasure getting to know each member. To Olya: I miss our chats and bubble tea! You have been a truly excellent friend, and I know you will thrive in your new job! I look forward to our next update. To Raymond: I can't wait to hear your thoughts on the next Marvel Movie (and the next, and the next…). Thank you for always being up for a chat. Tim, Lauren, Wenbin, Ben, Matt, Olivia, Andrew, Josh, Phillippa, Steven, Jamie, Daniel, Charlotte, Davide, James, Gangwei, Xiaofeng, Shirley, Changcheng, Ross, David, Erin: thank you for making the Bower group what it is. I have enjoyed getting to know you all.

To the Bristol CDT for giving me this opportunity. To Rachel, for being an amazing friend when I needed one the most. To Makenzie and Mark and Ben and Matt for being excellent housemates. I've never eaten so well as those weekly meals!

To my friends for keeping me (mostly) sane. A PhD is a truly challenging endeavour. A PhD during a pandemic is another level of challenge. I am so lucky to have incredible supporters. To Lucas: exploring stories with gave me the escape I needed. To Kelly, Katie, Priyasha, and Jasmine: I love you all. You four are my solid ground, and I don't know what I would have done without our phone calls.

To my family. Mum: for always having the best advice when I need it the most. John: I will endeavour to always live by your example; to never give up, to vouch for myself, and to love deeply. Dad and Debbie: for always encouraging me to work hard and push for my potential. My army of siblings: Giles, Loz, Ben, Charlie, SJ: for making sure I remember to have fun! I will always love our games nights.

To Edward: thank you. For always answering my calls. For always being at my side. You make the hardest days joyful, and the lightest days that much brighter. I'm eternally grateful for your love and support, and I am so glad I didn't have to try and do this without you.

Table of Contents

Abbreviations

ADHD	Attention-deficit/hyperactivity disorder
cod	Cyclooctadiene
DBA	Dibenzylideneacetone
DBU	1,8-Diazabicyclo[5.4.0]undec-7-ene
DCE	Dichloroethane
DFT	Density Functional Theory
DIPEA	Diisopropylethylamine
DMA	Dimethylacetamide
DME	Dimethoxyethane
DMF	Dimethylformamide
DPPB	1,4-Bis(diphenylphosphino)butane
DMSO	Dimethylsulfoxide
EDO	Electron-deficient olefin
e.e	Enantiomeric excess
e.r.	Enantiomeric ratio
HAA	Halogen Atom Abstraction
HASPO	Heteroatom-substituted Secondary Phosphine Oxide
HMPA	Hexamethylphosphoramide
Mes	Mesityl
NHC	*N*-Heterocyclic carbene
NMP	*N*-Methyl-2-pyrrolidine
PA	Phosphinous acid
PC	Photocatalyst
SET	Single-electron transfer
SPO	Secondary Phosphine Oxide
TBAF	Tetra-*n*-butylammonium fluoride
TBAT	Tetra-*n*-butylammonium difluorophenylsilicate
TBME	*tert*-Butyl methyl ether
TFAA	Trifluoroacetic anhydride

Chapter 1. Introduction

Out of the top 200 small molecule pharmaceuticals by retail value, 90% contain at least one nitrogen atom.[1] The high prevalence of C–N bonds in organic compounds means that their formation and cleavage is imperative for the diversification and synthesis of complex molecules.[2,3,4] This chapter outlines existing methods for the cleavage of C–N bonds in aryl amines, benzylamines, strained cyclic amines, and non-strained cyclic amines.

1.1 An Overview Regarding the C–N Bond and its Common Chemical Environments

The C–N bond can be found in a diverse range of steric and electronic environments. Transition metal-mediated cleavage of the C–N bond is often challenging due to its relatively inert nature (C_6H_5–NH_2 bond enthalpy = 104.2±0.6 kcal mol^{-1}; C_6H_5–Br bond enthalpy = 84±1 kcal mol^{-1}; $C_6H_5CH_2$–NH_2 bond enthalpy = 71.7±0.7 kcal mol^{-1}; $C_6H_5CH_2$–Br bond enthalpy = 63±1 kcal mol^{-1}).[5] Despite this, several advancements have been made in recent years,[2] including methods for the oxidative addition of aryl C–N bonds and benzylic C–N bonds, and the ring opening of strained cyclic amines and non-strained cyclic amines (Scheme 1). Within each of these chemical environments, the amine target may be primary, secondary, tertiary, or quaternary (Scheme 1). Each of these substitution patterns provides unique challenges for metal insertion into the C–N bond.

Primary, secondary, and tertiary amines contain an available lone pair on the nitrogen atom, and so are nucleophilic in nature. For alkyl amines, this nucleophilicity increases with increased substitution ($EtNH_2$ < Et_2NH < Et_3N) (Mayr's nucleophilicity: $EtNH_2$ = 12.9 (H_2O); Et_2NH = 14.7 (H_2O), 15.1 (MeCN); Et_3N = 17.1 (MeCN)).[6,7,8] This is because the availability of the lone pair increases with substitution due to the inductive electron-donating nature of the alkyl groups. Conversely, the C–N bond of quaternary ammonium salts is much weaker. This is because the C–N bond is strongly polarised. Quaternary ammonium salts are therefore more susceptible to bond cleavage or oxidative addition by a transition metal. Consequently, a common strategy to enable facile oxidative addition into C–N bonds is to exploit the nucleophilic nature of primary, secondary, and tertiary amines by forming a quaternary ammonium salt prior to oxidative addition.[9] Comparing different amine environments demonstrates that primary alkylamines, allylamines, and anilines have similar nucleophilicities ($EtNH_2$ = 12.9 (H_2O); Allylamine = 13.21 (H_2O); $PhNH_2$ = 13.0 (H_2O)),[6] while benzylamines have a higher nucleophilicity ($BnNH_2$ = 13.4 (H_2O)).[6] Cyclic amines increase in nucleophilicity with decreasing ring size (*N*-methyl piperidine = 18.7 (MeCN) vs *N*-methyl pyrrolidine = 20.6 (MeCN)).[8] This pattern is likely caused by increased ring strain, which ensures that the nitrogen lone pair is more available for nucleophilic attack. The increased nucleophilicity of more strained cyclic amines suggests that quaternisation and subsequent oxidative addition into the C–N bond should be more facile.

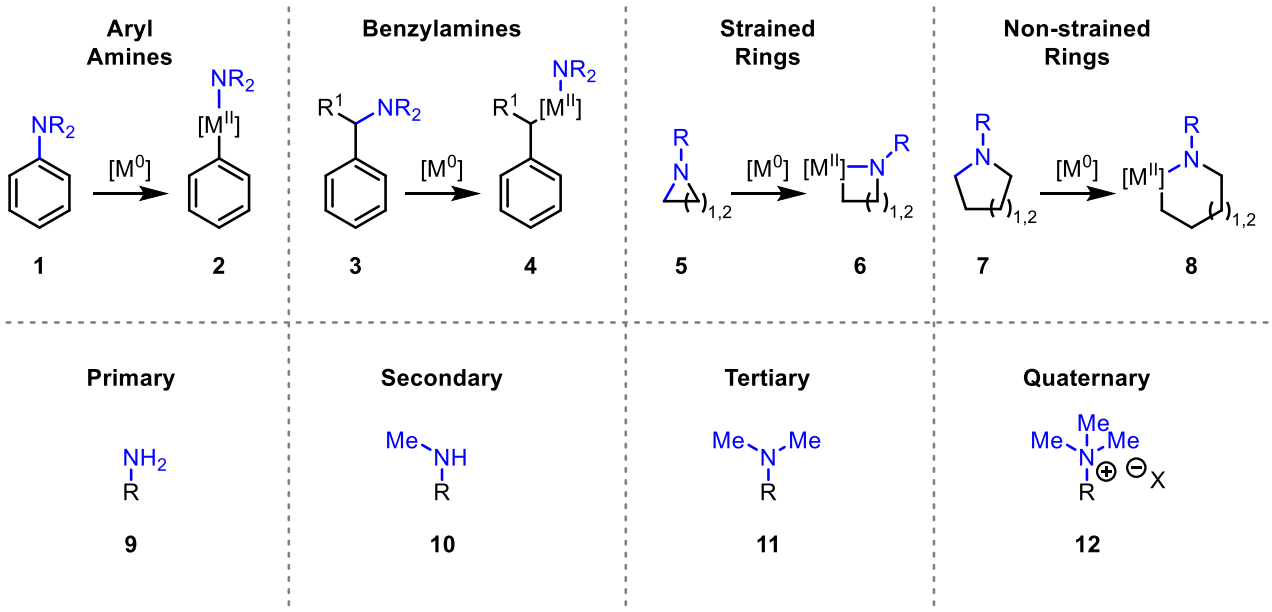

Scheme 1. *Common structural and electronic environments of the C–N bond*

1.2 Methods Involving the Oxidative Addition of Aryl C–N Bonds

The formation of diaryl compounds by Suzuki cross-coupling is one of the most prevalent reactions utilised in medicinal chemistry for the construction of biologically active targets.[10] The Suzuki cross-coupling typically involves reaction of an aryl halide with a boronic acid in the presence of a palladium catalyst, in order to generate new C–C bonds.[11] Aryl halides are traditionally employed, as oxidative addition into the C–X bond is facile; however, this reactivity also means that aryl halides can be difficult to carry through long synthetic sequences. Comparatively, tertiary anilines (aryl amines) are stable moieties, which may be synthesised and maintained through complex multi-step syntheses without undesired reactivity.[12] However, this also limits their availability for cross-coupling, due to the high dissociation energy of the aryl C–N bond which is typically inert due to conjugation of the nitrogen lone pair with the aromatic ring.[13] Despite this, protocols for the cross-coupling of aryl amines have been developed and proceed by three different routes; (1) by quaternisation of the nitrogen moiety, (2) by directing group mediation, or (3) by direct oxidative addition into a neutral C–N bond.

1.2.1. Aryl C–N Bond Activation via Quaternisation of the Nitrogen Centre

For the conversion of tertiary amine **13** into quaternary amine **14**, two alternative sets of reagents and conditions have been reported. However, both involve the use of highly corrosive (MeOTf) or highly toxic (MeI, DCE) reagents. Additionally, quaternary amine **14** typically requires isolation and

drying prior to its use in subsequent C–N cross-coupling reactions to give products **15**.[14–17] The use of less toxic reagents for the formation of quaternary amines is therefore of interest.

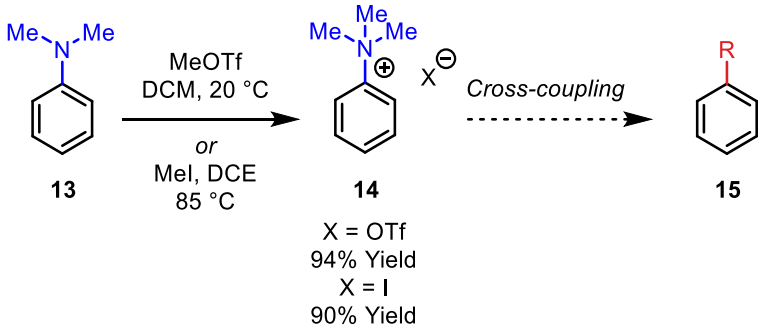

Scheme 2. *Synthesis of activated quaternary anilines* ***14***

In 1988, Wenkert and co-workers reported the first processes that involve oxidative addition of an aryl C–N bond to a transition metal. This involved a Kumada cross-coupling of trimethylammonium iodide salt **16** with a Grignard species. Here, a Ni^0 catalyst was employed to promote insertion into the C–N bond of **16** (NEt_3, benzene, reflux, 14 h).[16] This work was the first example of the exploitation of a simple quaternisation step to convert *N*,*N*-dialkyl anilines into suitable substrates for C–N bond insertion. However, this protocol is limited due to the poor substrate scope and reaction efficiency. Additionally, cross-coupling product **17** was formed in low yields of 11-63%. It was also found that trimethylammonium aryl iodide **16** was often unstable to the reaction conditions, as degradation to *N*,*N*-dimethylaniline side products **18** was observed.

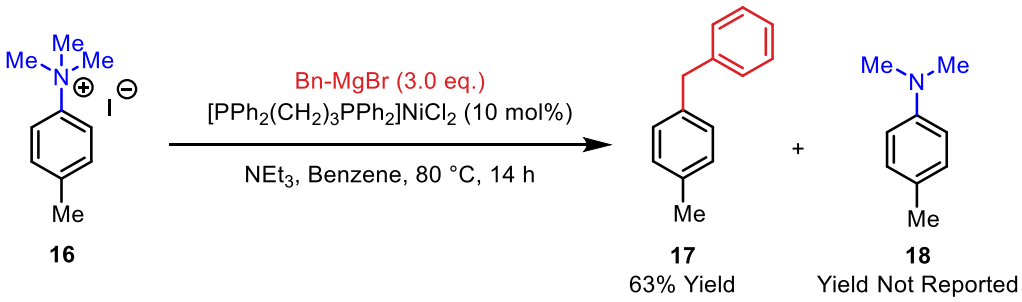

Scheme 3. *Cleavage of trimethylammonium iodide salt* ***16*** *as reported by Wenkert and co-workers*

The Kumada cross-coupling of trimethylammonium salts has advanced substantially since Wenkert's original publication. In 2010, Reeves and co-workers reported the room temperature Kumada cross-coupling of trimethylammonium triflate salts **19** with aryl Grignard reagents **20** ($PdCl_2(PPh_3)_2$, THF, 1 h) (Scheme 4A).[17] Fifteen examples were reported, with differing substitution patterns on both the aniline **19** and Grignard species **20**, with yields ranging between 79-94%. A telescoped process for the cross-coupling of *N*,*N*-dimethylaniline **13** and **20** via the in situ formation of trimethylammonium triflate salt **19** was also described (Scheme 4B). Here, cross-coupled product **21** was formed in 88% yield.

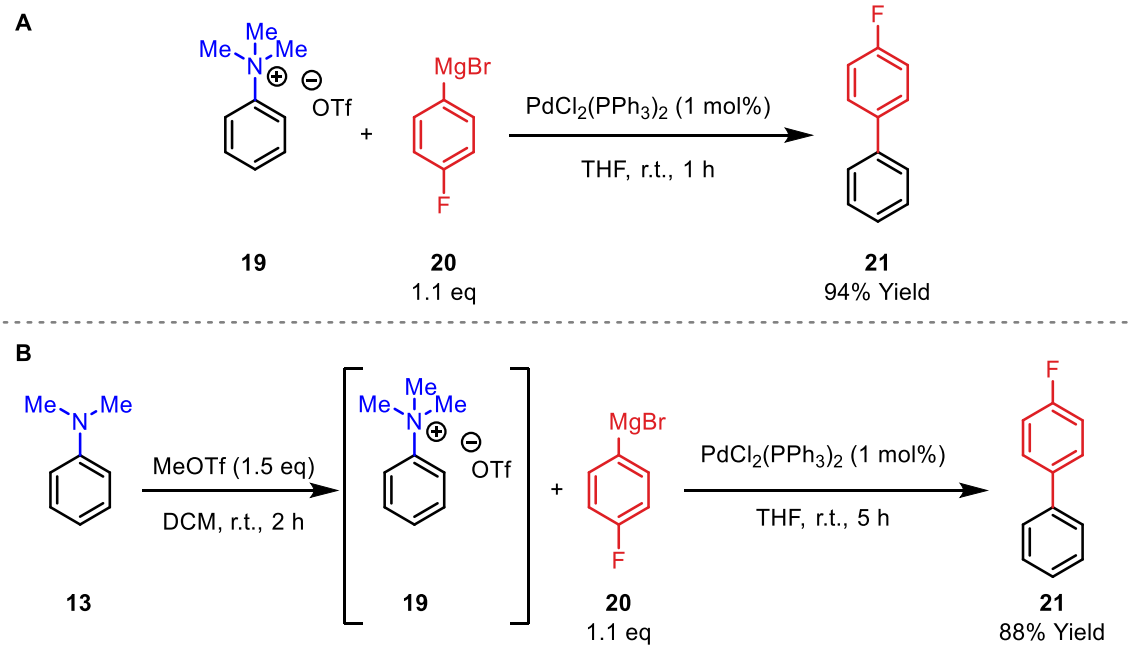

Scheme 4. *The advanced Kumada cross-coupling of trimethylammonium triflate salts* ***19***

The use of quaternary ammonium salts has been advanced to include a vast array of cross-coupling protocols. In 2003, the first Suzuki cross-coupling of trimethylammonium triflate **22** with boronic acid **23** was reported by MacMillan and co-workers ($Ni(cod)_2$, iMes•HCl, CsF, dioxane, 80 °C, 12 h) (Scheme 5A).[14] The authors demonstrated that the reaction tolerates a wider scope of substitution patterns around the aromatic ring of both trimethylammonium triflates **22** and boronic acids **23**, with 21 examples reported in 79-98% yields. Other cross-couplings of aryl trimethylammonium salts for the formation of diaryls include Negishi cross-couplings (**14**, **25**, $Ni(PCy_3)_2Cl_2$, THF/NMP, 90 °C, 8 h) (Scheme 5B);[17] Stille cross-couplings (**19**, **27**, $Ni(cod)_2$, ICy•HBF_4, CsF, dioxane, 80 °C, 12 h) (Scheme 5C);[18] and Murahashi cross-couplings (**28**, **29**, $PdCl_2(PPh_3)_2$, THF, r.t., 12 h) (Scheme 5D).[19]

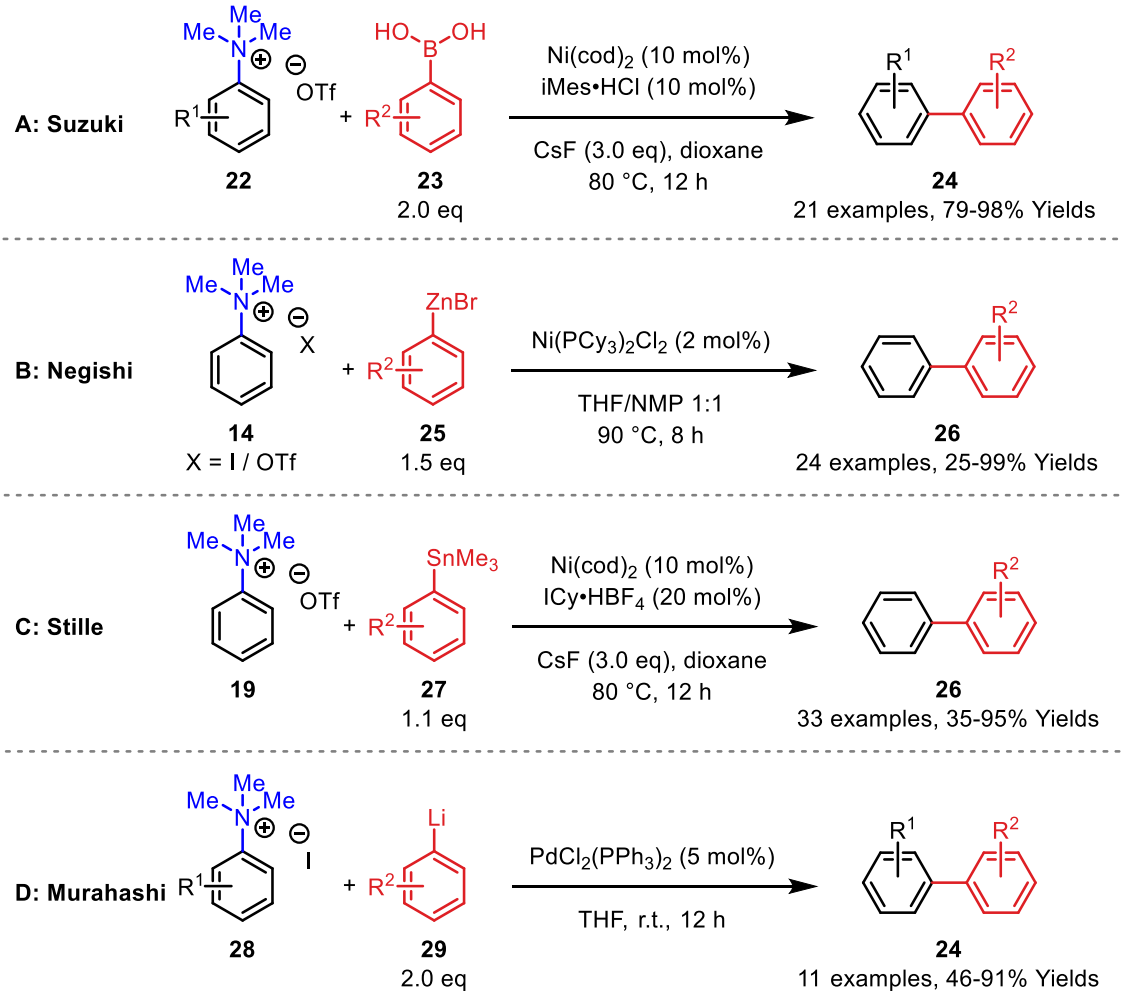

Scheme 5. *Protocols for the cross-coupling of trimethylammonium salts*

The mechanisms for each of these protocols are fundamentally similar. Firstly, the nickel or palladium catalyst **I** cleaves the aryl C–N bond of trimethylammonium salt **30** through oxidative addition, forming complex **II** (Scheme 6). Subsequent transmetalation with aryl coupling partner **31** ([M'] = MgBr; $B(OH)_2$; ZnBr; $SnMe_3$; Li) generates metal complex **III**, which undergoes reductive elimination to return the original metal catalyst **I** and diaryl product **33**. The aforementioned examples demonstrate that the conversion of *N*,*N*-dimethylanilines into trimethylammonium salts is an effective strategy for enabling the cleavage of aryl C–N bonds. It should be noted that limitations arise from the toxicity of methyl triflate and methyl iodide, and from the need to isolate the intermediate trimethylammonium salts; a telescoped two-step process from the commercially available *N*,*N*-dimethylanilines is not suitable for many processes, and results in notable decreases in yield.[17]

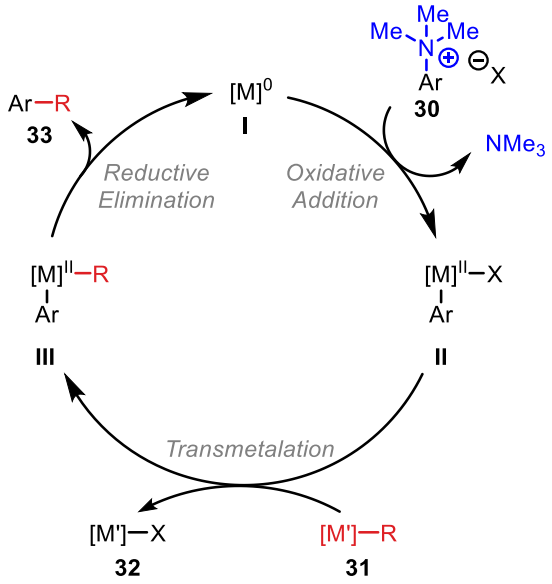

Scheme 6. *General transition-metal catalysed cross-coupling of aryl trimethylammonium salts* ***30***

1.2.2. Aryl C–N Activation using Tethered Directing Groups

An alternative strategy for the cross-coupling of aryl C–N bonds involves the use of directing groups. Here, the metal catalyst is held in closer proximity to the C–N bond, which reduces the entropic cost of oxidative addition.[13,20–23] One example of this strategy was reported by Kakiuchi and colleagues in 2007. In this report, ketone-directed cross-couplings of primary, secondary, and tertiary anilines **34a**, **34b**, and **34c** were achieved under Ru-catalysed conditions (**35**, $RuH_2(CO)(PPh_3)_2$, toluene, reflux, 20 h) (Scheme 7).[20] This protocol demonstrates an effective method for the cross-coupling of aryl amines with differing amine environments, an advantage over the previously discussed quaternisation protocol. However, the necessity of the directing group is a notable limitation for the scope and application of this protocol in target-directed settings.

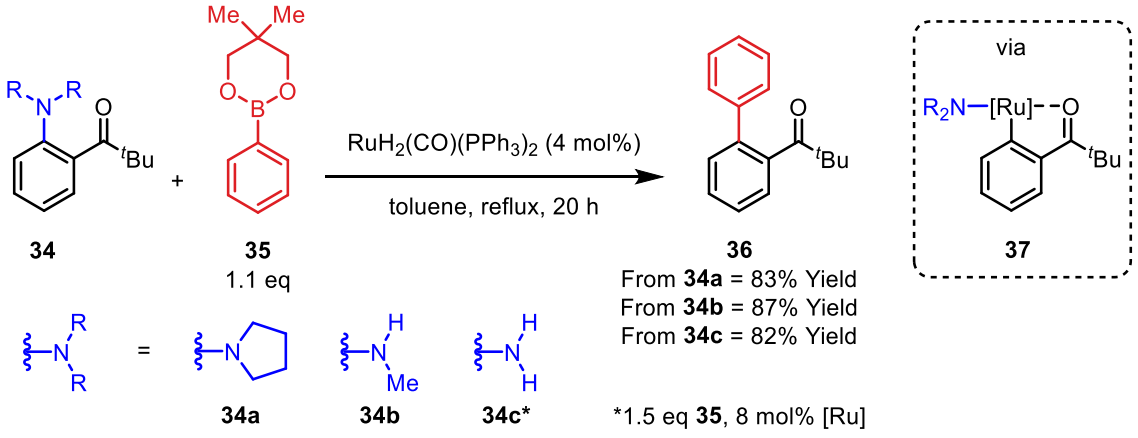

Scheme 7. *Cross-coupling of primary, secondary, and tertiary anilines by use of a directing group*

Directing groups have also been used for the carbonylation of aryl C–N bonds. Wu and co-workers demonstrated that 2-pyridyl systems of type **38** may be used in conjunction with $Ru_3(CO)_{12}$ for the conversion of tertiary aryl amines into diaryl ketones under a pressurised atmosphere of CO (**35**, *o*-xylene, 160 °C) (Scheme 8A).[13] In the report, four examples of alternative substitution patterns on the aniline ring were demonstrated and, though cyclic pyrrolidine and *N*,*N*-diethyl substitution were tolerated on the aniline moiety (70%, 45% yields respectively), primary and secondary amines were not tolerated. The proposed mechanism for this carbonylation commences with coordination of ruthenium to CO, which generates active catalyst **I** (Scheme 8B). As CO is a π-acidic ligand, the electron density at the ruthenium centre decreases, making oxidative addition more challenging. The pyridine directing group of substrate **38** is therefore crucial; coordination of **I** to aniline **38** occurs, forming **II**. The ruthenium centre then inserts into the aniline C–N bond to generate structure **III** which, following transmetalation with boronic ester **35**, provides intermediate **IV**. Subsequent carbonylation may occur by two separate pathways: (1) by insertion into the C**1**–Ru bond, forming **V**, or (2) by insertion into the C**2**–Ru bond, forming **V'**. Both intermediates **V** and **V'** may then generate product **39** by reductive elimination and, upon coordination of another molecule of CO, catalyst **I** is regenerated.

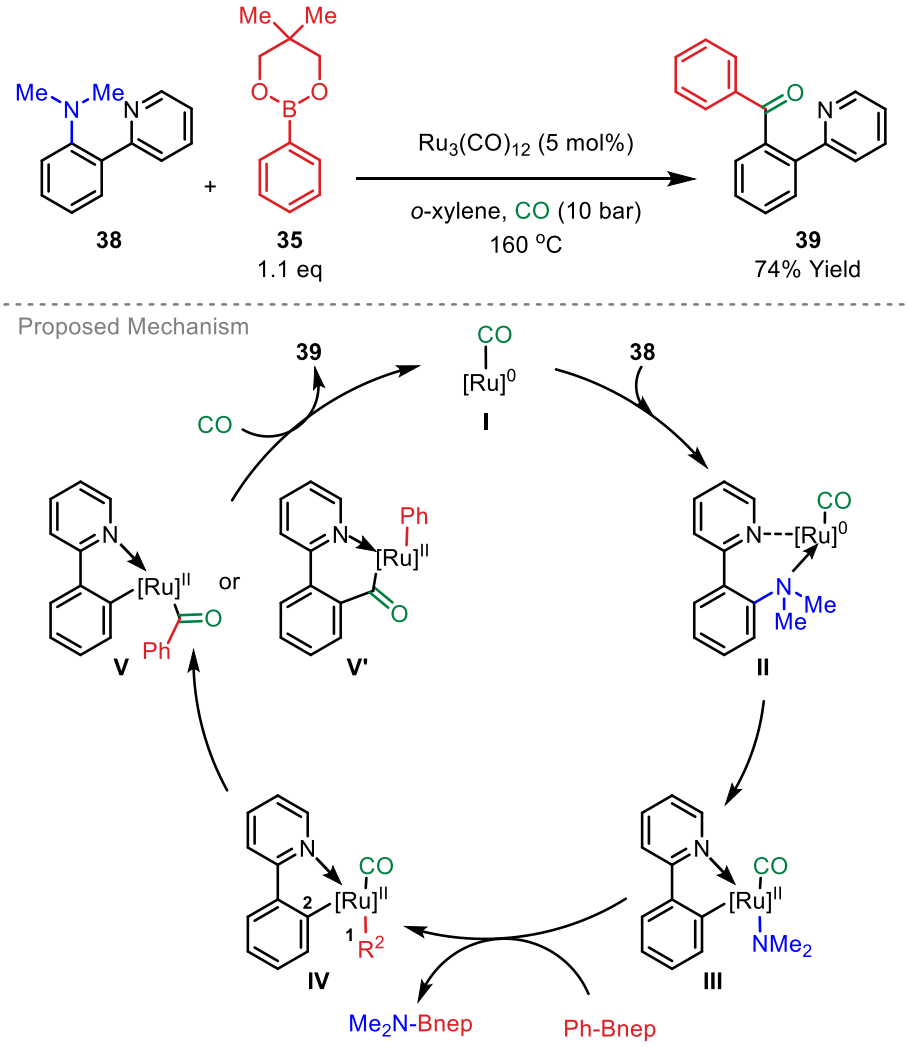

Scheme 8. *Procedure for the carbonylation of aniline* ***38*** *facilitated by a pyridine directing group*

1.2.3. Oxidative Additions of Neutral Aryl C–N Bonds in the Absence of Directing Groups

Current methods for the direct cross-coupling of neutral aryl amines without a directing group are still limited. Despite this, Shi reported a nickel-catalysed cross-coupling of aryl amines **40** in 2018 (**35**, $NiBr_2$, $iMes^{Me}$, Mg, THF, 135 °C, 36 h) (Scheme 9).[24,25] This protocol requires a highly electron-donating NHC (N-heterocyclic carbene) ligand to promote oxidative addition of the neutral C–N bond with nickel. The role of magnesium within this cross-coupling is unconfirmed; while it likely acts as an initiating reductant of nickel, other metal reductants (e.g. Zn, Mn, Na, Al, Sn) were unsuccessful, suggesting magnesium has an additional role within the cross-coupling. The scope of this process is somewhat limited, as deviation from the extended π-system of the naphthyl group of **40** resulted in an extreme loss of reactivity. In the report, 23 substrates were cross-coupled, with yields ranging between 12 and 93%, and only non-polar boronic ester coupling partners such as **35** were utilised. The proposed mechanism for this transformation is depicted in Scheme 9 and involves a Ni^{I}–Ni^{III} oxidative process. First, nickel species **I** is formed by ligand exchange of $iMes^{Me}$ with substrate **40**; coordination of the nickel is likely assisted by the extended π-system of the naphthyl unit. Oxidative addition into the aryl C–N bond generates structure **II**, which undergoes transmetalation with boronic ester **35** to give intermediate **III**. Reductive elimination regenerates the active catalyst and provides cross-coupled product **41**.

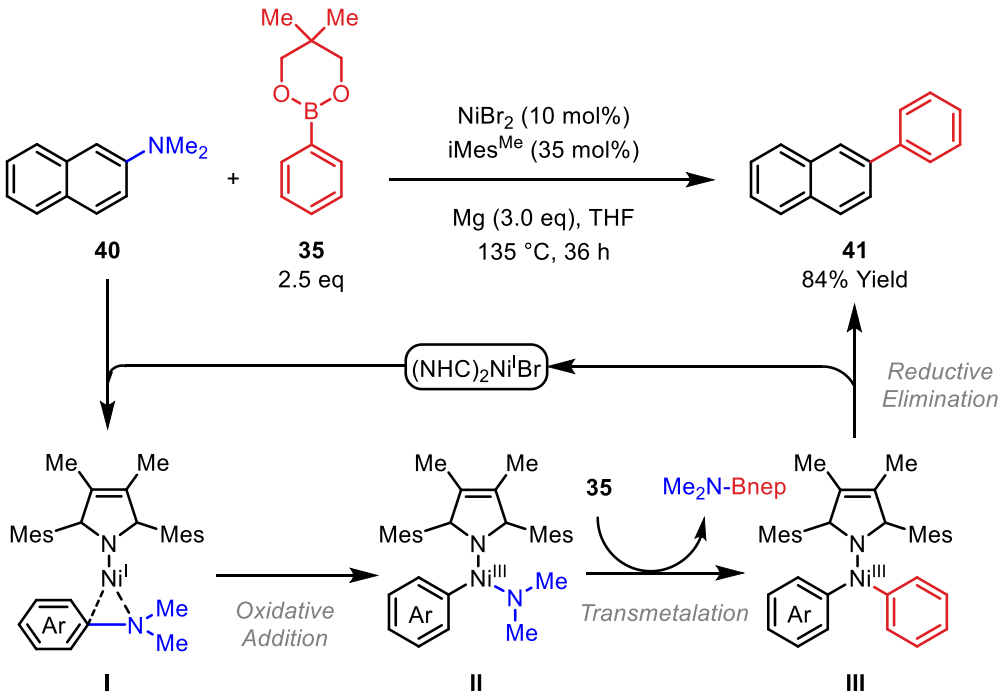

Scheme 9. *The cross-coupling of neutral aryl amines*

1.3 Benzylic C–N Bond Activation

The development of new methods for the cross-coupling of benzylic C–N bonds (Scheme 10A) has progressed substantially alongside methods for aryl C–N cross-coupling (Section 1.2). The resulting diarylmethanes **43** (R^2 = Ar) and triarylmethanes **45** or **46** (R^2, R^3 = Ar) are important substructures in dye precursors and photochromic agents, as well as in anti-cancer and antibacterial compounds used in the pharmaceutical industry.[26,27] Common and efficient strategies for the formation of these substructures typically involve the use of benzylic electrophiles, which are generated through the cleavage of activated C–H bonds,[28,29] non-activated C–H bonds,[27] C–O bonds,[30,31] C–[M] bonds,[32] or C–X bonds.[33] A notable challenge for the cross-coupling of benzylic amines arises from the chiral centre at the benzylic α position of **44** ($R^3 \neq H$) (Scheme 10B). Enantiospecific and enantioselective transformations are important for drug design because one enantiomer of a compound may have a substantially different pharmacological profile to its mirror image, either rendering half of a treatment ineffective, or even toxic.[22] Benzylic amine cross-coupling protocols that offer excellent enantiocontrol are still limited.

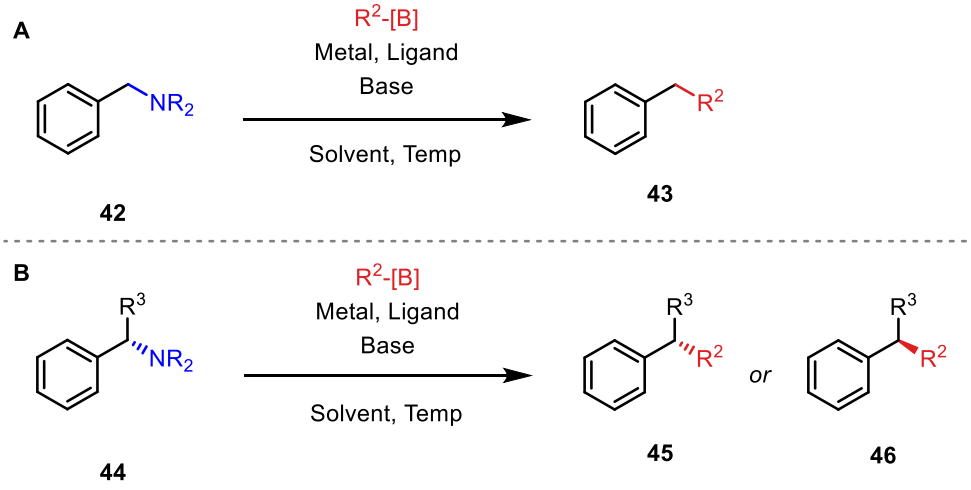

Scheme 10. *Cross-coupling of α-primary and α-secondary benzylamines*

1.3.1. Benzylic C–N Activation by Quaternisation of the Nitrogen Centre

1.3.1.1. The use of Trimethylammonium salts for the Cross-Coupling of Benzylic C–N Bonds

The first cross-coupling of benzylic trimethylammonium triflate salts was reported by Watson and co-workers in 2013 (Scheme 11A).[34] Here, Ni^0 catalyst $Ni(cod)_2$ was employed to convert quaternary benzylamine **45** into diarylmethane **17** in 84% yield (**46**, PPh_2Cy, K_3PO_4, dioxane, 40 °C, 24 h). The report also detailed the first cross-coupling of α-secondary naphthyl substrate **48**. Here, **48** was converted to diarylethane **49** in 72% yield and 97% e.e. (**46**, $Ni(cod)_2$, P(*o*-Tol)$_3$, K_3PO_4, dioxane,

70 °C, 6 h). For the cross-coupling of α-primary benzylamine **45**, a broad scope of 22 boronic acids and 9 benzylamines was demonstrated, with yields of 49% to quantitative. For the cross-coupling of α-secondary systems **48**, a more modest scope was reported, with 10 different boronic acid coupling partners and 5 different benzylic amines tolerated, with yields ranging from 37% to 96%, and enantioselectivities ranging from 52% to 99%.

Despite the successful cross-coupling of benzylic trimethylammonium triflate salts, there are several limitations associated with this approach. As with aryl trimethylammonium triflate salts, the use of toxic methyl triflate is required to form starting materials **45** and **48**, and isolation of these starting materials was carried out prior to cross-coupling. Furthermore, for the cross-coupling of α-secondary systems, different conditions (base, ligand, metal and ligand loading) were required for each substrate. To enable the wider application of this cross-coupling process, a more general procedure is required.

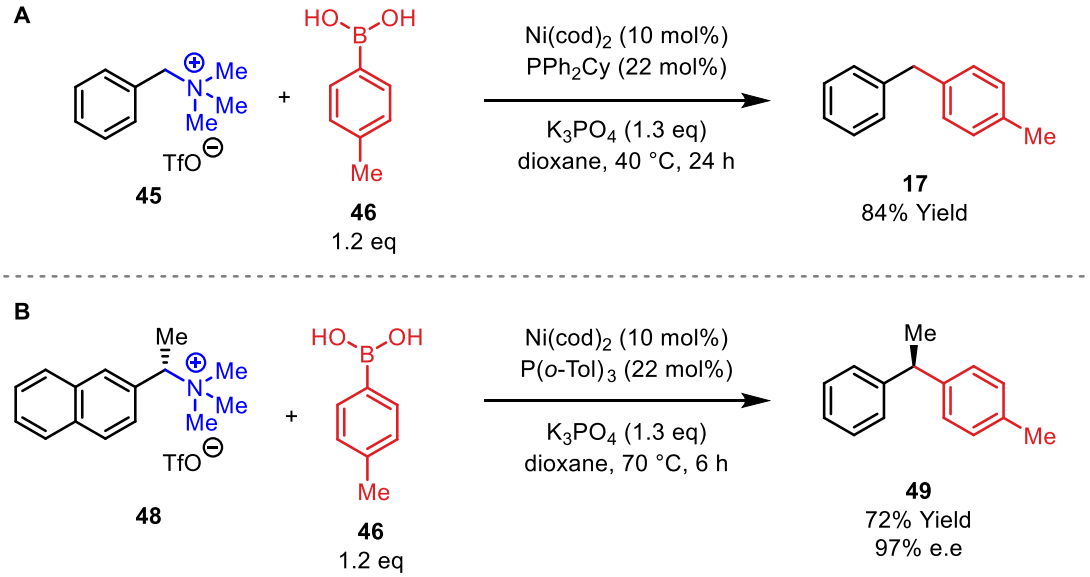

Scheme 11. *The first reported cross-coupling of benzylic trimethylammonium triflate salts*

Various alternative cross-couplings have since been developed which harness the reactivity of benzylic trimethylammonium triflate salts (Scheme 12). In 2019, Shu and co-workers demonstrated the cross-electrophile coupling of C–N and C–O electrophiles **50** and **51** in the presence of a Ni^{II} catalyst ($NiBr_2$(diglyme), BPhen, Mn, NaOAc, DMF, 80 °C) (Scheme 12A).[35] In the report, a wide substrate scope was demonstrated, including various benzylic ammonium salts, and aromatic, aliphatic, and cyclic alkenyl acetates. Processes involving aryl ammonium salts were also exemplified. The viability of using vinyl triflate coupling partners instead of vinyl acetates was also demonstrated. Radical clock experiments were used to gain insight into the reaction mechanism. For these studies, it was proposed that oxidative addition of the C–N bond may proceed by a radical mechanism instead of the typical 2-electron process implicated in Watson and co-workers' study. Further cross-couplings of benzylic C–N bonds include: Sonogashira cross-couplings (**45**, **53**, $Pd(PPh_3)_4$, K_2CO_3, PhMe:DMSO, 100 °C, 12

h) (Scheme 12B),[36] Hiyama cross-couplings (**45**, **55**, $PdCl_2(CH_3CN)_2$, PPh_2Cy, TBAF, EtOH, 120 °C, 24 h) (Scheme 12C),[37] and Suzuki cross-couplings (**57**, **58**, $PdCl_2$, PPh_3, Na_2CO_3, 100 °C, 24 h) (Scheme 12D).[38]

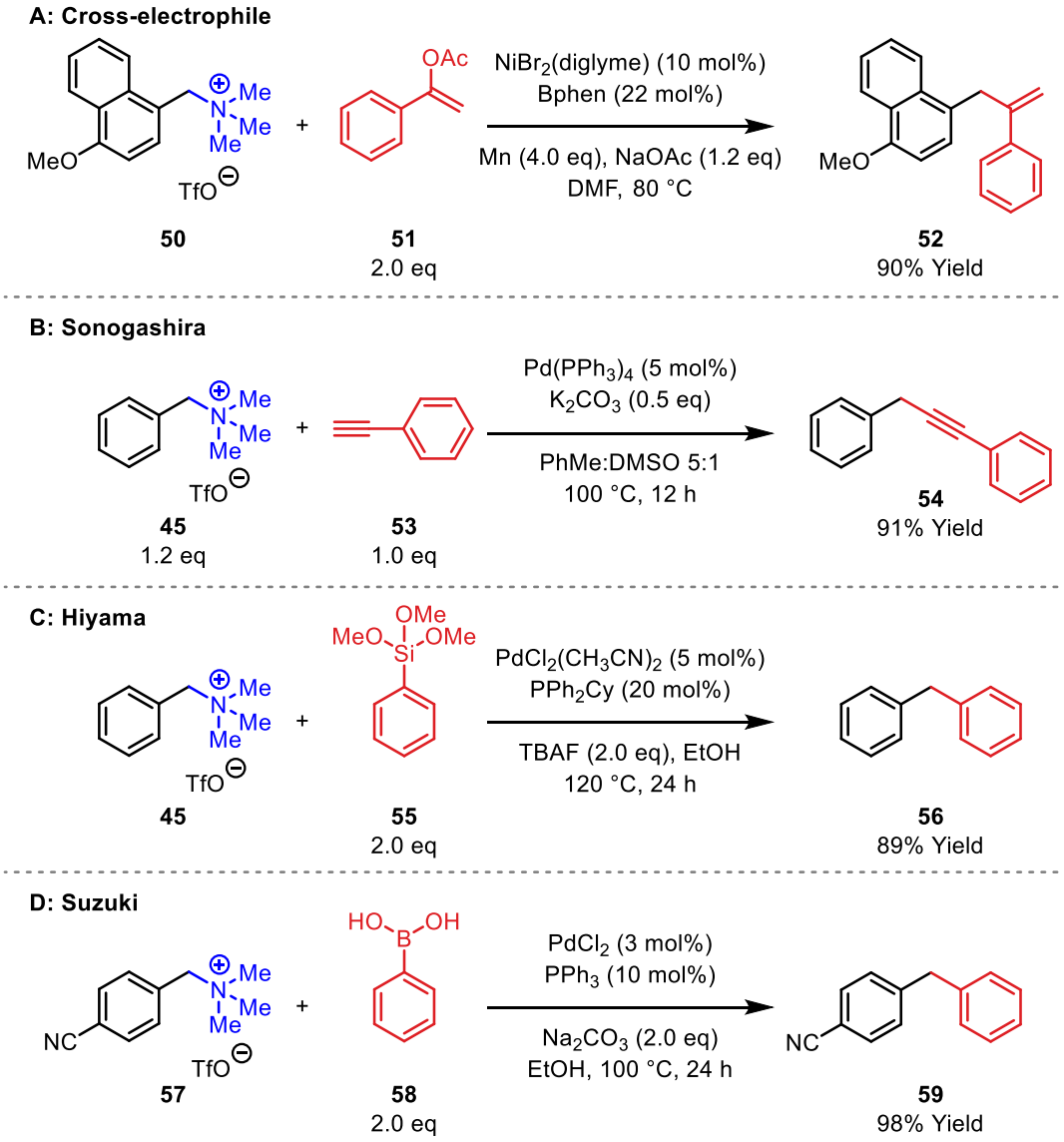

Scheme 12. *Cross-couplings of benzyl trimethylammonium triflate salts*

The proposed mechanism for the Sonogashira, Hiyama, and Suzuki cross-couplings is shown in Scheme 13. As with the cross-coupling of aryl trimethylammonium triflates, the nickel or palladium catalyst **I** undergoes oxidative addition of the polarised C–N bond of **60** to provide metal complex **II**. If starting material **60** is enantioenriched, the chirality is inverted during this 2-electron oxidative addition step. Cross-coupling partner **31** then undergoes transmetalation to give metal complex **III** which, following reductive elimination, delivers product **62** and regenerates active catalyst **I**.

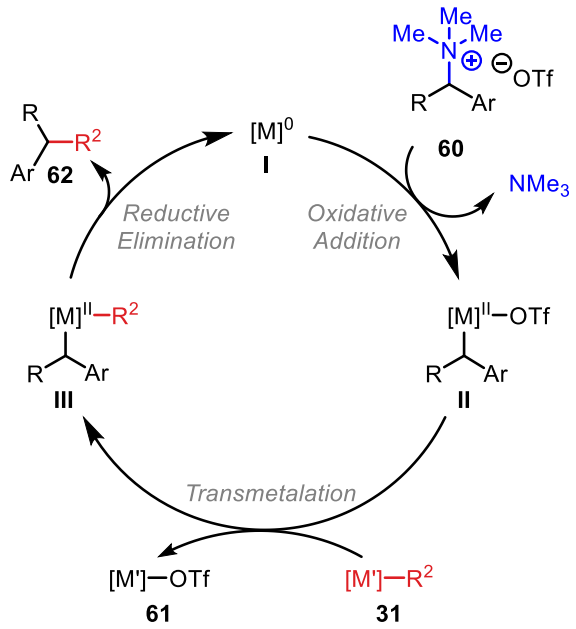

Scheme 13. *Transition-metal catalysed cross-coupling of benzylic trimethylammonium salts* ***60***

1.3.1.2. The use of Pyridinium Katritzky salts for the Cross-Coupling of Benzylic C–N Bonds

An alternative method for the activation of benzylic amines involves the use of pyridinium Katritzky salts (Scheme 14). This method was first demonstrated by Watson and colleagues in 2018, who reported that primary amines such as **63** can be converted to pyridinium Katritzky salts **64** in yields of up to 94% (**47**, EtOH, reflux). Substrates of type **64** can then undergo cross-coupling in the presence of a nickel catalyst to give diarylmethane products such as **65** (PhenNi(OAc)$_2$•H$_2$O, K$_3$PO$_4$, EtOH, dioxane, 60 °C, 5 h) (Scheme 14A).[26] Altering the cross-coupling protocol to a one-pot, two-step procedure, without isolation of Katritzky salt intermediate **64** decreased the yield from 94% to 76%.

The proposed mechanism of this protocol (Scheme 14B) commences with a single-electron transfer from Ni^{I} catalyst complex **I** to the pyridinium salt of **64**, generating intermediate **66** and Ni complex **II**.[39,40] A cascade radical transfer follows, generating benzylic radical **67**. A second SET occurs between metal complex **II** and benzylic radical **67**, giving intermediate **68** which then undergoes reductive elimination to furnish product **69**. The formation of radical **67** severely limits the scope of this process, because any benzylic enantioenrichment within starting material **64** is eroded. This is likely why there are few published examples of α-secondary benzylamine cross-couplings using Katritzky pyridinium salts. Additionally, this protocol is hindered by the poor atom economy of the transformation. Despite this, there are also many advantages to this cross-coupling. Most notably, primary benzylamines **63** function as precursors to Katritzky salts **64** rather than the tertiary amine starting materials employed for the cross-coupling of trimethylammonium triflate salts **60** (Section 1.3.1.1). In 2018, the Pfizer internal store contained 5208 primary benzylamines, compared to 1843

benzyl chlorides and 1020 benzyl bromides.[26] This substrate availability demonstrates the value of developing cross-coupling strategies with primary benzylamines.

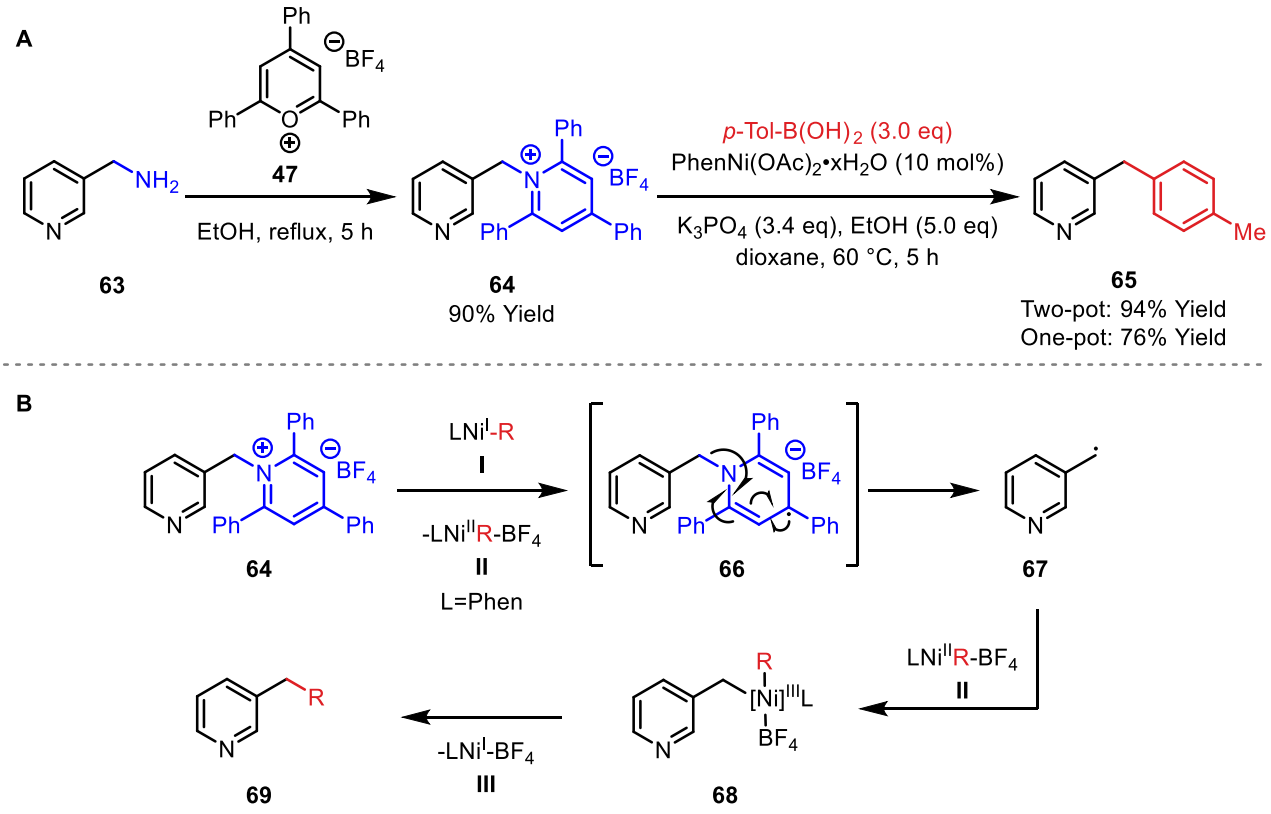

Scheme 14. *Using Katritzky salts for the cross-coupling of primary benzylamines*

1.3.2. Oxidative Addition of Neutral Benzylic C–N Bonds Without Directing Groups

The first processes involving oxidative addition of a neutral benzylic C–N bond without the use of any directing groups were reported by Wu and co-workers in 2018. Here, a palladium catalyst was employed for the oxidative addition of the C–N bond of benzylamines **42** to provide intermediate **I**, which then underwent carbonylation to **II**, followed by nucleophilic attack of methanol to give ester products **70** (MeOH, $Pd_2(dba)_3$, DPPB, dimethyl carbonate, CO, 140 °C, 24 h) (Scheme 15).[41] Primary, secondary, and tertiary benzylamines **42** were found to be suitable substrates, giving methyl esters **70** in yields ranging from 51% to quantitative. Additionally, ethanol was tolerated in place of methanol, providing the ethyl ester analogue of **70** in 89% yield. To demonstrate utility, the method was applied to the synthesis of methylphenidate, a drug used for the treatment of ADHD and narcolepsy.

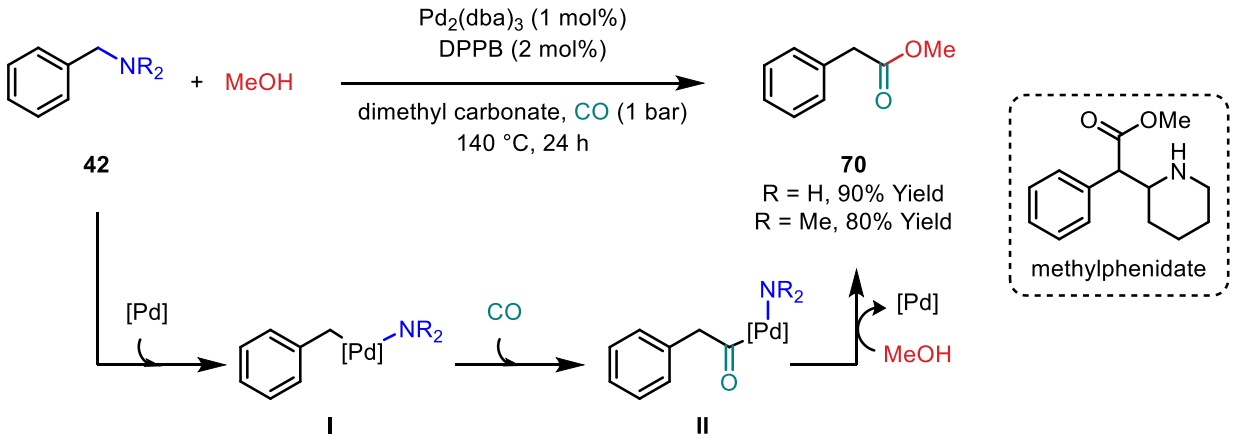

Scheme 15. *The carbonylation of neutral benzylamines* ***42*** *to give esters* ***70***

1.4 C–N Bond Activation via Strain Release of Cyclic Amines

Another class of C–N bonds are those found within small, nitrogen-containing rings such as aziridines and azetidines **71**. The inherent strain within these systems facilitates oxidative addition (Scheme 16A) and nucleophilic displacement of the C–N bond (Scheme 16B. This is discussed further in Section 5.1.1).[42,43] Aziridines and azetidines can be highly functionalised systems with defined stereochemistry often installed on the backbone of the ring. Ring opening protocols can therefore provide enantioenriched products **73**, which contain high levels of 3-dimensionality, and may be of use to medicinal chemistry.[44]

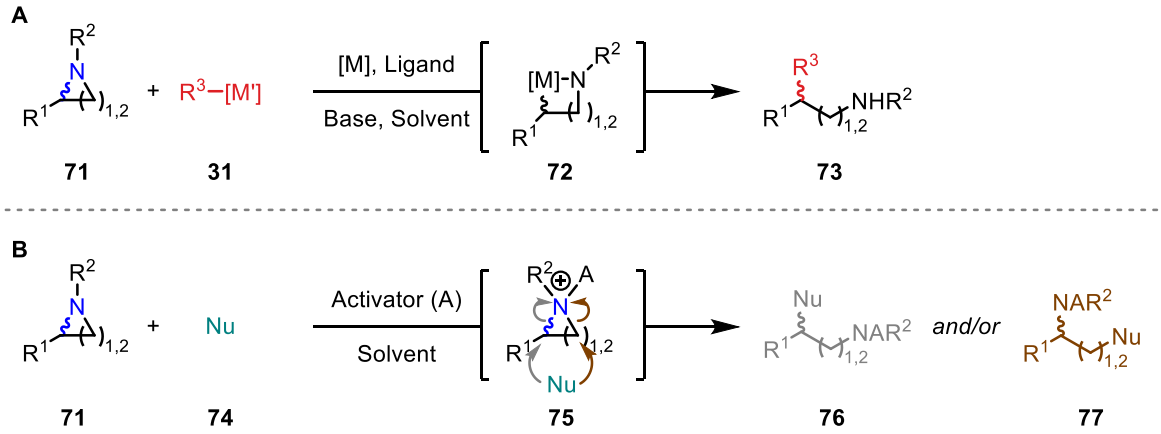

Scheme 16. *C–N bond activation via strain release of cyclic amines*

1.4.1. Metal-Catalysed Cross-Couplings of Aziridines

The first example of a transition-metal-catalysed cross-coupling of aziridines **78** was the Negishi alkylation reported by Doyle and co-workers. Here, SET oxidative addition of the strained C–N bond was achieved using a nickel catalyst ligated with an electron-deficient olefin ($NiCl_2$•glyme, **80**, ^{n}BuZnBr, dioxane/DMA, r.t., 6 h) (Scheme 17A).[45] Ring opening occurred exclusively on the more hindered benzylic C–N bond, likely facilitated by metal coordination to the aromatic ring prior to oxidative addition and stabilisation of the benzylic radical formed via SET oxidative addition. One limitation of this methodology is that it only tolerates *N*-tosyl substrates. The enantiospecificity of this transformation was examined by the application of the *R*-enantiomer of aziridine **78** to the reaction conditions. Unfortunately, product **79** was generated in only 11% e.e., demonstrating poor enantiospecificity. Later work in this area expanded the scope of this reaction to include di-substitution on the benzylic position for the formation of more highly substituted systems (see Section 5.1.1).[46,47]

Investigations into the mechanism of this alkylation and the role of the requisite electron-deficient olefin (EDO) ligand (e.g. **80**) were reported in 2020 (Scheme 17B).[48] Through isolation of intermediates **II** and **III**, it was discovered that the mechanism progresses through a Ni^0–Ni^{II} redox cycle, which suggests that the alkyl zinc bromide coupling partner (e.g. ^{n}BuZnBr) has a secondary purpose as a reducing agent, reducing $Ni^{II}Cl_2$•glyme to Ni^0 catalyst complex **I**. Oxidative addition of the C–N bond of aziridine **78** by **I** likely proceeds via an irreversible SET to give catalyst complex **II**, which undergoes transmetalation with the organozinc coupling partner, generating intermediate **III**. Dissociation of the EDO ligand, and association of the DMA solvent generates off-cycle species **IV**, which undergoes competitive β-hydride elimination and C–H reductive elimination to form side products **81** and **82**. When EDO ligand **80** is ligated to metal complex **III**, β-hydride elimination is suppressed, as evidenced by the ability to isolate **III**. Following C–C reductive elimination to provide **V**, metal complex **V** undergoes elimination to give **79** and Ni^0 catalyst complex **I**.

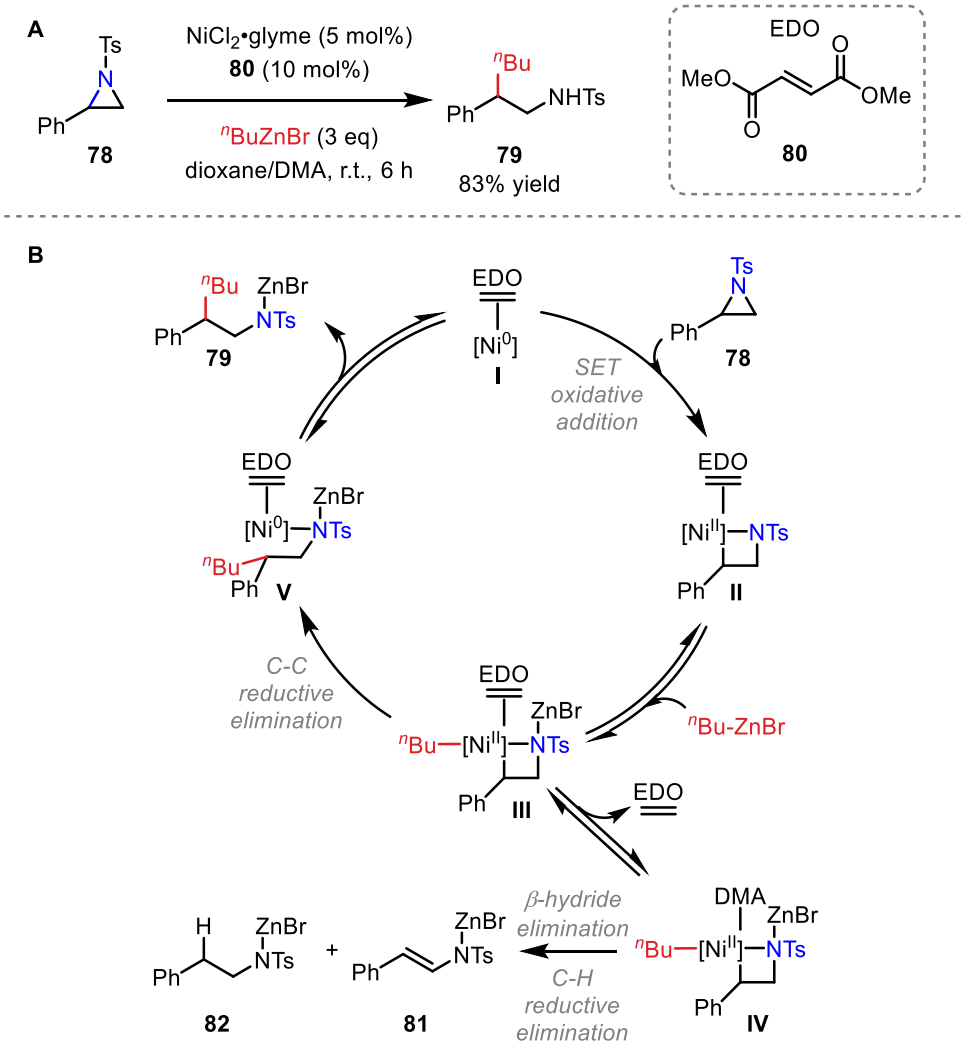

Scheme 17. *Negishi alkylation of aziridines using electron-deficient olefin ligands*

Doyle and co-workers subsequently reported an advance of the aforementioned Negishi coupling in 2013. In the report, the requirement for benzylic activation of the C–N bond was addressed ($NiBr_2$•DME, *p*-TolZnBr, LiCl, THF, r.t., 12 h) (Scheme 18A).[49] Aryl and alkyl nucleophiles were demonstrated, as well as a few aziridine substrates with different substitutions in the C**1** position. Disubstitution in the C**1** position, however, was not tolerated. Substrate scope was further limited by the required *N*-Cn moiety. The alkene group on this unit is essential as it directs the nickel catalyst for C–N oxidative addition. The inherent regioselectivity seen within the previous protocol (Scheme 17) was not observed within this system, as linear and branched products **84** and **85** were generated in a 3.8:1 ratio. A similar protocol for the ring opening of alkyl-substituted aziridines **86** was published by Jamison and co-workers in 2014 ($((CH_3)_2CH(CH_2)_2ZnBr$, $NiCl_2$, Me_4phen, DCE/THF, r.t., 18 h) (Scheme 18B).[49] Higher regioselectivities were observed under these conditions, with linear product **87** favoured in >20:1 selectivity. Further studies using enantiopure aziridines suggested that the oxidative addition step is S_N2-like, resulting in inversion of stereochemistry.

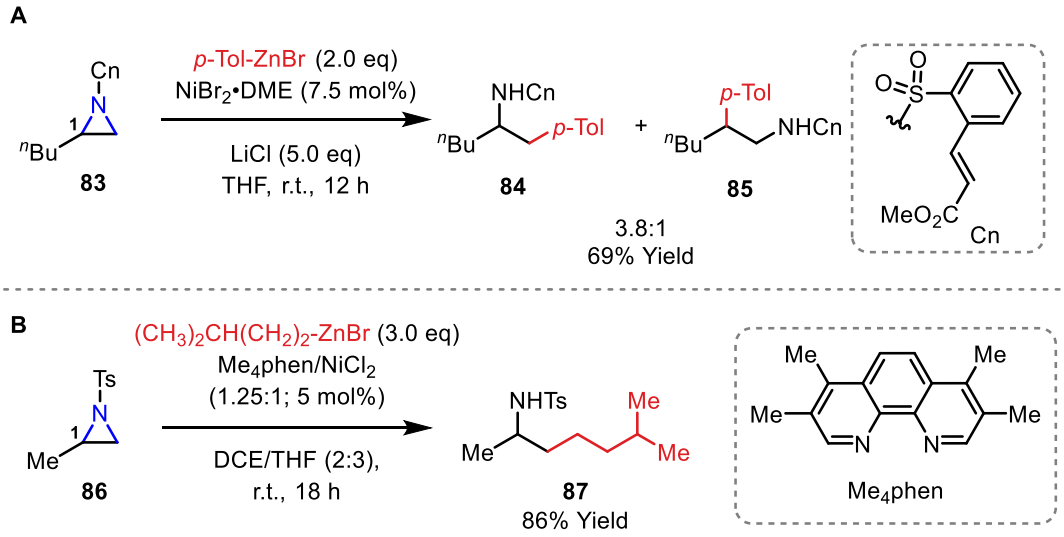

Scheme 18. *Advancements in the Negishi alkylation of aziridines*

Palladium-catalysed aziridine ring openings have also been demonstrated within the context of Suzuki cross-couplings (Scheme 19). One example was reported by Michael and Duda, who employed aryl boronic acids **58** with $Pd(dba)_2$ for the regioselective ring opening of aziridines **88** (PNp_3, Cs_2CO_3, *m*-ClC_6H_4OH, THF, 35 °C) (Scheme 19A).[50] Advances of this Suzuki cross-coupling were reported by Michael and Teh, who expanded the scope to encompass alkenyl boronic acid coupling partners such as **90** (**86**, $Pd(dba)_2$, PNp_3, *m*-$NO_2C_6H_4OH$, THF, 35 °C) (Scheme 19B).[51] This work also included examples using hindered 1,1-disubstituted alkenyl boronic acids. Both protocols display high regiocontrol for the linear product (**89**, **91**) over the branched product.

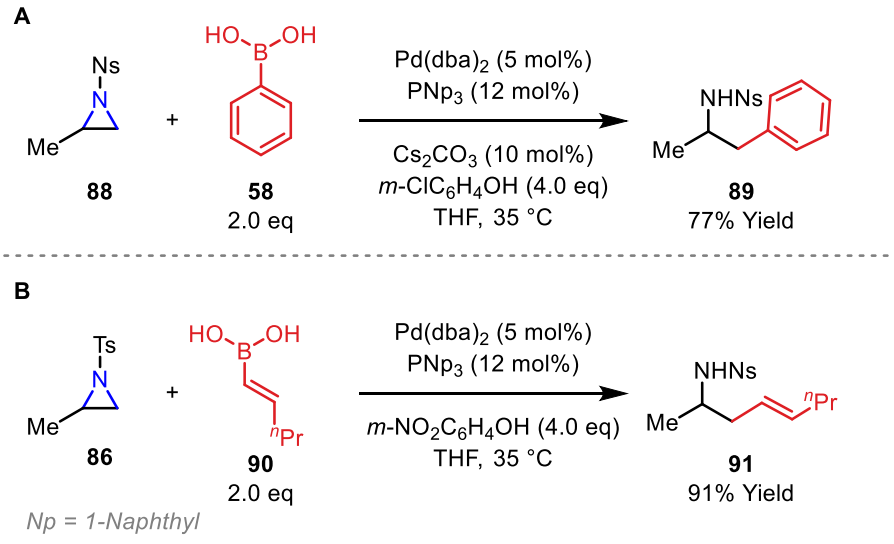

Scheme 19. *The palladium-catalysed Suzuki cross-coupling of aziridines*

1.4.2. Photoredox Chemistry for the Ring Opening of Strained Cyclic Amines

Another method for the ring opening of aliphatic aziridines was reported by Doyle and co-workers in 2020. Specifically, a photoredox cross-electrophile coupling protocol was developed, which converts differentially substituted aziridines **92** into highly substituted products **94** (**93**, $NiBr_2$•DME, dtbbpy, 4CzIPN, NEt_3, THF, photoreactor, 24 h) (Scheme 20).[52] The proposed mechanism for this reaction progresses as shown in Scheme 20. First, Ni^0 catalyst **I** cleaves the aryl iodide bond of **93** by oxidative addition, generating Ni^{II} complex **II**. Simultaneously, the iodide anion attacks aziridine **92** to form ring-opened intermediate **95**. Single-electron transfer (with **IV** or 4CzIPN$^{-\bullet}$), or halogen-atom abstraction of **95** then generates alkyl radical **96**. This radical is then trapped by **II**, generating Ni^{III} species **III**. From **III**, reductive elimination provides product **94** and Ni^{I} species **IV**, which is subsequently reduced by photocatalyst 4CzIPN (PC) to regenerate Ni^0 **I**. The activated photocatalyst PC* then abstracts an electron from triethylamine and reforms PC$^{-\bullet}$. $Et_3N^{+\bullet}$ is then used for the in situ generation of HI which is used to mediate the cleavage of aziridine **92**, and thus the cycle continues. Due to the radical nature of this cross-coupling, no enantioselective examples were reported.

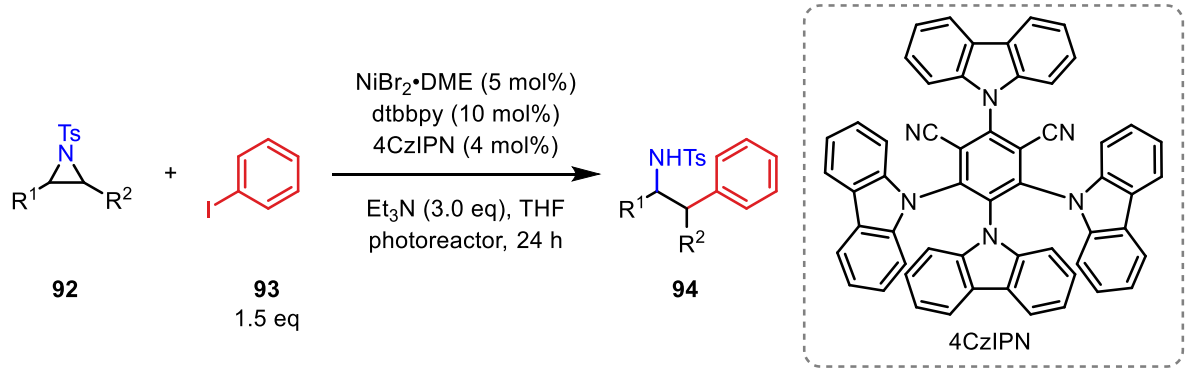

Proposed Mechanism

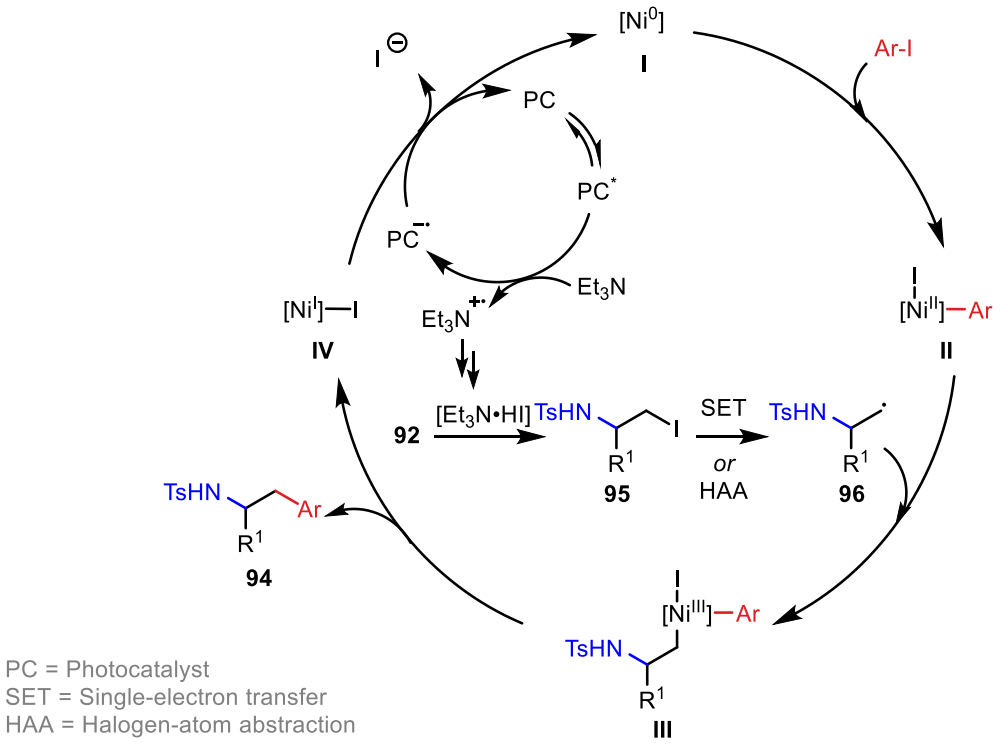

PC = Photocatalyst
SET = Single-electron transfer
HAA = Halogen-atom abstraction

Scheme 20. *The photoredox cross-electrophile coupling of aliphatic aziridines*

1.4.3. Stereocontrolled Ring Expansion of Aziridines

The ring expansion of aziridines by carbonylation provides a method for the synthesis of β-lactams. The first catalytic carbonylation of aziridines **97** was reported by Alper and co-workers in 1983, who employed a rhodium catalyst for the stereoretentive oxidation addition of the aziridine C–N bond, forming β-lactams **98** via intermediate **99** ($[RhCl(CO)_2]_2$, CO, benzene, 90 °C, 2 days) (Scheme 21A).[53] While the highly regiospecific transformation demonstrated the excellent viability of this protocol, high reaction temperatures (90 °C) and CO pressures (20 atm), and slow reaction times (2 days) were required. In 2002, Coates and co-workers expanded on this work, providing a mechanistically distinct method for the stereoinvertive oxidative addition of aziridines **100** for the formation of β-lactams **101** via intermediate **102** ($[CpTi(THF)_2]^+[Co(CO)_4]^-$, CO, DME, 60 °C, 5 h) (Scheme 21B).[54] This protocol is postulated to progress via Lewis-acid assisted nucleophilic attack of the C**1** centre, giving intermediate **102** in a stereoinvertive manner. This method offers high yields and regioselectivity, as well as lower reaction temperatures (60 °C), though high CO pressures (60 atm) were required.

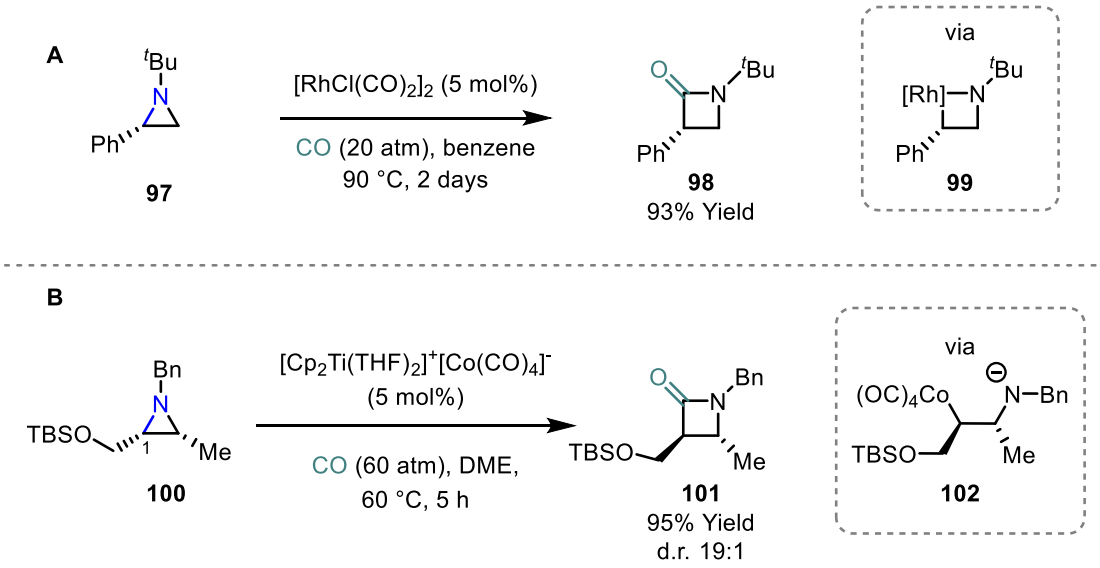

Scheme 21. *Methods for the stereoretentive and stereoinvertive carbonylation of aziridines*

In 2010, Aggarwal and co-workers reported an alternative method for the stereospecific carbonylation of aziridines **102** and **103**, which gave β-lactams **104** in high diastereomeric excess ($Pd_2(dba)_3$•$CHCl_3$, PPh_3, CO, toluene, r.t., 2 h) (Scheme 22A).[55] The substrate scope reported was limited to alkenyl-substituted aziridines, though ambient reaction temperatures (r.t.) and pressures (1 bar) provide definite improvements to the Alper conditions. A similar protocol for the carboxylation of

aziridines **102** was also reported by Aggarwal and co-workers.[56] This protocol provides a method for the conversion of aziridines **102** into oxazolidinones **105** using a Pd^0 catalyst for the cleavage of the C–N bond ($Pd_2(dba)_3$•$CHCl_3$, PPh_3, TBAT, CO_2, toluene, 0 °C, 2 h) (Scheme 22B). The reported scope was similarly limited to alkenyl-substituted aziridines. The mechanism for this transformation is proposed to proceed as shown in Scheme 22B, wherein aziridine **102** reacts with the Pd^0 catalyst to form π-allyl palladium intermediate **I**. Capture of **I** by CO_2 then forms intermediate **II** which may undergo cyclisation to oxazolidinones **105**.

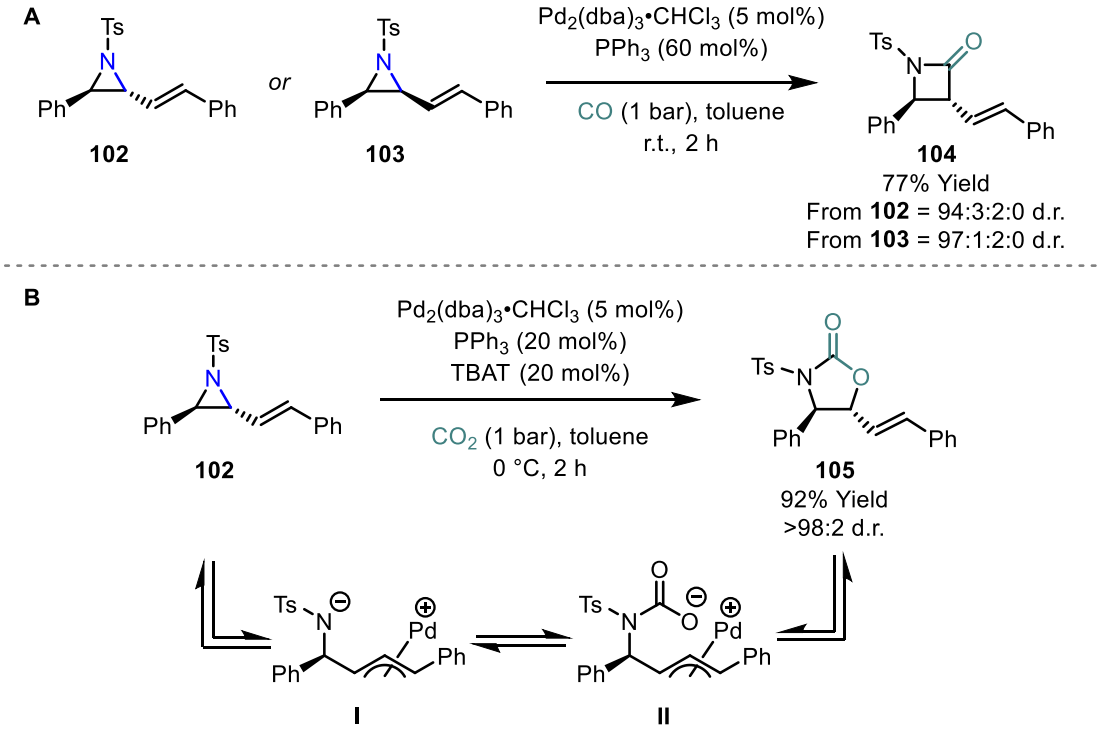

Scheme 22. *The advanced stereoselective carbonylation and carboxylation of aziridines*

1.5. Methods for the Ring Opening of Non-Strained Cyclic Amines

The ring opening of non-strained cyclic amines is inherently more challenging than the ring opening of strained cyclic amines. Because of this, there are few existing methods for the ring opening of pyrrolidines and piperidines by C–N cleavage, and those that do exist offer severely limited scope. The methods that have been developed can be divided into three different categories: (1) reductive cleavage, (2) oxidative cleavage, and (3) von Braun-type cleavage (Scheme 23).[57] Within this chapter, reductive cleavage and oxidative cleavage are explored; von Braun-type cleavage is further examined in Section 5.2.1.

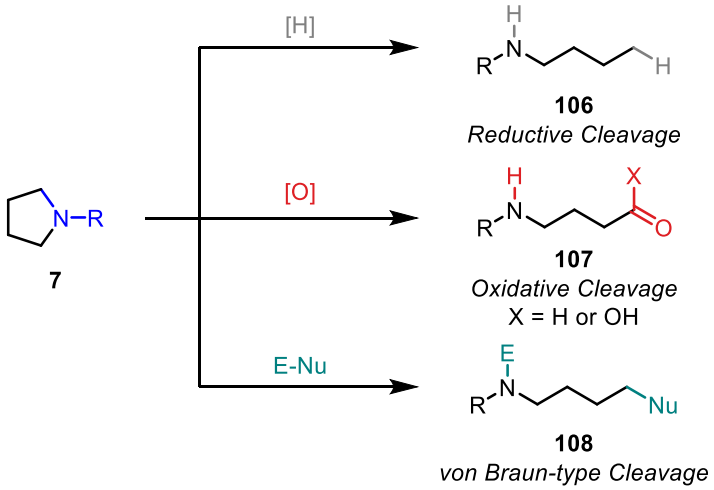

Scheme 23. *Methods for the ring opening of non-strained cyclic amines*

1.5.1. Using *Reductive Cleavage* for the Ring Opening of Non-Strained Cyclic Amines

The typical approach for the reductive cleavage of non-strained cyclic amines employs transition metal catalysed hydrogenation conditions to give hydrocarbon frameworks such as **106**. One example was reported by Tourwé and co-workers in 1997. Here, H_2 and palladium on carbon were employed for the ring opening of cyclic amine **109** to form amino acid **110** (MeOH/H_2O, r.t., 8 h) (Scheme 24A).[58] In this instance, substrate scope was limited, with only two examples reported, and benzylic activation is required to enable C–N bond cleavage. An alternative method for the reductive cleavage of non-strained cyclic amines was reported by Honda and Ishikawa in 1999, in which methanol was used as the proton source and SmI_2 as the reductant (**111**, HMPA, THF, 0 °C to r.t., 9 h) (Scheme 24B).[59] A broader substrate scope was demonstrated, including pyrrolidine and piperidine substrates. The mechanism commences with single electron transfer from SmI_2 to the carbonyl moiety, giving **112**. A second electron transfer follows, providing intermediate **113** which, following elimination, gives the enol tautomer of product **114**. The use of reductive cleavage for the ring opening of non-strained cyclic amines is limited by the utility of the hydrocarbon frameworks generated, as their lack of functional handles render further transformations challenging.

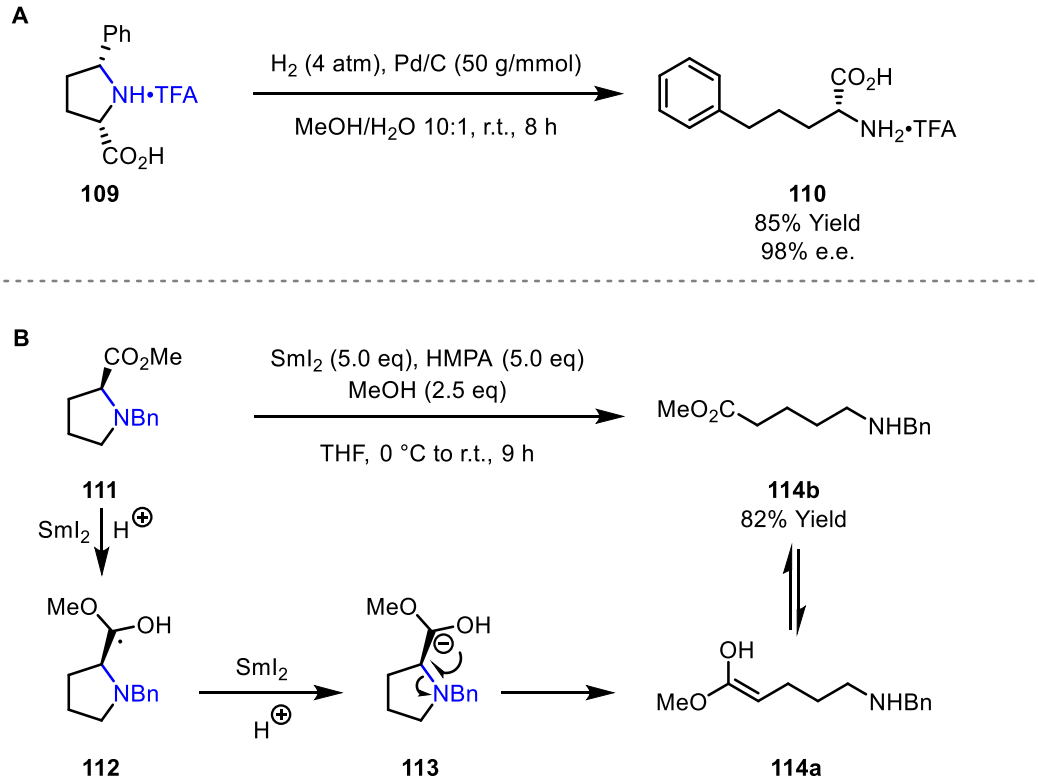

Scheme 24. *Applying reductive cleavage conditions for the ring opening of non-strained cyclic amines*

1.5.2. Using *Oxidative Cleavage* for the Ring Opening of Non-Strained Cyclic Amines

The use of oxidative cleavage over reductive cleavage for the ring opening of non-strained cyclic amines has seen broader methodological application. One reason is that this approach usually provides functional handles in the ring opened products, making them more useful for synthetic protocols. The use of ruthenium porphyrin Ru(TMP)Cl_2 together with 2,6-dichloropyridine *N*-oxide has been demonstrated as an effective system for the oxidation and ring opening of cyclic amides such as **115** (benzene, 40 °C, ~18 h) (Scheme 25A).[60] This technique also proved effective for the ring opening of 5-, 6-, and 7-membered rings. A similar ring opening method was reported by Che and co-workers in 2011, who instead employed an iron catalyst for the oxidative ring opening of cyclic amines such as **115** (**M1**, Oxone, MeCN/H_2O, 80 °C, 6 h; $Fe(ClO_4)_2$•$6H_2O$, Oxone, 80 °C, 6 h) (Scheme 25B).[61] The report also demonstrated that this method may be applied to the epoxidation of alkenes, the oxidation of arenes, the oxidation of alkanes, and the demethylation of tertiary amines. While the yields for this ring opening protocol are lower than those generated by use of the ruthenium catalyst, the use of iron catalysts is highly desirable as they are more biocompatible. Both of these protocols are limited, however, by their low functional group tolerance; for example, oxidatively sensitive functionality is not tolerated.

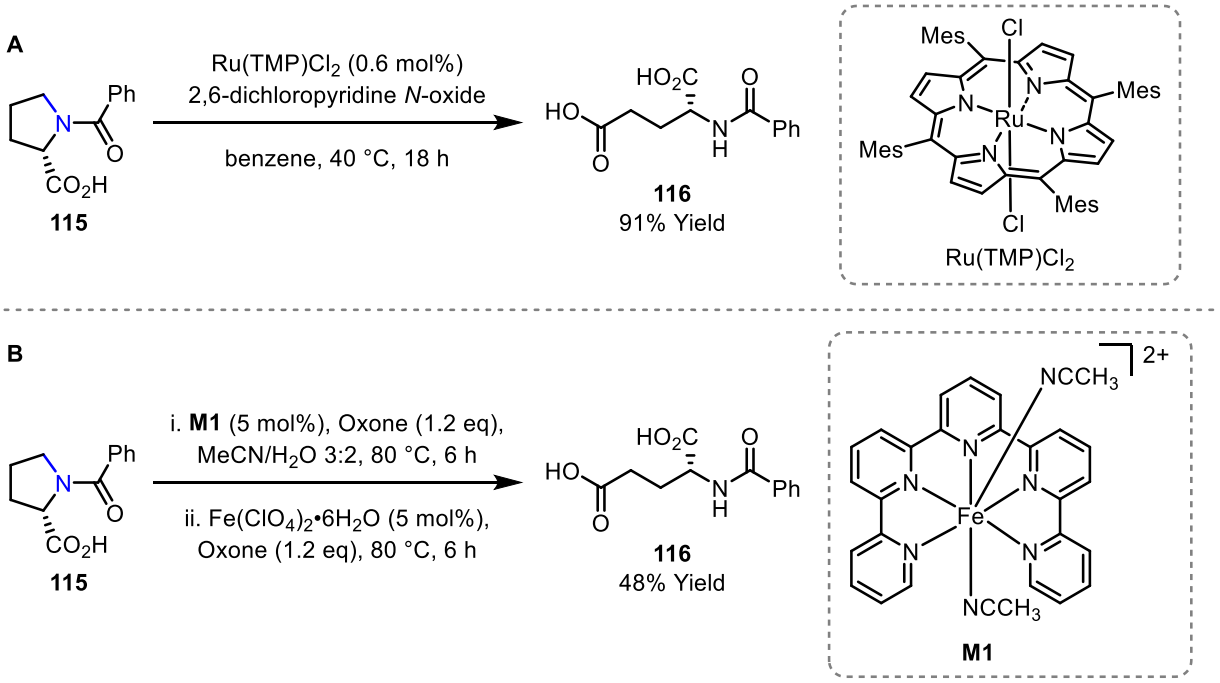

Scheme 25. *Applying oxidative cleavage conditions for the ring opening of non-strained cyclic amines*

Photooxidation may also be used for the oxidative cleavage of non-strained cyclic amines. Ferroud and co-workers demonstrated this in the ring opening of pyrrolidine and piperidine systems **117** to provide linear products **121**. The process requires photocatalyst **122** and oxygen (hν >630 nm, MeCN/MeOH, 20 °C, 4 h), and is highly regioselective (Scheme 26).[62] The scope of this protocol is limited by the required bulky *N*-substituent, and substitutions on the pyrrolidine and piperidine backbones were limited to methyl or ethyl groups. The proposed mechanism for the ring opening is shown in Scheme 26. Photooxidation of **117** generates hydrazinium **118** which, upon attack of the nucleophile, gives hemiaminal **119**. A second photooxidation gives **120** which, upon subsequent nucleophilic attack of methanol, gives product **121**. When water is used in place of methanol, this final step produces an aldehyde product.

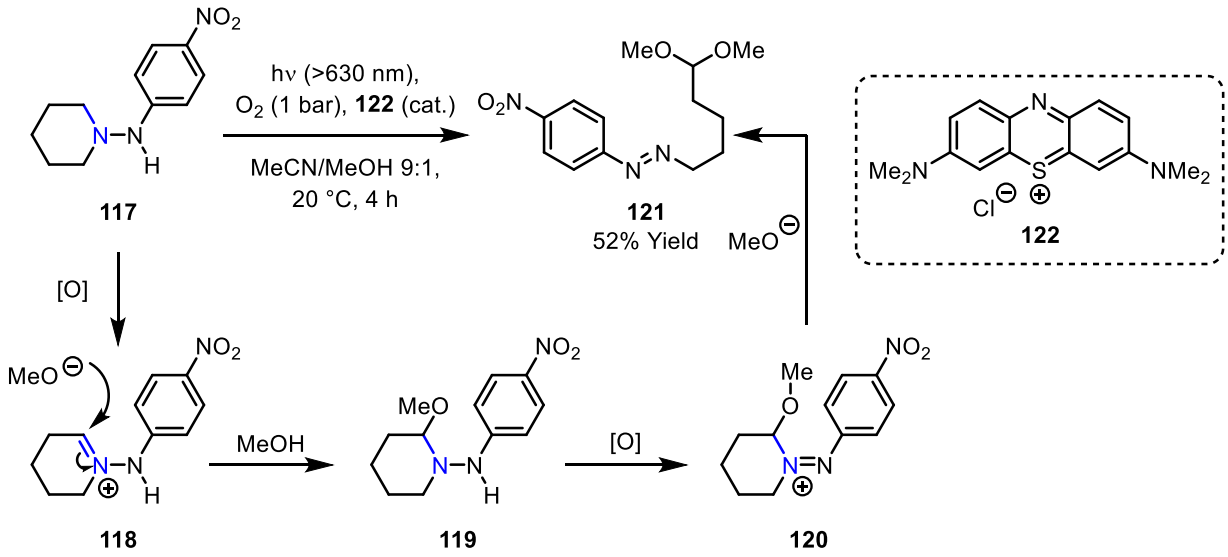

Scheme 26. *Applying photooxidation conditions for the oxidative cleavage of non-strained cyclic amines*

1.6. Project Aims and Thesis Overview

As outlined within this chapter, a variety of methods for the cleavage of C–N bonds have been developed, each with their own scope and limitations. For the cleavage of aryl C–N bonds, the formation and isolation of quaternary ammonium salts results in an additional synthetic step, whereas the use of directing groups severely limits substrate scope. Methods involving the oxidative addition of readily available neutral aryl amines are very rare (Section 1.2). Predominant methods for the cleavage of benzylic C–N bonds require either a quaternisation event or initial conversion to pyridinium salts, resulting in an extra synthetic step. As with aryl amines, methods for the oxidative addition of neutral benzylamines are rare (Section 1.3). C–N bond activations of strained aziridine and azetidine rings offer an excellent platform to synthesise highly functionalised products, though the current literature is limited in terms of substrate scope, especially with respect to the *N*-substituent. Additionally, there are limitations with respect to stereocontrol, which limits access to enantioenriched products (Section 1.4). Protocols for the ring opening of non-strained pyrrolidine and piperidine rings are more sparse than those for strained rings. Existing methods are limited by poor functional group tolerability, and there are few protocols for the synthesis of products containing useful synthetic handles (Section 1.5).

The aim of the work described in this thesis was to discover a new method, or methods, for the in situ activation of C–N bonds in aryl and benzylic systems, as well as strained and non-strained rings. The work described in Chapter 2 details initial studies into the employment of secondary phosphine oxides as amphoteric ligands for the oxidative addition of aryl and benzylic C–N bonds. It was proposed

that the ability of secondary phosphine oxides to coordinate a soft Lewis acid and hard Lewis acid simultaneously would promote the oxidative addition of C–N bonds (Scheme 27).

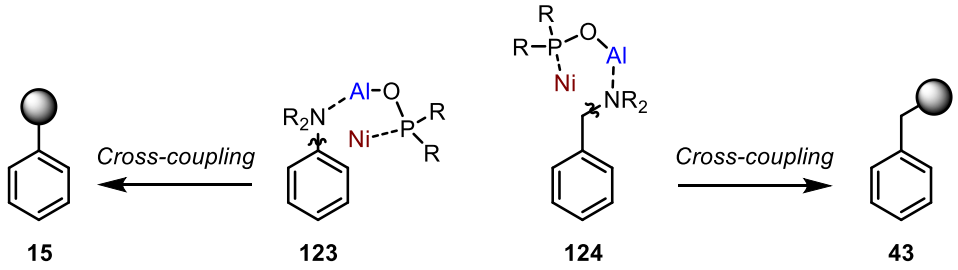

Scheme 27. *Employment of secondary phosphine oxides to promote oxidative addition of C–N bonds*

The goal of Chapter 3 was to develop a new protocol for the cross-coupling or nucleophilic substitution of α-primary benzylamines **125** via their corresponding benzyl iodides **126** (Scheme 28). It was proposed that the use of a stochiometric acyl chloride or anhydride activator in combination with an iodide source may be advantageous, and that a telescoped one-pot process for iodination and cross-coupling or nucleophilic substitution to give **127** or **128**, respectively, may be achieved.

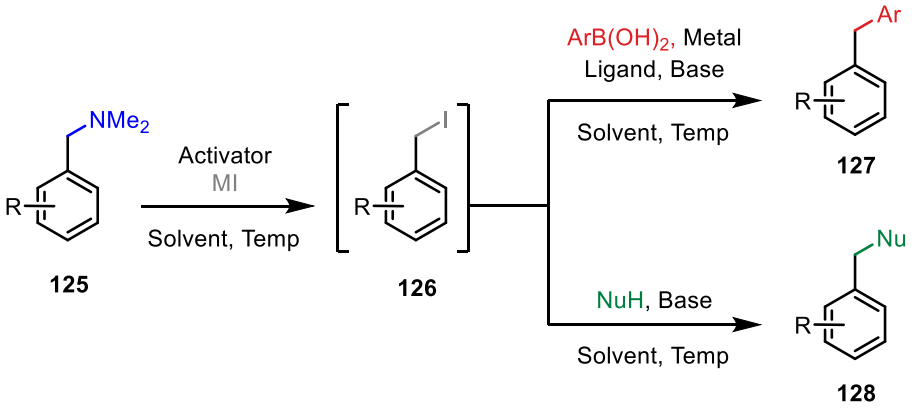

Scheme 28. *The proposed cross-coupling and/or nucleophilic substitution of α-primary benzylamines via intermediary benzyl iodides*

The goal of Chapter 4 was to expand the scope of the proposed benzylamine cross-coupling to include more complex α-secondary benzylamines **129** (Scheme 29). It was understood that a different protocol may be required for this cross-coupling, due to additional complexity and steric diversity in the α position. It was also recognised that boronic acids such as those employed in Chapter 3 may not be viable cross-coupling partners.

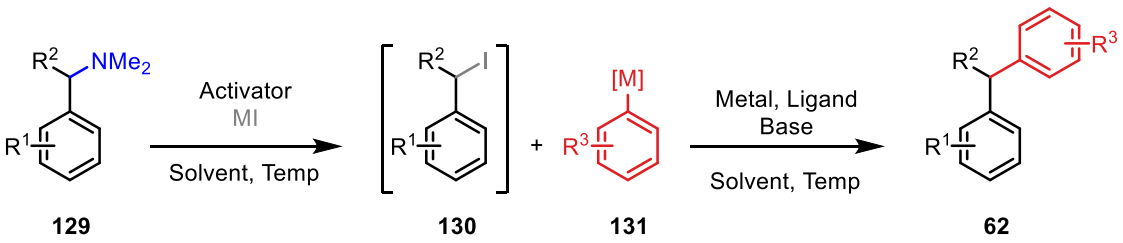

Scheme 29. *Proposed cross-coupling of α-secondary benzylamines via intermediary benzyl iodides*

Chapter 5 describes investigations to expand further the scope of this methodology to the ring opening of strained cyclic amines **71** (Scheme 30A) and unstrained cyclic amines **135** (Scheme 30B). It was proposed that the formation of intermediate alkyl or benzylic iodides **132** or **136** would allow for the development of telescoped aziridine and pyrrolidine cross-coupling and nucleophilic substitution protocols. In these instances, the activator employed for polarisation of the C–N bond is maintained in the product, so exploration of the scope of different activators was also proposed.

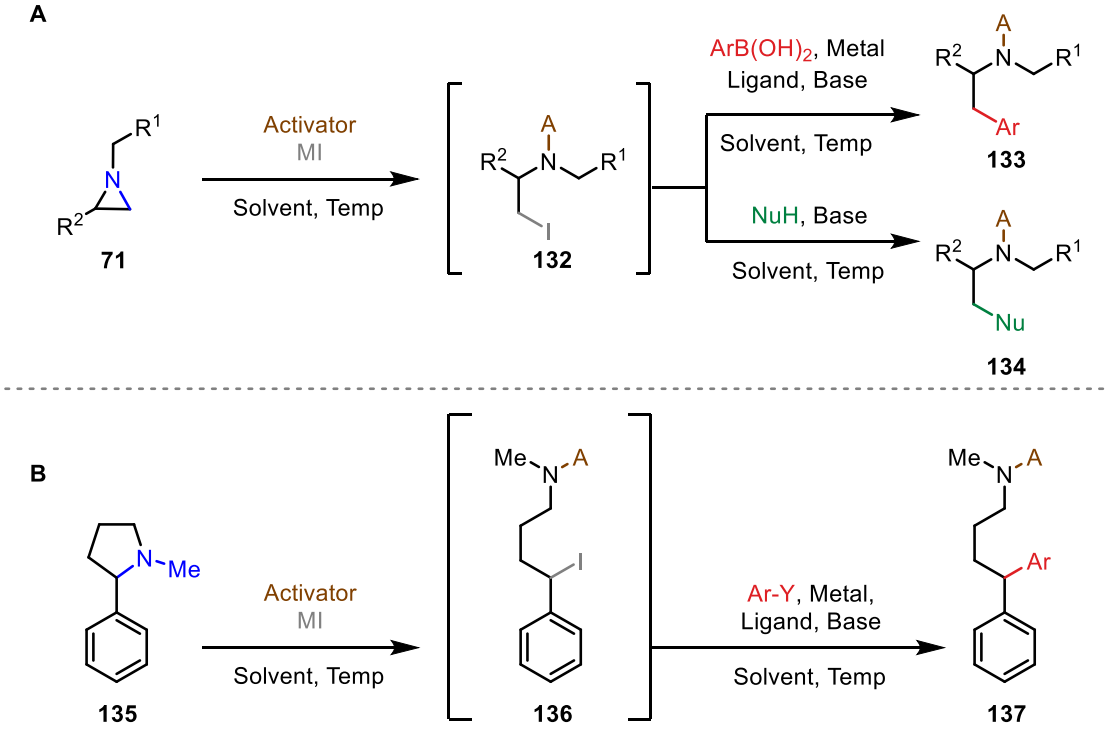

Scheme 30. *A proposed telescoped process for the cross-coupling or nucleophilic substitution of aziridines and pyrrolidines*

Chapter 2. SPO Ligands as Amphoteric Catalysts for the Activation of Aryl C–N bonds

As reported in Section 1.2, methods for the activation and cross-coupling of aryl C–N bonds are limited in terms of variety and scope. Nevertheless, as a ubiquitous functional group, methods for the diversification of anilines are highly desirable for total synthesis and late-stage functionalisation applications. This chapter outlines investigations into the use of Secondary Phosphine Oxides (SPOs) as amphoteric ligands for the proposed activation and cross-coupling of anilines and benzylamines.

2.1. Secondary Phosphine Oxides

2.1.1. Tautomerisation and Binding Abilities of Secondary Phosphine Oxides

Secondary Phosphine Oxides (SPOs) are particularly useful ligands: their ability to exist in equilibrium between two tautomeric forms **138** and **140** provides them with two reactive binding sites while maintaining high stability. Tautomerisation of SPOs strongly favours pentavalent oxide form **138** (Scheme 31); it was reported by Börner and colleagues in 2010 that, in non-coordinating conditions, phosphinous acid tautomer **140** (PA; Scheme 31) is only observed for SPOs with extremely electron-withdrawing substituents (e.g. $–C_5F_4N$).[63] This preference for the pentavalent form is ideal, as these are much more air- and moisture-stable than their corresponding phosphine ligands containing the same backbone (PR_3 vs $HP(O)R_2$).[64] In coordinating conditions, however, pentavalent phosphine oxide **138** is able to tautomerise into trivalent phosphinous acid **140**, which can act as a P-donor or an O-donor ligand; this provides the active form of the ligand.[65–68]

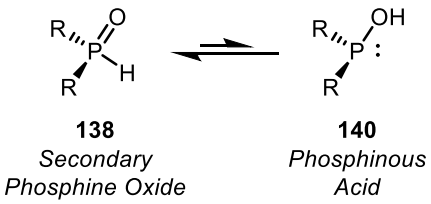

Scheme 31. *Structure and Tautomerisation of Secondary Phosphine Oxides*

There has been much speculation surrounding the mechanism of tautomerisation in SPOs.[69] In 2007, two potential pathways were proposed by Hong and co-workers,[70] proceeding either by unimolecular or bimolecular pathways (Scheme 32). In the proposed unimolecular pathway, tautomerism occurs via intramolecular proton exchange of the hydroxyl proton, whereas the bimolecular pathway involves hydroxyl proton exchange via 6-centred transition state **141**. In 2015, this work was advanced by Montchamp, Janesko, and co-workers, who demonstrated that water-catalysed tautomerisation involves simultaneous dissociation of the phosphine oxide P–H proton and formation of the phosphinous acid O–H bond.[71] This suggests that the inclusion of water may alter the pathway through which tautomerisation occurs. Furthermore, it was reported that the uncatalysed

unimolecular pathway is highly challenging for SPOs due to the strain within the required 3-membered transition state **139** (R = H; $\Delta G^{\ddagger}$ = 59.1 kcal mol^{-1}), and so, in the absence of catalytic water, the bimolecular pathway is likely to dominate.

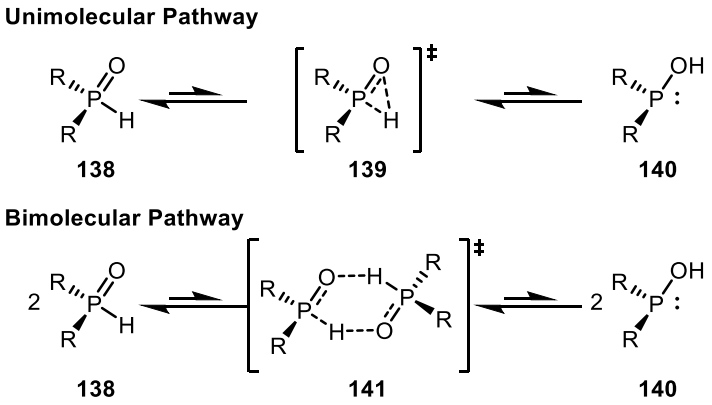

Scheme 32. *The mechanism for the tautomerisation of SPOs*

The complexation of SPO ligands is defined by this tautomerisation. As previously stated, the prevalent form of **138** is comparatively air- and moisture-stable,[67,72,73] which facilitates purification via flash chromatography, and makes the ligands easier to handle than less stable phosphines with similar chemical groups and structural backbones. As described later, SPOs do degrade slowly in air (Section 2.3), but they still demonstrate stability beyond that of many other phosphine ligand classes.[74]

Another advantage of SPO tautomerisation resides in the bifunctional reactivity offered by phosphinous acid form **140** (Scheme 33). As previously mentioned, this phosphinous acid is an ambidentate donor: it is able to coordinate via its P- or O-terminus, in a selective manner. The soft Lewis basic nature of the P-terminus means it ligates readily to soft Lewis acidic metals, such as Ni, Fe, Pd, Ir, Au, Pt, Rh, and Ru (forming **143**). In contrast, the hard Lewis basic O-terminus ligates preferentially to hard Lewis acids and early transition metals such as Ti, Cr, Mo, W, Mn, Re, and Ru (forming **142**).[69] Accordingly, complexation to these transition metals can shift the tautomerisation equilibrium in favour of the phosphinous acid form.

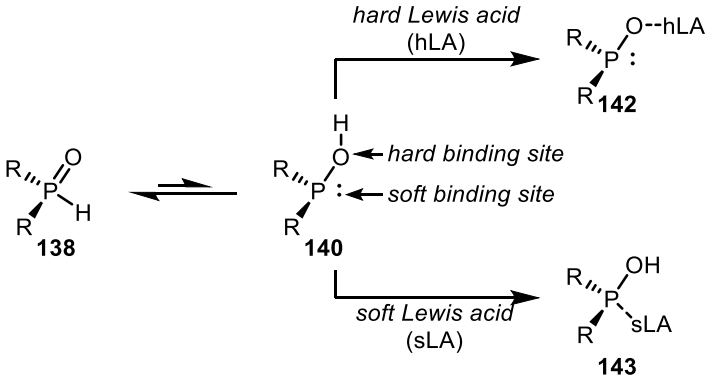

Scheme 33*. SPO ligands as ambidentate donors*

Further versatility of the PA form of SPOs lies in its electronic tunability. In the presence of base, the weakly acidic phosphinous acid is easily deprotonated. This allows coordination to a metal in a pseudobidentate manner, wherein two SPOs come together and form a hydrogen-bonded bridge (**144**, Figure 1). This structure can be extremely stable, because the P=O moiety is one of the strongest hydrogen-bond acceptors[68] ($((C_2H_5)_2HP{=}O{-}HOPh$ binding ΔH = -11.5 kcal mol^{-1} vs $(CH_3)_2C{=}O{-}HOPh$ binding ΔH = -4.66 kcal mol^{-1}).[75,76] In this pseudobidentate form, PAs become highly electron-donating ligands, comparable to *N*-heterocyclic carbene (NHC) ligands in their electron-donating ability (Figure 1).[69,77,78] Furthermore, it has been demonstrated that this hydrogen-bonded backbone (M = H) makes these ligands highly useful in hydroformylation, hydrogen-transfer, and hydrogenation reactions.[68] Alternatively, without this deprotonation, coordinated phosphinous acids are less donating even than their corresponding trisubstituted phosphorus counterparts, including tertiary phosphines, phosphite, and aminophosphine structures,[79] and so the electronic nature of SPOs is highly diverse, making them highly useful ligands.

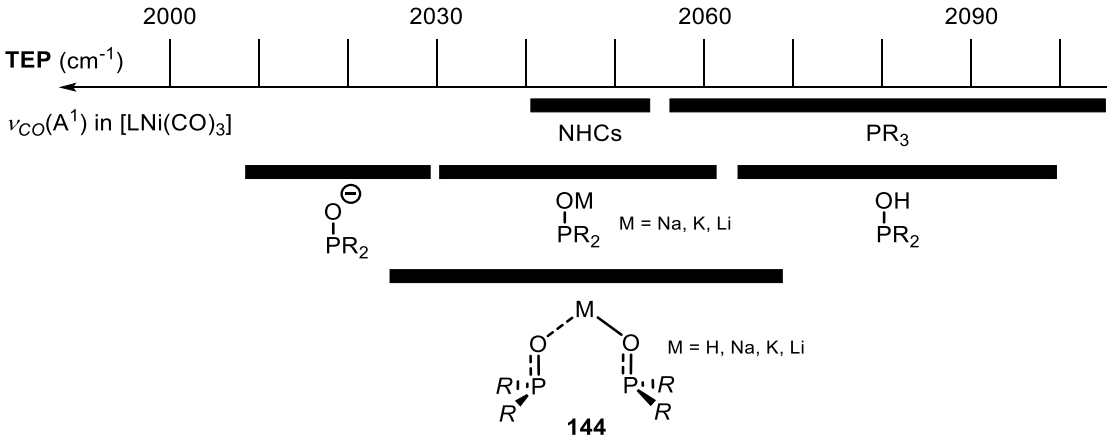

Figure 1. *Tolman's electronic parameter (TEP) of various phosphine and SPO ligands*

The ability of SPOs to bind via their P- or O-terminus suggests their utility in the design of amphoteric catalysts (Scheme 34). Furthermore, the highly electron-donating nature of pseudobidentate SPOs **144** suggests they may be viable ligands for challenging oxidative additions, such as those involving cleavage of relatively stable C–N, C–O, and C–H bonds. Scheme 34 shows a potential C–X bond cleavage, wherein X represents any electronegative element able to bind with a tethered Lewis acid. Indeed, there are reports of SPO ligands facilitating challenging oxidative additions in this manner, as discussed further in Section 2.1.3.

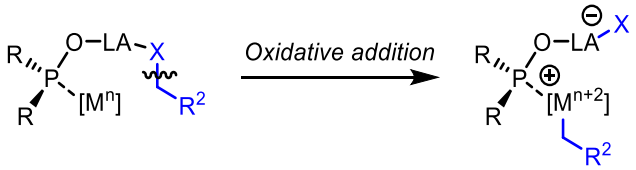

Scheme 34. *Applying the dual binding ability of SPO ligands for the cleavage of C–X bonds*

2.1.2 Methods for the Synthesis of SPO Ligands

SPO ligands typically fall under one of four structural classes (Figure 2). Dialkyl or diaryl SPOs **145** can be symmetrical or asymmetrical ($R^1 = R^2$; or $R^1 \neq R^2$), and they have a carbon-based backbone. Heteroatom-substituted SPOs (HASPOs) **146** contain heteroatom based subunits tethered to the phosphorus atom (X = O, N). They typically have a cyclic backbone, which can be chiral or achiral—this provides a very different electronic and steric alternative to dialkyl or diaryl SPOs **145**. SPOs **138** contain their chiral information at the phosphorus centre, rather than in the backbone of the molecule. Bidentate SPO-phosphine ligands **147** contain both an SPO centre and a phosphine centre, allowing for chelate binding to a metal. There are different methods of synthesis for each of these structural variants which, in turn, order different reactivities when the SPO is coordinated to a transition metal.

145 *Dialkyl/Diaryl SPO* | **146** *HASPO* | **138** *SPO with stereogenic P* | **147** *Bidentate SPO-Phosphine*

Figure 2. *Four structural classes of SPO ligand*

Achiral dialkyl or diaryl SPOs **145** (Figure 2) are commonly formed by Grignard displacement of an alkoxide from a monosubstituted phosphinic ester **148** (Scheme 35A)—this method was utilised in the research described later (Section 2.3).[73,80,81] Oxidation of secondary phosphines **149** to their corresponding secondary phosphine oxide **145** may also be employed (Scheme 35B), though various over-oxidised side-products are commonly formed, reducing the applicability of this method.[82] Another method for the synthesis of SPOs **152** proceeds via hydrolysis of the corresponding phosphine halide (Scheme 35C).[83] Compared to diaryl SPOs **145** (R = Ar), dialkyl SPOs **145** (R = Alk) are more challenging to synthesise due to the higher Lewis basicity of their oxygen centre, which leads to the formation of P–O–P side products **153** (Scheme 35).[69]

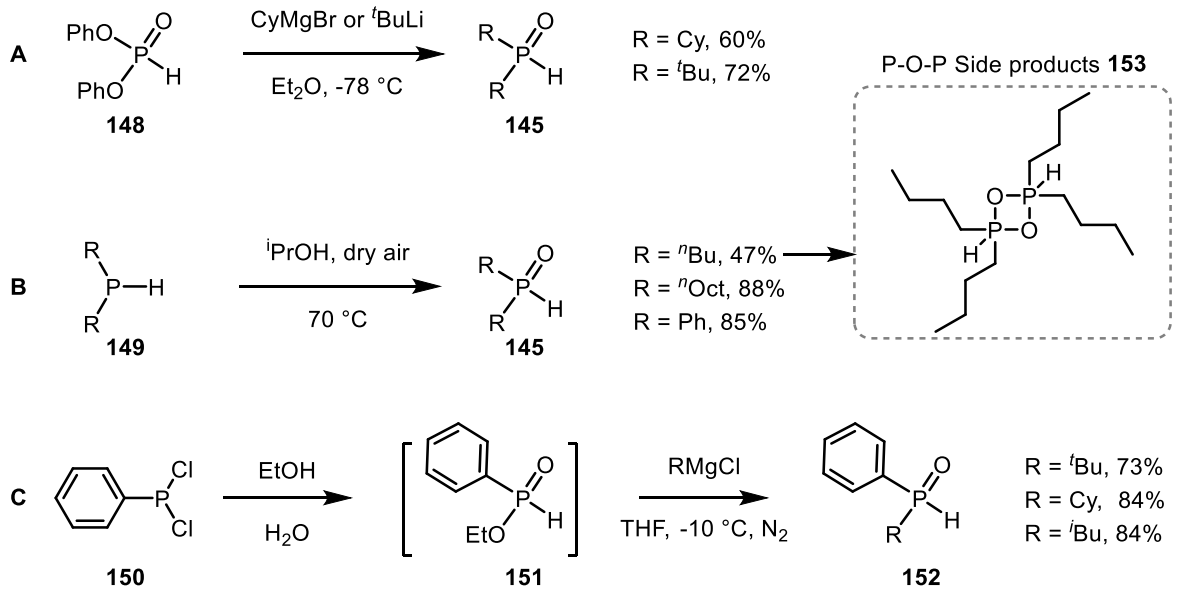

Scheme 35. *Various protocols for the synthesis of dialkyl or diaryl SPOs*

HASPO ligands **146**[67,72] may be synthesised from their corresponding diamines, diols, or amino alcohols in a two-step manner such as that shown in Scheme 36. Here, enantioenriched TADDOL **154** was employed for the synthesis of HASPO ligand **156** with a chiral backbone. The nucleophilic alcohol units of TADDOL first attack PCl_3 in an S_N2 manner, displacing chloride and forming phosphine chloride **155**. This is followed by hydrolysis, which generates HASPO target **156** in 82% yield. The facile nature of this synthesis makes highly diverse HASPO ligands accessible.[84]

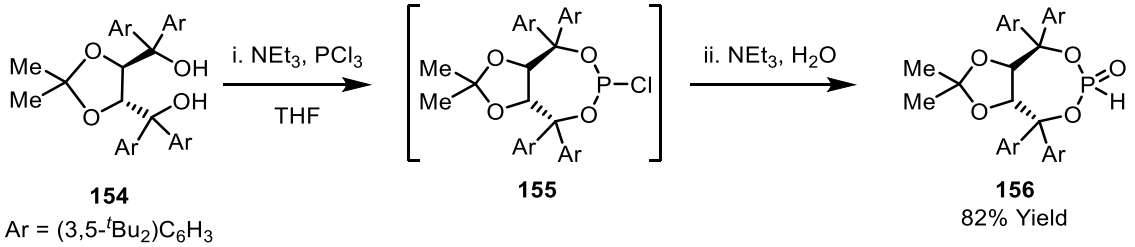

Scheme 36. *The synthesis of TADDOL-based HASPO ligand **156***

Although the majority of chiral SPO ligands developed contain their chiral information in the backbone of their structure, one method for the synthesis of an SPO with a stereogenic phosphorus atom was reported by Hamada and co-workers in 2005 (Scheme 37). Here, chiral triamine **157** reacts with PCl_3 (NEt_3) to form chiral phosphine **158**, which is then oxidised (H_2O, SiO_2) to generate chiral HASPO **159** in >99% e.e. This work demonstrates an elegant method for the incorporation of chirality into the phosphorus centre of the product, as well as in the backbone.[85] This ligand has since been used in various asymmetric allylic alkylations and substitutions.[85–88]

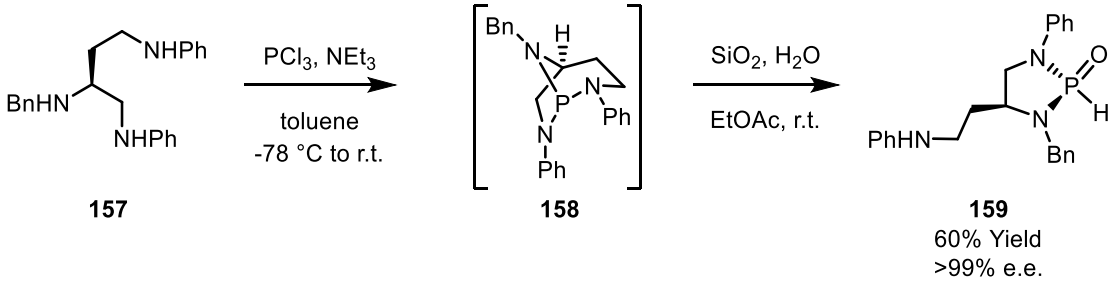

Scheme 37. *Synthesis of SPO* ***159*** *with a stereogenic phosphorous atom*

Bidentate SPO-phosphine ligands are less well explored. This class of ligand contains both a phosphine group and an SPO group, and it is hypothesised that this may facilitate coordination of a metal to both phosphorus atoms in a bidentate manner, as in Structure **164** (Scheme 38).[67,89] The synthesis of ligand **163** commences with aryl bromide **160**, which undergoes lithium-halogen exchange to aryl lithium **161** (^{n}BuLi, THF, hexane, TBME, -78 °C, 2 h), followed by S_N2 displacement of the P–Cl bond of $PhPCl_2$ (0 to 20 °C, 1.5 h), providing **162**. Finally, as is well-documented, the resulting phosphine chloride is hydrolysed with water to provide SPO **163** (Scheme 38).[90] This category of ligand comes with all the limitations of using phosphine ligands; the unstable nature of phosphines in air makes isolation of these products more challenging, though the bidentate binding may promote improved metal-ligand binding, and assist in tautomerisation of the SPO into its active PA form. These ligands perform well in certain rhodium-catalysed asymmetric hydrogenation reactions.[89]

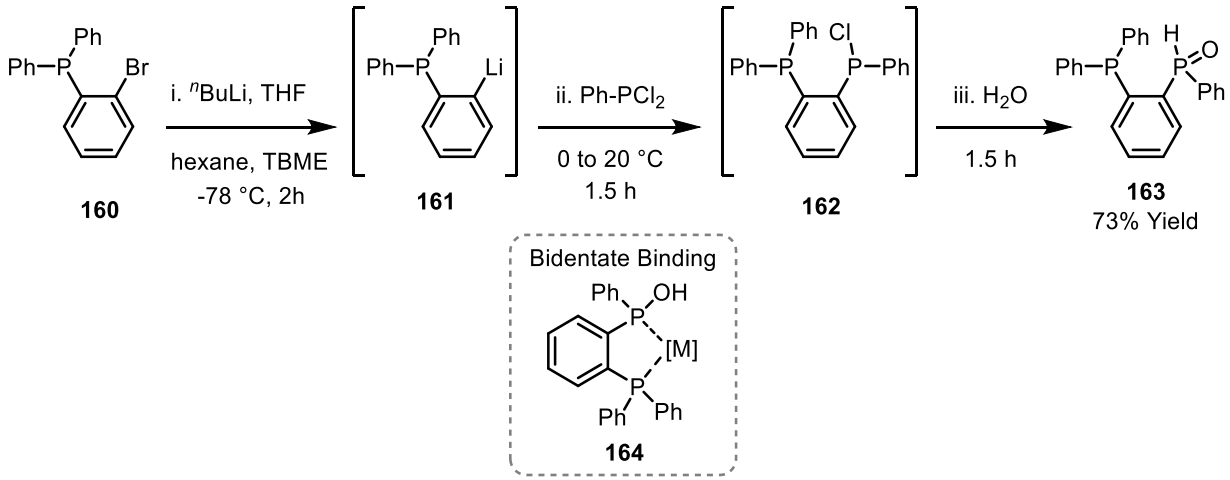

Scheme 38*. Synthesis of bidentate SPO-phosphine* ***163***

2.1.3 Secondary Phosphine Oxides as Amphoteric Ligands

So far, only a handful of reactions have been developed that take advantage of the built-in dual reactivity of SPOs.[67,89,91] Cramer and co-workers demonstrated the utility of this strategy in 2013, for the activation of the relatively stable C–H bond of formamide **165** under Ni-catalysed conditions

($Ni(cod)_2$, HASPO **167**, PPh_3, $AlMe_3$, toluene, 40 °C, 12 h) (Scheme 39A). This enabled a stereoselective intramolecular cyclisation to provide γ-lactam **166** in 96% yield and 97:3 e.r., with the latter controlled by the chiral backbone of HASPO ligand **167**.[67] It was proposed that the mechanism commences with tautomerisation of HASPO ligand **167** to its phosphinous acid **168** (Scheme 39B). This allows the formation of **I**, wherein the O- and P- termini are ligated to the hard Al and soft Ni centres, respectively. Subsequently, the carbonyl oxygen of formamide **165** coordinates to the Al-centre of **I**, which polarises the double bond and simultaneously brings the nickel centre into the proximity of the formamide C–H bond, giving structure **II**. This amphoteric mechanism lowers the enthalpic cost of oxidative addition. Following its insertion into the C–H bond, nickel coordinates to the alkene in advance of hydrometallation and C–C reductive elimination, which provides target **166**.

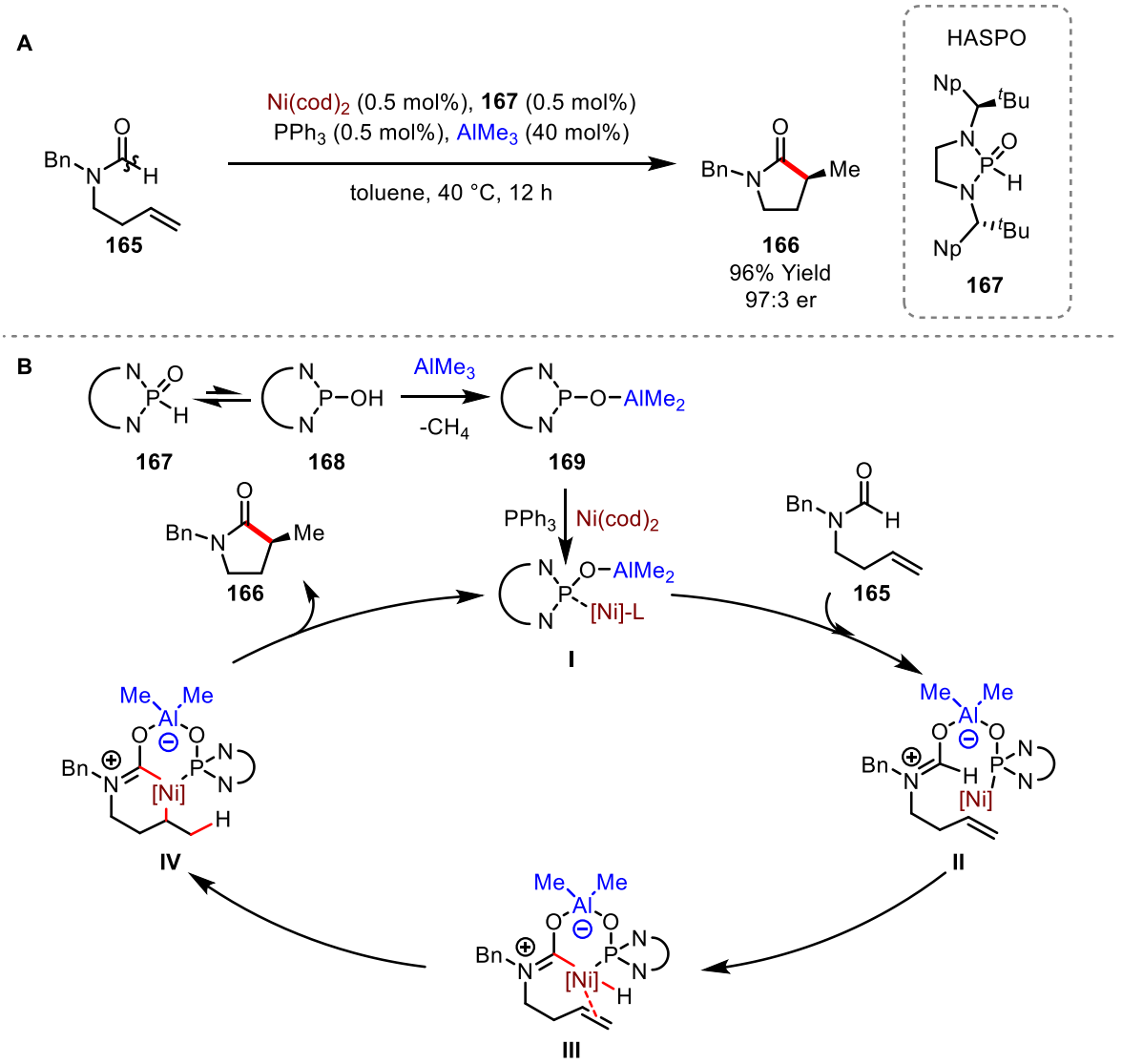

Scheme 39. *Procedure and mechanism of formamide C–H cleavage using HASPO ligand* ***167***

An alternative reaction which utilises the dual binding ability of SPOs was reported by Ye and colleagues in 2017. This ring expansion procedure employs achiral diaryl SPO ligand **172** for the

activation of the strained C–C bond of a cyclopropane moiety (Scheme 40).[80] Similarly to Cramer's protocol, Ni^0 pre-catalyst $Ni(cod)_2$, PPh_3, and $AlMe_3$ were used, but this time achiral SPO **172** (rather than HASPO **167**) was employed under more forcing conditions (130 °C). The mechanism for this transformation is similar to that described above: the in situ generated SPO-nickel-aluminium species **I** (Scheme 39) binds to the carbonyl to give **170** in advance of oxidative addition of the cyclopropyl ring, which forms metallocyclobutane **173**. Dissociation of the phosphine centre allows for the Ni-centre to coordinate to the alkyne partner, which inserts into the metallocyclobutane and, following C–C bond forming reductive elimination, gives 5-membered product **171**. It was proposed that the SPO-nickel-aluminium system facilitates the process in a threefold manner: (1) by bringing the nickel into proximity to the cyclopropane for oxidative addition; (2) by polarising the adjacent amide bond and destabilising the cyclopropane ring; and (3) by stabilising metallocyclobutane **173**.

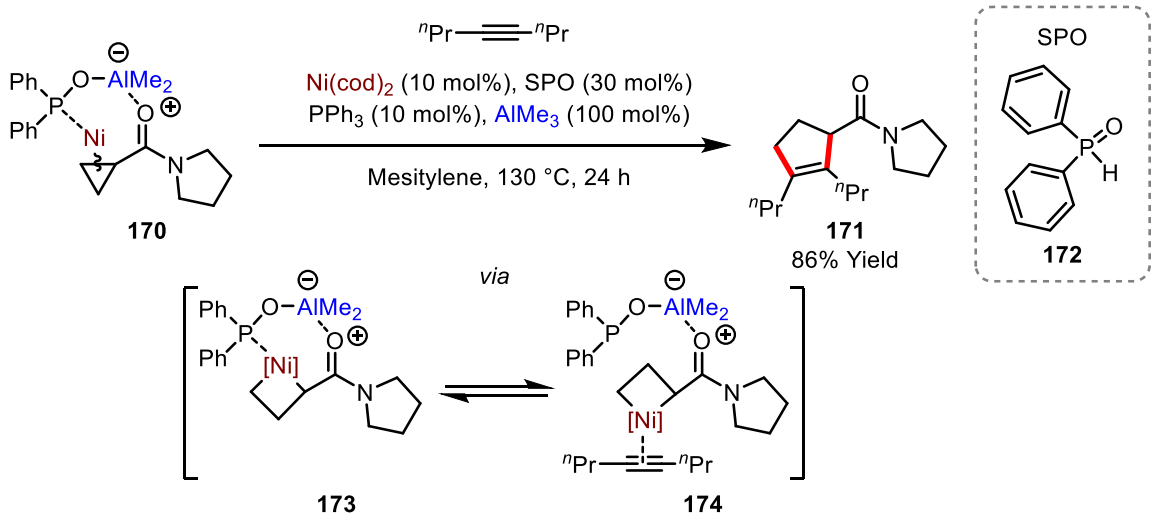

Scheme 40. *SPO amphoteric ligands for cyclopropane ring expansion*

In 2018, Ye and co-workers also reported the sequential C–H activation and cyclisation of benzoimidazoles in an enantiospecific manner ($Ni(cod)_2$, $AlMe_3$, HASPO **156**, 100 °C, 1 h) (Scheme 41).[91] Under these conditions, alkene hydroheteroarylation products **176** were formed in up to 98% yield and >99% e.e. Similar to the previous proposed mechanisms, it was posited that the SPO-nickel-aluminium complex (see Scheme 39) coordinates to the Lewis basic imidazole nitrogen, forming structure **175**. This polarises the C=N double bond and facilitates oxidative addition of the C–H bond to give **177**. Coordination of the nickel to the pendant alkenyl unit promotes hydrometallation to give **178** which, following C–C bond forming reductive elimination, forms product **176**.

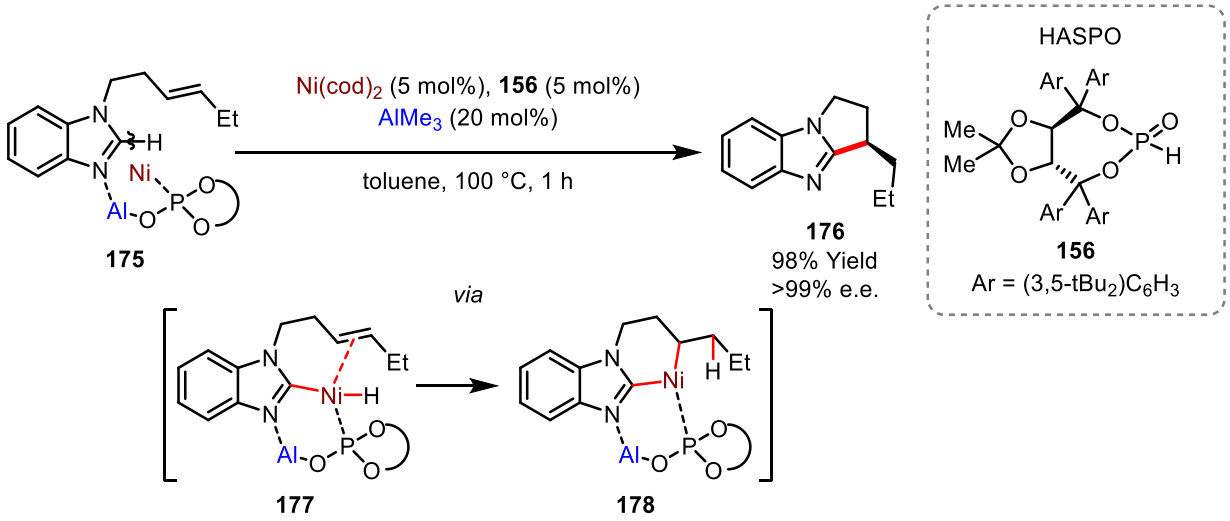

***Scheme 41**. SPO amphoteric catalysts for C–H cleavage and cyclisation*

2.2. The Proposed use of SPO Ligands in Amphoteric Catalysts for the Cleavage of C–N Bonds

The advantage of developing a ligand with built-in dual reactivity is that its use may bypass the need for complex directing groups for the cleavage of stable bonds. Within this project, it was proposed that an SPO dual binding system may be used to activate and cleave aryl and/or benzylic C–N bonds. This hypothetical system utilises a hard Lewis acid, such as aluminium, which may bind directly to the Lewis basic nitrogen centre of the target substrate. Addition of an SPO ligand and a soft Lewis basic metal capable of oxidative addition, such as nickel, provides a system where the redox active metal is held in close proximity to the target C–N bond (**123** and **124**) (Scheme 42). This arrangement should promote oxidative addition in a twofold manner: (1) because the process is now intramolecular, and (2) because the C–N bond is polarised (weakened) by coordination of the hard Lewis acid. If utilised in an appropriate manner, the proposed strategy could be used to access products such as **15** and **43**, and has evident potential for the activation of other strong bonds, such as Ar–OMe; Bn–OMe; C(O)–C; or C(O)–H bonds.

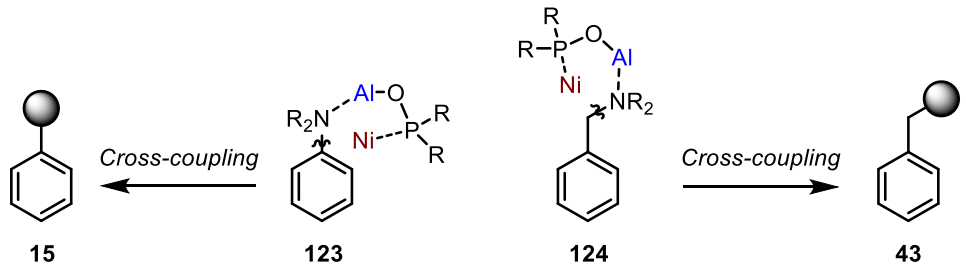

***Scheme 42**. Proposed system for C–N bond activation using SPOs as amphoteric ligands*

2.3 Synthesis of SPO Ligands

For the purpose of probing the applicability of various types of SPO ligand and their functionalities within the proposed aryl C–N bond activation, representative SPOs from each category defined in Figure 2 were chosen for synthesis. Diaryl SPO **180** and dialkyl SPO **181** were synthesised in a very similar manner, using the appropriate aryl or alkyl bromide as the starting material. The first step involved the formation of the corresponding Grignard reagent in THF (Mg, cat. I_2, 70 °C).[92] The intermediate solution was then reacted with diethylphosphite, and targets **180** and **181** were isolated in 78% and 47% yield, respectively, following purification via flash column chromatography (FCC) or recrystallisation. The yield for diaryl SPO **180** was significantly higher than that obtained for dialkyl SPO **181**. This difference is attributed to the competing formation of P–O–P side products during the synthesis of **181** (see Section 2.1.2, Scheme 35).[69]

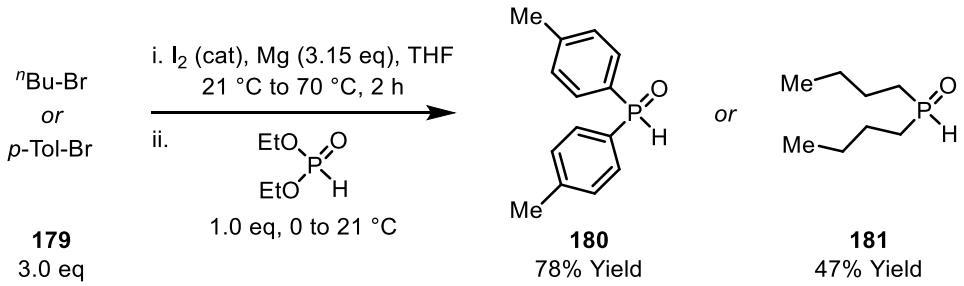

Scheme 43*. Synthesis of dialkyl and diaryl secondary phosphine oxides*

Inspired by the diaminophosphine oxide ligands used by Cramer and co-workers (Scheme 39),[67] HASPO ligand **185** was designed and synthesised. An achiral backbone was chosen, as the proposed aryl C–N activation was to be carried out on an sp^2 centre, giving achiral products. The synthesis of **185** was carried out in two steps; first, the reductive amination of benzaldehyde **183** with amine **182** (MeOH; $NaBH_4$ reduction; r.t.) provided diamine **184** in excellent yield following work up. The diamine was then phosphorylated (DCM, NEt_3, PCl_3, -78 °C) to form the N–P bonds of **185**, and the remaining P–Cl bond was hydrolysed (H_2O, -78 °C) to form the SPO of **185**. It was discovered that HASPO **185** is relatively unstable in solution, and this complicated purification, resulting in a low yield of 28%. HASPO **185** has a lower ^{31}P NMR shift than alkyl SPO **181** and aryl SPO **180** (HASPO **185** ^{31}P NMR δ = 15.9 ppm; SPO **181** ^{31}P NMR δ = 35.1 ppm; SPO **180** ^{31}P NMR δ = 22.2 ppm). This indicates that the P-centre of HASPO **185** has a lower electron density, and therefore is more susceptible to tautomerisation than **180** or **181**.[63]

Another challenge for the isolation of **185** was its decomposition on silica, likely via hydrolysis of its phosphinous acid tautomer. After some trials, it was discovered that FCC with oven-dried silica and fast elution through the column gave higher yields of isolated product. Rapid removal of the solvent

under reduced pressure also improved yields. Unfortunately, it was later discovered that the non-solvated compound is still subject to slow degradation if left in air—a new phosphorus NMR peak at δ = 8.5 ppm arose. Reported data for the NMR shift of $(Me_2N)_2P(O)H$ (^{31}P NMR δ = 21.8 ppm in $CDCl_3$)[93] vs $(Me_2N)_2P(O)(OH)$ (^{31}P NMR δ = 19.3 ppm in D_2O)[94] suggests this slight upfield shift likely corresponds to formation of phosphinic acid **186**. Subsequently, **185** was stored in a glove box, and this provided long-term stability.

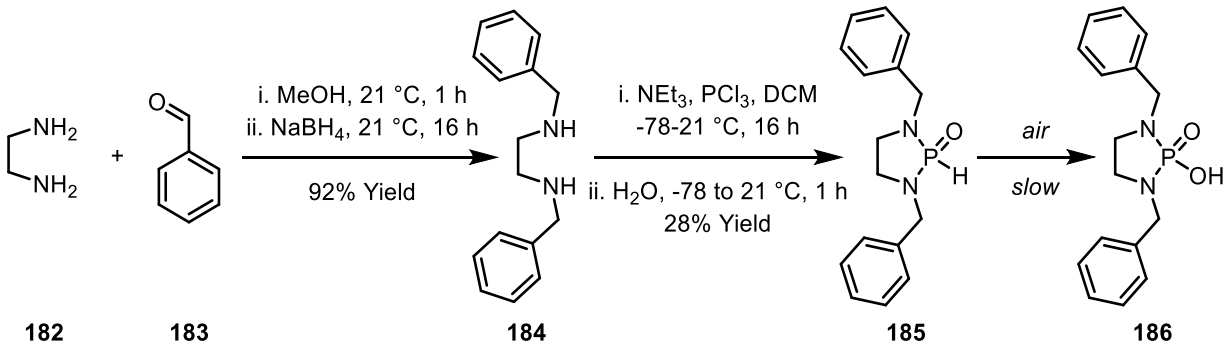

Scheme 44**. Synthesis of diaminophosphine oxide **185

The next SPO synthesised was chelating SPO-phosphine **163**. The first step in this synthesis was the halogen-lithium exchange of aryl bromide **160** (^{n}BuLi, THF, TMBE, -78 °C). The generated organolithium **161** was then added to $PhPCl_2$ (TBME, 0 °C) via cannula to give diaryl phosphine chloride **162**. This was hydrolysed (H_2O, 0 °C) to provide the desired SPO group of **163**. Following work up and purification via FCC (dry silica required), the product was isolated in 47% yield. As with diaminophosphine oxide **185**, partial degradation of the SPO (^{31}P NMR δ = 22.4 ppm)[95] to its equivalent phosphinic acid (^{31}P NMR δ = 34.9 ppm)[96] was seen, likely caused by reaction with adventitious oxygen. To prevent degradation, **163** was thereafter stored in a glove box.

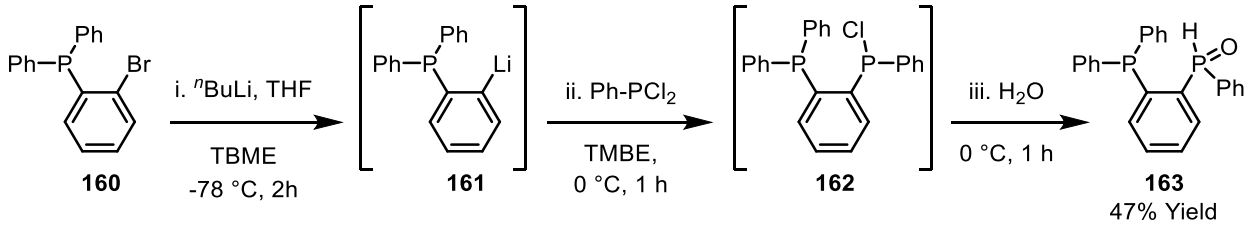

***Scheme 45**. Synthesis of bidentate SPO-phosphine*

2.4 Probing the Proposed C–N Activation Protocol

As discussed in Section 2.2, it was proposed that SPO-based amphoteric catalyst systems may be used for the activation and cleavage of aryl and benzylic C–N bonds (Section 2.2; Scheme 42). The chemical environment initially applied was based on those reported by Cramer and Ye (Section 2.1.3;

Schemes 39 and 40), who both employed highly electron-donating $Ni(cod)_2$, together with PPh_3 and $AlMe_3$. Aniline **18** and neopentyl glycolato borane (Bnep) coupling partner **35** were therefore exposed to these components at 130 °C in mesitylene, in an attempt to generate cross-coupled product **187**. Promisingly, initial yields of 17% by GC-MS analysis were observed. The Bnep coupling partner was selected over the more commonly utilised Bpin or boronic acid coupling partner, as the 6-membered ring increases the bond angle around the boron atom, making it more available for transmetalation.[97]

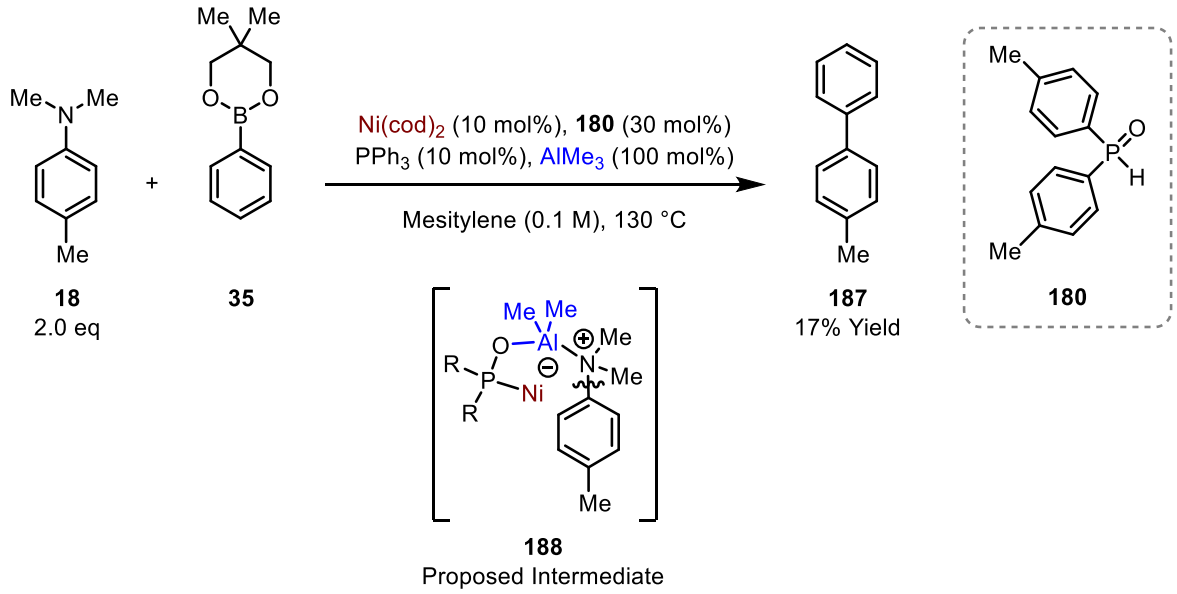

Scheme 46. *Applying aryl amines into proposed C–N cross-coupling conditions*

Bolstered by this initial result, alternative conditions inspired by aryl C–O bond activation methods were explored. In 2019, Ackermann and co-workers reported the use of SPO ligands in the Kumada-Corriu cross-coupling of phenol esters **189** ($NiCl_2$(DME), **181**, THF, r.t., 16 h).[97] This work exploited the ability of SPO ligands to assemble and form monoanionic pseudobidentate chelates **192**. As outlined in Section 2.1.1, chelates of this type are highly electron-donating, which makes them ideal ligands for oxidative additions involving relatively stable bonds. We considered that chelate structure **192** may have two roles within the reaction: (1) as a highly electron-donating ligand, and (2) as a Lewis acidic activator. For the latter, chelate **192** may interact with the methoxy group of **189** to form tethered chelate **193**, which promotes oxidative addition by polarising the C–O bond and bringing the Ni-centre into close proximity.

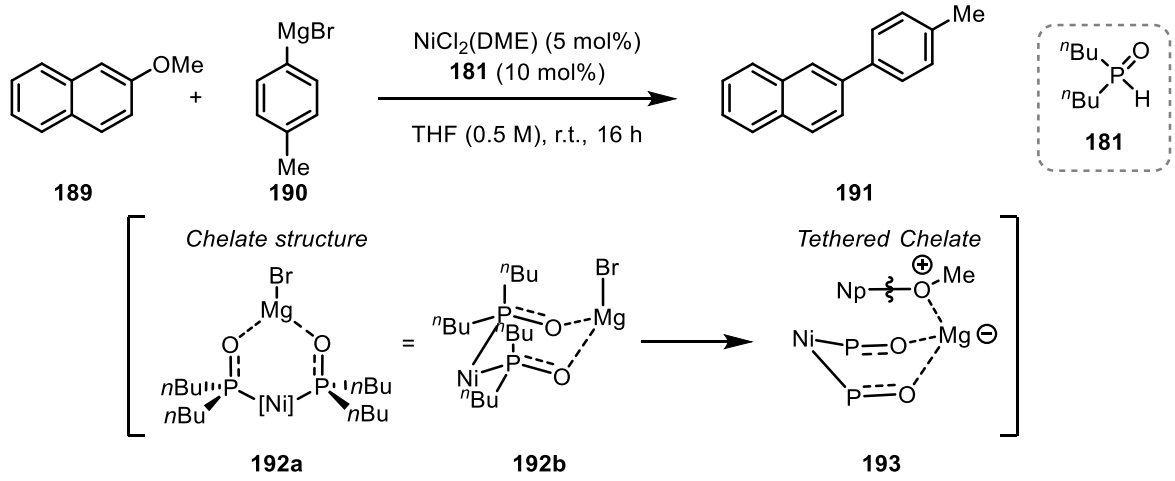

Scheme 47. *Aryl C–O Activation reported by Ackermann and co-workers*

The conditions reported by Ackermann and co-workers seemed promising for the potential activation of aryl C–N bonds; however, use of these conditions ([$NiCl_2$(DME)], SPO ligand, THF) for the cross-coupling of Grignard **195** and *N*,*N*-dimethylaniline **194** delivered no detectable product at r.t (Table 1, Entry 1). Undeterred, further variants of the process were explored, including the use of higher temperatures (70 °C), mono-methylated and free anilines **194** (A = NHMe; A = NH_2, respectively), and alternative SPO ligands (e.g. **181** and **186**). Unfortunately, in each case, no cross-coupled product **187** was obtained. In the case of HASPO **186**, some homo-coupling of Grignard **195** was observed by GCMS (Table 1, Entries 1 and 2), although this product was not quantified.

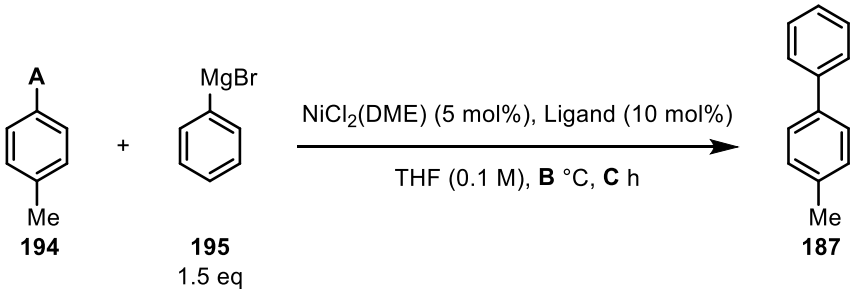

Entry	A	Ligand	B	C	Yield (%)
1	NMe_2	**186**	25	17	0
2	NMe_2	**186**	70	17	0
3	NMe_2	**181**	25	68	0
4	NHMe	**181**	25	68	0
5	NH_2	**181**	25	68	0
6	NMe_2	**181**	70	68	0
7	NHMe	**181**	70	68	0
8	NH_2	**181**	70	68	0

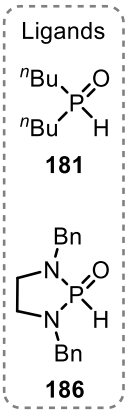

Table 1. *Application of aryl amine **194** into the Ackermann cross-coupling conditions*

In 2018, Shi and co-workers reported the Suzuki cross-coupling of naphthyl C–N bonds using a Ni-complex modified with $iMes^{Me}$ ($NiBr_2$, Mg, THF, 130 °C, 36 h) (Scheme 48),[25] and this was advanced in the same year to include borylation of naphthyl amines **40**.[24] In this process, magnesium metal was used for the in situ reduction of the $NiBr_2$ precatalyst to Ni^I. Unfortunately, the scope of this protocol is mostly limited to naphthyl or biaryl aniline substrates. However, this process uses a highly electron-donating *N*-heterocyclic carbene ligand to facilitate oxidative addition, and this suggested that an improvement in scope may be possible by instead using a chelating SPO. As explained in Section 2.1.1, this ligand class can be considered as electron-donating as NHC ligands. Therefore, Shi's conditions were trialled, but utilising SPO ligand **180** in place of the $iMes^{Me}$ carbene (Table SI:1, Entries 9 and 10). Unfortunately, only starting material was returned, and no cross-coupling was observed.

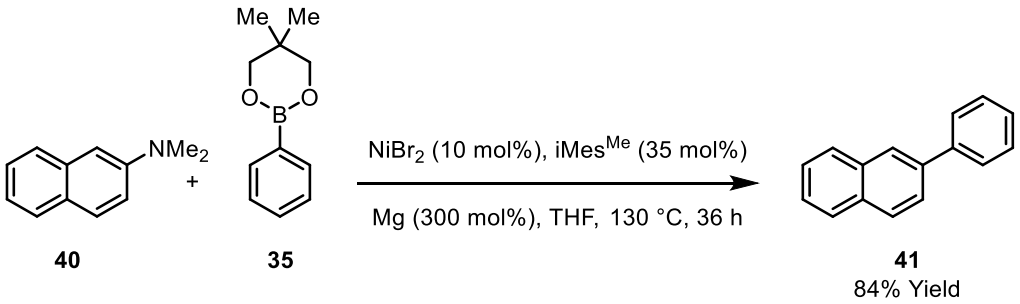

Scheme 48. *Reported aryl C–N activation by Shi and co-workers.*

Following these disappointing results, attention returned to the successful result shown in Scheme 46, as the low but promising yield of 17% could potentially be improved through optimisation studies. Preliminary experiments aimed to establish whether all of the reagents are vital for the formation of product **187**. To this end, a series of reactions were carried out (1) in absence of PPh_3, (2) at lower temperatures of 100 °C and 70 °C, (3) in the absence of the $AlMe_3$ Lewis acid and (4) in the presence of water. All of these deviations from the original conditions led to only recovery of starting material **18** (see Table SI:1) and cross-coupled product was not observed. Additionally, use of the conditions in Scheme 46 on mono-methylated and free aniline **194** (A = NHMe; A = NH_2, respectively) did not lead to any cross-coupling.

Next, the use of alternative Lewis acids was investigated. Trimethylaluminium is highly reactive and unstable in the presence of air or water;[98] it was proposed that this instability may lead to low turnover numbers. A variety of less reactive Lewis acids were trialled, including $Y(OTf)_2$, $FeCl_3$, $MgBr_2$, HBpin, and $SnCl_4$, each at loadings of 30 and 100 mol%. Unfortunately, in all cases, cross-coupling was not observed and only starting aniline **18** was returned (see Table SI:1).

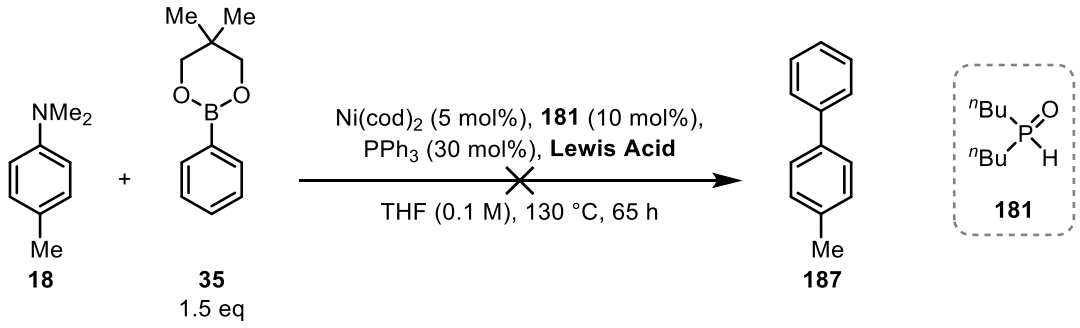

Scheme 49. *Exploration of alternate Lewis Acids*

It was considered that optimising the formation of proposed pseudobidentate structure **192**, reported by Ackermann and colleagues, for the activation of C–O bonds (Scheme 47) might improve the yield of **187** (Scheme 49). In 2011, Gérard Buono and co-workers described the effect of different bases on the electronic properties of SPO ligands.[79] In this study, SPO **181** and an inorganic base were used to form pseudobidentate structures **196** (Figure 3), with various group 1 metals (M) coordinated between the two oxygen atoms. By studying CO stretching frequencies of molybdenum complexes **197**, it was discovered that systems where M = Mg possess similar electronic properties to their analogous phosphinous acid (M = H)—these ligands are less electron donating. Alternately, systems where M = Na or K are strongly electron-donating, comparable to NHCs (**197** ν(CO): 2054 cm^{-1}; **198** (M = Na) ν(CO): 2052 cm^{-1}; **198** (M = K ν(CO): 2047 cm^{-1}).

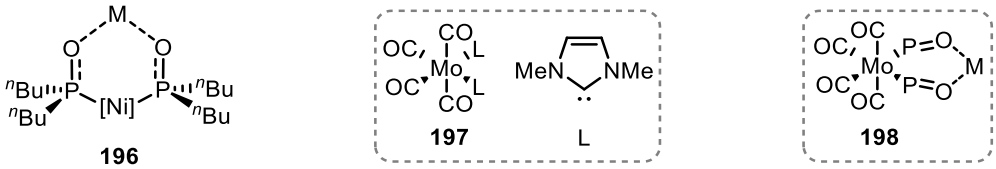

Figure 3. *Proposed pseudobidentate ligand structure activated by various metals (M)*

As NHC ligands have been successfully applied to C–N activation reactions,[25] the use of these highly electron-rich pseudobidentate SPO ligands was considered as a potential tactic to improve cross-coupling yields. To this end, ligand **180** was stirred with $Ni(cod)_2$, PPh_3 and Na_2CO_3 for 3 h prior to the reaction, to see if preformation of the catalyst showed any increase in yield. Unfortunately, no improvement in results was observed. Inclusion of Na_2CO_3 without extensive stirring prior to the reaction also proved to have no effect on yield. Additional studies into preformation of the aniline-Lewis acid complex by stirring of amine **18** and $AlMe_3$ before the reaction also proved ineffectual.

It was thought that the lack of improved reactivity may result from the poor solubility of Na_2CO_3 in mesitylene. To this end, ligand **180** was stirred with $Ni(cod)_2$, PPh_3 and Na_2CO_3 for 3 h in DMF prior to the reaction (Scheme 50). The subsequent cross-coupling was then carried out in a mixture of DMF and mesitylene, generating reduced yields of 11%. While DMF may promote formation of a

more active catalyst than mesitylene, it may also have a negative effect on the cross-coupling reaction, therefore showing no overall increase in yield.

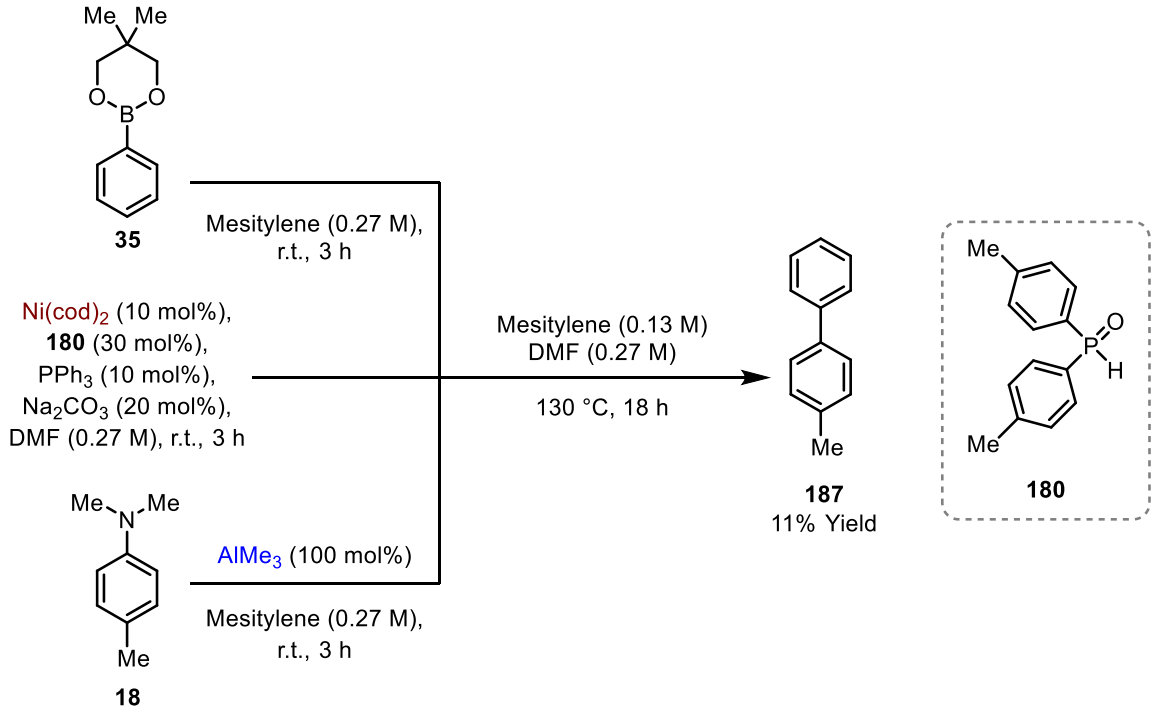

Scheme 50. *Trialling the pre-formation of pseudobidentate SPO complex* ***196***

Following these studies, no clear avenues for further alteration of the reaction conditions seemed productive, and so it was decided that the project would move away from the use of SPO-based amphoteric catalysts for the cross-coupling of aryl C–N bonds. However, it was still of interest to ascertain whether these catalysts may be feasible for the cleavage of *benzylic* C–N bonds instead. To this end, benzylamine **199** was synthesised by reductive amination (see Section 3.1.3, Scheme 60), and was subjected to cross-coupling with **35** under the conditions shown in Table 2. Unfortunately, in all cases, target diarylmethane **17** was not observed. No further investigations into this avenue were undertaken at this time.

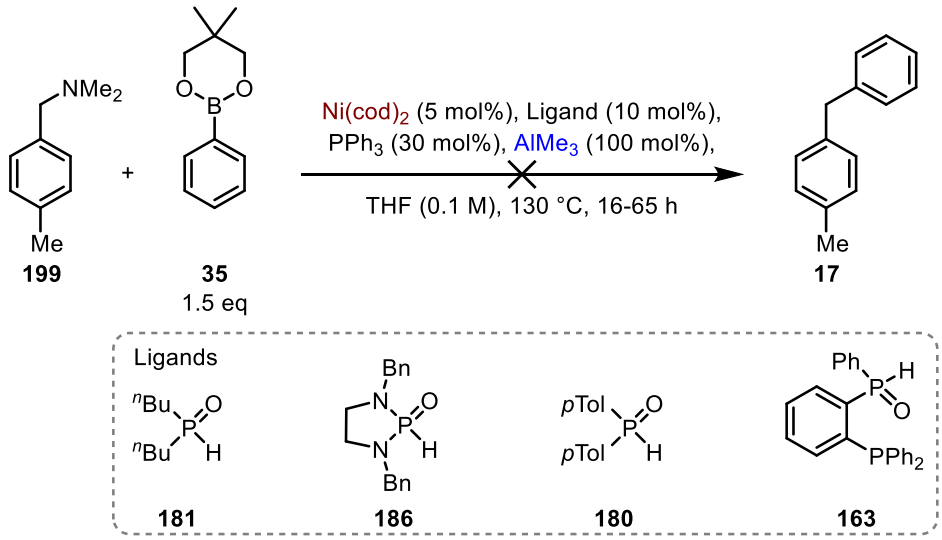

Table 2. *Application of benzylamine to established conditions*

2.5 Chapter Summary and Future Work

In this chapter, amphoteric catalysts derived from Secondary Phosphine Oxides (SPOs) have been explored for the activation of aryl and benzylic C–N bonds. The use of SPO **180** with $AlMe_3$, PPh_3, and $Ni(cod)_2$ provided proof of concept for the C–N activation of aryl amine **18**, by generating cross-coupled product **187** with 17% GC-MS yield (Scheme 46). Unfortunately, it was discovered that any alteration to these initial conditions resulted in the complete failure of the reaction. Additionally, application of these conditions to benzylic system **199** did not result in cross-coupled product **17**.

Future work in this area could examine further the use of different solvents for the preformation of the catalyst or the cross-coupling. One potentially powerful option would be to use a Lewis acid that can also function as the cross-coupling partner, as shown in Scheme 51. Here, hydrometallation of an alkyne with a Lewis acidic aluminium hydride should form organometallics such as **201**.[99] These could then react with the SPO, leading to systems **202** where, following oxidative addition, transmetalation would be facilitated by the proximity of the alkenyl metal reagent (Structure **203**).

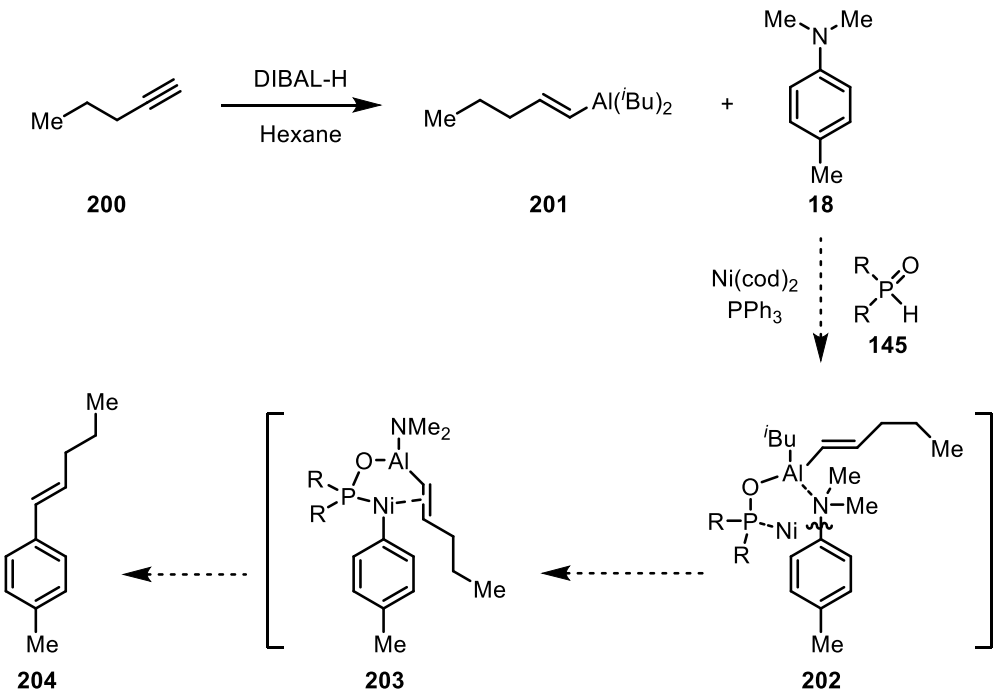

Scheme 51. *Proposed potential C–N activation using activated alkenes*

Chapter 3. Benzyl C–N Activation and Cross-Coupling

As discussed in Section 1.3, the activation and cross-coupling of benzylamines is highly desirable for the purpose of late-stage functionalisation, as the benzylamine moiety is ubiquitous in natural products and drug molecules. This chapter discusses a novel method for the activation and cleavage of tertiary benzylamines **125** for the formation of benzyl iodides **126** (Scheme 52). These iodides may be used subsequently in situ for cross-coupling and nucleophilic substitution reactions (providing **127** and **128**, respectively). Both steps of the process have been optimised to excellent yields, and a telescoped procedure has been developed that offers a broad scope.

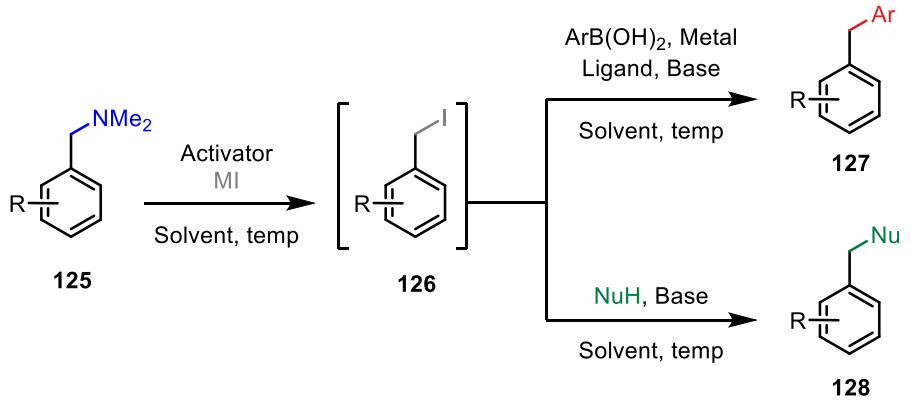

Scheme 52. *Benzylamine cleavage and subsequent in situ reactions explored within this chapter*

3.1 Benzylamine Conversion to Benzyl Halides

3.1.1 Background

As described in Chapter 2, attempts to use secondary phosphine oxides as amphoteric ligands for the activation and cross-coupling of benzylic C–N bonds proved unsuccessful, so investigations into alternative, stochiometric activators of the C–N bond were carried out. As outlined in Chapter 1 (Section 1.3), existing methods for the cross-coupling of benzylic C–N bonds are mostly limited to two avenues. The first uses highly toxic methyl triflate for the conversion of tertiary benzylamines into trimethylammonium triflate salts (Scheme 53A),[4,34,36,100] and the second uses bulky Katritzky pyridinium salts which provide benzyl radicals following single-electron transfer (SET) activation (Scheme 53B and 53C).[12,39,101] There are substantial drawbacks to both methods. Isolation of the trimethylammonium triflate salt (**45**) is required before cross-coupling can be carried out, thus increasing time and energy requirements for the transformation. Pyridinium Katritzky salts (**64** or **207**) are not atom economical, and SET cleavage of the C–N bond suggests that transfer of defined benzylic stereochemistry is not possible (Scheme 53C).[26,39] The goal of this project was to find a new method for benzylic C–N cross-coupling that addresses these limitations.

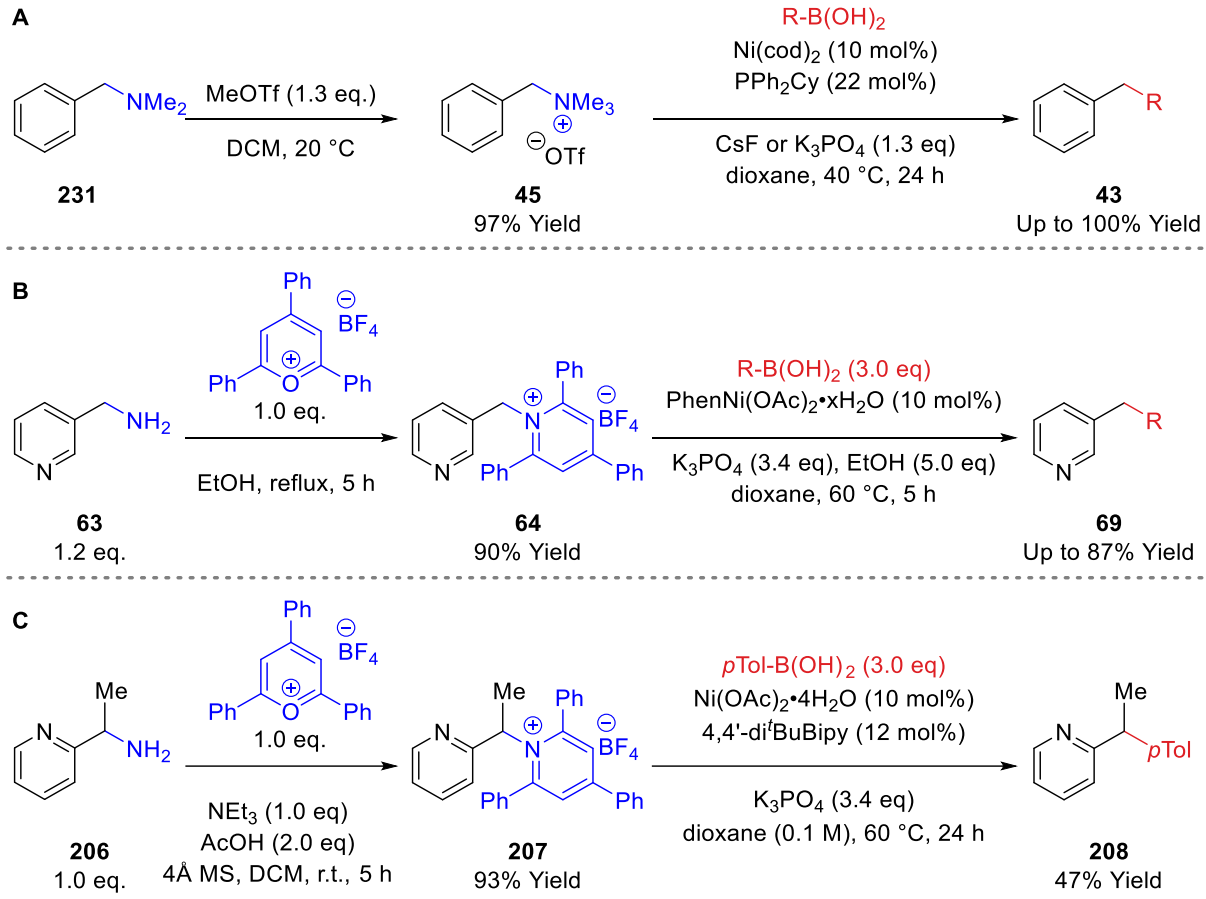

Scheme 53. *Existing methods for cross-coupling of benzylamine substrates*

An alternative category of reactions for the cleavage of benzylic C–N bonds focuses instead on activation (weakening) of the C–N bond by an external activator and subsequent substitution with a nucleophile. In 2019, Kunishima and co-workers reported the activation of gramine **209** by activator CDMT for the formation of products **213** (**214**, Et_3N, LiCl, MeCN, THF)(Scheme 54).[102] The scope of this reaction was limited to malonate nucleophiles and electron-rich gramines, and the mechanism progresses as shown in Scheme 54. First, the lone pair on the benzylic nitrogen displaces chloride from CDMT, generating salt **210**, which now possesses an activated C–N bond. The high leaving ability of triazine **211** facilitates the triethylamine-promoted E2' elimination to form key intermediate indolenine **212**. Malonate nucleophiles such as **214** were then employed to give substituted gramine **213**. This method requires no transition metals for the C–N bond cleavage, though the demonstrated atom economy is poor, due to the bulky nature of the CDMT activator.

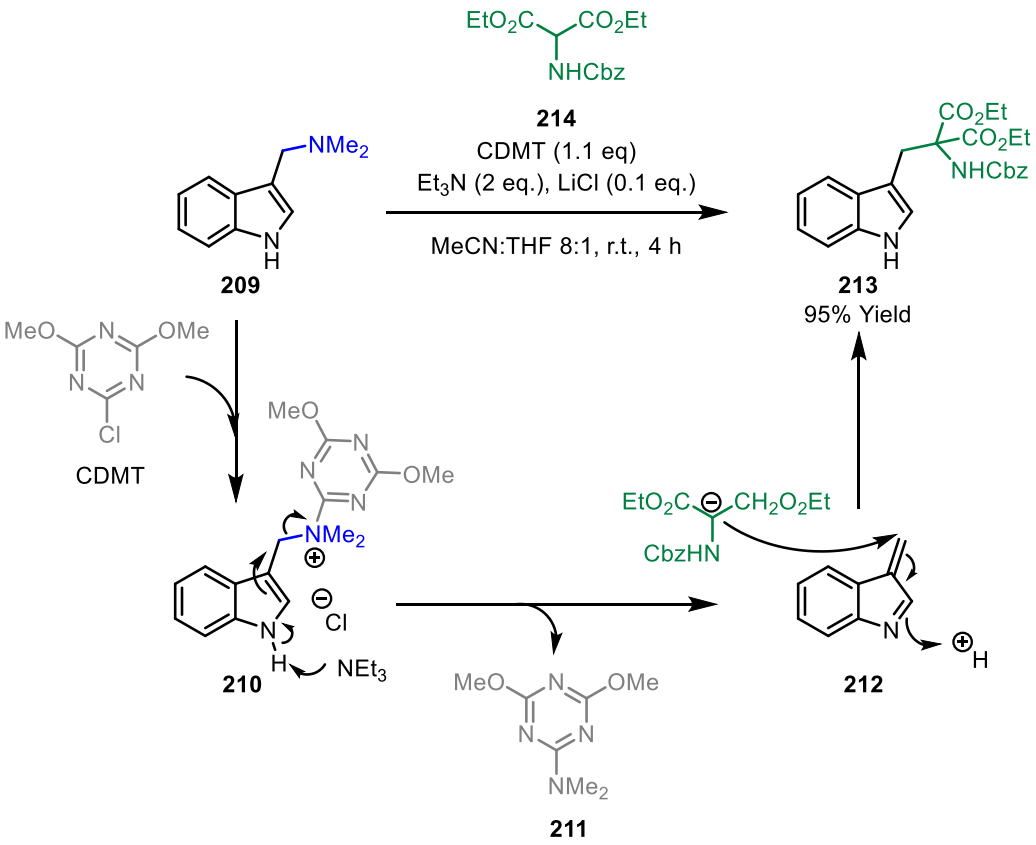

Scheme 54. *Use of a triazine-based activating agent for the C–N cleavage of gramines*

Chloroformates have also been explored as activators of benzylic C–N bonds, resulting in the formation of benzyl halides **216** (Scheme 55).[101,103,104,105,106] Due to the highly reactive nature of ethyl chloroformates, slow addition and demanding temperatures of -78 °C are required (K_2CO_3, THF, 12 h). Additionally, while application to various substrates has been demonstrated, this procedure is mostly limited to electron-rich systems like substrate **215**. The proposed mechanism for this transformation is shown in Scheme 55B: the nucleophilic amine reacts with the chloroformate to generate salt **217**. The released chloride anion is then available to attack the electrophilic carbon atom in an S_N2 displacement of carbamate **218**, generating benzyl halide **216**. This method also proceeds without the need for transition metal catalysts, though the toxic nature of the chloroformate and low temperature conditions are notable limitations.

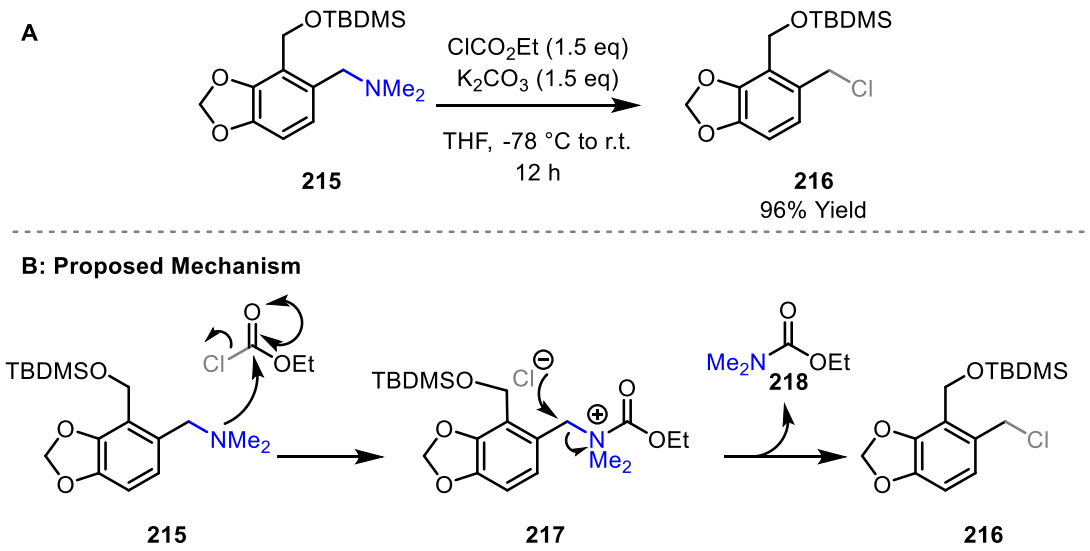

Scheme 55. *Using chloroformates for the activation of benzylic C–N bonds*

The use of an acyl chloride activator was demonstrated in 1993 by Nikiforov and co-workers.[107,108] This nucleophilic substitution reaction was used to convert benzylic C–N bonds (**219**) into C–S bonds (**222**) via proposed *N*-acyl ammonium species **221** (AcCl, acetone, r.t.; KSCN, r.t.) (Scheme 56). The process was only investigated with electron-rich benzylamine **219**, though a variety of nucleophiles were demonstrated. The proposed mechanism progresses with attack of acetyl chloride **220** by benzylamine **219** to give *N*-acyl ammonium **221**. Nucleophiles such as thiocyanate are then added to promote S_N2 displacement, generating products such as **222**.

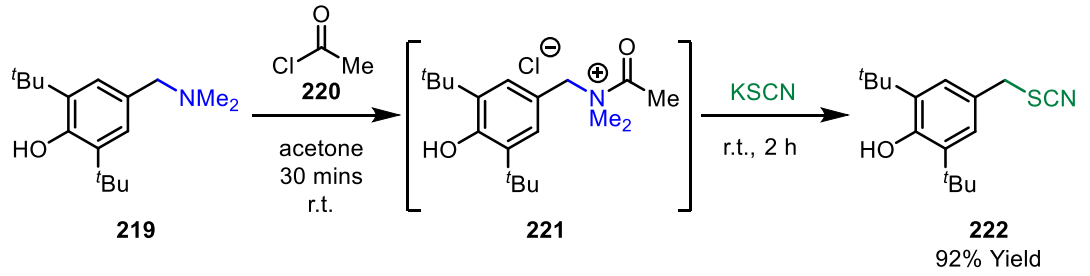

Scheme 56. *The activation of electron-rich benzylamines by acyl chlorides*

3.1.2. Initial Research Results

To improve on the limitations demonstrated in the methodologies described above (Schemes 53-56), it was proposed that acyl halides and anhydrides may be effective as low molecular weight and less toxic alternatives to methyl triflate and Katritzky pyridinium salts for C–N activation. It was first postulated that exposure of benzylamine **199** to acetyl chloride would provide *N*-acyl ammonium species **223** (Scheme 57). Due to the increased polarisation of the benzylic C–N bond of **223**, it was proposed that C–N oxidative addition of a transition metal may be possible, allowing for a Suzuki cross-

coupling to take place with boronic acid **58**. Nickel was selected as the metal catalyst, due to its established utility in the C–N cleavage of benzyl trimethylammonium triflate salts and its extensive application in a broad range of Suzuki cross-couplings.[4,34,36,100,109] In the event, when benzylamine **199** was stirred with acetyl chloride **220** in the presence of $AlCl_3$, phenylboronic acid **58**, $Ni(OAc)_2•4H_2O$, phenanthroline ligand **261**, and K_3PO_4 at 70 °C, none of desired product **17** was observed. Instead, traces of benzyl chloride **224** formed, as evidenced by GC-MS analysis and subsequently confirmed by ^1H NMR analysis.

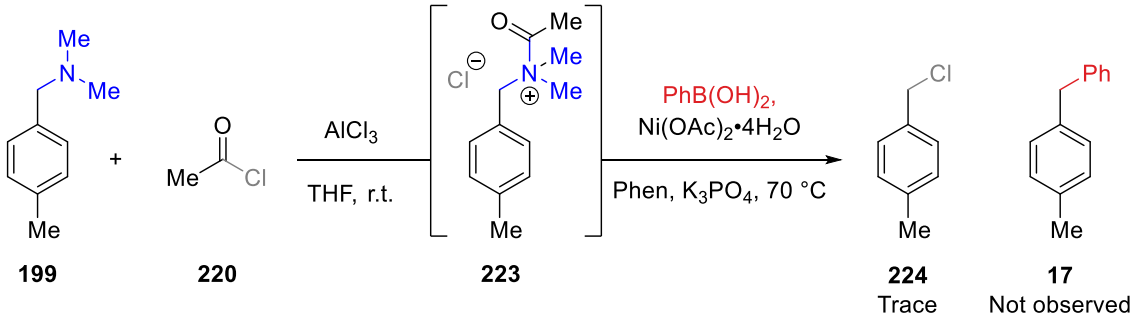

Scheme 57. *Initial benzylic C–N cleavage using acyl chloride activators*

As described in Section 3.1.1, toxic chloroformate reagents are regularly employed for the conversion of benzylamines into benzyl halides, requiring low temperatures (-78 °C, THF). Furthermore, the scope of these reactions is typically limited to systems with electron-rich aromatic units. Notably, the formation of benzyl chloride **224** uses a simple acyl chloride activator and involves an electron-neutral aryl substituent (Scheme 57). It was therefore proposed that acyl halides or anhydrides could be employed for the cleavage of benzylamine C–N bonds, leading to the formation of benzyl halides (Scheme 58). Once formed, these benzyl halides could undergo further transformations, ideally in situ, via either metal-catalysed cross-coupling or nucleophilic substitution protocols (Scheme 58). Extensive literature exists to support the viability of these subsequent processes,[110] so we envisaged that this two-step C–N activation-substitution sequence could offer wide scope for the diversification of challenging C–N bonds.

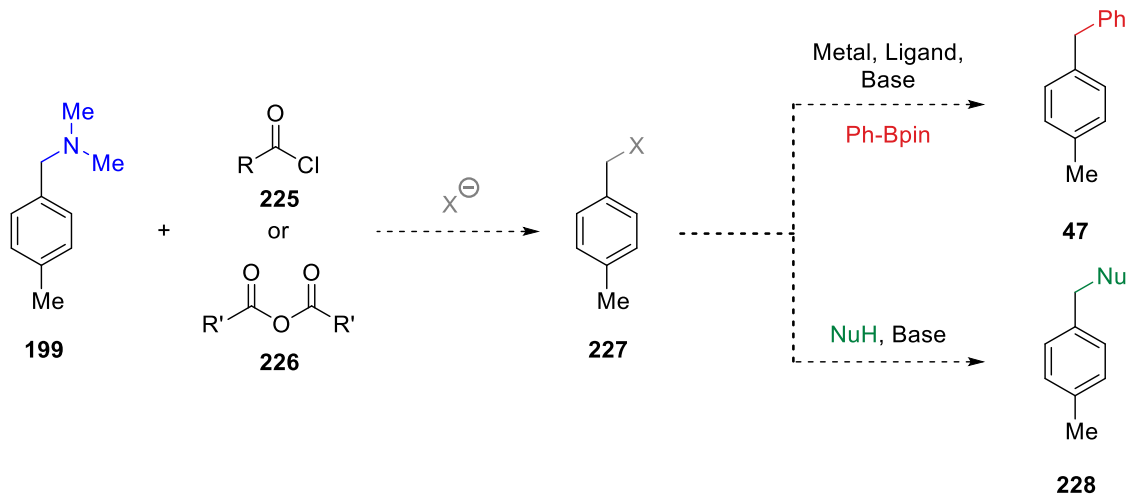

Scheme 58. *Benzylic C–N activation and subsequent proposed transformations*

Benzyl iodide **233** was selected as the target intermediate, as C–I bonds are more labile than C–Cl bonds,[110] and it was envisaged that this would facilitate subsequent manipulations. Furthermore, it was considered that intermediate **233** would be easier to access than chloride **224**, because a regime was envisaged wherein the presence of iodide would accelerate both the *N*-acylation and C–N displacement steps (Scheme 59). Specifically, exposure of an acyl chloride or anhydride (**229**) to an iodide source should generate a highly electrophilic acyl iodide **230** in situ (as Williams and co-workers reported, adding benzylamine to a mixture of benzoyl chloride and benzoyl iodide sees immediate consumption of benzoyl iodide but not of benzoyl chloride).[111] Nucleophilic attack by benzylamine **231** gives *N*-acyl ammonium species **232**. The iodide anion is a highly effective nucleophile (the Swain-Scott equation gives nucleophilicity values of H_2O = 1.0; Cl^- = 3.0; I^- = 5.0),[112] so this can promote nucleophilic substitution of the C–N bond of **232**, generating benzyl iodide **233** in an S_N1 or S_N2 manner. This step is driven by the establishment of amide resonance in by-product **234**. It was envisaged that the mild nature of the reagents and by-products may allow the solution of benzyl iodide **233** to be used directly in further cross-coupling or nucleophilic substitution reactions, as demonstrated in Scheme 58. Therefore, the aims of this project were (1) to optimise the formation of benzyl iodide **233** from benzylamine **231**; (2) to optimise the two-step, telescoped iodination-cross-coupling sequence; and (3) to optimise a complimentary two-step iodination-nucleophilic substitution sequence.

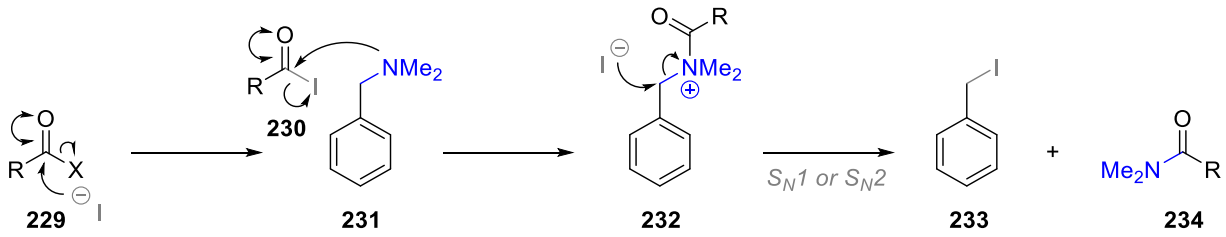

Scheme 59. *Proposed mechanism of benzylamine conversion to benzyl iodide*

3.1.3 Optimisation of the Conversion of a Tertiary Benzylamine to a Benzyl Iodide

For investigations into the conversion of benzylamines to benzyl iodides, tertiary benzylamine **199** was synthesised from benzaldehyde **235** (Scheme 60A). This was achieved by reductive amination of **235** using $HNMe_2$ ($Ti(O^iPr)_4$, MeOH, $NaBH_4$, r.t.), which provided **199** in 99% yield. The mechanism for this transformation is well understood,[110] and is outlined in Scheme 60B. The *p*-methyl substituent of **199** was selected to aid ^1H NMR analysis of crude reaction mixtures.

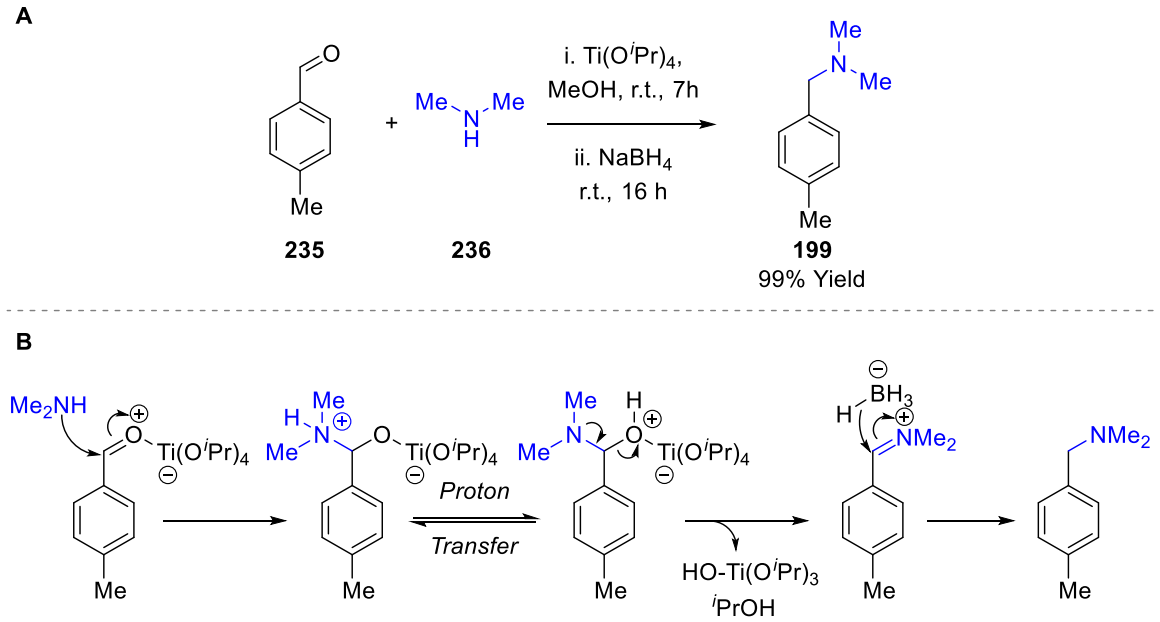

***Scheme 60**. (A) Synthesis of benzylamine **199** and (B) the reductive amination mechanism*

With substrate **199** in hand, attention focussed on its desired conversion to benzyl iodide **237**. Initial studies investigated the use of sodium iodide in the presence of three different activators: two acyl chlorides, acetyl chloride **220** and benzoyl chloride **239**, and trifluoroacetic anhydride (TFAA; **240**). These activators were evaluated in various solvents, ranging from polar aprotic variants (THF) to less polar (dioxane) and non-coordinating options (toluene and hexane). The initial reaction procedure commenced with the addition of sodium iodide and benzylamine **199** to the reaction tube. Solvent was added, followed by neat activator. As shown in Table 3, the combination of TFAA and THF showed the most promise, giving iodide **237** in 60% yield. It was also discovered that use of TFAA in either dioxane, toluene, or hexane generates high quantities of ester side product **238** (27%; 10%; and 25% yields, respectively), in which the trifluoroacetate leaving group has functioned as a nucleophile at the stage of either **232** or **233** (Scheme 59). The formation of **238** was completely suppressed using THF as the solvent (<1% yield). One explanation is that polar solvents increase solvation of trifluoroacetate, which removes it from the proximity to *N*-acyl ammonium salt **232**, thereby suppressing nucleophilic attack (Scheme 59). Alternatively, the limited solvation of iodide by THF (witnessed by dissolution of sodium iodide only upon addition of TFAA) may hold the iodide anion in proximity of *N*-acyl

ammonium **232**, which promotes attack of iodide onto **232**. It is postulated that TFAA is the most effective of the three evaluated activators due to its high electrophilicity, which may facilitate both the formation of the acyl iodide **230** as well as subsequent attack by amine **231**.

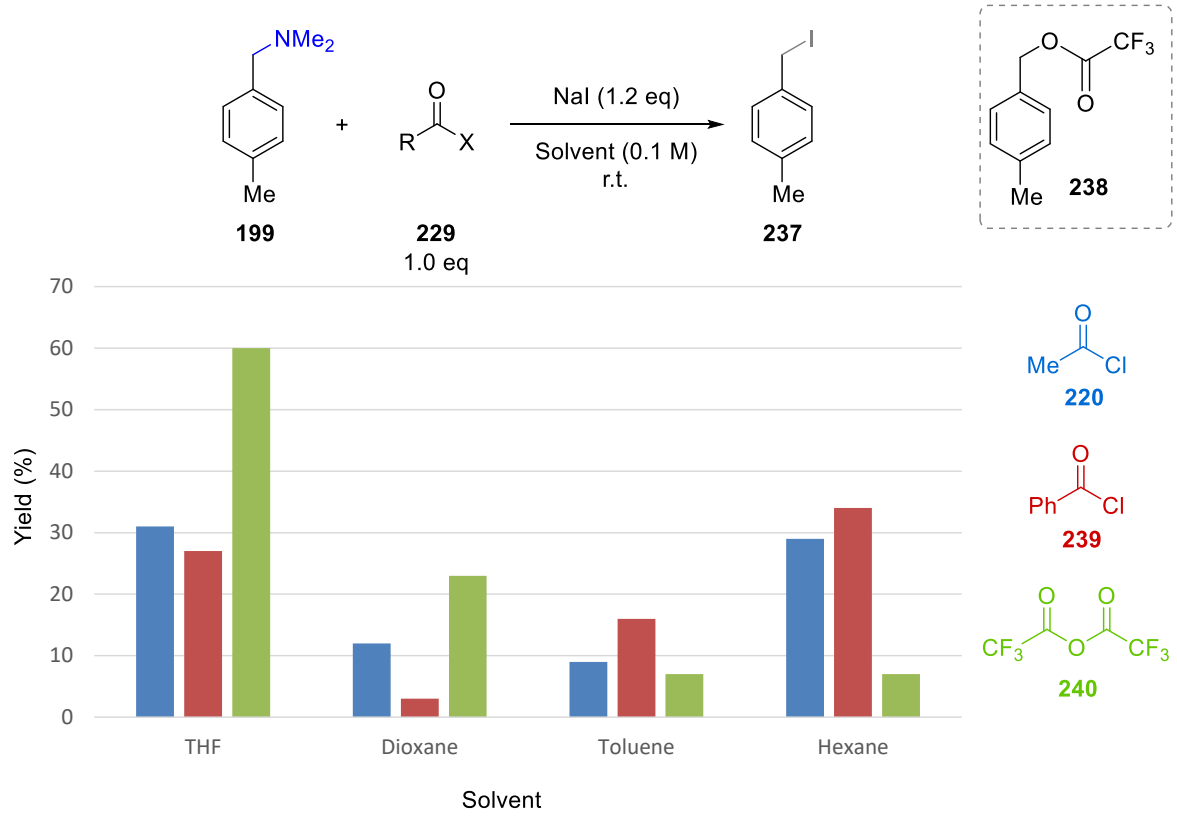

Table 3. *Optimisation of solvent and activator for the formation of benzyl iodide* ***237***

With the promising early result of 60% yield using TFAA in THF, further studies carried out in collaboration with Dr Javier García-Cárceles focussed on altering the equivalents of TFAA and NaI. Other factors, including the use of different iodide sources, reaction times and temperatures were also investigated (Table 4, Entries 1-8). It was discovered that 1.2 equivalents of both TFAA and of NaI is optimal (Entry 5), and that the alternate iodide sources (e.g. TBAI and KI) are less effective (Entries 9 and 10). Furthermore, it was found that consistent results were only obtained using *anhydrous* NaI, so this reagent was dried and handled in a glovebox. Under these conditions, a reaction time of 18 hours at room temperature provided the highest yield (Entry 5).

To improve the yield further, procedural alterations were investigated. It was discovered that first stirring NaI in THF, followed by the sequential addition of a 0.5 M solution of benzylamine **199** and a 0.5 M solution of TFAA gave significantly increased yields. When this procedure was applied on a 0.4 mmol scale, **237** was obtained in an isolated yield of 92% (Entry 11). Pre-dissolution of TFAA in THF may improve the yield because it allows slower addition into the NaI-amine suspension, which may facilitate the formation of acyl iodide **230**. It is likely that the efficiency of the process is even

higher than the 92% yield indicates, as some degradation of **237** occurred during purification by FCC and subsequent analysis.

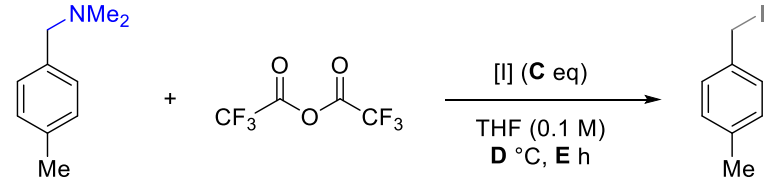

Entry	A	B	[I]	C	D	E	Yield
1	0.2	1.0	NaI	1.2	r.t.	18	60%
2	0.2	1.0	NaI	1.2	r.t.	3	40%
3	0.2	1.0	NaI	1.2	r.t.	7	47%
4	0.2	1.0	NaI	1.2	50	7	63%
5	0.2	1.2	NaI	1.2	r.t.	18	76%
6	0.2	1.5	NaI	1.2	r.t.	18	72%
7	0.2	1.2	NaI	1.0	r.t.	18	29%
8	0.2	1.2	NaI	2.0	r.t.	18	44%
9	0.2	1.2	TBAI	1.2	r.t.	18	0%*
10	0.2	1.2	KI	1.2	r.t.	18	38%*
11	0.4	1.2	NaI	1.2	r.t.	18	92%*[a]

[a] *0.5 M solutions of amine and TFAA added sequentially*

Table 4. *Optimisation of the conversion of **199** to benzyl iodide **237***

**This reaction was carried out by Dr Javier García-Cárceles*

Efforts were undertaken to determine whether acyl iodide **230** is generated in situ (Scheme 59). Unfortunately, ^{19}F NMR analyses were ineffective, as TFAA, trifluoroacetic acid (TFA), and the mixture of TFAA and NaI gave the same shift of δ = -76 ppm. It has been reported by Voronkov and co-workers that acetyl or benzoyl chlorides are able to react with tertiary amines (leading to C–N bond cleavage and the formation of amides, cf. **234**), but elevated temperatures of 170-200 °C are required.[113] Voronkov also reported that use of acetyl or benzoyl iodides allows the analogous reaction to occur at room temperature, which suggested that C–N cleavage is the result of acyl iodide formation. Williams and co-workers reported a study wherein acyl chlorides were stirred with iodide salts to facilitate acyl transfer. Mechanistic studies demonstrated a rate enhancement and increased yields when 60 mol% potassium iodide was used in anhydrous acetonitrile.[111] ^{13}C NMR analysis showed that the acyl iodide is generated as a minor component (20%) in equilibrium with the starting acyl chloride. These results are not directly comparable to the use of highly electrophilic TFAA, as described here, where direct attack by amine **199** is still a possibility.

Further studies revealed that removal of NaI from the reaction mixture does not prevent C–N cleavage from taking place. Instead, two different products were generated: ester **238** and ether **241**, which were formed in 18% and 39% yield, respectively (Scheme 61A). The proposed mechanism commences with acylation of benzylamine **199** to generate *N*-acyl ammonium salt **242**. In the absence of iodide, the half life of **242** is prolonged, which increases the chance of S_N1 or S_N2 attack by THF solvent, forming activated ether **245**. Carboxylate **244** may then react in one of two ways: (1) attack at the benzylic position generates ester **238** (pink arrows), whereas (2) attack at the α-position of THF opens the 5-membered ring and forms ether **241** (blue arrows). For the formation of **238**, a mechanism involving direct substitution of **242** by trifluoroacetate **244** may also be operative. Ether **241** was not observed when NaI was used, which highlights the importance of having an effective nucleophile present. In line with Williams and co-workers' study, the combined yield for the conversions of **199** to **238** and **241** (57% vs 92% with NaI) suggests that TFAA alone is less effective for the acylation of benzylamine **199**.

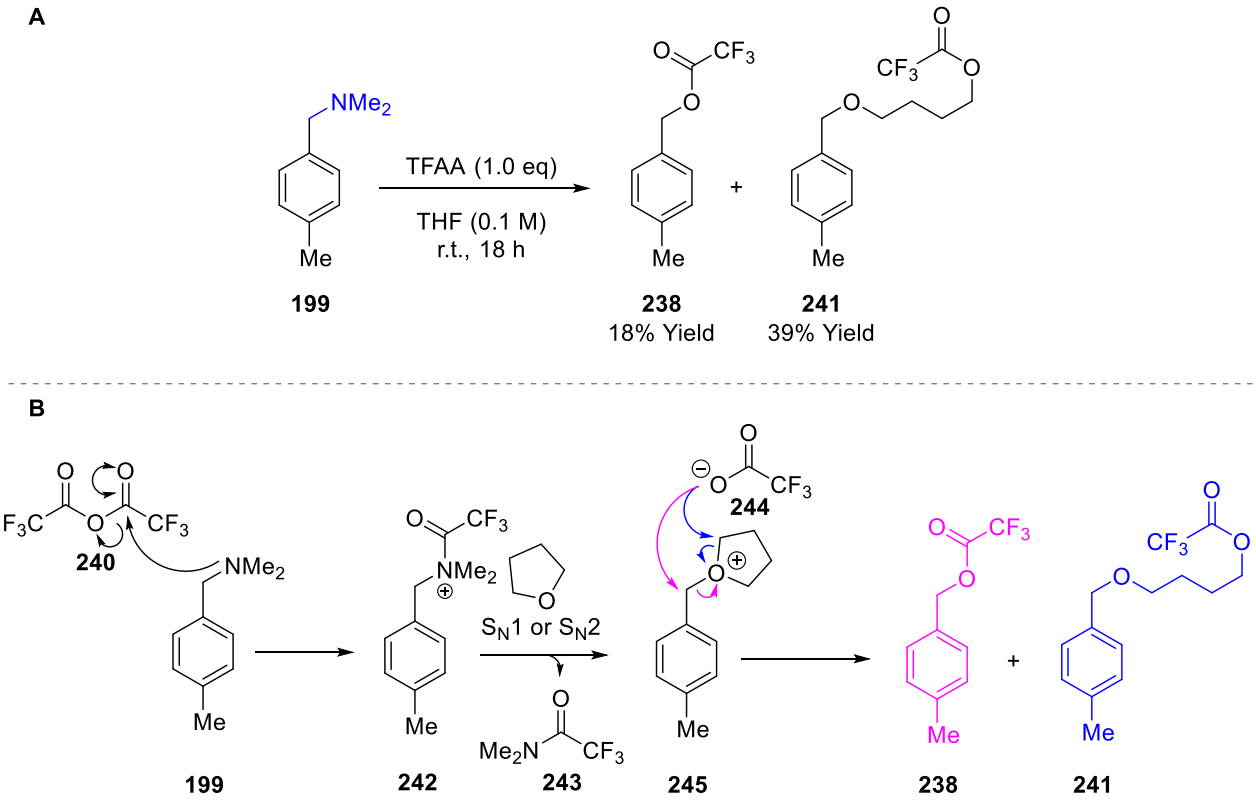

Scheme 61. *Proposed mechanism for the cleavage of benzylamine **199** in the absence of iodide*

3.2 A Telescoped Benzylamine Activation and Cross-coupling Sequence

3.2.1 Optimisation of the Telescoped Benzylamine Activation and Cross-coupling Process

With optimal conditions in hand for the conversion of benzylamine **199** into benzyl iodide **237**, investigations into the cross-coupling step were carried out. To this end, substrate **233** was synthesised from benzyl alcohol **246** using CsI in the presence of BF_3•OEt_2 (MeCN, r.t.).[114] In contrast to the reported conditions, this reaction did not give yields of 96% within 5 minutes, but instead required 2 hours for the highest yield of 58%. The reduced yield may be caused by degradation of the product during purification by FCC. Because of its sensitivity, iodide **233** was prepared freshly and employed immediately in the cross-coupling investigations.

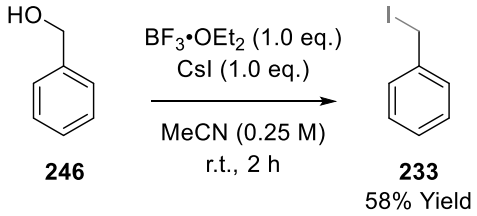

Scheme 62**. Synthesis of iodide substrate **233

Various conditions for the cross-coupling of benzyl iodide **233** were trialled. As palladium and nickel are both well-established metals employed in related cross-coupling reactions,[115,116] four metal catalyst complexes were selected: $Pd(OAc)_2$ as a Pd^{II} precursor catalyst; $Pd_2(dba)_3$ as a Pd^0 catalyst; $Ni(acac)_2$ as a Ni^{II} precursor catalyst; and $Ni(cod)_2$ as a Ni^0 catalyst. In all cases, PPh_3 was employed as the ligand and boronic acid **58** as the nucleophile due to their established broad utility in related cross-couplings (Na_2CO_3, THF, 100 °C).[117–119] As shown in Table 5, use of palladium catalysts gave high quantities of undesirable homo-coupled **247** (Entries 1 and 2, 19% and 31%) compared to $Ni(acac)_2$ (Entry 4, 2%). Of the four metal catalyst complexes, the highest yields of target product **56** were obtained with $Pd(OAc)_2$ (Entry 1, 27%) and $Ni(acac)_2$ (Entry 4, 23%), suggesting a preference for M^{II} species over M^0 species. This is a curious observation, given that oxidative addition requires a low oxidation state.[110] One potential reason as to why $Pd(OAc)_2$ performs particularly well as a precursor was advanced by Amatore and Jutand; they invoked that coordination of an acetate anion to palladium forms $[Pd^0(PPh_3)_2{}^-OAc]$ as the active catalyst instead of $[Pd^0(PPh_3)_4]$, with the former having a higher electron density, thereby promoting oxidative addition.[120] The success of $Ni(acac)_2$ over $Ni(cod)_2$ in this case may be due to its increased stability, which has been shown to increase yield—$Ni(cod)_2$ is highly unstable and decomposes rapidly in contact with air.[121]

Exploration of different phosphine ligands together with $Pd(OAc)_2$ or $Ni(acac)_2$ revealed that the latter offered consistently higher cross-coupling yields (Entries 5-8, Yields 0-17% vs Entries 9-12, Yields 26-51%). The highest yield of **56** obtained under Pd-catalysed conditions was 17% (Entry 8);

here, an additional 22% yield of homo-coupled **247** was also observed. Alternatively, under Ni-catalysed conditions, **56** could be accessed in 51% yield (Entry 12), accompanied by a 6% yield of **247** and an 8% yield of unreacted **233**. This result suggested that further improvements in yield were possible. Therefore, further work focussed on the use of different nickel complexes.

Nickel is an ideal metal for cross-coupling due to its relatively electropositive nature, which facilitates oxidation from Ni^0 to Ni^{II}, or from Ni^I to Ni^{III}, therefore allowing oxidative addition to occur readily.[122,123] Additionally, a broad range of oxidation states are easily accessible by nickel, which allows for alternative modes of reactivity, including radical-based mechanisms. Indeed, oxidative insertion of the C–I bond of **233** could occur by 2-electron or single electron transfer (SET) oxidative addition mechanisms.[122] The exact pathway can be heavily influenced by a delicate balance of ligand and substrate structure, with relatively small changes leading to large alterations in behaviour.[115] Therefore, investigations into the use of a wide variety of ligands were carried out.

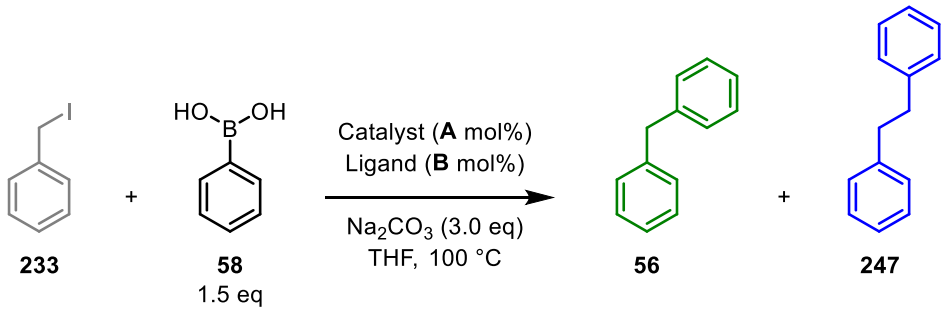

233 + **58** 1.5 eq → **56** + **247**

Entry	Catalyst	A	Ligand	B	Scale (mmol)	233	56	247
1[a]	M2	20	248	40	0.1	6%	27%	19%
2[a]	M3	20	248	40	0.1	8%	13%	31%
3	M4	10	248	20	0.2	53%	0%	23%
4	M5	10	248	20	0.2	37%	23%	2%
5	M2	10	249	20	0.2	49%	0%	5%
6	M2	10	250	20	0.2	24%	14%	16%
7	M2	10	251	20	0.2	48%	4%	13%
8	M2	10	252	20	0.2	14%	17%	22%
9	M5	10	249	20	0.2	13%	26%	8%
10	M5	10	250	20	0.2	27%	45%	<1%
11	M5	10	251	20	0.2	43%	32%	12%
12	M5	10	252	20	0.2	8%	51%	6%

M2 = $Pd(OAc)_2$; **M3** = Pd_2dba_3; **M4** = $Ni(cod)_2$; **M5** = $Ni(acac)_2$; [a]1.0 eq **58**, 6.0 eq Na_2CO_3; *Yields were obtained by ^1H NMR analysis against 1,4-dinitrobenzene*

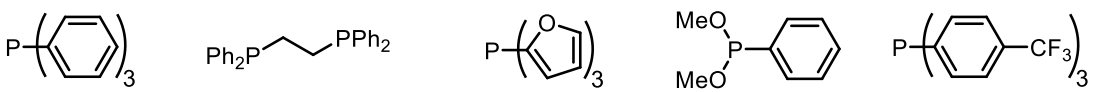

248 **249** **250** **251** **252**

Table 5. *Initial evaluation of pre-catalysts and ligands for the conversion of **233** to **56***

Due to the unstable nature of benzyl iodide **233**, further optimisation focussed on the development of the one-pot process wherein benzylamine **199** is converted to diarylmethane **17** via the intermediary of in situ generated benzyl iodide **237**. In preliminary efforts, it was established that the solution of benzyl iodide **237**, formed from **199** using TFAA/NaI, could be used directly in the cross-coupling step; no intermediate purification was required. Following the promising results using $Ni(acac)_2$ (Table 5), various ligands were investigated (Table 6). Bipyridine ligand **254** provided a 60% yield of **17** over the two-step, telescoped procedure, and so a wide variety of other bipyridyl ligands were investigated, encompassing variants possessing electronically distinct pyridyl rings (ligands **256-263**). No clear patterns were observed for ligands **256-263**, though a particularly low yield of 9% was observed with rigid phen ligand **261**, suggesting that some flexibility may be required. Electron withdrawing ester- and CF_3-substituted ligands **262** and **263** gave the most promising yields of 67% and 71% respectively, and so these were taken forward for further investigation.

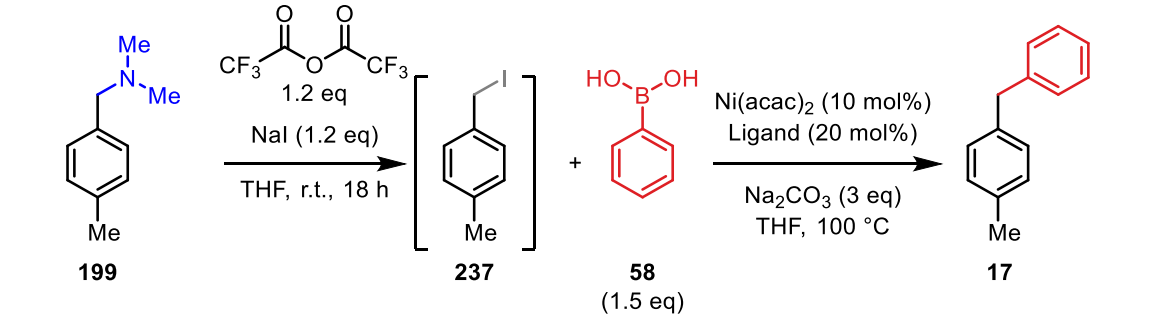

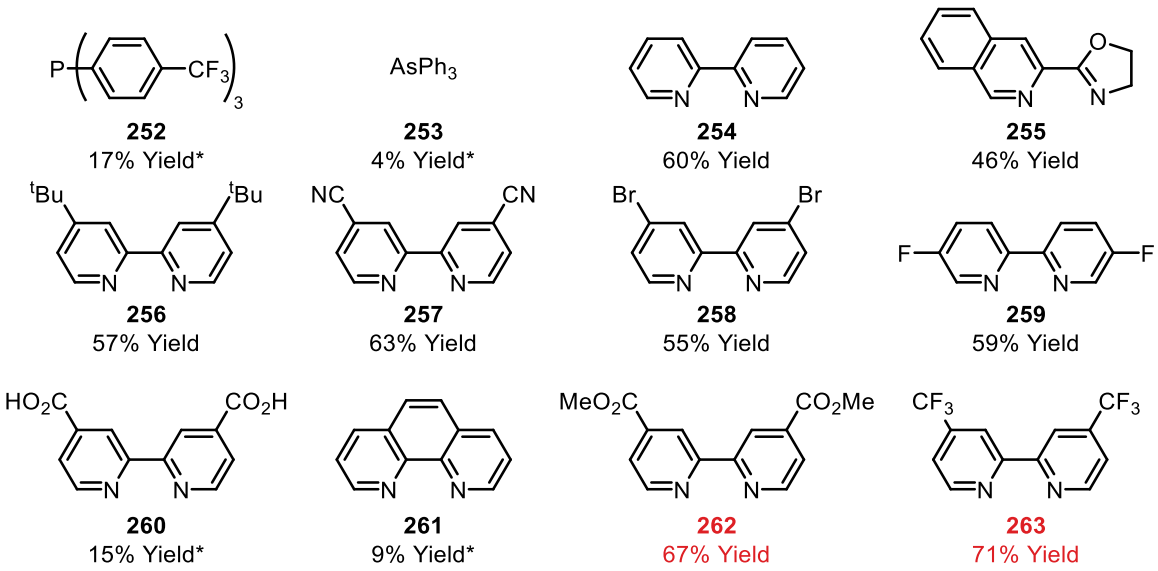

**Yield provided by ^1H NMR analysis against 1,4-dinitrobenzene; product not isolated*

Table 6. *Ligand trials for the conversion of **199** to **17***

The reasoning behind why ligands **262** and **263** were so effective in this cross-coupling was investigated. Bipyridyl ligands have been broadly employed for the cross-coupling of alkyl and aryl halides in combination with nickel catalysts,[123–126] and mechanistic studies suggest that they promote

SET oxidative addition by outer-sphere electron transfer (Scheme 63).[45,115,127,128] It is therefore likely that the oxidative addition step in this cross-coupling occurs by an SET mechanism, rather than via concerted 2-electron or S_N2-type pathways. In the present case, SET oxidative addition is likely facilitated by the stability of intermediate benzylic radical **264** (Scheme 63).[129] However, oxidative addition of benzylic halides by nickel complexes is well-known and facile,[45,115] and so it is unlikely that this is the rate limiting step for the conversion of **237** to **17**. Instead, transmetalation or reductive elimination are more likely to be the most challenging steps.

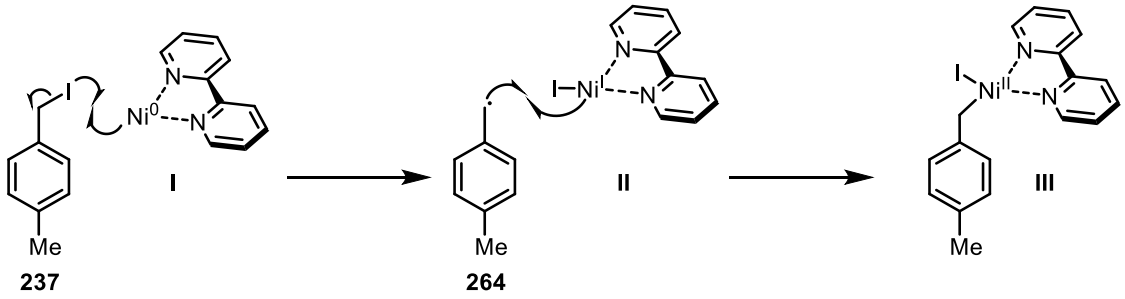

Scheme 63. *SET oxidative addition*

Two potential pathways for transmetalation are shown in Scheme 64, both demonstrating the essential role of the carbonate base. Pathway 1 (Scheme 64A) was inspired by the findings of Itami and co-workers,[130] who reported the formation of chelates such as **IV** prior to boronic acid coordination. DFT studies were employed to evidence the step-wise formation of **IV** and **V**. Pathway 2 (Scheme 64B) was inspired by the findings of Sun and co-workers, who used NMR studies to evidence the formation of boronate structures **265** when carbonate bases are used with boronic acids in anhydrous THF.[131] This pathway progresses through the same chelate **V** which, following transmetalation, gives structure **VI**. Sun and co-workers used palladium as the metal centre, whereas Itami and co-workers used nickel, and so pathway 1 is proposed to be the most likely pathway for transmetalation in this case. Reductive elimination of **VI** (Scheme 64C) provides product **17** and regenerates Ni^0 catalyst **I**. Xu and colleagues reported that the reductive elimination of four-coordinate nickel species is facilitated by coordination of a fifth electron-poor ligand, assisted by the redox active nature of the pyridyl ligands.[45,128,132] As both transmetalation and reductive elimination are facilitated by a lower electron density around the metal centre, this might explain why the electron poor ester- and CF_3-substituted bipyridyl ligands **262** and **263** are the most effective.

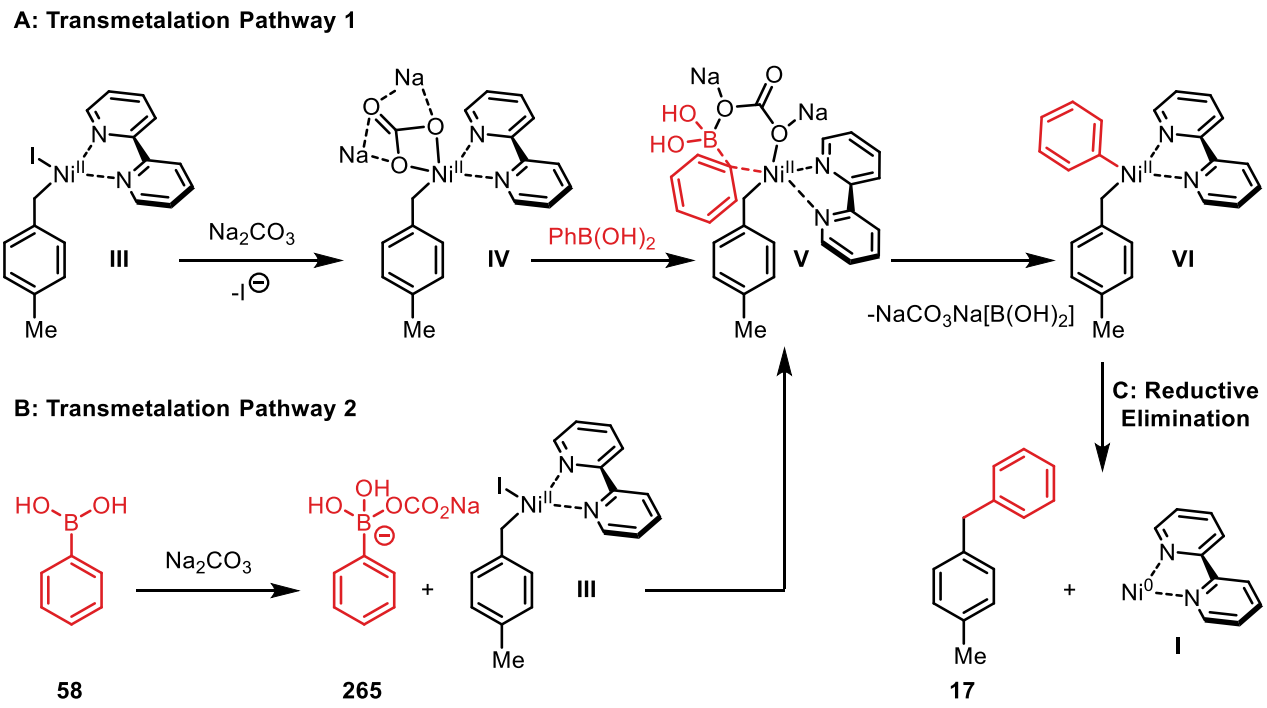

Scheme 64. *Carbonate-facilitated transmetalation and reductive elimination*

In collaboration with Dr. Javier García-Cárceles, optimisation studies continued, investigating next the role of different Ni^{II} sources, and optimal metal:ligand ratios and the catalyst loading. These results are summarised in Table 7. Electron poor bis(hexafluoroacetylacetonato)nickel^{II} hydrate (**M6**; $Ni(hfac)_2$; Entries 3 and 4) and nickel^{II} octanoate hydrate (**M7**; Entries 5 and 6) gave higher yields than $Ni(acac)_2$ (**M5**; Entries 1 and 2) and $Ni(THMD)_2$ (**M8**; Entries 7 and 8), and so they were studied further in different ratios and loadings (**M6**; Entries 9-11. **M7**; Entries 14 and 15). It was also discovered that increasing the scale to 0.6 mmol gave higher isolated yields and, at this scale, a 1:2 ratio of $Ni(hfac)_2$ (10 mol%) and ligand **262** gave **17** in an excellent yield of 95% over the two steps (Entry 11). Optimised conditions using nickel^{II} octanoate hydrate gave a yield of 87% using ligand **262**, with metal and ligand loadings of 2.5 mol% each (Entry 14). Attempts to use fewer than 1.5 equivalents of boronic acid **58** also caused a decrease in yield (Entries 12, 13, and 16). Replacement of boronic acid **58** with its equivalent boronic ester was also investigated, but this modification gave a 0% yield of **17** (Table SI:2). Other avenues investigated include use of alternative bases and base loadings, but all deviations from 3 equivalents of Na_2CO_3 proved detrimental to the yield (Table SI:2). Ligand **263** was also investigated but gave lower yields (Table SI:2). From these studies, the conditions shown in Entry 11 were chosen as optimal.

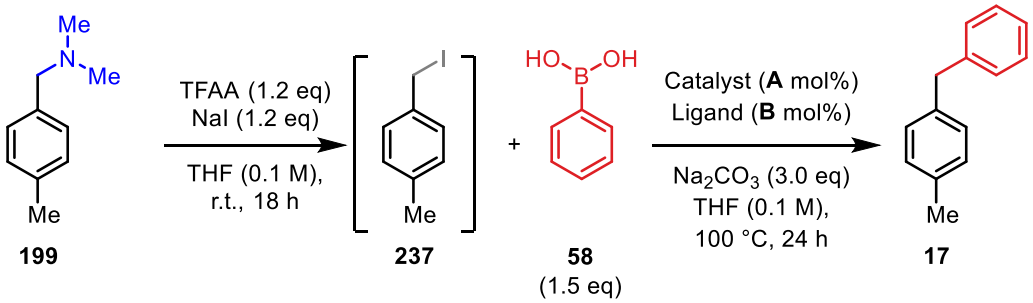

Entry	Catalyst	A	Ligand	B	Scale (mmol)	Yield
1	M5	10	262	20	0.4	67%
2	M5	10	263	20	0.4	71%
3	M6	10	262	20	0.4	81%
4	M6	10	263	20	0.4	85%
5	M7	10	262	20	0.4	75%
6	M7	10	263	20	0.4	81%
7	M8	10	262	20	0.4	68%
8	M8	10	263	20	0.4	76%
9*	M6	2.5	262	5	0.6	57%
10*	M6	5	262	5	0.6	72%
11	M6	5	262	10	0.6	95%
12[a]*	M6	5	262	10	0.6	65%
13[b]*	M6	5	262	10	0.6	79%
14*	M7	2.5	262	2.5	0.6	87%
15*	M7	2.5	262	5	0.6	81%
16[b]*	M7	2.5	262	2.5	0.6	62%

M5 = $Ni(acac)_2$; **M6** = Bis(hexafluoroacetylacetonato)nickel(II) hydrate; **M7** = Nickel(II) octanoate hydrate; **M8** = $Ni(TMHD)_2$; [a]1.0 eq **58**; [b]1.2 eq **58**

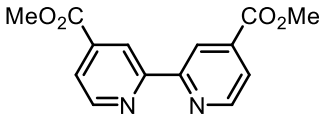

262

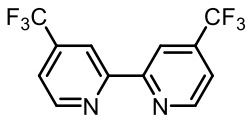

263

Table 7. *Optimisation of nickel and ligand ratios for benzyl iodide cross-coupling*

**This data was obtained by Dr Javier García-Cárceles*

3.2.2 Probing the Tolerability of the C–N Iodination Cross-Coupling Protocol

3.2.2.1 Synthesis of Benzylamine Substrates

For investigations into reaction scope, a variety of benzylamine substrates were synthesised, the majority of which were accessed by reductive amination ($HNMe_2$ then $NaBH_4$) of the corresponding benzaldehyde (Table 8). A wide variety of differentially substituted substrates were accessed. This included systems with sterically hindered *ortho*-positions (**271** and **272**), basic heteroarenes (**275** and

276), and potentially reactive functionality (e.g. ester **273**). This work was carried out in collaboration with Dr. Javier García-Cárceles.

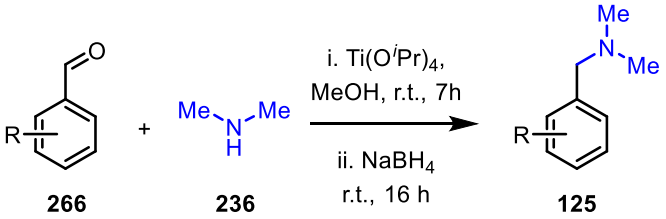

266 **236** **125**

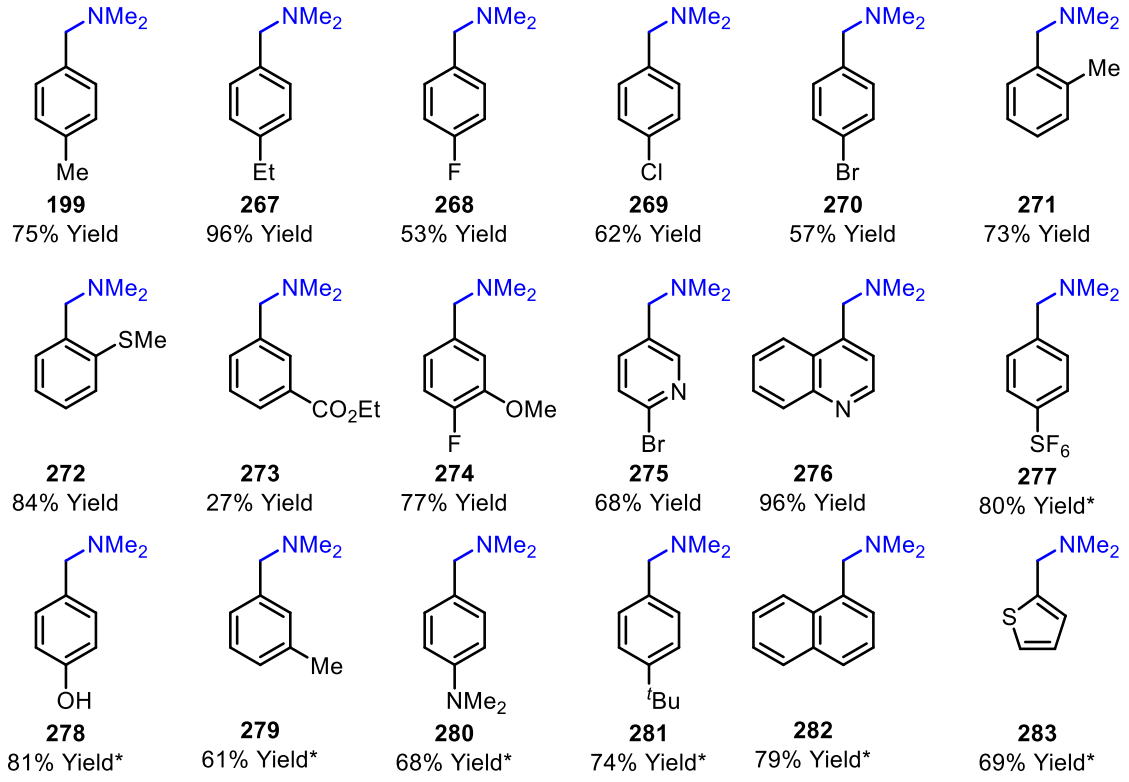

Table 8. *Reductive amination for the formation of benzylamine substrates*

**This reaction was carried out by Dr Javier García-Cárceles*

For the synthesis of pyrrolidine and piperidine systems **287** and **288**, an alternative strategy was employed. This involved base-promoted (KOH) nucleophilic displacement of benzyl bromide **284** with pyrrolidine **285** or piperidine **286**, which generated **287** and **288** in 58% and 76% yield, respectively (Scheme 65A). In a similar manner, bulky diphenyl substrate **290** was synthesised from benzyl bromide **284** ($HNPh_2$, DIPEA, MeCN, 80 °C, 3 days) (Scheme 65B).[133] Attempts to access **287** and **288** by reductive amination were compromised by the difficulty in achieving condensation to the imine.

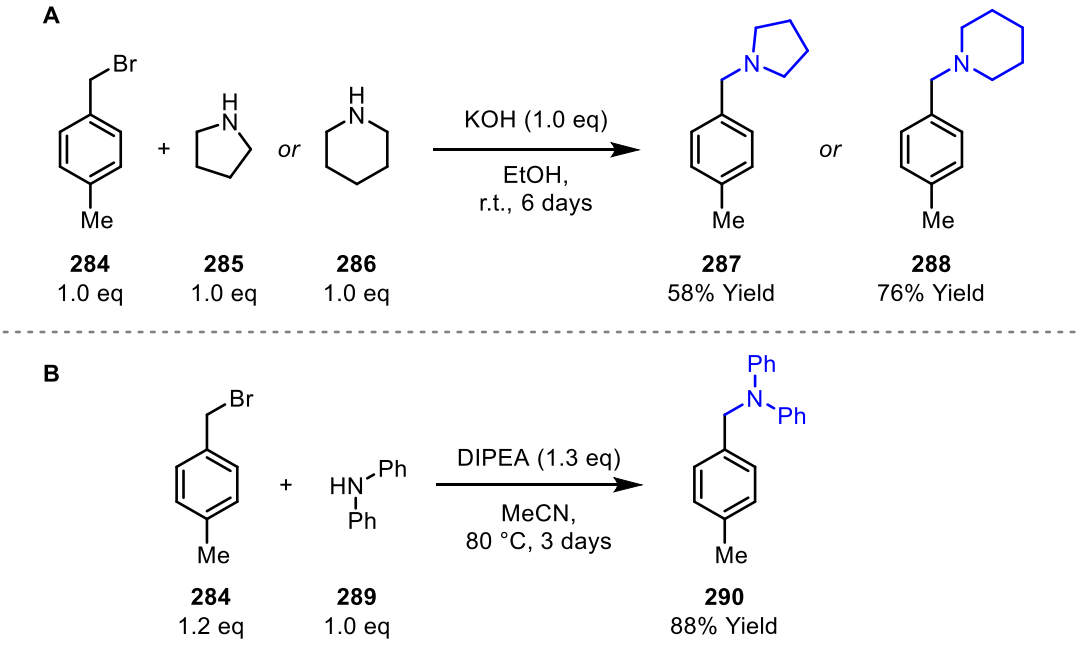

Scheme 65. *Procedures for the synthesis of alternative N-substituted benzylamines*

The substrates shown in Scheme 66 were synthesised by Dr Javier García-Cárceles. Dicyclohexylamine substituted substrate **291** was synthesised from benzaldehyde **235** using a $Ti(O^iPr)_4$ promoted reductive amination protocol (i. $HNCy_2$, $Ti(O^iPr)_4$, MeOH, r.t.; ii. $NaBH_4$, r.t.), whereas diisopropylamine substituted substrate **292** was synthesised by nucleophilic displacement of bromide **284** (HN^iPr_2, K_2CO_3, MeCN, reflux). Finally, compound **294**, which contains a peracetylated sugar, was synthesised from phenol **278** (mannose **293**, BF_3•OEt_2, DCM, 0 °C to r.t.).

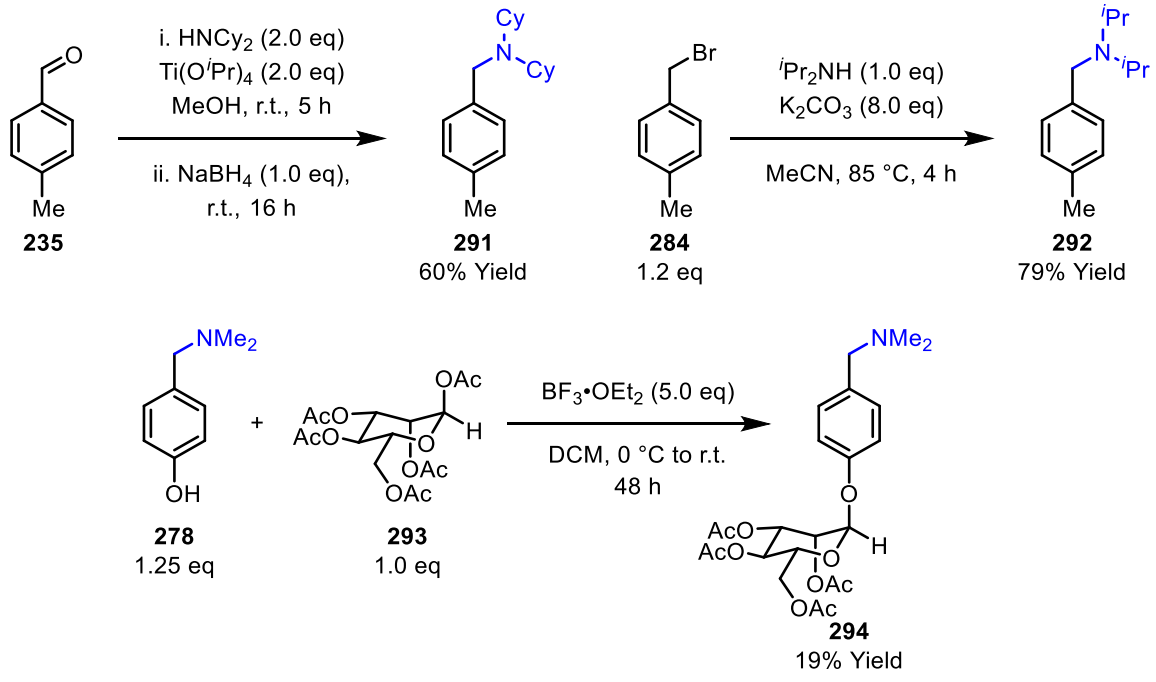

Scheme 66. *Methods used for synthesis of benzylamine substrates*

These reactions were carried out by Dr Javier García-Cárceles

3.2.2.2. Application of Benzylamine Substrates to the Established Cross-Coupling Protocol

With a representative range of amine substrates in hand, the scope of the cross-coupling protocol was probed. Initially, the tolerance of alternative steric environments around the amino unit was evaluated, with bulky dicyclohexylamine **291** progressing to form **17** with 59% yield (Table 9). Cyclic pyrrolidine and piperidine systems **284** and **288** participated to give **17** in 80% and 64% yield, respectively. These results demonstrate that C–N cleavage occurs preferentially at the benzylic position over the alkyl positions, possibly driven by the increased stability of the S_N2 transition state that the former offers. This selectivity was especially exciting because it suggested that C–N activation may be effective for more complex systems containing more varied amine groups.

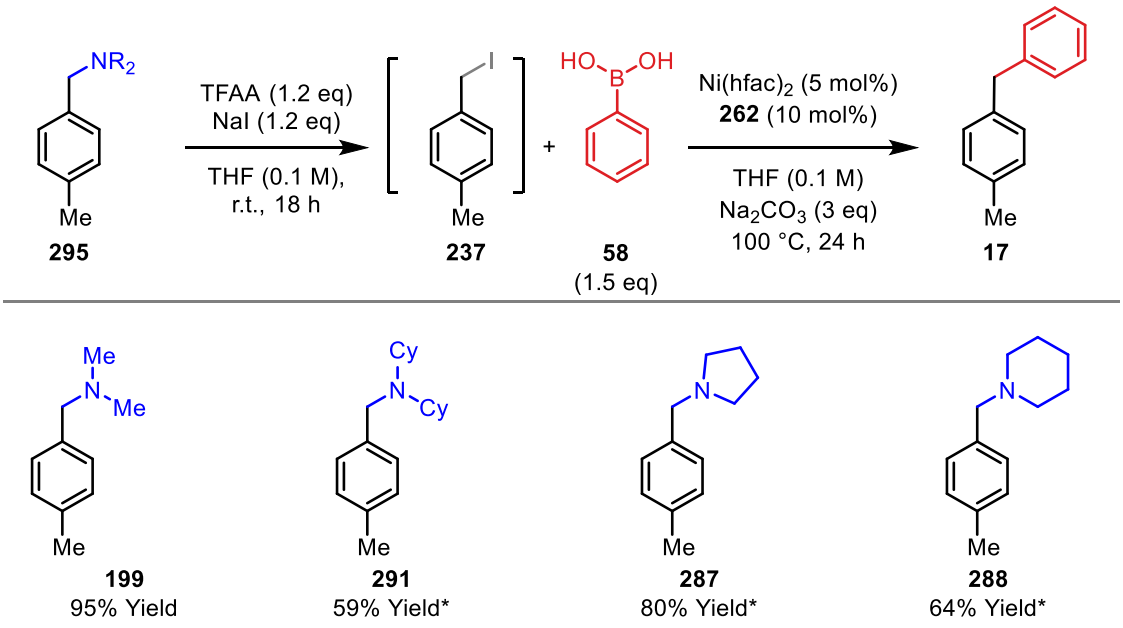

Table 9. *Tolerance of the developed cross-coupling for different amino groups*

**This data was obtained by Dr Javier García-Cárceles*

Although the results in Table 9 were exciting, it was found that some amino moieties were less well tolerated. For example, subjection of secondary amine **298** to the reaction conditions gave amide **299** with 74% yield and, unsurprisingly, this could not be converted to the corresponding iodide. Primary amines such as **205** were also ineffective, though in this case a complex mixture was generated and no specific products were identified. It was also found that although pyrrolidine and piperidine substrates **287** and **288** were well-tolerated, diphenyl and diisopropyl substrates **290** and **292** did not provide desired diarylmethanes **17**. The reasons for the failure of the latter are not clear as a complex

mixture of products was obtained. For diphenyl substrate **290**, the amine lone pair is delocalised such that it is less available for acylation (see Scheme 59), which may provide an explanation.

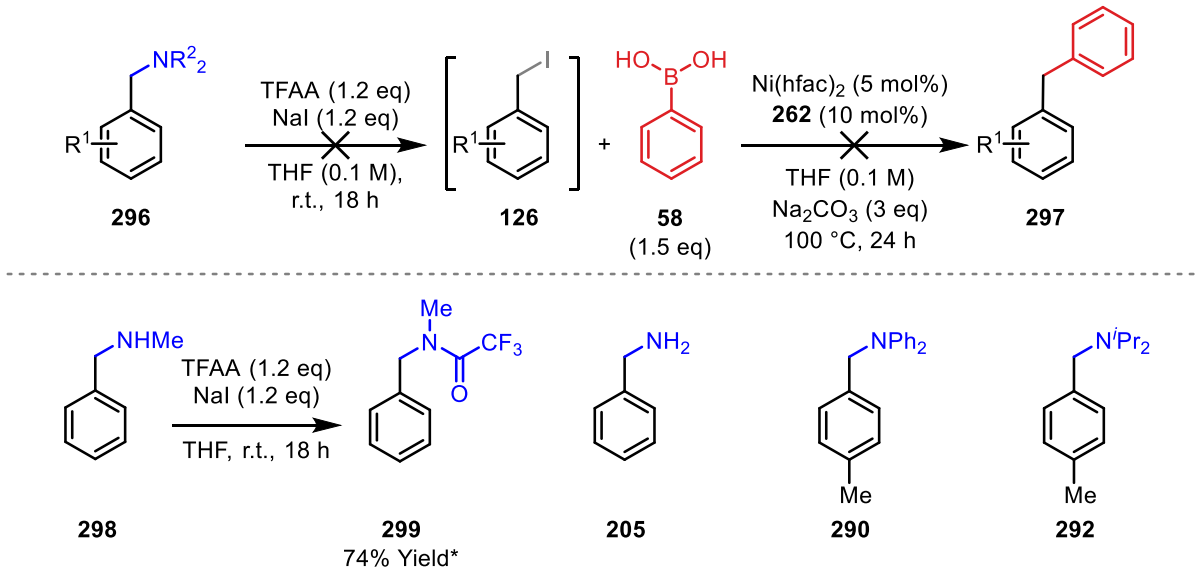

Scheme 67. *Amino groups unsuited to the developed cross-coupling protocol*

**This reaction was carried out by Dr Javier García-Cárceles*

The tolerance of the protocol to substitution on the aromatic unit of a range of benzylamines was also investigated (Table 10). Sterically demanding systems were well-tolerated, with naphthyl system **301** and *ortho*-substituted system **303** forming in 80% and 79% yield, respectively. Products **304**, **307**, and **310**, which contain electron-withdrawing functionality were accessed in moderate to good yields. Electron-donating substituents were also tolerated, as demonstrated by the high yielding formation of **306**, **308**, and **309**. Notably, even systems with competing nucleophilic functionality participated; for example, phenol systems **305** and aniline **312** were generated in appreciable yield. In these cases, more equivalents of the TFAA activator were required, likely to acylate the competing nucleophilic functionality, while maintaining enough TFAA for reaction with the desired benzylamine site. Presumably, the sacrificial acyl groups underwent hydrolysis during aqueous work-up. Substrate **294**, which possesses a peracetylated sugar, was converted to **311** in 90% yield.[134]

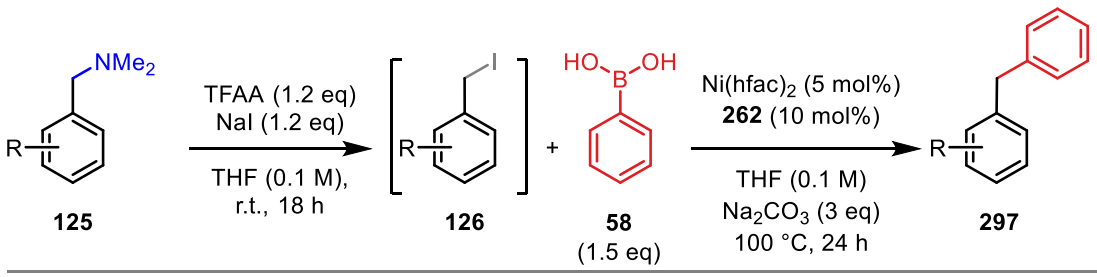

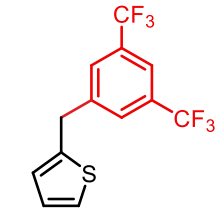

300
96% Yield*

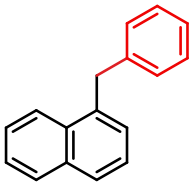

301
80% Yield*

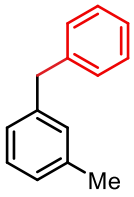

302
71% Yield*

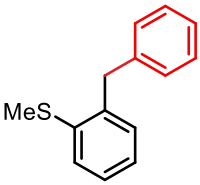

303
79% Yield*

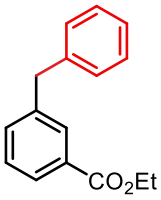

304
48% Yield[a]*

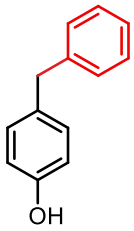

305
45% Yield[c]*

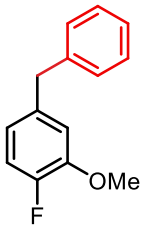

306
70% Yield*

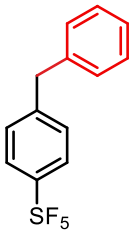

307
71% Yield*

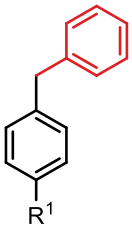

308
R[1]=Et, 79% Yield*
309
R[1]=*t*Bu, 88% Yield*

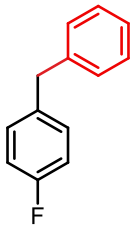

310
72% Yield*

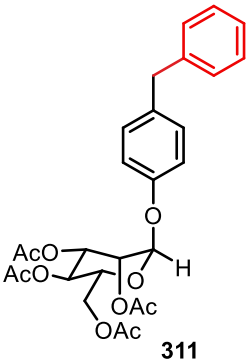

311
90% Yield[b]*

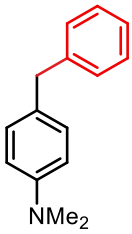

312
35% Yield[c]*

[a]*0.35 mmol scale;* [b]*0.20 mmol scale;* [c]*2.0 eq of TFAA and NaI at 0 °C*

Table 10. *Tolerance for benzylamine derivatives*

**This data was obtained by Dr Javier García-Cárceles*

Some aromatic units were not tolerated (Scheme 68). Subjection of quinoline **276** to the cross-coupling conditions generated a complex mixture from which no identifiable products could be obtained. This is likely caused by complications associated with the heteroaromatic nitrogen centre, which may react with TFAA and/or coordinate to the nickel catalyst. Substrates **275**, **269**, and **270** containing aryl chlorides or bromides also resulted in complex reaction mixtures, likely due to competing $C(sp^2)$–$C(sp^2)$ cross-coupling.

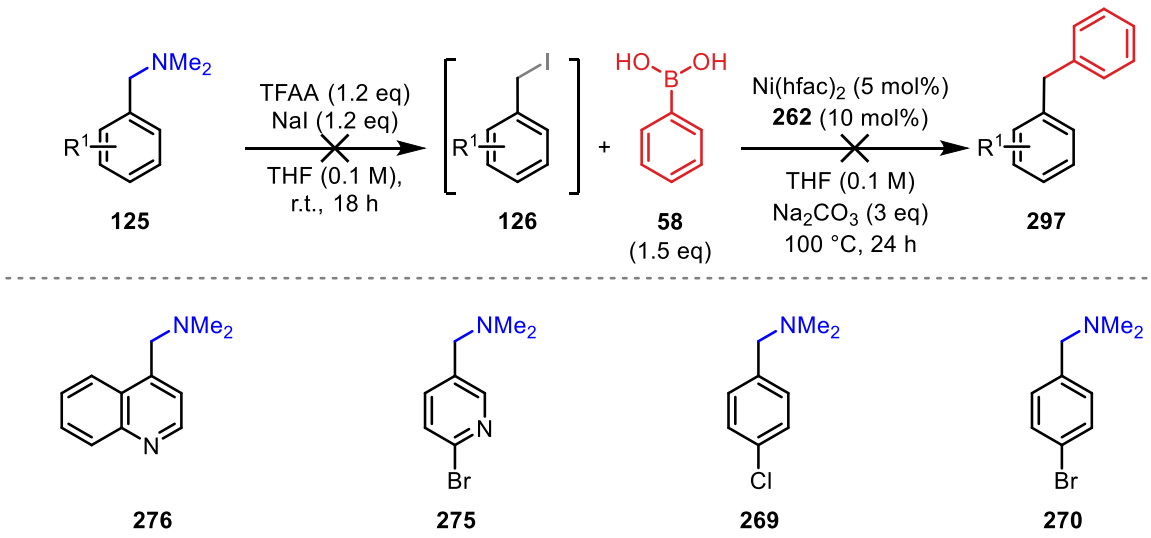

Scheme 68. *Tertiary benzylamine substrates unsuited to the cross-coupling protocol*

These reactions were carried out by Dr Javier García-Cárceles

To define the limits of this method, non-benzylic systems were also evaluated. Cyclohexyl substrate **315** gave a complex mixture of products, indicating that a benzylic C–N bond is a necessity. This was rationalised further by subjecting phenethylamine **316** to the iodination step. Iodination product **314** was not observed; instead, amide **317** formed in 33% yield. This shows that in this case, competing methyl C–N cleavage is more favourable. This result indicates that further investigations into the use of non-benzylic C–N bonds are warranted, especially to establish whether selective processes can be achieved.

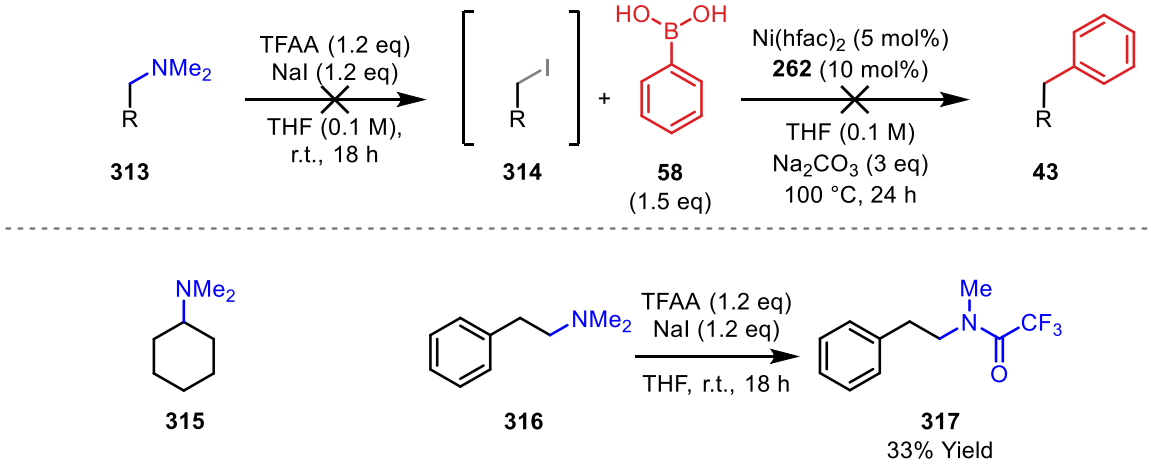

Scheme 69. *Tertiary amine substrates unsuited to cross-coupling*

These reactions were carried out by Dr Javier García-Cárceles

3.2.2.3. Examining the Tolerability of the Cross-Coupling to Alternative Boronic Acid Coupling Partners

Having established the scope and limitations of the protocol with respect to the amino-partner, investigations into the scope of the boronic acid coupling partner were undertaken (Table 11). Products **319**, **320**, and **321**, furnished with electron-withdrawing substituents were formed in 86%, 79%, and 78% yield, respectively. Electron-donating substituents were also well-tolerated; products **322** and **326** formed in 83% and 79% yield, respectively. Heteroaromatic boronic acids were also effective for this cross-coupling, forming pyridine-containing and benzothiophene-containing products **323** and **324** in 49% and 80% yield, respectively. The successful formation of **323** shows that the conditions can tolerate coordinating functionality, although in this case, the cross-coupling step required a higher temperature (150 °C) and higher catalyst loading. Product **325**, containing *ortho*-substituted aryl bromide was formed in 68% yield. In this case, no competing $C(sp^2)$–$C(sp^2)$ cross-coupling was observed. This result suggests that there is kinetic selectivity for cross-coupling at the benzylic position over the aryl position. Once product **325** was formed, further $C(sp^2)$–$C(sp^2)$ cross-coupling was prevented by steric crowding of the tethered aryl group. The scope demonstrated here and above indicates that this telescoped method for C–N cross-coupling may be an effective tool for total synthesis as well as for the functionalisation of various natural products and drug molecules.

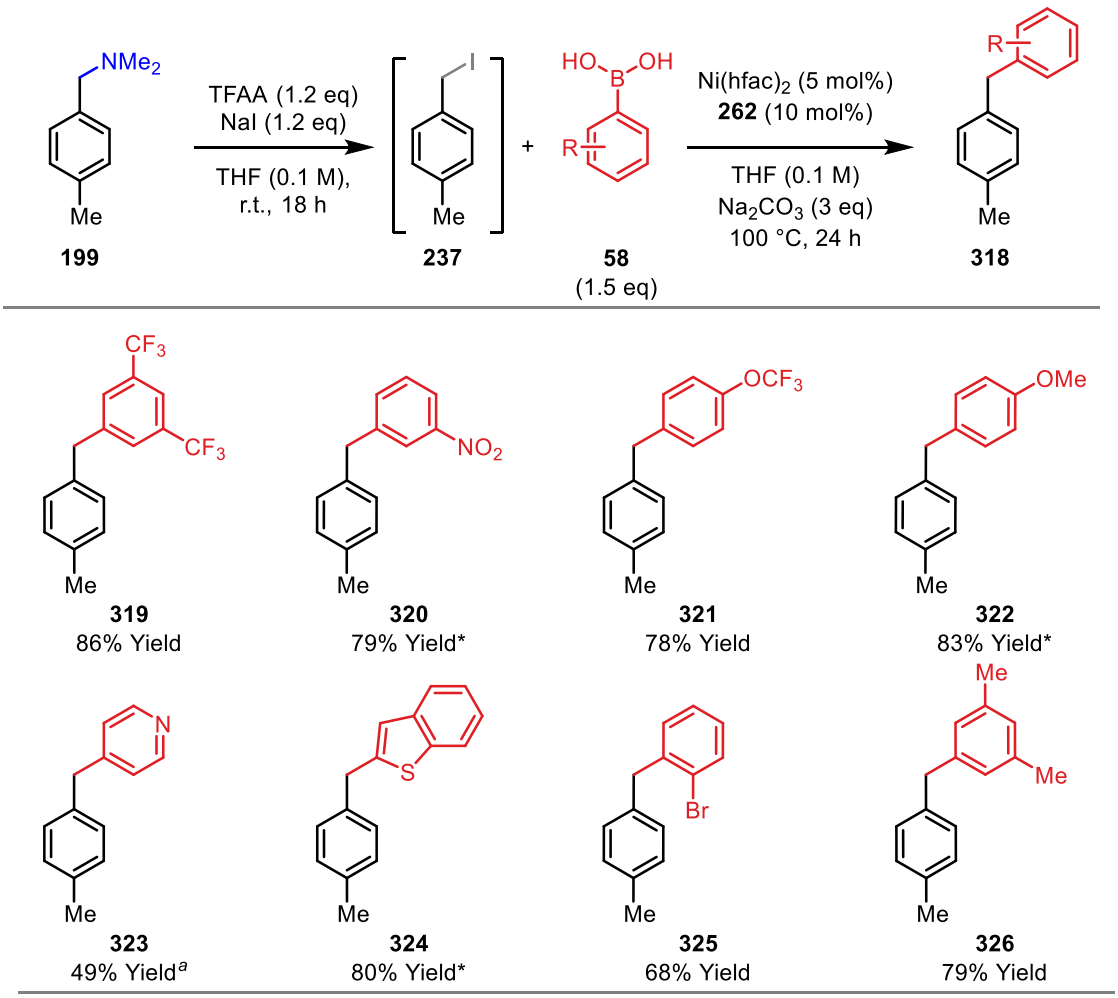

[a] *10 mol% Ni(hfac)$_2$, 20 mol% **262**, 150 °C*

Table 11. *Tolerance of the cross-coupling for alternative boronic acid coupling partners*
**This data was obtained by Dr Javier García-Cárceles*

3.3 The Development of a C–N Iodination/Nucleophilic Substitution Protocol

Due to the excellent leaving ability of halides in S_N2 reactions,[110] it was hypothesised that the optimised method described in Section 3.1.2 for converting benzylamines **199** into benzyl iodides **237** might be a useful first step in a telescoped two-step protocol for nucleophilic substitution of benzylamines (Scheme 70).

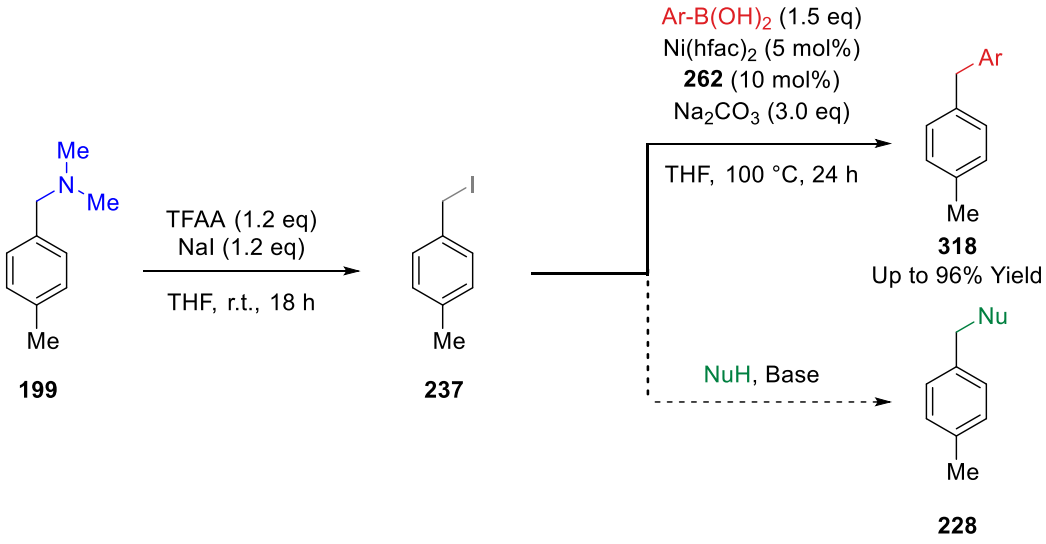

Scheme 70. *Proposed C–N iodination/nucleophilic substitution protocol*

This reaction was first trialled with phenolate as the nucleophile, which was generated in situ by treatment of phenol with either KO^{t}Bu or NaH. A one-step process, wherein phenol, the base and the iodination reagents were added at the outset did not lead to formation of product **327** (Scheme 71A). However, deprotonation of the nucleophile prior to exposure to **237** was advantageous. Preformation of a solution of sodium phenolate, and then addition of a solution of benzyl iodide **237** gave target **327** in 39% yield (Scheme 71B).

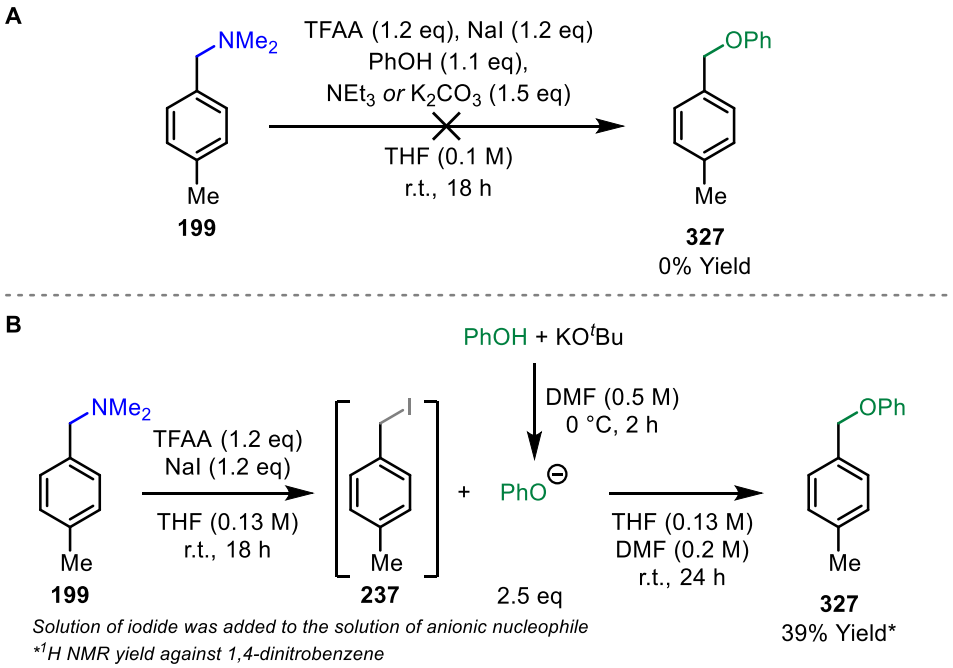

Scheme 71. *Initial conditions for the telescoped nucleophilic substitution of benzylamine **199***

Subsequent studies were undertaken by MSci student Joshua Thomson (Table 12). It was discovered that, in THF, the use of NaH and KO^{t}Bu offered comparable results (Entries 1 and 2, 51%

vs 52% yield). Changing the solvent used for the deprotonation step to DMF increased the yield of **327** (76% with NaH vs 57% with KO^{t}Bu) (Entries 3 and 4). It was discovered that decreasing or increasing the temperature (0 °C or 80 °C) decreased the yield to 23% and 31%, respectively (KO^{t}Bu, DMF, Entries 5 and 6). The use of different bases such as DBU and CsOPiv also resulted in decreased yields (Entries 7 and 8). Finally, it was discovered that inverting the order of addition, so the solution of the *nucleophile* was added into the solution of benzyl iodide **237** (dropwise over 5 minutes), increased the yield substantially. For example, with this procedural modification, **327** was accessed in 97% yield (NaH, DMF, r.t., Entry 9). Further studies confirmed that reducing the equivalents of base or nucleophile caused a decrease in yield.

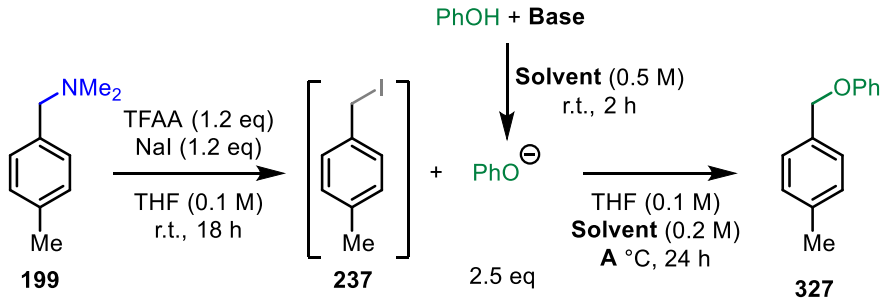

Entry	Base	Solvent	A	Yield
1	NaH	THF	r.t.	51%[a]
2	KO^{t}Bu	THF	r.t.	52%[a]
3	NaH	DMF	r.t.	76%[a]
4	KO^{t}Bu	DMF	r.t.	57%[a]
5	KO^{t}Bu	DMF	0 °C	23%[a]
6	KO^{t}Bu	DMF	80 °C	31%[a]
7	DBU	DMF	r.t.	12%[a]
8	CsOPiv	DMF	r.t.	26%[a]
9	NaH	DMF	r.t.	97%[b]
10	KO^{t}Bu	THF	r.t.	90%[b]

[a] *The solution of benzyl iodide was added to the solution of nucleophile;*
[b] *The solution of nucleophile was added dropwise to the solution of benzyl iodide over 5 minutes*

Table 12. *Optimisation of benzylamine activation and nucleophilic substitution*
This work was carried out by Joshua Thomson

This telescoped benzylamine nucleophilic substitution protocol was applied to three different nucleophiles: phenol, thiophenol, and diethyl malonate (Table 13). All were effective, thereby showing that the method can convert benzylic C–N bonds into new C–O, C–S, and C–C bonds.

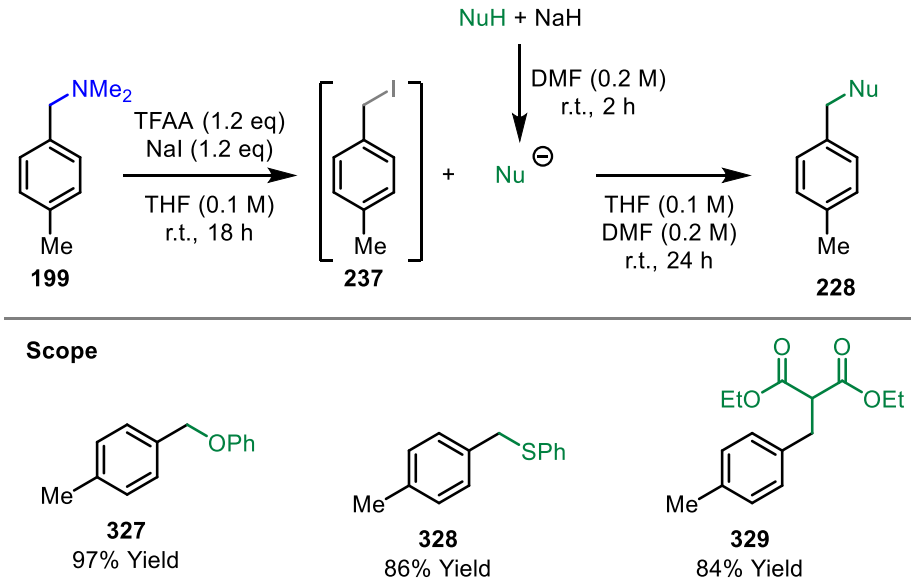

Table 13. *Benzylamine activation and nucleophilic substitution*

This work was carried out by Joshua Thomson

Unfortunately, application of a pyrrolidine nucleophile to the reaction conditions in Table 12, Entry 9 did not give target **287** (Scheme 72A). Clearly, the reactivity profile of **284** is different to that of e.g. phenol (PhOH pKa = 10; pyrrolidine pKa = 44), and so further investigations are required to establish effective conditions for the second step. This should be possible because, as outlined in Scheme 65 (Section 3.2.2.1), target **287** has previously been synthesised from benzyl bromide. Accordingly, different bases (e.g. KOH, DIPEA), and solvents (e.g. THF or MeCN) should be evaluated for the second step. If successful, this would provide a new method for converting benzylamines into new, alternative benzylamines. This may prove useful in late-stage functionalisation for drug-discovery because it would allow the direct exploration of comparable steric and electronic environments around a nitrogen centre (Scheme 72B).

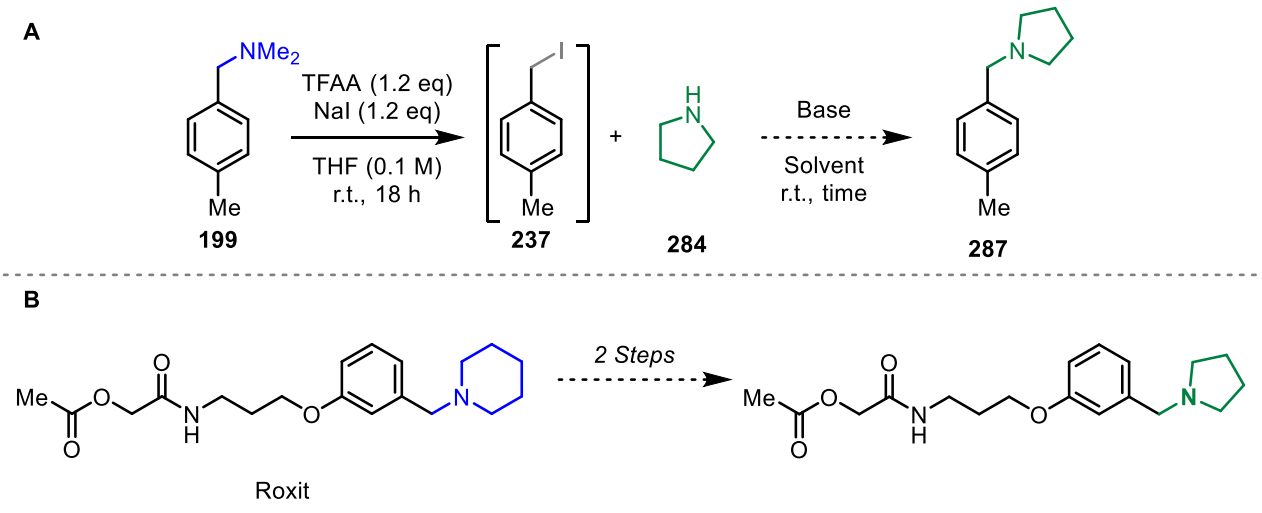

Scheme 72. *Proposed pyrrolidine nucleophilic substitution and its use in late-stage functionalisation*

3.4 Chapter Summary and Future Work

Described within this chapter is the development and optimisation of a novel method for the substitution of benzylic amines. The process involves the in situ conversion of benzylamines **125** to benzyl iodides **126**, followed by a telescoped cross-coupling or nucleophilic substitution (Scheme 73). These transformations have all been achieved with excellent yields. This chemistry potentially has broad applicability within the late-stage functionalisation of drug molecules and natural products, as well as providing a useful new tool for total synthesis.

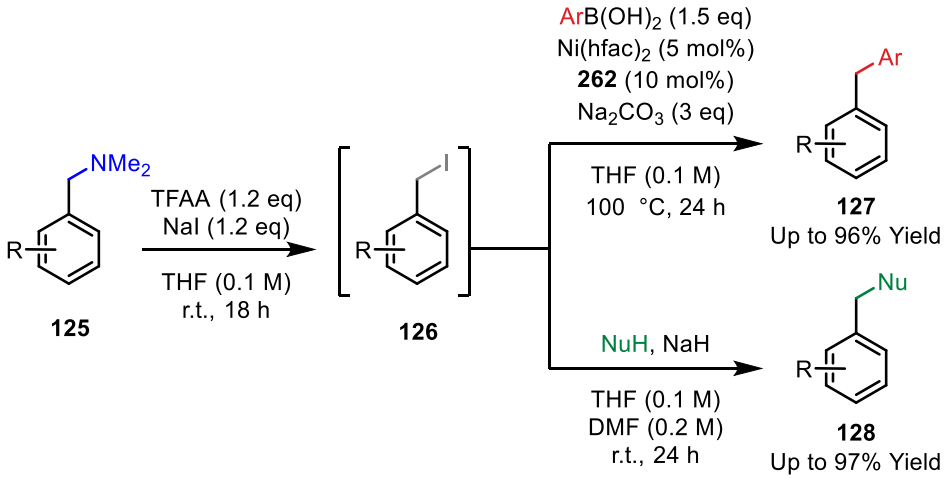

Scheme 73. *Optimised cross-coupling and nucleophilic substitution described in this chapter*

Future work within this project could focus on expanding the scope of nucleophilic substitution to include amine nucleophiles,[133] as well as a broader range of alcohol and thiol nucleophiles (Scheme 74A). Additionally, the application of the strategy to more complex systems, such as those with substitution at the α-position of the benzylamine substrate, is highly desirable (Scheme 74B). This work is explored in Chapter 4. As natural products are highly diverse, this formal C–N activation method could have wide-ranging applications if more complex systems can be tolerated.

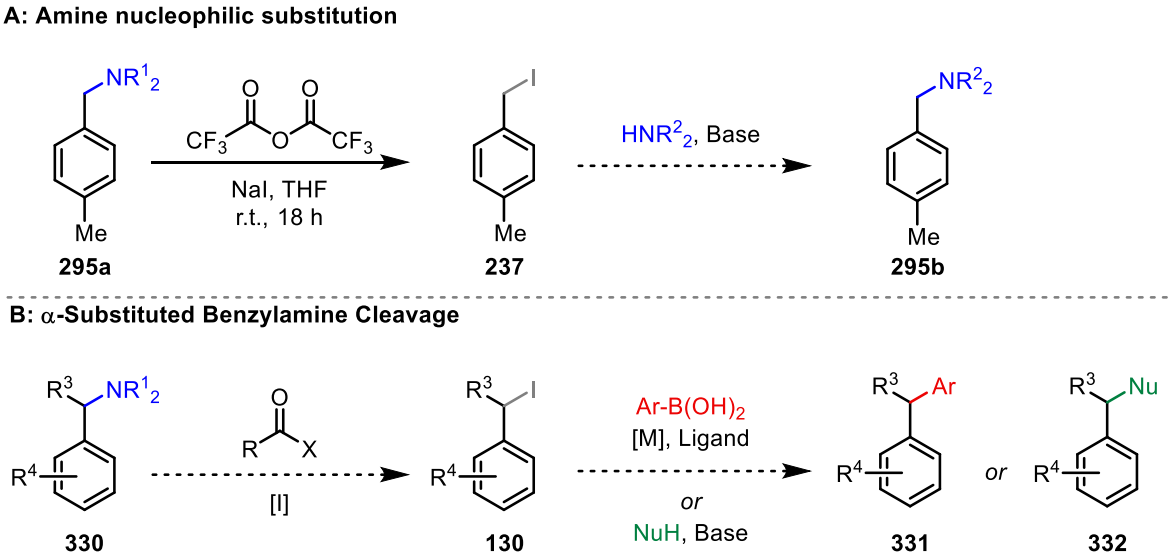

Scheme 74. *Future work in C–N bond activation*

Chapter 4. α-Substituted Benzylic C–N Activation and Cross-Coupling

In Chapter 3, a novel protocol for the cross-coupling or nucleophilic substitution of benzylic C–N bonds was described. In this chapter, the cross-coupling methodology is extended to tolerate more complex α-secondary benzylic amines (Scheme 75). Natural products and drug molecules often contain complex functionality and steric diversity in the α position, and so this logical extension of the C–N cross-coupling protocol may offer significant benefits.

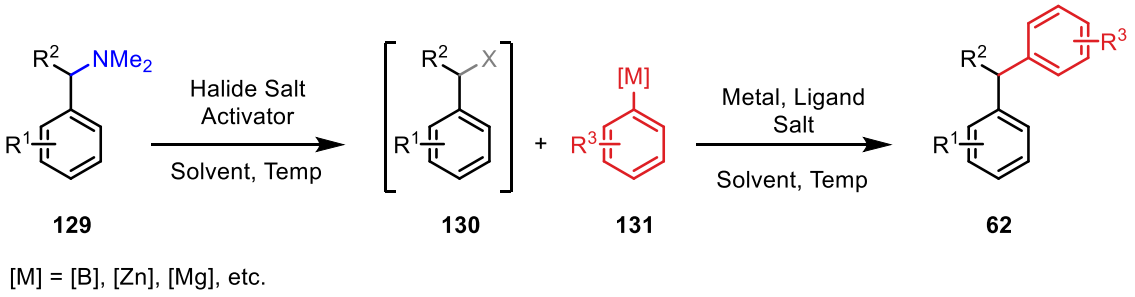

Scheme 75. *Extending the cross-coupling protocol to include α-substituted benzylamine substrates*

4.1. Background

As described in Section 1.3, there are few methods available for the cross-coupling of α-secondary benzylamines. Those that have been reported employ quaternary trimethylammonium triflate salts **334** (Scheme 76A)[4] or *N*-ditosylates **336** (Scheme 76B),[135] illustrating that considerable polarisation of the C–N bond is required for success. Myriad additional challenges are associated with the cross-coupling of α-secondary systems, specifically (1) the chiral centre present within the starting material introduces an enantiomeric control aspect, (2) greater steric hindrance at the benzylic centre may inhibit oxidative addition or substitution, potentially promoting more favourable side reactions, and (3) the introduction of a new group adjacent to the reactive centre may promote alternative side reactions such as β-hydride elimination. As shown in Scheme 76A, the use of trimethylammonium triflate salts can offer enantiomeric control, as inversion of stereochemistry occurs during the cross-coupling (i.e. the process is stereospecific). Watson and co-workers demonstrated this within a telescoped 2-step cross-coupling of α-secondary benzylamine **333** to diarylethane **335** via in situ formation of trimethylammonium triflate salt **334** (MeOTf, Et_2O, 0 °C, 0.5 h; **46**, $Ni(cod)_2$, K_3PO_4, dioxane, 80 °C, 6 h), which generated product **335** in 71% yield and 83% e.e., with the benzylic stereocentre undergoing inversion during the cross-coupling.[4] Alternatively, the cross-coupling protocol developed by Tian and colleagues, in which *N*-ditosylate **336** is converted into **337** (PMPMgBr. CuI, THF, 70 °C, 2 h) (Scheme 76B) uses achiral starting materials.[135] The level of enantiospecificity of this process was not described.

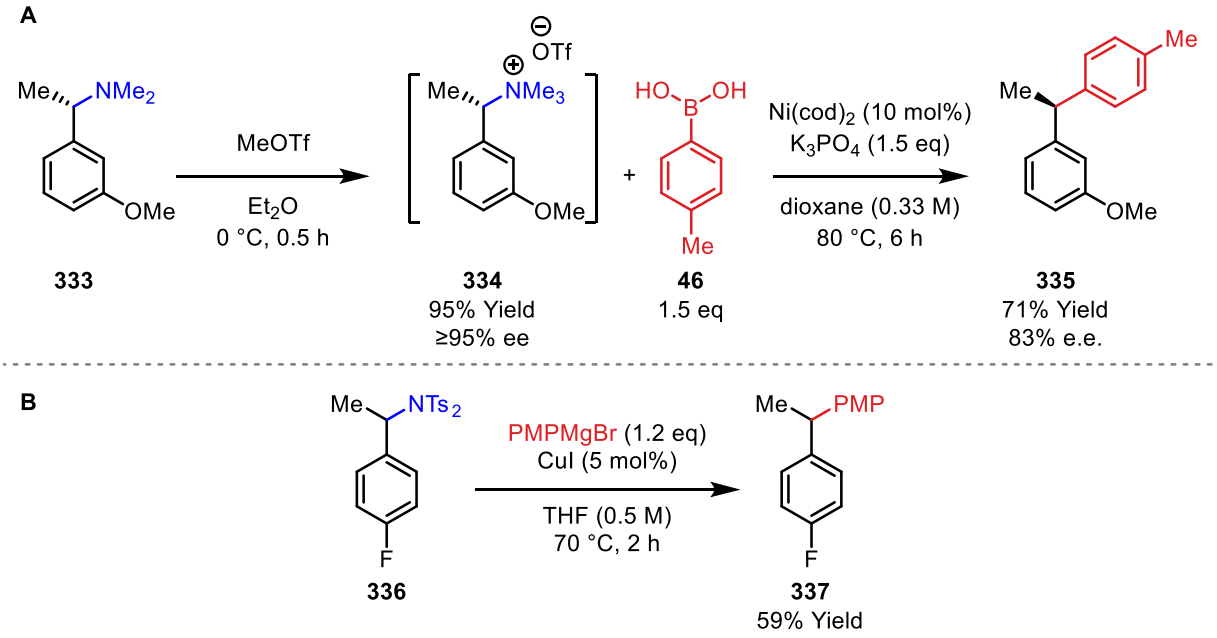

Scheme 76. *Existing protocols for the cross-coupling of α-secondary benzylamines*

4.2. Optimisation of the Telescoped α-Substituted Benzylamine Cross-Coupling Protocol

4.2.1. Synthesis of α-Substituted Benzylamine 339

To investigate whether α-secondary benzylamines could be tolerated within the cross-coupling protocol developed in Chapter 3, α-secondary substrate **339** was synthesised. An Eschweiler-Clark dimethylation was employed in this instance, utilizing a large excess of formic acid and formaldehyde at 100 °C (Scheme 77) to give **339** in a 62% isolated yield. Alterations to the reaction conditions were examined, but reductions in reaction time or the quantity of formaldehyde and/or formic acid led to considerably lower yields (<10%). One potential explanation for this is the reversible nature of iminium formation (**340** to **341**) under these conditions. Because aqueous formaldehyde is used, the equilibrium presumably favours starting material **340**. Consequentially, forcing conditions are required to achieve reasonable efficiencies. It should be noted that much of the optimisation described later utilised optically pure benzylamine **358**—this substrate was synthesised in the same manner, from commercially available and enantiopure **338**, which is cheaper than racemic **338** shown in Scheme 77.

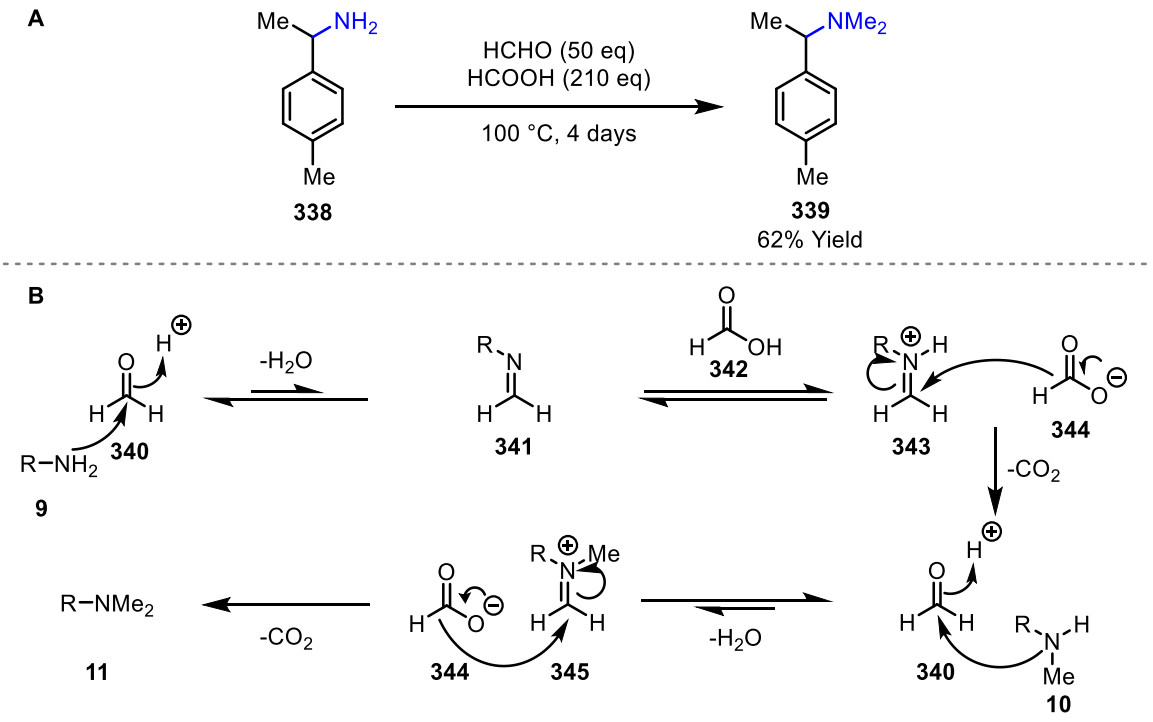

Scheme 77. *Synthesis of α-substituted benzylamine* ***339*** *and its mechanism*

4.2.2. Application of Substrate 339 to the Established Cross-Coupling Protocol

With α-secondary benzylamine substrate **339** in hand, investigations were undertaken to establish whether it was viable for the cross-coupling protocol developed in Chapter 3 (Scheme 73). Unfortunately, the previously optimised conditions returned only a 21% yield of desired diarylethane **347**. ^{1}H NMR analysis showed signals indicative of an alkene side-product, which was most likely styrene **348**. Mechanistically, this observation indicated that β-hydride elimination was competing with the transmetalation step, a situation likely exacerbated by the high reaction temperature (100 °C).

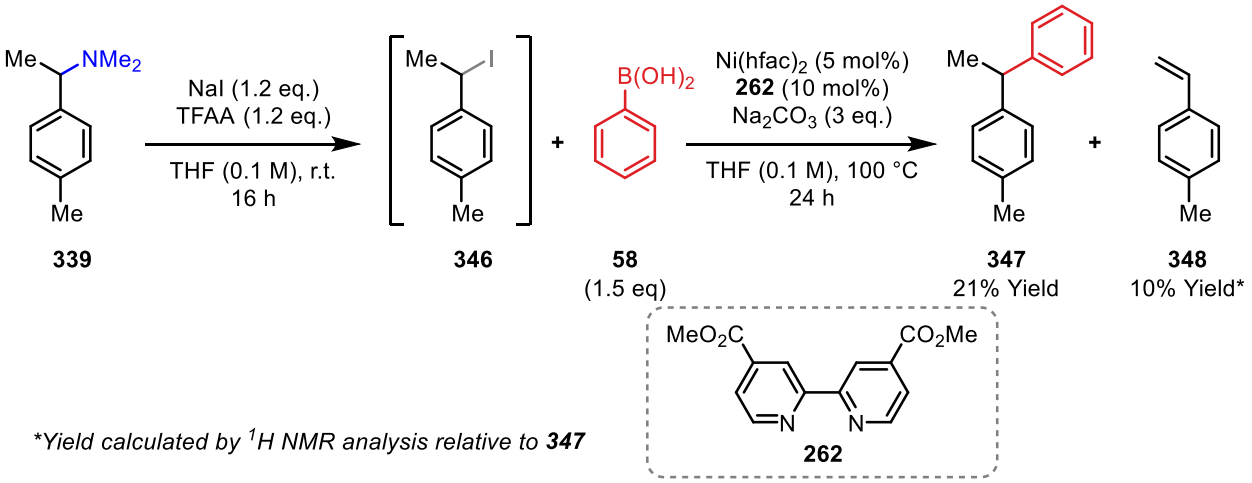

Yield calculated by ^{1}H NMR analysis relative to* ***347*

Scheme 78. *Applying **339** to optimal conditions for α-primary benzylamine cross-coupling*
This work was carried out by Dr Javier García-Cárceles

4.2.3. Exploration of Boronate Coupling Partners

Evaluation of the literature on the cross-coupling of α-substituted benzyl halides indicated that boronic acid coupling partners are not typically used. Instead, established cross-couplings of benzyl halides employ more nucleophilic coupling partners such as alkyl zinc halides,[136,137] aryl zinc halides,[138] aryl Grignard reagents,[139] activated boronic esters,[140] and indium organometallics[141] (Scheme 79). The use of a more nucleophilic coupling partner increases the rate of the transmetalation step, therefore decreasing the propensity of β-hydride elimination from intermediate **346** (Scheme 78). It also allows the reaction to take place at lower temperatures which further reduces the formation of side products, generating the product with higher yields and greater selectivity.

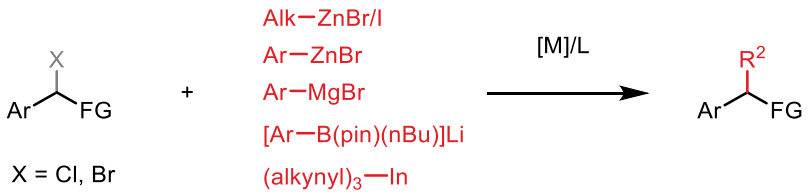

Scheme 79. *Alternative nucleophiles for cross-coupling of α-secondary benzyl halides*

Boronate salts have been historically employed to facilitate challenging cross-couplings that employ metals with a lower propensity for transmetalation. Examples include iron,[142] zinc,[143] and cobalt.[144] Boronate salts have also been employed for Ni and Pd catalysed cross-coupling reactions, and a useful feature of these reactions is their ability to proceed at low temperatures, which can often reduce competing undesirable reaction pathways.[140,145] In 2017, Shen and co-workers reported the use of lithium boronate salt **350** for the cross-coupling of secondary benzyl bromide **349** at 10 °C ($NiBr_2$•DME, **351**, THF). Here, the low temperature was required to improve the enantioselectivity (Scheme 80).[140]

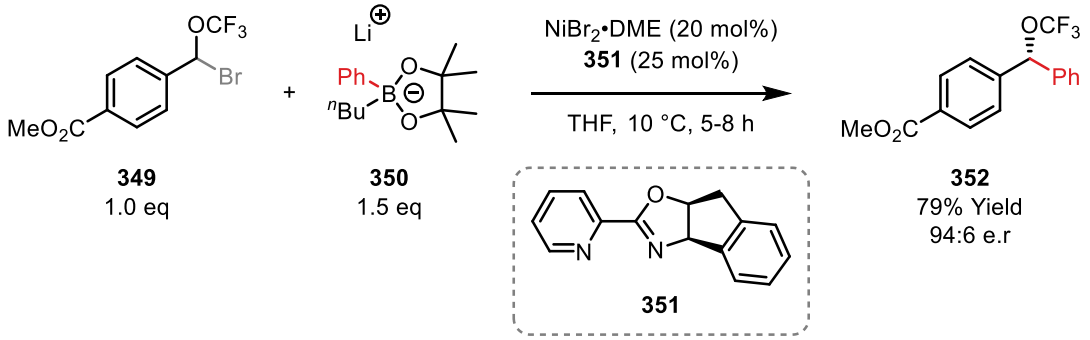

Scheme 80. *Enantioselective cross-coupling of α-OCF_3 benzyl halides by Shen and co-workers*

Inspired by the work of Shen and co-workers, boronate salts **356** and **357** were prepared (Scheme 81).[138] The *para*-methoxy unit was selected to add polarity to diarylethane **331** and assist in purification by FCC. These boronates were synthesised in two steps; first, commercially available boronic acid **353** was reacted with pinacol (Na_2SO_4, Et_2O, r.t.), providing boronic ester **355** in quantitative yield following filtration. Boronic ester **355** was then converted to boronate salt **356** by reaction with *n*-butyllithium (THF, -20 °C to r.t.), or to **357** by reaction with *tert*-butyllithium (THF, -40 °C to r.t.). The products were dried under vacuum and stored in the glovebox due to their rapid degradation in air.

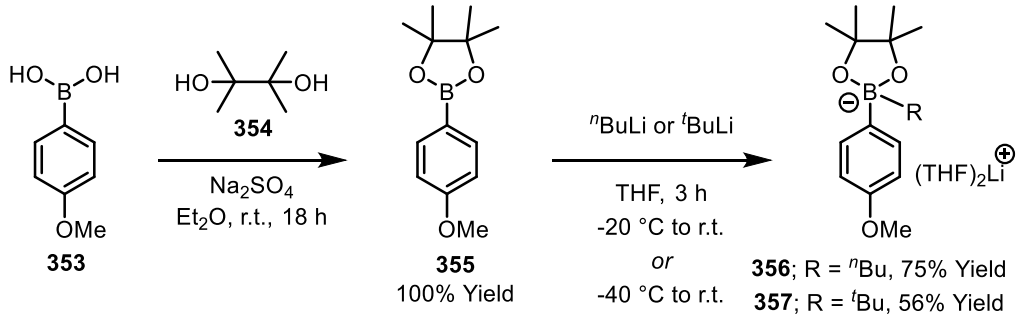

Scheme 81. *Synthesis of boronates **356** and **357***

Application of these boronate salts to the cross-coupling protocol was explored (Table 14). Similar yields for the cross-coupling of benzylamine **358** were achieved using boronic acid **353** at 100 °C (25% yield), and *n*-butyl activated boronate **356** at room temperature (26% yield) with $Ni(hfac)_2$ as the catalyst (Row 1). This confirmed that boronate salts enable this cross-coupling to occur at lower temperatures. Using $NiBr_2$(glyme) as the precatalyst gave an *increased* yield using boronate salts **357** and **356** at room temperature (51%, 52% yield), compared to boronic acid **353** at 130 °C (27% yield) (Row 2). *t*-Butyl activated boronate **357** and *n*-butyl activated boronate **356** gave similar yields under the same conditions (51% isolated yield vs 52% isolated yield), which suggested similar levels of reactivity. Accordingly, further studies with the former were not pursued, because its preparation requires ^{t}BuLi, which is a highly pyrophoric and unstable reagent. Boronic acid **353** and boronic ester **355** were not sufficiently reactive to give any cross-coupling at room temperature (Row 3; $NiBr_2$(diglyme)). From these results, boronate **356** was established as the most suitable cross-coupling partner for this process.

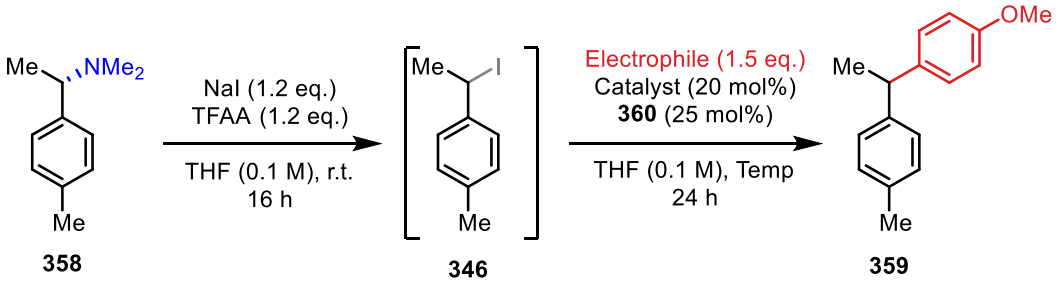

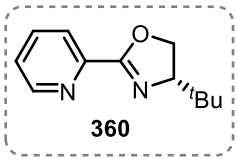

360

Catalyst	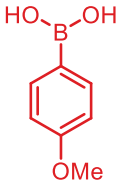 **353**	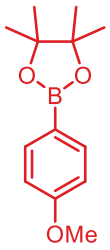 **355**	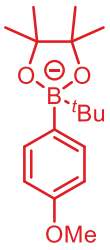 **357**	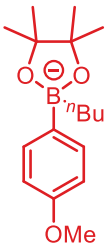 **356**
$Ni(hfac)_2$	25% Yield[a,b] (100 °C)			26% Yield[b] (r.t.)
$NiBr_2(glyme)$	27% Yield[a,b] (130 °C)		51% Yield (r.t.)	52% Yield (r.t.)
$NiBr_2(diglyme)$	20% Yield[a,b] (100 °C)			
	0% Yield[b] (r.t.)	0% Yield[b] (r.t.)		62% Yield (r.t.)

*[a]10 mol% of [Ni], 20 mol% of **360**, 3.0 eq Na_2CO_3, and achiral amine **339** was used; [b]Yield obtained by ^1H NMR analysis against 1,4-dinitrobenzene*

***Table 14.** Evaluation of various nucleophiles and metals for cross-coupling*

4.2.4. Optimising the Cross-Coupling of α-Secondary Benzylamine 358

With *n*-butyl boronate **356** selected as the best coupling partner, a variety of different metal and ligand combinations were examined to establish optimal cross-coupling conditions (Table 15). It was discovered that $Ni(hfac)_2$, the optimal catalyst complex in the cross-coupling of α-primary benzylamines (Chapter 3), and $Ni(acac)_2$ were outperformed by both $NiBr_2(glyme)$ and $NiBr_2(diglyme)$ when pyridine-oxazole ligand **360** was employed (Entries 1, 2, 3, and 5). Examining these two metals with alternative nitrogen-based ligands confirmed that pyridine-oxazole **360** was optimal of those tested (62% yield, $NiBr_2(diglyme)$; 52% yield, $NiBr_2(glyme)$) (Entries 3 and 4). Ligand **360** outperformed ester-substituted bipyridine ligand **262** (44% yield, $NiBr_2(glyme)$) (Entry 5), as well as isoquinoline-based ligand **255** (Entry 6), and various others (Table SI:3). Notably, electron-poor variant ligand **361** also gave a lower yield (44% yield, $NiBr_2(diglyme)$) (Entry 7). This suggests that the limiting step for

this mechanistic cycle is different to that for the cross-coupling of α-primary benzylamines, which was facilitated by electron-poor ligands (Chapter 3). Further examination of metal-ligand loadings indicated that a decrease in these was not possible under these conditions without loss of yield (Entries 8 and 9).

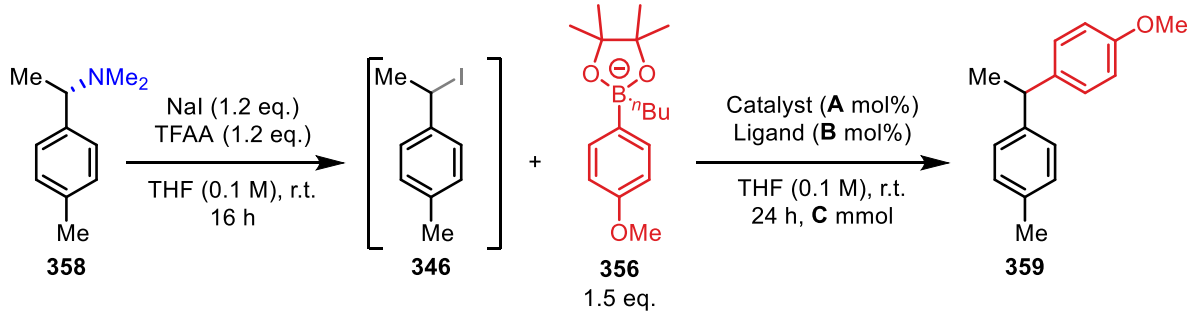

Entry	Catalyst	A	Ligand	B	C	Yield
1	M6	20	360	25	0.4	26%[a]
2	M5	20	360	25	0.4	19%[a]
3	M9	20	360	25	0.4	52%
4	M10	20	360	25	0.4	62%
5	M9	20	262	25	0.4	44%
6	M9	20	255	25	0.4	41%
7	M10	20	361	25	0.6	44%
8	M10	10	360	12	0.6	19%
9	M10	5	360	6	0.4	41%

M6 = $Ni(hfac)_2$; **M5** = $Ni(acac)_2$; **M9** = $NiBr_2(glyme)$; **M10** = $NiBr_2(diglyme)$. [a]*Yield obtained by GC-MS analysis against* [n]*dodecane*

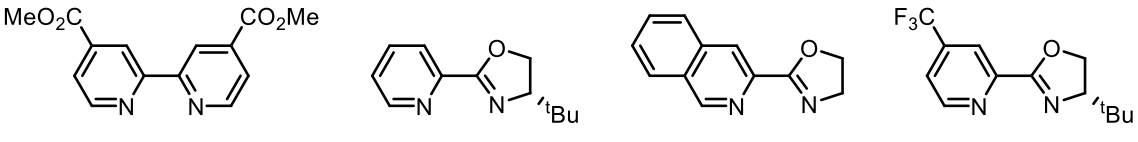

Table 15. *Optimisation of metal and ligand combinations for the cross-coupling protocol*

It is theorised that transmetalation is the rate-limiting step for this transformation. This challenging step is facilitated by the use of nickel catalysts, which have a much lower propensity for β-hydride elimination than palladium catalysts.[146] Chelating nitrogen-based ligands used in combination with these nickel catalysts further suppresses β-hydride elimination.[122] These findings are supported by the work of Fu and co-workers, who demonstrated that β-hydride elimination can be suppressed using tricoordinate pybox ligands such as **491** (Table SI:3). The authors suggested that this effect was due to coordinative saturation of the nickel catalyst.[128,147] Unfortunately, pybox ligand **491** was found to decrease the yield of cross-coupling here. This may be explained by steric hindrance preventing the

bulky boronate from accessing the metal centre. As discussed in Chapter 3, Section 3.2.1, the ability of nickel to access a wide variety of oxidation states and the versatile electronic nature of pyridine-based ligands (caused by their ability to take part in metal backbonding) means that there is a high propensity for these reactions to occur via SET oxidative addition (Scheme 82),[45,115,127,128] and so this is the mode of oxidative addition likely occurring within this cross-coupling as well.

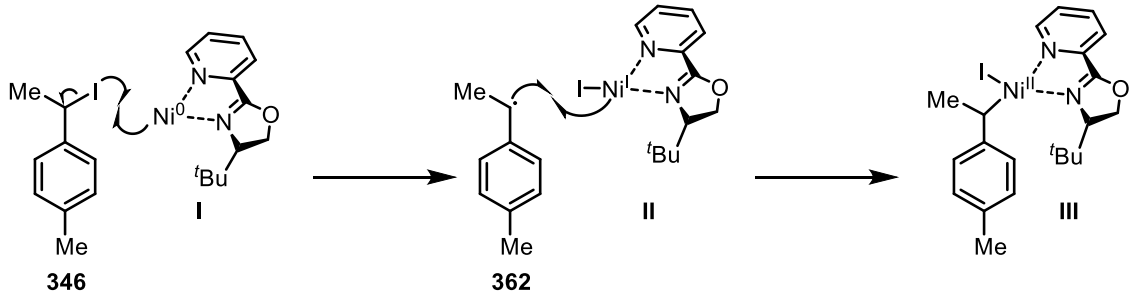

Scheme 82. *SET oxidative addition mechanism for the cross-coupling of α-secondary benzylamines*

Unfortunately, attempts to improve the yield of this process were unsuccessful. Furthermore, repetition of Entry 4 (Table 15) gave inconsistent yields between 57% and 68%, so alternative avenues were pursued. Zinc salts were considered as an additive: in 2019, Shen and colleagues reported the use of $ZnBr_2$ to increase the reactivity of boronate salts by their in situ conversion to lithium aryl zincates (Scheme 83A).[138] This was further supported by the zinc-catalysed cross-coupling of benzyl bromide **284** and boronate salt **364** reported by Ingleson and colleagues in 2017 (Scheme 83B), and further reports by Fu and co-workers in 2016.[143,146] Unfortunately, introduction of $ZnBr_2$ into the reaction conditions gave no increase in yield, and so this avenue was not explored further (Table SI:3).

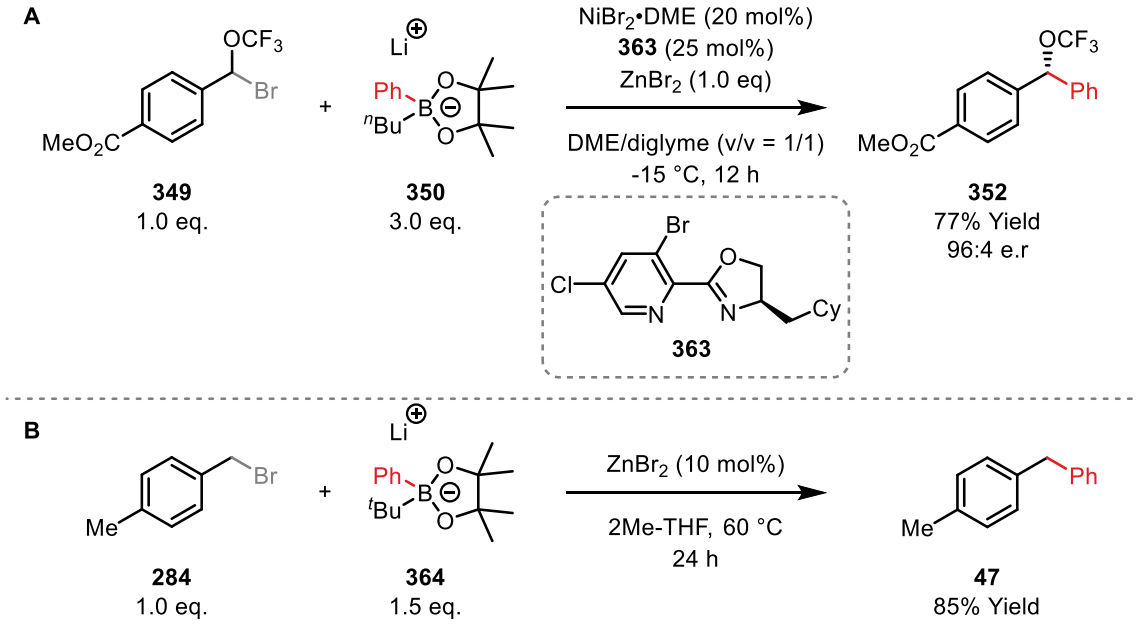

Scheme 83. *The use of $ZnBr_2$ to facilitate boronate cross-couplings*

Control experiments to establish whether the cross-coupling takes place solely using benzyl iodide **346** and boronate salt **356** were undertaken, but only trace quantities of product were observed in the absence of metal and/or ligand. Other reaction modifications that were examined include: conducting the reaction in the dark; varying the solvent (2-MeTHF, Et_2O, dioxane and TBME); heating to 40 °C; and varying the equivalents of boronate salt **356**. All modifications to the procedure resulted in a decrease in yield (Table SI:3).

Subsequently, the conversion of benzylamine **358** to benzyl iodide **346** was re-examined, as detailed in Table 16. Here, the quartet seen at δ = 5.44 ppm (circled in grey) corresponds to the C**1** proton of benzyl iodide **346**, and the two doublets at δ = 5.73 and 5.21 ppm (circled in red) correspond to C**2**Ha and C**2**Hb of styrene **348**. When the conditions shown in Table 16 were applied (TFAA (1.2 eq), NaI (1.2 eq), THF (0.1 M), r.t., 18 h; 62% cross-coupling yield), an ^{1}H NMR yield of just 48% was observed, with an iodide:styrene ratio of 1:0.04 (Entry 1). As evidenced by the higher overall two-step yield (see Table 15), it is likely that the in situ yield of **346** is higher than 48%, with the instability of the product being a major factor. Increasing either the equivalents of NaI or the reaction concentration saw a decrease in both the yield and iodide:styrene ratio (Entries 2 and 5). Exploring variations in temperature proved more advantageous: conducting the reaction at -10 °C for the first hour (then r.t. for 17 h) increased the ^{1}H NMR yield of **346** to 58%, though the iodide:styrene ratio of 1:0.04 was unchanged (Entry 3). Decreasing the reaction time to 5 h gave an increased ^{1}H NMR yield of 60%, but a lower ratio of iodide:styrene of 1:0.12 (Entry 4). Thereafter, alterations in temperature and reaction times were reexplored. Conducting the iodination at -10 °C for the full 5 h gave an improved yield of 63% and an iodide:styrene ratio of 1:0.10 (Entry 6). Finally, conducting the reaction at -10 °C for 1 h, then at r.t. for 4 h, gave a lower yield of 51%, but an improved iodide:styrene ratio of 1:0.02 (Entry 7). It became clear that a balance between reaction time and temperature was required, and so reaction times and temperature alterations were explored further within the two-step cross-coupling protocol.

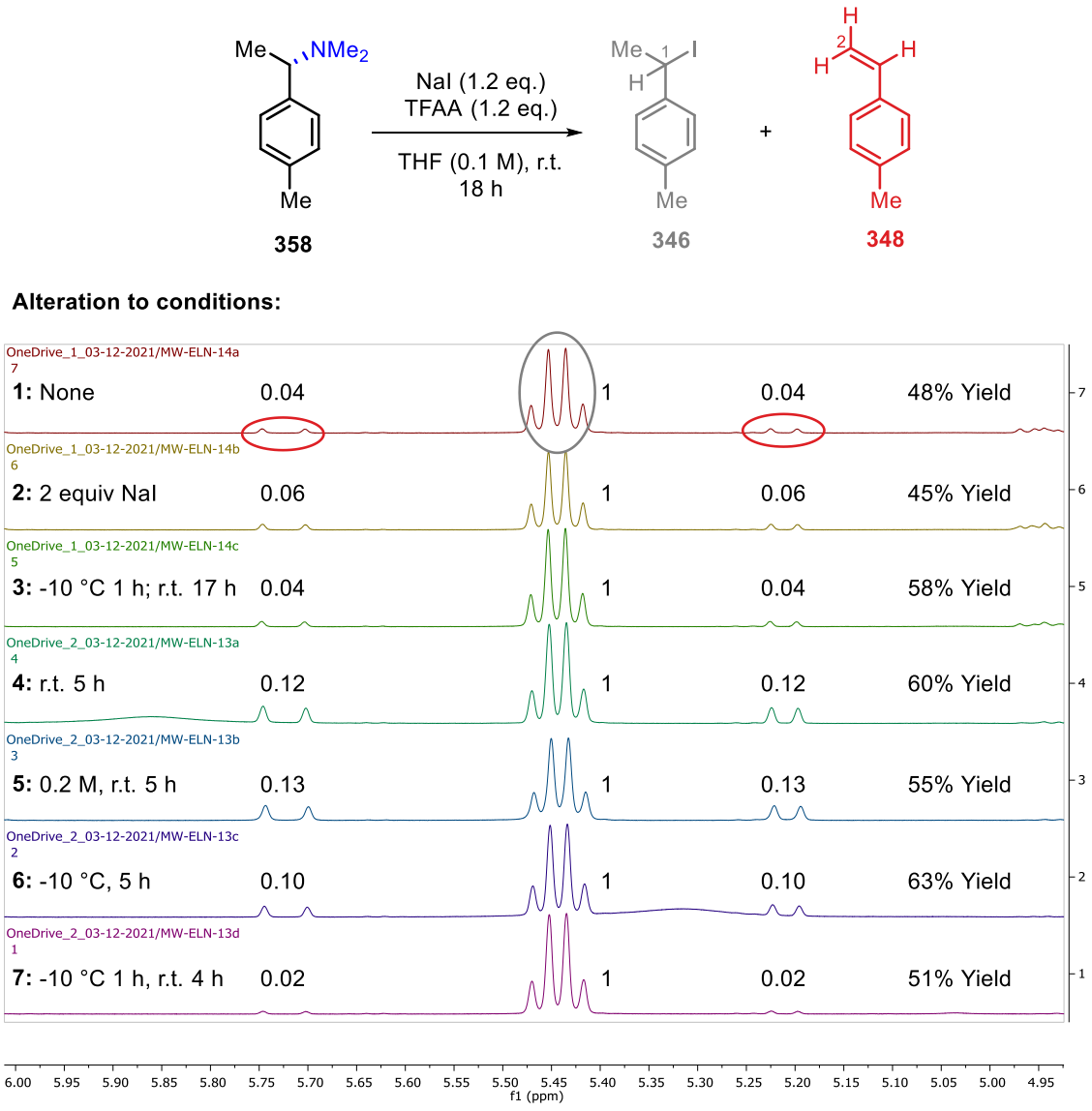

Table 16. *Reevaluation of the α-substituted iodination protocol*

While optimisation of the iodination protocol was being carried out, it was also considered whether it might instead be advantageous to target the analogous benzyl bromide. The synthesis of benzyl bromide **365** was attempted by replacement of NaI with NaBr. ^{1}H NMR analysis of the crude showed 80% conversion to a new species, which possessed a quartet for the benzylic proton at δ = 6.0 ppm. This does not match the literature value of bromide **365**,[148] but it does match the literature value for ester **366**.[149] It was therefore concluded that using NaBr in place of NaI is not a viable alternative for this substrate class. The preferential formation of **366** in this case may reflect the diminished nucleophilicity of bromide vs iodide.

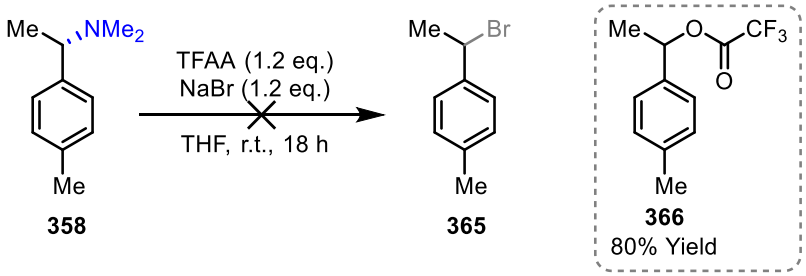

Scheme 84. *Probing the efficacy of sodium bromide for the halogenation of benzylamine* ***356***

Temperature and reaction time variations within the first step were incorporated into the two-step cross-coupling and the optimal conditions were determined. It was discovered that carrying out the first step at 0 °C for the first hour, then at room temperature for 17 hours gave improved yields compared to shorter reaction times of 6 hours, and colder temperatures of -10 °C (Table SI:3). It was also discovered that carrying out the second cross-coupling step at 0 °C for 24 hours gave the highest yields and most consistent results, leading to the final optimised conditions shown in Scheme 85. The yield obtained was lower than for α-primary systems, and this is likely due to a combination of the following factors: (1) the elimination side reaction that occurs in the first step, (2) increased steric hindrance around the reacting centre, and (3) competing β-hydride elimination during the cross-coupling step.

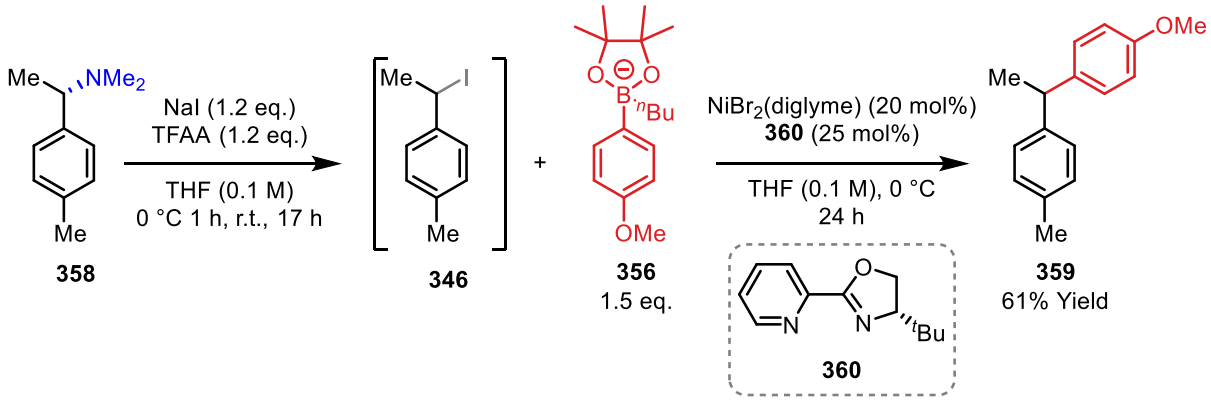

Scheme 85. *Optimised conditions for the cross-coupling of α-secondary benzylamine* ***358***

This reaction was conducted with enantiopure starting material **358** and so the resulting diarylethane **359** was analysed to determine if any enantiomeric excess was maintained. Unfortunately, but as expected based on the possible S_N1 iodination pathway and/or the proposed SET oxidative addition mechanism, analysis of product **359** by chiral HPLC gave an enantiomeric ratio of 45:55 (see Section 7.5). Additional investigations into the enantiopurity of benzyl iodide **346** were unfortunately unsuccessful because its high instability prevented purification for analysis.

Based on these observations, a proposed mechanism for this transformation is as shown in Scheme 86. As with the cross-coupling explored in Chapter 3, and supported by the loss of enantiopurity during the reaction (though it is possible this also occurs in the iodination step) and the optimal use of

a nitrogen-based ligand (**360**), an SET oxidative addition is proposed. Benzyl radical **362** is formed, and this recombines with Ni^{I} species **II** to generate metal complex **III**. β-Hydride elimination from **III** may form styrene side product **348**, giving metal hydride **IV**. This step is suppressed by use of boronate **356**, which allows transmetalation to outcompete β-hydride elimination, thereby forming metal complex **V** which, following reductive elimination, generates desired diarylethane **359**.

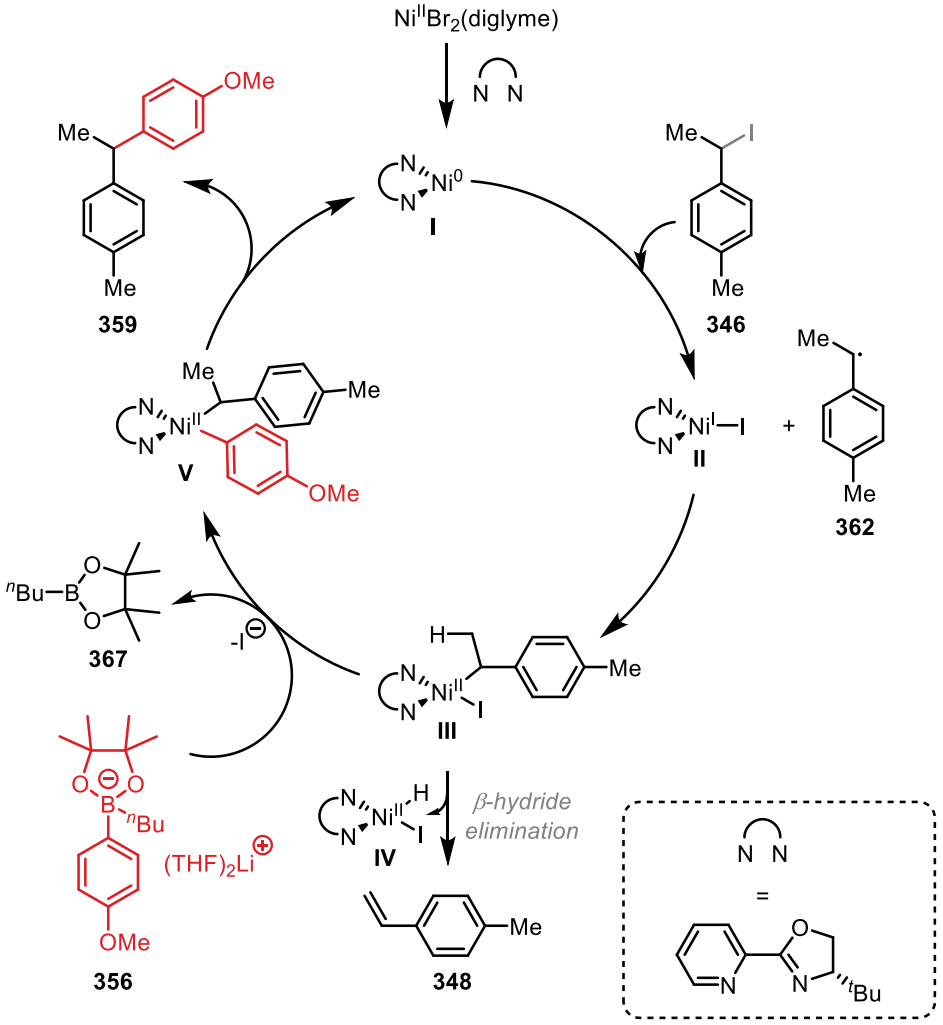

Scheme 86. *Proposed mechanism for the cross-coupling of α-substituted benzyl iodide* ***346***

Future work exploring alternative metal-ligand complexes that promote S_N2 oxidative addition rather than SET oxidative addition may prevent the formation of benzyl radical **362**. In combination with the development of an enantiospecific S_N2 iodination protocol, a wholly enantiospecific cross-coupling process may be demonstrated. Alternatively, different chiral ligands may be explored to induce asymmetry following radical formation. Enantioconvergent SET oxidative additions have been reported in other contexts. For example, Tyrol and co-workers reported the enantioconvergent iron-catalysed Suzuki-Miyaura cross-coupling of benzyl chlorides **368** using enantioenriched metal-ligand complex **M11** (**369**, ^{Ph}CNBox, LiNMeEt, 1,3,5-TMB, 1,2-DFB, -15 °C, 24 h) (Scheme 87).[150] This protocol delivers enantioenriched products from achiral starting materials because the recombination of

intermediate radical **371** and chiral metal complex **372** is reversible, and so this thermodynamically controlled scenario leads to the observed enantioselectivity for **370** (Scheme 87).

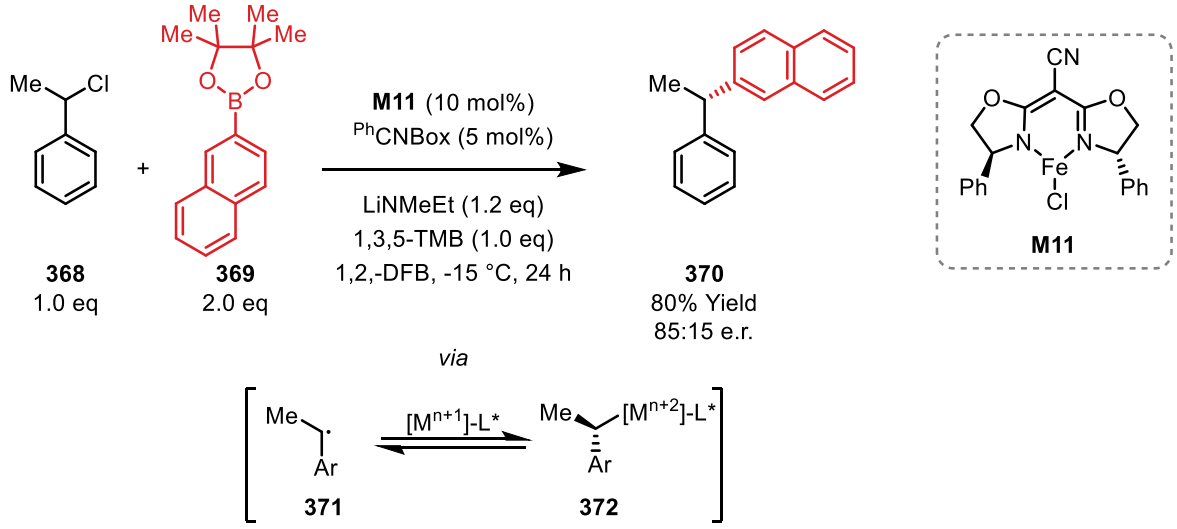

Scheme 87. *Iron-catalysed enantioconvergent synthesis of diarylethanes*

4.3. Evaluation of the Scope of the Telescoped α-Substituted Benzylamine Cross-Coupling

4.3.1. Synthesis of α-Secondary Benzylamine Substrates

To examine the scope of this cross-coupling, a variety of α-substituted benzylamines were synthesised (Table 17). The majority of these were accessed by methylation of their respective primary benzylamines using the Eschweiler-Clark reaction explored in Section 4.2.1, Scheme 77. Systems with a variety of different electronic and steric environments were selected. *Ortho*-methoxy substrate **375** was chosen to probe the effects of electron-donating substituents and steric hindrance, whereas the *meta*-trifluoromethyl group of **376** was chosen as an electron-withdrawing substrate. Systems with alternative groups in the R^2 position were also synthesised using this method: ethyl-substituted **377** has an altered steric environment at the α position (A values: methyl = 1.70, ethyl = 1.75), while CF_3 and phenyl substituted systems **378** and **379** were designed to investigate whether the absence of a β-hydrogen provides a superior substrate. For the reasons discussed in Section 4.2.1, low to moderate yields were generally obtained for the methylation reaction and optimisation was not pursued. The particularly low yields for *ortho*-methoxy and α-phenyl systems **375** and **379** may reflect increased steric hindrance.

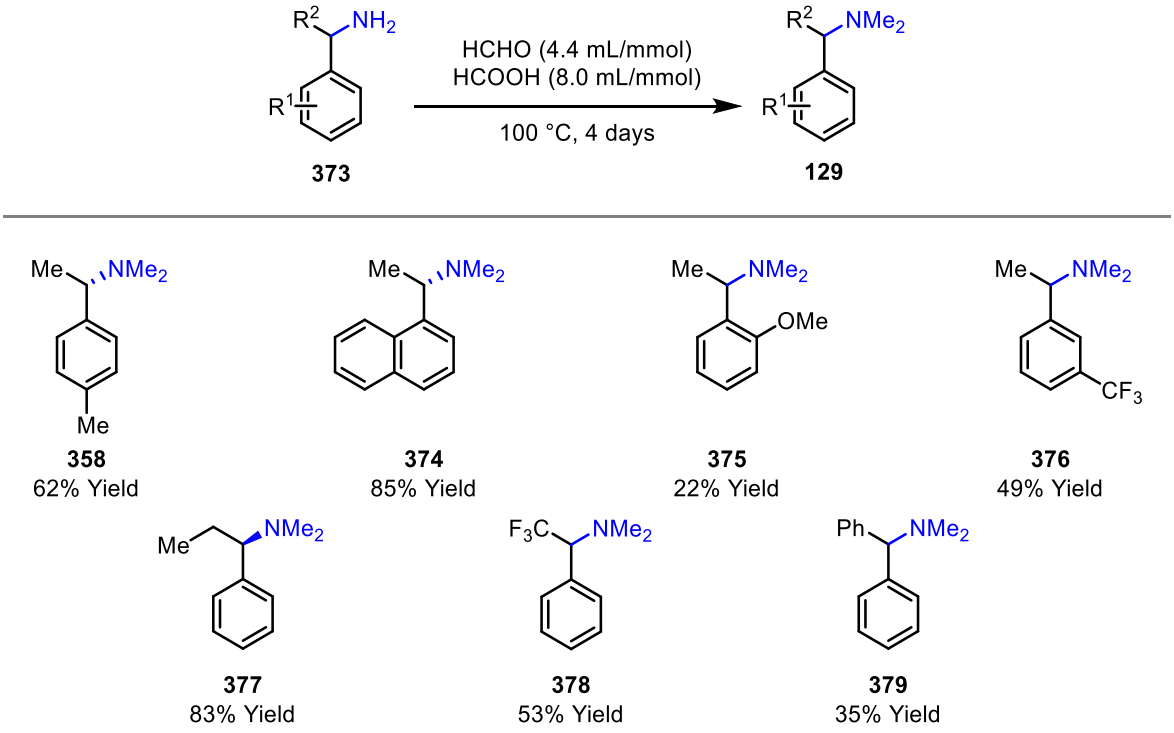

Table 17. *Methylation of α-substituted benzylamines*

Certain substrates, such as amino ester **381**, were not accessed by Eschweiler-Clark methylation. Here, bromide **380** was instead chosen as the precursor, and S_N2 displacement using $HNMe_2$ as the nucleophile (Na_2CO_3, THF) provided product **381** in 50% yield (Scheme 88).

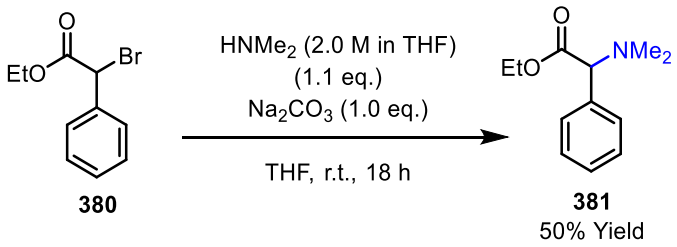

Scheme 88. *Synthesis of amino ester **381***

Alkyne and alkene substrates **384** and **387** were also synthesised to enable an understanding of whether amine cleavage and cross-coupling is viable for non-benzylic systems (Scheme 89). The synthesis of alkyne **384** (Scheme 89A) commenced with a Sonogashira cross-coupling between alkyne **382** and phenyl iodide ($Pd(PPh_3)_2Cl_2$, CuI, NEt_3, DMF, r.t.) to form alcohol **383**. Tertiary amine **384** was then formed via a two-step procedure; alcohol **383** was first converted into its mesylate (MsCl, NEt_3, THF), and subsequent addition of $HNMe_2$ (THF, 50 °C) formed tertiary amine **384** in 67% yield. Alkene **387** (Scheme 89B) was then synthesised over two steps from ketone **385**. First, a reductive amination was employed to form amine **386** (Step 1: NH_4OH, NaOH, EtOH, H_2O; Step 2: Zn, EtOH,

AcOH). This was then exposed to dibromopentane in order to form tertiary amine **387** ($NaHCO_3$, toluene). This step required demanding conditions (115 °C) to form product **387** in 43% yield.

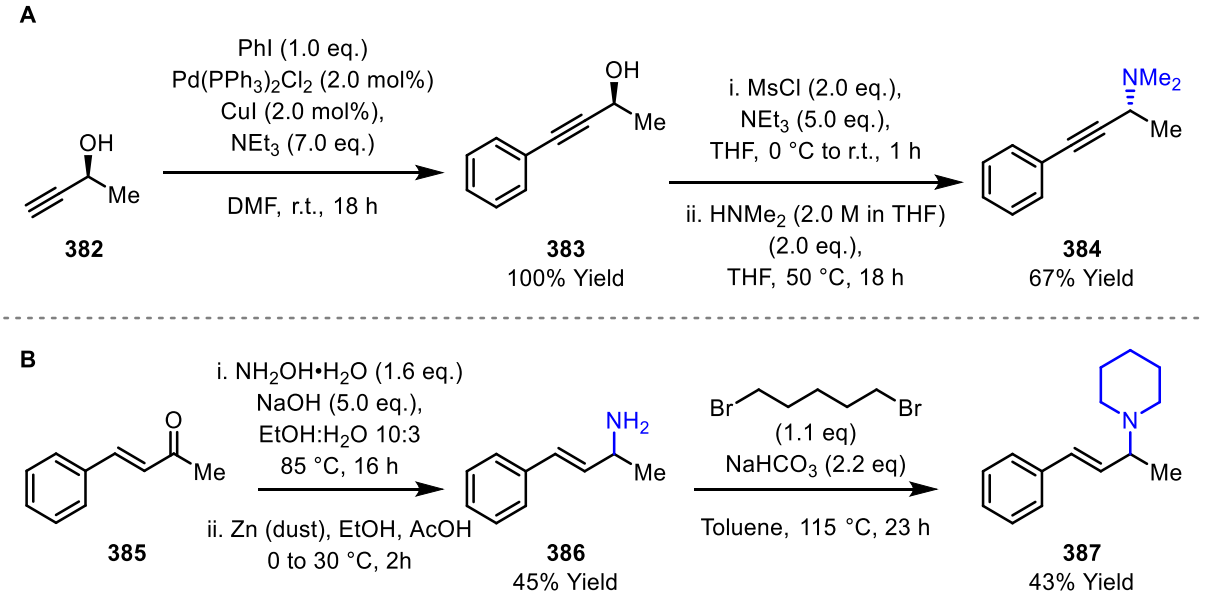

Scheme 89. *Synthesis of non-benzylic α-substituted amines*

4.3.2. Probing the Tolerability of the Cross-Coupling Protocol to Alternative Benzylamines

With substrates **374-379**, **381**, **384**, and **387** in hand, the scope of the cross-coupling was examined by applying the optimised conditions outlined in Section 4.2.4 (Scheme 85). Unfortunately, as shown in Table 18, in all cases the yields were considerably lower than the 61% obtained with **359**. For example, *ortho*-methoxy product **390** and *meta*-CF_3 product **391** were isolated in 17% and 22% yield, respectively. Due to their low polarity, and the formation of side products, isolation of **390** and **391** was challenging, with multiple purifications by FCC required to obtain clean samples. Ethyl-substituted product **389** was obtained in 32% isolated yield, which does demonstrate some variability of the α-substituent of the benzylamine.

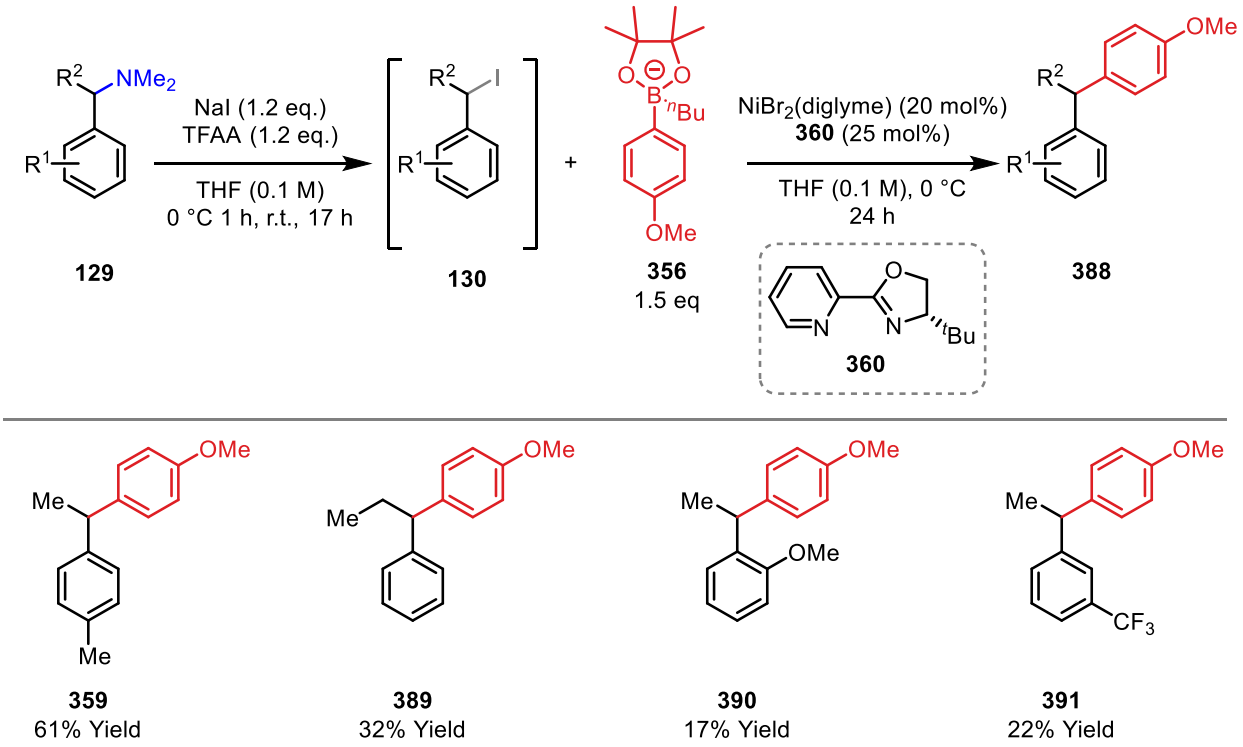

Table 18. *Tolerability of the cross-coupling protocol for α-substituted benzylamines*

Further attempts to expand the scope of this reaction with respect to the amine were unsuccessful. It was previously theorised that α-CF_3 substrate **378** may be effective in the cross-coupling due to its lack of a problematic β-hydrogen atom. Unfortunately, attempts to convert this tertiary amine into benzyl iodide **392** gave only ammonium salt **393**, in quantitative yield. This data was obtained by Dr. Karim Bahou.

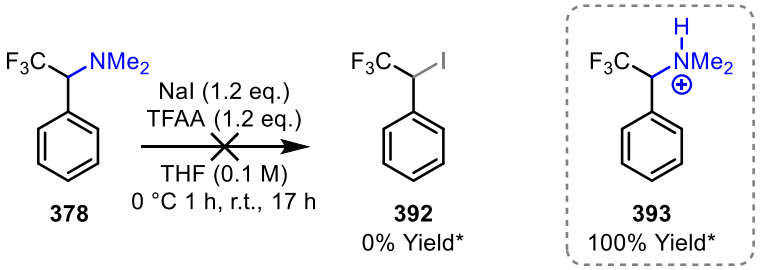

Scheme 90. *Probing the tolerability of the iodination protocol for substrate **378***

**This data was obtained by Dr Karim Bahou*

Similarly, α-phenyl substrate **379** did not give any cross-coupled product, though in this case conversion to iodide **130** was possible (as confirmed by Dr. Karim Bahou). **130** (R^1 = H, R^2 = Ph) was found to be highly unstable, which is possibly why the subsequent cross-coupling step was unsuccessful. Another reason could be the increased steric hindrance around the benzylic centre, or increased stabilisation of the benzylic radical within the SET oxidative addition step, which greatly decreases the reactivity of the radical and its ability to complete oxidative addition. Alkyne and alkene

substrates **384** and **387**, as well as naphthyl substrate **374** generated complex mixtures, from which purification to obtain definitive results was challenging.

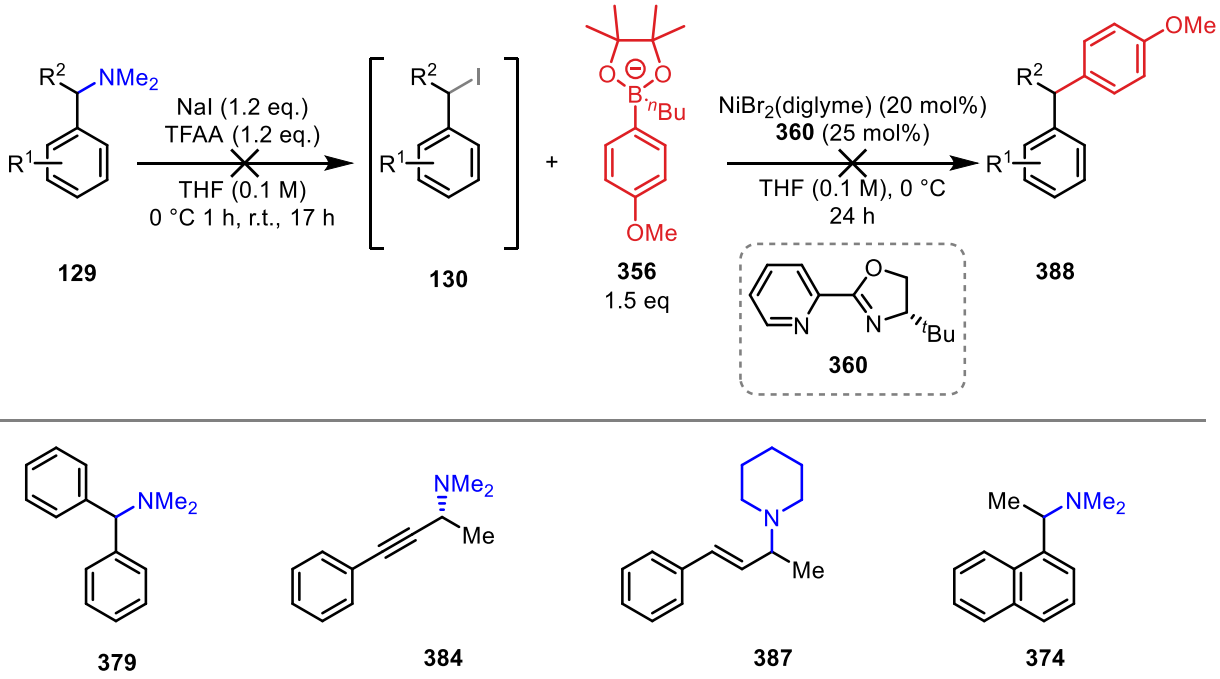

Table 19. *Unsuccessful amine substrates applied to the cross-coupling protocol*

4.3.3. Synthesis of Boronate salt Nucleophiles

The synthesis of five different *n*-butyl activated boronate salts was carried out in the same manner as **356** (Scheme 81), starting from their respective boronic acids or boronic esters, depending on commercial availability. The esterification progressed readily for most substrates, including sterically hindered trimethyl boronic acid **399** (Table 20). Activation using ^{n}BuLi required Schlenk techniques, due to the unstable nature of ^{n}BuLi and the facile degradation of boronate products **395** in air. Reasonable to good yields were obtained for all substrates except trimethylboronic ester **400**, in which only unreacted boronic ester starting material was returned. This is likely due to its lack of solubility in THF.

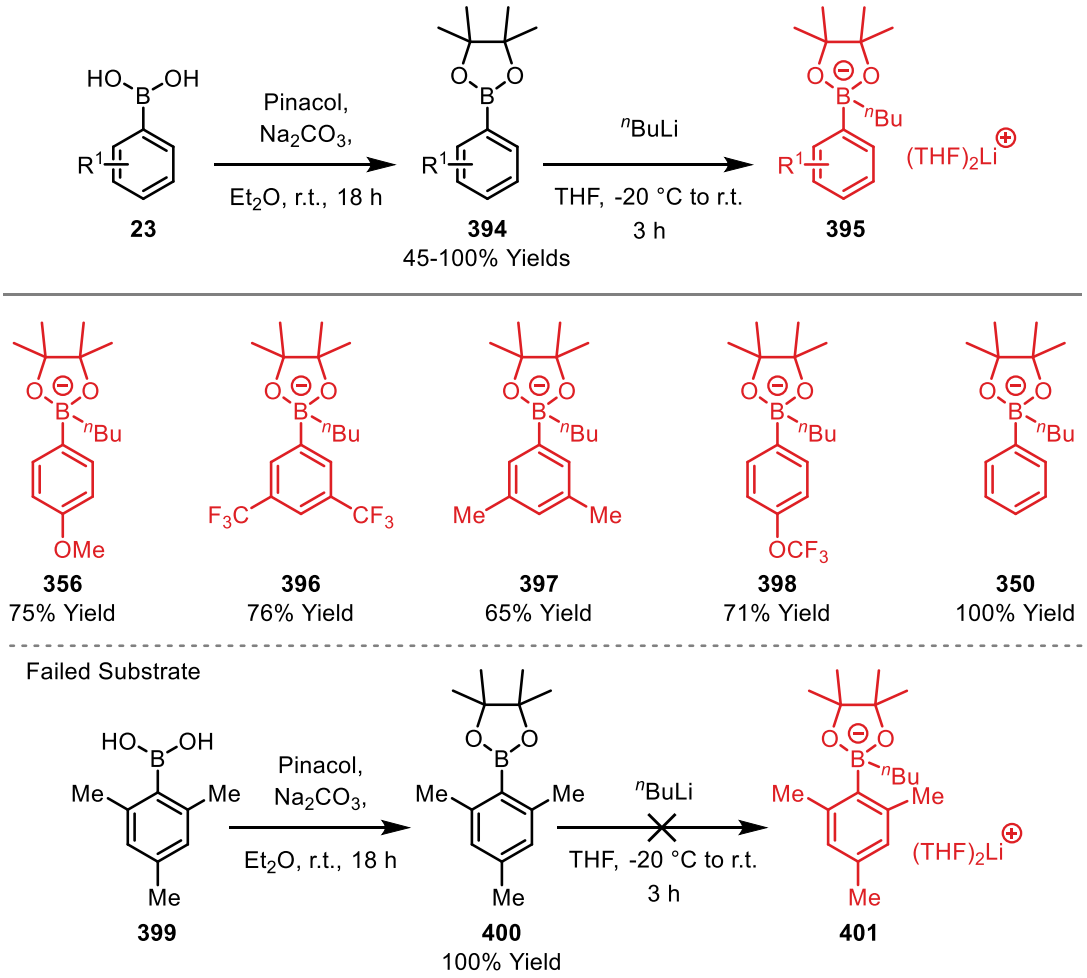

Table 20. *Synthesis of boronate coupling partners*

4.3.4. Probing the Tolerability of the Cross-Coupling to Alternative Boronate Coupling Partners

Boronate coupling partners **350** and **396-398** were applied to the established cross-coupling conditions (Table 21). Dimethyl-substituted **405** was isolated in 54% yield, a result that is similar to optimised *para*-methoxy **359**. Yields of 50% and 30% were obtained for electron-poor variants **403** and **404**, showing some tolerance for different electronic environments, and simple phenyl system **347** was formed in 36% yield. These results show promise given the complexity of the desired cross-coupling, which must occur at the expense of competing styrene formation in both the iodide formation and cross-coupling steps.

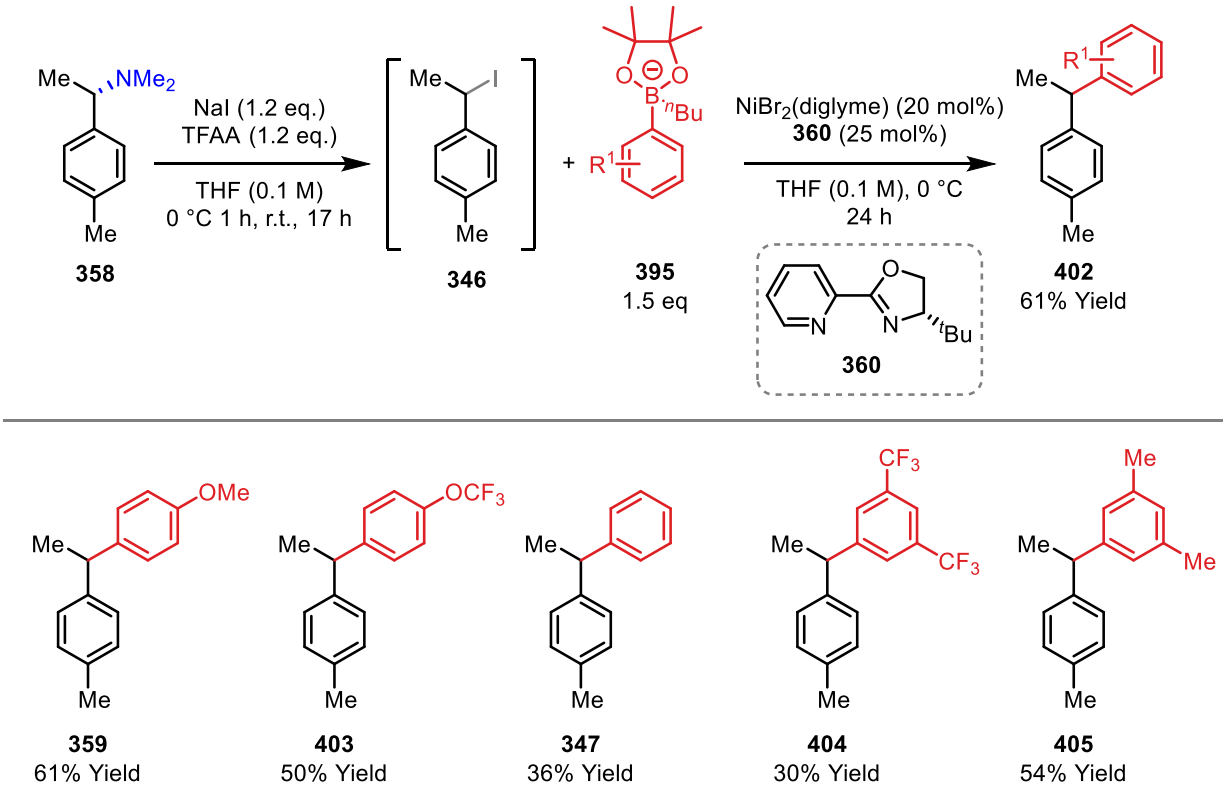

Table 21. *Tolerability of the cross-coupling protocol to boronate coupling partners*

4.4. Exploration of Alternative Conditions for the Cross-Coupling of α-Substituted Benzylamines

Though the established cross-coupling conditions maintained reasonably high yields for the complex 2-step transformation with respect to alternative boronate coupling partners **350**, and **396-398**, the poor yields and complex mixtures obtained when applying alternative benzylamine substrates **374-379**, **381**, **384**, and **387** were problematic (Table 18, Table 19, Scheme 90). Therefore, attention returned to literature examples of benzyl halide cross-couplings to determine whether the yields and poor reaction scope could be improved with different conditions.

In 2009, Carretero and colleagues reported the cross-coupling of α-methyl benzyl bromide **406** using Grignard **407** as the coupling partner (Scheme 91A).[139] This cross-coupling uses low metal and ligand loadings of 3 mol% ($Pd(CH_3CN)_2Cl_2$, Xantphos). The optimal reaction solvent here was THF, which would conveniently allow our THF solution of benzyl iodide **346** to be used directly under this strategy. Unfortunately, no product was seen upon application of benzylamine **358** to these conditions (Scheme 91B). Instead, 25% yield of styrene was observed and this procedure was not explored further. This cross-coupling may be hindered by the reaction of *N*,*N*-dimethyl-2,2,2-trifluoroacetamide **243** (generated as a by-product within the iodination protocol) with Grignard **407**, giving carbonyl addition products.[151] Future work could probe whether this reaction is effective with greater equivalents of Grignard **407** to overcome this side process.

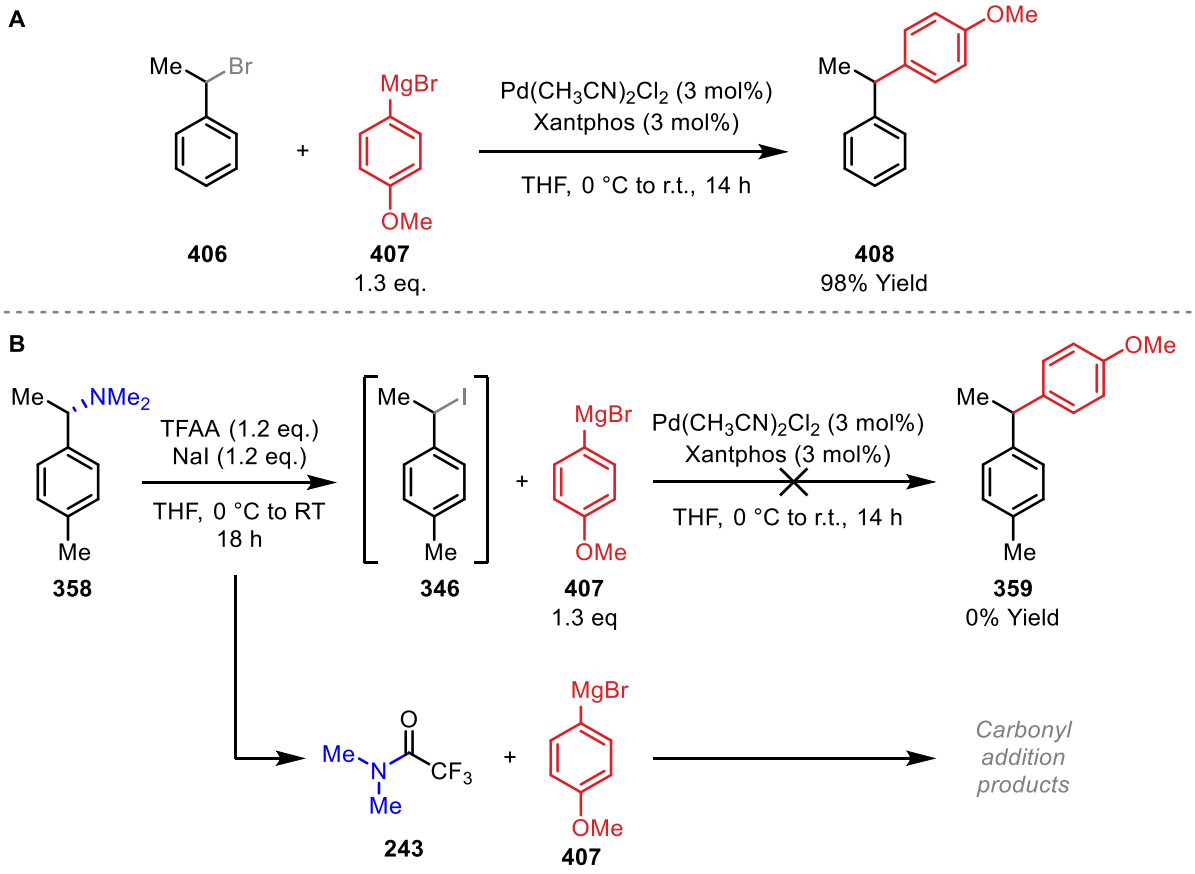

Scheme 91. *Application of benzylamine **358** to Carretero and co-workers' cross-coupling conditions*

Next, conditions reported by Zhang and co-workers for the reductive cross-coupling of α-methyl benzyl chloride **368** with aryl bromide **409** were investigated.[152] These conditions employed NiI_2 as the metal catalyst complex together with ligand **410**, reductant Zn, and additive KF (DMA, r.t.). A reasonably broad scope of electron-rich cross-coupling partners were demonstrated, with phenyl bromide coupling in 92% yield (Scheme 92A). Alternative conditions were required for electron-poor substrates. Zhang and co-workers suggest that Zn is required for the in situ formation of benzyl fluoride, which was theorised to be the active substrate. Applying the same conditions to benzyl iodide **346** gave a 2-step ^{1}H NMR yield of 40%, which demonstrates that this reductive cross-coupling shows great potential as an alternative method, if iodide formation can be improved (Scheme 92B).

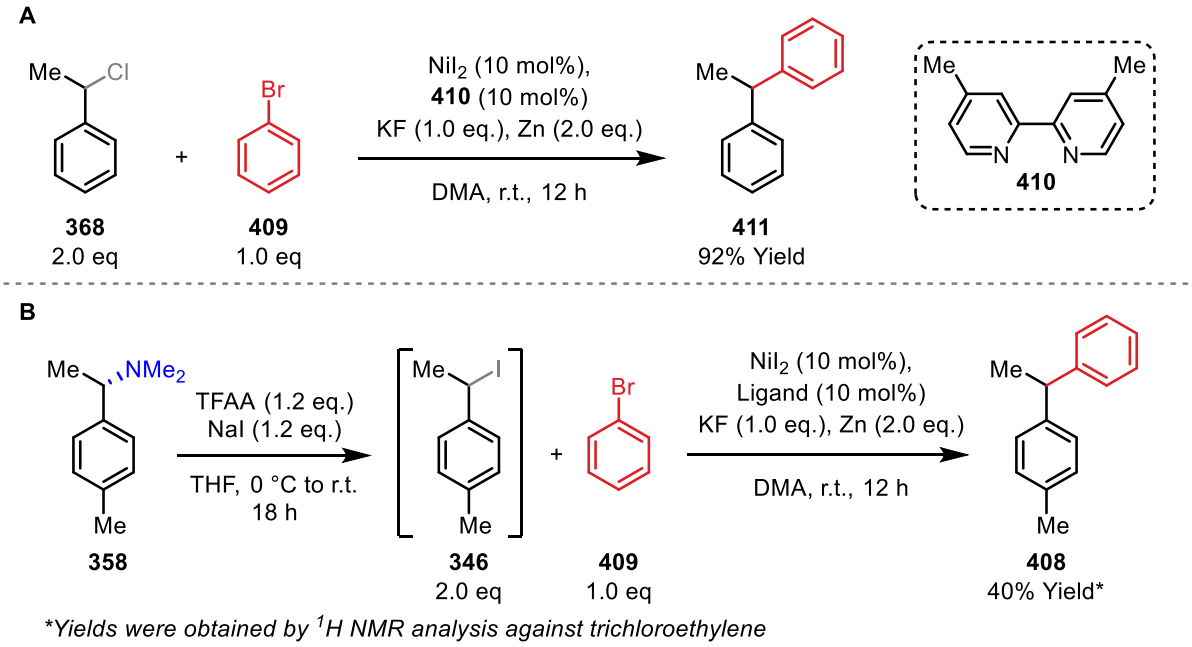

Scheme 92. *Application of benzylamine* ***358*** *to Zhang and co-workers' cross-coupling conditions*

4.5. Summary and Future Work

In this chapter, a new method for the activation of α-substituted benzylamines, via their conversion to α-substituted benzyl iodides, and subsequent cross-coupling is described. Since both steps suffer from competing styrene formation, the yields obtained for this 2-step method were lower than desired, and more work is required to optimise this cross-coupling. Future work will require improvements to the first step wherein the benzylamines are converted to their benzyl halides. This might involve the exploration of different halide salts, different reaction temperatures, and different reaction setups. Studies into the enantiospecificity of this iodination with isolable halide intermediates should also be carried out. Additionally, efforts to improve the scope to include α-CF_3 substrates should be undertaken, as fluorine-containing products are highly sought after in the medicinal chemistry industry (Scheme 93A).[153]

New methods for cross-coupling should be explored, including cross-electrophile couplings such as that described in Section 1.3.1.1. These reactions often take place at low temperatures, which may inhibit styrene formation. Use of boronate salts could also be explored further, with different metal complexes and ligands being used to alter the mode of oxidative addition away from SET. This aspect is potentially important because it could render the cross-coupling enantiospecific. For the conditions explored within this chapter, complete racemisation of the reacting centre was observed. This could be addressed in one of two ways: (1) the use of chiral ligands may allow enantioconvergent SET oxidative addition (Scheme 93B),[150,154] or (2) alteration of the benzyl iodide to another, more stable halide such

as bromide or chloride, may alter the oxidative addition pathway to a stereospecific variant (e.g. S_N2 oxidative addition; Scheme 93C).[155] In this instance, an enantiospecific S_N2 halogenation protocol must also be assured.

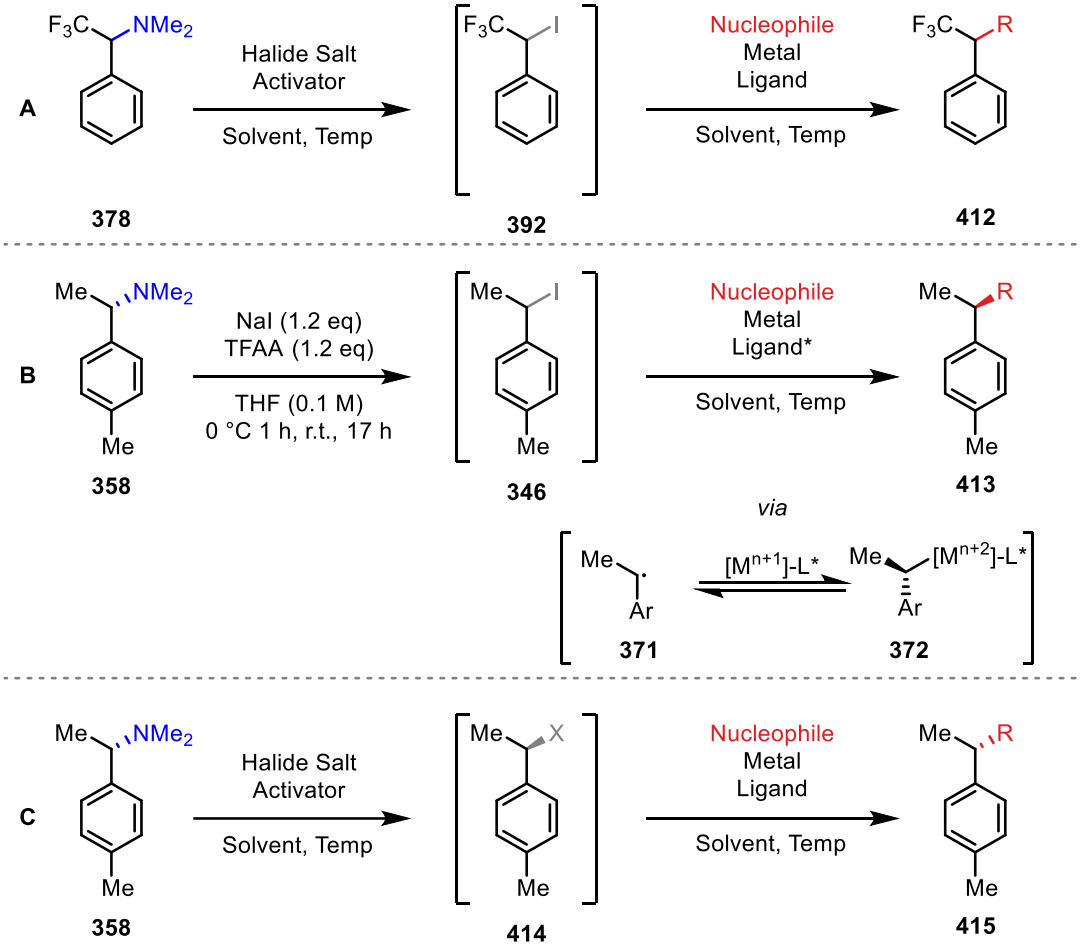

Scheme 93. *Future work on the cross-coupling of α-substituted benzylamines*

Chapter 5. Cyclic Amines and Ring Opening Reactions

Chapters 3 and 4 describe new methods for the cleavage and cross-coupling of benzylic C–N bonds of α-primary and α-secondary benzylamines. Within this chapter, studies are described that aim to extend the procedure to include the ring opening of strained and non-strained cyclic amines. Initial studies into the application of this chemistry to the ring opening of strained aziridines are discussed (Scheme 94A). This proposed reaction converts aziridines **71** into alkyl iodides **132**. The effect this ring opening has on the substrate is three-fold: (1) the cyclic geometry becomes linear, (2) a new C–I bond has formed, which potentially allows for further cross-coupling or nucleophilic substitution, and (3) a new amide functionality is introduced. The diverse new reactivity formed within a single reaction step suggests that this ring opening may be highly effective for the late-stage functionalisation of drug molecules and natural products. Procedures for iodide cross-coupling or nucleophilic substitutions are proposed to give structures **133** and **134**, respectively. Second, and in a similar manner, the proposed ring opening of 2-aryl pyrrolidines **135** to give intermediates **136** is demonstrated (Scheme 94B). For both processes, the cyclic amine starting material becomes a conjunctive component of the targets (**133**, **134**, and **137**).

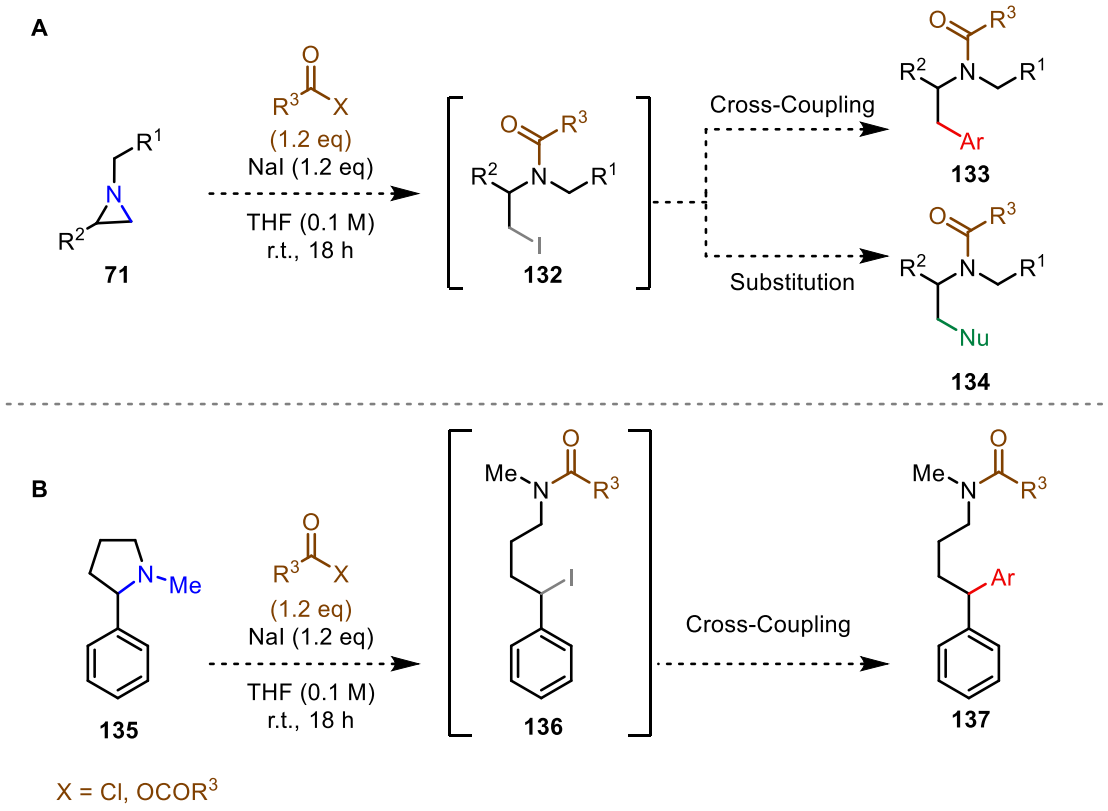

Scheme 94. *Proposed ring opening of aziridines **71** and 2-aryl pyrrolidines **135***

5.1. Ring Openings of Strained Cyclic Amines

5.1.1. Established Protocols for the Ring Opening of Strained Cyclic Amines

Due to the strained nature of aziridine rings, it was proposed that effective ring opening may be achieved using TFAA-promoted C–N cleavage, as utilised within Chapters 3 and 4. Existing methods for the ring opening of aziridines are elaborated in Section 1.4 and are typically carried out either (1) by oxidative addition of a transition metal (usually nickel) into the strained C–N bond (Scheme 95A),[48,156,157] (2) by coordination of an activator and subsequent nucleophilic attack (Scheme 95B),[158–160,161] or (3) by use of an *N*-bound electron withdrawing group and subsequent nucleophilic attack (Scheme 95C).[162] One example of the former was reported by Doyle and co-workers, who demonstrated a nickel-catalysed ring opening from the sterically hindered quaternary centre of **416** ($Ni(acac)_2$, Fro-DO, ^{n}BuZnBr, DMA, r.t.).[48] The proposed mechanism commences with insertion of the metal into the C–N bond to give metallocyclobutane **417**, which may undergo further interactions with the organozinc coupling partner to give product **418** in 68% yield. This procedure is limited to substrates containing aromatic substitution on the aziridine ring, likely due to the increased lability of the benzylic C–N bond; this lability also offers high regioselectivity for this transformation. One example of a two-step activator-promoted nucleophilic attack was reported by Xu and Wu in 2022, who demonstrated the use of 1,2,3-thiodiazoles **419** and aziridines **420** for the synthesis of thiazolines **423** (K_2CO_3, DMF, MW 130 °C) (Scheme 95B).[159] This protocol proceeds via thioketene intermediate **421**, which reacts with aziridine **420** to give species **422**, in advance of an intramolecular ring-opening. This protocol is limited by high reaction temperatures (130 °C), and requires a microwave reactor. The use of *N*-bound electron-withdrawing groups together with a nucleophile was exploited by Nenajdenko and co-workers in 2001, who demonstrated that the use of *N*-tosyl aziridines such as **424** may undergo ring opening with Grignard reagents to form products such as **425** (PhMgBr, CuI, THF, -78 °C to r.t., 1 h) (Scheme 95C).[163] Unfortunately, this protocol suffers from a lack of regiocontrol, even with use of bulky isopropyl substituents, and requires low reaction temperatures (-78 °C).

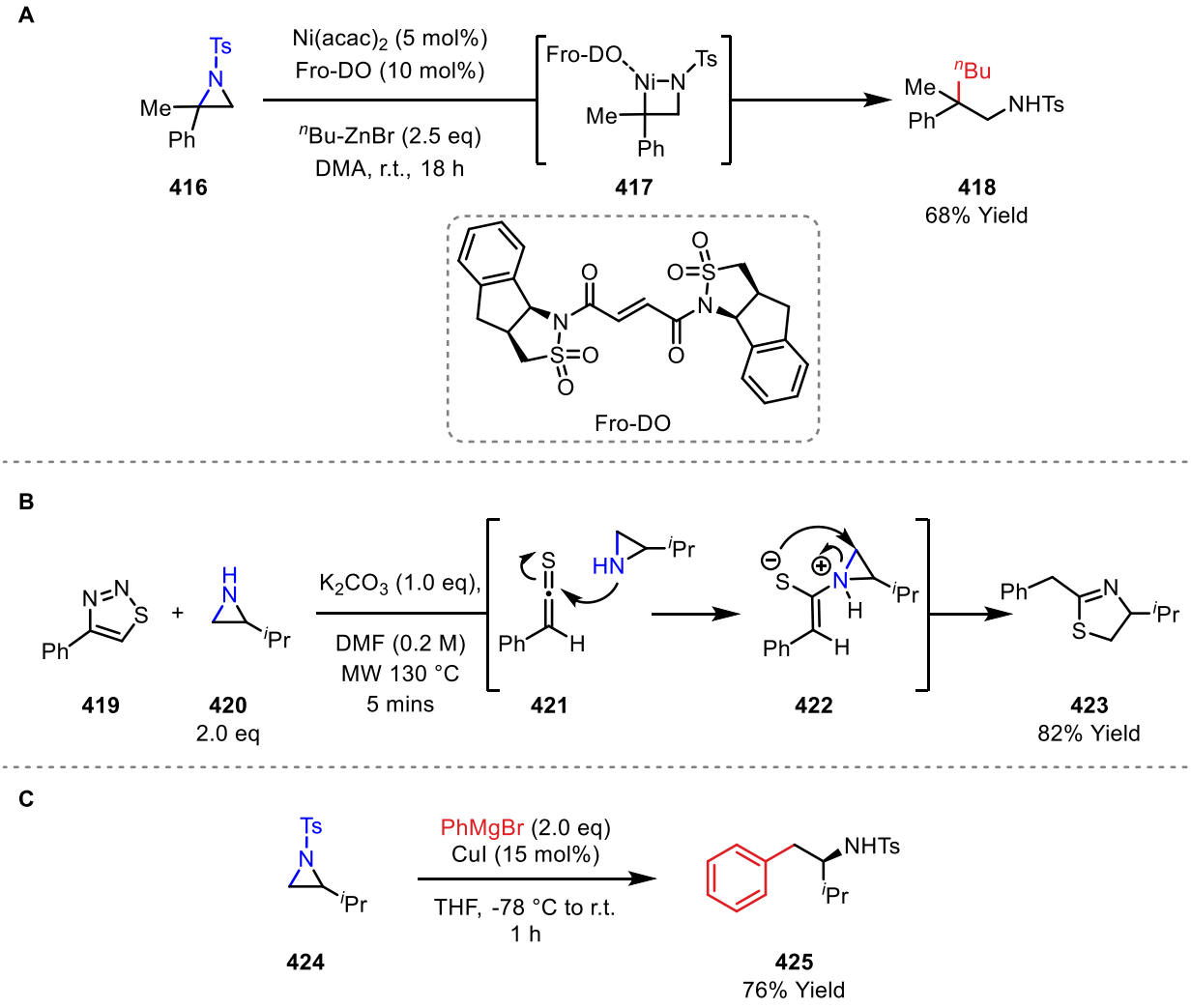

Scheme 95. *Established procedures for the ring opening of aziridines*

Chloroformate reagents have also been employed as activators for the nucleophilic ring opening of aziridines. In 1997, Shipman and co-workers reported the successful ring opening of methyleneaziridines **426** by reaction with chloroformates **427** (DCM, r.t., 24 h) (Scheme 96A).[161] A limited scope of substrates containing different *N*-substituents was demonstrated, though all contained the same aziridine backbone as **426**, with the methylene unit enhancing the strain of the system. In 2012, de Kimpe and co-workers demonstrated that a similar protocol could be used for the ring opening of azetidines **429**, forming methyl carbamates **430** (**427**, DCM, 40 °C, 4 h). It was also demonstrated that the carbamate products are effective precursors for the ring-closing formation of oxazinanones **431** (DMF, 140 °C, 30 mins, microwave reactor) (Scheme 96B).[164] The scope demonstrated for this protocol was limited to various substitutions on the *N*-benzyl group. These limitations suggest that improved methods for the ring opening of aziridines and azetidines are desirable. In particular, and as in previous chapters, a protocol that is efficient enough to be telescoped with a subsequent cross-coupling step was deemed desirable.

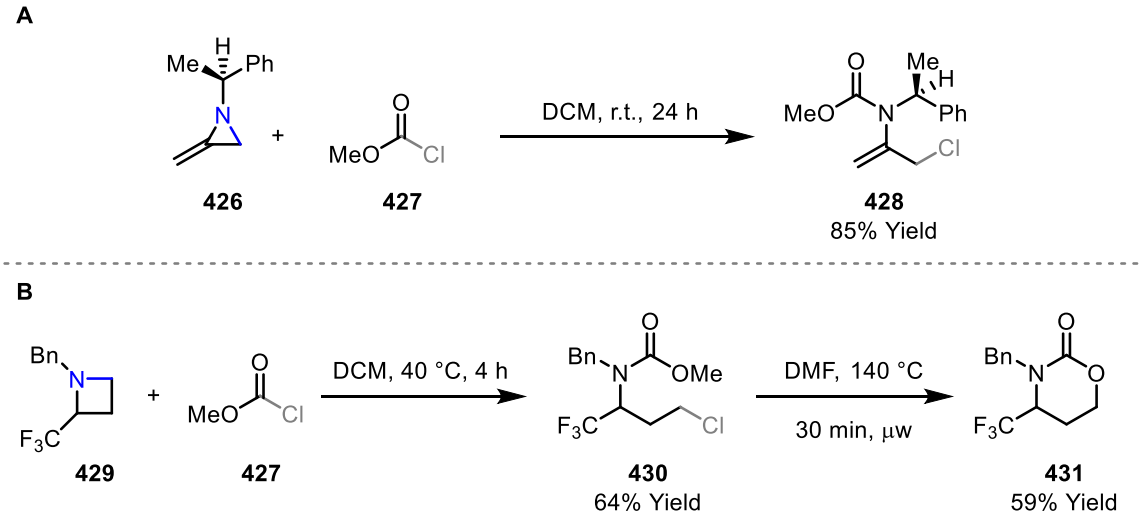

Scheme 96. *Chloroformate activators for the ring opening of strained cyclic amines*

5.1.2. Synthesis of Aziridine Substrates

To probe whether the TFAA-promoted C–N cleavage protocol is effective for aziridine substrates, benzyl-substituted aziridine **436** was synthesised over three steps (Scheme 97A). First, the amide coupling of L-phenylalanine derivative **432** and acyl chloride **433** (DIPEA, DCM, 0 °C to r.t.) formed amide **434** in excellent yield. Subsequent reduction of the ester and amide groups ($LiAlH_4$, THF, 70 °C) provided alcohol **435** in a quantitative yield. High temperatures were required for this reduction due to the stability of the amide group. A modified Wenker reaction was then employed for the synthesis of aziridine **436** (chlorosulfonic acid, toluene, 0 °C to r.t.; NaOH, 120 °C), which was generated in 52% isolated yield. Due to the instability of the aziridine, some product was likely lost during purification. The mechanism for the Wenker reaction is outlined in Scheme 97B.

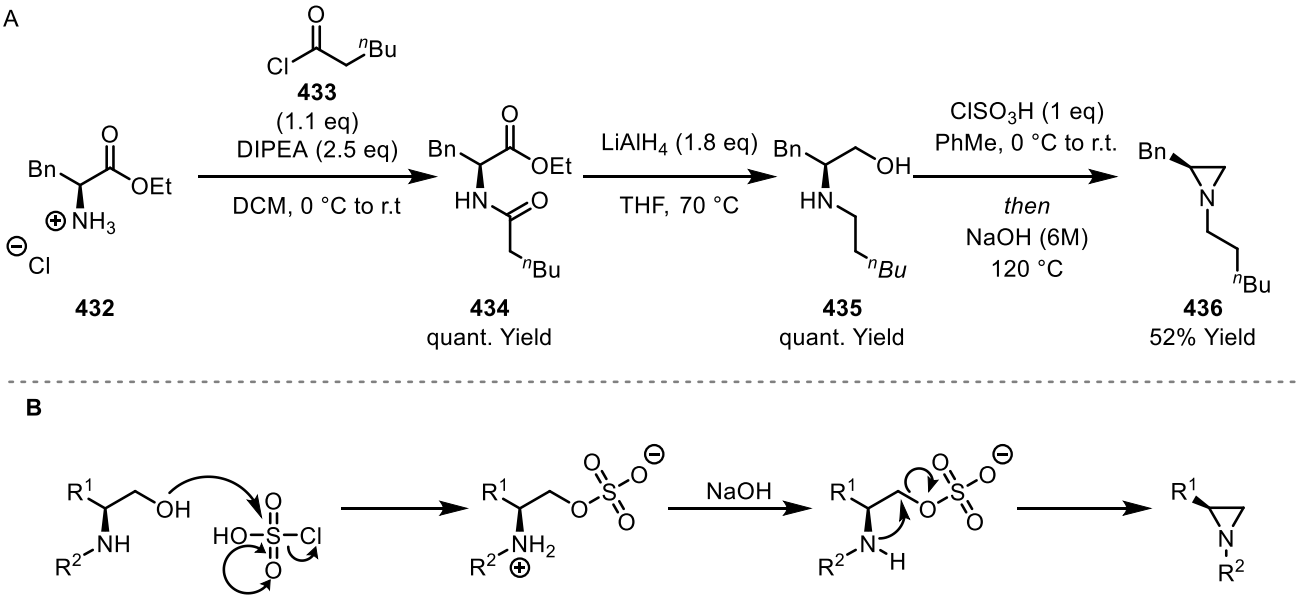

Scheme 97. *Synthesis of aziridine* ***436***

5.1.3. Exploring the Viability of the Proposed Aziridine Ring Opening Procedure

When aziridine **436** was applied to the established C–N cleavage conditions shown in Scheme 98A, expected product **437** was not observed. MSci student Joshua Thomson investigated further, determining that the major product for this reaction was structural isomer **440**. It was hypothesised that this product was formed via the mechanism outlined in Scheme 98B. Following polarisation of the C–N bond by TFAA, the tethered phenyl group of **438** attacks the electrophilic carbon atom, breaking the aziridine C–N bond to form phenonium ion **439**. It is postulated that phenonium ion formation is faster than the desired iodide attack because the former is intramolecular. Product **440** can then be generated by attack of iodide onto phenonium ion **439**, breaking open the 3-membered ring and restoring aromaticity. The successful ring opening of this aziridine demonstrates that TFAA/NaI is an effective activator for the cleavage of aziridine C–N bonds. For the purpose of further studies, the synthesis of an alternative aziridine without the alkyl-tethered benzyl group should be completed, because this would obviate competing phenonium ion formation during ring opening.

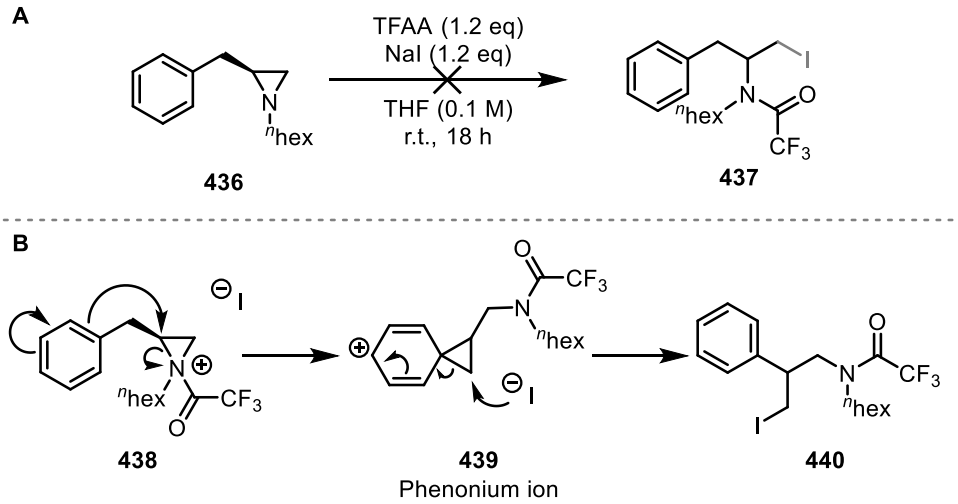

Scheme 98. *Studies into the ring opening of aziridines by use of TFAA/NaI*

5.1.4. Aziridine Ring Opening Summary and Future work

Aziridine **436** has been synthesised and applied to C–N cleavage conditions, with successful ring opening occurring via an unusual intramolecular phenonium ion mediated pathway. Future work within this project may focus on synthesising alternative aziridine targets and applying them to the same reaction conditions. Following this, optimisation of the ring opening and development of conditions for subsequent cross-coupling and nucleophilic substitutions should be explored (Scheme 99).

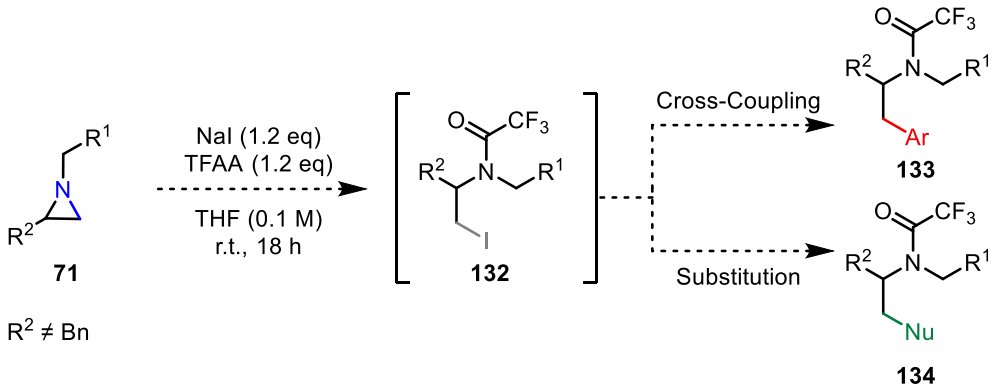

Scheme 99. *Proposed future work for the ring opening of aziridine substrates*

5.2. Pyrrolidine Ring Opening

5.2.1. Established Protocols for the Ring Opening of Non-Strained Cyclic Amines

As explored in Section 1.5, three general methods are typically employed for the ring opening of non-strained cyclic amines: (1) reductive cleavage, (2) oxidative cleavage, and (3) von Braun type cleavage.[57] The last of these is relevant to this project. Von Braun cleavage utilises cyanogen bromide (BrCN) in the ring-opening of cyclic amines such as piperidine **441** (DCM, r.t.) (Scheme 100A).[165–167] The scope of this ring opening is limited to benzylic piperidines and fused ring systems. In this procedure, cyanide acts as the activator, coordinating to the nitrogen atom and polarising the C–N bond. This facilitates attack of bromide anion at the benzylic carbon of intermediate **442**, opening the piperidine ring and generating linear product **443**. Cyanogen bromide is highly toxic, and may undergo explosive trimerisation to cyanuric bromide, or decompose to dangerous hydrogen cyanide, making it an undesirable reagent.[168]

An alternative method for the ring opening of non-strained cyclic amines was reported by Cho and co-workers, in which the ring-opening of pyrrolidines **444** was achieved using chloroformate reagents **445** (DCM, r.t., 2 h) (Scheme 100B).[169] This promising advancement allows the cleavage of various *N*-alkyl pyrrolidine rings, though scope expansion to larger ring sizes or alternative *N*-substitutions was not reported. The proposed mechanism for this transformation is similar to that of the von Braun procedure, with the chloroformate activator polarising the C–N bond of **446** via acylation, and the chloride anion acting as the ring-opening nucleophile. However, as discussed in Section 3.1.1, chloroformates are also toxic reagents, and their diversity is limited, providing poor synthetic flexibility.

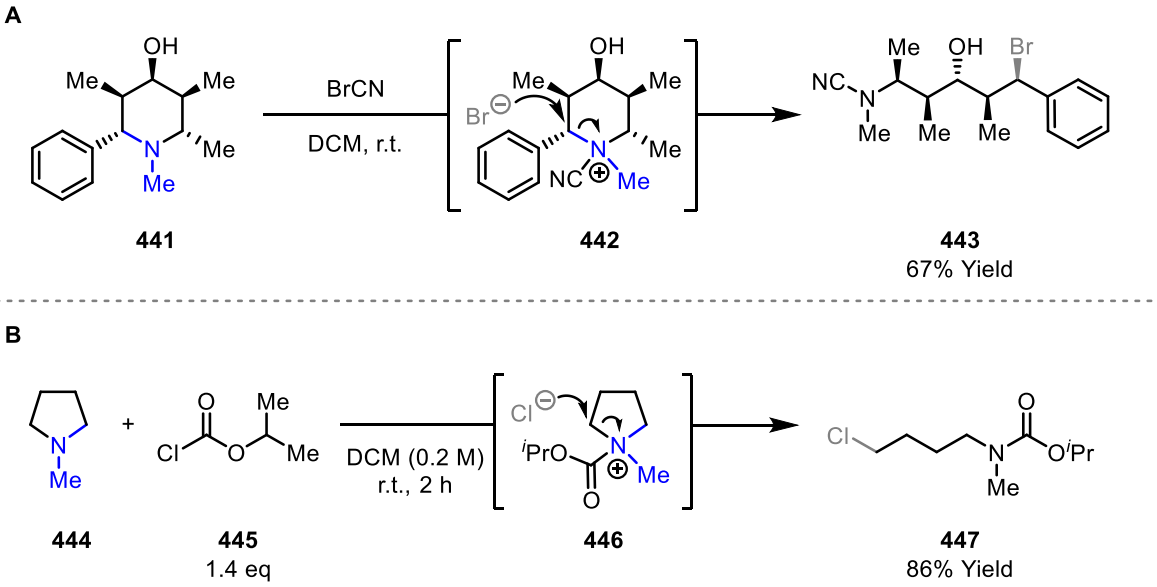

Scheme 100. *Established methods for the ring-opening of non-strained cyclic amines*

5.2.2. Synthesis of 2-Aryl Pyrrolidine

It was proposed that the previously demonstrated TFAA/NaI system may promote the effective ring opening of non-strained 2-aryl pyrrolidines. To evaluate the viability of this proposal, *N*-methyl system **135** was synthesised from commercially available 2-aryl pyrrolidine **448**. This was achieved utilising Eschweiler-Clark conditions with formic acid and formaldehyde, and reaction times of 2 days (100 °C), as previously discussed in Section 4.2.1. Following purification by FCC, product **135** was obtained in 97% yield.

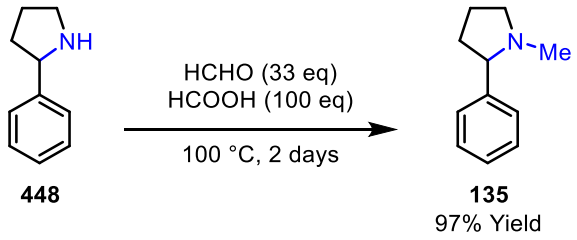

Scheme 101. *Synthesis of 2-aryl pyrrolidine substrate **135***

5.2.3. Optimisation of the 2-Aryl Pyrrolidine Ring Opening

Applying 2-aryl pyrrolidine **135** to the optimised iodination conditions outlined in Section 4.2.4 (NaI (1.2 eq), TFAA (1.2 eq), THF (0.1 M), 0 °C to r.t., 18 h) provided a 1:1 ratio of iodide **449** (circled in grey) and alkene **450** (circled in brown), as determined by ^{1}H NMR analysis (Scheme 102). While ring opening to **449** was promising, the lack of selectivity for **449** vs **450** was undesirable. Substrate

135 was therefore adopted for further optimisation studies to determine (1) if the selectivity for the formation of iodide **449** over alkene **450** could be improved, and (2) whether activators other than TFAA may be suitable for this transformation, as this would improve the scope of accessible products.

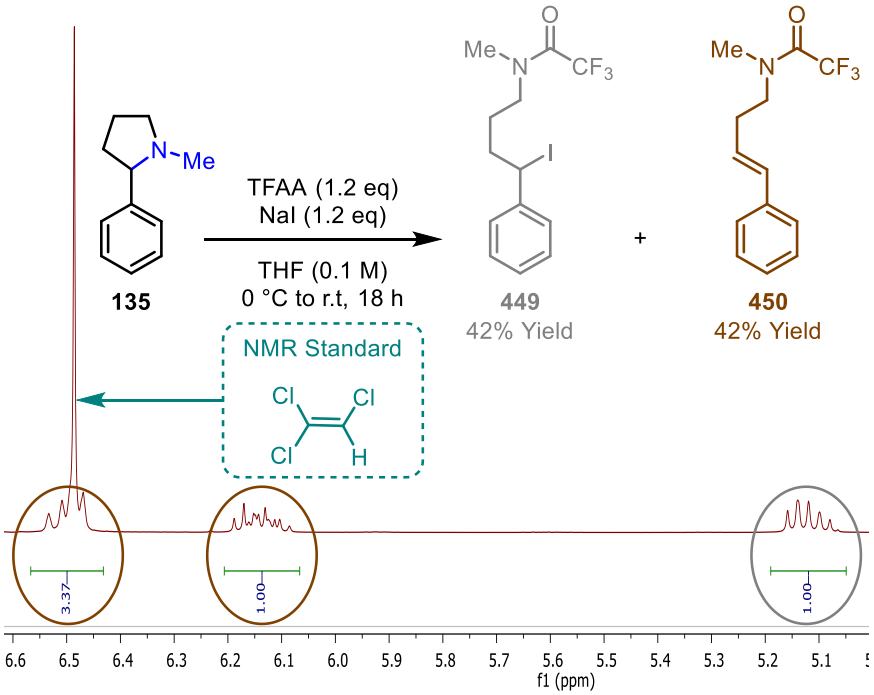

Scheme 102. *Initial 2-aryl pyrrolidine ring opening studies*

The proposed mechanism for this transformation is shown in Scheme 103B. First, TFAA reacts with sodium iodide to give highly electrophilic acyl iodide **230**, as described in Section 3.1.3. The nitrogen atom of 2-aryl pyrrolidine **135** then attacks acyl iodide **230** to provide *N*-acyl ammonium salt **451**. Iodide anion may then attack at the benzyl position of **451**, generating desired iodide **449** in an S_N1 or S_N2 reaction (Scheme 103B; grey arrows). However, E1 or E2 elimination may also occur, leading to the formation of alkene **450** (Scheme 103B; brown arrows). Additionally, it was observed that the ratio of iodide **449**: alkene **450** increased upon attempts to purify by FCC. This suggests that elimination of iodide **449** can also lead to alkene **450**.

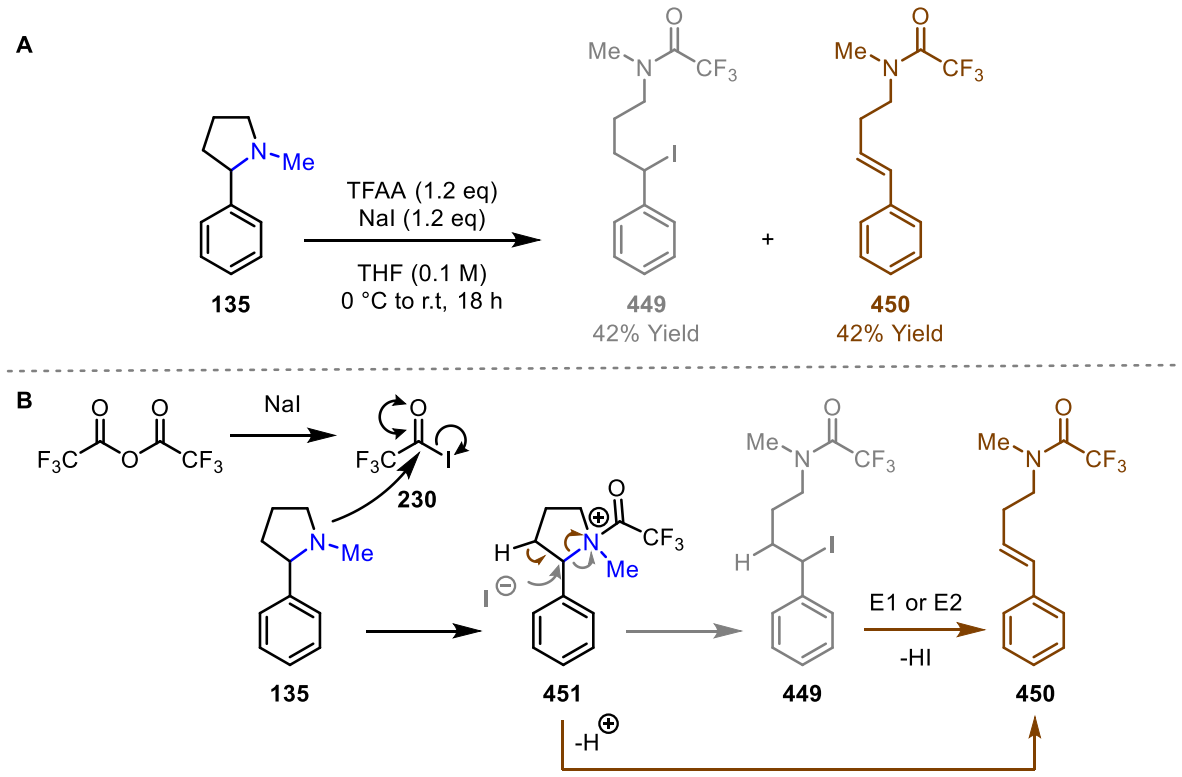

Scheme 103. *Initial 2-aryl pyrrolidine ring opening and a proposed mechanism*

With the goal of improving both the yield and selectivity of this transformation, various alterations to the established reaction conditions were explored (Table 22). It was considered that the labile nature of the benzylic C–I bond of **452a** may facilitate formation of alkene **450**, so use of sodium bromide in place of sodium iodide was trialled (Entry 2). Gratifyingly, improvements in both the yield of **452** formation and the ratio of **452**:**450** were observed. It was also noted that while use of sodium iodide leads to the formation of benzylic iodide **452a**, when sodium bromide was employed as the salt, benzylic acetate **452b** formed instead of the desired benzyl halide. While benzyl halide formation was predominantly desired, benzylic acetates are highly versatile intermediates which can undergo hydrolysis to alcohols and also participate in cross-couplings.[170–174] Therefore, optimisation for the formation of acetate **452b** was continued. Increasing the equivalents of sodium bromide from 1.2 to 2.5, as well as increasing the reaction concentration to 0.2 M gave a notable increase in yield from 53% to 61% (Entry 3). Trialling sodium iodide in these new conditions gave a lower yield of 46% and higher quantities of alkene **450** (Entry 4). Next, the optimal solvent for this ring opening was established (Entries 5-7), with 2-MeTHF providing the highest ^{1}H NMR yield of 68%. Investigations into the reaction temperature (Entries 8-9) proved that 50 °C was superior, giving product **452** in 76% yield. Further studies evaluated reaction times, alternative halide salts, and a broader range of solvents, though any alteration from the conditions in entry 9 proved detrimental (Table SI:4). Subsequent investigation carried out by Peter Ledwith examined the ring opening without sodium bromide, providing acetate

452b in 76% yield, with just 14% yield of alkene **450** (Entry 10). This suggests that, in the presence of trifluoroacetate, the bromide anion is not competitive for C–N bond cleavage.

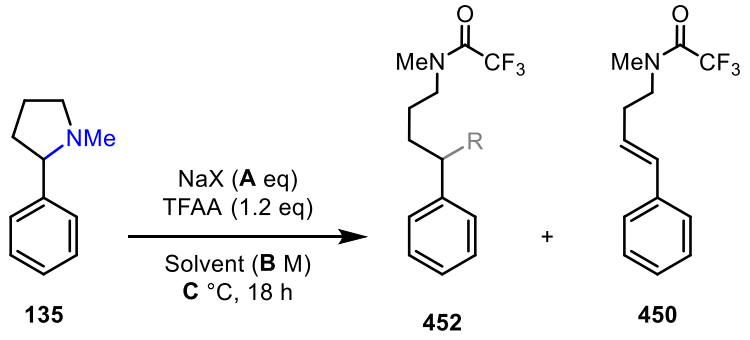

Entry	NaX	A	Solvent	B	Temp	Yield 452	Yield 450
1	NaI	1.2	THF	0.1	0 °C to r.t.	42%[a]	42%
2	NaBr	1.2	THF	0.1	0 °C to r.t.	53%[b]	14%
3	NaBr	2.5	THF	0.2	0 °C to r.t.	61%[b]	17%
4	NaI	2.5	THF	0.2	0 °C to r.t.	46%[a]	22%
5	NaBr	2.5	Et_2O	0.2	0 °C to r.t.	66%[b]	17%
6	NaBr	2.5	MeCN	0.2	0 °C to r.t.	40%[b]	15%
7	NaBr	2.5	2-MeTHF	0.2	0 °C to r.t.	68%[b]	17%
8	NaBr	2.5	2-MeTHF	0.2	40 °C	52%[b]	18%
9	NaBr	2.5	2-MeTHF	0.2	50 °C	76%[b]	23%
10*	-	-	THF	0.1	r.t.	76%[b]	14%

Table 22. *Optimisation of 2-aryl pyrrolidine ring opening conditions*

**This reaction was carried out by Peter Ledwith*

5.2.4. Exploring the Tolerability of Alternative Activators for Pyrrolidine Ring Opening

Exploration of the scope of the ring opening commenced with trials of various activators in place of TFAA. As the activator remains tethered to final compound **453**, the use of different activators is a key aspect of scope expansion. Furthermore, it was theorised that employing acyl chloride activators in place of an anhydride would eliminate any acetate formation in favour of benzylic bromide formation. As shown in Scheme 104, three different acyl chloride activators were trialled. Of these, acetyl chloride was most promising, providing target bromide **455** in 71% ^{1}H NMR yield, with a 16% ^{1}H NMR yield of alkene **456**. Unfortunately, separation of **455** and **456** by FCC proved challenging. Use of benzoyl chloride provided product **457** alongside alkene **458**, but accurate yields were not easily determined due to the complex mixture generated. Instead, key peaks were identified by low temperature ^{1}H NMR analysis of a partially purified mixture, which gave a bromide: alkene ratio of 0.34:1 (this ratio could not be accurately determined from the crude mixture). Finally, when using acryloyl chloride, definitive

evidence for the formation of bromide **459** could not be obtained, but alkene **460** was isolated in 19% yield. These preliminary results demonstrate that the ring opening of 2-aryl pyrrolidine **135** is possible using different activators, though further work is required to explore the breadth, and to improve the yields and selectivity.

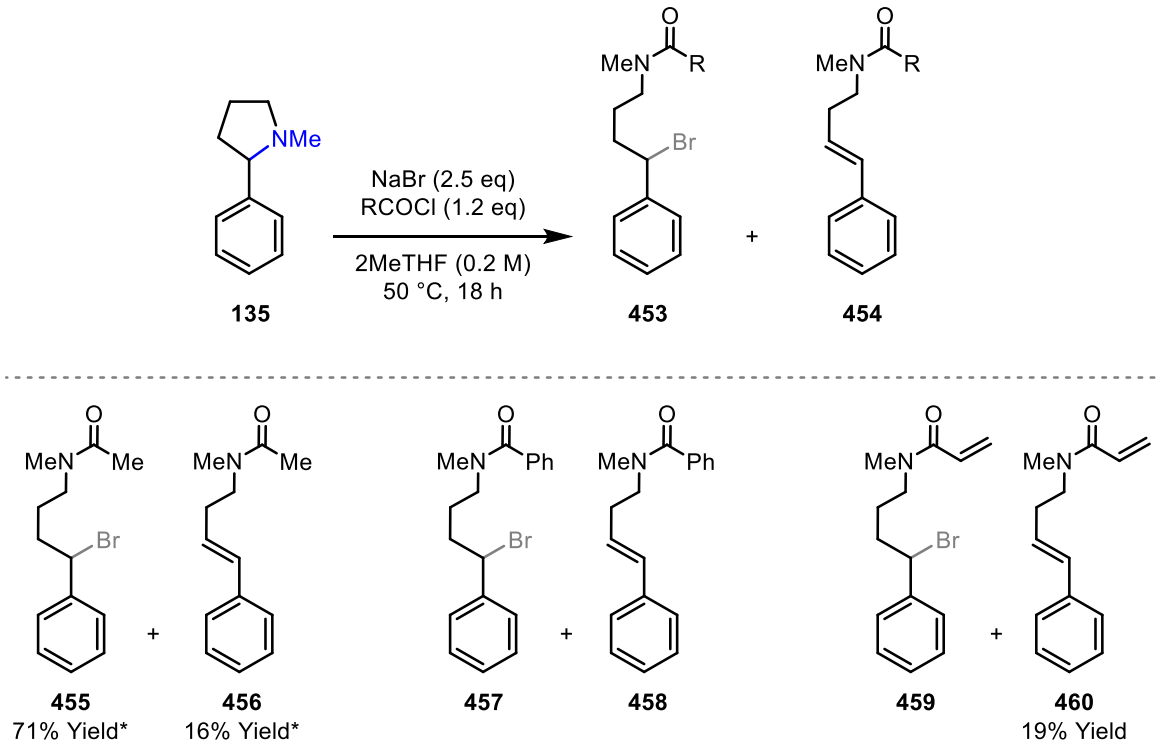

Scheme 104. *Alternate activators trialled within the ring opening of 2-aryl pyrrolidine* ***135***

5.2.5. Exploring Alternative Unstrained Rings Within the Established Ring-Opening Protocol

Tetrahydrofuran substrate **463** and pyrrolidine **466** were synthesised to determine whether the 2-aryl pyrrolidine ring opening protocol could be applied to cyclic ethers or non-benzylic pyrrolidines. The two-step synthesis of benzofuran **463** commenced with reduction of the ketone and carboxylic acid of commercially available **461** ($LiAlH_4$, Et_2O, r.t.) to provide diol **462** in 71% yield following FCC. A subsequent cyclodehydration was then employed (NEt_3, $P(OEt)_3$, I_2, DCM, -78 °C to r.t.) to give tetrahydrofuran **463** in 94% yield (Scheme 105A).[175] Pyrrolidine **466** was synthesised in one step and 37% yield from amine **464** via double *N*-alkylation with dibromide **465** (K_2CO_3, MeCN, 90 °C) (Scheme 105B).

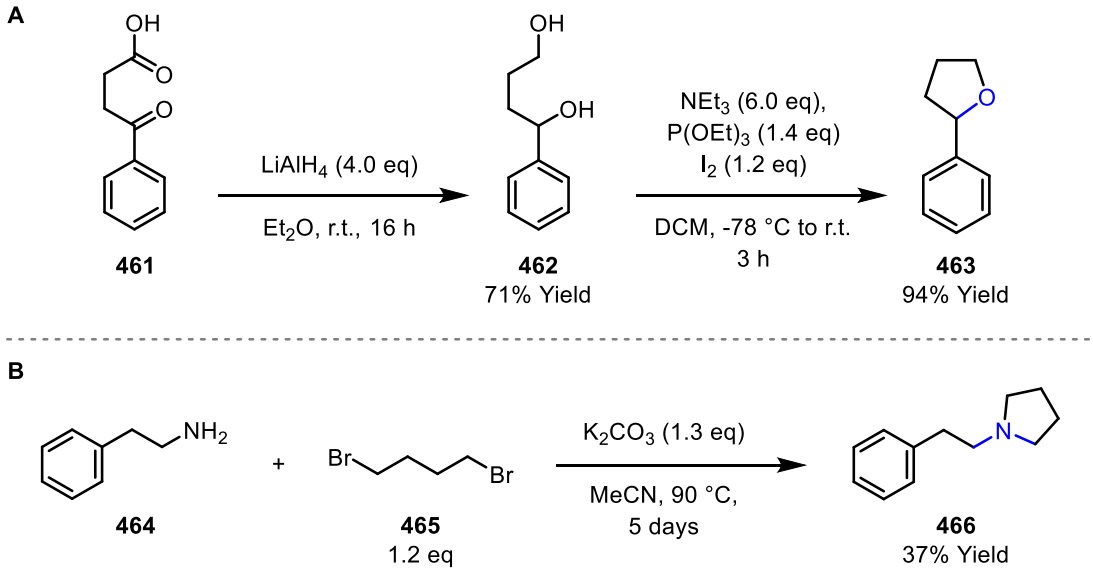

Scheme 105. *Synthesis of alternative cyclic substrates*

When tetrahydrofuran **463** was applied to the optimised ring opening conditions described in Table 22, only starting material was returned (Scheme 106A). This suggests that any coordination to oxygen by the TFAA activator does not weaken the C–O bond sufficiently to promote bond cleavage by bromide anion or carboxylate. An alternative explanation is that TFAA is not electrophilic enough to coordinate to the oxygen centre. The use of TFAA/NaI may be effective for this ring opening, because trifluoroacetyl iodide is expected to be a much more electrophilic acylating agent and iodide is a better nucleophile. Similarly, no ring opening was seen when pyrrolidine substrate **466** was applied to the same conditions. Instead, only the TFA salt of **466** was formed (Structure **469**). This is likely generated during work-up or handling due to adventitious water hydrolysing unreacted TFAA into TFA.

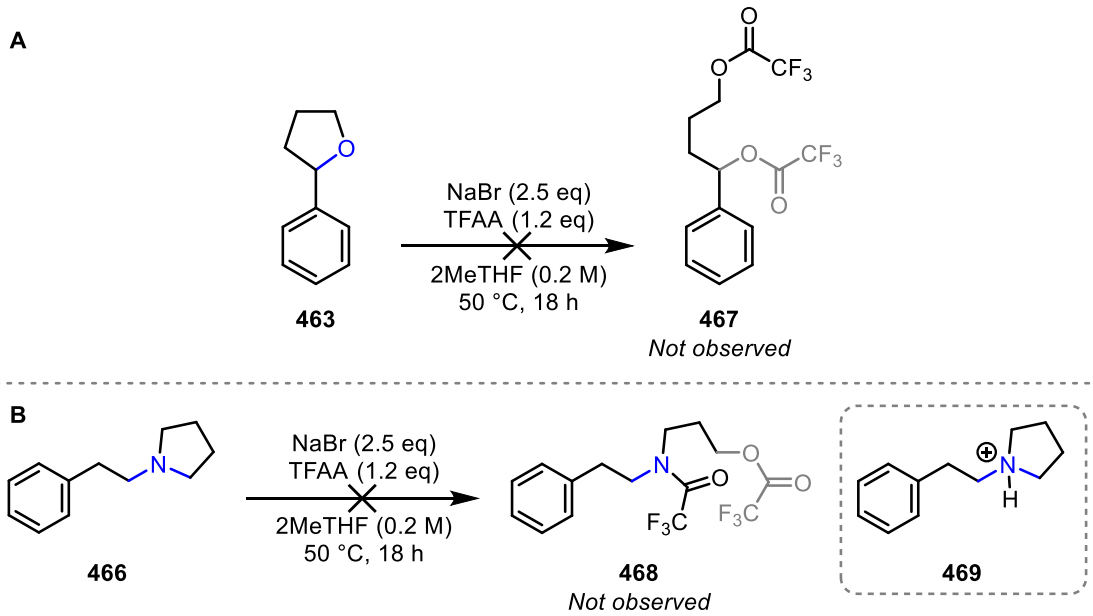

Scheme 106. *Probing the tolerability of alternative cyclic substrates to the established ring opening*

5.2.6. Ongoing Advancements into the Selective Formation of Bromide Intermediates

While benzylic esters are highly versatile reagents, their utility as intermediates within a 2-step cross-coupling protocol is notably lower than that of benzylic halides. Therefore, subsequent work carried out by PhD student Peter Ledwith has examined whether conditions for the formation of bromide **470** may be developed. Early investigations have determined that use of LiBr (3.0 eq) together with higher equivalents of TFAA (2.0 eq) gives bromide product **470** in 60% yield, with alkene **450** forming in 27% yield, and with no formation of acetate **471** (THF, r.t., 24 h) (Scheme 107A). This improved yield is likely the result of the greater solubility of LiBr (vs NaBr) in 2-MeTHF. Further optimisation studies are ongoing. Probing the viability of this generated bromide into a cross-coupling protocol was also carried out by Peter Ledwith, who demonstrated that applying bromide **470** to the optimised cross-coupling conditions developed within Chapter 4 (Section 4.2.4) gives product **472** with an isolated yield of 70%. This indicates the viability of these cyclic pyrrolidine substrates within a two-step one-pot cross-coupling protocol.

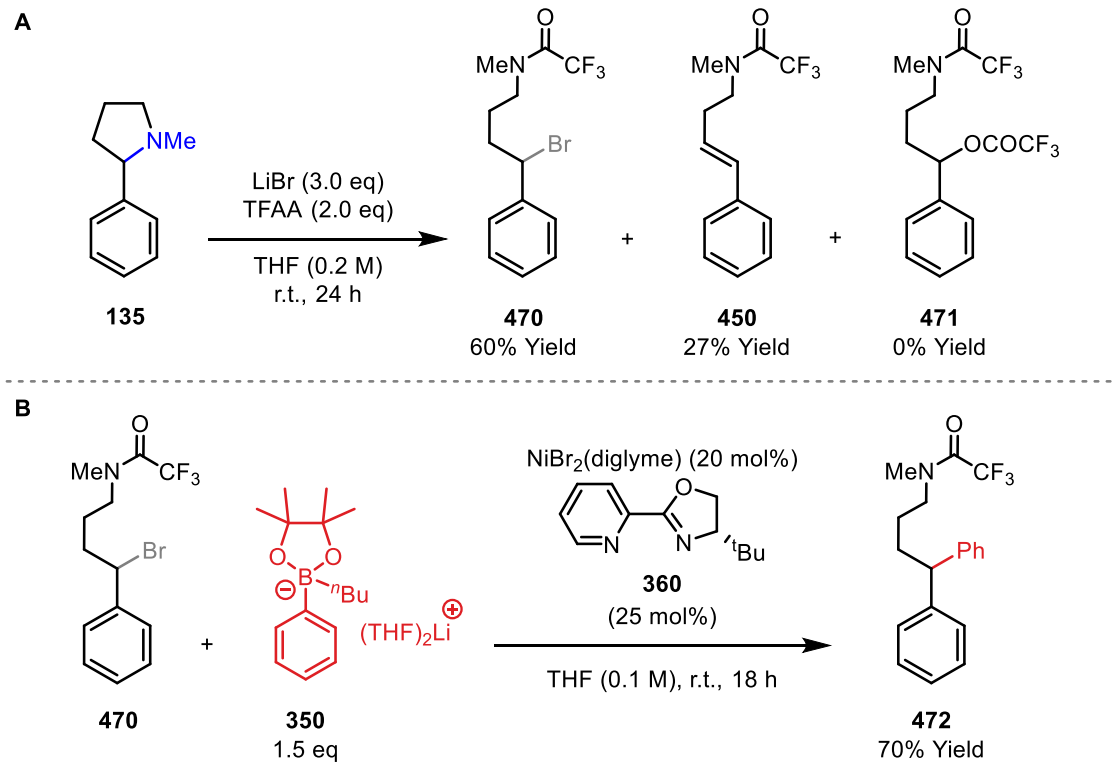

Scheme 107. *Advancements into the selective formation of bromide* ***470*** *and its subsequent cross-coupling*

This work was carried out by Peter Ledwith

5.2.7. Pyrrolidine Ring Opening Summary and Future work

A new method for the ring opening of 2-aryl pyrrolidine **135** using acetyl chloride and sodium bromide has been developed, with some tolerability for different acyl chloride and anhydride activators. The competing formation of alkene side products was observed, but conditions have been developed that minimise this. It was also observed that using TFAA/NaBr results in the formation of a benzylic acetate in favour of a benzylic bromide, and that this is suppressed when acyl chloride activators are used, or when LiBr is employed. Application of the conditions to a representative 2-aryl tetrahydrofuran and a non-arylated pyrrolidine were unsuccessful, and no ring opening was observed. Therefore, further work is required to complete optimisation of the formation of bromides **453** and to expand the scope of this ring opening protocol. Given the reasonable success of the ring opening of 2-aryl pyrrolidine **135**, future work should also focus on optimising an effective telescoped two-step procedure for ring opening and subsequent cross-coupling or nucleophilic substitution. This would allow the one pot conversion of 2-arylated pyrrolidines to products of type **137** or **473**.

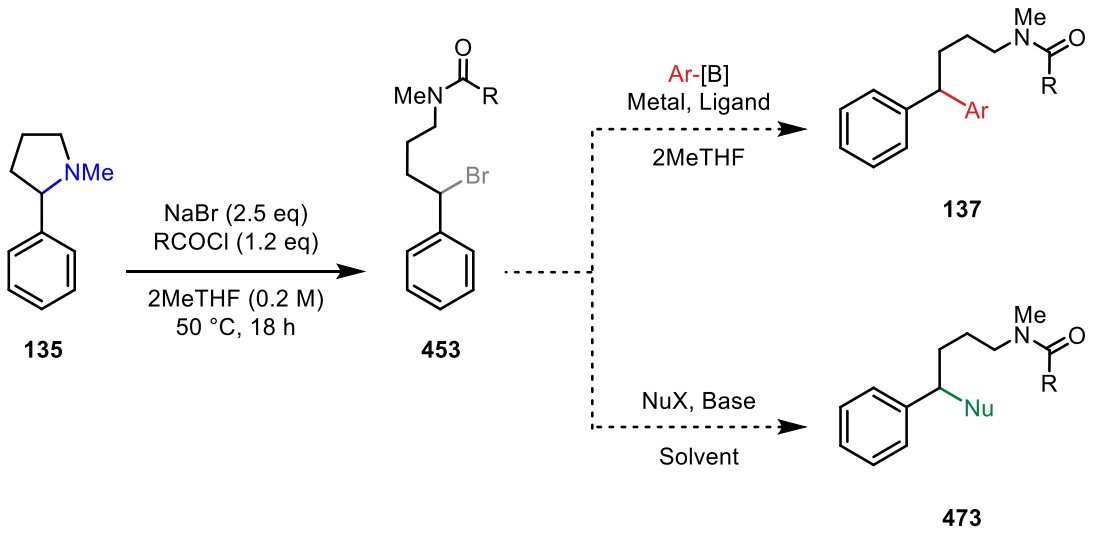

Scheme 108. *Future work for the ring opening of 2-aryl pyrrolidines*

Chapter 6. Overall Summary and Conclusions

This thesis describes the exploration of novel methods for the activation and cleavage of C–N bonds in aryl amines, benzyl amines, aziridines, and pyrrolidines. As reported within Chapter 2, experiments probing the viability of using SPO-based amphoteric catalysts for the activation of aryl C–N bonds have seen some success. The use of SPO ligand **180** with Ni^0 catalyst $Ni(cod)_2$ resulted in the successful C–N cleavage of aryl amine **18**, giving biaryl **187** in 17% yield (**35**, PPh_3, $AlMe_3$, Mesitylene, 130 °C). It is proposed that this activation is facilitated by the in situ formation of complex **188**. It was discovered that any alteration to the reaction conditions displayed in Scheme 109 resulted in a reduction in yield, or complete loss of reactivity.

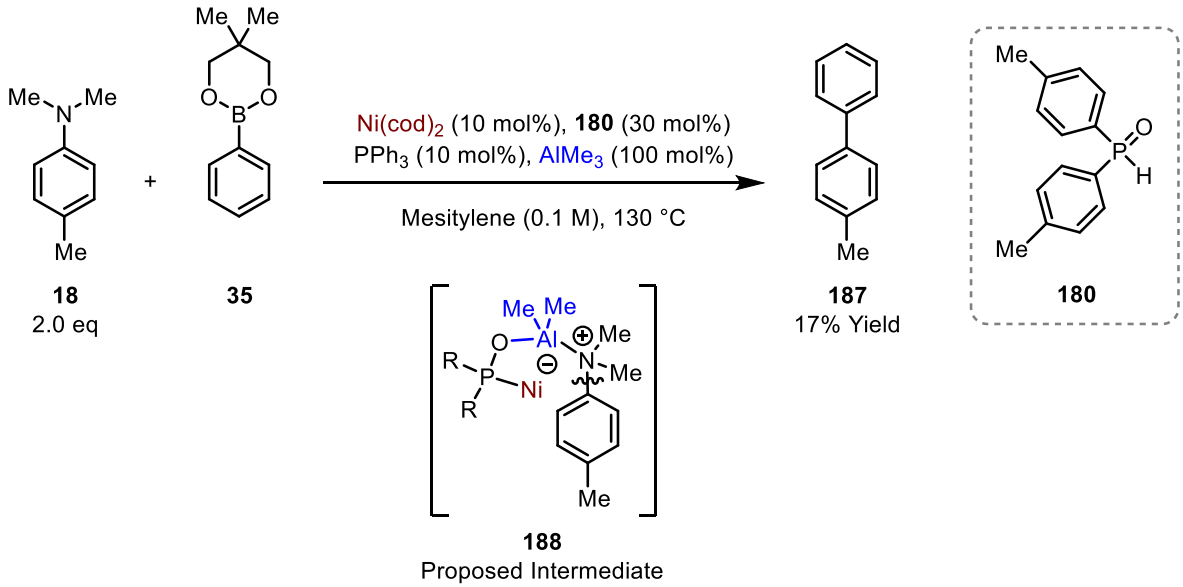

Scheme 109. *Cross-coupling of aryl amines using SPO ligands*

As described in Chapter 3, subsequent studies explored the use of acyl chlorides and anhydrides as in situ activators of benzylamine C–N bonds. A new synthetic method was discovered, wherein benzylamines **199** may be converted into benzyl iodides **237**, and this process was optimised to excellent yields (TFAA, NaI, THF, r.t., 18 h). Furthermore, this work demonstrated that the synthesised benzyl iodides **237** may be used as non-isolated intermediary species within cross-coupling and nucleophilic substitution protocols, in which benzylamines **199** are converted into diarylmethanes **318** ($ArB(OH)_2$, $Ni(hfac)_2$, **262**, Na_2CO_3, THF, 100 °C, 24 h), or substituted products **228** (i. NuH, NaH, DMF, r.t., 2 h; ii. **237**, Nu^-, THF, DMF, r.t., 24 h). This telescoped, two-step, one-pot protocol has a rich scope of substrates, tolerating a wide range of substitution patterns on both the amine and boronic acid substrates. Furthermore, oxygen-, sulfur-, and carbon-centred nucleophiles were demonstrated for the formation of products **228**.

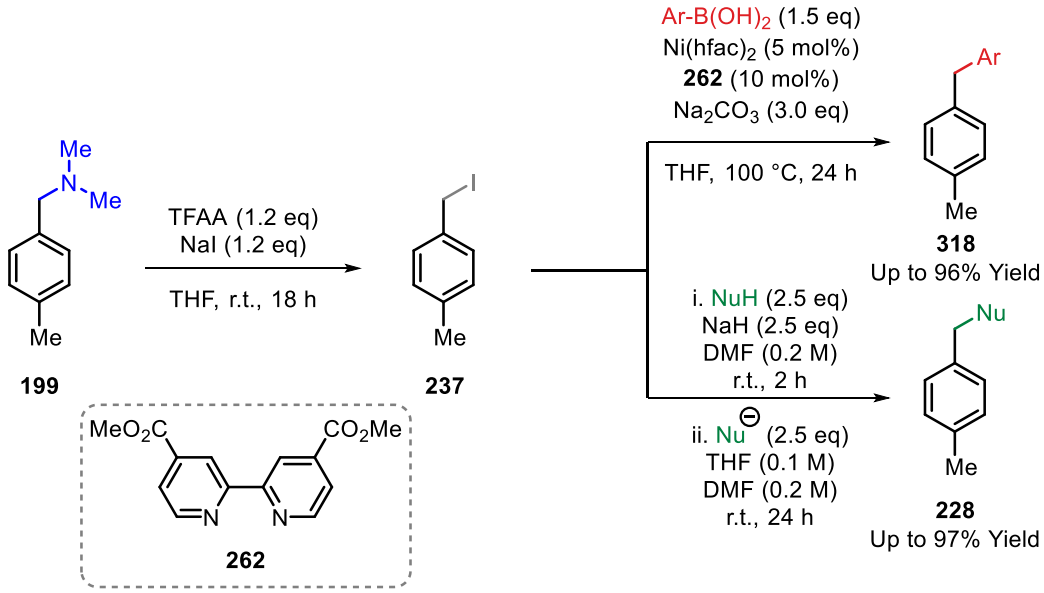

Scheme 110. *Cross-coupling and nucleophilic substitution of benzylamines*

As demonstrated within Chapter 4, subsequent studies expanded the application of this cross-coupling protocol to include α-secondary benzylamines **129**. Due to increased mechanistic complications, re-optimisation of the iodination protocol *and* the cross-coupling protocol was required. Following extensive studies, the telescoped two-step, one-pot method for the cross-coupling of α-secondary benzylamines was developed, giving products **62** with good yields (i. NaI, TFAA, THF, 0 °C 1 h, r.t. 17 h; ii. **395**, $NiBr_2$(diglyme), **360**, THF, 0 °C, 24 h). The substrate scope was found to be limited, with all alternative benzylamines resulting in a distinct decrease in yield, and few variations tolerated on the R^2 portion of the molecule. Further work within the Bower group is ongoing to address these limitations.

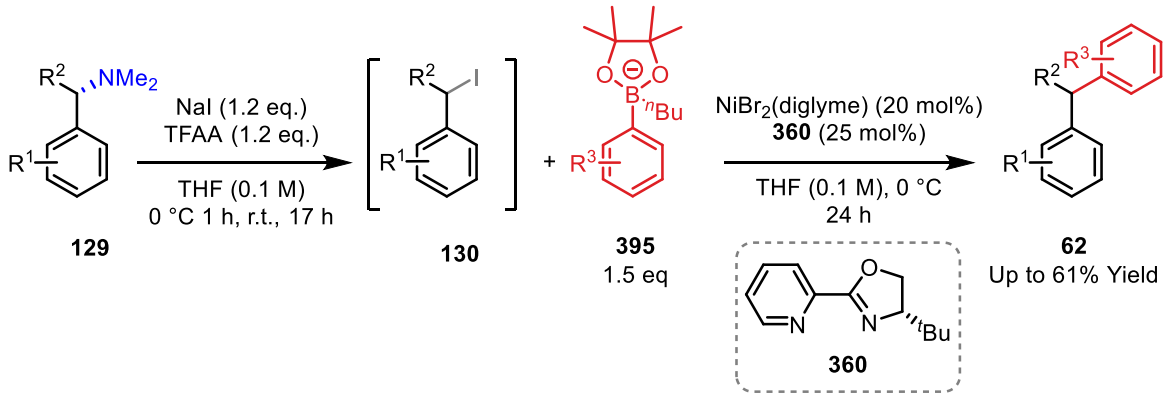

Scheme 111. *Cross-coupling of α-secondary benzylamines*

Chapter 5 describes studies into the expansion of this protocol to include the ring opening of strained cyclic amines such as aziridines, and non-strained cyclic amines such as pyrrolidines. Studies into the ring opening of strained aziridine rings resulted in the successful ring opening of aziridine **436** to give product **440** (NaI, TFAA, THF, r.t., 18 h) (Scheme 112A). It was determined that an

intramolecular mechanism resulted in the formation of **440** over **437**. Further work within the Bower group is ongoing to improve this limitation. For the ring opening of pyrrolidines **135**, the successful formation of halides **455** has been optimised to good yields (Scheme 112B). The competing side formation of alkene **456** has been diminished through optimisation studies, and a limited substrate scope of alternative acyl chloride activators have been demonstrated. Further work within the Bower group is ongoing to complete this optimisation and improve upon the existing limitations.

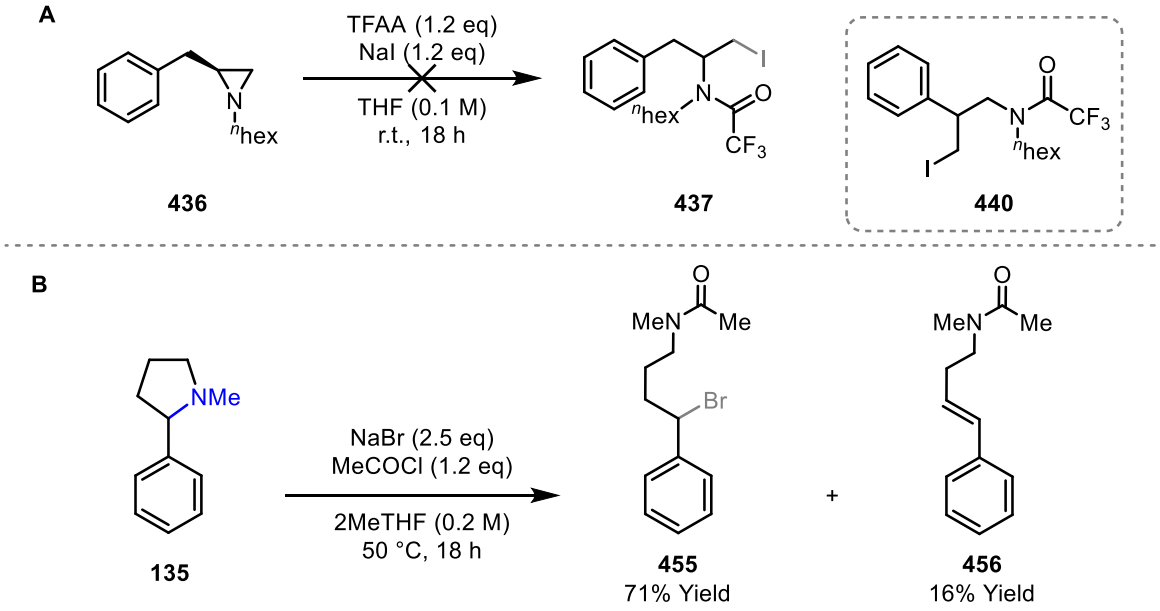

Scheme 112. *Ring opening of strained and non-strained cyclic amines*

Chapter 7. Experimental

7.1. General Experimental Details

All materials for which a synthetic route is not described or referenced were purchased from commercial sources (Sigma-Aldrich, Acros, TCI, Alfa Aesar, Fluorochem, and Strem) and used as received unless otherwise stated. Anhydrous solvents were obtained by distillation using standard procedures or by passage through drying columns supplied by Anhydrous Engineering Ltd. The removal of solvents in vacuo was achieved both using a Büchi rotary evaporator (bath temperatures up to 40 °C) at a pressure of either 15 mmHg (diaphragm pump) or 0.1 mmHg (oil pump), as appropriate, and a high vacuum line at room temperature. Catalytic reactions were carried out inside oven/flame dried Young-type resealable tubes. Petrol refers to petroleum ether consisting of aliphatic hydrocarbons boiling in the range 40-60 °C. Flash column chromatography (FCC) was performed using silica gel (Aldrich 40-63 μm, 230-400 mesh). Thin layer chromatography was performed using aluminium backed 60 F_{254} silica plates. Visualisation was achieved by UV fluorescence or a basic $KMnO_4$ solution and heat. Proton nuclear magnetic resonance spectra (NMR) were recorded on the following spectrometers: JEOL ECS400, JEOL ECZ400, Varian 400-MR, Brucker Nano400, Brucker Avance I DPX-400, Brucker Avance III HD 400, and Brucker Avance III 500 with prodigy cryoprobe machines. ^{1}H NMR spectra were recorded at 400 MHz or 500 MHz as stated. ^{13}C NMR spectra were recorded at 101 MHz or 126 MHz as stated. ^{19}F NMR spectra were recorded at 400 MHz or 471 MHz as stated. ^{31}P NMR were recorded at 162 MHz. Chemical shifts (δ) are given in parts per million (ppm). Peaks are described as singlets (s), doublets (d), triplets (t), quartets (q), multiplets (m), and broad (br). Coupling constants (*J*) are quoted to the nearest 0.5 Hz. All assignments of NMR spectra were based on 2D NMR data (COSY, HSQC, HMBC). Where compounds were isolated as a mixture of isomers (e.g. rotamers), they are referred to as 'major rotamer' and 'minor rotamer'. NMR yields were determined by employing 1,4-dinitrobenzene or trichloroethylene as an internal standard. Mass spectra were recorded using the following instruments: Brucker Daltonics micrOTOF II (ESI), Agilent 6540 UHD Q-TOF LC/MS (ESI), Thermo Scientific Orbitap Elite (EI), or Agilent 7200 Q-TOF (CI) mass spectrometers. Infrared spectra were recorded on a Perkin Elmer Spectrum Two FT-IR spectrometer or a Perkin Elmer Spectrum 100 FT-IR as thin films or solids compressed on a diamond plate. Melting points were determined using Reichert melting point apparatus. Optical rotations were measured using an ADP440+ polarimeter at the concentration and temperature stated. Enantiometric excess was determined using an Agilent 1290 Infinity chiral SFC as stated for each compound. GC-FID/MS analysis was performed on an Agilent 7920A GC equipped with a 5977B MSD. Molar amounts of reaction components were determined by integration of peak areas relative to dodecane as an internal standard using calibration curves of $R^2 > 0.99$.

7.2. General Procedures

General Procedure 1: One-Pot Aryl Amine Cross-Coupling Protocol

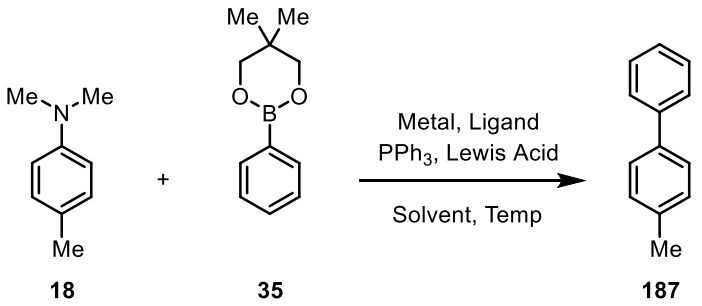

Air-stable reagents were loaded into a flame-dried Schlenk tube: PPh_3 (5.2 mg, 0.06 mmol); 5,5-dimethyl-2-phenyl-1,3,2-dioxaborinane **35** (0.2 mmol, 1.0 eq), Lewis acid (10 mol% or 100 mol%); $NiBr_2$ (0.02 mmol, 0.1 eq). The flask was then evacuated and flushed with N_2 × 3, before non-air-stable reagents were loaded inside the glove box: $Ni(cod)_2$ (0.02 mmol, 0.1 eq); SPO ligand (0.06 mmol, 0.3 eq). To the reagents was added anhydrous mesitylene (2 mL), *N*,*N*,4-trimethylaniline **18** (0.20 mmol, 1.0 eq), and $AlMe_3$ solution (2 M in toluene, 0.20 mmol, 1.0 eq). The reaction was then stirred at the specified temperature for the specified time. The reaction was then cooled to room temperature and a dodecane standard (1.0 eq) was added. A sample was analysed by GC-MS, and a yield calculated against the standard.

General Procedure 2: Three-Pot Aryl Amine Cross-Coupling Protocol

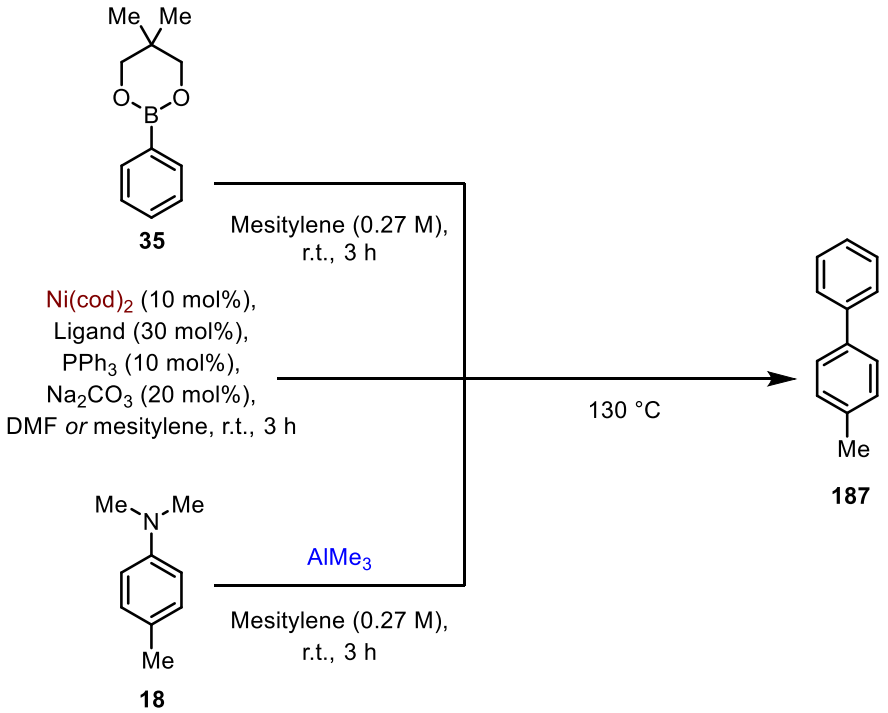

Into a flame-dried Schlenk tube (flask **1**) was loaded air-stable reagents: PPh_3 (0.06 mmol, 0.3 eq), and Na_2CO_3 (0.04 mmol, 0.2 eq). The flask was then evacuated and flushed with N_2 × 3, before non-air-stable reagents were loaded inside the glove box: $Ni(cod)_2$ (0.02 mmol, 0.1 eq); SPO ligand (0.06 mmol, 0.3 eq). To the reagents was added anhydrous mesitylene (1.0 mL) or DMF (0.75 mL), and the reaction was stirred at room temperature for 3 h.

Meanwhile, in a flame-dried Schlenk tube (flask **2**), *N*,*N*,4-trimethylaniline **18** (0.20 mmol, 1.0 eq) was dissolved in mesitylene (0.5 mL), and $AlMe_3$ (2 M solution in toluene; 0.03 mL, 0.06 mmol. 0.3 eq; or 0.1 mL, 0.20 mmol, 1.0 eq) was added. The reaction was stirred at room temperature for 3 h.

Meanwhile, in a flame-dried Schlenk tube (flask **3**), 5,5-dimethyl-2-phenyl-1,3,2-dioxaborinane **35** (0.20 mmol, 1.0 eq) was dissolved in mesitylene (0.5 mL). The reaction was stirred at room temperature for 3 h.

Flask **1** was added to flask **2** *via* syringe, and then flask **3** was added to the mixture *via* syringe. The reaction was then stirred at 130 °C for the specified time. The reaction was then cooled to room temperature and a dodecane standard (0.20 mmol, 1.0 eq) was added. A sample was analysed by GC-MS, and a yield calculated against the standard.

General Procedure 3: Reductive Amination

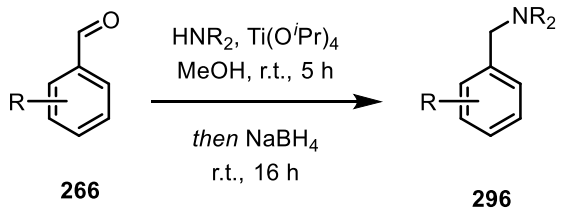

266 **296**

Titanium isopropoxide (2.0 eq.) was loaded into an argon-flushed round-bottom flask. Next, the corresponding disubstituted amine (2.0-4.0 eq. as specified) was added, followed by the appropriate aldehyde (1.0 eq.) dissolved in methanol (1.80 mL/mmol). The solution was then stirred at room temperature for 5 h before sodium borohydride (1.0 eq.) was added portion wise over 20 mins. The reaction was then stirred at room temperature for a further 18 h. The reaction was then quenched with water (1.00 mL/mmol), diluted with brine, and the product was extracted into Et_2O (×3). The organics were collected, washed with brine (15.0 mL), dried over Na_2SO_4, filtered, and concentrated to give the desired product. Further purification via FCC was carried out if required.

General Procedure 4: One-pot α-Primary Benzylamine C–N Activation/Suzuki Cross-Coupling

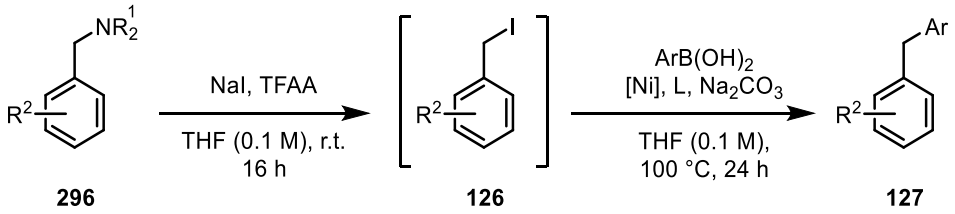

296 **126** **127**

Preparation of stock solution of the appropriate benzyl iodide. A resealable tube was flame-dried and taken to the glovebox, where NaI (1.2 eq.) was added. The tube was taken out of the glovebox and evacuated/backfilled with nitrogen (×3). Anhydrous THF (0.1 M total; 0.5 M solutions of other materials is required) was added, and the resulting mixture was stirred to form a fine suspension. The appropriate benzyl amine solution (1.0 eq., 0.5 M in THF), and then TFAA solution (1.2 eq., 0.5 M in THF) were sequentially added so that the final concentration was 0.1 M, and the mixture was stirred under nitrogen, at room temperature for 16 h.

Procedure for cross-coupling. After that time, into a flame-dried resealable tube was loaded the corresponding arylboronic acid (1.5 eq.), nickel (II) hexafluoroacetylacetonate hydrate (5 mol%), the appropriate ligand (10 mol%), and Na_2CO_3 (3.0 eq.). The tube was evacuated and backfilled with nitrogen (×3) before the appropriate volume of the in situ-prepared benzyl iodide (0.1 M in THF, 1.0 eq.) was added. The tube was sealed and the reaction was stirred at 100 ºC for 24 h. Next, the reaction was cooled to room temperature and the solvent was evaporated under reduced pressure. The crude residue was resuspended in water and EtOAc, the organic phase was separated, and the aqueous phase was extracted with EtOAc (×2). The combined organic phases were dried over Na_2SO_4, filtered, and concentrated under reduced pressure to afford the crude product, which was purified by FCC.

General Procedure 5: One pot α-Primary Benzylamine C–N Activation/Nucleophilic substitution

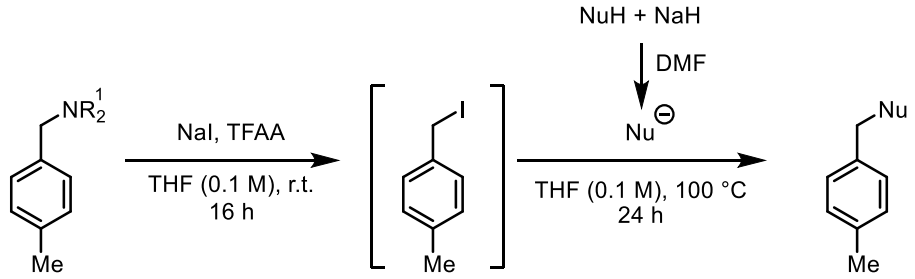

295 **237** **228**

Preparation of stock solution of 1-(1-iodoethyl)-4-methylbenzene. A sealed tube was flame-dried and taken to the glovebox, where NaI (1.2 eq.) was added. The tube was taken out of the glovebox and evacuated and backfilled with argon (×3). Next anhydrous THF, then *N*,*N*-dimethyl-1-(p-tolyl)ethan-1-

amine solution (1.0 equiv., 0.5 M in THF), and TFAA solution (1.2 eq., 0.5 M in THF) were sequentially added so that the final concentration was 0.1 M, and the mixture was stirred at room temperature for 16 h.

Preparation of stock solution of appropriate nucleophile. A separate sealed tube was flame-dried and loaded with NaH (1.0 equiv.). The tube was then evacuated and backfilled with argon (×3). Anhydrous DMF (0.5 M) was added, followed by the appropriate nucleophile (1.0 eq). The solution was stirred at room temperature for 2 h.

Stock solution of nucleophile (2.5 eq., 0.5 M in DMF) was then added dropwise to the stock solution of 1-(iodomethyl)-4-methylbenzene (1 eq. 0.1 M in THF). The reaction was then stirred for 18 h. Next, the solvent was evaporated under reduced pressure. The crude residue was resuspended in water/EtOAc, the organic phase was separated, and the aqueous phase was extracted with EtOAc (×2). The combined organic phases were dried over Na_2SO_4, filtered, and concentrated under reduced pressure to afford the crude product, which was purified by FCC.

General Procedure 6: Eschweiler-Clark

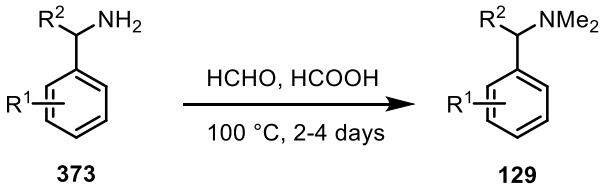

373 **129**

A mixture of the appropriate benzylic amine (1.0 eq.), formaldehyde (37% in water, 4.40 mL/mmol) and formic acid (8.00 mL/mmol) was heated to 100 ºC for 2-4 days. After that time, volatiles were removed under reduced pressure and the aqueous phase was basified using solid NaOH. The product was then extracted with Et_2O (×3), and the combined organic phases were dried over Na_2SO_4, filtered, and concentrated to give the desired product. Further purification *via* FCC was carried out if required.

General Procedure 7: One-pot α-Secondary Benzylamine C–N Activation/Suzuki Cross-Coupling

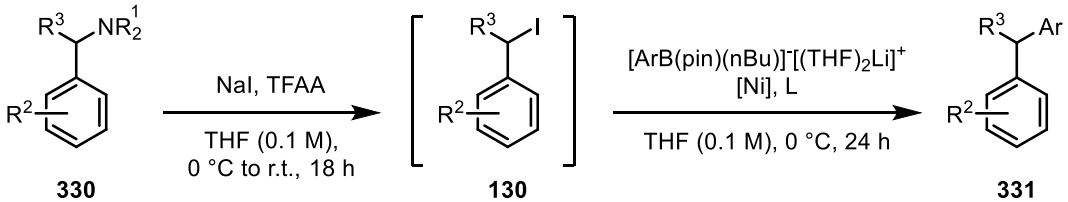

330 **130** **331**

Preparation of stock solution of the appropriate α-substituted benzyl iodide. A resealable tube was flame-dried and taken to the glovebox, where NaI (1.2 eq.) was added. The tube was taken out of the glovebox and evacuated/backfilled with nitrogen (×3). Anhydrous THF (0.1 M total; 0.5 M solutions of other materials is required) was added, and the resulting mixture was stirred to form a fine suspension. The appropriate α-substituted benzyldisubstituted amine solution (1.0 eq., 0.5 M in THF), and then TFAA solution (1.2 eq., 0.5 M in THF) were sequentially added so that the final concentration was 0.1 M, and the mixture was stirred under pressure of nitrogen, at 0 °C for 1 h, then room temperature for 17 h.

Procedure for α-substituted cross-coupling. After that time, into a flame-dried resealable tube was loaded the corresponding arylboronate (1.5 eq.), nickel (II) bromide 2-methoxyethyl ether complex (20 mol%), and the appropriate ligand (25 mol%). The tube was evacuated and backfilled with nitrogen (×3) before the appropriate volume of the *in situ*-prepared benzyl iodide (0.1 M in THF, 1.0 eq.) was added. The tube was sealed and the reaction was stirred at 0 ºC for 24 h. Next, the reaction was cooled to room temperature and the solvent was evaporated under reduced pressure to afford the crude product, which was purified by FCC.

General Procedure 8: Reduction of *N*-Acyl Amino Esters

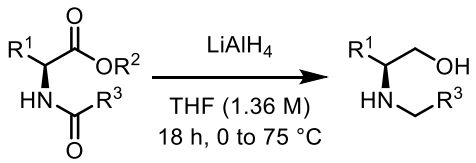

434 **435**

To a solution of acylated amino ester in anhydrous THF (1.36 M) at 0 °C, was added $LiAlH_4$ (1.0 M in THF, 1.8 eq) dropwise. The mixture was heated at reflux and stirred overnight. The reaction was then cooled to 0 °C and quenched with H_2O (0.06 mL/mmol), then 4.0 M NaOH (0.06 mL/mmol), then H_2O (0.02 mL/mmol). The mixture was filtered through Celite®, washed with EtOAc and concentrated in vacuo. The products were used in the next step without further purification.

General Procedure 9: Synthesis of Non-Activated Aziridines Under Modified Wenker Conditions

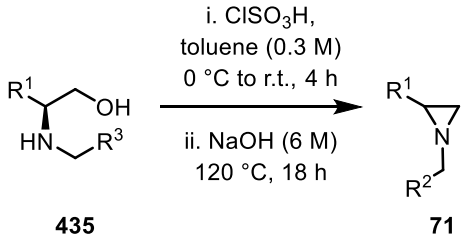

435 **71**

The amino alcohol was dissolved in anhydrous toluene (0.30 M) and the solution was cooled to 0 °C. $ClSO_3H$ (1.00 eq) was added dropwise, and the resulting heterogeneous solution was stirred at r.t. for 4 h. NaOH (6.0 M) was added to result in a 1:1 biphasic solution and the solution was heated to 120 °C overnight. The mixture was cooled to r.t. and the organic phase was isolated. The remaining aqueous phase was then extracted with EtOAc (×3). The organics were combined, dried over Na_2SO_4, concentrated in vacuo, and purified by FCC.

General Procedure 10: C–N Activation of Cyclic Benzyl Pyrrolidines

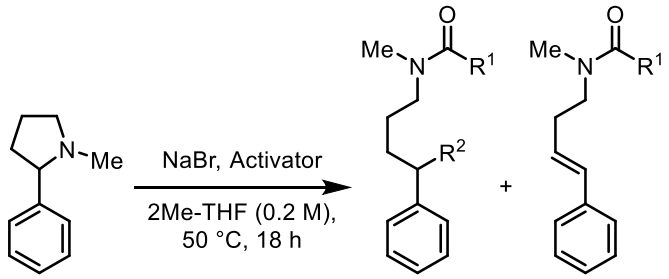

135 **474** **454**

A resealable tube was flame-dried and loaded with NaBr (2.5 eq.). The tube was evacuated/backfilled with nitrogen (×3). Anhydrous 2Me–THF (0.2 M total; 0.5 M solutions of other materials is required) was added, and the resulting mixture was stirred to form a fine suspension. The appropriate 2-aryl pyrrolidine solution (1.0 eq., 0.5 M in 2Me–THF), and then activator solution (1.2 eq., 0.5 M in 2Me–THF) were sequentially added so that the final concentration was 0.2 M. The tube was sealed and the mixture stirred at 50 °C for 18 h to afford the crude product, which was purified by FCC.

7.3. Experimental Procedures for the Studies in Chapter 2

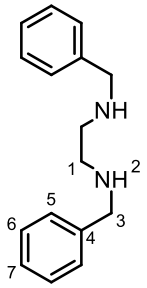

184

***N*¹,*N*²-Dibenzylethane-1,2-diamine (184):** Benzonitrile (0.91 mL, 9.00 mmol) was dissolved in MeOH (12 mL). Ethylenediamine (0.30 mL, 4.50 mmol) was added dropwise and the reaction was stirred at room temperature for 16 h. Sodium borohydride (681 mg, 18.0 mmol) was added portionwise over 25 minutes, and the reaction was stirred at room temperature for 3 h. The reaction was concentrated and the residue partitioned between H_2O (50 mL) and CH_2Cl_2 (3 × 15 mL). The organic extracts were combined, washed with brine (60 mL), dried over Na_2SO_4, filtered and concentrated *in vacuo* to give the title product (993 mg, 4.13 mmol, 92%) as a colourless oil. δ_H (400 MHz, $CDCl_3$) 7.35-7.29 (8H, m, C**5**-H, C**6**-H), 7.26-7.21 (2H, m, C**7**-H), 3.78 (4H, s, C**3**-H_2), 2.77 (4H, s, C**1**-H_2), 1.56 (2H, s, N**2**-H). δ_C (101 MHz, $CDCl_3$) 140.6 (C**4**), 128.5 (C**5**), 128.3 (C**6**), 127.0 (C**7**), 54.1 (C**3**), 49.0 (C**1**).

The spectroscopic properties were consistent with the data available in the literature.[176]

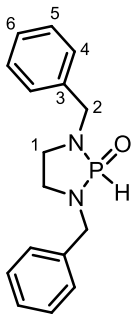

185

1,3-Dibenzyl-1,3,2-diazaphospholidine 2-oxide (185): *N*¹,*N*²-Dibenzylethane-1,2-diamine **184** (927 mg, 3.86 mmol) was loaded into a round-bottom flask and flushed with Ar. Anhydrous CH_2Cl_2 (15 mL) was added and the reaction was cooled to -78 °C. Anhydrous NEt_3 (4.30 mL, 30.9 mmol) was added, then distilled PCl_3 (0.34 mL, 3.86 mmol) was added dropwise over 5 mins. The reaction was warmed slowly to room temperature over 15 h before being cooled again to -78 °C. H_2O (70.0 μL, 3.86 mmol) was added and the reaction was stirred at room temperature for 1 h. The reaction was concentrated *in vacuo*, suspended in Et_2O (2×20 mL), filtered through celite (washed with 20 mL Et_2O) and concentrated *in vacuo* to give a yellow oil (697 mg). FCC (short plug, 100% Et_2O then 100% MeCN) gave the title product (309 mg, 1.08 mmol, 28%) as a yellow oil. δ_H (400 MHz, $CDCl_3$) 7.57 (1H, d, *J*

= 610 Hz, P(O)H), 7.36-7.26 (10 H, m, C**4**-H, C**5**-H, C**6**-H), 4.26 (2H, dd, *J* = 15.0, 8.5 Hz, C**2**-H_2), 4.18 (2H, dd, *J* = 15.0, 8.5 Hz, C**2**-H_2), 3.18-3.09 (2H, m, C**1**-H_2), 3.07-3.00 (2H, m, C**1**-H_2). δ_C (101 MHz, $CDCl_3$) 128.8, 128.3, 127.7 (C**3**, C**4**, C**5**, C**6**), 49.0 (d, *J* = 7.0 Hz, C**2**), 44.7 (C**1**). δ_P (162 MHz, $CDCl_3$) 15.9. (ESI^+) HRMS: Calculated for $C_{16}H_{19}N_2OP$: 287.1308. Found $[M + H]^+$: 287.1299.

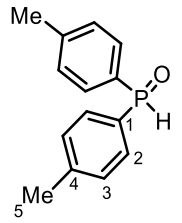

180

Di-*p*-tolylphosphine oxide (180): Into a flame-dried 3-neck flask, fitted with condenser, was loaded Mg turnings (77 mg, 3.15 mmol), I_2 (1 crystal), and THF (5 mL). 4 drops of 4-bromotoluene were added and the reaction was heated to reflux using a heat gun. The remaining 4-bromotoluene (total: 513 mg, 3.00 mmol) in THF (1.5 mL) was added dropwise, maintaining reflux. The reaction was stirred at 70 °C for a further 1 h, and was then cooled to 0 °C. Diethyl phosphonate (0.13 mL, 1.00 mmol) was added dropwise and the reaction was stirred at room temperature for 2 h. The reaction was then cooled to 0 °C and quenched with aqueous HCl (1.00 M, 3.00 mL). CH_2Cl_2 (4 mL) was added. The solution was filtered through celite with additional CH_2Cl_2, dried over Na_2SO_4, filtered, and concentrated *in vacuo* to a pale yellow oil (211 mg). FCC (50-100% EtOAc in petrol) provided the title product (177 mg, 0.77 mmol, 77%) as a colourless solid. δ_H (400 MHz, $CDCl_3$) 8.03 (1H, d, *J* = 477 Hz, P(O)H), 7.57 (4H, dd, *J* = 13.5, 8.0 Hz, ArH), 7.30 (4H, dd, *J* = 8.0, 2.5 Hz, ArH), 2.41 (6H, s, C**5**-H_3). δ_C (101 MHz, $CDCl_3$) 143.2 (d, *J* = 2.5 Hz, C**4**), 130.9 (d, *J* = 12.0 Hz, C**3**), 129.7 (d, *J* = 13.0 Hz, C**2**), 129.3 (d, *J* = 31.0 Hz, C**1**), 21.8 (C**5**). δ_P (162 MHz, $CDCl_3$) 22.2.

The spectroscopic properties were consistent with the data available in the literature.[95]

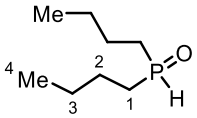

181

Dibutylphosphine oxide (181): Into a flame-dried, 3-neck flask, fitted with condenser, was loaded Mg turnings (230 mg, 9.45 mmol), which was then activated by stirring under vacuum whilst heating with a heat gun for 10 mins. After allowing the flask to cool, I_2 (2 crystals) and THF (12 mL) were added. 4 drops of 1-bromobutane were added and the reaction was heated to reflux using a heat gun. The heat was then removed and the remainder of 1-bromobutane (total: 0.97 mL, 9.00 mmol) was added dropwise, maintaining reflux. The reaction was then stirred at 70 °C for 1 h. The reaction was then cooled to 0 °C, and diethyl phosphonate (0.39 mL, 3.00 mmol) was added dropwise. The reaction was

then stirred at room temperature for 2 h, before being cooled again to 0 °C, quenched with aqueous HCl (1 M, 9 mL) and diluted with CH_2Cl_2 (20 mL). The solution was then filtered through celite, dried over Na_2SO_4, filtered and concentrated to a yellow oil (530 mg). The crude was then purified *via* recrystallisation from hot hexane to give the title product (227 mg, 1.40 mmol, 47%) as a colourless solid. δ_H (400 MHz, $CDCl_3$) 6.88 (1H, d, *J* = 446.0 Hz, P(O)H), 1.93-1.73 (4H, m, C**1**-H_2), 1.73-1.55 (4H, m, C**2**-H_2), 1.55-1.41 (4H, m, C**3**-H_2), 0.97 (6H, t, *J* = 7.5 Hz, C**4**-H_3). δ_C (101 MHz, $CDCl_3$) 28.1 (d, *J* = 64.5 Hz, C**1**), 24.0 (d, *J* = 9.5 Hz, C**2**), 23.9 (d, *J* = 8.5 Hz, C**3**), 13.7 (C**4**). δ_P (162 MHz, $CDCl_3$) 35.1.

The spectroscopic properties were consistent with the data available in the literature.[83]

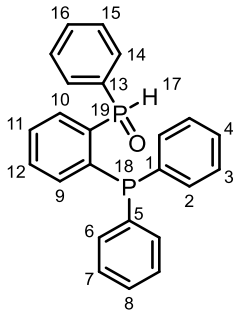

163

(2-(Diphenylphosphaneyl)phenyl)(phenyl)phosphine oxide (163): (2-Bromophenyl) diphenylphosphane (341 mg, 1.00 mmol) was dissolved in THF (1 mL) and TBME (1 mL). The reaction was cooled to -78 °C. *n*-BuLi (1.55 M in hexanes, 0.65 mL, 1.00 mmol) was added dropwise and the reaction was stirred at -78 °C for 2 h. In a separate flask, dichloro(phenyl)phosphane (0.14 mL, 1.00 mmol) was dissolved in TBME (0.50 mL) and cooled to 0 °C. The contents of the first flask were then transferred to the second flask *via* syringe, and the reaction was stirred at 0 °C for 1 h. H_2O (4 mL) was added and the reaction was stirred at 0 °C for a further 70 mins. Brine (40 mL) was added to the reaction mixture and the organics were extracted into 10:1 EtOAc:CH_2Cl_2 (20 mL), then EtOAc (15 mL), then toluene (15 mL), then CH_2Cl_2 (15 mL). The organic extracts were combined, dried over Na_2SO_4, filtered, and concentrated to a beige oil (346 mg). FCC (oven-dried silica; 75 % EtOAc in petrol) provided the title product (181 mg, 0.47 mmol, 47%) as a colourless oil. δ_H (400 MHz, $CDCl_3$) 8.75 (1H, dd, *J* = 499.5, 4.0 Hz, P(O)H), 8.20-8.13 (1H, m, Ar-H), 7.79-6.94 (18H, m, Ar-H). δ_P (162 MHz, $CDCl_3$) 16.6 (1P, d, *J* = 81.0 Hz, P**19**), -17.8 (1P, d, *J* = 81.0 Hz, P**18**). *Carbon NMR analysis could not be obtained due to concentration issues.*

The spectroscopic properties were consistent with the data available in the literature.[90]

7.4. Experimental Procedures for the Studies in Chapter 3

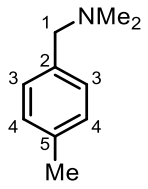

199

***N*,*N*-Dimethyl-1-(*p*-tolyl)methanamine (199):** General procedure **3** *(Reductive Amination)* was followed using 4-methylbenzaldehyde (3.60 mL, 30.0 mmol), *N*,*N*-dimethylamine (2.0 M in methanol, 30.0 mL, 60.0 mmol), titanium isopropoxide (18.3 mL, 60.0 mmol) and $NaBH_4$ (1.16 g, 30.0 mmol). FCC (40-50% EtOAc/hexane) gave the title product (3.360 g, 75%) as a yellow oil. δ_H (400 MHz, $CDCl_3$) 7.19 (2H, d, *J* = 8.0 Hz, C**4**-H), 7.13 (2H, d, *J* = 8.0 Hz, C**3**-H), 3.38 (2H, s, C**1**-H_2), 2.34 (3H, s, C**5**-CH_3), 2.23 (6H, s, N(CH_3)$_2$). δ_C (101 MHz, $CDCl_3$) 136.7 (C**5**), 135.9 (C**2**), 129.2 (C**3**), 129.1 (C**4**), 64.3 (C**1**), 45.5 (N(CH_3)$_2$), 21.2 (C**5**-CH_3).

The spectroscopic properties were consistent with the data available in the literature.[177]

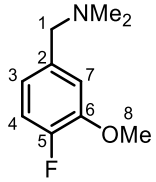

274

1-(4-Fluoro-3-methoxyphenyl)-*N*,*N*-dimethylmethanamine (274): General procedure **3** *(Reductive Amination)* was followed using 4-fluoro-3-methoxybenzaldehyde (540 mg, 3.50 mmol), *N*,*N*-dimethylamine (2.0 M in methanol, 3.50 mL, 7.00 mmol), titanium isopropoxide (2.10 mL, 7.00 mmol) and $NaBH_4$ (133 mg, 3.50 mmol). FCC (10% methanol/CH_2Cl_2) gave the title product (495 mg, 77%) as a yellow oil. R_f: 0.45 (10% MeOH/CH_2Cl_2). ν_{max} / cm^{-1}: 2941 (m), 2816 (m), 2768 (m), 1610 (m), 1514 (s), 1456 (s), 1416 (s), 1274 (s), 1213 (s), 1148 (s), 1035 (s). δ_H (400 MHz, $CDCl_3$): 7.03-6.95 (2H, m, C**3**-H, C**4**-H), 6.82-6.75 (1H, m, C**7**-H), 3.90 (3H, s, C**8**-H_3), 3.38 (2H, s, C**1**-H_2), 2.24 (6H, s, N(CH_3)$_2$). δ_C (101 MHz, $CDCl_3$): 151.6 (d, *J* = 244.5 Hz, C**5**), 147.7 (d, *J* = 10.5 Hz, C**6**), 135.3 (d, *J* = 3.5 Hz, C**2**), 121.3 (d, *J* = 6.5 Hz, C**7**), 115.5 (d, *J* = 18.0 Hz, C**4**), 113.9 (d, *J* = 1.5 Hz, C**3**), 64.1 (C**1**), 56.3 (C**8**), 45.4 (N(CH_3)$_2$). δ_F (400 MHz, $CDCl_3$): -137.9. *m/z* (ESI^+) HRMS: Calculated for $C_{10}H_{15}FNO$: 184.1132. Found $[M+H]^+$: 184.1123.

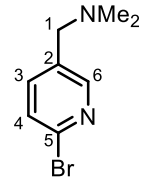

275

1-(6-Bromopyridin-3-yl)-*N*,*N*-dimethylmethanamine (275): General procedure **3** *(Reductive Amination)* was followed using 6-bromonicotinaldehyde (651 mg, 3.50 mmol), *N*-*N*-dimethylamine (2.0 M in methanol, 3.50 mL, 7.00 mmol), titanium isopropoxide (2.10 mL, 7.00 mmol) and $NaBH_4$ (133 mg, 3.50 mmol). FCC (10% methanol/CH_2Cl_2) gave the title product (514 mg, 68%) as a yellow oil. R_f: 0.55 (10% MeOH/CH_2Cl_2). ν_{max} / cm^{-1}: 2942 (m), 2818 (m), 2769 (m), 1561 (m), 1452 (s), 1086 (s), 1019 (s). δ_H (400 MHz, $CDCl_3$): 8.27 (1H, d, *J* = 2.0 Hz, C**6**-H), 7.55 (1H, dd, *J* = 8.0, 2.0 Hz, C**3**-H), 7.44 (1H, d, *J* = 8.0 Hz, C**4**-H), 3.39 (2H, s, C**1**-H_2), 2.24 (6H, s, N(CH_3)$_2$). δ_C (101 MHz, $CDCl_3$): 150.6 (C**6**), 140.9 (C**2**), 139.4 (C**3**), 133.8 (C**5**), 128.0 (C**4**), 60.7 (C**1**), 45.4 (N(CH_3)$_2$). *m/z* (ESI^+) HRMS: Calculated for $C_8H_{12}{}^{79}BrN_2$: 215.0178. Found $[M+H]^+$: 215.0180.

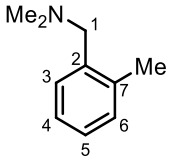

271

***N*,*N*-Dimethyl-1-(*o*-tolyl)methanamine (271):** General procedure **3** *(Reductive Amination)* was followed using 2-methylbenzaldehyde (0.40 mL, 3.50 mmol), *N*-*N*-dimethylamine (2.0 M in methanol, 3.50 mL, 7.00 mmol), titanium isopropoxide (2.10 mL, 7.00 mmol) and $NaBH_4$ (133 mg, 3.50 mmol). FCC (10% methanol/CH_2Cl_2) gave the title product (383 mg, 73%) as an orange oil. δ_H (400 MHz, $CDCl_3$): 7.28-7.23 (1H, m, C**3**-H), 7.18-7.12 (3H, m, C**4**-H, C**5**-H, C**6**-H), 3.39 (2H, s, C**1**-H_2), 2.37 (3H, s, C**7**-CH_3), 2.25 (6H, s, N(CH_3)$_2$). δ_C (101 MHz, $CDCl_3$): 137.4 (C**7**), 137.1 (C**2**), 130.3 (C**5**), 130.0 (C**3**), 127.2 (C**4**), 125.7 (C**6**), 62.1 (C**1**), 45.7 (N(CH_3)$_2$)., 19.3 (Ar-CH_3).

The spectroscopic properties were consistent with the data available in the literature.[178]

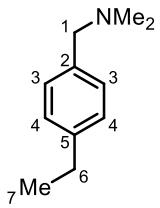

267

1-(4-Ethylphenyl)-*N*,*N*-dimethylmethanamine (267): General procedure **3** *(Reductive Amination)* was followed using 4-ethylbenzaldehyde (0.59 mL, 3.50 mmol), *N*-*N*-dimethylamine (2.0 M in

methanol, 3.50 mL, 7.00 mmol), titanium isopropoxide (2.10 mL, 7.00 mmol) and $NaBH_4$ (133 mg, 3.50 mmol). FCC (100% EtOAc) gave the title product (546 mg, 96%) as a yellow oil. δ_H (400 MHz, $CDCl_3$): 7.22 (2H, d, *J* = 8.0 Hz, C**3**-H), 7.15 (2H, d, *J* = 8.0 Hz, C**4**-H), 3.41 (2H, s, C**1**-H_2), 2.64 (2H, q, *J* = 7.5 Hz, C**6**-H_2), 2.24 (6H, s, N(CH_3)$_2$), 1.23 (3H, t, *J* = 7.5 Hz, C**7**-H_3). δ_C (101 MHz, $CDCl_3$): 143.2 (C**2**), 136.1 (C**5**). 129.3 (C**3**), 127.9 (C**4**), 64.2 (C**1**), 45.4 (N(CH_3)$_2$), 28.7 (C**6**), 15.7 (C**7**).

The spectroscopic properties were consistent with the data available in the literature.[179]

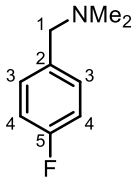

268

1-(4-Fluorophenyl)-*N*,*N*-dimethylmethanamine (268): General procedure **3** *(Reductive Amination)* was followed using 4-fluorobenzaldehyde (0.38 mL, 3.50 mmol), *N*,*N*-dimethylamine (2.0 M in methanol, 3.50 mL, 7.00 mmol), titanium isopropoxide (2.10 mL, 7.00 mmol) and $NaBH_4$ (133 mg, 3.50 mmol). FCC (100% EtOAc) gave the title product (285 m, 53%) as a pale yellow oil. δ_H (400 MHz, $CDCl_3$): 7.32-7.24 (2H, m, C**3**-H), 7.01 (2H, dd, *J* = 8.5, 8.5 Hz, C**4**-H), 3.41 (2H, s, C**1**-H_2), 2.25 (6H, s, N(CH_3)$_2$). δ_C (101 MHz, $CDCl_3$): 152.5 (d, *J* = 244 Hz, C**5**), 134.5 (C**2**), 130.8 (d, *J* = 7.0 Hz, C**3**), 115.2 (d, *J* = 21.0, C**4**), 63.6 (C**1**), 45.3 (N(CH_3)$_2$). δ_F (376 MHz, $CDCl_3$): -115.8.

The spectroscopic properties were consistent with the data available in the literature.[178]

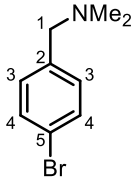

270

1-(4-Bromophenyl)-*N*,*N*-dimethylmethanamine (270): General procedure **3** *(Reductive Amination)* was followed using 4-bromobenzaldehyde (648 mg, 3.50 mmol), *N*,*N*-dimethylamine (2.0 M in methanol, 3.50 mL, 7.00 mmol), titanium isopropoxide (2.10 mL, 7.00 mmol) and $NaBH_4$ (133 mg, 3.50 mmol). FCC (100% EtOAc) gave the title product (482 mg, 57%) as a colourless oil. δ_H (400 MHz, $CDCl_3$): 7.44 (2H, d, *J* = 8.0 Hz, C**3**-H), 7.19 (2H, d, *J* = 8.0 Hz, C**4**-H), 3.38 (2H, s, **C**1-H_2), 2.23 (6H, s, N(CH_3)$_2$). δ_C (101 MHz, $CDCl_3$): 137.8 (C**2**), 131.5 (C**3**), 130.9 (C**4**), 121.0 (C**5**), 63.7 (C**1**), 45.4 (N(CH_3)$_2$).

The spectroscopic properties were consistent with the data available in the literature.[178]

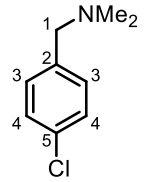

269

1-(4-Chlorophenyl)-*N*,*N*-dimethylmethanamine (269): General procedure **3** *(Reductive Amination)* was followed using 4-chlorobenzaldehyde (492 mg, 3.50 mmol), *N*,*N*-dimethylamine (2.0 M in methanol, 3.50 mL, 7.00 mmol), titanium isopropoxide (2.10 mL, 7.00 mmol) and $NaBH_4$ (133 mg, 3.50 mmol). FCC (100% EtOAc) gave the title product (396 mg, 62%) as a colourless oil. δ_H (400 MHz, $CDCl_3$): 7.35-7.21 (4H, m, C**3**-H, C**4**-H), 3.39 (2H, s, C**1**-H_2), 2.24 (6H, s, N(CH_3)$_2$). δ_C (101 MHz, $CDCl_3$): 137.4 (C**2**), 132.9 (C**5**), 130.5 (C**3**), 128.5 (C**4**), 63.7 (C**1**), 45.4 (N(CH_3)$_2$).

The spectroscopic properties were consistent with the data available in the literature.[178]

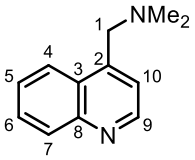

276

***N*,*N*-Dimethyl-1-(quinolin-4-yl)methanamine (276):** General procedure **3** *(Reductive Amination)* was followed using quinoline-4-carbaldehyde (550 mg, 3.50 mmol), *N*,*N*-dimethylamine (2.0 M in methanol, 3.50 mL, 7.00 mmol), titanium isopropoxide (2.10 mL, 7.00 mmol) and $NaBH_4$ (133 mg, 3.50 mmol) to give the title product (624 mg, 96%) as a yellow oil. R_f: 0.15 (50% EtOAc/hexane). ν_{max} / cm^{-1}: 2942 (m), 2817 (m), 2768 (s), 1593 (s), 1508 (s), 1464 (s), 830 (s), 759 (s). δ_H (400 MHz, $CDCl_3$): 8.86 (1H, d, *J* = 4.5 Hz, C**9**-H), 8.22 (1H, dd, *J* = 8.5, 1.5 Hz, C**7**-H), 8.12 (d, *J* = 8.5 Hz, C**4**-H), 7.71 (1H, ddd, *J* = 8.5, 7.0, 1.5 Hz, C**6**-H), 7.56 (1H, ddd, *J* = 8.5, 7.0, 1.5 Hz, C**5**-H), 7.39 (1H, d, *J* = 4.5 Hz, C**10**-H), 3.84 (2H, s, C**1**-H_2), 2.32 (6H, s, N(CH_3)$_2$). δ_C (101 MHz, $CDCl_3$): 150.3 (C**9**), 148.6 (C**8**), 144.7 (C**3**), 130.1 (C**4**), 129.2 (C**6**), 127.8 (C**2**), 126.6 (C**5**), 124.2 (C**7**), 121.6 (C**10**), 61.2 (C**1**), 46.0 (N(CH_3)$_2$). *m/z* (ESI^+) HRMS: Calculated for $C_{12}H_{15}N_2$: 187.1230. Found $[M+H]^+$: 187.1233.

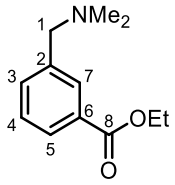

273

Ethyl 3-((dimethylamino)methyl)benzoate (273): General procedure **3** *(Reductive Amination)* was followed using ethyl 3-formylbenzoate (624 mg, 3.50 mmol), dimethylamine (2.0 M in methanol, 1.75 mL, 3.50 mmol), titanium isopropoxide (2.10 mL, 7.00 mmol) and $NaBH_4$ (133 mg, 3.50 mmol) to give

the title product (198 mg, 27%) as a yellow oil. R_f: 0.175 (50% EtOAc/hexane). ν_{max} / cm^{-1}: 2977 (m), 2818 (m), 2771 (m), 1717 (s), 1280 (s), 1194 (s), 1103 (s), 749 (s). δ_H (400 MHz, $CDCl_3$): 7.98-7.93 (2H, m, C**7**-H, C**5**-H), 7.53 (1H, d, *J* = 7.5 Hz, C**3**-H), 7.40 (1H, dd, *J* = 7.5, 7.5 Hz, C**4**-H), 4.37 (2H, q, *J* = 7.0 Hz, OCH_2), 3.49 (2H, s, C**1**-H_2), 2.26 (6H, s, $N(CH_3)_2$), 1.39 (3H, t, *J* = 7.0 Hz, C-CH_3). δ_C (101 MHz, $CDCl_3$): 166.8 (C**8**), 139.1 (C**6**), 133.8 (C**3**), 130.7 (C**2**), 130.3 (C**5**), 128.6 (C**7**), 128.5 (C**4**), 64.0 (C**1**), 61.1 (OCH_2), 45.4 ($N(CH_3)_2$), 14.5 (C-CH_3). *m/z* (ESI^+) HRMS: Calculated for $C_{12}H_{18}NO_2$: 208.1332. Found $[M+H]^+$: 208.1340.

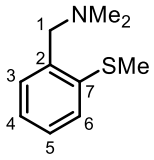

272

***N,N*-Dimethyl-1-(2-(methylthio)phenyl)methanamine (272):** General procedure **3** *(Reductive Amination)* was followed using 2-(methylthio)benzaldehye (0.45 mL, 3.50 mmol), dimethylamine (2.0 M in methanol, 3.50 mL, 7.00 mmol), titanium isopropoxide (2.10 mL, 7.00 mmol) and $NaBH_4$ (133 mg, 3.50 mmol) to give the title product (534 mg, 84%) as a yellow oil. R_f: 0.44 (50% EtOAc/hexane). ν_{max} / cm^{-1}: 2940 (m), 2813 (s), 2766 (s), 1438 (s), 1025 (s), 747 (s). δ_H (400 MHz, $CDCl_3$): 7.28 (3H, m, C**3**-H, C**5**-H, C**6**-H), 7.11 (1H, ddd, *J* = 7.0, 7.0, 1.5 Hz, C**4**-H), 3.46 (2H, s, C**1**-H), 2.46 (3H, s, SCH_3), 2.26 (6H, s, $N(CH_3)_2$). δ_C (101 MHz, $CDCl_3$): 138.9 (C**7**), 136.8 (C**2**), 129.9 (C**6**), 127.8 (C**5**), 125.1 (C**4**), 124.4 (C**3**), 62.2 (C**1**), 45.5 ($N(CH_3)_2$), 15.7 (SCH_3). *m/z* (ESI^+) HRMS: Calculated for $C_{10}H_{16}NS$: 182.0998. Found $[M+H]^+$: 182.1001.

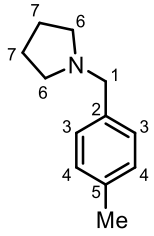

287

1-(4-Methylbenzyl)pyrrolidine (287): To 1-(bromomethyl)-4-methylbenzene (648 mg, 3.50 mmol) in EtOH (10 mL) was added pyrrolidine (0.300 mL, 3.50 mmol) and potassium hydroxide (196 mg, 3.50 mmol). The solution was stirred at room temperature for 5 days, 17 h. The reaction was then partitioned between brine (20 mL) and EtOAc (3×10 mL). The organics were collected and combined, dried over Na_2SO_4, filtered, and concentrated to give a yellow oil (539 mg). FCC (10-40% EtOAc/Hexane) gave the title product (358 mg, 58%) as a pale yellow oil. δ_H (400 MHz, $CDCl_3$): 7.22 (2H, d, *J* = 8.0 Hz, C**3**-H), 7.12 (2H, d, *J* = 8.0 Hz, C**4**-H), 3.59 (2H, s, C**1**-H_2), 2.57-2.46 (4H, m, C**6**-H_2), 2.33 (3H, s, C**5**-CH_3), 1.84-1.74 (4H, m, C**7**-H_2). δ_C (101 MHz, $CDCl_3$): 136.5 (C**5**), 136.4 (C**2**), 129.0 (C**3**) 128.9 (C**4**), 60.5 (C**1**), 54.1 (C**6**), 23.5 (C**7**), 21.1 (C**5**-CH_3).

The spectroscopic properties were consistent with the data available in the literature.[180]

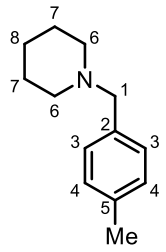

288

1-(4-Methylbenzyl)piperidine (288): To 1-(bromomethyl)-4-methylbenzene (648 mg, 3.50 mmol) in EtOH (10.0 mL) was added piperidine (0.350 mL, 3.50 mmol) and potassium hydroxide (196 mg, 3.50 mmol). The solution was stirred at room temperature for 5 days, 17 h. The reaction was then partitioned between brine (20 mL) and EtOAc (3×10 mL). The organics were collected and combined, dried over Na_2SO_4, filtered, and concentrated to give a yellow oil (626 mg). FCC (50% EtOAc/Hexane; 10-50% EtOAc/Hexane) gave the title product (503 mg, 76%) as a pale yellow oil. δ_H (400 MHz, $CDCl_3$): 7.20 (2H, d, *J* = 8.0 Hz, C**3**-H), 7.12 (2H, d, *J* = 8.0 Hz, C**4**-H), 3.44 (2H, s, C**1**-H_2), 2.45-2.35 (4H, m, C**6**-H_2), 2.34 (3H, s, C**5**-CH_3), 1.61-1.53 (4H, m, C**7**-H_2), 1.47-1.37 (2H, m, C**8**-H_2). δ_C (101 MHz, $CDCl_3$): 136.5 (C**5**), 135.6 (C**2**), 129.3 (C**3**), 128.9 (C**4**), 63.7 (C**1**), 54.5 (C**6**), 26.1 (C**7**), 24.5 (C**8**), 21.2 (C**5**-CH_3).

The spectroscopic properties were consistent with the data available in the literature.[181]

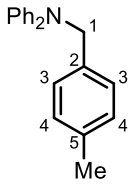

290

***N*-(4-methylbenzyl)-*N*-phenylaniline (290):** To a solution of diphenylamine (592 mg, 3.50 mmol) in acetonitrile (15 mL) was added 1-(bromomethyl)-4-methylbenzene (777 mg, 4.20 mmol) and DIPEA (0.800 mL, 4.55 mmol). The solution was stirred at 80 °C for 3 days. The volatiles were removed under reduced pressure, and the residue partitioned between water (10 mL) and CH_2Cl_2 (3×10 mL). The organics were combined, dried over Na_2SO_4, filtered and concentrated to an orange oil (1.136 g). FCC (0-10% EtOAc/hexane) gave the title product (838 mg, 88%) as a pale yellow oil. δ_H (400 MHz, $CDCl_3$): 7.28-7.20 (6H, m, ArCH), 7.14-7.04 (6H, m, ArCH), 6.93 (2H, ddt, *J* = 7.5, 7.5, 1.0 Hz, ArCH), 4.97 (2H, s, C**1**-H), 2.31 (3H, s, C**5**-CH_3). δ_C (101 MHz, $CDCl_3$): 148.2 (ArC), 136.5 (C**5**), 136.2 (C**2**), 129.5 (ArCH), 129.4 (C**4**), 126.6 (C**3**), 121.4 (ArCH), 120.8 (ArCH), 118.0 (ArCH), 56.2 (C**1**), 21.2 (C**5**-CH_3).

The spectroscopic properties were consistent with the data available in the literature.[182]

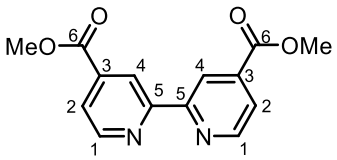

262

Dimethyl [2,2'-bipyridine]-4,4'-dicarboxylate (262): [2,2'-bipyridine]-4,4'-dicarboxylic acid suspended in methanol (17.0 mL) was added to H_2SO_4 (concentrated, 2.0 mL), washing with 3.0 mL methanol. The reaction was then heated at 85 °C for 66 h. The reaction was then cooled to room temperature, before pouring onto water (75 mL). The slurry was then adjusted to pH 8 using aqueous sodium hydroxide (25% w/v) and the product extracted into $CHCl_3$ (3×50 mL). The organics were collected and combined, dried over Na_2SO_4, filtered, and concentrated to give the title product (900 mg, 81%) as a colourless solid. δ_H (400 MHz, $CDCl_3$) 8.97 (2H, dd, *J* = 1.5, 1.0 Hz, C**4**-H), 8.87 (2H, dd, *J* = 5.0, 1.0 Hz, C**1**-H), 7.91 (2H, dd, *J* = 5.0, 1.5 Hz, C**2**-H), 4.00 (6H, s, OCH_3). δ_C (101 MHz, $CDCl_3$) 165.7 (C**6**), 156.6 (C**5**), 150.3 (C**1**), 138.8 (C**3**), 123.4 (C**2**), 120.7 (C**4**), 52.9 (OCH_3).

The spectroscopic properties were consistent with the data available in the literature.[183]

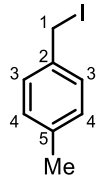

237

1-(Iodomethyl)-4-methylbenzene (237): General procedure General Procedure **4** (*preparation of benzyl iodide*) was followed using *N*,*N*-dimethyl-1-(*p*-tolyl)methanamine (0.5 M in THF, 3.60 mL, 1.80 mmol), TFAA (0.5 M in THF, 4.32 mL, 2.16 mmol), and NaI (324 mg, 2.16 mmol) in THF (10.1 mL). The solution of the compound obtained was taken directly into the next step. δ_H (400 MHz, $CDCl_3$): 7.27 (2H, d, *J* = 8.0 Hz, C**3**-H), 7.10 (2H, d, *J* = 8.0 Hz, C**4**-H), 4.45 (2H, s, C**1**-H_2), 2.31 (3H, s, C**5**-CH_3). δ_C (101 MHz, $CDCl_3$): 138.0 (C**2**), 136.4 (C**5**), 129.7 (C**3**), 128.8 (C**4**), 21.4 (C**5**-CH_3), 6.3 (C**1**).

The spectroscopic properties were consistent with the data available in the literature.[184]

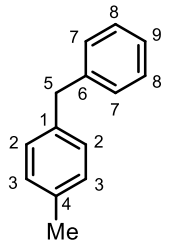

17

1-Benzyl-4-methylbenzene (17): General Procedure **4** *(One-pot α-Primary Benzylamine C–N Activation/Suzuki Cross-Coupling)* was followed using phenylboronic acid (110 mg, 0.90 mmol), nickel (II) hexafluoroacetylacetonate hydrate (14.2 mg, 0.030 mmol), dimethyl [2,2'-bipyridine]-4,4'-dicarboxylate ligand (16.3 mg, 0.06 mmol), Na_2CO_3 (190.8 mg, 1.80 mmol), and 1-methyl-4-(iodomethyl)benzene (0.1 M in THF, 6.00 mL, 0.60 mmol). Using *N*,*N*-dimethyl-1-(*p*-tolyl)methanamine (**358**), *N*-cyclohexyl-*N*-(4-methylbenzyl)cyclohexanamine (**291**), 1-(4-methylbenzyl)pyrrolidine (**287**) or 1-(4-methylbenzyl)piperidine (**288**) as starting materials, 105 mg (95%), 65 mg (59%), 87 mg (80%) and 70 mg (64%) were obtained of the title compound, respectively, as a yellow oil. FCC was carried out using 100% hexane in all cases. δ_H (400 MHz, $CDCl_3$): 7.31-7.25 (2H, m, C**8**-H), 7.22-7.16 (3H, m, C**7**-H, C**9**-H), 7.13-7.06 (4H, m, C**2**-H, C**3**-H), 3.95 (2H, s, C**5**-H_2), 2.32 (3H, s, C**4**-CH_3). δ_C (101 MHz, $CDCl_3$): 141.6 (C**4**), 138.2 (C**6**), 135.7 (C**1**), 129.3 (C**7**), 129.0 (C**2**), 128.9 (C**8**), 128.6 (C**3**), 126.1 (C**9**), 41.7 (C**5**), 21.1 (C**4**-CH_3).

The spectroscopic properties were consistent with the data available in the literature.[185]

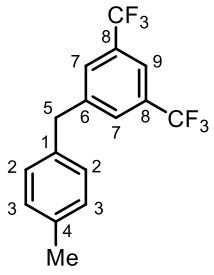

319

1-(4-Methylbenzyl)-3,5-bis(trifluoromethyl)benzene (319): General Procedure **4** *(One-pot α-Primary Benzylamine C–N Activation/Suzuki Cross-Coupling)* was followed using (3,5-bis(trifluoromethyl)phenyl)boronic acid (232 mg, 0.90 mmol), nickel (II) hexafluoroacetylacetonate hydrate (14.2 mg, 0.03 mmol), dimethyl [2,2'-bipyridine]-4,4'-dicarboxylate ligand (16.3 mg, 0.060 mmol), Na_2CO_3 (191 mg, 1.80 mmol), and 1-(iodomethyl)-4-methylbenzene (0.1 M in THF, 6.00 mL, 0.600 mmol) prepared from *N*,*N*-dimethyl-1-(*p*-tolyl)methanamine (**358**). FCC (100% hexane) gave the title compound (165 mg, 86%) as a colourless oil. δ_H (400 MHz, $CDCl_3$): 7.72 (1H, s, C**9**-H), 7.63 (2H, s, C**7**-H), 7.15 (2H, d, *J* = 8.0 Hz, C**3**-H), 7.06 (2H, d, *J* = 8.0 Hz, C**2**-H), 4.06 (2H, s, C**5**-H_2), 2.34 (3H, s, C**4**-CH_3). δ_C (101 MHz, $CDCl_3$): 144.0 (C**6**), 136.7 (C**4**), 135.9 (C**1**), 131.8 (q, *J* = 33.5 Hz, C**8**),

129.8 (C**3**), 129.1 (q, *J* = 3.5 Hz, C**7**), 128.9 (C**2**), 123.5 (q, *J* = 273.0 Hz, C**8**-$\underline{C}F_3$), 120.3 (sept, *J* = 4.0 Hz, C**9**), 41.2 (C**5**), 21.2 (C**4**-$\underline{C}H_3$). δ_F (376 MHz, $CDCl_3$): -62.7.

The spectroscopic properties were consistent with the data available in the literature.[186]

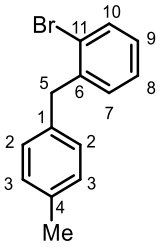

325

1-Bromo-2-(4-methylbenzyl)benzene (325): General Procedure **4** *(One-pot α-Primary Benzylamine C–N Activation/Suzuki Cross-Coupling)* was followed using (2-bromophenyl)boronic acid (181 mg, 0.90 mmol), nickel (II) hexafluoroacetylacetonate hydrate (14.2 mg, 0.03 mmol), dimethyl [2,2'-bipyridine]-4,4'-dicarboxylate ligand (16.3 mg, 0.06 mmol), Na_2CO_3 (191 mg, 1.80 mmol), and 1-(iodomethyl)-4-methylbenzene (0.1 M in THF, 6.00 mL, 0.60 mmol) prepared from *N*,*N*-dimethyl-1-(*p*-tolyl)methanamine (**358**). FCC (100% hexane) gave the title compound (107 mg, 68%) as a colourless oil. δ_H (400 MHz, $CDCl_3$): 7.56 (1H, dd, *J* = 8.0, 1.0 Hz, C**10**-$\underline{H}$), 7.22 (1H, ddd, *J* = 7.5, 1.0, 1.0 Hz, C**7**-$\underline{H}$), 7.15-7.05 (6H, m, C**2**-$\underline{H}$, C**3**-$\underline{H}$, C**8**-$\underline{H}$, C**9**-$\underline{H}$), 4.08 (2H, s, C**5**-$\underline{H}_2$), 2.33 (3H, s, C**4**-$C\underline{H}_3$). δ_C (101 MHz, $CDCl_3$): 140.7 (C**6**), 136.5 (C**1**), 135.9 (C**4**), 133.0 (C**10**), 131.1 (C**8**), 129.3 (C**3**), 129.0 (C**2**), 127.9 (C**9**), 127.6 (C**7**), 125.0 (C**11**), 41.5 (C**5**), 21.2 (C**4**-$\underline{C}H_3$).

The spectroscopic properties were consistent with the data available in the literature.[187]

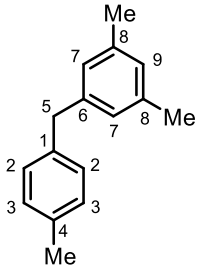

326

1,3-Dimethyl-5-(4-methylbenzyl)benzene (326): General Procedure **4** *(One-pot α-Primary Benzylamine C–N Activation/Suzuki Cross-Coupling)* was followed using (3,5-dimethylphenyl)boronic acid (135 mg, 0.90 mmol), nickel (II) hexafluoroacetylacetonate hydrate (14.2 mg, 0.03 mmol), dimethyl [2,2'-bipyridine]-4,4'-dicarboxylate ligand (16.3 mg, 0.06 mmol), Na_2CO_3 (191 mg, 1.80 mmol), and 1-(iodomethyl)-4-methylbenzene (0.1 M in THF, 6.00 mL, 0.60 mmol) prepared from *N*,*N*-dimethyl-1-(*p*-tolyl)methanamine (**358**). FCC (100% hexane) gave the title compound (100 mg, 79%) as a colourless oil. R_f: 0.29 (100% Hexane). ν_{max} / cm^{-1}: 3015 (m), 2916 (s), 1604 (s), 1513 (s), 1459 (m), 807 (m). δ_H (400 MHz, $CDCl_3$): 7.10 (4H, s, C**2**-$\underline{H}$, C**3**-$\underline{H}$), 6.84 (1H, s, C**9**-$\underline{H}$), 6.82 (2H, s, C**7**-$\underline{H}$),

3.87 (2H, s, C**5**-$\underline{H}_2$), 2.33 (3H, s, C**4**-C$\underline{H}_3$), 2.28 (6H, s, C**8**-C$\underline{H}_3$). δ_C (101 MHz, $CDCl_3$): 141.4 (C**6**), 138.5 (C**1**), 138.0 (C**8**), 135.6 (C**4**), 129.5 (C**3**), 128.7 (C**2**), 127.1 (C**9**), 126.9 (C**7**), 41.5 (C**5**), 21.5 (C**8**-$\underline{C}H_3$), 21.4 (C**4**-$\underline{C}H_3$). *m/z* (ESI^+) HRMS: Calculated for $C_{16}H_{18}Na$: 233.1301. Found $[M+Na]^+$: 233.1296.

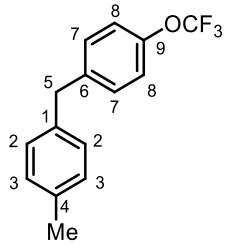

321

1-Methyl-4-(4-(trifluoromethoxy)benzyl)benzene (321): General Procedure **4** *(One-pot α-Primary Benzylamine C–N Activation/Suzuki Cross-Coupling)* was followed using (4-(trifluoromethoxy)phenyl)boronic acid (185 mg, 0.90 mmol), nickel (II) hexafluoroacetylacetonate hydrate (14.2 mg, 0.03 mmol), dimethyl [2,2'-bipyridine]-4,4'-dicarboxylate ligand (16.3 mg, 0.06 mmol), Na_2CO_3 (191 mg, 1.80 mmol), and 1-(iodomethyl)-4-methylbenzene (0.1 M in THF, 6.00 mL, 0.60 mmol) prepared from *N*,*N*-dimethyl-1-(*p*-tolyl)methanamine (**358**). FCC (100% hexane) gave the title compound (125 mg, 78%) as a colourless oil. R_f: 0.56 (100% Hexane). ν_{max} / cm^{-1}: 2921 (m), 1507 (s), 1256 (s), 1221 (s), 1161 (s), 804 (m). δ_H (400 MHz, $CDCl_3$): 7.19 (2H, d, *J* = 8.0 Hz, C**7**-$\underline{H}$), 7.12 (4H, d, *J* = 8.0 Hz, C**3**-$\underline{H}$, C**8**-$\underline{H}$), 7.07 (2H, d, *J* = 8.0 Hz, C**2**-$\underline{H}$), 3.94 (2H, s, C**5**-$\underline{H}_2$), 2.33 (3H, s, C**4**-C$\underline{H}_3$). δ_C (101 MHz, $CDCl_3$): 147.7 (C**9**), 140.3 (C**1**), 137.5 (C**6**), 136.0 (C**4**), 130.2 (C**2**), 129.4 (C**3**), 128.9 (C**7**), 126.3 (q, *J* = 361.5 Hz, O$\underline{C}F_3$), 121.2 (C**8**), 40.9 (C**5**), 21.2 (C**4**-$\underline{C}H_3$). δ_F (376 MHz, $CDCl_3$): -57.8.

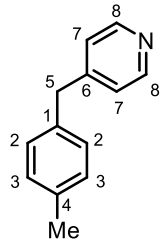

323

4-(4-Methylbenzyl)pyridine (323): General Procedure **4** *(One-pot α-Primary Benzylamine C–N Activation/Suzuki Cross-Coupling)* was followed using pyridin-4-ylboronic acid (111 mg, 0.90 mmol), nickel (II) hexafluoroacetylacetonate hydrate (28.4 mg, 0.06 mmol), dimethyl [2,2'-bipyridine]-4,4'-dicarboxylate ligand (32.6 mg, 0.12 mmol), Na_2CO_3 (191 mg, 1.80 mmol), and 1-(iodomethyl)-4-methylbenzene (0.1 M in THF, 6.00 mL, 0.60 mmol) prepared from *N*,*N*-dimethyl-1-(*p*-tolyl)methanamine (**358**), and was carried out at 150 °C. FCC (10-25% EtOAc/hexane), followed by preparative TLC (2% MeOH/CH_2Cl_2) gave the title compound (50 mg, 45%) as an orange oil. δ_H (400

MHz, $CDCl_3$): 8.47 (2H, br s, C**8**-H), 7.14-7.04 (6H, m, C**2**-H, C**3**-H, C**7**-H), 3.93 (2H, s, C**5**-H_2), 2.33 (3H, s, C**4**-CH_3). δ_C (101 MHz, $CDCl_3$): 149.9 (C**8**), 136.4 (C**4**), 135.9 (C**1**), 129.6 (C**3**), 129.1 (C**2**), 127.6 (C**6**), 124.3 (C**7**), 41.0 (C**5**), 21.2 (C**4**-CH_3).

The spectroscopic properties were consistent with the data available in the literature.[188]

7.5. Experimental Procedures for the studies in Chapter 4

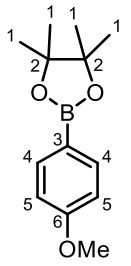

355

2-(4-Methoxyphenyl)-4,4,5,5-tetramethyl-1,3,2-dioxaborolane (355): (4-methoxyphenyl)boronic acid (5.19 g, 34.1 mmol) was dissolved in Et_2O (100 mL). Pinacol (4.03 g, 34.1 mmol) was added and the reaction was stirred for 1 h. Two spatulas of Na_2SO_4 were added (approx. 2.0 g), and the reaction was stirred at room temperature for 17 h. The solution was filtered and concentrated to give the title compound (7.98 g, 100%) as a colourless oil. δ_H (400 MHz, $CDCl_3$): 7.75 (2H, d, *J* = 8.5 Hz, C**4**-H), 6.90 (2H, d, *J* = 8.5 Hz, C**5**-H), 3.83 (3H, s, OCH_3), 1.33 (12H, s, C**1**-H_3). δ_C (101 MHz, $CDCl_3$): 162.3 (C**6**), 136.7 (C**4**), 113.5 (C**5**), 83.7 (C**2**), 55.2 (OCH_3), 2.50 (C**1**). *Carbon C**3** was not detected due to quadrupolar broadening.*

The spectroscopic properties were consistent with the data available in the literature.[189]

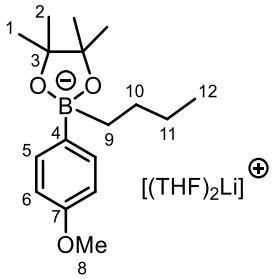

356

2-Butyl-2-(4-methoxyphenyl)-4,4,5,5-tetramethyl-1,3,2-dioxaborolan-2-uide tetrahydrofuran iodide complex (356): 2-(4-Methoxyphenyl)-4,4,5,5-tetramethyl-1,3,2-dioxaborolane (2.00 g, 8.54 mmol) was loaded into a flame-dried Schlenk flask and dried under vacuum. THF (15 mL) was added and the solution was cooled to -20 °C. *n*Butyllithium (1.3 M in hexanes, 6.25 mL, 8.12 mmol) was added over 15 mins and the reaction was stirred at -20 °C for 2 h, and then stirred at room temperature

for 1 h. Solvents were removed *in vacuo* and product was dried *in vacuo* to give the title compound (2.83 g, 6.40 mmol, 75%) as a colourless solid. δ_H (500 MHz, $CDCl_3$): 7.21 (2H, d, *J* = 8.0 Hz, C**5**-H), 6.76 (2H, d, *J* = 8.0 Hz, C**6**-H), 3.73 (8H, br s, C**8**-H_3, THF 2×OCH_2), 1.85 (8H, br s, THF-2×CH_2), 1.31-1.16 (2H, m, C**9**), 1.14 (3H, s, C**8**), 1.07 (6H, s, C**1/2**-H_3), 0.94 (6H, s, C**2/1**-H_3), 0.91-0.82 (2H, m, C**10**-H_2), 0.78 (3H, t, *J* = 7.5 Hz, C**12**-H_3), 0.44-0.37 (2H, m, C**11**-H_2). δ_C (126 MHz, $CDCl_3$): 158.0 (C**7**), 132.3 (C**5**), 113.9 (C**6**), 79.0 (C**3**), 68.1 (THF-OCH_2), 55.1 (C**8**), 30.1 (C**10**), 27.2 (C**11**), 26.7 (C**1/2**), 26.5 (C**2/1**), 25.7 (THF-CH_2), 14.2 (C**12**). *Carbons C**4** and C**9** were not detected due to quadrupolar broadening.*

The spectroscopic properties were consistent with the data available in the literature.[144]

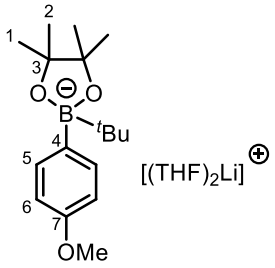

357

2-(*tert*-Butyl)-2-(4-methoxyphenyl)-4,4,5,5-tetramethyl-1,3,2-dioxaborolan-2-uide tetrahydrofuran iodide complex (357): 2-(4-Methoxyphenyl)-4,4,5,5-tetramethyl-1,3,2-dioxaborolane (1.42 g, 6.07 mmol) was loaded into a flame-dried Schlenk flask and dried under vacuum. THF (13 mL) was added and the solution was cooled to -40 °C. *tert*-Butyllithium (1.7 M in hexanes, 3.40 mL, 5.76 mmol) was added over 15 mins and the reaction was stirred at -40 °C for 40 mins, and then stirred at room temperature for 45 mins. Solvents were removed *in vacuo* to form a colourless gum. Hexane (15 mL) was added and the solution was sonicated for 1 h and solvents were removed *via* cannula filtration to give a colourless solid. Product was dried *in vacuo* for 18 h to provide the title compound (1.50 g, 3.39 mmol, 56%) as a colourless solid. δ_H (400 MHz, THF-d8): 7.27 (2H, d, *J* = 8.5 Hz, C**5**-H), 6.54 (2H, d, *J* = 8.5 Hz, C**6**-H), 3.65 (3H, s, OCH_3), 1.11 (6H, s, C**1/2**-H_3), 0.82 (6H, s, C**2/1**-H_3), 0.61 (9H, s, C(CH_3)$_3$). δ_C (101 MHz, THF-d8): 157.3 (C**7**), 134.0 (C**5**), 111.5 (C**6**), 78.3 (C**3**), 54.8 (OCH_3), 30.8 (C(CH_3)$_3$), 28.9 (C(CH$_3$)$_3$), 28.6 (C**1/2**), 28.1(C**2/1**). *Carbon C**4** was not detected due to quadrupolar broadening.*

The spectroscopic properties were consistent with the data available in the literature.[144]

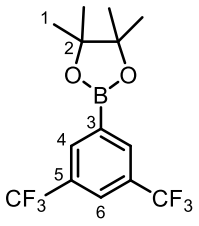

475

2-(3,5-Bis(trifluoromethyl)phenyl-4,4,5,5-tetramethyl-1,2,3-dioxaborolane (475): (3,5-Bis (trifluoromethyl)phenyl)boronic acid (1.29 g, 5.00 mmol) was dissolved in Et_2O (20 mL). Pinacol (591 mg, 5.00 mmol) was added and the reaction was stirred for 1 h. One spatula of Na_2SO_4 was added (approx.1.0 g), and the reaction was stirred at room temperature for 16 h. The solution was filtered and concentrated to give the title compound (769 mg, 45%) as a colourless solid. M.P. = 65-66 °C.[190] δ_H (400 MHz, $CDCl_3$): 8.23 (2H, s, C**4**-H), 7.94 (1H, s, C**6**-H), 1.37 (12H, s, C**1**). δ_C (101 MHz, $CDCl_3$): 134.8 (q, *J* = 2.0 Hz, C**4**), 131.0 (q, *J* = 33.0 Hz, C**5**), 125.0-124.8 (m, C**6**), 123.6 (q, *J* = 274.0 Hz, CF_3), 122.3 (C**3**), 85.0 (C**2**), 25.0 (C**1**). δ_F (376 MHz, $CDCl_3$): -62.7 (s).

The spectroscopic properties were consistent with the data available in the literature.[190]

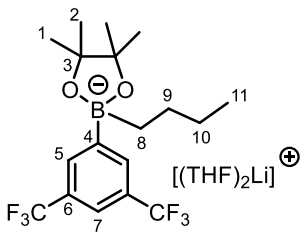

396

2-(3,5-Bis(trifluoromethyl)phenyl)-2-butyl-4,4,5,5-tetramethyl-1,3,2-dioxaborolane-2-uide tetrahydrofuran iodide complex (396): 2-(3,5-Bis(trifluoromethyl)phenyl-4,4,5,5-tetramethyl-1,2,3-dioxaborolane (3.48 g, 10.2 mmol) was loaded into a flame-dried Schlenk flask and dried under vacuum. THF (21 mL) was added and the solution was cooled to -20 °C. *n*Butyllithium (2.3 M in hexanes, 5.77 mL, 13.3 mmol) was added over 15 mins and the reaction was stirred at -20 °C for 2 h, and then stirred at room temperature for 1 h. Solvents were removed *in vacuo* and product was washed with hexane (15 mL), then dried *in vacuo* for 18 h to give the title compound (4.27 g, 10.2 mmol, 76%) as a colourless solid. δ_H (500 MHz, $CDCl_3$): 7.83 (2H, s, C**5**-H), 7.59 (1H, s, C**7**-H), 3.71 (8H, br s, THF 2×OCH_2), 1.86 (8H, br s, THF 2×CH_2), 1.20 (6H, s, C**1**/C**2**-H_3), 1.18-1.14 (2H, m, C**10**-H_2), 1.03 (6H, s, C**2**/C**1**-H_3), 0.89-0.80 (2H, m, C**9**-H_2), 0.71 (3H, t, *J* = 7.5 Hz, C**11**-H_3), 0.50-0.40 (2H, m, C**8**-H_2). δ_C (126 MHz, $CDCl_3$): 130.8 (br s, C**5**), 124.2 (br s, C**6**), 117.9 (br s, C**7**), 70.0 (THF 2×OCH_2), 79.0 (C**3**), 29.5 (C**9**), 27.0 (C**10**), 26.0 (C**1**/C**2**), 25.7 (THF 2×CH_2), 25.6 (C**2**/C**1**), 14.0 (C**11**). δ_F (471 MHz, $CDCl_3$): -62.4. *Due to solubility challenges, a greater concentration of ^{13}C NMR was not obtained and due to*

*splitting, the CF_3 carbon was not observed. Carbons C**4** and C**8** were not detected due to quadrupolar broadening.*

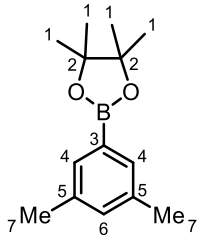

476

2-(3,5-Dimethylphenyl)-4,4,5,5-tetramethyl-1,3,2-dioxaborolane (476): (3,5-Dimethylphenyl)boronic acid (1.98 g, 13.2 mmol) was dissolved in Et_2O (50 mL). Pinacol (1.56 g, 13.2 mmol) was added and the reaction was stirred for 1 h. One spatula of Na_2SO_4 was added (approx. 1.0 g), and the reaction was stirred at room temperature for 16 h. The solution was filtered and concentrated to give the title compound (3.06 g, 100%) as a colourless solid. M.P. = 100-101 °C.[211] δ_H (500 MHz, $CDCl_3$): 7.44 (2H, s, C**4**-H), 7.10 (1H, s, C**6**-H), 2.32 (6H, s, C**7**-H_3), 1.35 (12H, s, C**1**-H_3). δ_C (101 MHz, $CDCl_3$): 137.3 (C**5**), 133.1 (C**6**), 132.5 (C**4**), 83.8 (C**2**), 25.0 (C**1**), 21.3(C**7**). *Carbon C**3** was not detected due to quadrupolar broadening.*

The spectroscopic properties were consistent with the data available in the literature.[191]

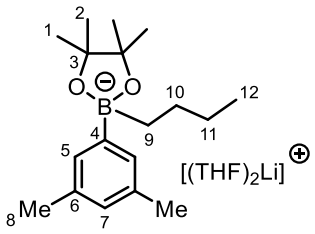

397

2-Butyl-2-(3,5-dimethylphenyl)-4,4,5,5-tetramethyl-1,3,2-dioxaborolane-2-uide tetrahydrofuran iodide complex (397): 2-(3,5-Dimethylphenyl)-4,4,5,5-tetramethyl-1,3,2-dioxaborolane (4.53 g, 13.9 mmol) was loaded into a flame-dried Schlenk flask and dried under vacuum. THF (28 mL) was added and the solution was cooled to -20 °C. *n*Butyllithium (2.3 M in hexanes, 6.04 mL, 13.9 mmol) was added over 15 mins and the reaction was stirred at -20 °C for 2 h, and then stirred at room temperature for 1 h. Solvents were removed *in vacuo* and product was dried *in vacuo* for 18 h to a colourless solid. Starting material remained, so the reaction was repeated using the crude product, with THF (28 mL) and *n*Butyllithium (2.3 M in hexanes, 6.04 mL, 13.9 mmol), washing with hexane (20 mL) to give the title compound (3.96 g, 13.9 mmol, 65%) as a colourless solid. δ_H (500 MHz, $CDCl_3$): 6.85 (2H, s, C**5**-H), 6.74 (1H, s, C**7**-H), 3.71 (8H, br s, THF 2×OCH_2), 2.17 (6H, s, C**8**-H_3), 1.86 (8H, br s, THF 2×CH_2), 1.36-0.65 (19H, m, C**1**-H_3, C**2**-H_3, C**10**-H_2, C**11**-H_2, C**12**-H_3), 0.42 (2H, m, C**9**-H_2). δ_C (126 MHz,

$CDCl_3$): 137.5 (C**6**), 128.3 (C**5**), 127.7 (C**7**), 79.0 (C**3**), 68.2 (THF O<u>C</u>H_2), 30.1 (C**10**), 27.1 (C**11**), 26.8-26.0 (br m, C**1**, C**2**, C**12**), 25.7 (THF <u>C</u>H_2), 21.7 (C**8**), 14.1 (C**12**). *Carbons C**4** and C**9** were not detected due to quadrupolar broadening.*

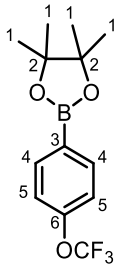

477

<u>4,4,5,5-Tetramethyl-2-(4-(trifluoromethoxy)phenyl)-1,3,2-dioxaborolane (477):</u> (4-(Trifluoromethoxy)phenyl)boronic acid (2.72 g, 13.2 mmol) was dissolved in Et_2O (50 mL). Pinacol (1.56 g, 13.2 mmol) was added and the reaction was stirred for 1 h. One spatula of Na_2SO_4 was added (approx. 1.0 g), and the reaction was stirred at room temperature for 16 h. The solution was filtered and concentrated to give title compound (3.68 g, 97%) as a colourless oil. δ_H (500 MHz, $CDCl_3$): 7.84 (2H, d, *J* = 8.5 Hz, C**4**-<u>H</u>), 7.20 (2H, d, *J* = 8.5 Hz, C**5**-<u>H</u>), 1.34 (12H, s, C**1**-<u>H_3</u>). δ_C (101 MHz, $CDCl_3$): 151.8 (q, *J* = 1.5 Hz, C**6**), 136.7 (C**4**), 120.6 (q, *J* = 261 Hz, O<u>C</u>F_3), 120.0 (C**5**), 84.2 (C**2**), 25.0 (C**1**). δ_F (376 MHz, $CDCl_3$): -57.6. *Carbon C**3** was not detected due to quadrupolar broadening.*

The spectroscopic properties were consistent with the data available in the literature.[192]

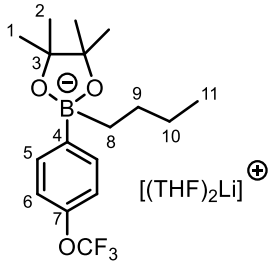

398

<u>2-Butyl-4,4,5,5-tetramethyl-2-(4-(trifluoromethoxy)phenyl)-1,3,2-dioxaborolane-2-uide tetrahydrofuran iodide complex (398):</u> 4,4,5,5-Tetramethyl-2-(4-(trifluoromethoxy)phenyl)-1,3,2-dioxaborolane (3.64 g, 12.6 mmol) was loaded into a flame-dried Schlenk flask and dried under vacuum. THF (26 mL) was added and the solution was cooled to -20 °C. *n*Butyllithium (2.3 M in hexanes, 7.12 mL, 16.4 mmol) was added over 15 mins and the reaction was stirred at -20 °C for 2 h, and then stirred at room temperature for 1 h. Solvents were removed *in vacuo* and product was washed with hexane (20 mL), then dried *in vacuo* for 18 h to provide the title compound (4.41 g, 8.89 mmol, 71%) as a colourless solid. δ_H (400 MHz, $CDCl_3$): 7.33 (2H, d, *J* = 7.0 Hz, C**5**-<u>H</u>), 7.02 (2H, d, *J* = 7.0 Hz, C**6**-<u>H</u>), 3.70 (8H, br s, THF 2×OC<u>H_2</u>), 1.83 (8H, br s, THF 2×C<u>H_2</u>), 1.21-1.16 (2H, m, C**10**-<u>H_2</u>), 1.09 (6H, s, C**1/2**-<u>H_3</u>),

0.95 (6H, s, C**2/1**-$\underline{H}_3$), 0.91-0.81 (2H, m, C**9**-$\underline{H}_2$), 0.76 (3H, t, *J* = 7.0 Hz, C**11**-$\underline{H}_3$), 0.49-0.35 (2H, m, C**8**-$\underline{H}_2$). δ_C (101 MHz, $CDCl_3$): 154.1 (C**4**), 147.8 (br, C**7**), 132.3 (C**6**), 120.8 (q, *J* = 256.0 Hz, O$\underline{C}F_3$) 120.3 (C**5**), 79.2 (C**3**), 68.2 (THF O$\underline{C}H_2$), 30.1 (C**9**), 27.0 (C**8**), 26.5 (C**1,2**), 25.7 (THF $\underline{C}H_2$), 25.2 (C**10**), 14.0 (C**11**). δ_F (376 MHz, $CDCl_3$): -57.8.

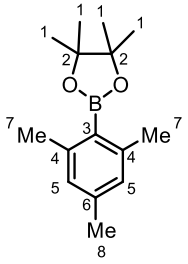

400

2-Mesityl-4,4,5,5-tetramethyl-1,3,2-dioxaborolane (400): 2,4,6-Trimethylphenylboronic acid (1.64 g, 10.0 mmol) was dissolved in Et_2O (40 mL). Pinacol (1.18 g, 10.0 mmol) was added and the reaction was stirred for 2 days. The solution was concentrated to give the title compound (2.64 g, 100%) as a colourless oil. δ_H (400 MHz, $CDCl_3$): 6.83 (2H, s, C**5**-$\underline{H}$), 2.35 (6H, s, C**7**-$\underline{H}_3$), 2.27 (3H, s, C**8**-$\underline{H}_3$), 1.23 (12H, s, C**1**-$\underline{H}_3$). δ_C (101 MHz, $CDCl_3$): 139.8 (C**4**), 138.8 (C**6**), 127.4 (C**5**), 75.2 (C**2**), 25.0 (C**1**), 22.2 (C**7**), 21.3 (C**8**). *Carbon C**3** was not detected due to quadrupolar broadening.*

The spectroscopic properties were consistent with the data available in the literature.[193]

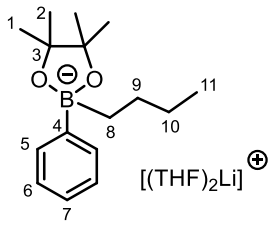

350

2-Butyl-4,4,5,5-tetramethyl-2-phenyl-1,3,2-dioxaborolan-2-uide tetrahydrofuran iodide complex (350): 2-Mesityl-4,4,5,5-tetramethyl-1,3,2-dioxaborolane (2.08 g, 10.2 mmol) was loaded into a flame-dried Schlenk flask and dried under vacuum. THF (21 mL) was added and the solution was cooled to -20 °C. *n*Butyllithium (2.3 M in hexanes, 5.8 mL, 13.3 mmol) was added over 15 mins and the reaction was stirred at -20 °C for 2 h, and then stirred at room temperature for 1 h. Solvents were removed *in vacuo* and product was washed with hexane (20 mL), then dried *in vacuo* for 18 h to provide the title compound (2.65 g, 10.2 mmol, 100%) as a colourless solid. δ_H (500 MHz, $CDCl_3$): 7.28 (2H, d, *J* = 7.0 Hz, C**5**-$\underline{H}$), 7.21 (2H, dd, *J* = 7.0, 7.0 Hz, C**6**-$\underline{H}$), 7.12 (1H, dd, *J* = 7.0, 7.0 Hz, C**9**-$\underline{H}$), 3.74-3.67 (8H, m, THF 2×OC$\underline{H}_2$), 1.87-1.80 (8H, m, THF 2×C$\underline{H}_2$), 1.25-1.67 (2H, m, C**10**-$\underline{H}_2$), 1.08 (6H, s, C**1/2**-$\underline{H}_3$), 0.94 (6H, s, C**2/1**-$\underline{H}_3$), 0.91-0.84 (2H, m, C**9**-$\underline{H}_2$), 0.76 (3H, t, *J* = 7.5 Hz, C**11**-$\underline{H}_3$), 0.46-0.39 (2H, m, C**8**-$\underline{H}_2$). δ_C (127 MHz, $CDCl_3$): 130.5 (C**5**), 128.4 (C**6**), 125.8 (C**7**), 19.2 (C**3**), 68.2 (THF O$\underline{C}H_2$), 30.0

(C**9**), 27.1 (C**10**), 26.5 (C**1/2**), 26.3 (C**2/1**), 25.7 (THF $\underline{C}H_2$), 14.1 (C**11**). *Carbons C**4** and C**8** were not detected due to quadrupolar broadening.*

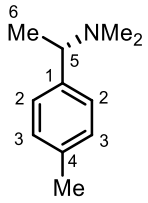

358

***(S)-N,N*-Dimethyl-1-(*p*-tolyl)ethan-1-amine (358):** General Procedure **6** (*Eschweiler-Clark reaction)* was followed using *(S)*-1-(p-tolyl)ethan-1-amine (2.55 mL, 17.5 mmol), formaldehyde (77 mL) and formic acid (140 mL). Purification by FCC (0-4% MeOH/CH_2Cl_2) provided the title compound (1.76 g, 62%) as a yellow oil. R_f = 0.19 (4% MeOH in CH_2Cl_2). ν_{max} / cm^{-1}: 2974 (m), 2813 (m), 2765 (s), 1453 (s), 1079 (s), 955 (s), 821 (s). δ_H (400 MHz, $CDCl_3$): 7.18 (2H, d, *J* = 8.0 Hz, C**2**-$\underline{H}$), 7.13 (2H, d, *J* = 8.0 Hz, C**3**-$\underline{H}$), 3.25 (1H, q, *J* = 6.5 Hz, C**5**-$\underline{H}$), 2.34 (3H, s, C**4**-C$\underline{H}_3$), 2.20 (6H, s, N(C$\underline{H}_3$)$_2$), 1.37 (3H, d, *J* = 6.5 Hz, C**6**-$\underline{H}_3$). δ_C (101 MHz, $CDCl_3$): 140.8 (C**1**), 136.7 (C**4**), 129.1 (C**3**), 127.6 (C**2**), 65.8 (C**5**), 43.3 (N($\underline{C}H_3$)$_2$), 21.2 (C**4**-$\underline{C}H_3$), 20.3 (C**6**). *m/z* (ESI^+) HRMS: Calculated for $C_{11}H_{17}N$: 163.1361. Found $[M+H]^+$: 164.1439. $[\alpha]^{24}_D$ = -56.88 (c 0.235, $CHCl_3$).

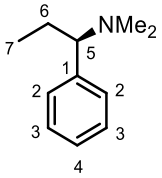

377

***(R)-N,N*-Dimethyl-1-phenylpropan-1-amine (377):** General Procedure **6** (*Eschweiler-Clark reaction)* was followed using *(R)*-1-phenylpropan-1-amine (0.43 mL, 3.00 mmol), formaldehyde (13 mL), and formic acid (24 mL). Purification by FCC (2% NEt_3 in EtOAc) provided the title compound (408 mg, 83%) as a colourless oil. R_f = 0.28 (2% NEt_3 in EtOAc). ν_{max} / cm^{-1}: 2959 (m), 2815 (m), 2768 (m), 1600 (m), 1452 (s), 766 (s), 702 (s). δ_H (400 MHz, $CDCl_3$): 7.35-7.29 (2H, m, C**3**-$\underline{H}$), 7.28-7.20 (3H, m, C**2**-$\underline{H}$, C**4**-$\underline{H}$), 3.07 (1H, dd, *J* = 9.5, 4.5 Hz, C**5**-$\underline{H}$), 2.19 (6H, s, N(C$\underline{H}_3$)$_2$), 2.01-1.89 (1H, m, C**6**-$\underline{H}_a$), 1.80-1.68 (1H, m, C**6**-$\underline{H}_b$), 0.72 (3H, t, *J* = 7.5 Hz, C**7**-$\underline{H}_3$). δ_C (101 MHz, $CDCl_3$): 140.6 (C**1**), 128.8 (C**2**), 128.1 (C**3**), 127.2 (C**4**), 72.8 (C**5**), 43.1 (N($\underline{C}H_3$)$_2$), 26.2 (C**6**), 11.0 (C**7**). *m/z* (ESI^+) HRMS: Calculated for $C_{11}H_{17}N$: 163.1361. Found $[M+H]^+$: 164.1439. $\mathbf{[\alpha]^{24}_D}$ = 12.25 (c 0.2205, $CHCl_3$).

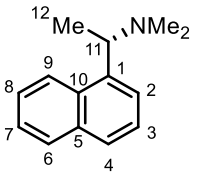

374

***(S)-N,N*-Dimethyl-1-(napthalen-1-yl)ethan-1-amine (374):** General Procedure **6** *(Eschweiler-Clark reaction)* was followed using *(S)*-1-(naphthalen-1-yl)ethan-1-amine (0.48 mL, 3.00 mmol), formaldehyde (13 mL) and formic acid (24 mL). FCC (2% NEt_3; 49% EtOAc in hexane) provided the title compound (438 mg, 85%) as a yellow oil. R_f = 0.36 (2% NEt_3 in EtOAc). ν_{max} / cm^{-1}: 2975 (m), 2814 (m), 2765 (m), 1455 (m), 800 (s), 778 (s). δ_H (400 MHz, $CDCl_3$): 8.38 (1H, d, *J* = 8.5 Hz, C**9**-H), 7.86 (1H, d, *J* = 8.0 Hz, Ar-H), 7.75 (1H, d, *J* = 8.0 Hz, Ar-H), 7.61 (1H, d, *J* = 7.0 Hz, Ar-H), 7.54-7.41 (3H, m, 3×Ar-H), 4.05 (1H, q, *J* = 6.5 Hz, C**11**-H), 2.30 (6H, s, $N(CH_3)_2$), 1.50 (3H, d, *J* = 6.5 Hz, C**12**-H_3). δ_C (101 MHz, $CDCl_3$): 139.3 (C**1**), 134.1 (ArC), 131.7 (ArC), 129.0 (ArCH), 127.5 (ArCH), 125.8 (ArCH), 125.6 (ArCH), 125.5 (ArCH), 124.6 (ArCH), 123.9 (C**9**), 62.4 (C**11**), 43.7 ($N(CH_3)_2$), 19.2 (C**12**). *m/z* (ESI^+) HRMS: Calculated for $C_{14}H_{17}N$: 200.1443. Found $[M+H]^+$: 200.1443. $[\alpha]^{24}_D$ = -66.34 (c 0.250, $CHCl_3$).

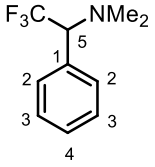

378

2,2,2-Trifluoro-*N,N*-dimethyl-1-phenylethan-1-amine (378): General Procedure **6** (*Eschweiler-Clark reaction)* was followed using 2,2,2-trifluoro-1-phenylethan-1-amine (525 mg, 3.00 mmol), formaldehyde (13 mL), and formic acid (24 mL). Purification by FCC (10% EtOAc/Hexane) provided the title compound (323 mg, 53%) as a colourless oil. δ_H (400 MHz, $CDCl_3$): 7.43-7.33 (5H, m, C**2**-H, C**3**-H, C**4**-H), 3.95 (1H, q, *J* = 8.5 Hz, C**5**-H), 2.34 (6H, s, $N(CH_3)_2$). δ_C (101 MHz, $CDCl_3$): 132.2 (C**1**) 129.5 (C**2**), 128.8 (C**4**), 128.6 (C**3**), 128.4 (q, *J* = 254.5 Hz, CF_3), 70.9 (q, *J* = 27.5 Hz, C**5**), 43.3 ($N(CH_3)_2$). δ_F (400 MHz, $CDCl_3$): -67.2 (d, *J* = 8.5 Hz).

The spectroscopic properties were consistent with the data available in the literature.[194]

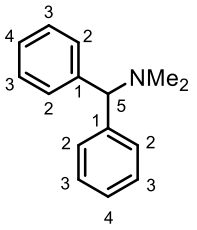

379

***N,N*-Dimethyl-1,1-diphenylmethanamine (379):** General Procedure **6** (*Eschweiler-Clark reaction)* was followed using diphenylmethanamine (2.13 g, 11.6 mmol), formaldehyde (51 mL), and formic acid (94 mL). Purification by FCC (0-25% EtOAc/Hexane; 0-4% MeOH/CH_2Cl_2) provided the title compound (849 mg, 35%) as a colourless solid. M.P.: 63-64 °C.[195] δ_H (500 MHz, $CDCl_3$): 7.41 (4H, d, *J* = 7.5 Hz, C**3**-H), 7.25 (4H, dd, *J* = 7.5, 7.5 Hz, C**2**-H), 7.16 (2H, dd, *J* = 7.5, 7.5 Hz, C**4**-H), 4.05 (1H, s, C**5**-H), 2.19 (6H, s, N(CH_3)$_2$). δ_C (126 MHz, $CDCl_3$): 143.6 (C**1**), 128.6 (C**2**), 127.9 (C**3**), 127.0 (C**4**), 78.2 (C**5**), 44.9 (N(CH_3)$_2$).

The spectroscopic properties were consistent with the data available in the literature.[195]

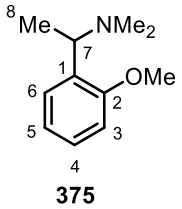

375

1-(2-Methoxyphenyl)-*N,N*-dimethylethan-1-amine (375): General Procedure **6** (*Eschweiler-Clark reaction)* was followed using 1-(2-methoxyphenyl)ethan-1-amine (454 mg, 3.00 mmol), formaldehyde (13 mL), and formic acid (24 mL). FCC (100% EtOAc to 2% NEt_3/EtOAc) provided the title compound (117 mg, 22%) as a pale yellow oil. R_f = 0.04 (100% EtOAc). ν_{max} / cm^{-1}: 2975 (m), 2944 (m), 2814 (m), 2765 (m), 1724 (m), 1455 (m), 1239 (s), 1030 (s), 754 (s). δ_H (400 MHz, $CDCl_3$): 7.38 (1H, dd, *J* = 7.5, 2.0 Hz, C**6**-H), 7.20 (1H, ddd, *J* = 8.0, 7.5, 2.0 Hz, C**4**-H), 6.95 (1H, dd, *J* = 7.5, 7.5, 1.0 Hz, C**5**-H), 6.87 (1H, dd, *J* = 8.0, 1.0 Hz, C**3**-H), 3.85 (1H, q, *J* = 7.0 Hz, C**7**-H), 3.82 (3H, s, OCH_3), 2.21 (6H, s, N(CH_3)$_2$), 1.31 (3H, d, *J* = 7.0 Hz, C**8**-H_3). δ_C (101 MHz, $CDCl_3$): 157.1 (C**2**), 132.2 (C**1**), 127.9 (C**6**), 127.7 (C**4**), 120.6 (C**5**), 110.7 (C**3**), 57.1 (C**7**), 55.6 (OCH_3), 43.3 (N(CH_3)$_2$), 19.6 (C**8**). *m/z* (ESI^+) HRMS: Calculated for $C_{11}H_{17}NO$: 180.1388. Found $[M+H]^+$: 180.1383.

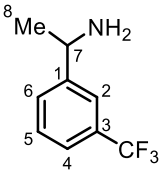

478

1-(3-(Trifluoromethyl)phenyl)ethan-1-amine (478): $Ti(O^iPr)_4$ (5.92 mL, 20.0 mmol) was loaded into a flame dried, 2-neck flask with attached condenser. Ammonia (7.0 M in MeOH; 4.30 mL, 30.0 mmol), then 1-(3-(trifluoromethyl)phenyl)ethan-1-one (1.52 mL, 10.0 mmol) in MeOH (20 mL) was added. The reaction was then stirred at 50 °C for 17.5 h, and cooled to room temperature. Sodium borohydride (378 mg, 10 mmol) was added portionwise, and the reaction was stirred at room temperature for a further 3.5 h. The solution was then filtered and concentrated to a colourless paste (2.00 g). FCC (2% CH_2Cl_2/MeOH) provided the title compound (611 mg, 32%) as a yellow oil. δ_H (400 MHz, $CDCl_3$):

7.62 (1H, s, C**2**-H), 7.55 (1H, d, *J* = 7.5 Hz, C**6**-H), 7.50 (1H, d, *J* = 7.5 Hz, C**4**-H), 7.44 (1H, dd, *J* = 7.5, 7.5 Hz, C**5**-H), 4.20 (1H, q, *J* = 6.5 Hz, C**7**-H), 1.65 (2H, s, NH_2), 1.40 (3H, d, *J* = 6.5 Hz, C**8**-H_3). δ_C (101 MHz, $CDCl_3$): 148.6 (C**1**), 130.9 (d, *J* = 32.0 Hz. C**3**), 129.4 (C**6**), 129.1 (C**5**), 124.4 (q, *J* = 272.0 Hz, CF_3), 123.8 (q, *J* = 3.5 Hz, C**4**), 122.8 (q, *J* = 3.5 Hz, C**2**), 51.2 (C**7**), 25.9 (C**8**). δ_F (400 MHz, $CDCl_3$): -62.4.

The spectroscopic properties were consistent with the data available in the literature.[196]

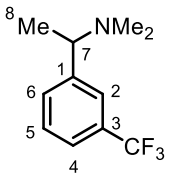

376

***N,N*-Dimethyl-1-(3-trifluoromethyl)phenyl)ethan-1-amine (376):** General Procedure **6** (*Eschweiler-Clark reaction)* was followed using 1-(3-(trifluoromethyl)phenyl)ethan-1-amine (611 mg, 3.20 mmol), formaldehyde (14 mL), and formic acid (26 mL). FCC (100% EtOAc) provided title compound (339 mg, 49%) as a colourless oil. R_f = 0.32 (2% NEt_3 in EtOAc). ν_{max} / cm^{-1}: 2980 (m), 2820 (m), 2771 (m), 1446 (m), 1324 (s), 1269 (m), 1163 (s), 1123 (s), 1071 (m), 705 (m). δ_H (400 MHz, $CDCl_3$): 7.56 (1H, s, C**2**-H), 7.52-7.48 (2H, m, C**4**-H, C**6**-H), 7.43 (1H, dd, *J* = 7.5, 7.5 Hz, C**5**-H), 3.31 (1H, q, *J* = 6.5 Hz, C**7**-H), 2.20 (6H, s, $N(CH_3)_2$), 1.37 (3H, d, *J* = 6.5 Hz, C**8**-H_3). δ_C (101 MHz, $CDCl_3$): 145.5 (C**1**), 130.7 (q, *J* = 32.0 Hz, C**3**), 130.1 (C**6**), 128.9 (q, *J* = 1.5 Hz, C**5**), 124.4 (q, *J* = 273.0 Hz, CF_3), 124.3 (q, *J* = 4.0 Hz, C**2**), 124.0 (q, *J* = 4.0 Hz, C**4**), 65.8 (C**7**), 43.3 ($N(CH_3)_2$), 20.3 (C**8**). δ_F (376 MHz, $CDCl_3$): -62.3. *m/z* (ESI^+) HRMS: Calculated for $C_{11}H_{15}F_3N$: 217.1078. Found $[M+H]^+$: 218.1151.

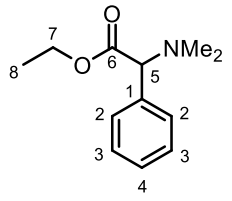

381

Ethyl 2-(dimethylamino)-2-phenylacetate (381): Ethyl 2-bromo-2-phenylacetate (0.70 mL, 4.00 mmol) was dissolved in THF (15 mL), and Na_2CO_3 (424 mg, 4.00 mmol) was added. Dimethylamine solution (2.0 M in THF, 2.2 mL, 4.4 mmol) was added dropwise to the stirred solution, and the reaction was stirred at room temperature for 18 h. The reaction was then filtered under pressure, and washed with EtOAc. The filtrate was concentrated and partitioned between CH_2Cl_2 (3×15 mL) and H_2O (20 mL). The organics were combined and collected, dried over Na_2CO_3, filtered, and concentrated to a pale yellow oil (911 mg). FCC (25% EtOAc/Hexane) provided the title compound (413 mg, 50%) as a colourless oil. δ_H (400 MHz, $CDCl_3$): 7.46-7.41 (2H, m, C**2**-H), 7.37-7.28 (3H, m, C**3**-H, C**4**-H), 4.25-

4.08 (2H, m, C**7**-H$_2$), 3.85 (1H, s, C**5**-H), 2.25 (6H, s, N(CH$_3$)$_2$), 1.21 (3H, t, *J* = 7.0 Hz, C**8**-H$_3$). δ_C (101 MHz, $CDCl_3$): 171.9 (C**6**), 136.6 (C**1**), 128.9 (C**2**), 128.7 (C**3**), 128.5 (C**4**), 75.6 (C**5**), 61.1 (C**7**), 43.6 (N(CH$_3$)$_2$), 14.2 (C**8**).

The spectroscopic properties were consistent with the data available in the literature.[197]

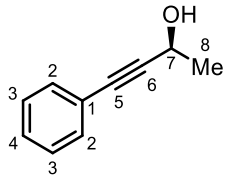

383

***(S)*-4-Phenylbut-3-yn-2-ol (383):** Into a dry 2-neck flask was loaded copper iodide (11.5 mg, 0.06 mmol) and $Pd(PPh_3)_2Cl_2$ (42 mg, 0.06 mmol). The flask was purged with nitrogen, and DMF (1.5 mL) was added, followed by iodobenzene (0.34 mL, 3.00 mmol), *(S)*-but-3-yn-2-ol (0.24 mL, 3.00 mmol), and NEt_3 (2.93 mL, 21.0 mmol). The mixture was then stirred at room temperature for 18 h, before quenching with saturated NH_4Cl solution (15 mL). The aqueous was then extracted with EtOAc (3×9 mL), the organics were combined, washed with brine (15 mL), dried over Na_2SO_4, filtered and concentrated to a brown oil (688 mg). FCC (10% EtOAc/hexane) gave the title compound (438 mg, 100%) as an orange oil. δ_H (400 MHz, $CDCl_3$): 7.45-7.40 (2H, m, C**2**-H), 7.33-7.28 (3H, m, C**3**-H, C**4**-H), 4.76 (1H, q, *J* = 6.5 Hz, C**7**-H), 1.63 (1H, br s, OH), 1.56 (3H, d, *J* = 6.5 Hz, C**8**-H$_3$). δ_C (101 MHz, $CDCl_3$): 131.8 (C**2**), 128.5 (C**4**), 128.4 (C**3**), 122.7 (C**1**), 91.1 (C**6**), 84.2 (C**5**), 59.0 (C**7**), 24.5 (C**8**). $[\alpha]^{24}_D$ = -32.36 (c 0.244, $CHCl_3$).

The spectroscopic properties were consistent with the data available in the literature.[198]

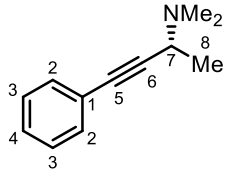

384

***(R)*-*N*,*N*-Dimethyl-4-phenylbut-3-yn-2-amine (384):** *(S)*-4-Phenylbut-3-yn-2-ol (398 mg, 2.72 mmol) was dissolved in THF (7 mL). Triethylamine (1.90 mL, 13.6 mmol) was added, and the solution was cooled to 0 °C. Mesyl chloride (0.42 mL, 5.44 mmol) was added, and the reaction was stirred at room temperature for 1 h. Dimethylamine solution (2.0 M in THF; 6.8 mL, 13.6 mmol) was added, and the reaction was stirred at 50 °C for 18 h. The solution was cooled, filtered through a Celite pad, washed with Et_2O, and concentrated to a brown oil (487 mg). FCC (25% EtOAc/hexane) provided the title compound (318 mg, 67%) as a brown oil. δ_H (400 MHz, $CDCl_3$): 7.45-7.40 (2H, m, C**2**-H), 7.32-7.28 (3H, m, C**3**-H, C**4**-H), 3.70 (1H, q, *J* = 7.0 Hz, C**7**-H), 2.34 (6H, s, N(CH$_3$)$_2$), 1.41 (3H, d, *J* = 7.0 Hz,

C**8**-H). δ_C (101 MHz, $CDCl_3$): 131.8 (C**2**), 128.3 (C**3**), 128.0 (C**4**), 123.4 (C**1**), 87.7 (C**6**), 85.4 (C**5**), 52.9 (C**7**), 41.4 ($N(CH_3)_2$), 20.1 (C**8**). $[\alpha]^{24}_D$ = 43.157 (c 0.276, $CHCl_3$).

The spectroscopic properties were consistent with the data available in the literature.[199]

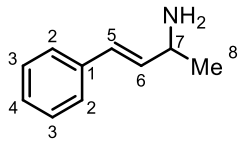

386

***(E)*-4-Phenylbut-3-en-2-amine (386):** *Step 1:* 4-Phenyl-3-buten-2-one (1.46 g, 10.0 mmol) and hydroxylammonium chloride (1.11 g, 16.0 mmol) were dissolved in ethanol (10 mL) and water (3 mL). NaOH (4.00 g, 50.0 mmol) was added portionwise, and the solution was stirred at 85 °C for 16 h. The reaction was cooled to room temperature, acidified to pH 2 with HCl (4.0 M, aqueous), then extracted with CH_2Cl_2 (3×20 mL). The organics were combined and concentrated to form the oxime intermediate, which was used directly in step 2.

Step 2: The oxime intermediate was dissolved in ethanol (8 mL) and acetic acid (glacial, 8 mL). The solution was cooled to 0 °C, and zinc dust (3.27 g, 50.0 mmol) was added portionwise. The reaction was stirred at 30 °C for 2 h, then filtered through celite. The filtrate was concentrated and the residue dissolved in HCl (4.0 M, 100 mL) and extracted with CH_2Cl_2 (3×30 mL). The aqueous layer was then basified to pH 12 using NaOH (12 M, aqueous), and extracted again with CH_2Cl_2 (3×30 mL). The organics were combined, washed with brine (20 mL), dried over $MgSO_4$, and concentrated to give the title compound (657 mg, 45%) as an orange oil. δ_H (400 MHz, $CDCl_3$): 7.37 (2H, d, *J* = 7.0 Hz, C**2**-H), 7.30 (2H, dd, *J* = 7.0, 7.0 Hz, C**3**-H), 7.22 (1H, dd, *J* = 7.0, 7.0 Hz, C**4**-H), 6.49 (1H, d, *J* = 16.0 Hz, C**5**-H), 6.22 (1H, dd, *J* = 16.0, 6.5 Hz, C**6**-H), 3.71 (1H, td, *J* = 6.5, 6.5 Hz, C**7**-H), 2.29 (2H, br s, NH_2), 1.29 (3H, d, *J* = 6.5 Hz, C**8**-H_3). δ_C (101 MHz, $CDCl_3$): 137.2 (C**1**), 135.2 (C**6**), 128.7 (C**3**), 128.6 (C**5**), 127.5 (C**4**), 126.5 (C**2**), 49.5 (C**7**), 23.6 (C**8**).

The spectroscopic properties were consistent with the data available in the literature.[200]

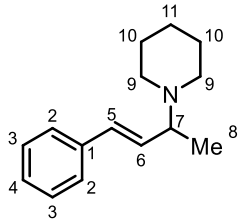

387

***(E)*-1-(4-Phenylbut-3-en-2-yl)piperidine (387):** Into a flame-dried Schlenk tube was loaded *(E)*-4-phenylbut-3-en-2-amine (291 mg, 1.98 mmol), dibromopentane (0.30 mL, 2.18 mmol), and sodium bicarbonate (366 mg, 4.36 mmol). The flask was evacuated and backfilled with nitrogen (×3), before

anhydrous toluene (3 mL) was added. The reaction tube was sealed, then stirred at 115 °C for 23 h before cooling to room temperature and concentrating *in vacuo*. FCC (75% EtOAc/1% NEt_3/Hexane) provided the title product (185 mg, 1.98 mmol, 43%) as an orange oil. δ_H (500 MHz, $CDCl_3$): 7.39-7.35 (2H, m, C**3**-H), 7.33-7.28 (2H, m, C**2**-H), 7.21 (1H, dddd, *J* = 7.5, 7.5, 1.5, 1.5 Hz, C**4**-H), 6.42 (1H, d, *J* = 16.0 Hz, C**5**-H), 6.24 (1H, dd, *J* = 16.0, 8.0 Hz, C**6**-H), 3.07 (1H, dt, *J* = 6.5, 6.5 Hz, C**7**-H), 2.59-2.43 (4H, m, C**9**-H_2), 1.65-1.55 (4H, m, C**10**-H_2), 1.46-1.39 (2H, m, C**11**-H_2), 1.25 (3H, d, *J* = 6.5 Hz, C**8**-H_3). δ_C (126 MHz, $CDCl_3$): 137.4 (C**1**), 133.1 (C**6**), 130.6 (C**5**), 128.7 (C**2**), 127.4 (C**4**), 126.4 (C**3**), 63.1 (C**7**), 51.2 (C**9**), 26.5 (C**10**), 24.8 (C**11**), 17.9 (C**8**).

The spectroscopic properties were consistent with the data available in the literature.[201]

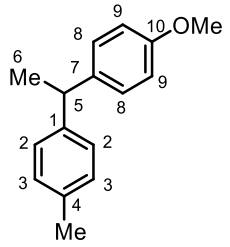

359

1-Methoxy-4-(1-(*p*-tolyl)ethyl)benzene (359): General Procedure **7** *(One-pot α-Secondary Benzylamine C–N Activation/Suzuki Cross-Coupling)* was followed using 2-butyl-2-(4-methoxyphenyl)-4,4,5,5-tetramethyl-1,3,2-dioxaborolan-2-uide tetrahydrofuran iodide complex (398 mg, 0.90 mmol), nickel (II) bromide 2-methoxyethyl ether complex (42.3 mmol, 0.12 mmol), *(S)*-4-*tert*-butyl-2-(2-pyridyl)oxazoline (30.6 mg, 0.15 mmol), and 1-(1-iodoethyl)-4-methylbenzene (0.1 M in THF, 0.60 mmol) prepared from *N*,*N*-dimethyl-1-(*p*-tolyl)ethan-1-amine (98 mg, 0.60 mmol). FCC (10% toluene/Hexane) provided the title product (83 mg, 61%) as a pale yellow oil. δ_H (400 MHz, $CDCl_3$): 7.13 (2H, d, *J* = 9.0 Hz, C**9**-H), 7.10 (4H, s, C**2**-H, C**3**-H), 6.82 (2H, d, *J* = 9.0 Hz, C**8**-H), 4.07 (1H, q, *J* = 7.0 Hz, C**5**-H), 3.78 (3H, s, OCH_3), 2.31 (3H, s, C**4**-CH_3), 1.60 (3H, d, *J* = 7.0 Hz, C**6**-H_3). δ_C (101 MHz, $CDCl_3$): 157.9 (C**10**), 144.0 (C**1**), 138.9 (C**7**), 135.5 (C**4**), 129.2 (C**3**), 128.6 (C**8**), 127.5 (C**2**), 113.8 (C**9**), 55.4 (OCH_3), 43.7 (C**5**), 22.3 (C**6**), 21.1 (C**4**-CH_3). $[\alpha]^{24}_D$ = 0.00 (c 0.235, $CHCl_3$). HPLC: tR = 11.560 mins, 45.1%; tR = 12.432 mins, 54.9%. (Chiral ART Amylose-SA, 150 x 4.6 mml.D., S-5 µm, 100% hexane, 0.75 mL/min).

The spectroscopic properties were consistent with the data available in the literature.[4]

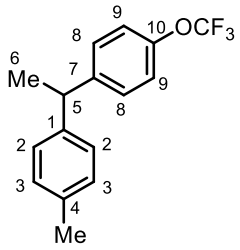

403

1-Methyl-4-(1-(4-(trifluoromethoxy)phenyl)ethyl)benzene (403): General Procedure **7** *(One-pot α-Secondary Benzylamine C–N Activation/Suzuki Cross-Coupling)* was followed using 2-butyl-4,4,5,5-tetramethyl-2-(4-(trifluoromethoxy)phenyl)-1,3,2-dioxaborolan-2-uide tetrahydrofuran iodide complex (447 mg, 0.90 mmol), nickel (II) bromide 2-methoxyethyl ether complex (42.3 mmol, 0.12 mmol), *(S)*-4-*tert*-butyl-2-(2-pyridyl)oxazoline (30.6 mg, 0.15 mmol), and 1-(1-iodoethyl)-4-methylbenzene (0.1 M in THF, 0.60 mmol) prepared from *N*,*N*-dimethyl-1-(*p*-tolyl)ethan-1-amine (98 mg, 0.60 mmol). FCC (100% hexane) provided the title product (84 mg, 50%) as a pale yellow oil. R_f = 0.05 (100% hexane). ν_{max} / cm^{-1}: 2969 (m), 2918 (m), 1508 (m), 1256 (s), 1222 (s), 1161 (s), 1018 (m), 814 (m). δ_H (400 MHz, $CDCl_3$): 7.22 (2H, d, *J* = 9.0 Hz, C**9**-H), 7.14-7.07 (6H, m, C**2**-H, C**3**-H, C**8**-H), 4.12 (1H, q, *J* = 7.0 Hz, C**5**-H), 2.32 (3H, s, C**4**-CH_3), 1.61 (3H, d, *J* = 7.0 Hz, C**6**-H_3). δ_C (101 MHz, $CDCl_3$): 145.5 (C**1**/**7**), 142.9 (C**7**/**1**), 136.0 (C**4**), 129.3 (C**3**), 128.9 (C**2**/**8**), 127.5 (C**8**/**2**), 121.0 (C**9**), 120.7 (q, *J* = 253.5 Hz, OCF_3), 43.9 (C**5**), 22.1 (C**6**), 21.1 (C**4**-CH_3). δ_F (471 MHz, $CDCl_3$): -57.9. *m/z* (CI^+) HRMS: Calculated for $C_{16}H_{16}F_3O$: 281.1153. Found $[M+H]^+$: 281.1507.

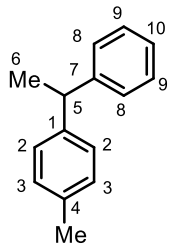

347

1-Methyl-4-(1-phenylethyl)benzene (347): General Procedure **7** *(One-pot α-Secondary Benzylamine C–N Activation/Suzuki Cross-Coupling)* was followed using 2-butyl-4,4,5,5-tetramethyl-2-phenyl-1,3,2-dioxaborolan-2-uide tetrahydrofuran iodide complex (371 mg, 0.90 mmol), nickel (II) bromide 2-methoxyethyl ether complex (42.3 mmol, 0.12 mmol), *(S)*-4-*tert*-butyl-2-(2-pyridyl)oxazoline (30.6 mg, 0.15 mmol), and 1-(1-iodoethyl)-4-methylbenzene (0.1 M in THF, 0.60 mmol) prepared from *N*,*N*-dimethyl-1-(*p*-tolyl)ethan-1-amine (98 mg, 0.60 mmol). FCC (100% hexane) provided the title product (42 mg, 36%) as a colourless oil. δ_H (500 MHz, $CDCl_3$): 7.30-7.26 (2H, m, C**9**-H), 7.23-7.20 (2H, m, C**8**-H), 7.17 (1H, dddd, *J* = 7.0, 7.0, 1.5, 1.5 Hz, C**10**-H), 7.13-7.08 (4H, m, C**2**-H, C**3**-H), 4.12 (1H, q, *J* = 7.0 Hz, C**5**-H), 2.31 (3H, s, C**4**-CH_3), 1.63 (3H, d, *J* = 7.0 Hz, C**6**-H_3). δ_C (126 MHz, $CDCl_3$): 146.7

(C**1**/**7**), 143.6 (C**7**/**1**), 135.6 (C**4**), 129.2 (C**2**/**3**), 128.5 (C**9**), 127.7 (C**3**/**2**), 127.6 (C**8**), 126.1 (C**10**), 44.5 (C**5**), 22.1 (C**6**), 21.1 (C**4**-CH_3).

The spectroscopic properties were consistent with the data available in the literature.[202]

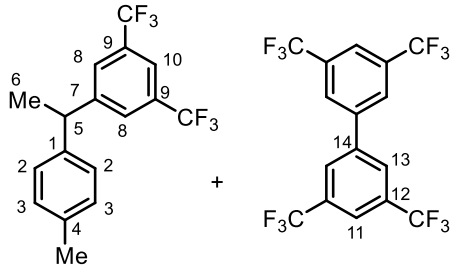

404 **479**

1-(1-(*p*-Tolyl)ethyl)-3,5-bis(trifluoromethyl)benzene (404): General Procedure **7** *(One-pot α-Secondary Benzylamine C–N Activation/Suzuki Cross-Coupling)* was followed using 2-(3,5-bis (trifluoromethyl)phenyl)-2-butyl-4,4,5,5-tetramethyl-1,3,2-dioxaborolan-2-uide tetrahydrofuran iodide complex (494 mg, 0.90 mmol), nickel (II) bromide 2-methoxyethyl ether complex (42.3 mmol, 0.12 mmol), *(S)*-4-*tert*-butyl-2-(2-pyridyl)oxazoline (30.6 mg, 0.15 mmol), and 1-(1-iodoethyl)-4-methylbenzene (0.1 M in THF, 0.60 mmol) prepared from *N*,*N*-dimethyl-1-(*p*-tolyl)ethan-1-amine (98 mg, 0.60 mmol). FCC (100% hexane) provided title products **404** and **479** (98 mg, **404**:**479** 2:1, **404** = 30%) as a colourless oil. R_f = 0.41 (100% hexane). ν_{max} / cm^{-1}: 2973 (m), 1371 (m), 1276 (s), 1167 (s), 1127 (s), 896 (m), 706 (m), 682 (s). δ_H (400 MHz, $CDCl_3$): 8.03 (2H, s, C**13**-H), 7.99 (1H, s, C**11**-H), 7.71 (1H, s, C**10**-H), 7.66 (2H, s, C**8**-H), 7.14 (2H, d, *J* = 8.0 Hz, C**3**-H), 7.09 (2H, d, *J* = 8.0 Hz, C**2**-H), 4.24 (1H, q, *J* = 7.0 Hz, C**5**-H), 2.34 (3H, s, C**4**-CH_3), 1.68 (3H, d, *J* = 7.0 Hz, C**6**-H_3). δ_C (101 MHz, $CDCl_3$): 149.3 (C**1**/**7**), 141.3 (C**7**/**1**), 140.6 (C**14**), 136.6 (C**4**), 133.1 (q, *J* = 32.0 Hz, C**12**), 131.7 (q, *J* = 33.0 Hz, C**9**), 129.7 (C**3**), 127.9 (q, *J* = 3.5 Hz, C**8**), 127.7 (q, *J* = 3.5 Hz, C**13**), 127.5 (C**2**), 123.6 (q, *J* = 272.0 Hz, CF_3), 123.2 (q, *J* = 274.5 Hz, CF_3), 122.8 (q, *J* = 4.0 Hz, C**11**), 120.3 (q, *J* = 4.0 Hz, C**10**), 44.4 (C**5**), 21.9 (C**6**), 21.1 (C**4**-CH_3). δ_F (400 MHz, $CDCl_3$): -62.8 (6F, s, C**9**-CF_3), -62.9 (6F, s, C**12**-CF_3). *m/z* (CI^+) HRMS: Calculated for $C_{17}H_{15}F_6$: 333.1078. Found $[M+H]^+$: 333.1438.

*The spectroscopic properties for product **479** were consistent with the data available in the literature.*[203]

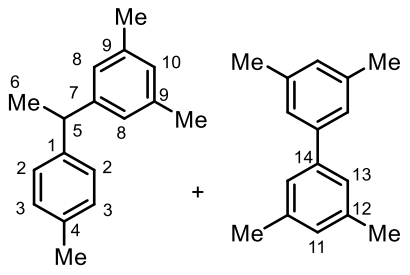

405 **480**

1,3-Dimethyl-5-(1-(p-tolyl)ethyl)benzene (405): General Procedure **7** *(One-pot α-Secondary Benzylamine C–N Activation/Suzuki Cross-Coupling)* was followed using 2-butyl-2-(3,5-dimethylphenyl)-4,4,5,5-tetramethyl-1,3,2-dioxaborolan-2-uide tetrahydrofuran iodide complex (396 mg, 0.90 mmol), nickel (II) bromide 2-methoxyethyl ether complex (42.3 mmol, 0.12 mmol), *(S)*-4-*tert*-butyl-2-(2-pyridyl)oxazoline (30.6 mg, 0.15 mmol), and 1-(1-iodoethyl)-4-methylbenzene (0.1 M in THF, 0.60 mmol) prepared from *N*,*N*-dimethyl-1-(*p*-tolyl)ethan-1-amine (98 mg, 0.60 mmol). FCC (100% hexane) provided title products **405** and **480** (79 mg, **405**:**480** = 12:1, **405** = 54%) as a colourless oil. R_f = 0.33 (100% hexane). ν_{max} / cm^{-1}: 3018 (m), 2965 (m), 2919 (m), 1601 (m), 1513 (s), 1451 (m), 848 (s), 817 (s), 701 (s). δ_H (500 MHz, $CDCl_3$): 7.19 (0.33H, s, C**13**-H), 7.12 (2H, d, *J* = 8.0 Hz, C**2**-H), 7.09 (2H, d, *J* = 8.0 Hz, C**3**-H), 6.94 (0.16H, s, C**11**-H), 6.83 (2H, s, C**8**-H), 6.82 (1H, s, C**10**-H), 4.04 (1H, q, *J* = 7.0 Hz, C**5**-H), 2.38 (1H, s, C**12**-CH_3), 2.31 (3H, s, C**4**-CH_3), 2.27 (6H, s, C**9**-CH_3), 1.59 (3H, d, *J* = 7.0 Hz, C**6**-H_3). δ_C (126 MHz, $CDCl_3$): 146.6 (C**7**), 143.8 (C**1**), 141.6 (C**14**), 138.2 (C**12**), 137.9 (C**9**), 135.5 (C**4**), 129.1 (C**3**), 128.6 (C**11**), 127.8 (C**2**), 127.6 (C**10**), 125.5 (C**8**), 125.3 (C**13**), 44.4 (C**5**), 22.1 (C**6**), 21.6 (C**12**-CH_3), 21.5 (C**9**-CH_3), 21.1 (C**4**-CH_3). *m/z* (CI^+) HRMS: Calculated for $C_{17}H_{21}$: 225.1643. Found $[M+H]^+$: 225.1947.

*The spectroscopic properties for product **480** were consistent with the data available in the literature.*[204]

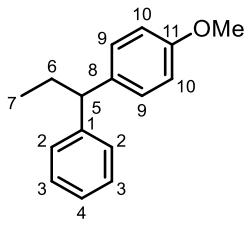

389

1-Methoxy-4-(1-phenylpropyl)benzene (389): General Procedure **7** *(One-pot α-Secondary Benzylamine C–N Activation/Suzuki Cross-Coupling)* was followed using 2-butyl-2-(4-methoxyphenyl)-4,4,5,5-tetramethyl-1,3,2-dioxaborolan-2-uide tetrahydrofuran iodide complex (398 mg, 0.90 mmol), nickel (II) bromide 2-methoxyethyl ether complex (42.3 mmol, 0.12 mmol), *(S)*-4-*tert*-butyl-2-(2-pyridyl)oxazoline (30.6 mg, 0.15 mmol), and (1-iodopropyl)benzene (0.1 M in THF, 0.60 mmol) prepared from *N*,*N*-dimethyl-1-phenylpropan-1-amine (98 mg, 0.60 mmol). FCC (0-5% EtOAc/Hexane) provided title product (44 mg, 32%) as a colourless oil. δ_H (500 MHz, $CDCl_3$): 7.30-.25 (2H, m, C**2**-H), 7.24-7.20 (2H, m, C**3**-H), 7.18-7.13 (3H, m, C**9**-H, C**4**-H), 6.82 (2H, d, *J* = 8.5 Hz, C**10**-H), 3.77 (3H, s, OCH_3), 3.74 (1H, t, *J* = 7.5 Hz, C**5**-H), 2.04 (2H, dt, *J* = 7.5, 7.5 Hz, C**6**-H_2), 0.89 (3H, t, *J* = 7.5 Hz, C**7**-H_3). δ_C (126 MHz, $CDCl_3$): 158.0 (C**11**), 145.7 (C**1**), 137.5 (C**8**), 128.9 (C**9**), 128.5 (C**2**), 128.0 (C**3**), 126.1 (C**4**), 113.9 (C**10**), 55.4 (OCH_3), 52.5 (C**5**), 28.9 (C**6**), 12.9 (C**7**).

The spectroscopic properties were consistent with the data available in the literature.[205]

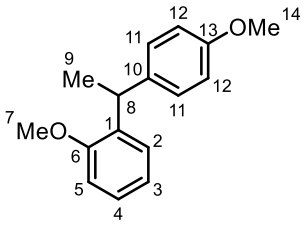

390

1-Methoxy-2-(1-(4-methoxyphenyl)ethyl)benzene (390): General Procedure **7** *(One-pot α-Secondary Benzylamine C–N Activation/Suzuki Cross-Coupling)* was followed using 2-butyl-2-(4-methoxyphenyl)-4,4,5,5-tetramethyl-1,3,2-dioxaborolan-2-uide tetrahydrofuran iodide complex (398 mg, 0.90 mmol), nickel (II) bromide 2-methoxyethyl ether complex (42.3 mmol, 0.12 mmol), *(S)*-4-*tert*-butyl-2-(2-pyridyl)oxazoline (30.6 mg, 0.15 mmol), and 1-(1-iodoethyl)-2-methoxybenzene (0.1 M in THF, 0.60 mmol) prepared from 1-(2-methoxyphenyl)-*N*,*N*-dimethylethan-1-amine (108 mg, 0.60 mmol). FCC (0-10% EtOAc/Hexane) provided the title product (25 mg, 17%) as a pale yellow oil. δ_H (500 MHz, $CDCl_3$): 7.19-7.14 (3H, m, C**11**-H, C**5**-H), 7.13 (1H, dd, *J* = 7.5, 1.5 Hz, C**2**-H), 6.90 (1H, ddd, *J* = 7.5, 7.5, 1.0 Hz, C**3**-H), 6.84 (1H, dd, *J* = 7.5, 1.5 Hz, C**4**-H), 6.83-6.79 (2H, m, C**12**-H), 4.53 (1H, q, *J* = 7.0 Hz, C**8**-H), 3.79 (3H, s, OC**14**-H_3), 3.78 (3H, s, OC**7**-H_3), 1.55 (3H, d, *J* = 7.0 Hz, C**9**-H_3). δ_C (126 MHz, $CDCl_3$): 157.7 (C**13**), 156.9 (C**6**), 138.6 (C**10**), 135.4 (C**1**), 128.7 (C**11**), 127.7 (C**5**), 127.1 (C**2**), 120.6 (C**3**), 113.6 (C**12**), 110.7 (C**4**), 55.6 (C**7**), 55.3 (C**14**), 36.7 (C**8**), 21.2 (C**9**).

The spectroscopic properties were consistent with the data available in the literature.[206]

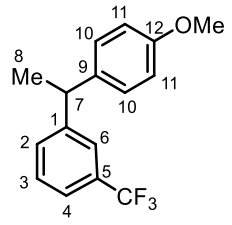

391

1-(1-(4-methoxyphenyl)ethyl)-3-(trifluoromethyl)benzene (391): General Procedure **7** *(One-pot α-Secondary Benzylamine C–N Activation/Suzuki Cross-Coupling)* was followed using 2-butyl-2-(4-methoxyphenyl)-4,4,5,5-tetramethyl-1,3,2-dioxaborolan-2-uide tetrahydrofuran iodide complex (398 mg, 0.90 mmol), nickel (II) bromide 2-methoxyethyl ether complex (42.3 mmol, 0.12 mmol), *(S)*-4-*tert*-butyl-2-(2-pyridyl)oxazoline (30.6 mg, 0.15 mmol), and 1-(1-iodoethyl)-3-(trifluoromethyl)benzene (0.1 M in THF, 0.60 mmol) prepared from *N*,*N*-dimethyl-1-(3-(trifluoromethyl)phenyl)ethan-1-amine (130 mg, 0.60 mmol). FCC (0-10% EtOAc/Hexane) provided title product (37 mg, 22%) as a colourless oil. $\mathbf{R_f}$ = 0.087 (100% hexane). $\mathbf{\nu_{max}}$ **/ cm^{-1}**: 2967 (m), 2935 (m), 1611 (m), 1511 (s), 1327 (s), 1246 (s), 1161 (s), 1121 (s), 1075 (s), 1035 (s), 831 (s), 802 (s), 702 (s). δ_H (500 MHz, $CDCl_3$): 7.48 (1H, s, C**6**-H), 7.46-7.42 (1H, m, C**4**-H), 7.39-7.36 (2H, m, C**2**-H, C**3**-H), 7.12 (2H, d, *J* = 8.5 Hz, C**10**-H), 6.85 (2H, d, *J* = 8.5 Hz, C**11**-H), 4.16 (1H, q, *J* = 7.0 Hz, C**7**-H),

3.79 (3H, s, OC<u>H</u>$_3$), 1.64 (3H, d, *J* = 7.0 Hz, C**8**-<u>H</u>$_3$). δ_C (126 MHz, $CDCl_3$): 158.2 (C**12**), 147.8 (C**1**), 137.6 (C**9**), 131.2 (C**2**), 130.7 (q, *J* = 32.0 Hz, C**5**), 128.9 (C**3**), 128.6 (C**10**), 124.4 (q, *J* = 273.0 Hz, <u>C</u>F$_3$), 124.3 (q, *J* = 4.0 Hz, C**6**), 123.0 (q, *J* = 4.0 Hz, C**4**), 114.1 (C**11**), 55.4 (O<u>C</u>H$_3$), 44.0 (C**7**), 22.1 (C**8**). δ_F (471 MHz, $CDCl_3$): -62.5 (s). *m/z* (ESI^+) HRMS: Calculated for $C_{16}H_{15}F_3O$: 280.1075. Found $[M]^+$: 280.0976.

7.6. Experimental Procedures for the Studies in Chapter 5

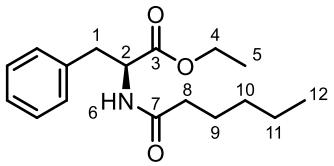

434

<u>Ethyl hexanoyl-*L*-phenylalaninate (434):</u> To a solution of L-phenylalanine ethyl ester hydrochloride (1.15 g, 5.0 mmol) in dry CH_2Cl_2 (0.10 M) was added DIPEA (2.2 mL, 12.5 mmol). The mixture was cooled to 0 °C and hexanoyl chloride (0.76 mL, 5.5 mmol) was added dropwise. The mixture was warmed to room temperature and stirred for 16 h. The mixture was washed with acidified brine (×3) and $NaHCO_3$ (sat. aq.). The organic extracts were dried over Na_2SO_4, filtered, and concentrated *in vacuo*. Purification by FCC (20% EtOAc/Hexane) provided the title compound (1.658 g, 100%) as a yellow oil. δ_H (400 MHz, $CDCl_3$): 7.32-7.22 (3H, m, Ar<u>H</u>), 7.13-7.08 (2H, m, Ar<u>H</u>), 5.95-5.87 (1H, m, N<u>H</u>), 4.92-4.85 (1H, m, C**2**-<u>H</u>), 4.18 (2H, q, *J* = 7.0 Hz, C**4**-<u>H</u>$_2$), 3.13 (2H, m, C**1**-<u>H</u>$_2$), 2.17 (2H, t, *J* = 7.5 Hz, C**8**-<u>H</u>$_2$), 1.60 (2H, dt, *J* = 7.5, 7.5 Hz, C**9**-<u>H</u>$_2$), 1.36-1.20 (7H, m, C**10**-<u>H</u>$_2$, C**11**-<u>H</u>$_2$, C**12**-<u>H</u>$_3$), 0.89 (3H, t, *J* = 7.0 Hz, C**5**-<u>H</u>$_3$). δ_C (101 MHz, $CDCl_3$): 172.8 (C**7**), 171.9 (C**3**), 136.1 (Ar<u>C</u>), 129.5 (Ar<u>C</u>H), 128.6 (Ar<u>C</u>H), 127.2 (Ar<u>C</u>H), 61.6 (C**4**), 53.1 (C**2**), 38.1 (C**1**), 36.7 (C**8**), 31.5 (C**10**), 25.4 (C**9**), 22.5 (C**11**), 14.3 (C**5**), 14.1 (C**12**).

The spectroscopic properties were consistent with the data available in the literature.[207]

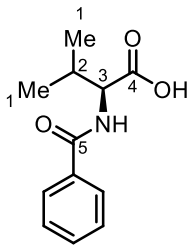

481

<u>Benzoyl-L-valine (481):</u> (*L*)-Valine (2.00 g, 17.1 mmol) and solid NaOH (0.79 g, 17.1 mmol) were dissolved in H_2O (5.00 mL). Et_2O (28.0 mL) was added, and the solution was cooled to 0 °C. To the mixture was alternately added benzoyl chloride (2.00 mL, 17.1 mmol) and a solution of NaOH (0.79 g,

17.1 mmol) in H_2O (1.8 mL) in equal portions to maintain a slightly alkaline solution. The reaction was then warmed to r.t. and stirred for 17 h. Volatiles were removed in vacuo, and the resulting aqueous was then acidified with HCl (aqueous, 3.0 M) to pH 2/3. The aqueous layer was then extracted with Et_2O (3×20 mL). The organics were combined, dried over Na_2SO_4, and concentrated to provide the title compound (3.45 g, 91%) as a colourless oil. δ_H (400 MHz, $CDCl_3$): 7.83-7.78 (2H, m, Ar<u>H</u>), 7.55-7.50 (1H, m, Ar<u>H</u>), 7.47-7.42 (2H, m, Ar<u>H</u>), 6.70 (1H, d, *J* = 8.5 Hz, N<u>H</u>), 4.80 (1H, dd, *J* = 8.5, 5.0 Hz, C**3**-<u>H</u>), 2.41-2.30 (1H, m, C**2**-<u>H</u>), 1.05 (3H, d, *J* = 7.0 Hz, C**1**-<u>H_3</u>), 1.03 (3H, d, *J* = 7.0 Hz, C**1**-<u>H_3</u>). δ_C (101 MHz, $CDCl_3$): 175.6 (C**4**), 168.1 (C**5**), 134.0 (Ar<u>C</u>), 132.1 (Ar<u>C</u>H), 128.8 (Ar<u>C</u>H), 127.3 (Ar<u>C</u>H), 57.6 (C**3**), 31.4 (C**2**), 19.2 (C**1**), 18.0 (C**1**).

The spectroscopic properties were consistent with the data available in the literature.[207]

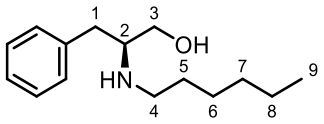

435

<u>(*S*)-2-(hexylamino)-3-phenylpropan-1-ol (435):</u> General Procedure **8** (*Reduction of* N-*Acyl Amino Esters*) was followed using ethyl hexanoyl-*L*-phenylalaninate **434** (1.29 g, 4.4 mmol) and $LiAlH_4$ (7.9 mL, 1.0 M in THF) to provide the title compound (1.26 g, 100%) as a colourless oil. δ_H (400 MHz, $CDCl_3$): 7.34-7.15 (5H, m, Ar<u>H</u>), 3.61 (1H, dd, *J* = 10.5, 4.0 Hz, C**3**-<u>H</u>), 3.31 (1H, dd, *J* = 10.5, 5.5 Hz, C**3**-<u>H</u>), 2.93-2.85 (1H, m, C**2**-<u>H</u>), 2.83-2.68 (2H, m, C**1**-<u>H_2</u>), 2.65-2.54 (2H, m, C**4**-<u>H_2</u>), 1.47-1.36 (2H, m, C**5**-<u>H_2</u>), 1.33-1.18 (8H, C**6**-<u>H_2</u>, C**7**-<u>H_2</u>, C**8**-<u>H_2</u>, N<u>H</u>, O<u>H</u>), 0.87 (3H, t, *J* = 7.0 Hz, C**9**-<u>H_3</u>). δ_C (101 MHz, $CDCl_3$): 138.8 (Ar<u>C</u>), 129.3 (Ar<u>C</u>H), 128.7 (Ar<u>C</u>H), 126.5 (Ar<u>C</u>H), 62.5 (C**3**), 60.1 (C**2**), 47.0 (C**4**), 38.4 (C**1**), 31.8 (C**7**), 30.4 (C**5**), 27.0 (C**6**), 22.8 (C**8**), 14.2 (C**9**).

The spectroscopic properties were consistent with the data available in the literature.[207]

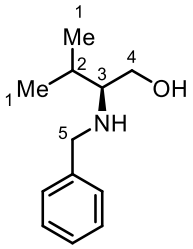

482

<u>(S)-2-(benzylamino)-3-methylbutan-1-ol (482):</u> General Procedure **8** (*Reduction of* N-*Acyl Amino Esters*) was followed using benzoyl-L-valine **481** (3.45 g, 15.6 mmol) and $LiAlH_4$ (28 mL, 1.0 M in THF) to provide the title compound (2.92 g, 97%) as a colourless oil. δ_H (400 MHz, $CDCl_3$): 7.35-7.32 (4H, m, Ar<u>H</u>), 7.29-7.25 (1H, m, Ar<u>H</u>), 3.83 (1H, d, *J* = 13.0 Hz, C**5**-<u>H</u>), 3.76 (1H, d, *J* = 13.0 Hz, C**5**-<u>H</u>), 3.65 (1H, dd, *J* = 10.5, 4.0 Hz, C**4**-<u>H</u>), 3.37 (1H, dd, *J* = 10.5. 7.0 Hz, C**4**-<u>H</u>), 2.48 (1H, ddd, *J* =

7.0, 7.0, 4.0 Hz, C**3**-H), 1.88 (1H, septet, *J* = 7.0 Hz, C**2**-H), 0.98 (3H, d, *J* = 7.0 Hz, C**1**-H_3), 0.92 (3H, d, *J* = 7.0 Hz, C**1**-H_3). δ_C (101 MHz, $CDCl_3$): 140.6 (ArC), 128.6 (ArCH), 128.3 (ArCH), 127.3 (ArCH), 64.0 (C**3**), 60.5 (C**4**), 51.5 (C**5**), 29.0 (C**2**), 19.7 (C**1**), 18.6 (C**1**).

The spectroscopic properties were consistent with the data available in the literature.[207]

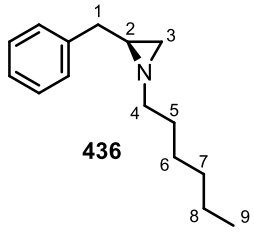

436

(S)-2-benzyl-1-hexylaziridine (436): General Procedure **9** (*Synthesis of Non-Activated Aziridines Under Modified Wenker Conditions)* was followed using (*S*)-2-(hexylamino)-3-phenylpropan-1-ol **435** (300 mg, 1.27 mmol) and $ClSO_3H$ (85 µL, 1.27 mmol). FCC (30% EtOAc/Hexane) provided the title compound (143 mg, 52%) as a pale yellow oil. δ_H (400 MHz, $CDCl_3$): 7.33-7.19 (5H, m, ArH), 2.75 (1H, dd, *J* = 14.5, 6.5 Hz, C**1**-H), 2.63 (1H, dd, *J* = 14.5, 6.0 Hz, C**1**-H), 2.23-2.32 (1H, m, C**4**-H), 2.17-2.08 (1H, m, C**4**-H), 1.67 (1H, d, *J* = 3.5 Hz, C**3**-H), 1.54-1.47 (1H, m, C**2**-H), 1.46-1.38 (2H, m, C**5**-H_2), 1.35-1.17 (7H, m, C**3**-H, C**6**-H_2, C**7**-H_2, C**8**-H_2), 0.87 (3H, t, *J* = 7.0 Hz, C**9**-H_3). δ_C (101 MHz, $CDCl_3$): 140.1 (ArC), 128.9 (ArCH), 128.5 (ArCH), 126.3 (ArCH), 61.7 (C**4**), 40.7 (C**2**), 39.8 (C**1**), 34.0 (C**3**), 32.0 (C**7**), 30.0 (C**5**), 27.3 (C**6**), 22.7 (C**8**), 14.2 (C**9**).

The spectroscopic properties were consistent with the data available in the literature.[207]

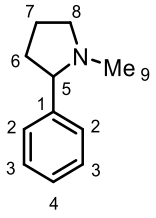

135

1-Methyl-2-phenylpyrrolidine (135): General Procedure **6** (*Eschweiler-Clark reaction)* was followed using 2-phenylpyrrolidine (1.00 g, 6.79 mmol), formaldehyde (18 mL), and formic acid (26 mL) over 2 days. FCC (100% EtOAc) provided the title compound (1.07 g, 97%) as a yellow oil. δ_H (500 MHz, $CDCl_3$): 7.36 (4H, m, C**2**-H, C**3**-H), 7.26-7.22 (1H, m, C**4**-H), 3.24 (1H, ddd, 9.5, 8.0, 2.0 Hz, C**8**-H), 3.03 (1H, dd, *J* = 9.0, 7.5 Hz, C**5**-H), 2.28 (1H, td, *J* = 9.5, 8.0 Hz, C**8**-H), 2.21-2.13 (4H, m, C**9**-H_3, C**6**-H), 2.01-1.90 (1H, m, C**7**-H), 1.84-1.72 (2H, m, C**6**-H, C**7**-H). δ_C (126 MHz, $CDCl_3$): 143.4 (C**1**), 128.5 (C**3**), 127.7 (C**2**), 127.2 (C**4**), 71.8 (C**5**), 57.3 (C**8**), 40.7 (C**9**), 35.3 (C**6**), 22.7 (C**7**).

The spectroscopic properties were consistent with the data available in the literature.[208]

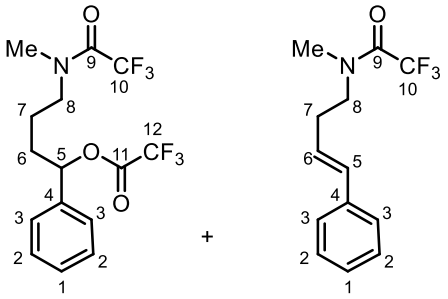

471 + **450**

1 - phenyl-4-(2,2,2-trifluoro-*N*-methylacetamido) butyl - 2,2,2 - trifluoroacetate (471) + (*E*)-2,2,2-trifluoro-*N*-methyl-*N*-(4-phenylbut-3-en-1-yl)acetamide (450): General Procedure **10** (*C–N Activation of Cyclic Benzyl Pyrrolidines*) was followed using 1-methyl-2-phenylpyrrolidine (48.4 mg, 0.30 mmol), trifluoroacetic anhydride (50 µL, 0.36 mmol), and sodium bromide (77 mg, 0.75 mmol). NMR analysis provides yields of 76% and 23% respectively. FCC (0-15% EtOAc/Hexane) provided ester **471** (47 mg, 46%) as a pale yellow oil, and alkene **450** (24 mg, 31%) as a colourless oil.

Ester 471: R_f = 0.34 (25% EtOAc/Hexane). ν_{max} / cm^{-1}: 3413 (br), 2921 (m), 1783 (m), 1681 (s), 1191 (s), 1142 (s), 1102 (s), 767 (s), 700 (s). δ_H (500 MHz, $CDCl_3$): 7.43-7.32 (5H, m, C**1**-**3**-H), 5.89 (0.66H, dd, *J* = 8.0, 6.0 Hz, C**5**-H, major rotamer), 5.87 (0.33H, dd, *J* = 8.0, 6.0 Hz, C**5**-H, minor rotamer), 3.53-3.38 (2H, m, C**8**-H_2), 3.07 (2H, q, *J* = 1.5 Hz, NCH_3, major rotamer), 2.96 (1H, s, NCH_3, minor rotamer), 2.10-2.01 (1H, m, C**6**-H), 1.95-1.86 (1H, m, C**6**-H), 1.76-1.63 (1H, m, C**7**-H), 1.63-1.57 (1H, m, C**7**-H). δ_C (126 MHz, $CDCl_3$): 157.2 (q, *J* = 38.5 Hz, C**9**), 157.0 (q, *J* = 35.5 Hz, C**9**), 156.9 (q, *J* = 42.5 Hz, C**11**), 137.7 (C**4**, major rotamer), 137.4 (C**4**, minor rotamer), 129.4 (C**1**, minor rotamer), 129.3 (C**1**, major rotamer), 129.2 (C**2**, minor rotamer), 129.1 (C**2**, major rotamer), 126.5 (C**3**, major rotamer), 126.5 (C**3**, minor rotamer), 116.6 (q, *J* = 286.0 Hz, C**10**-F_3, minor rotamer), 116.5 (q, *J* = 286.0 Hz, C**10**-F_3, major rotamer), 114.6 (q, *J* = 286.0 Hz, C**12**-F_3), 80.23 (C**5**, major rotamer), 80.0 (C**5**, minor rotamer), 48.9 (C**8**, minor rotamer), 48.8 (C**8**, major rotamer), 34.8 (q, *J* = 4.0 Hz, NCH_3, major rotamer), 34.4 (NCH_3, minor rotamer), 33.0 (C**6**, major rotamer), 32.7 (C**6**, minor rotamer), 24.0 (C**7**, minor rotamer), 22.5 (C**7**, major rotamer). δ_F (471 MHz, $CDCl_3$): -68.6 (C**10**-F_3, minor rotamer), 69.8 (C**10**-F_3, major rotamer), -75.1 (C**12**-F_3, major rotamer), -75.2 (C**12**-F_3, minor rotamer). *m/z* (ESI^+) HRMS: Calculated for $C_{15}H_{15}F_6NO_3$: 371.28. Found $[M\text{-}OCOCF_3]^+$: 258.1103.

Alkene 450: R_f = 0.38 (25% EtOAc/Hexane). ν_{max} / cm^{-1}: 2914 (m), 1687 (s), 1245 (m), 1191 (s), 1139 (s), 1100 (s), 967 (m), 744 (m), 695 (s), 669 (m). δ_H (500 MHz, $CDCl_3$): 7.36-7.28 (4H, m, C**2**-**3**-H), 7.26-7.20 (1H, m, C**1**-H), 6.48 (1H, dd, *J* = 16.0, 9.0 Hz, C**5**-H), 6.18-6.06 (1H, m, C**6**-H), 3.61-3.51 (2H, m, C**8**-H_2), 3.14 (1.85H, q, *J* = 1.5 H, NCH_3, major rotamer), 3.07 (1.15H, s, NCH_3, minor rotamer), 2.57-2.49 (2H, m, C**7**-H_2). δ_C (126 MHz, $CDCl_3$): 157.1 (q, *J* = 40.0 Hz, NC(O)CF_3), 137.2 (C**4**, major rotamer), 136.9 (C**4**, minor rotamer), 133.4 (C**5**, minor rotamer), 133.0 (C**5**, major rotamer), 128.8 (C**2**, minor rotamer), 128.7 (C**2**, major rotamer), 127.8 (C**1**, minor rotamer), 127.6 (C**1**, major rotamer),

126.3 (C**3**, minor rotamer), 126.2 (C**3**, major rotamer), 125.7 (C**6**, major rotamer), 124.7 (C**6**, minor rotamer), 49.4 (C**8**, major rotamer), 48.5 (C**8**, minor rotamer), 35.5 (q, *J* = 3.5 Hz, N<u>C</u>H$_3$, major rotamer), 34.8 (N<u>C</u>H$_3$, minor rotamer), 32.2 (C**7**, minor rotamer), 30.5 (C**7**, major rotamer). δ_F (471 MHz, $CDCl_3$): -68.6 (1.2F, s, minor rotamer), -69.8 (1.8F, s, major rotamer). *m/z* (ESI^+) HRMS: Calculated for $C_{13}H_{14}F_3N$): 257.1. Found $[M+H]^+$: 258.1104.

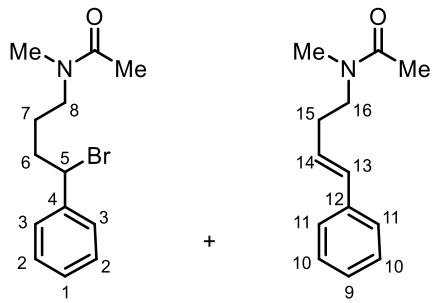

455 **456**

***N* - (4 – bromo – 4 - phenylbutyl) – *N* – methylacetamide (455) + (*E*) – *N* – methyl – *N* - (4 – phenylbut - 3 -en-1-yl)acetamide (456):** General Procedure **10** (*C–N Activation of Cyclic Benzyl Pyrrolidines*) was followed using 1-methyl-2-phenylpyrrolidine (96.7 mg, 0.60 mmol), acetyl chloride (51 µL, 0.72 mmol), and sodium bromide (154 mg, 1.5 mmol). ^{1}H NMR analysis provided yields of 71% and 16% respectively. R_f = 0.073 (50% EtOAc/hexane). ν_{max} / cm^{-1}: 3379 (br), 2918 (m), 2850 (m), 1619 (s), 1494 (m), 1451 (s), 1402 (s), 1026 (m), 969 (m), 747 (s), 700 (s). δ_H (500 MHz, $CDCl_3$): Key Peaks: 6.47 (0.5 H, t, *J* = 15.0 Hz, C**13**-<u>H</u>), 6.24-6.11 (0.5 H, m, C**14**-<u>H</u>), 5.06-4.84 (1H, m, C**5**-<u>H</u>), 3.03 (0.5H, s, NC<u>H</u>$_3$, major rotamer, alkene), 2.99 (0.4H, s, NC<u>H</u>$_3$, minor rotamer, alkene), 2.97 (1.4H, s, NC<u>H</u>$_3$, major rotamer, bromide), 2.90 (0.9H, s, NC<u>H</u>$_3$, minor rotamer, bromide), 2.08 (s, C(O)C<u>H</u>$_3$, alkene), 2.07 (s, C(O)C<u>H</u>$_3$, bromide). *m/z* (CI^+) HRMS: Calculated for $C_{13}H_{17}NO$ (alkene **456**): 203.13. Found $[M+H]^+$: 204.1726. *m/z* (ESI^-) HRMS: Calculated for $C_{13}H_{18}{}^{79}BrNO$ (bromide **455**): 283.20. Found $[M]^-$: 283.2631.

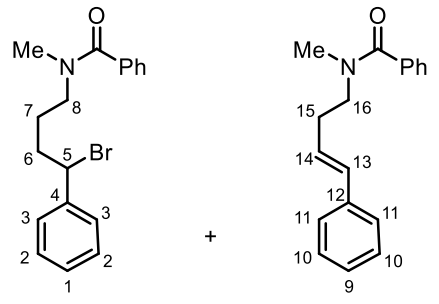

457 **458**

***N* - (4-bromo-4-phenylbutyl) - *N* – methylbenzamide (457) + (*E*) - *N* - methyl - *N* - (4 - phenylbut-3-en-1-yl) benzamide (458):** General Procedure **10** (*C–N Activation of Cyclic Benzyl Pyrrolidines*) was followed using 1-methyl-2-phenylpyrrolidine (96.7 mg, 0.60 mmol), benzoyl chloride (84 µL, 0.72 mmol), and sodium bromide (154 mg, 1.5 mmol). ^{1}H NMR analysis provided inconclusive yields. FCC

(0-30% EtOAc/Hexane) gave an impure mixture of the title compounds (unknown yields)**. R_f =** 0.106 (25% EtOAc in hexane). ν_{max} / cm^{-1}: 2919 (br m), 1714 (m), 1600 (s), 1447 (m), 1403 (m), 1265 (m), 1072 (m), 968 (m), 734 (s), 698 (s). δ_H (400 MHz, CD_2Cl_2, 263 K): Key Peaks: 6.54 (0.5H, d, *J* = 16.0 Hz, C**13**-H), 6.38 (0.5H, d, *J* = 16.0 Hz, C**13**-H), 6.36-6.26 (0.5H, m, C**14**), 6.02-5.91 (0.5H, m, C**14**), 4.85 (0.17H, t, *J* = 7.5 Hz, C**5**-H), 4.67 (0.14H, t, *J* = 10.0 Hz, C**5**-H), 3.10 (2.5H, s, NCH_3, alkene **458**, major rotamer), 3.01 (1.5H, s, NCH_3, alkene **458**, minor rotamer), 2.96 (2.9H, s, NCH_3, bromide **457**, major rotamer), 2.91 (1.1H, s, NCH_3, bromide **457**, minor rotamer). *m/z* (CI^+) HRMS: Calculated for $C_{13}H_{17}NO$ (alkene **458**): 265.36. Found $[M+H]^+$: 266.1615.

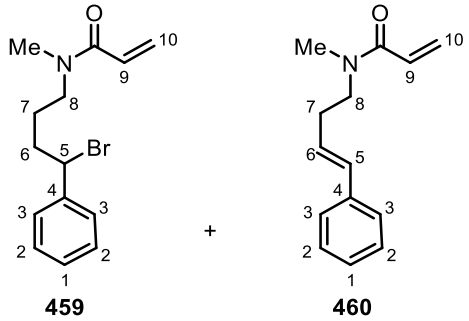

***N* - (4 – bromo - 4 - phenylbutyl) - *N* – methylacrylamide (459) + (*E*) - *N* – methyl - *N* - (4 - phenylbut-3-en-1-yl) acrylamide (460):** General Procedure **10** (*C–N Activation of Cyclic Benzyl Pyrrolidines*) was followed using 1-methyl-2-phenylpyrrolidine (96.7 mg, 0.60 mmol), 2-propenoyl chloride (59 µL, 0.72 mmol), and sodium bromide (154 mg, 1.5 mmol). ^{1}H NMR analysis gives inconclusive yields. FCC (0-50% EtOAc/Hexane) provided alkene **460** (0.12 mmol, 19%) as a colourless oil. R_f = 0.063 (25% EtOAc in hexane). ν_{max} / cm^{-1}: 2922 (m), 2851 (m), 1646 (s), 1610 (s), 1448 (m), 1417 (m), 1402 (m), 965 (s), 794 (m), 745 (m), 694 (m). δ_H (500 MHz, $CDCl_3$): 7.35-7.27 (4H, m, C**2**-H, C**3**-H), 7.25-7.17 (1H, m, C**1**-H), 6.58 (1H, ddd, *J* = 17.0 (rotamer splitting), 16.5, 10.5 Hz, C**9**-H, major + minor rotamer), 6.46 (1H, dd, *J* = 16.0 (rotamer splitting), 1.5 Hz, C**5**-H, major + minor rotamer), 6.32 (1H, ddd, *J* = 16.5, 8.0 (rotamer splitting), 2.0 Hz, C**10**-H, major + minor rotamer), 6.23-6.07 (1H, m, C**6**-H, major + minor rotamer), 5.67 (1H, dt, *J* = 10.5, 2.0 Hz, C**10**-H, major + minor rotamer), 3.54 (2H, dt, *J* = 34.5 (rotamer splitting), 7.5 Hz, C**8**-H_2, major + minor rotamer), 3.06 (3H, d, *J* = 20.5 Hz (rotamer splitting), NCH_3, major + minor rotamer), 2.49 (2H, dd, *J* = 7.5, 7.0 (rotamer splitting)Hz, C**7**-H_2). δ_C (126 MHz, $CDCl_3$): 166.6 (C(O), major rotamer), 166.4 (C(O), minor rotamer), 137.5 (C**4**, minor rotamer), 137.1 (C**4**, major rotamer), 132.9 (C**5**, major rotamer), 132.1 (C**5**, minor rotamer), 128.7 (C**3**, major rotamer), 128.6 (C**3**, minor rotamer), 128.0 (C**10**, minor rotamer), 127.8 (C**10**, major rotamer), 127.7 (C**9**, minor rotamer), 127.6 (C**9**, major rotamer), 127.3 (C**1**), 127.1 (C**6**, minor rotamer), 126.2 (C**2**), 125.6 (C**6**, major rotamer), 20.1 (C**8**, major rotamer), 48.1 (C**8**, minor rotamer), 36.1 (NCH_3, minor rotamer), 34.3 (NCH_3, major rotamer), 32.7 (C**7**, major rotamer), 31.2 (C**7**, minor rotamer). *m/z* (ESI^+) HRMS: Calculated for $C_{14}H_{17}NO$ (alkene **460**): 215.13. Found $[M+H]^+$: 216.1384.

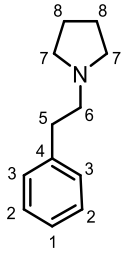

466

1-Phenethylpyrrolidine (466): To a solution of Phenethylamine (1.26 mL, 10.0 mmol) in MeCN (50 mL) was added 1,4-dibromobutane (1.43 mL, 12.0 mmol) and K_2CO_3 (1.80 g, 13.0 mmol). The solution was then stirred at 90 °C for 6 h before being cooled to r.t. The reaction was quenched by addition of H_2O (20 mL). The aqueous was extracted by CH_2Cl_2 (3×20 mL); the organics were combined and dried over $MgSO_4$, then concentrated to a yellow oil (1.37 g). FCC (1% NEt_3/EtOAc) provided the title compound (656 mg, 37%) as a yellow oil. δ_H (500 MHz, $CDCl_3$): 7.28 (2H, dd, *J* = 7.5, 7.5 Hz, C**2**-H), 7.23-7.17 (3H, m, C**3**-H, C**1**-H), 2.87-2.81 (2H, m, C**5**-H_2), 2.73-2.67 (2H, m, C**6**-H_2), 2.61-2.54 (4H, m, C**7**-H_2), 1.85-1.78 (4H, m, C**8**-H_2). δ_C (126 MHz, $CDCl_3$): 140.7 (C**4**), 128.8 (C**2**), 128.5 (C**3**), 126.1 (C**1**), 58.5 (C**6**), 54.4 (C**7**), 36.0 (C**5**), 23.6 (C**8**).

The spectroscopic properties were consistent with the data available in the literature.[209]

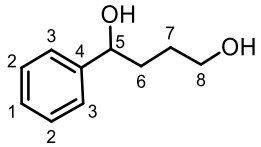

462

1-Phenylbutane-1,4-diol (462): To a suspension of $LiAlH_4$ (304 mg, 8.0 mmol) in dry Et_2O (25 mL) at 0 °C, 3-benzoylpropionic acid (356 mg, 2.0 mmol) was added portionwise over 30 mins. After stirring at r.t. for 2 h, the excess $LiAlH_4$ was destroyed by the addition of H_2O (2 mL) and NaOH (aq, 6.0 M, 0.5 mL). The solution was then dried over Na_2SO_4, filtered, and concentrated to a cloudy, colourless oil (308 mg). FCC (0-100% EtOAc/Hexane) provided the title compound (235 mg, 71%) as a colourless oil. δ_H (500 MHz, $CDCl_3$): 7.38-7.32 (4H, m, C**2**-H, C**3**-H), 7.31-7.26 (1H, m, C**1**-H), 4.75 (1H, t, *J* = 6.5 Hz, C**5**-H), 3.75-3.66 (2H, m, C**8**-H_2), 1.90-1.85 (2H, m, C**6**-H_2), 1.77-1.62 (2H, m, C**7**-H_2). δ_C (126 MHz, $CDCl_3$): 144.8 (C**4**), 128.6 (C**2**/**3**), 127.7 (C**1**), 125.9 (C**3**/**2**), 74.6 (C**5**), 63.1 (C**8**), 36.3 (C**6**), 29.3 (C**7**).

The spectroscopic properties were consistent with the data available in the literature.[210]

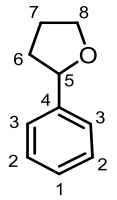

463

2-Phenyltetrahydrofuran (463): Under an atmosphere of argon, 1-phenylbutane-1,4-diol (235 mg, 1.41 mmol) was dissolved in NEt_3 (1.18 mL, 8.46 mmol) and dry CH_2Cl_2 (2.5 mL). The mixture was cooled to -78 °C and treated with $P(OEt)_3$ (0.34 mL, 1.97 mmol). Subsequently, iodine (429 mg, 1.69 mmol) was added and the mixture was stirred at -78 °C until complete dissolution of iodine (2.5 h). Then the reaction was stirred at r.t. for 30 mins. The reaction was then quenched with KOH (4.0 M in MeOH, 0.6 mL) and the solvent was removed in vacuo. The residue was partitioned between H_2O (3 mL) and hexane (3 mL). The organics were collected, and the aqueous washed with hexane (2×3 mL). The organics were combined and washed with H_2O (5×2 mL), then dried over $MgSO_4$ and concentrated to provide the title compound (1.96 mL, 94%) as a yellow oil. δ_H (500 MHz, $CDCl_3$): 7.35-7.31 (4H, m, C**3**-H, C**2**-H), 7.27-7.23 (1H, m, C**1**-H), 4.89 (1H, dd, *J* = 7.0, 7.0 Hz, C**5**-H), 4.10 (1H, ddd, *J* = 8.5, 6.5, 6.5 Hz, C**8**-H), 3.94 (1H, ddd, *J* = 8.5, 6.5 6.5 Hz, C**8**-H), 2.33 (1H, dddd, *J* = 12.5, 7.0, 7.0, 5.5 Hz, C**6**-H), 2.06-1.96 (2H, m, C**7**-H), 1.81 (1H, dddd, *J* = 12.5, 8.5, 8.5, 7.0 Hz, C**6**-H). δ_C (126 MHz, $CDCl_3$): 143.6 (C**4**), 128.4 (C**2**/**3**), 127.3 (C**1**), 125.8 (C**3**/**2**), 80.8 (C**5**), 68.8 (C**8**), 34.8 (C**6**), 26.2 (C**7**).

The spectroscopic properties were consistent with the data available in the literature.[175]

7.7. Spectra of Novel Compounds

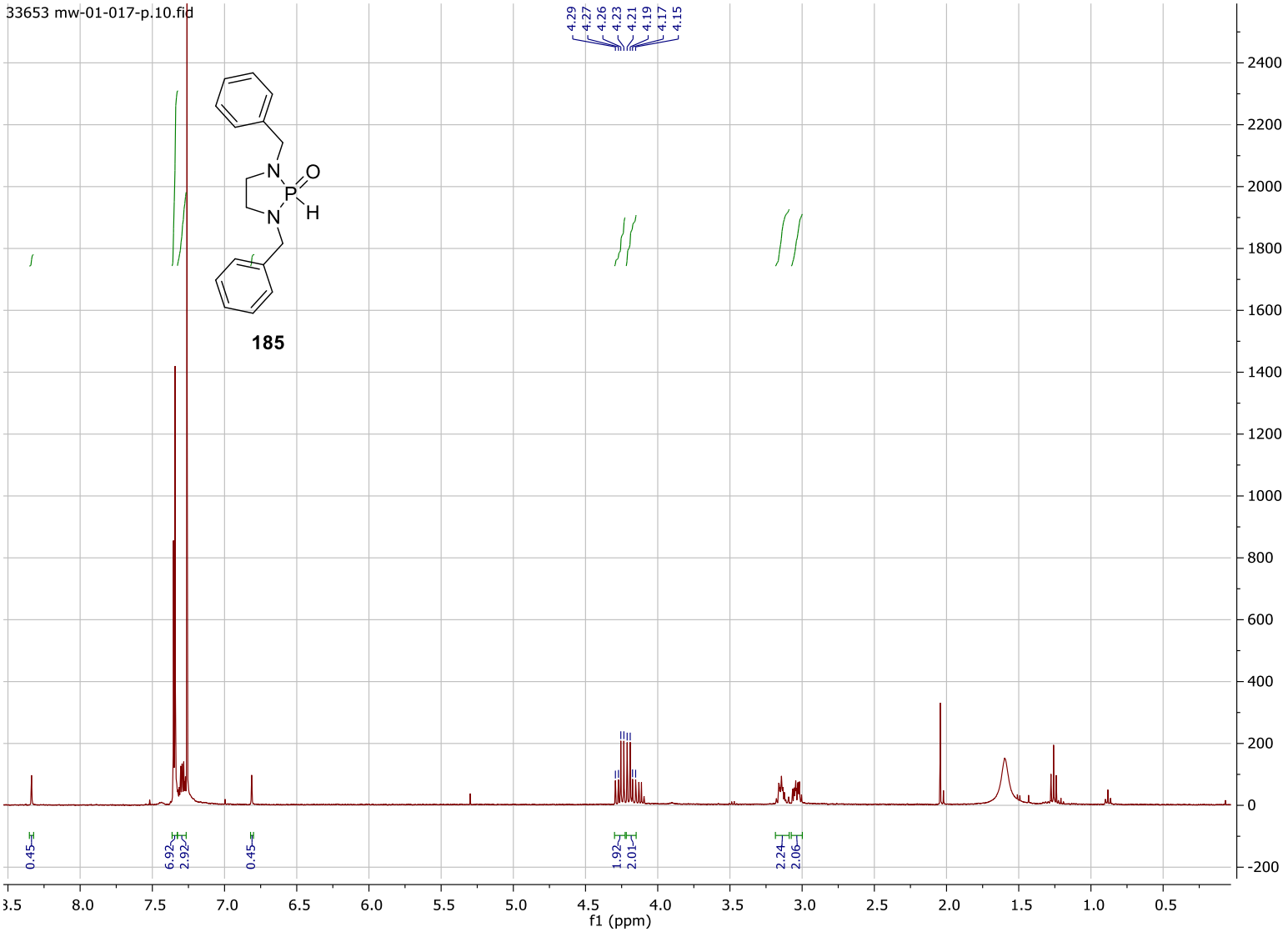

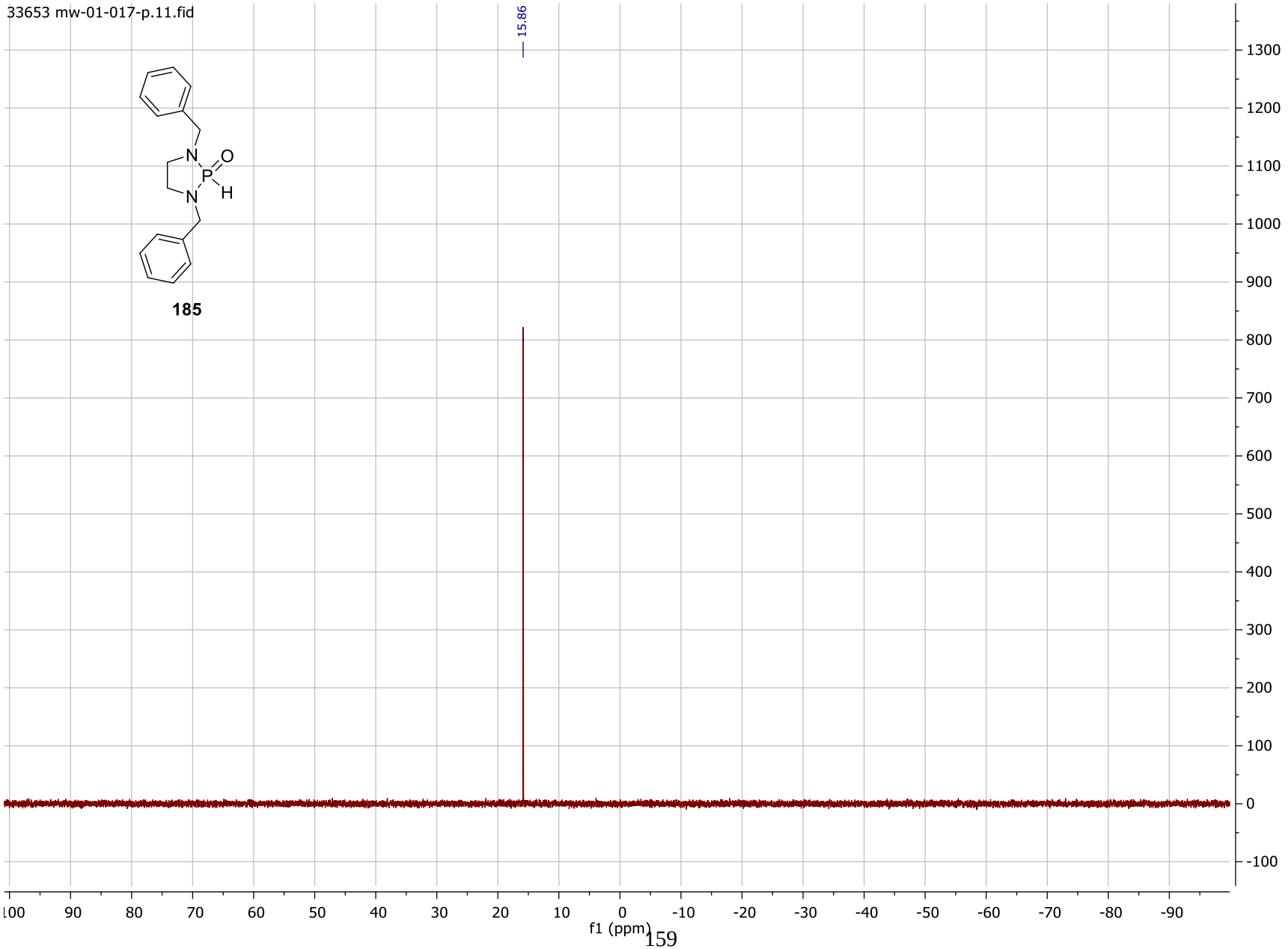
33653 mw-01-017-p.11.fid
15.86
185
1300
1200
1100
1000
900
800
700
600
500
400
300
200
100
0
-100
100
90
80
70
60
50
40
30
20
10
0
-10
-20
-30
-40
-50
-60
-70
-80
-90
f1 (ppm)

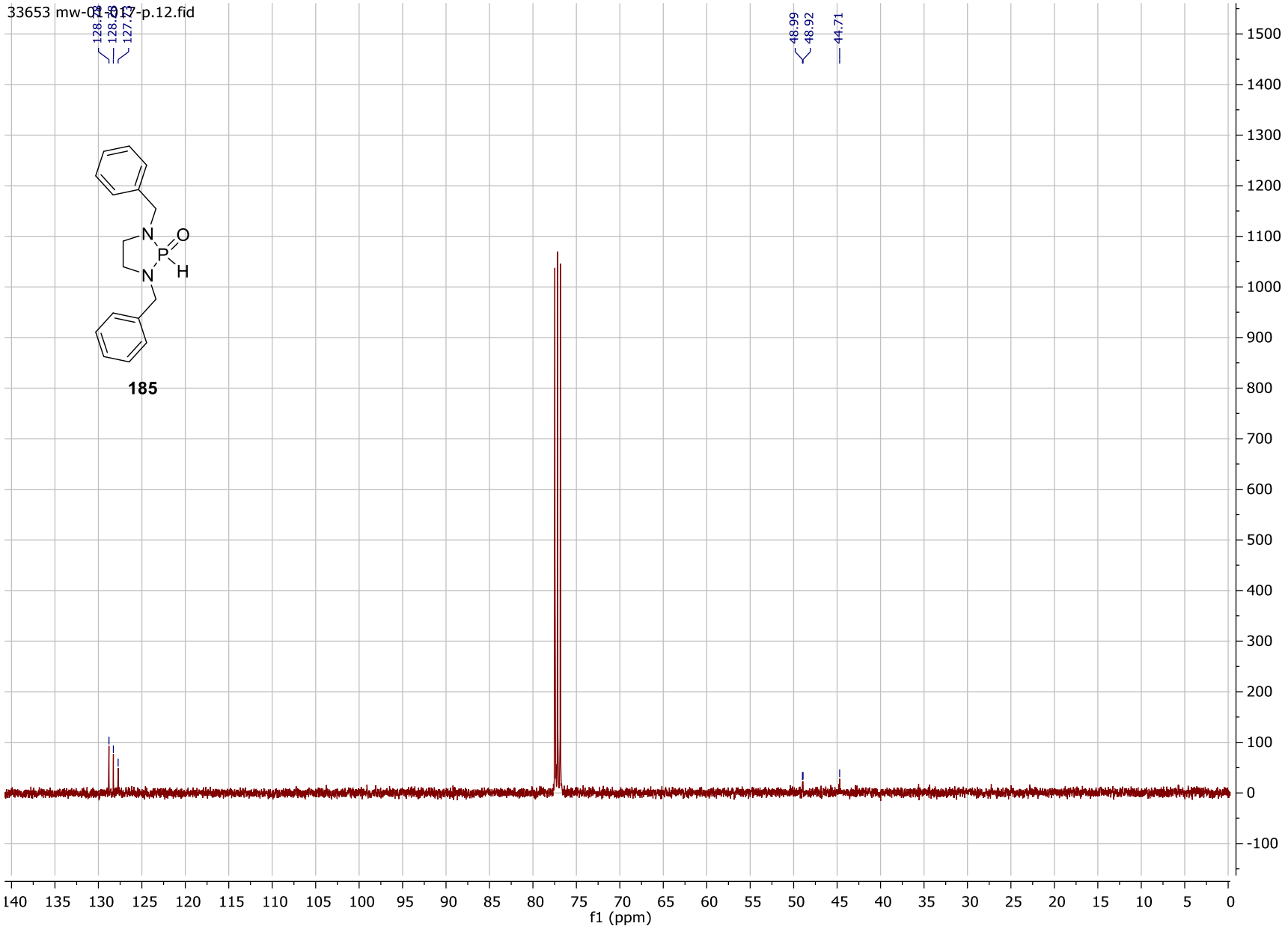
33653 mw-03-017-p.12.fid
128.73
128.47
127.47
48.99
48.92
44.71
N
O
P
H
N
185
1500
1400
1300
1200
1100
1000
900
800
700
600
500
400
300
200
100
0
-100
140 135 130 125 120 115 110 105 100 95 90 85 80 75 70 65 60 55 50 45 40 35 30 25 20 15 10 5 0
f1 (ppm)

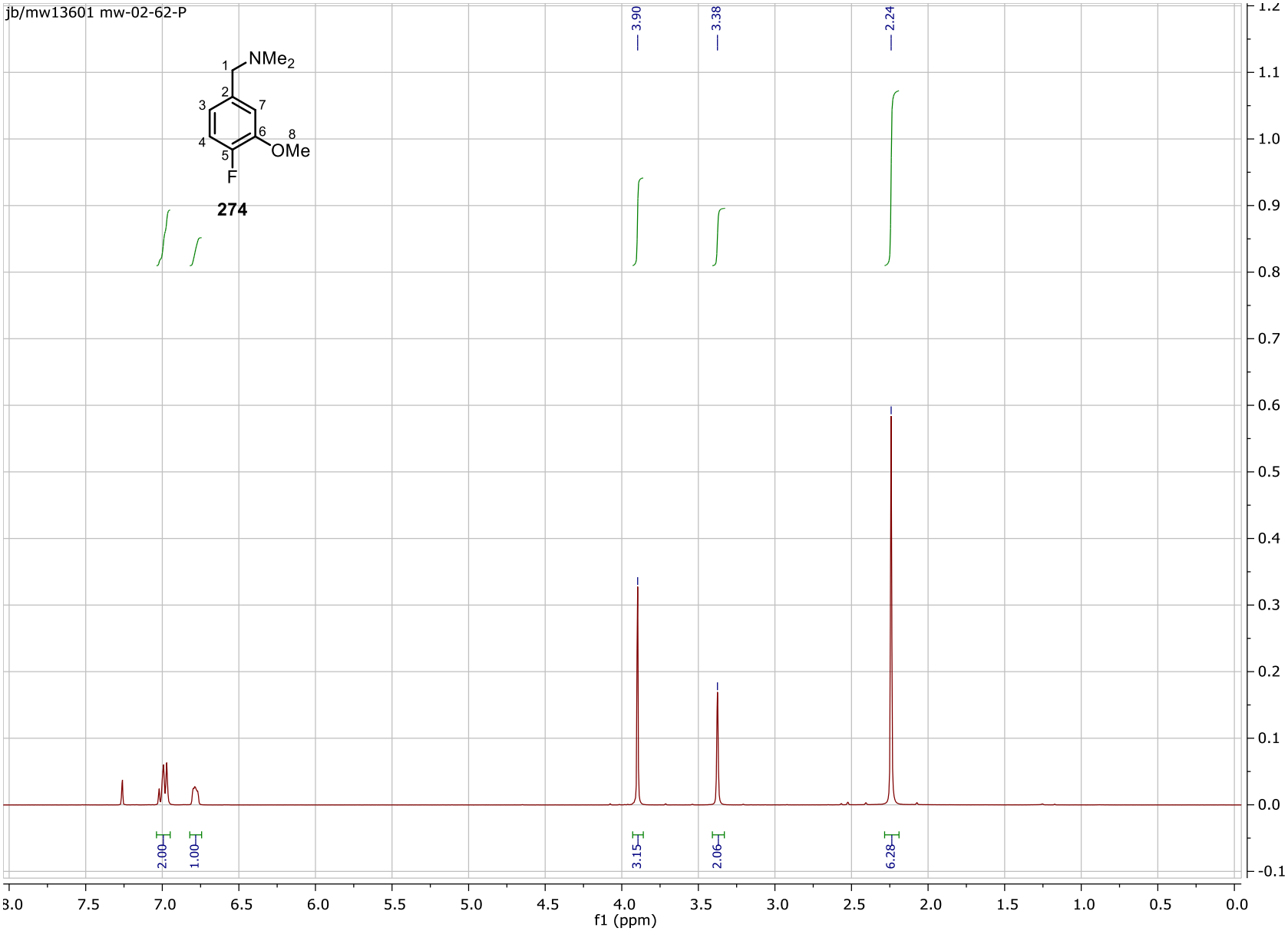
jb/mw13601 mw-02-62-P
NMe2
OMe
F
274
3.90
3.38
2.24
2.00
1.00
3.15
2.06
6.28
f1 (ppm)

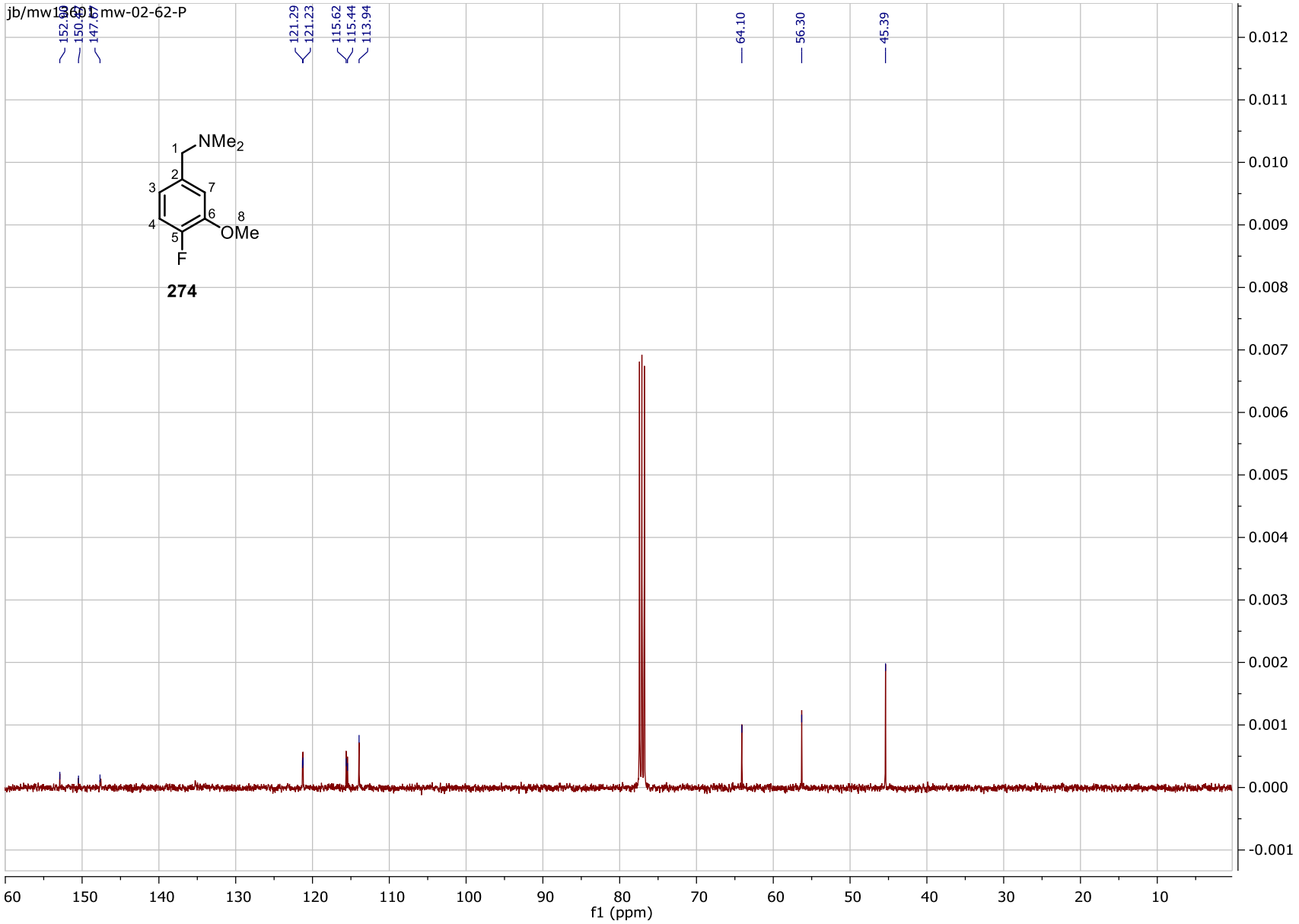
jb/mw13001/mw-02-62-P
152.38
150.01
147.67
121.29
121.23
115.62
115.44
113.94
64.10
56.30
45.39
NMe2
OMe
F
1
2
3
4
5
6
7
8
274
0.012
0.011
0.010
0.009
0.008
0.007
0.006
0.005
0.004
0.003
0.002
0.001
0.000
-0.001
60
150
140
130
120
110
100
90
80
70
60
50
40
30
20
10
f1 (ppm)

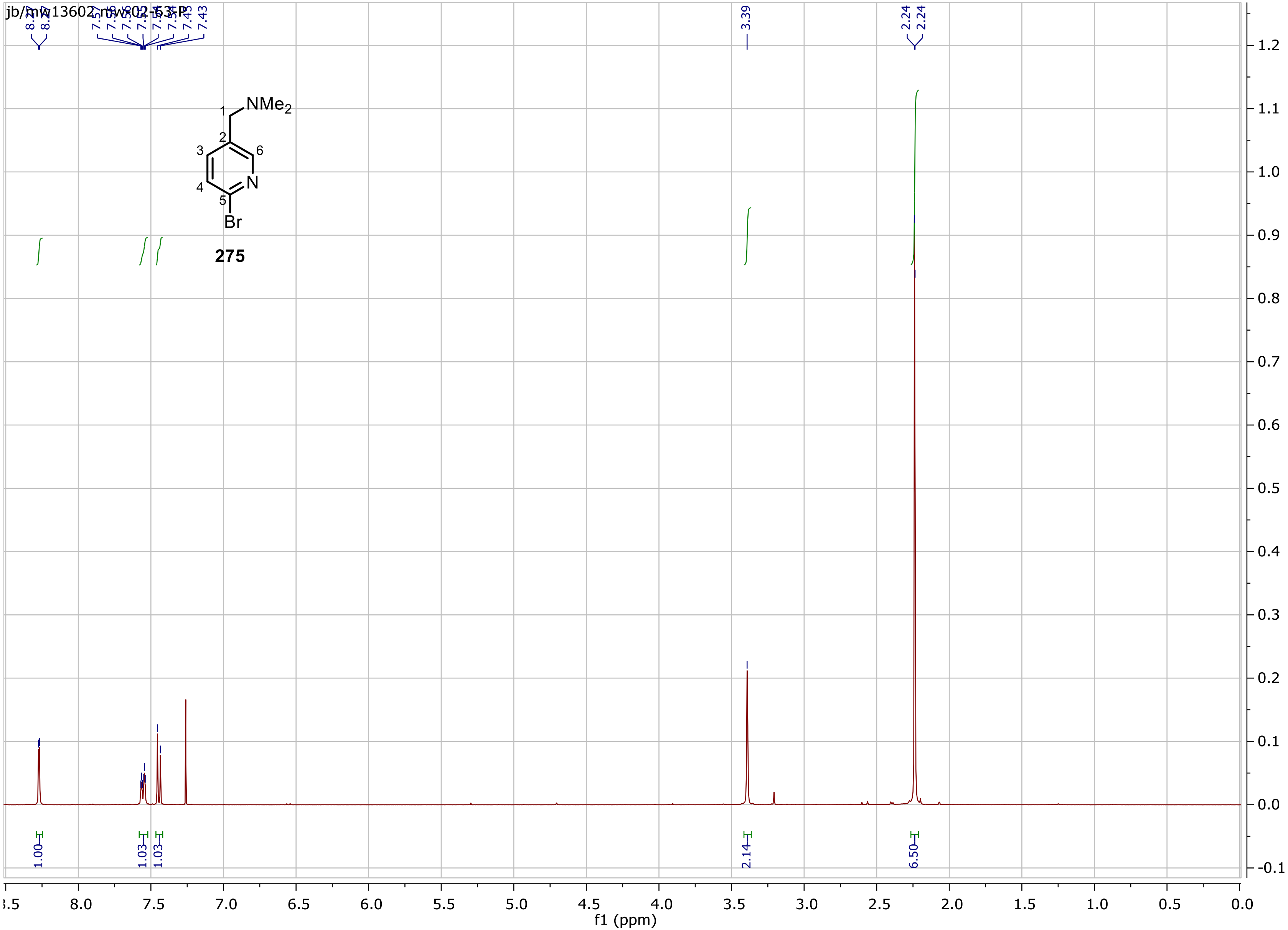

jb/mw13602_mw802-53-P
8.27
8.27
7.58
7.57
7.56
7.56
7.55
7.54
7.45
7.43
3.39
2.24
2.24
NMe2
1
2
3
6
N
4
5
Br
275
1.00
1.03
1.03
2.14
6.50
f1 (ppm)

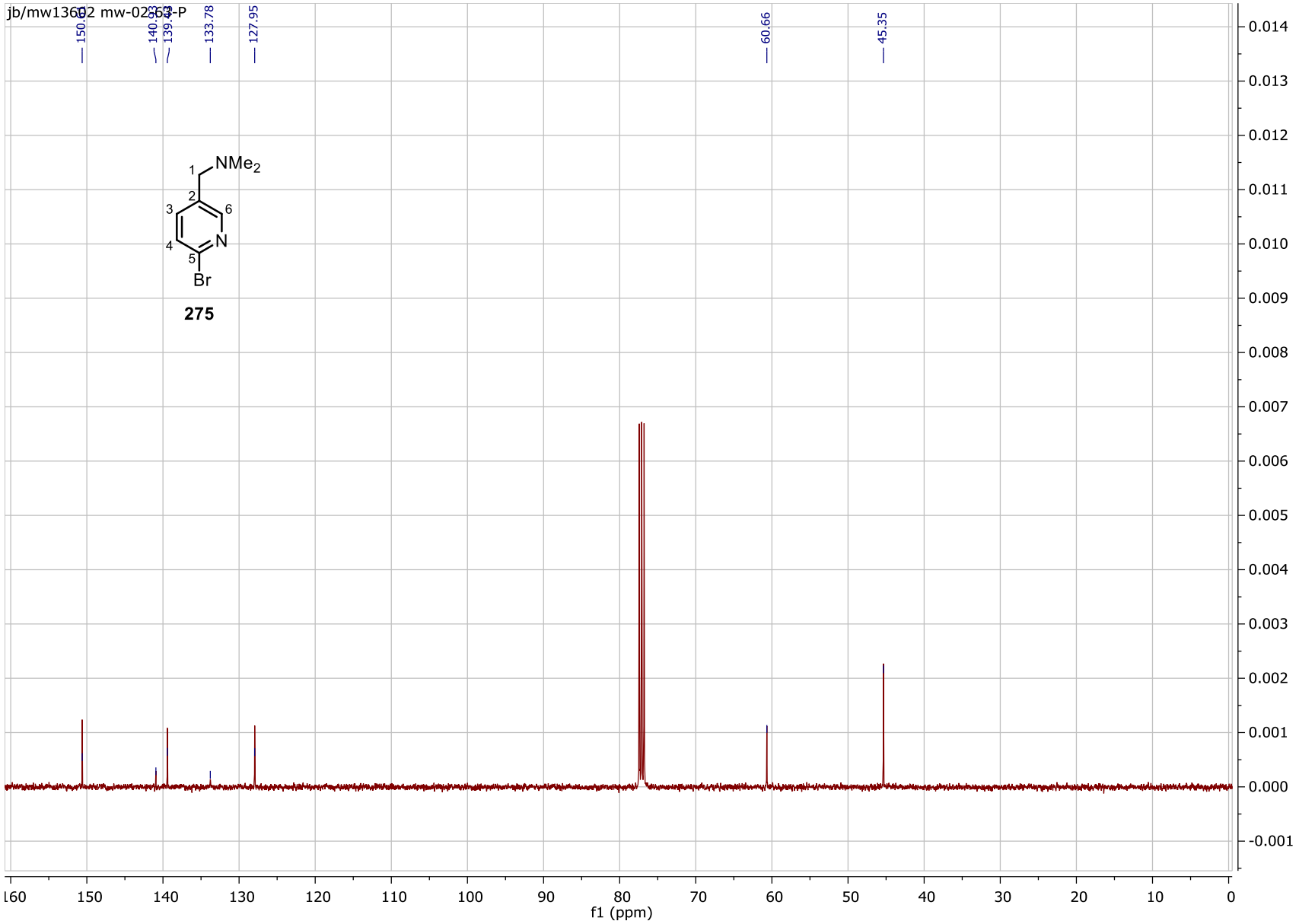
jb/mw13602 mw-02563-P
150.
140.
139.
133.78
127.95
60.66
45.35
NMe2
Br
275
f1 (ppm)

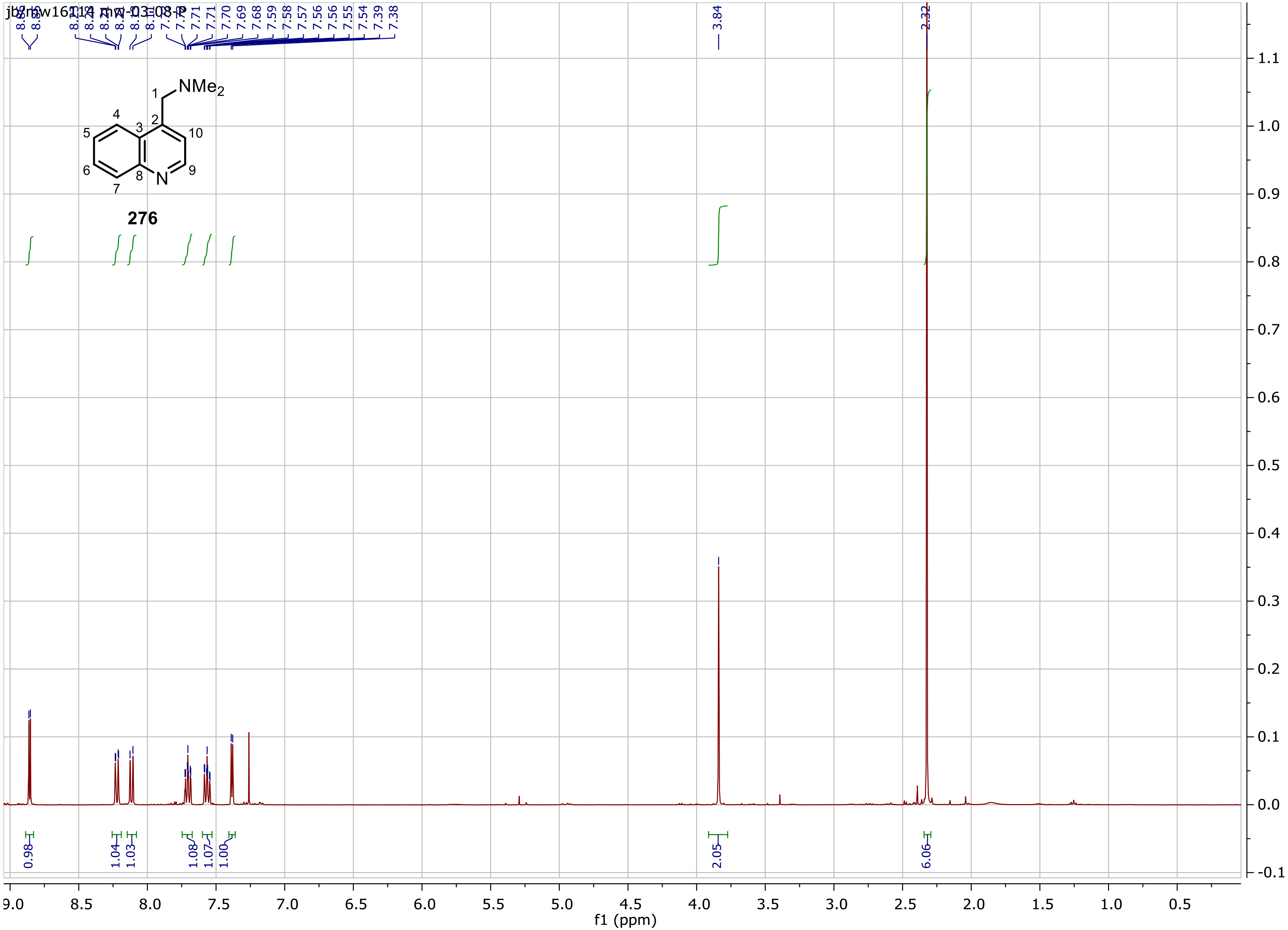
NMe2
1
2
3
4
5
6
7
8
9
10
N
276
3.84
2.32
0.98
1.04
1.03
1.08
1.07
1.00
2.05
6.06
f1 (ppm)

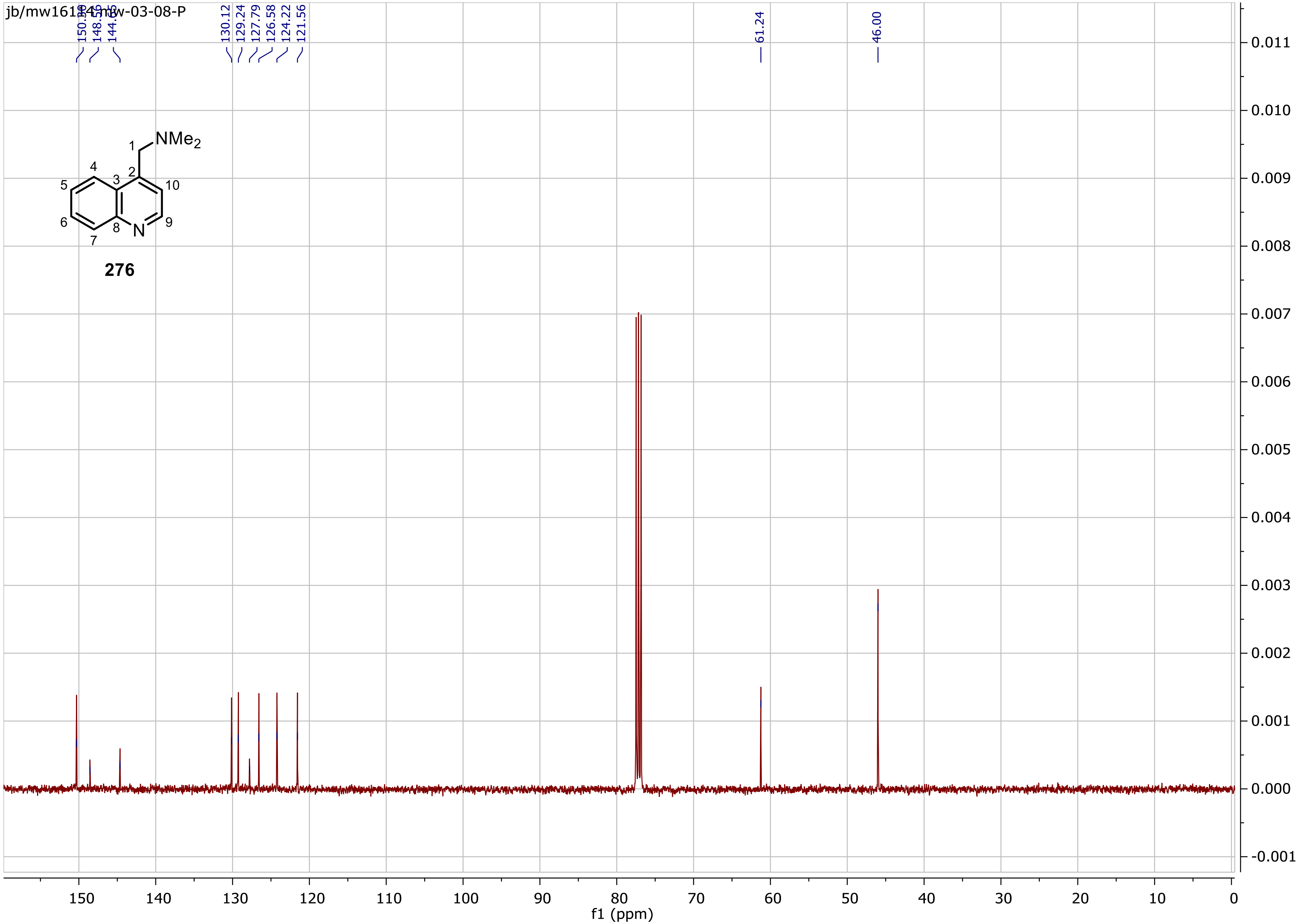
130.12
129.24
127.79
126.58
124.22
121.56
61.24
46.00
NMe2
1
2
3
4
5
6
7
8
9
10
N
276
0.011
0.010
0.009
0.008
0.007
0.006
0.005
0.004
0.003
0.002
0.001
0.000
-0.001
150
140
130
120
110
100
90
80
70
60
50
40
30
20
10
0
f1 (ppm)

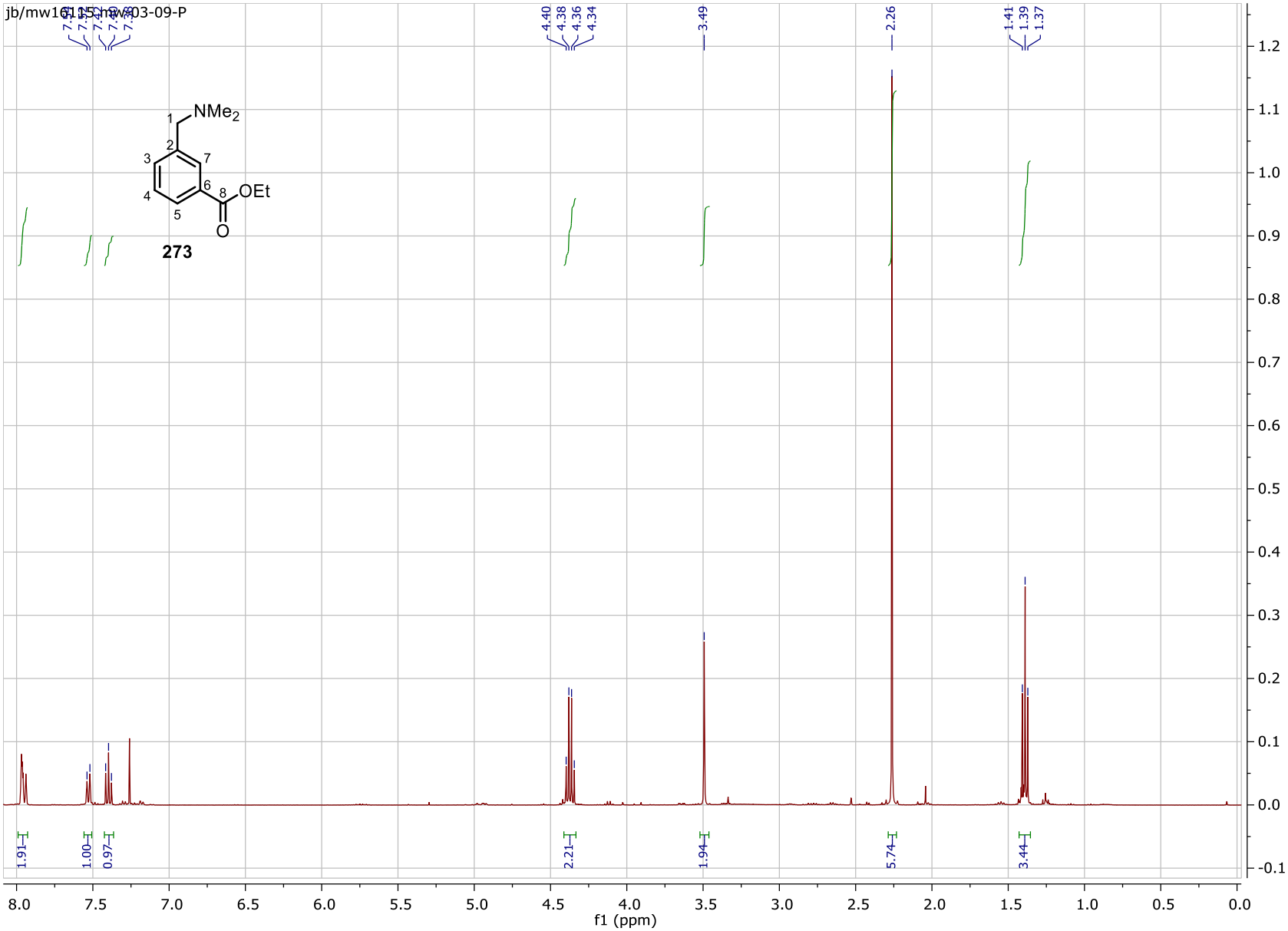
jb/mw161115_hmw303-09-P
7.51
7.50
7.49
7.48
7.38
4.40
4.38
4.36
4.34
3.49
2.26
1.41
1.39
1.37
NMe2
OEt
O
1
2
3
4
5
6
7
8
273
1.91
1.00
0.97
2.21
1.94
5.74
3.44
f1 (ppm)

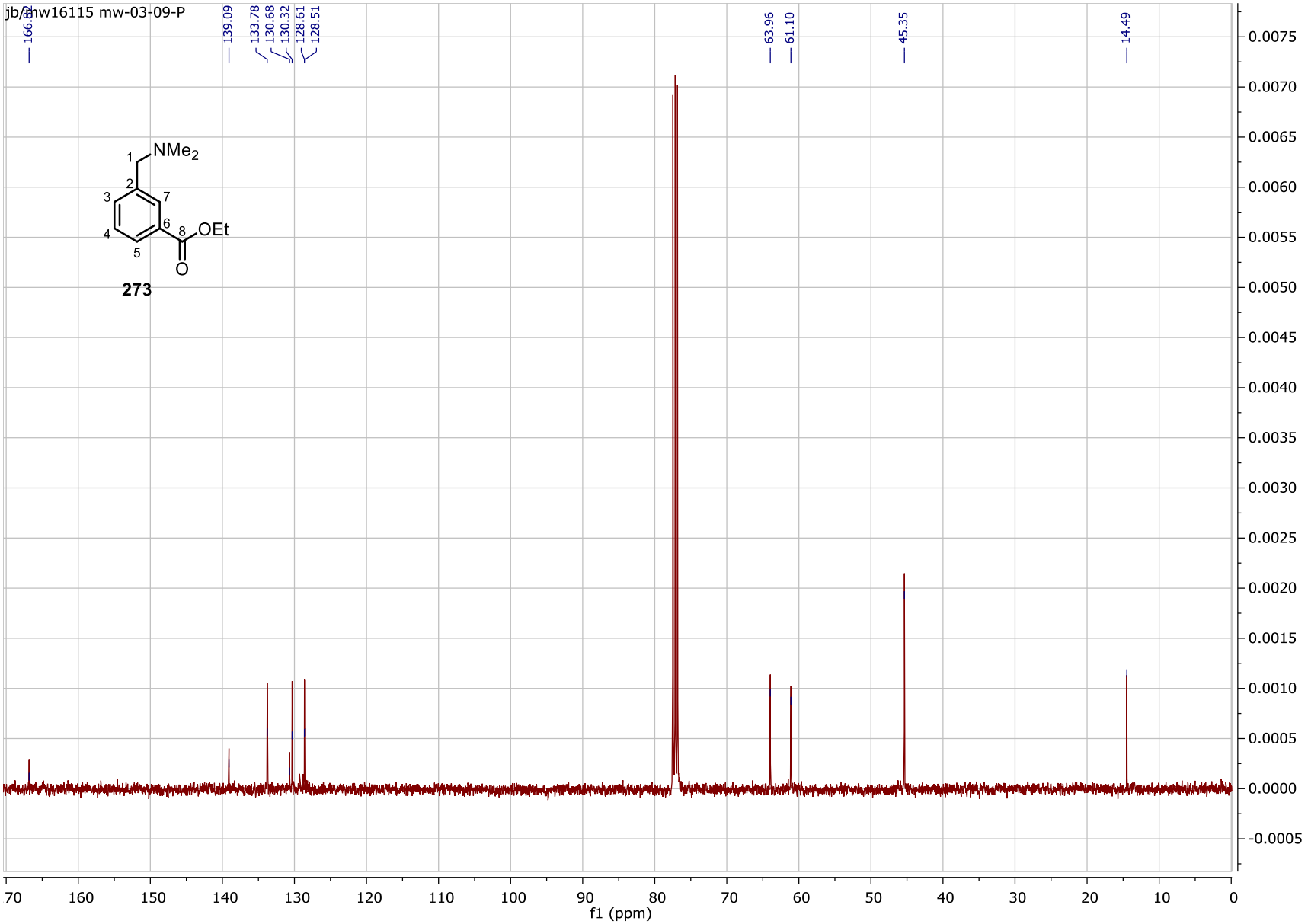
jb/mw16115 mw-03-09-P
166.48
139.09
133.78
130.68
130.32
128.61
128.51
63.96
61.10
45.35
14.49
NMe2
OEt
O
1
2
3
4
5
6
7
8
273
0.0075
0.0070
0.0065
0.0060
0.0055
0.0050
0.0045
0.0040
0.0035
0.0030
0.0025
0.0020
0.0015
0.0010
0.0005
0.0000
-0.0005
70
160
150
140
130
120
110
100
90
80
70
60
50
40
30
20
10
0
f1 (ppm)

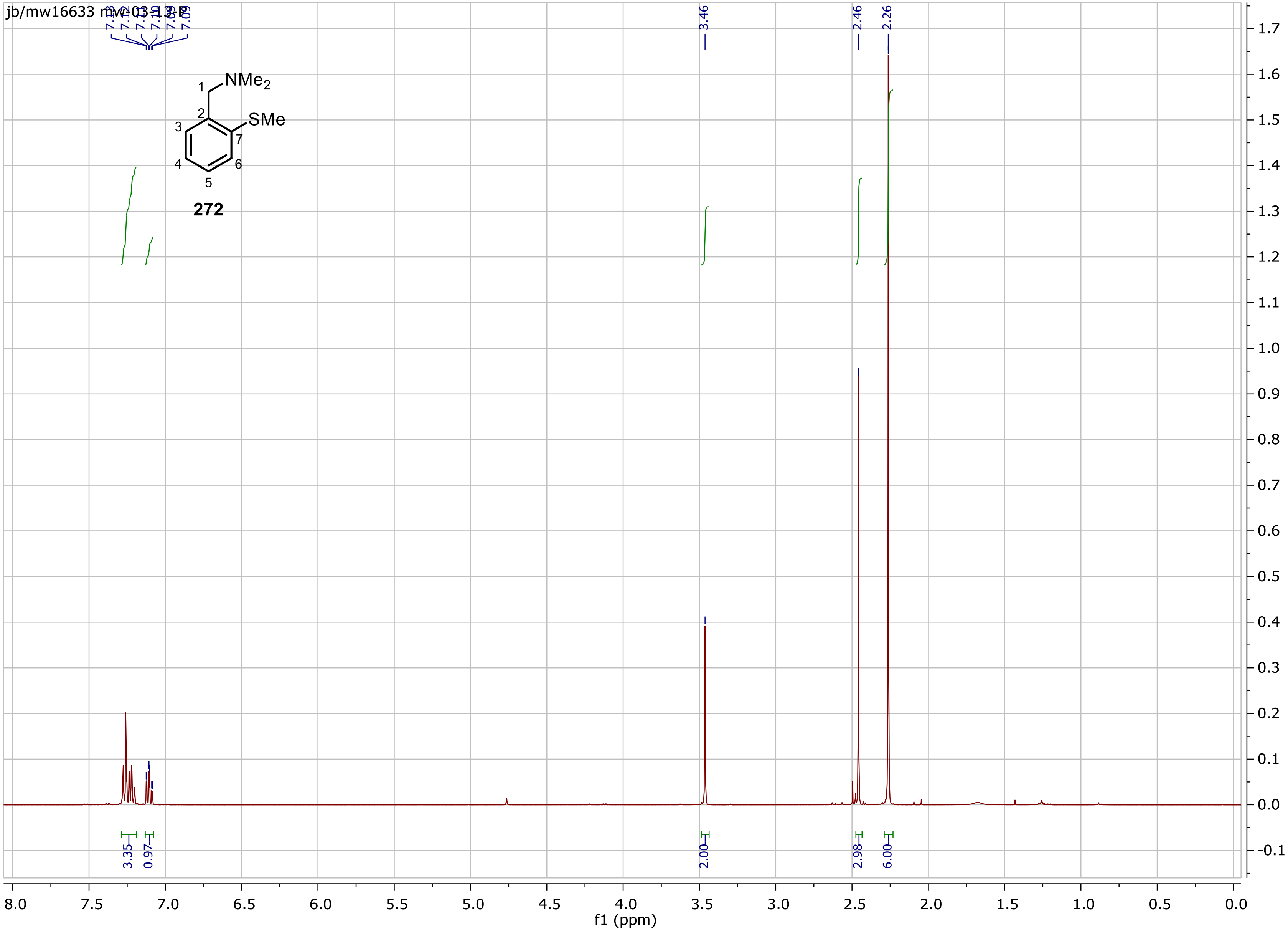
jb/mw16633 mw-03-19-P
3.46
2.46
2.26
NMe2
SMe
272
3.35
0.97
2.00
2.98
6.00
f1 (ppm)

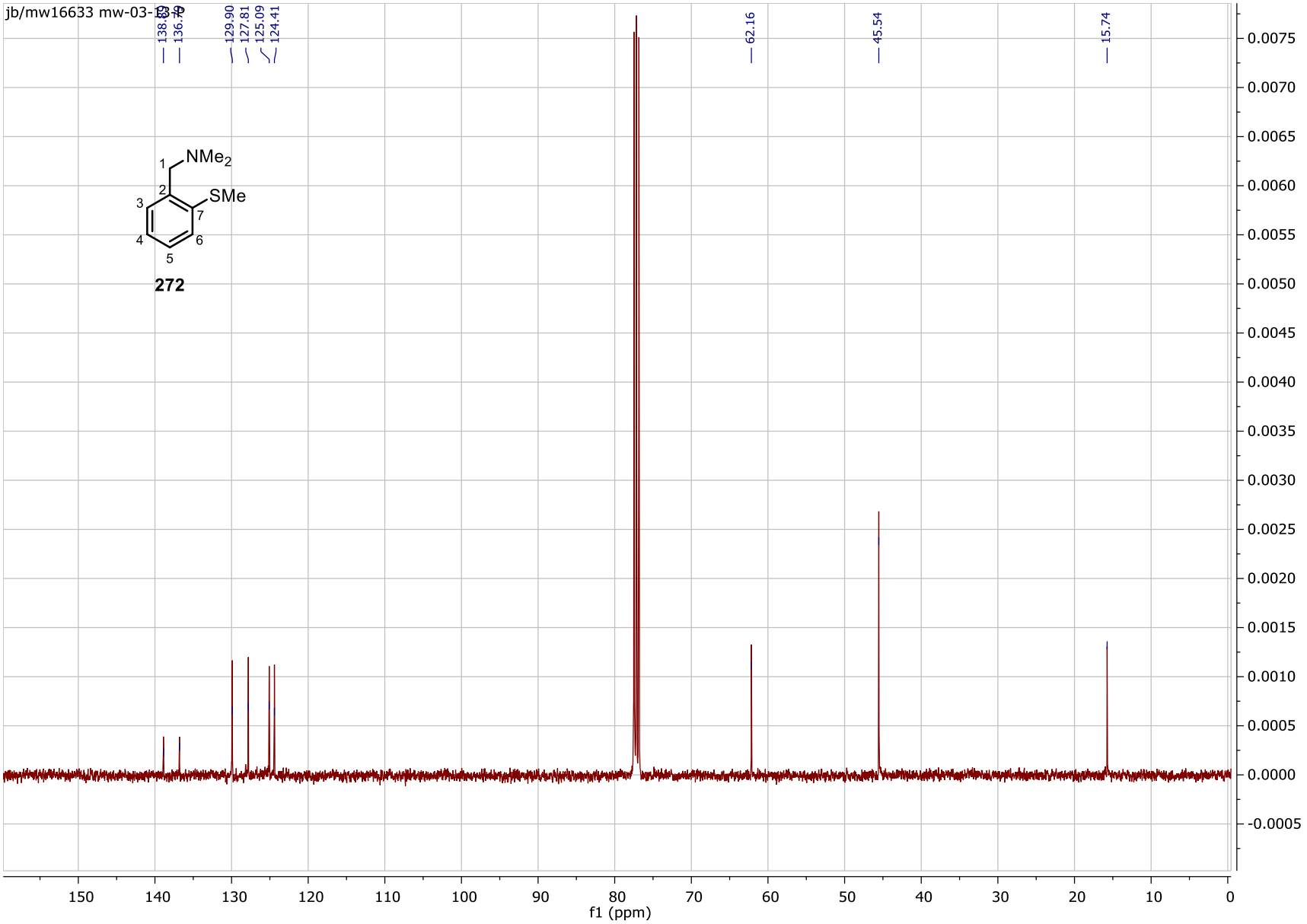
jb/mw16633 mw-03-
138.83
136.74
129.90
127.81
125.09
124.41
62.16
45.54
15.74
NMe2
SMe
1
2
3
4
5
6
7
272
0.0075
0.0070
0.0065
0.0060
0.0055
0.0050
0.0045
0.0040
0.0035
0.0030
0.0025
0.0020
0.0015
0.0010
0.0005
0.0000
-0.0005
150
140
130
120
110
100
90
80
70
60
50
40
30
20
10
0
f1 (ppm)

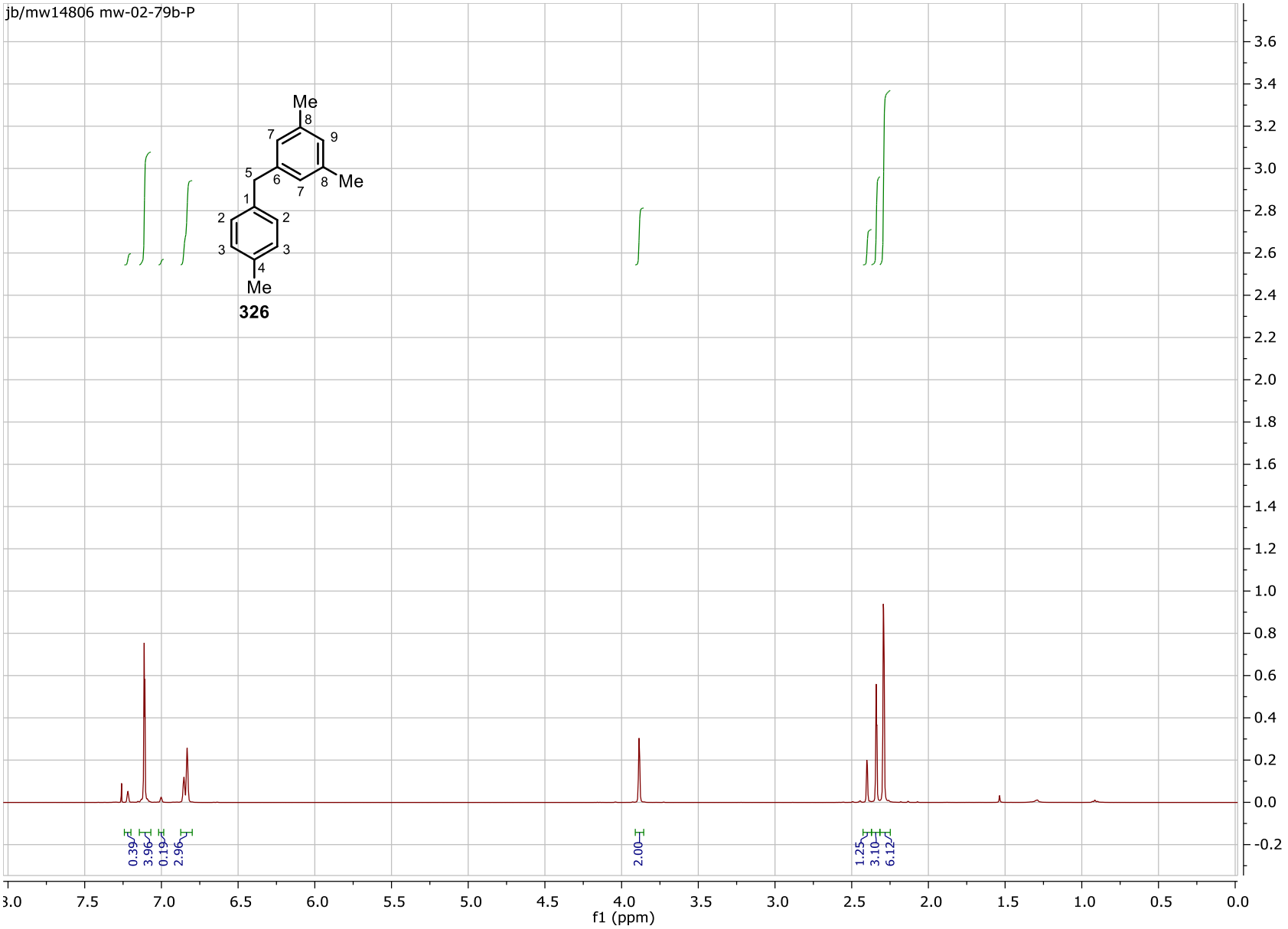
jb/mw14806 mw-02-79b-P
Me
Me
Me
326
0.39
3.96
0.19
2.96
2.00
1.25
3.10
6.12
f1 (ppm)

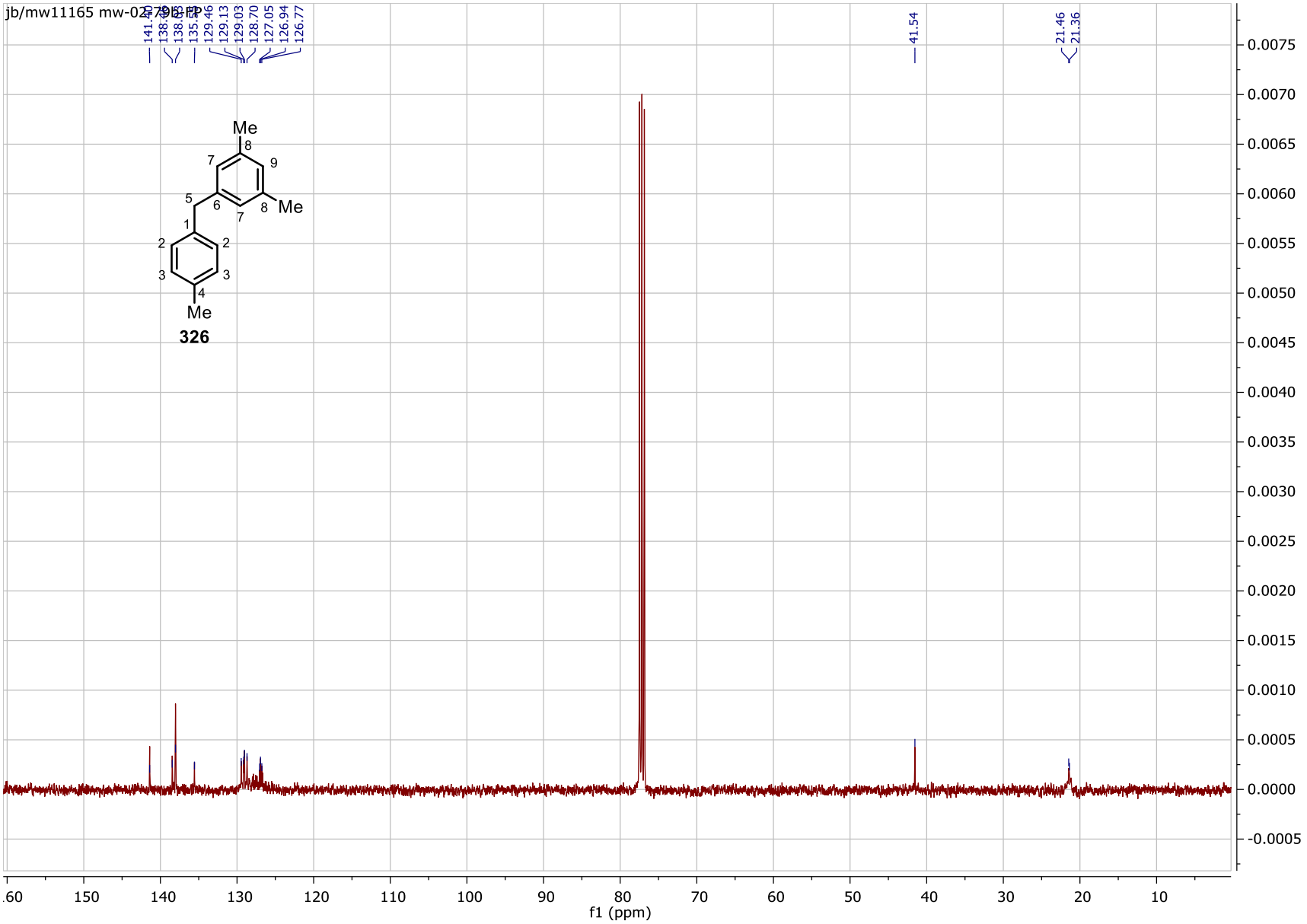
jb/mw11165 mw-02-79b-FP
141.47
138.63
138.54
135.54
129.46
129.13
129.03
128.70
127.05
126.94
126.77
41.54
21.46
21.36
Me
Me
Me
326
f1 (ppm)

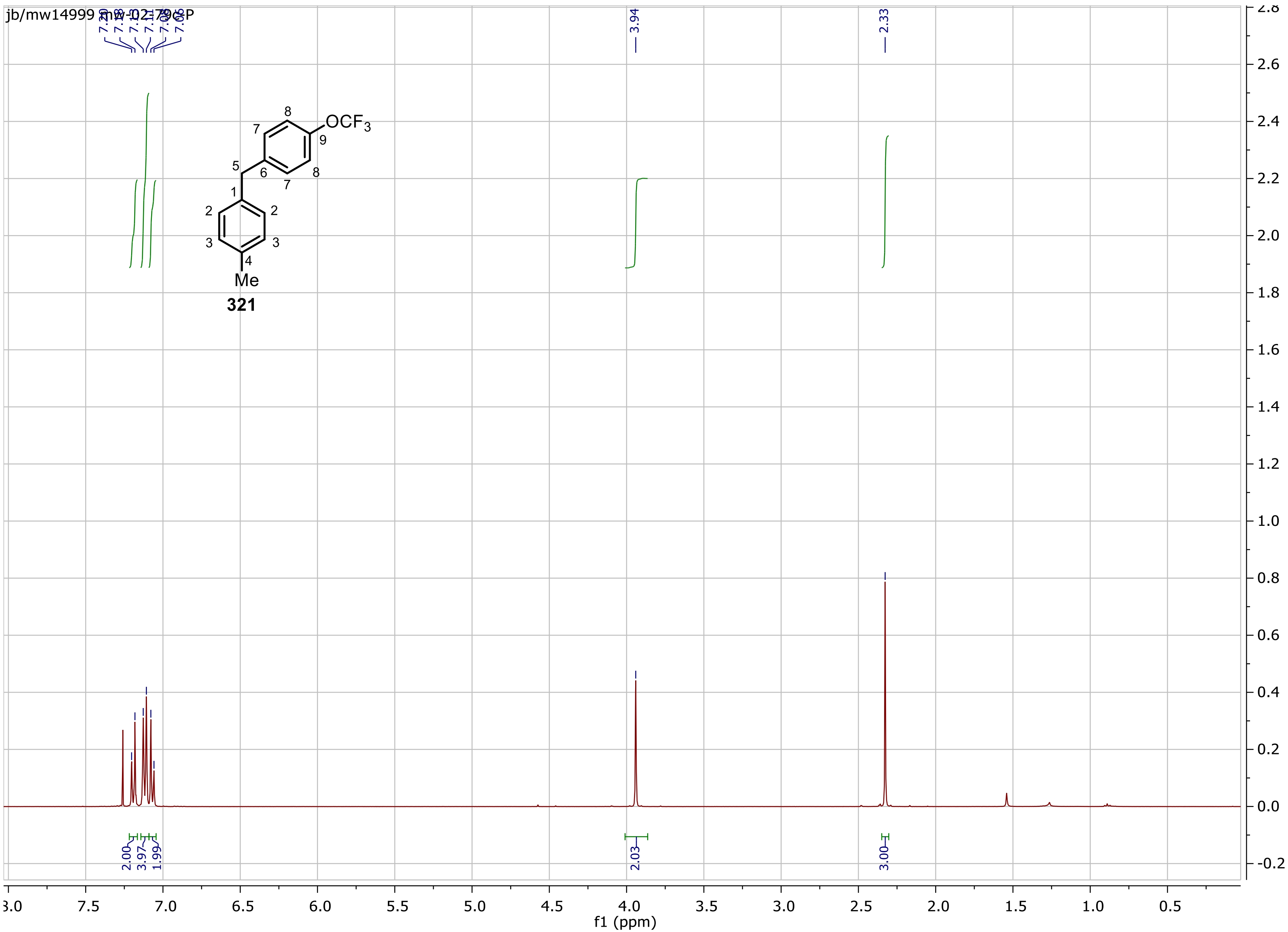
jb/mw14999 mw-02-79 SP
3.94
2.33
OCF3
Me
321
2.00
3.97
1.99
2.03
3.00
f1 (ppm)

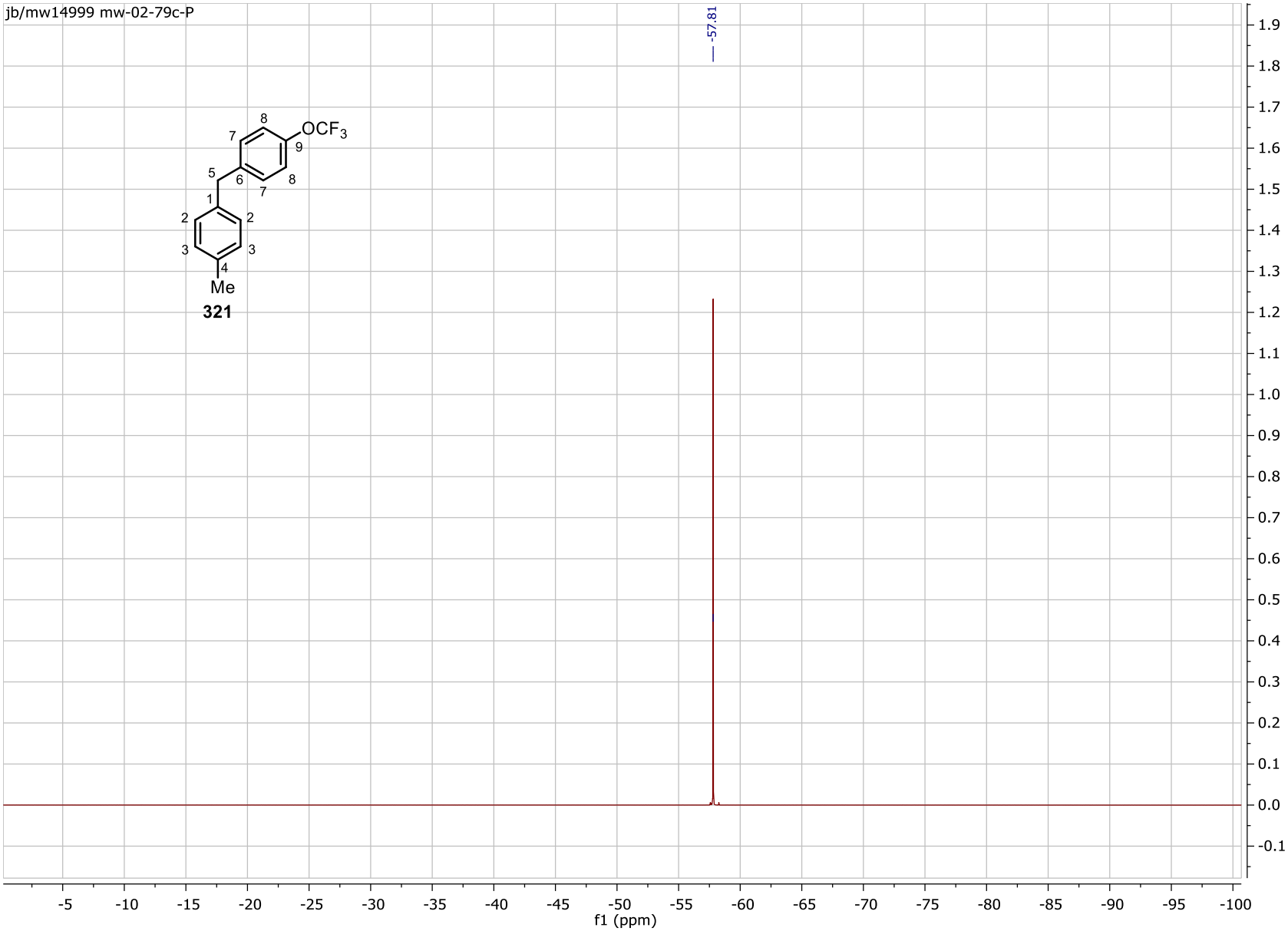
jb/mw14999 mw-02-79c-P
-57.81
OCF3
Me
321
f1 (ppm)

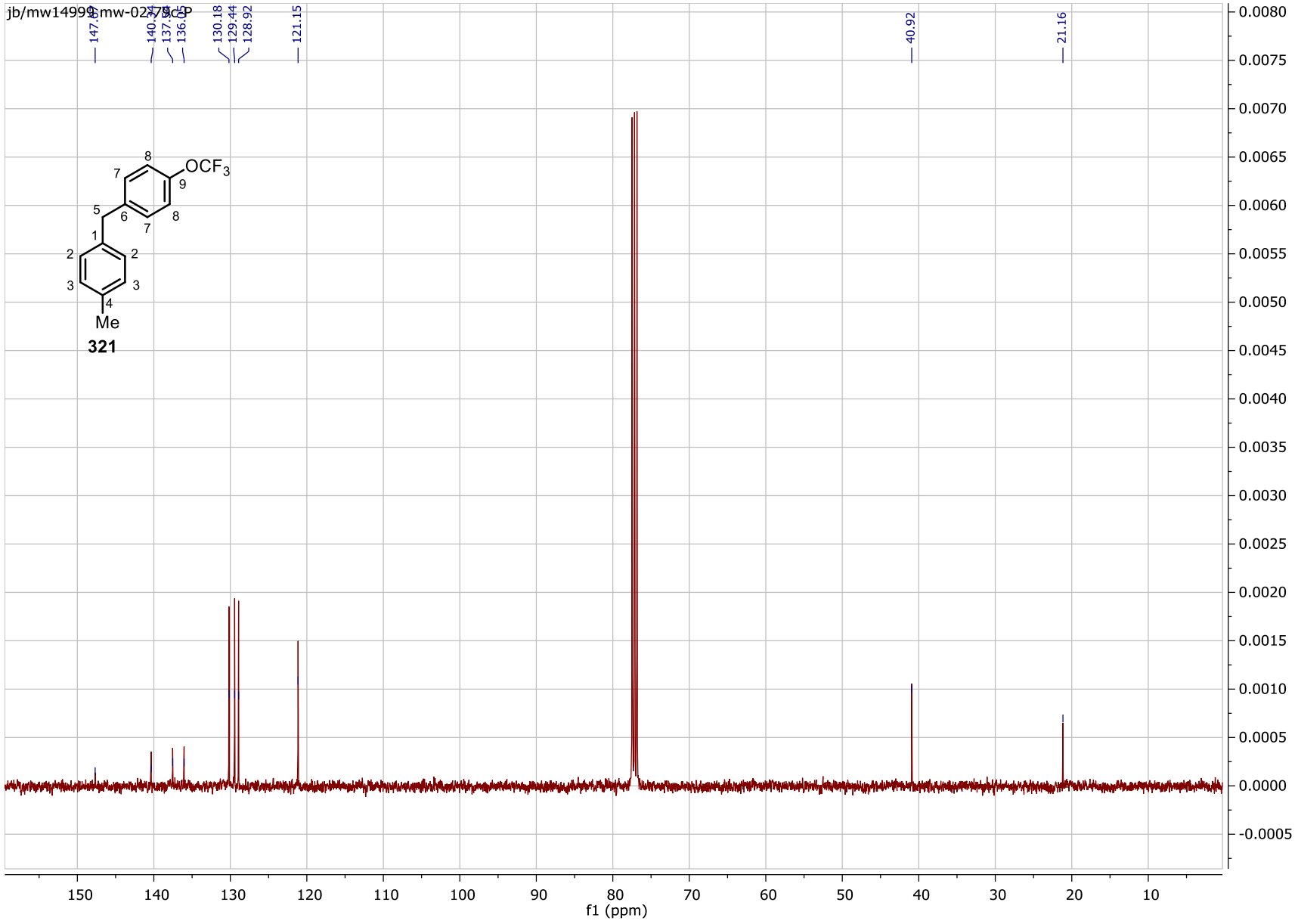
jb/mw14999-mw-027-9cD
147.87
140.47
137.45
136.05
130.18
129.44
128.92
121.15
40.92
21.16
OCF3
Me
321
f1 (ppm)

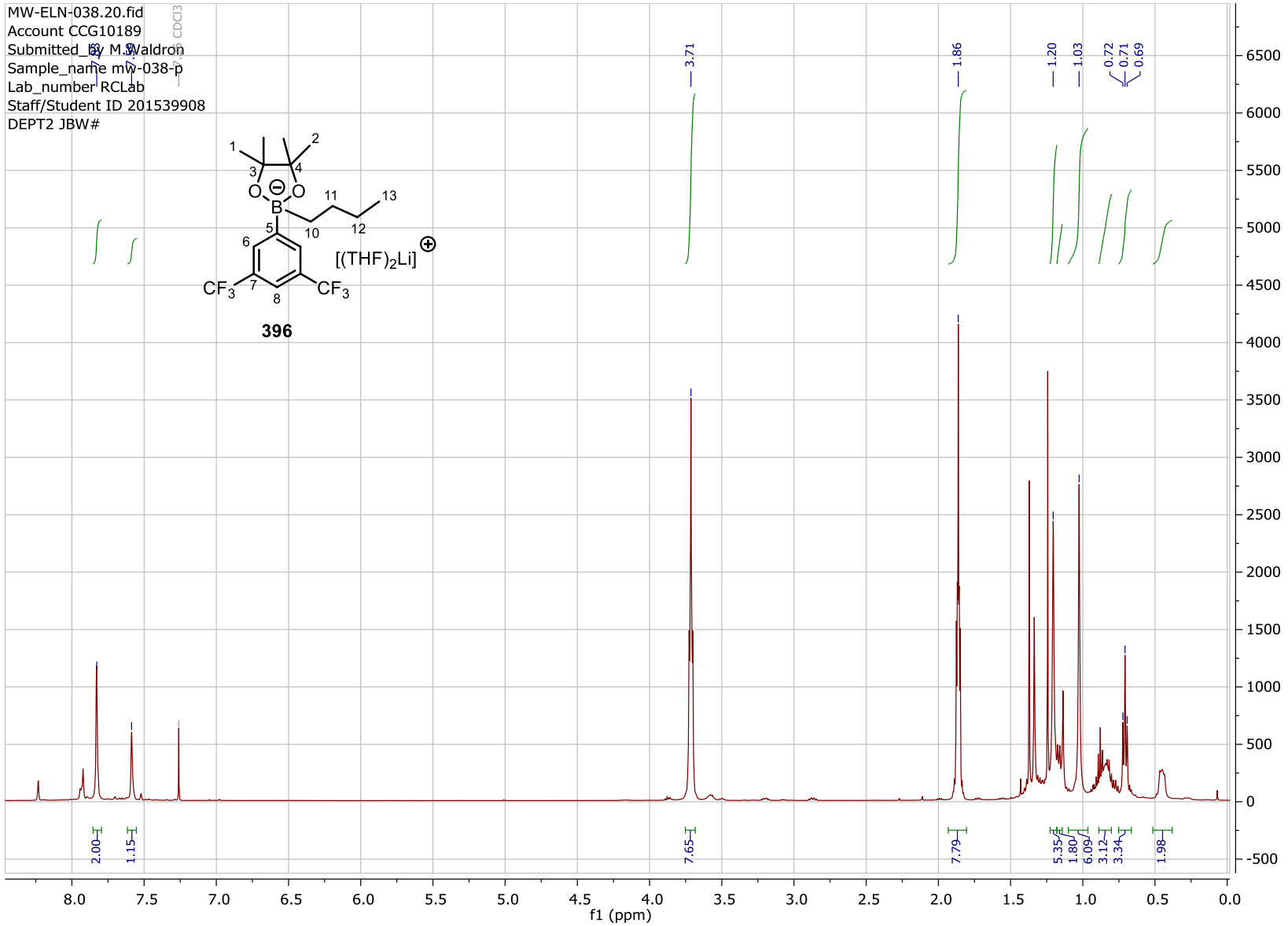
MW-ELN-038.20.fid
Account CCG10189
Submitted_by M.Waldron
Sample_name mw-038-p
Lab_number RCLab
Staff/Student ID 201539908
DEPT2 JBW#
CDCl3
[(THF)2Li]
CF3
CF3
396
3.71
1.86
1.20
1.03
0.72
0.71
0.69
2.00
1.15
7.65
7.79
5.35
1.80
6.09
3.12
3.34
1.98
f1 (ppm)

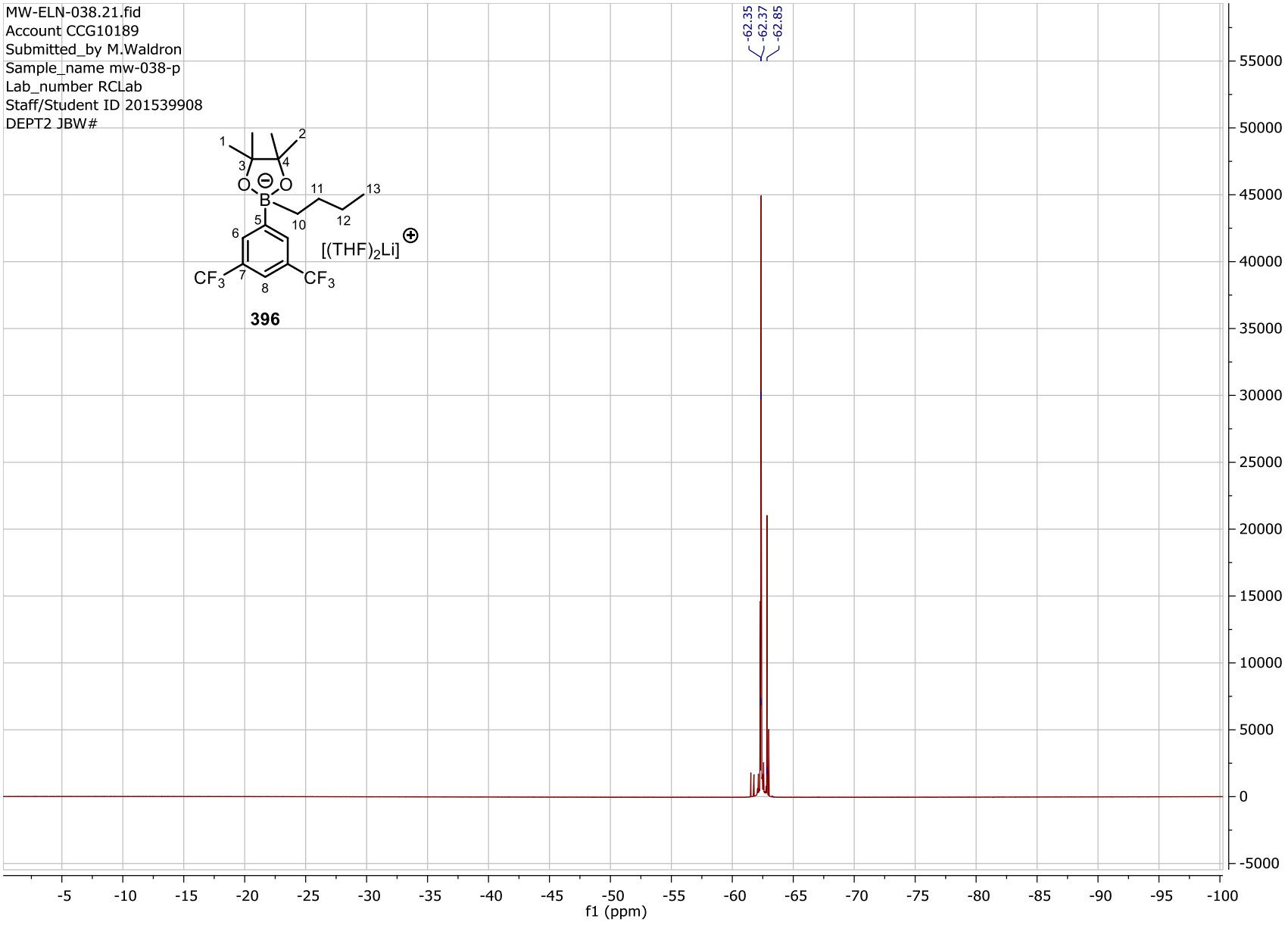
MW-ELN-038.21.fid
Account CCG10189
Submitted_by M.Waldron
Sample_name mw-038-p
Lab_number RCLab
Staff/Student ID 201539908
DEPT2 JBW#
-62.35
-62.37
-62.85
[(THF)2Li]
CF3
CF3
55000
50000
45000
40000
35000
30000
25000
20000
15000
10000
5000
0
-5000
-5
-10
-15
-20
-25
-30
-35
-40
-45
-50
-55
-60
-65
-70
-75
-80
-85
-90
-95
-100
f1 (ppm)

396

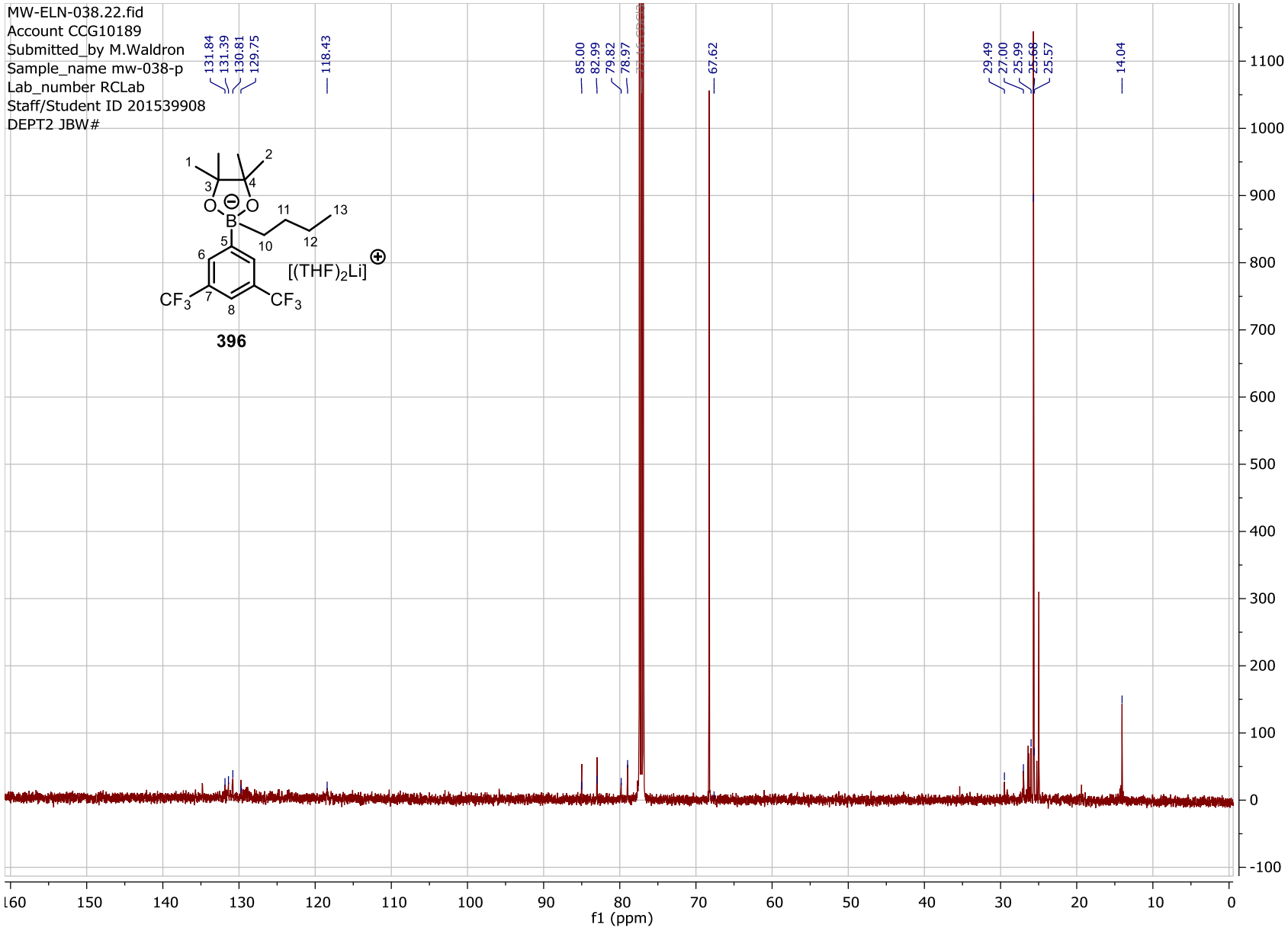
MW-ELN-038.22.fid
Account CCG10189
Submitted_by M.Waldron
Sample_name mw-038-p
Lab_number RCLab
Staff/Student ID 201539908
DEPT2 JBW#
131.84
131.39
130.81
129.75
118.43
85.00
82.99
79.82
78.97
67.62
29.49
27.00
25.99
25.68
25.57
14.04
[(THF)2Li]
CF3
CF3
f1 (ppm)

396

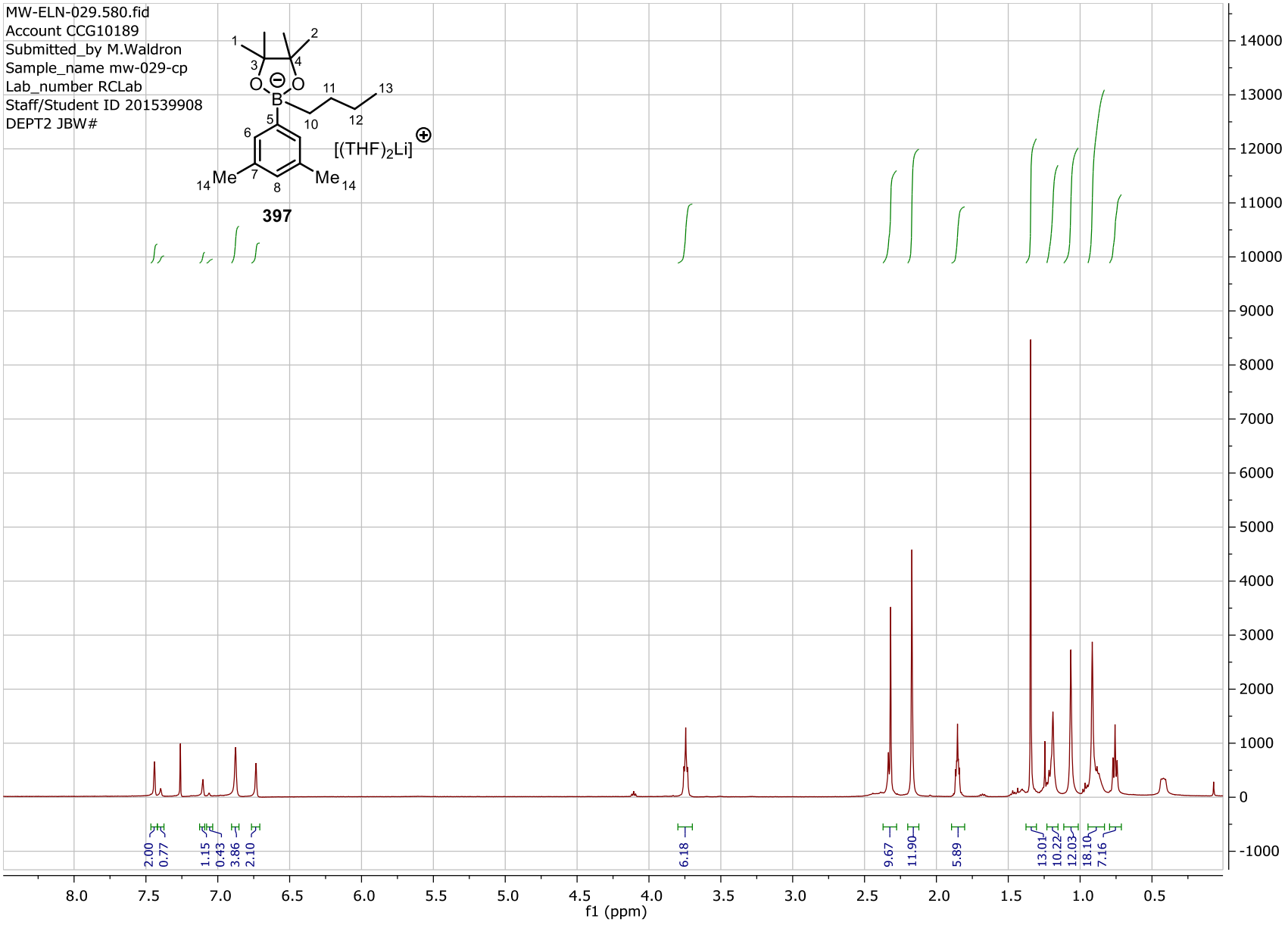
MW-ELN-029.580.fid
Account CCG10189
Submitted_by M.Waldron
Sample_name mw-029-cp
Lab_number RCLab
Staff/Student ID 201539908
DEPT2 JBW#
[(THF)2Li]
Me
Me
397
2.00
0.77
1.15
0.43
3.86
2.10
6.18
9.67
11.90
5.89
13.01
10.22
12.03
18.10
7.16
f1 (ppm)

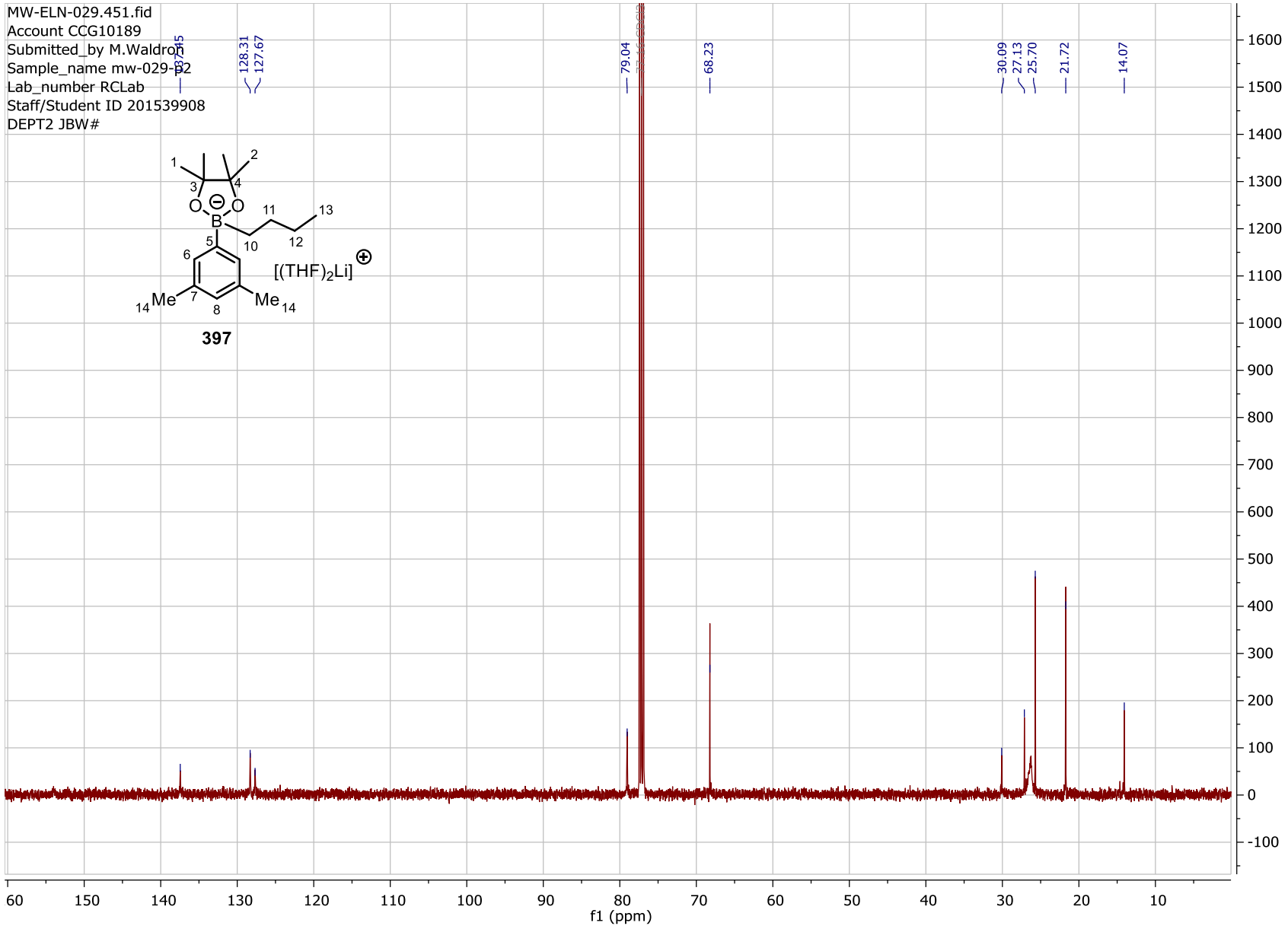
MW-ELN-029.451.fid
Account CCG10189
Submitted_by M.Waldron
Sample_name mw-029-02
Lab_number RCLab
Staff/Student ID 201539908
DEPT2 JBW#
128.31
127.67
79.04
68.23
30.09
27.13
25.70
21.72
14.07
[(THF)2Li]
Me
Me
f1 (ppm)

397

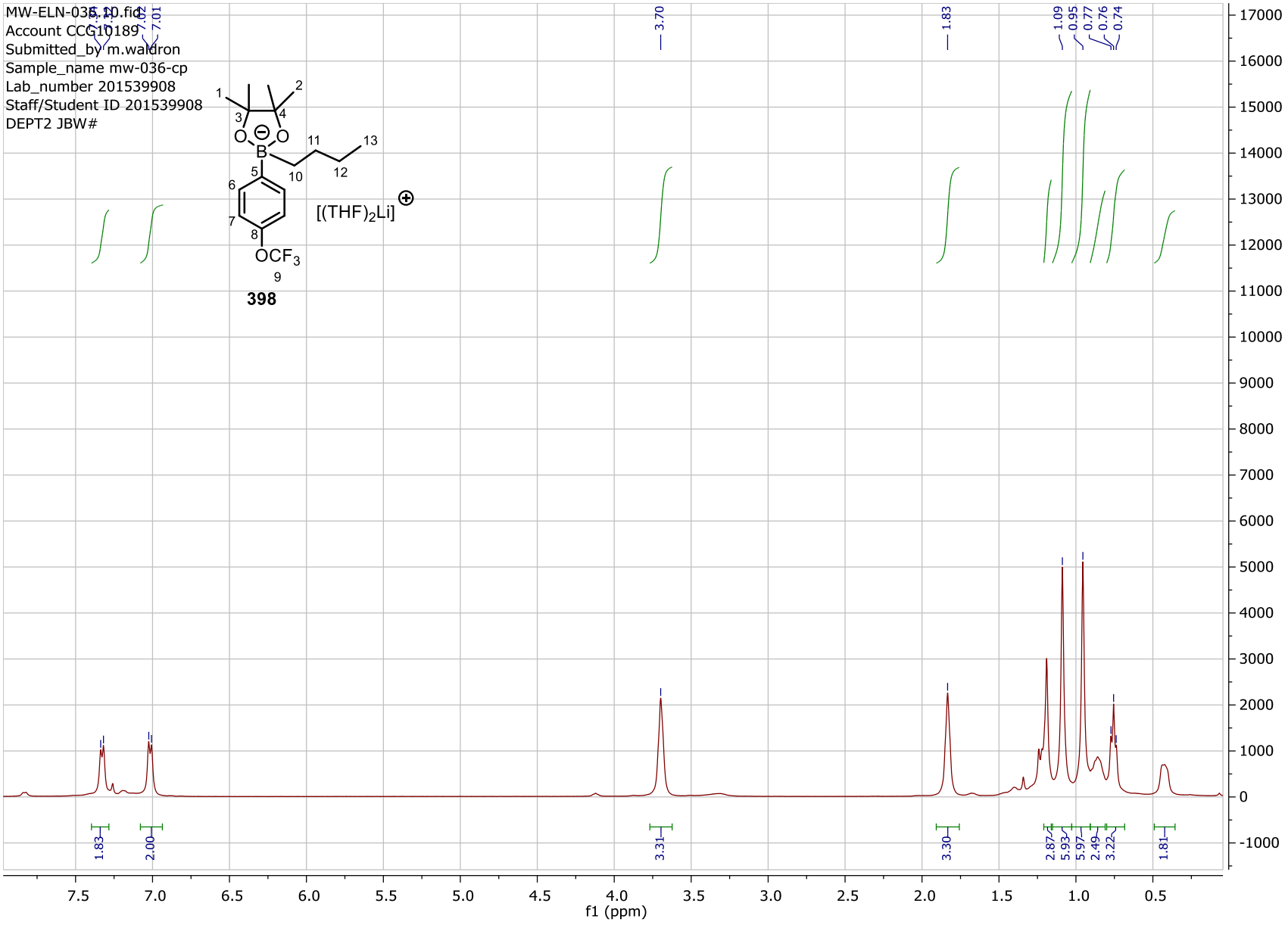
MW-ELN-036-10.fid
Account CCG10189
Submitted_by m.waldron
Sample_name mw-036-cp
Lab_number 201539908
Staff/Student ID 201539908
DEPT2 JBW#
[(THF)2Li]
398
f1 (ppm)

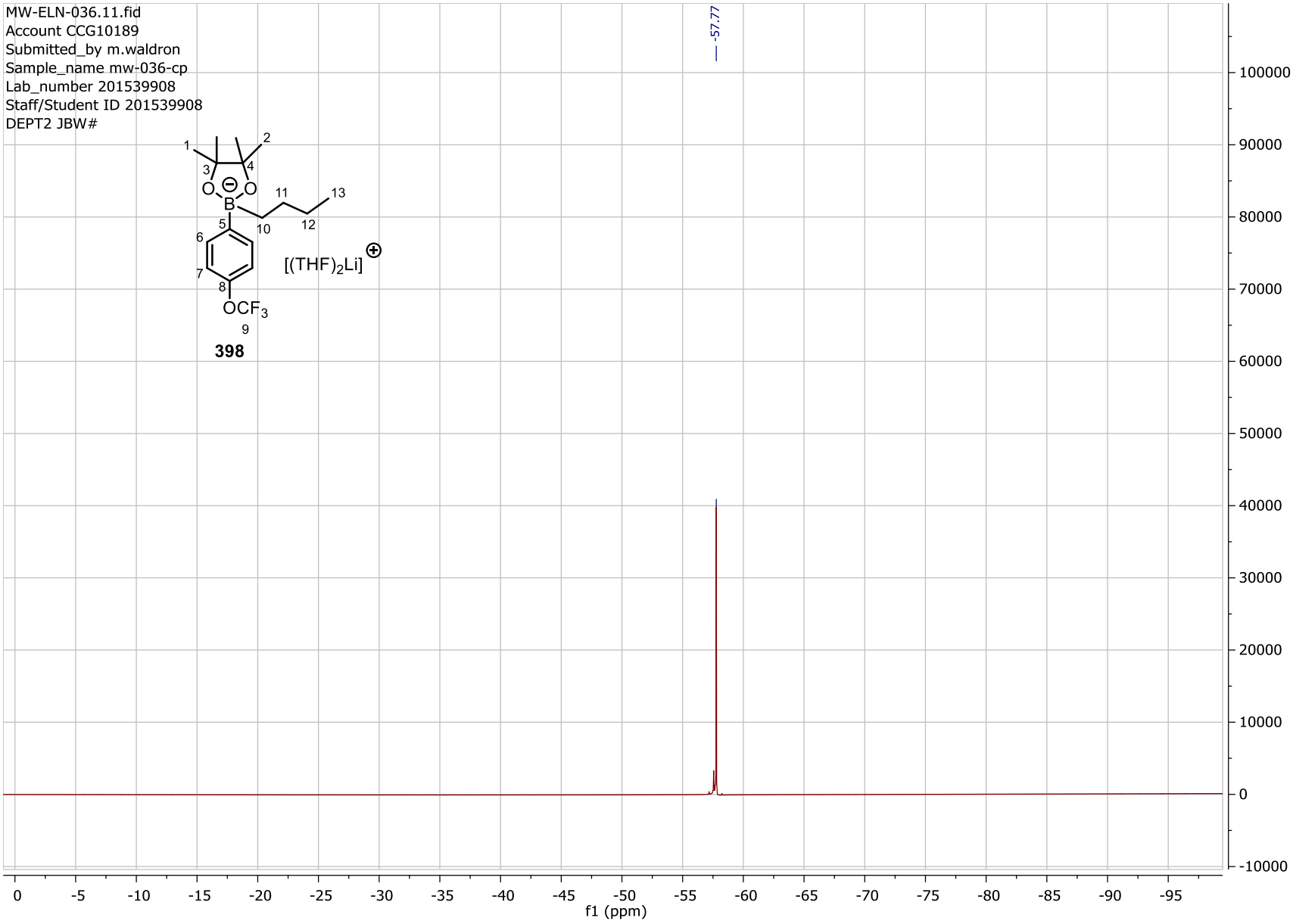
MW-ELN-036.11.fid
Account CCG10189
Submitted_by m.waldron
Sample_name mw-036-cp
Lab_number 201539908
Staff/Student ID 201539908
DEPT2 JBW#
-57.77
[(THF)2Li]
OCF3
398
f1 (ppm)

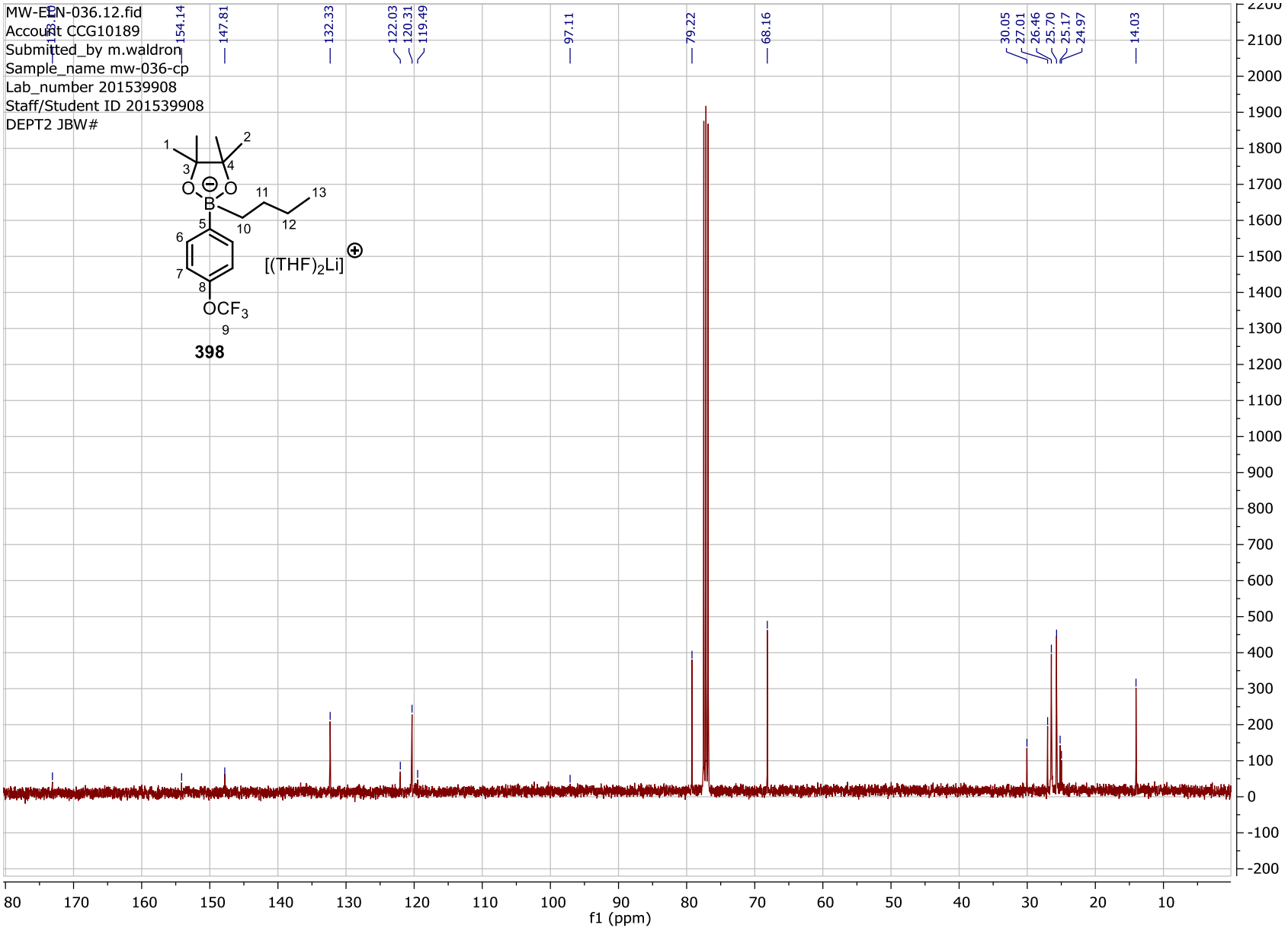
MW-EEN-036.12.fid
Account CCG10189
Submitted_by m.waldron
Sample_name mw-036-cp
Lab_number 201539908
Staff/Student ID 201539908
DEPT2 JBW#
154.14
147.81
132.33
122.03
120.31
119.49
97.11
79.22
68.16
30.05
27.01
26.46
25.70
25.17
24.97
14.03
[(THF)2Li]
OCF3
398
f1 (ppm)

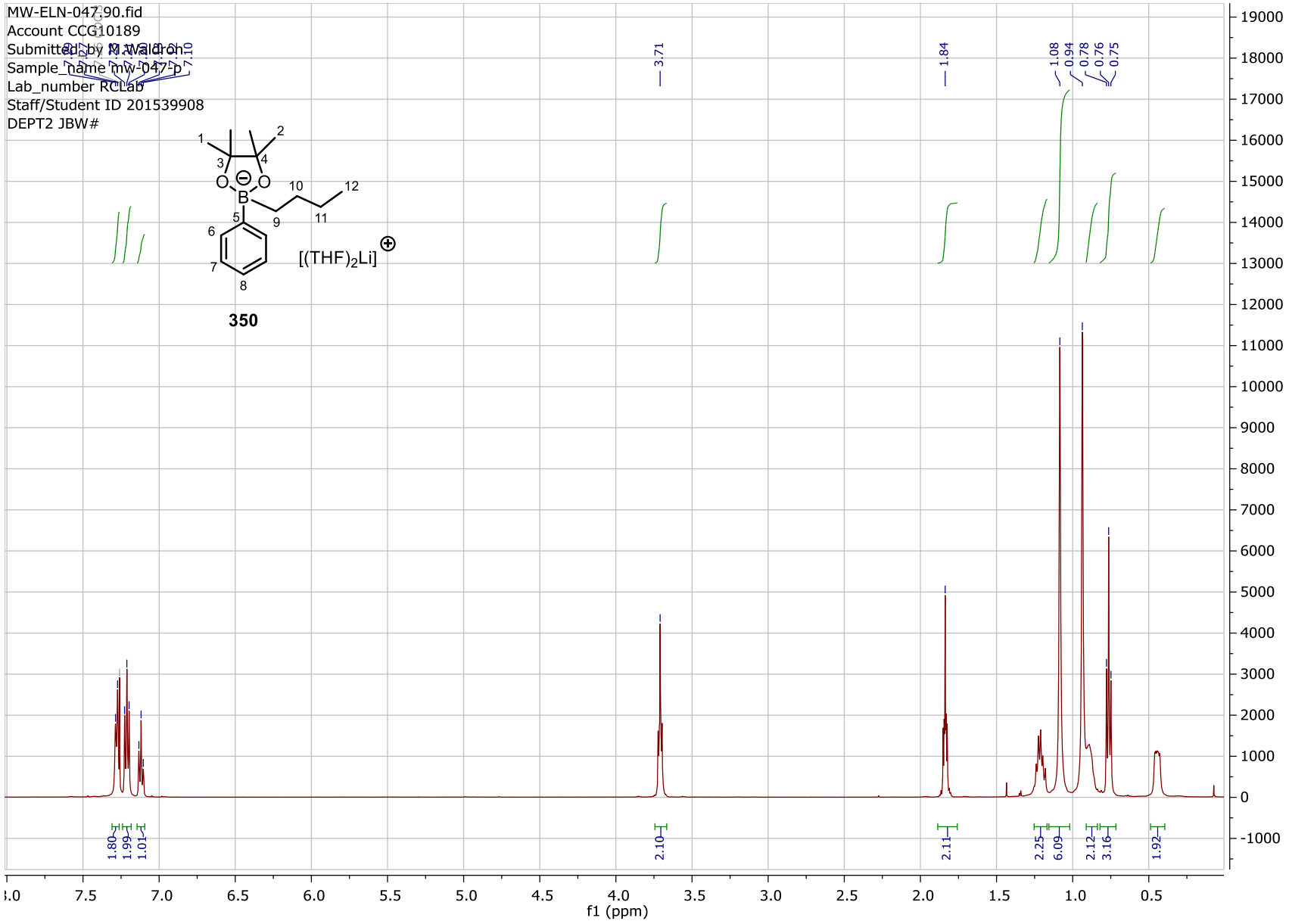
MW-ELN-047-90.fid
Account CCG10189
Submitted by M.Waldron
Sample_name mw-047-p
Lab_number RCLab
Staff/Student ID 201539908
DEPT2 JBW#
[(THF)2Li]
350
3.71
1.84
1.08
0.94
0.78
0.76
0.75
1.80
1.99
1.01
2.10
2.11
2.25
6.09
2.12
3.16
1.92
f1 (ppm)

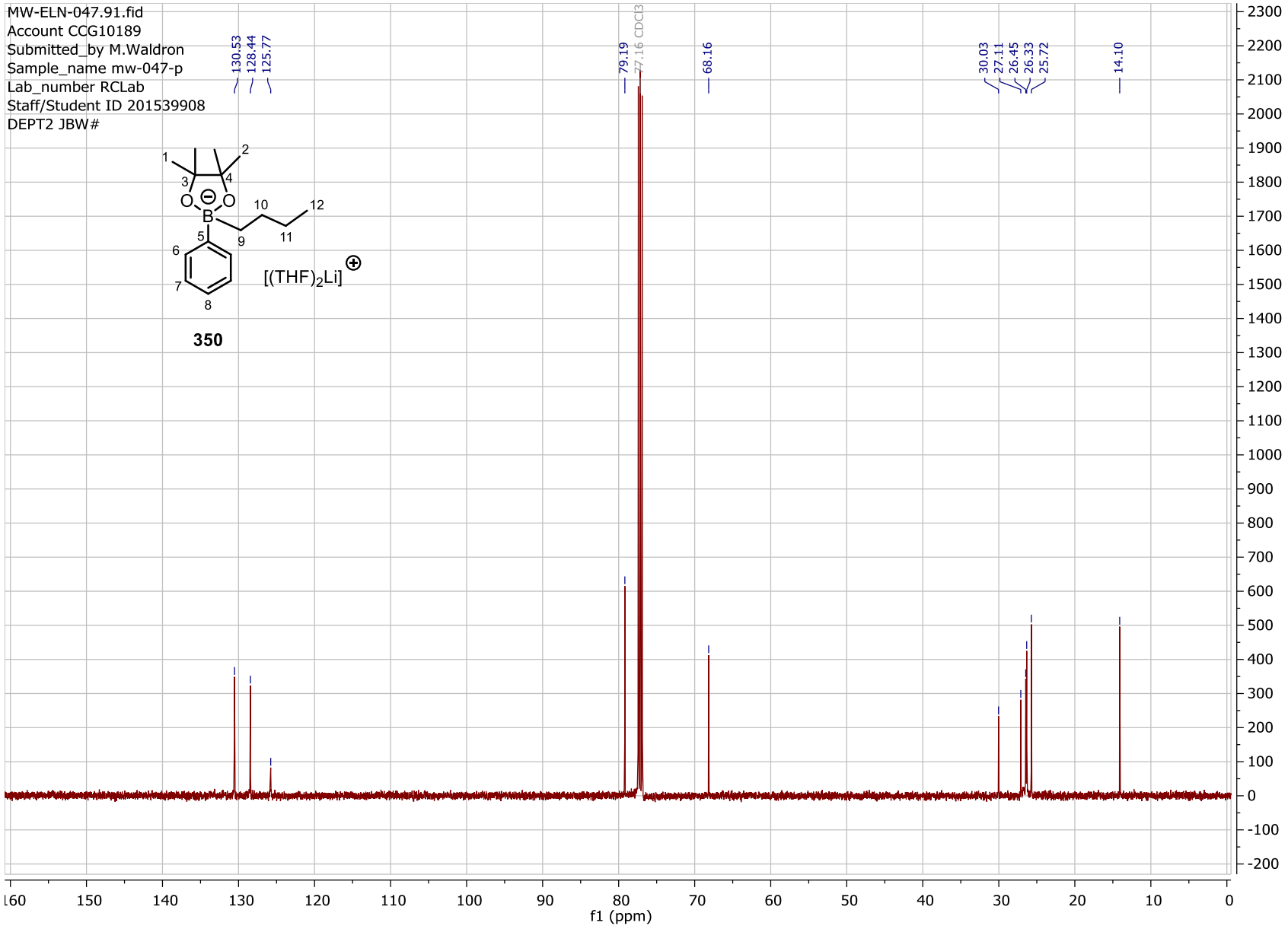
MW-ELN-047.91.fid
Account CCG10189
Submitted_by M.Waldron
Sample_name mw-047-p
Lab_number RCLab
Staff/Student ID 201539908
DEPT2 JBW#
130.53
128.44
125.77
79.19
77.16 CDCl3
68.16
30.03
27.11
26.45
26.33
25.72
14.10
[(THF)2Li]
350
f1 (ppm)

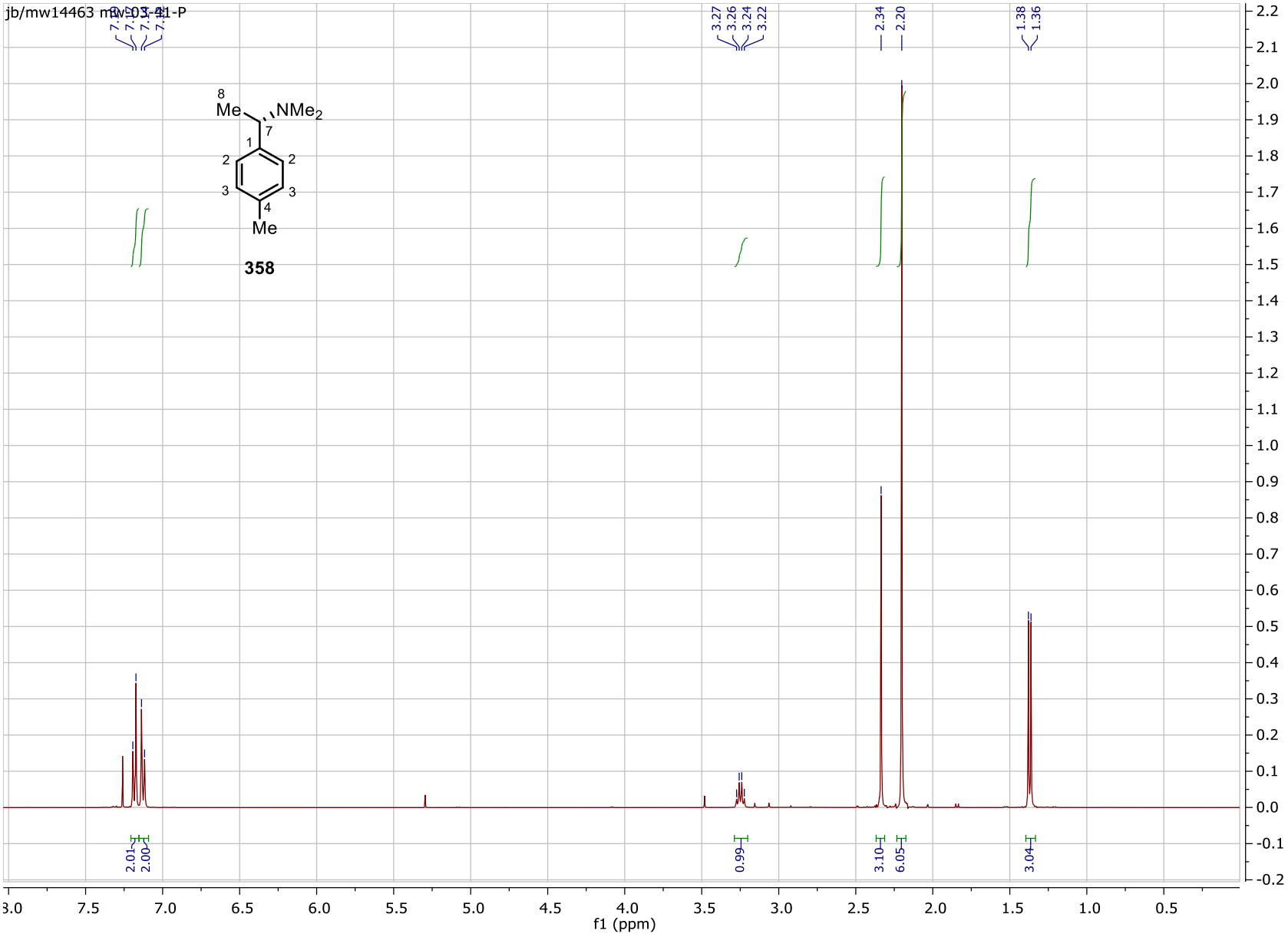
jb/mw14463 mw-03-41-P
7.26
7.25
7.24
7.22
3.27
3.26
3.24
3.22
2.34
2.20
1.38
1.36
Me
NMe2
Me
358
2.01
2.00
0.99
3.10
6.05
3.04
f1 (ppm)

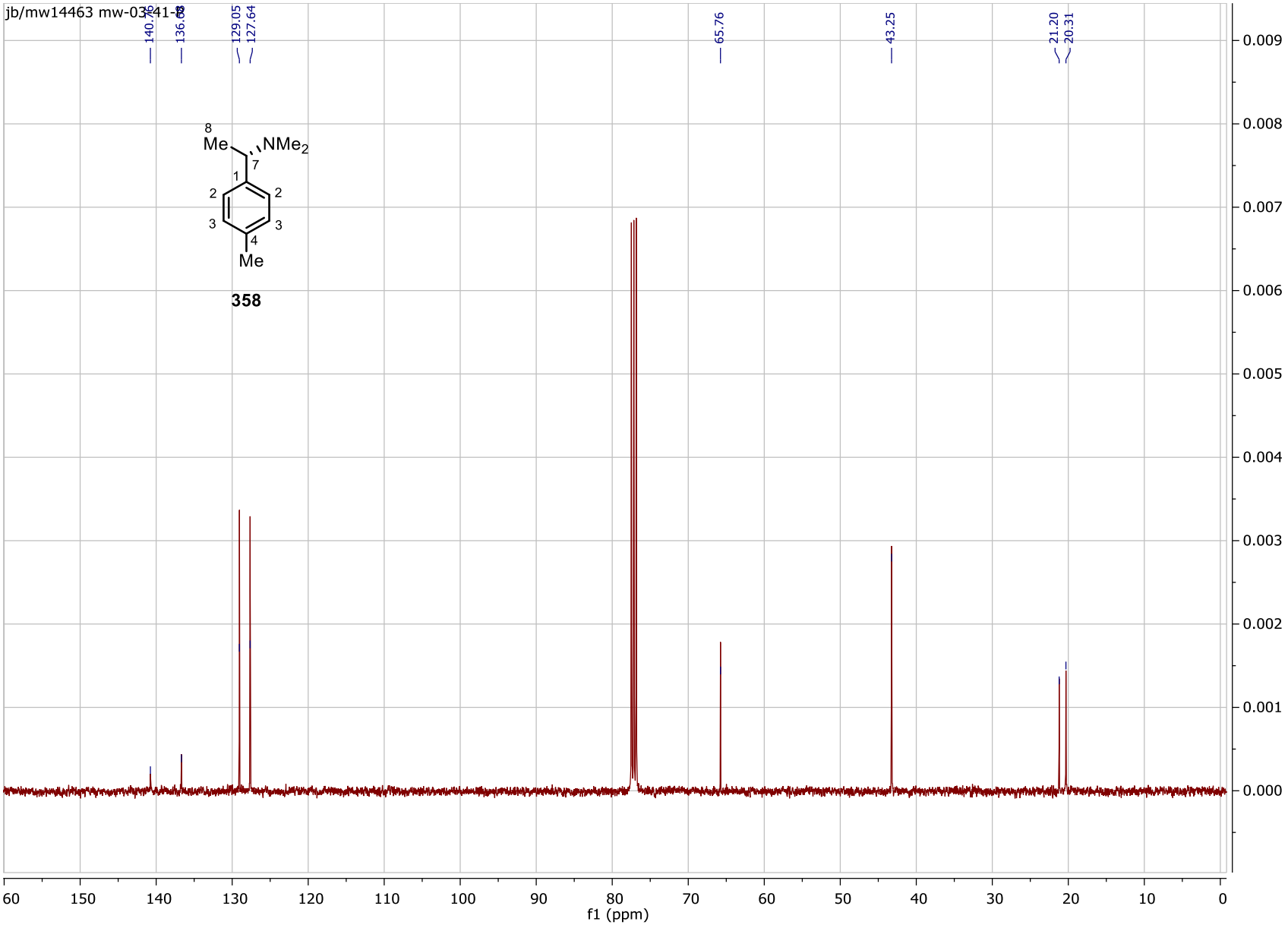
jb/mw14463 mw-03241-8
140.76
136.68
129.05
127.64
65.76
43.25
21.20
20.31
8
Me
NMe2
7
1
2
2
3
3
4
Me
358
0.009
0.008
0.007
0.006
0.005
0.004
0.003
0.002
0.001
0.000
60
150
140
130
120
110
100
90
80
70
60
50
40
30
20
10
0
f1 (ppm)

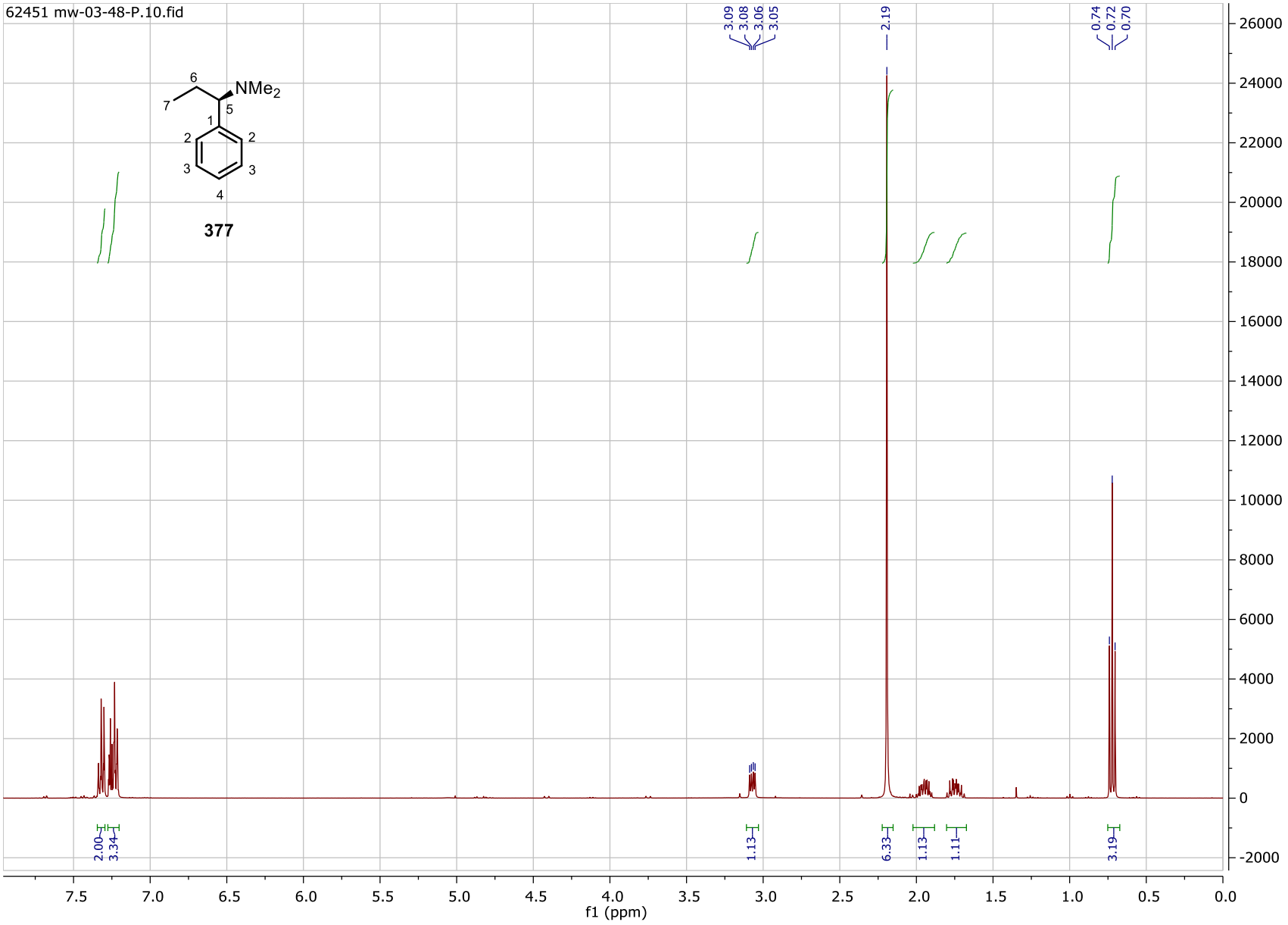
62451 mw-03-48-P.10.fid
3.09
3.08
3.06
3.05
2.19
0.74
0.72
0.70
NMe2
377
2.00
3.34
1.13
6.33
1.13
1.11
3.19
f1 (ppm)

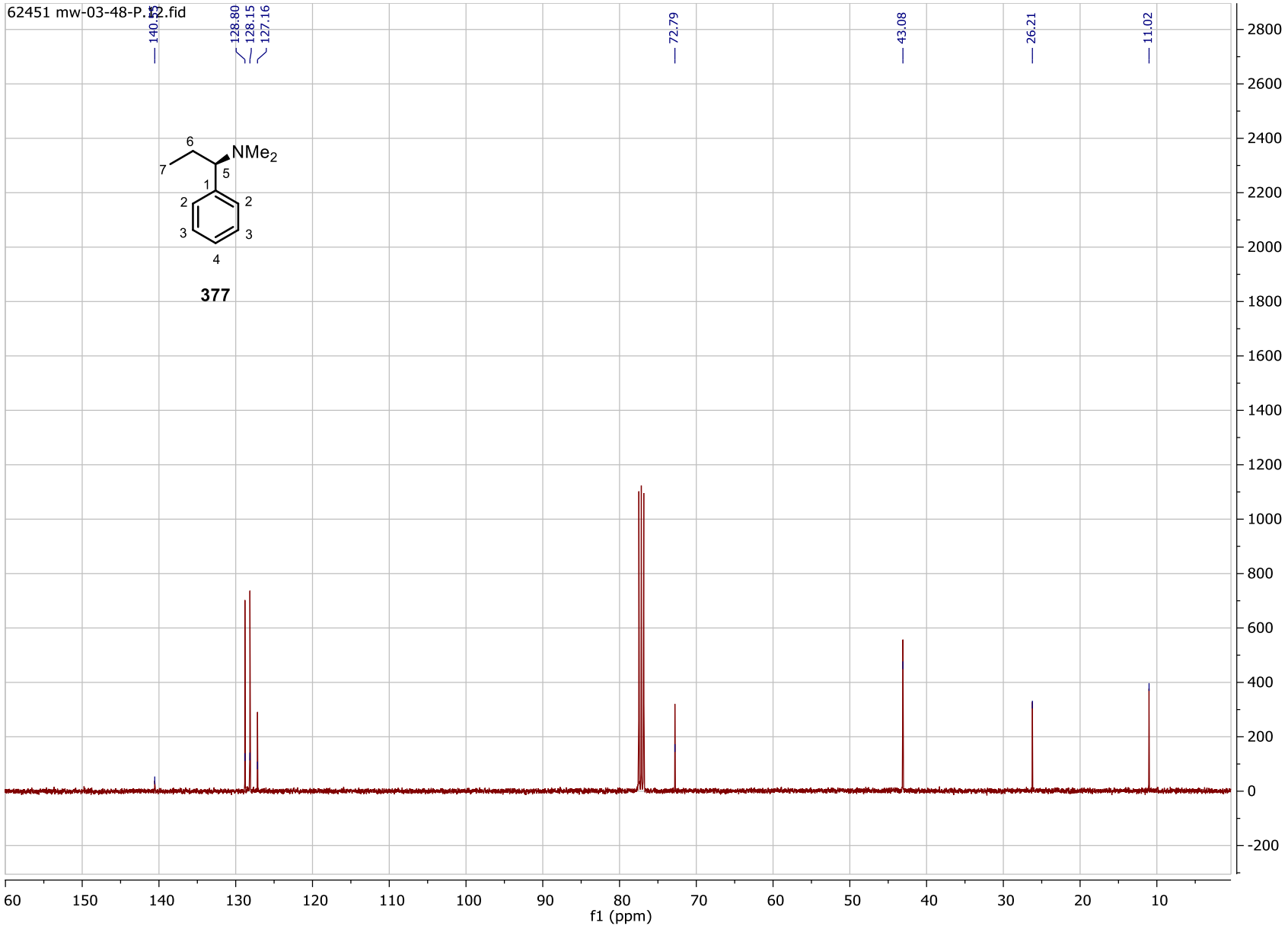
62451 mw-03-48-P.12.fid
140.12
128.80
128.15
127.16
72.79
43.08
26.21
11.02
NMe2
377
f1 (ppm)

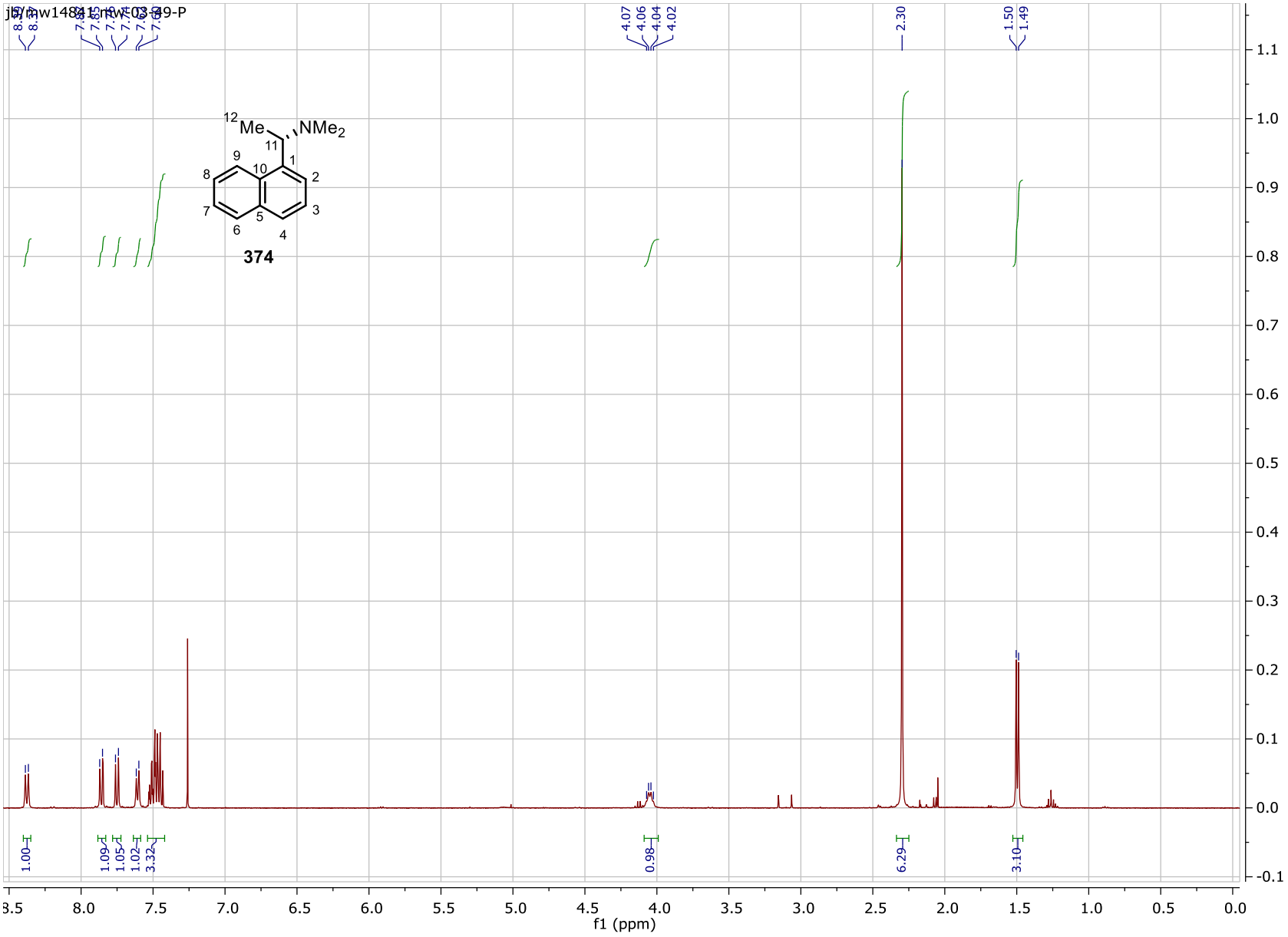
jb/mw14841-mw-03-39-P
8.31
8.30
7.85
7.84
7.77
7.76
7.63
7.62
4.07
4.06
4.04
4.02
2.30
1.50
1.49
12
Me
NMe2
11
1
2
3
4
5
6
7
8
9
10
374
1.00
1.09
1.05
1.02
3.32
0.98
6.29
3.10
f1 (ppm)

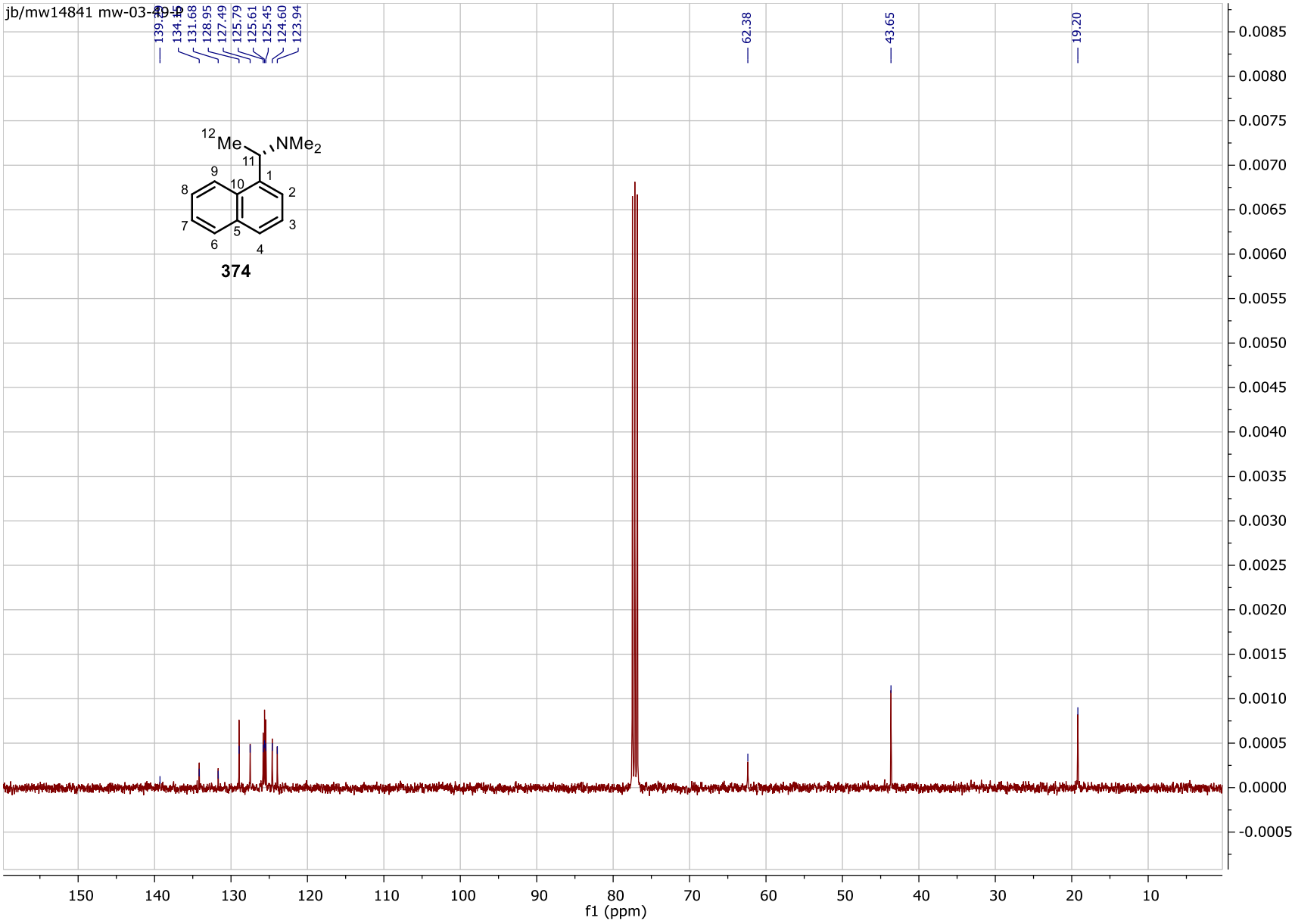
jb/mw14841 mw-03-49-b
139.78
134.14
131.68
128.95
127.49
125.79
125.61
125.45
124.60
123.94
62.38
43.65
19.20
12
Me
NMe2
11
1
2
3
4
5
6
7
8
9
10
374
0.0085
0.0080
0.0075
0.0070
0.0065
0.0060
0.0055
0.0050
0.0045
0.0040
0.0035
0.0030
0.0025
0.0020
0.0015
0.0010
0.0005
0.0000
-0.0005
150
140
130
120
110
100
90
80
70
60
50
40
30
20
10
f1 (ppm)

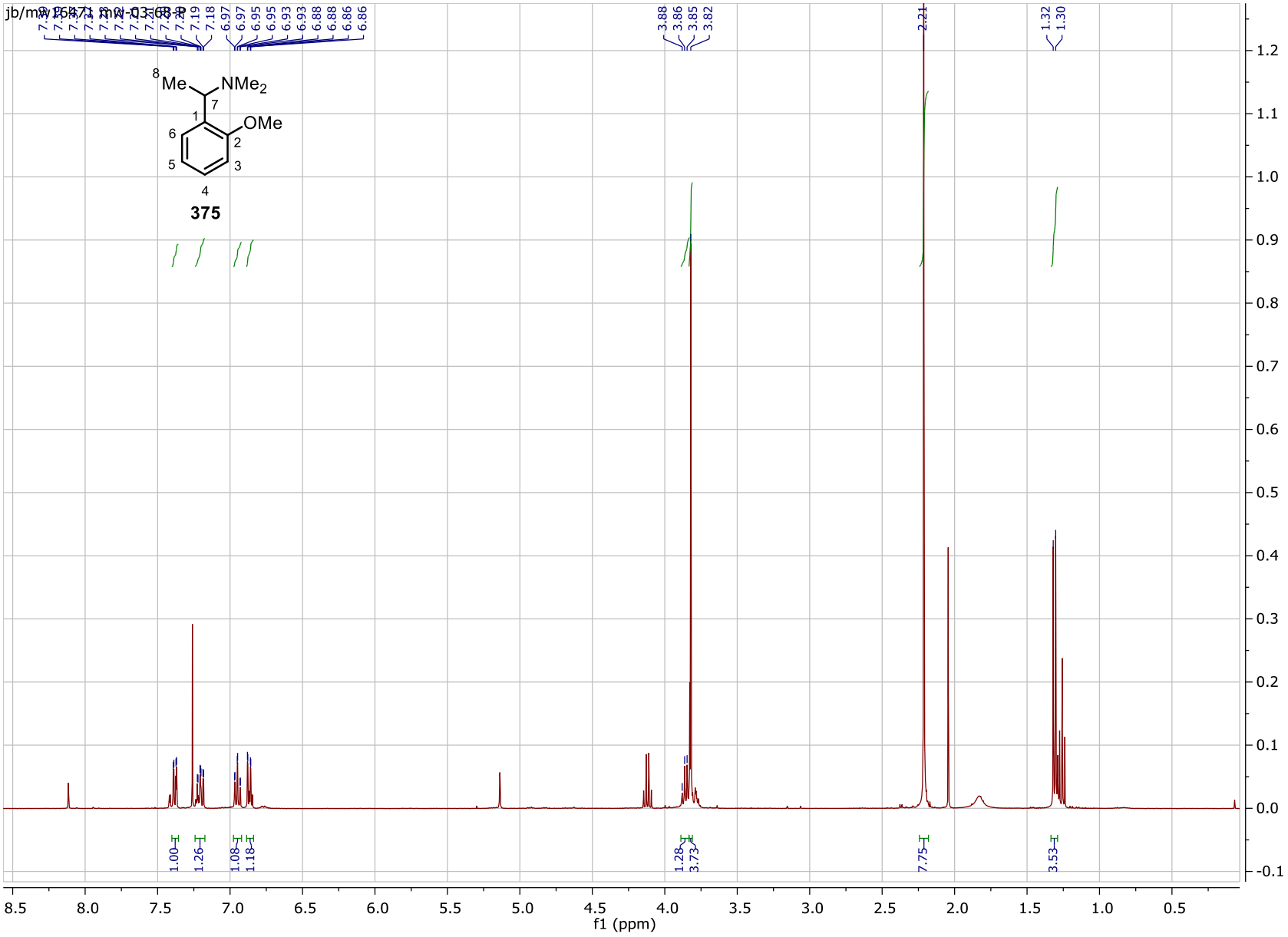
jb/mw/26471 mw-03-68-p
7.28
7.19
7.18
6.97
6.95
6.93
6.88
6.86
3.88
3.86
3.85
3.82
2.21
1.32
1.30
Me
NMe2
OMe
375
1.00
1.26
1.08
1.18
1.28
3.73
7.75
3.53
f1 (ppm)

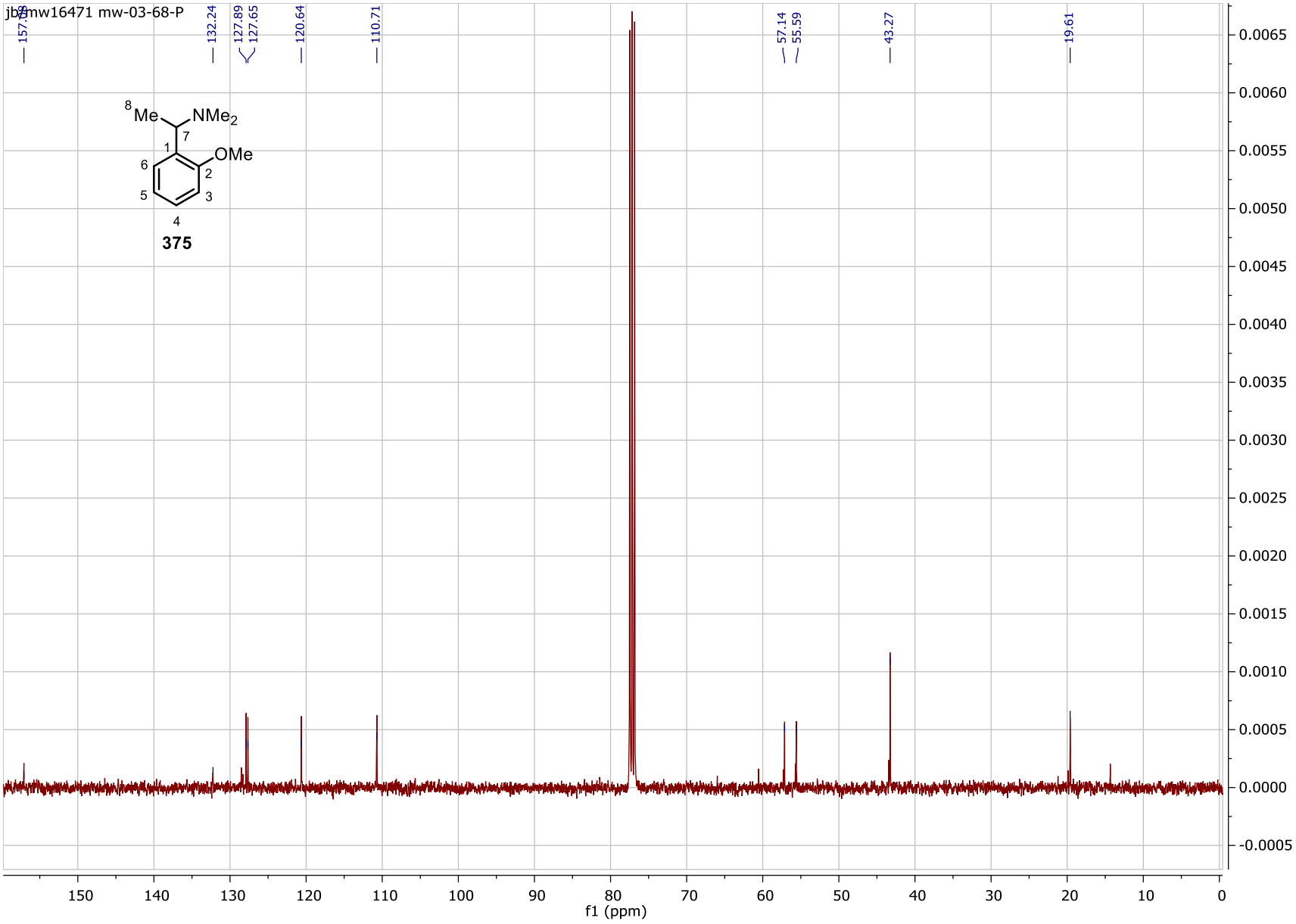
jb@mw16471 mw-03-68-P
157.88
132.24
127.89
127.65
120.64
110.71
57.14
55.59
43.27
19.61
8Me
NMe2
7
1
OMe
6
2
5
3
4
375
0.0065
0.0060
0.0055
0.0050
0.0045
0.0040
0.0035
0.0030
0.0025
0.0020
0.0015
0.0010
0.0005
0.0000
-0.0005
150
140
130
120
110
100
90
80
70
60
50
40
30
20
10
0
f1 (ppm)

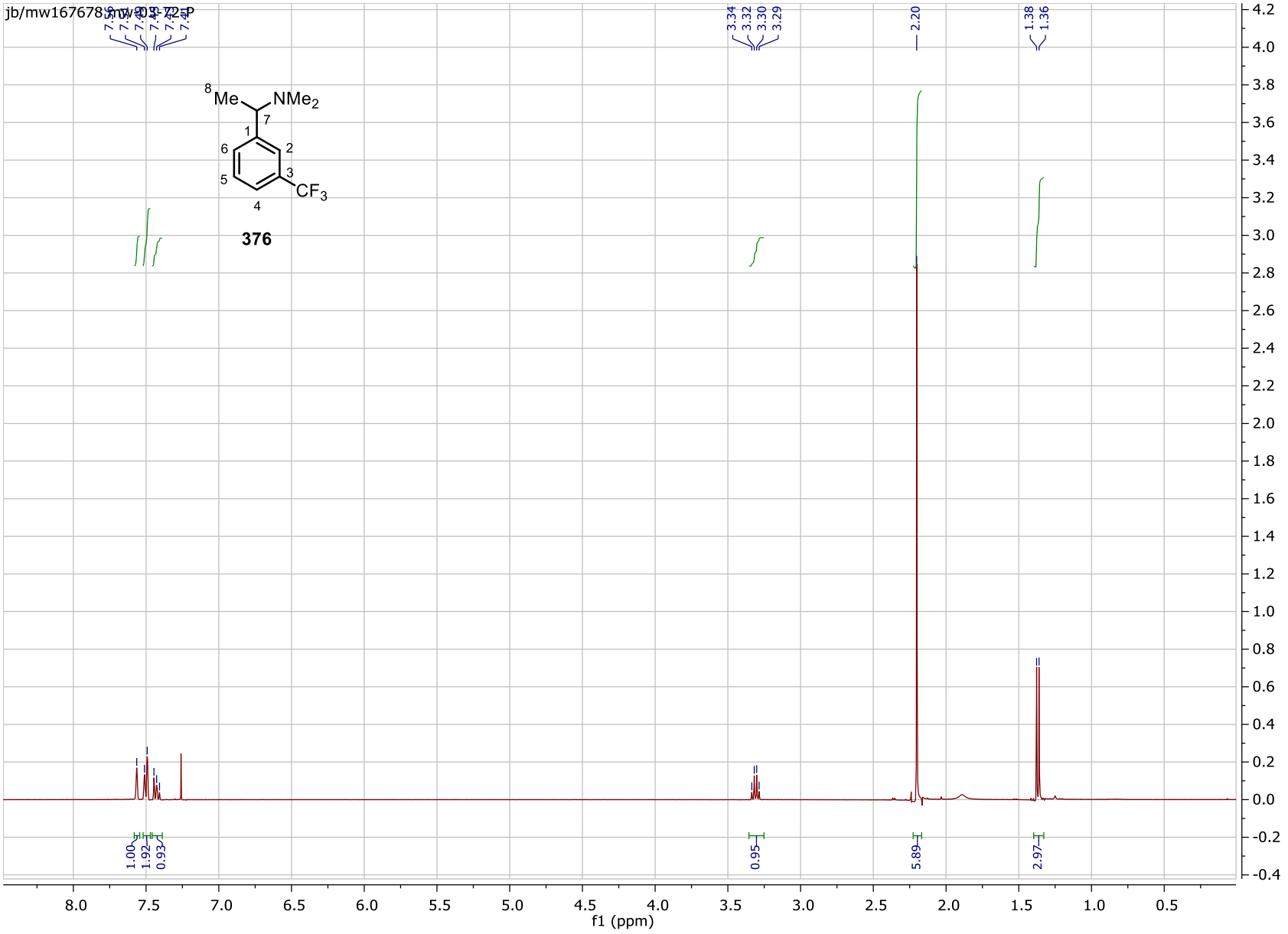
jb/mw167678/mw205-72-P
7.58
7.56
7.48
7.46
7.44
7.43
7.42
7.41
3.34
3.32
3.30
3.29
2.20
1.38
1.36
8
Me
NMe2
7
1
2
3
4
5
6
CF3
376
1.00
1.92
0.93
0.95
5.89
2.97
f1 (ppm)

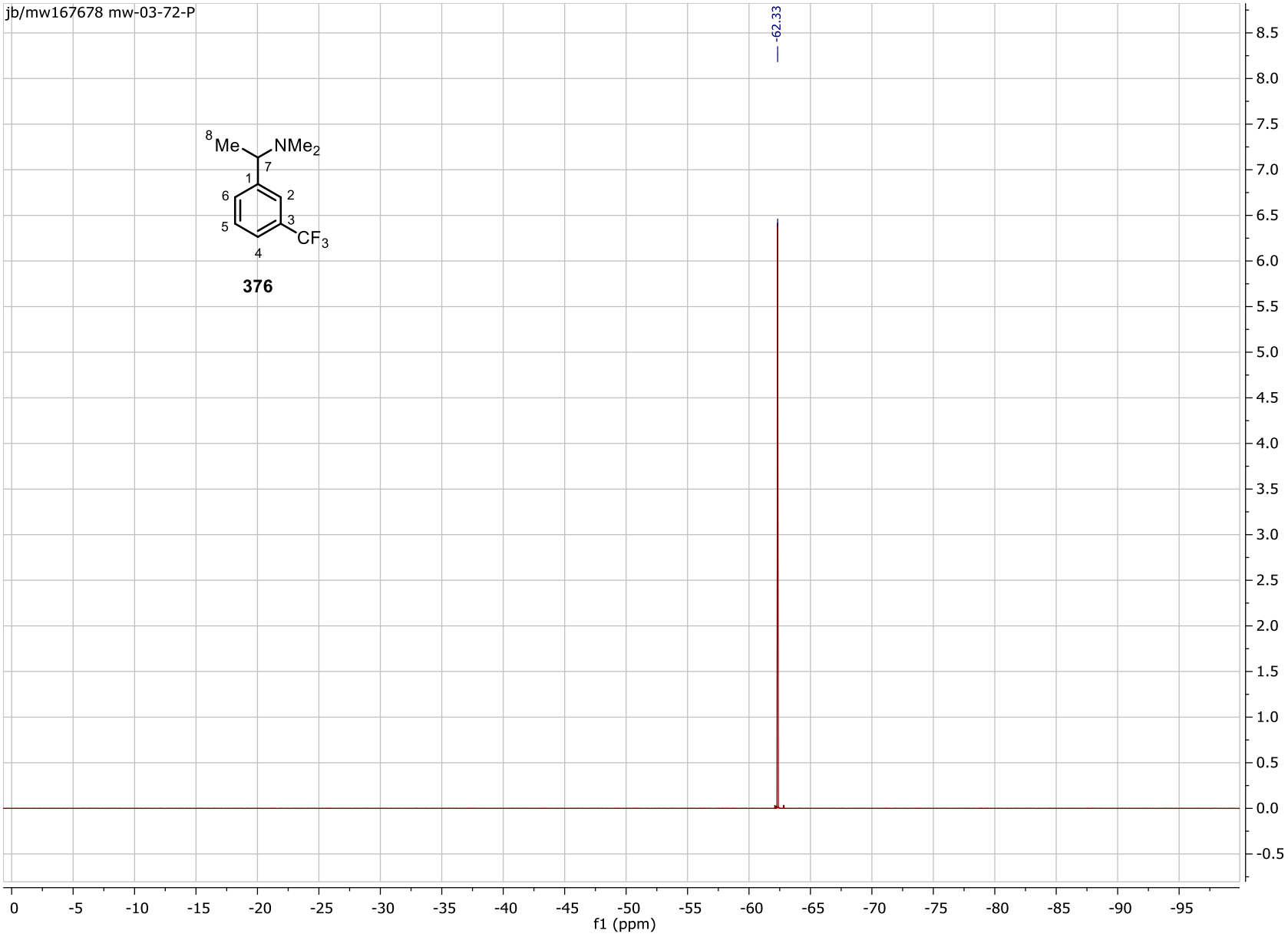
jb/mw167678 mw-03-72-P
-62.33
8
Me
NMe2
7
1
6
2
5
3
4
CF3
376
8.5
8.0
7.5
7.0
6.5
6.0
5.5
5.0
4.5
4.0
3.5
3.0
2.5
2.0
1.5
1.0
0.5
0.0
-0.5
0
-5
-10
-15
-20
-25
-30
-35
-40
-45
-50
-55
-60
-65
-70
-75
-80
-85
-90
-95
f1 (ppm)

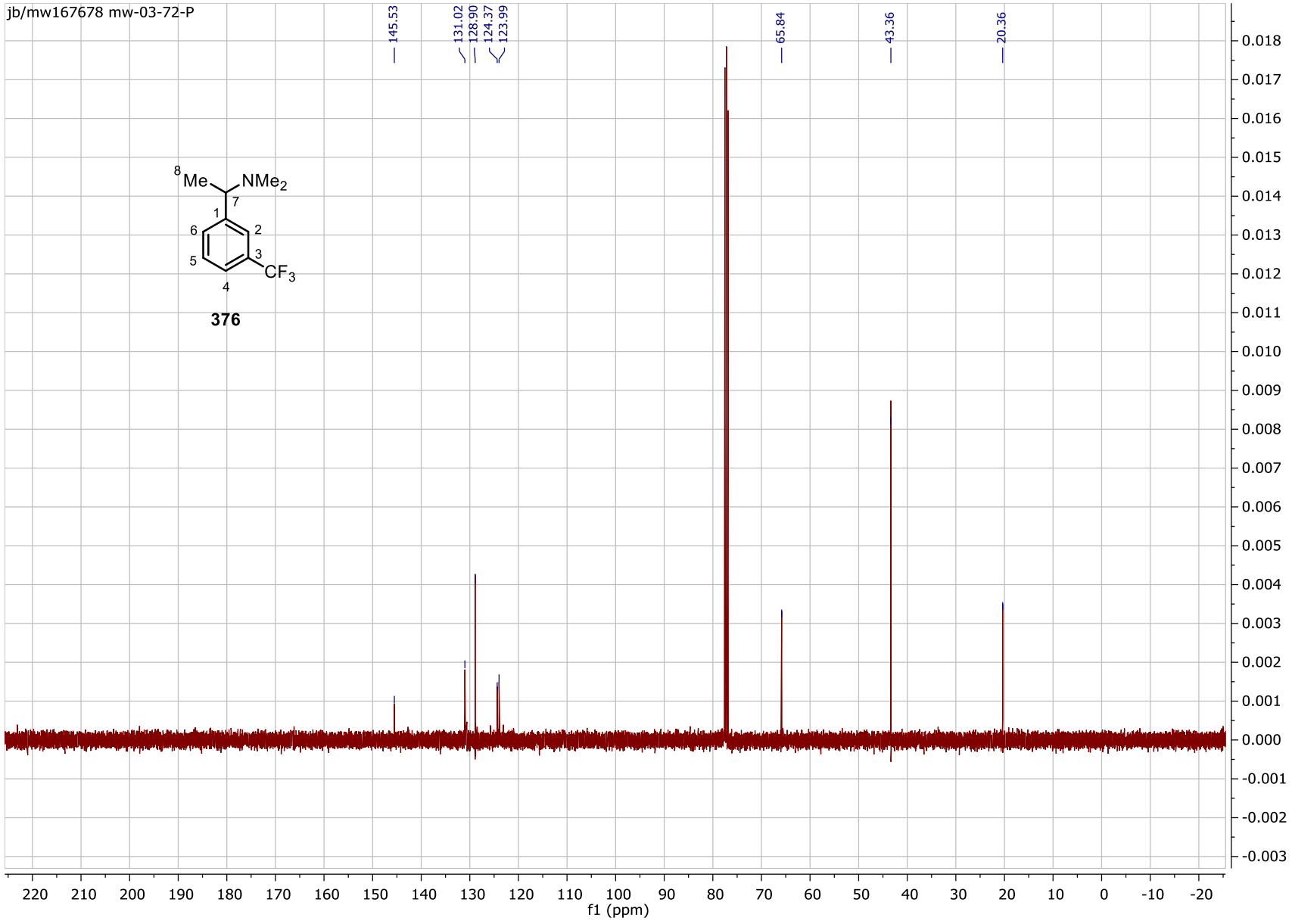
jb/mw167678 mw-03-72-P
145.53
131.02
128.90
124.37
123.99
65.84
43.36
20.36
Me
NMe2
CF3
376
f1 (ppm)

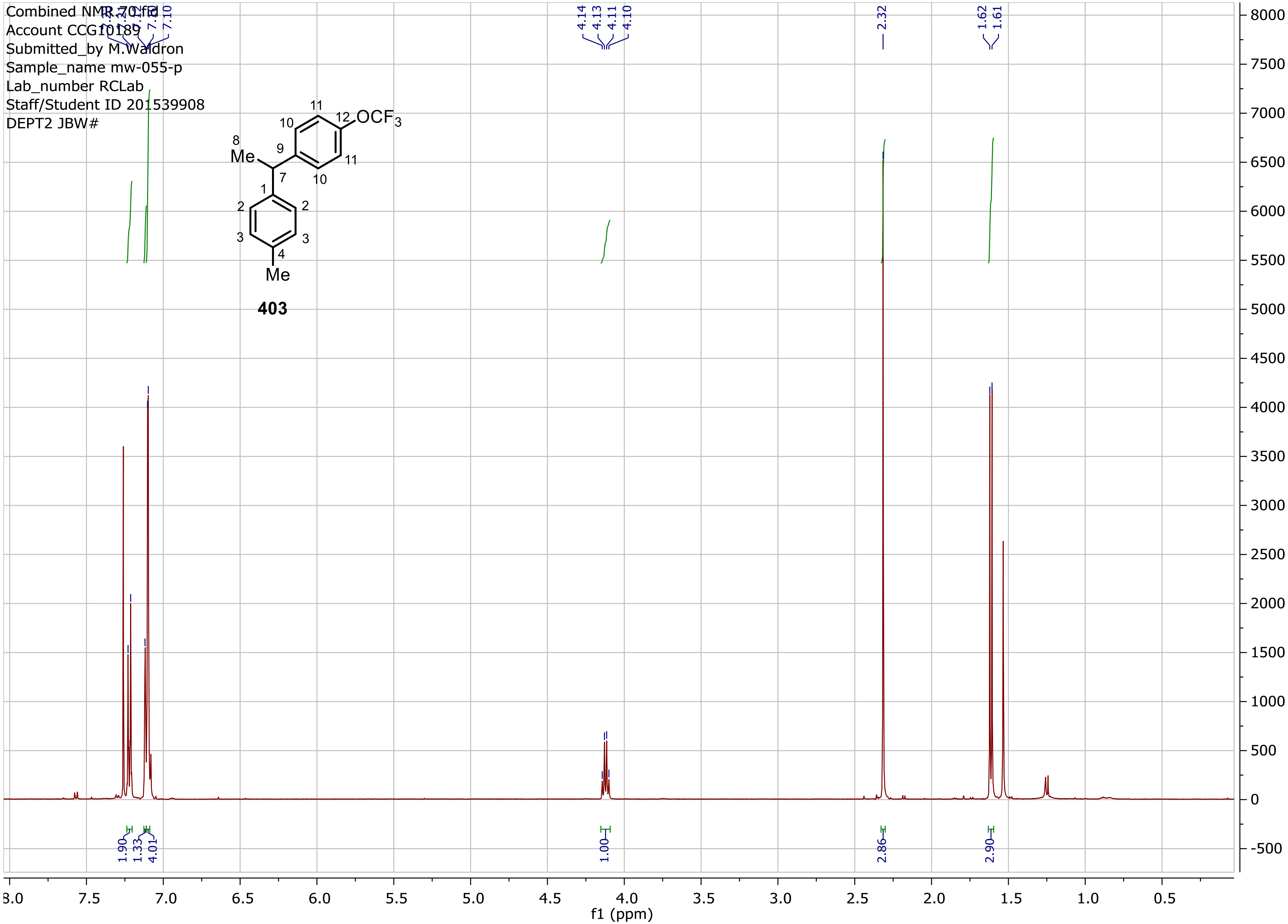
Combined NMR 70 fid
Account CCG10189
Submitted_by M.Waldron
Sample_name mw-055-p
Lab_number RCLab
Staff/Student ID 201539908
DEPT2 JBW#
7.10
4.14
4.13
4.11
4.10
2.32
1.62
1.61
OCF3
Me
Me
403
1.90
1.33
4.01
1.00
2.86
2.90
f1 (ppm)

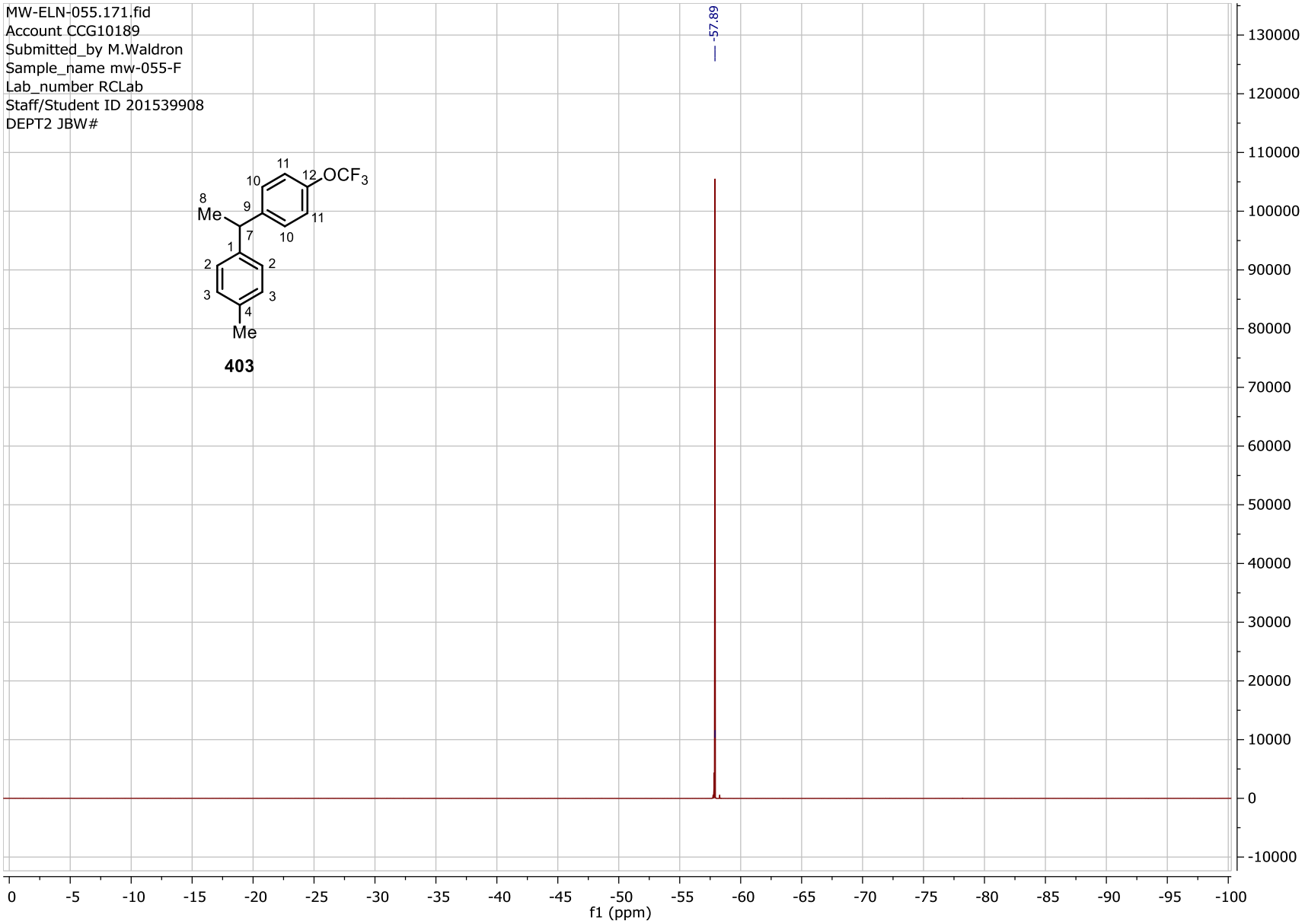
MW-ELN-055.171.fid
Account CCG10189
Submitted_by M.Waldron
Sample_name mw-055-F
Lab_number RCLab
Staff/Student ID 201539908
DEPT2 JBW#
-57.89
OCF3
Me
Me
403
f1 (ppm)

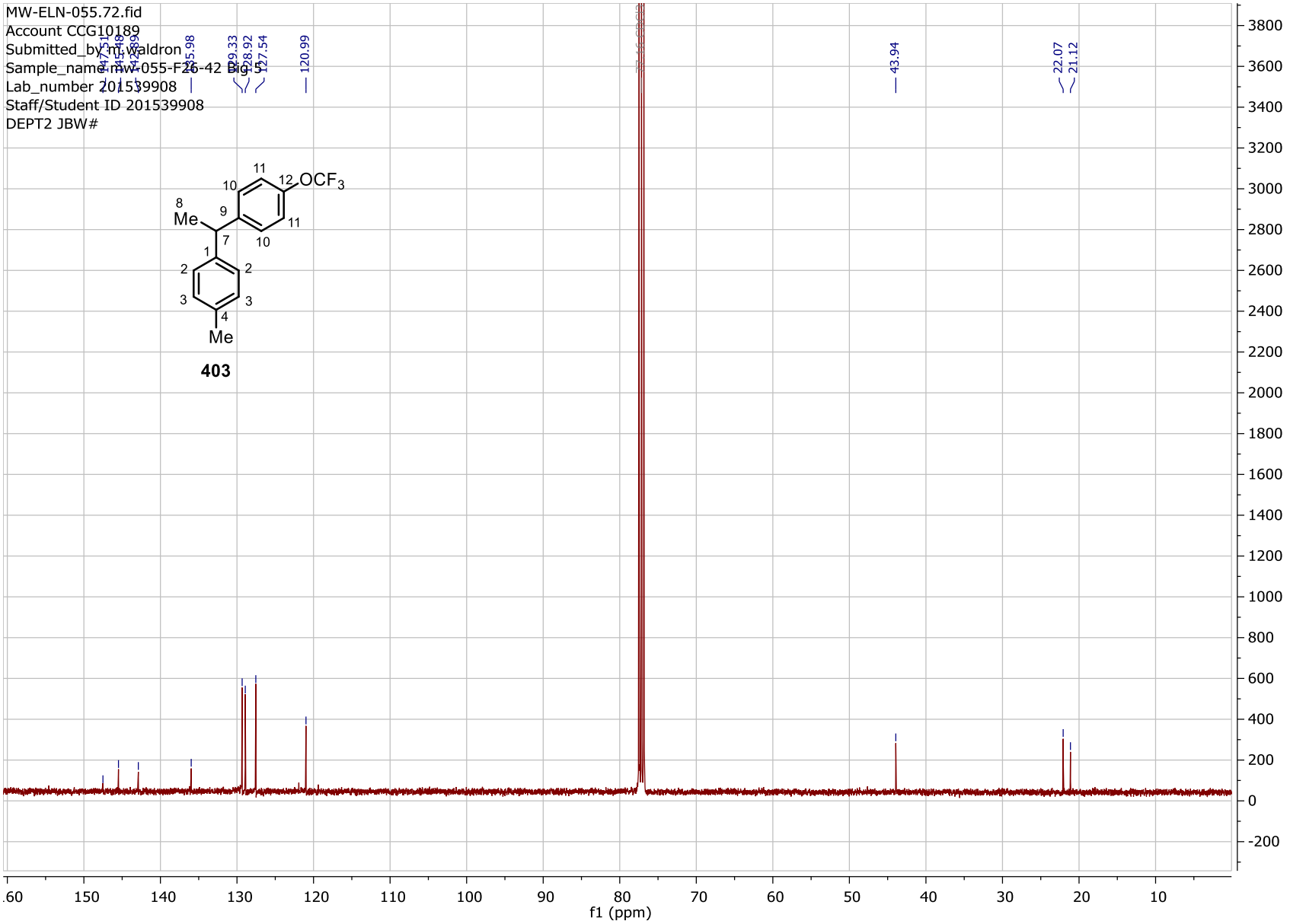
MW-ELN-055.72.fid
Account CCG10189
Submitted_by m.waldron
Sample_name mw-055-F26-42 Big-5
Lab_number 201539908
Staff/Student ID 201539908
DEPT2 JBW#
125.98
129.33
128.92
127.54
120.99
43.94
22.07
21.12
403
f1 (ppm)

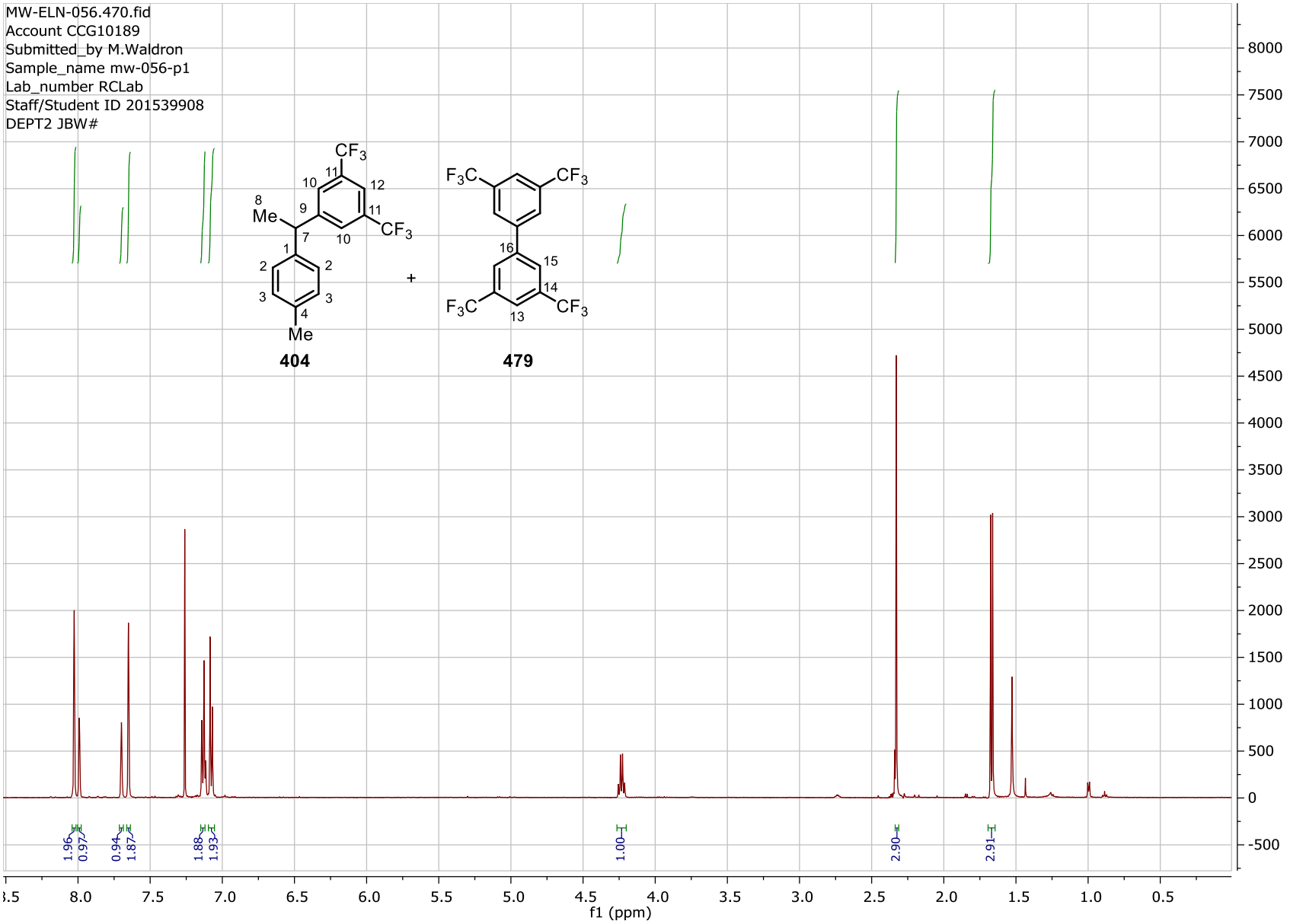
MW-ELN-056.470.fid
Account CCG10189
Submitted_by M.Waldron
Sample_name mw-056-p1
Lab_number RCLab
Staff/Student ID 201539908
DEPT2 JBW#
404
479
f1 (ppm)

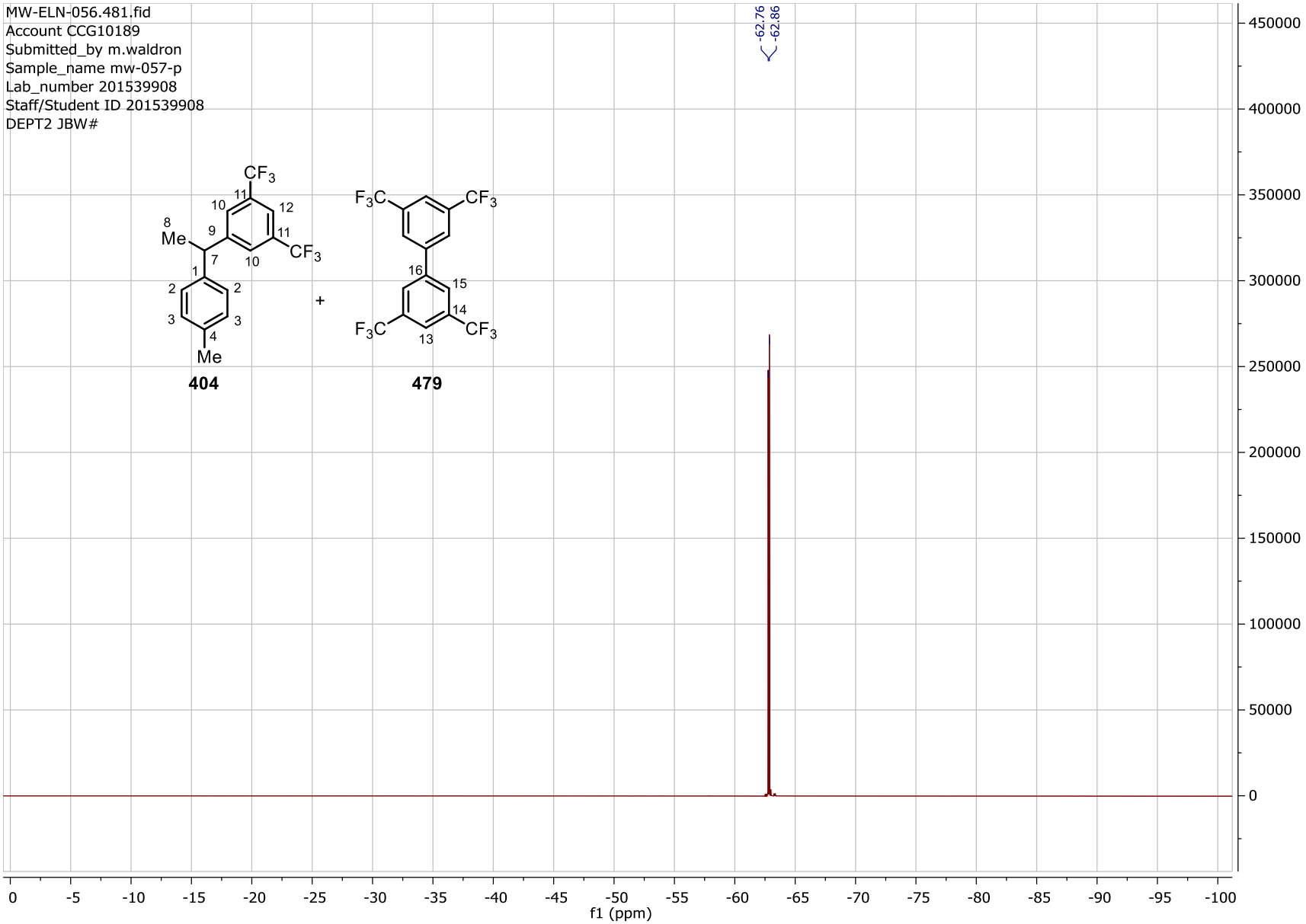
MW-ELN-056.481.fid
Account CCG10189
Submitted_by m.waldron
Sample_name mw-057-p
Lab_number 201539908
Staff/Student ID 201539908
DEPT2 JBW#
-62.76
-62.86
404
479
f1 (ppm)

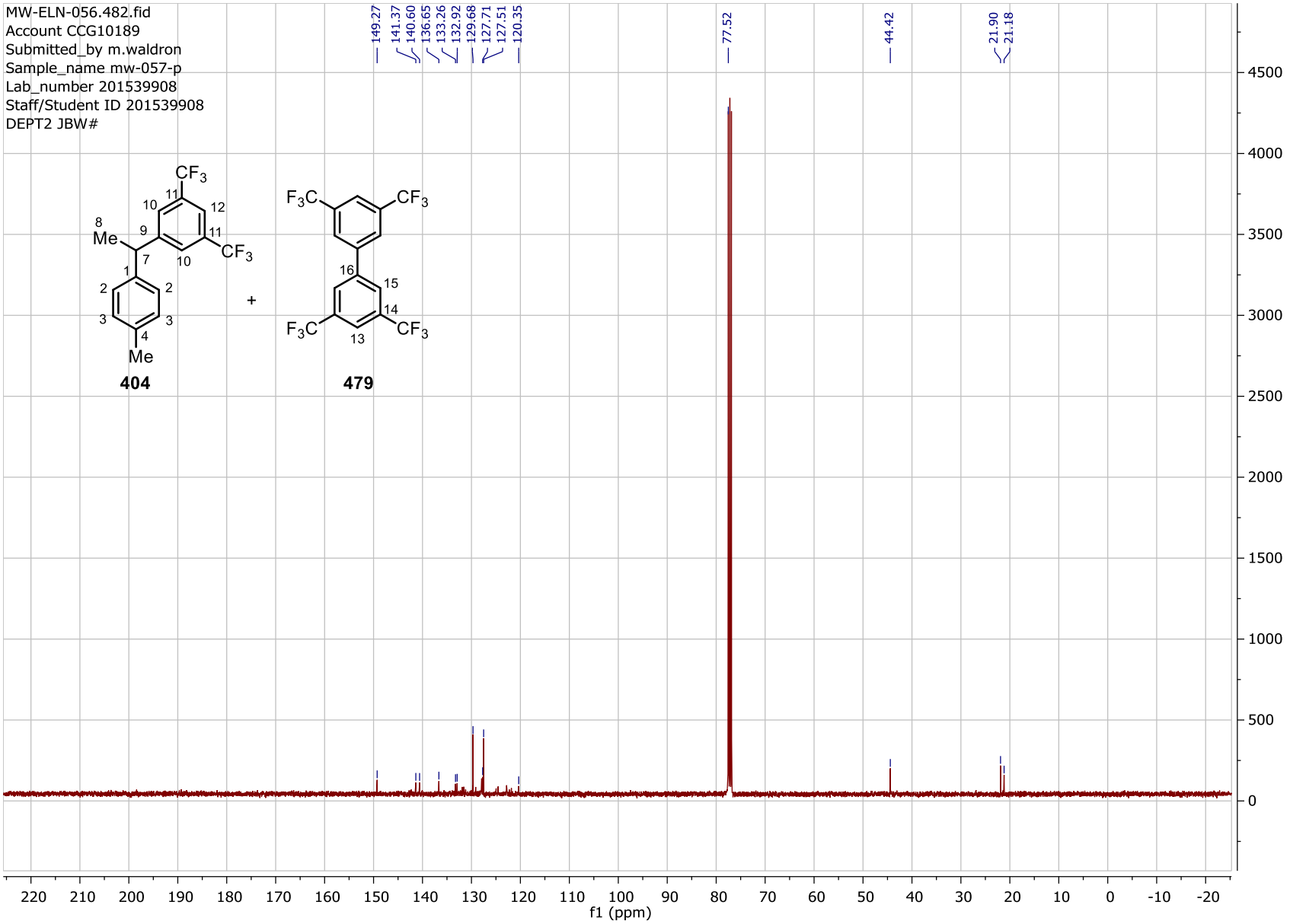
MW-ELN-056.482.fid
Account CCG10189
Submitted_by m.waldron
Sample_name mw-057-p
Lab_number 201539908
Staff/Student ID 201539908
DEPT2 JBW#
149.27
141.37
140.60
136.65
133.26
132.92
129.68
127.71
127.51
120.35
77.52
44.42
21.90
21.18
404
479
f1 (ppm)

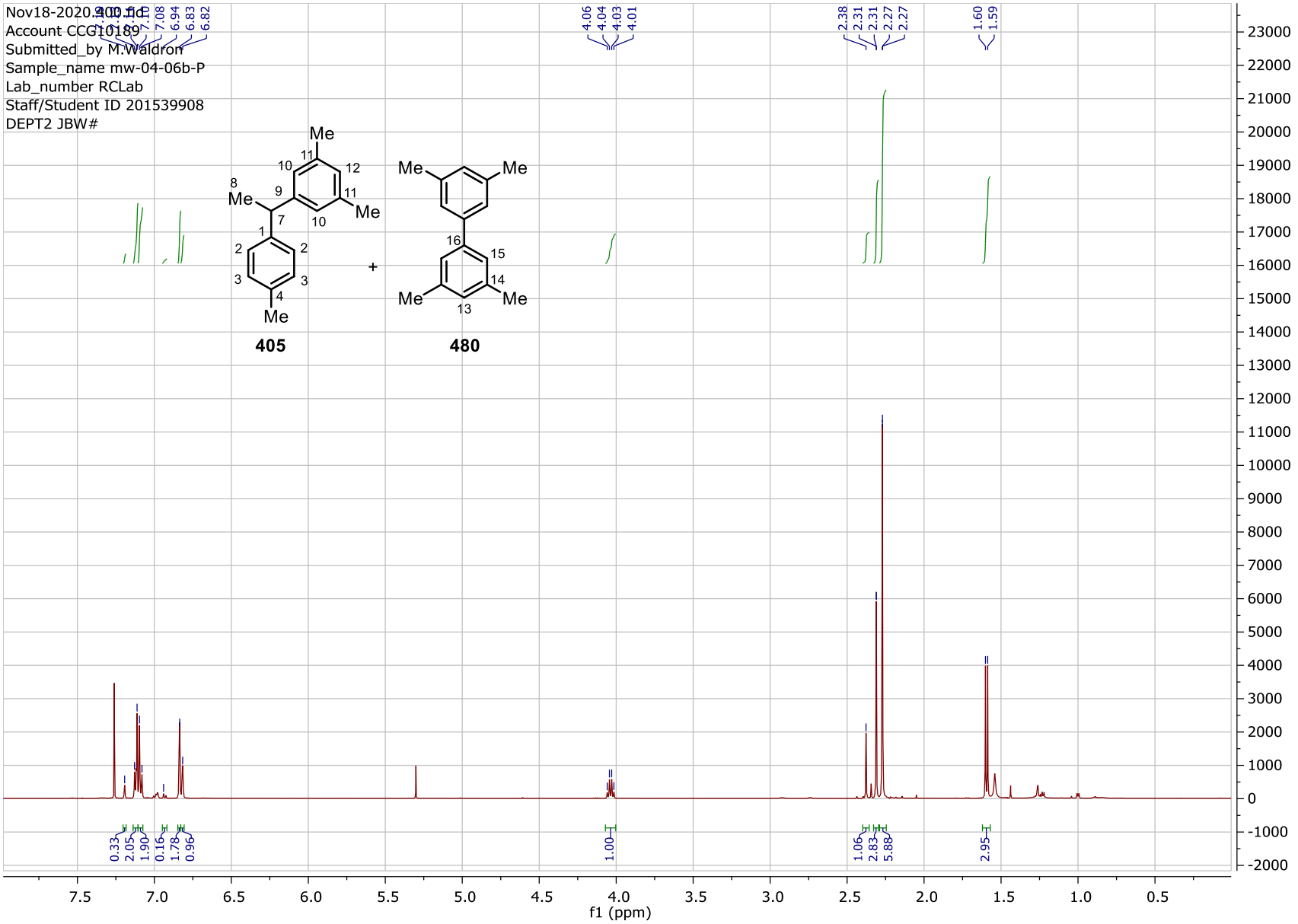
Nov18-2020.400.fid
Account CCG10189
Submitted_by M.Waldron
Sample_name mw-04-06b-P
Lab_number RCLab
Staff/Student ID 201539908
DEPT2 JBW#
405
480
f1 (ppm)

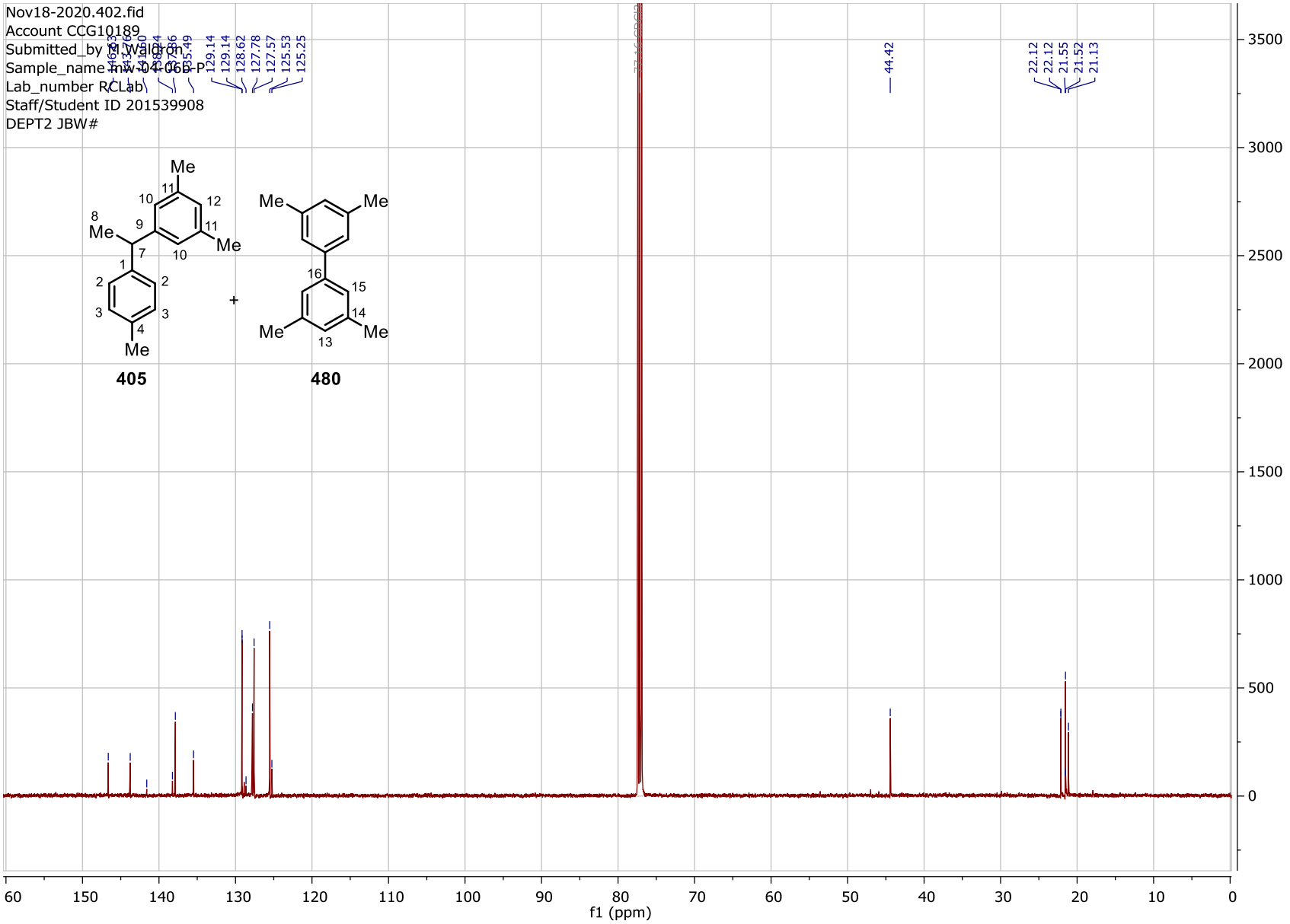
Nov18-2020.402.fid
Account CCG10189
Submitted_by M.Walton
Sample_name mw-04-06b-P
Lab_number RCLab
Staff/Student ID 201539908
DEPT2 JBW#
129.14
129.14
128.62
127.78
127.57
125.53
125.25
44.42
22.12
22.12
21.55
21.52
21.13
405
480
f1 (ppm)

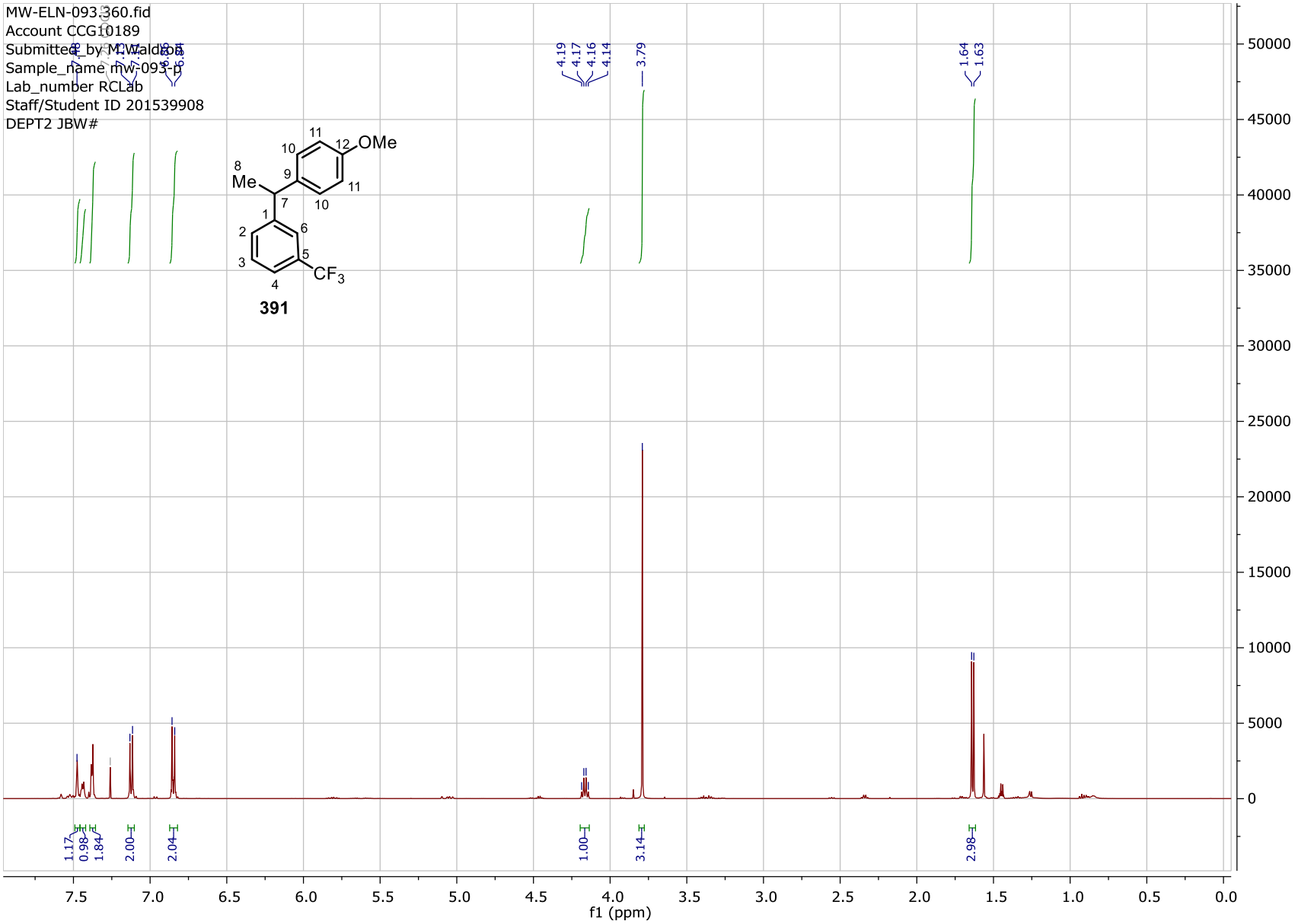
MW-ELN-093.360.fid
Account CCG10189
Submitted_by M.Waldron
Sample_name mw-093-p
Lab_number RCLab
Staff/Student ID 201539908
DEPT2 JBW#
391
4.19
4.17
4.16
4.14
3.79
1.64
1.63
1.17
0.98
1.84
2.00
2.04
1.00
3.14
2.98
f1 (ppm)

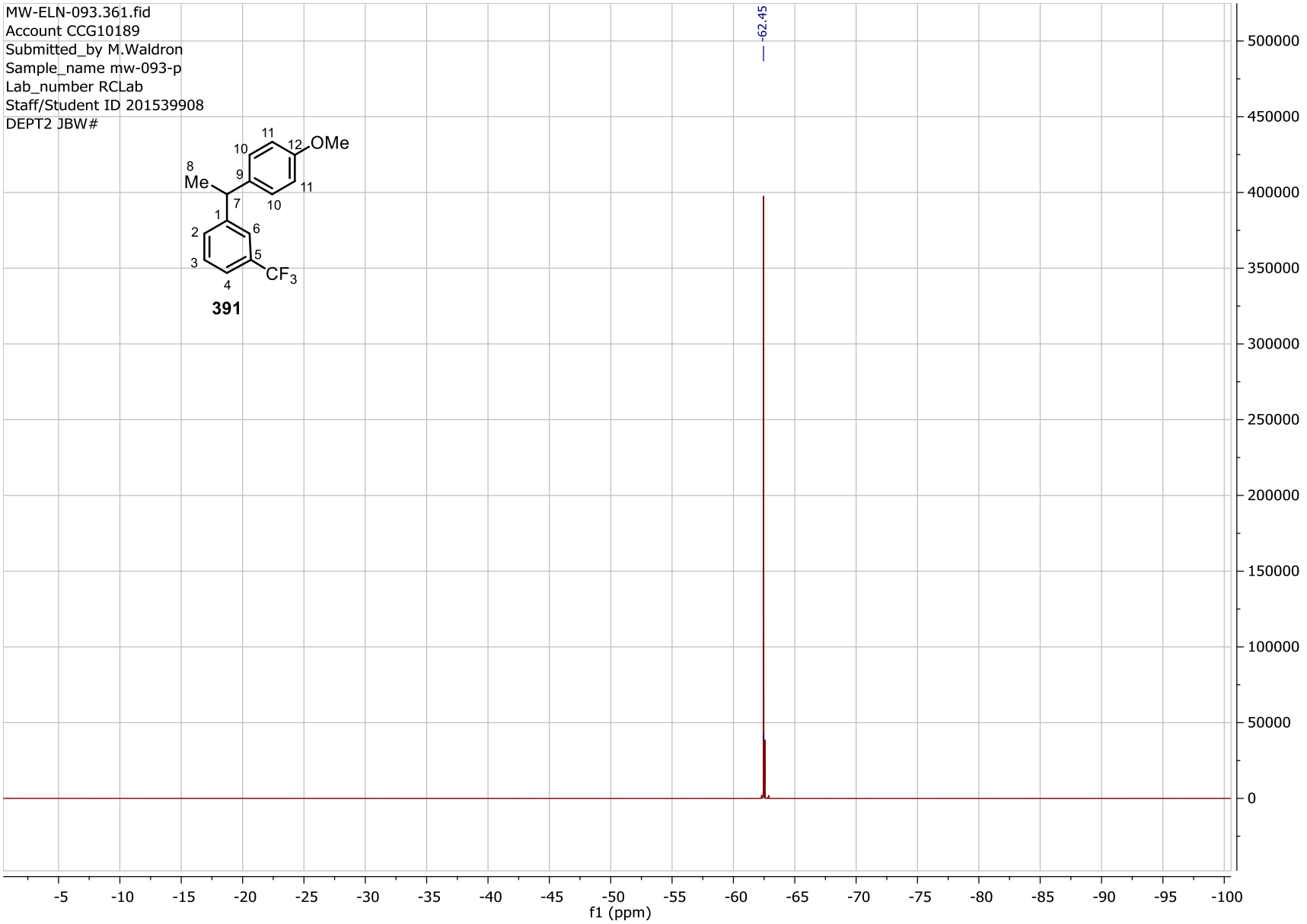
MW-ELN-093.361.fid
Account CCG10189
Submitted_by M.Waldron
Sample_name mw-093-p
Lab_number RCLab
Staff/Student ID 201539908
DEPT2 JBW#
-62.45
OMe
Me
CF3
391
f1 (ppm)

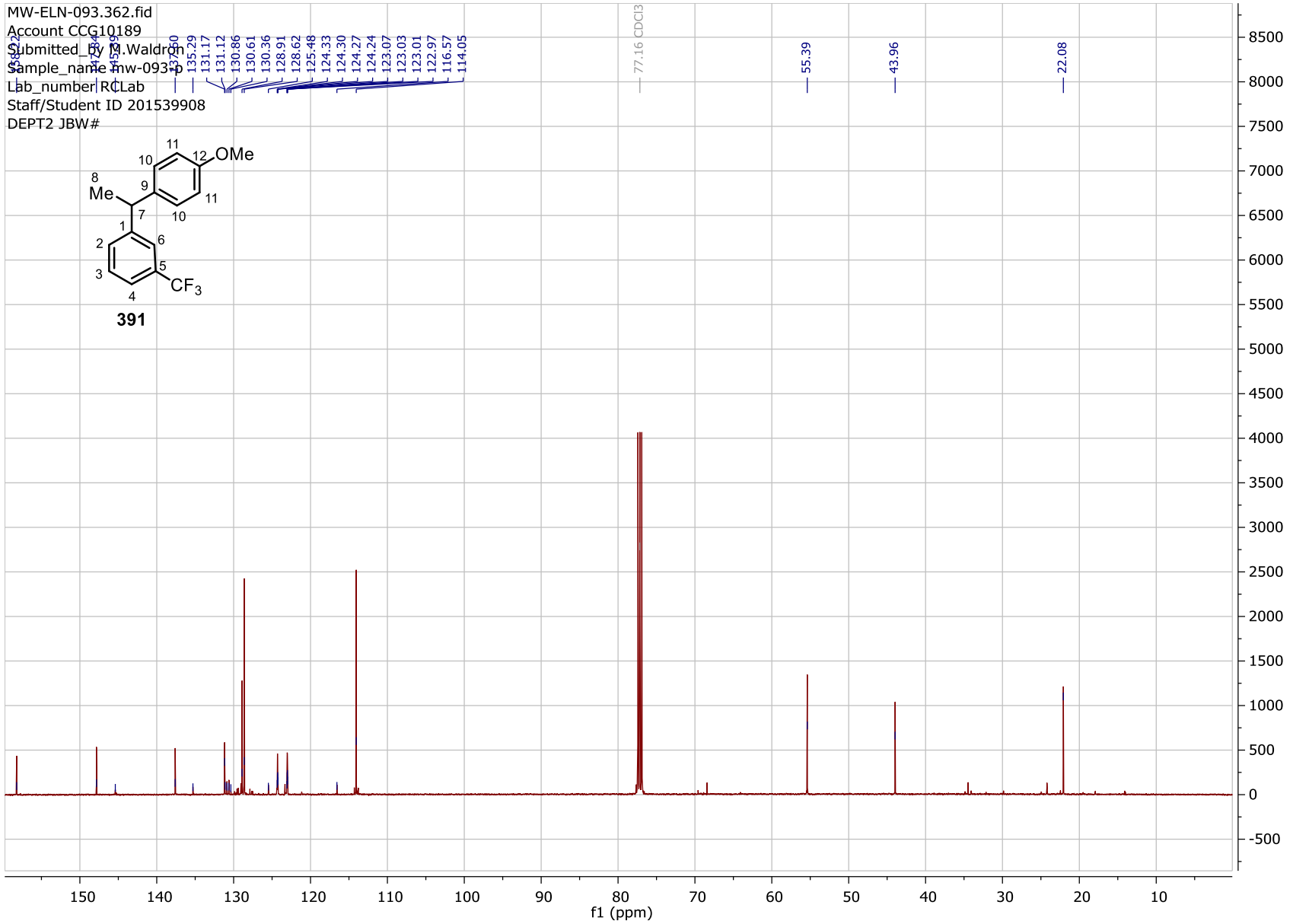
MW-ELN-093.362.fid
Account CCG10189
Submitted_by M.Waldron
Sample_name mw-093-p
Lab_number RCLab
Staff/Student ID 201539908
DEPT2 JBW#
135.29
131.17
131.12
130.86
130.61
130.36
128.91
128.62
125.48
124.33
124.30
124.27
124.24
123.07
123.03
123.01
122.97
116.57
114.05
77.16 CDCl3
55.39
43.96
22.08
OMe
Me
CF3
391
f1 (ppm)

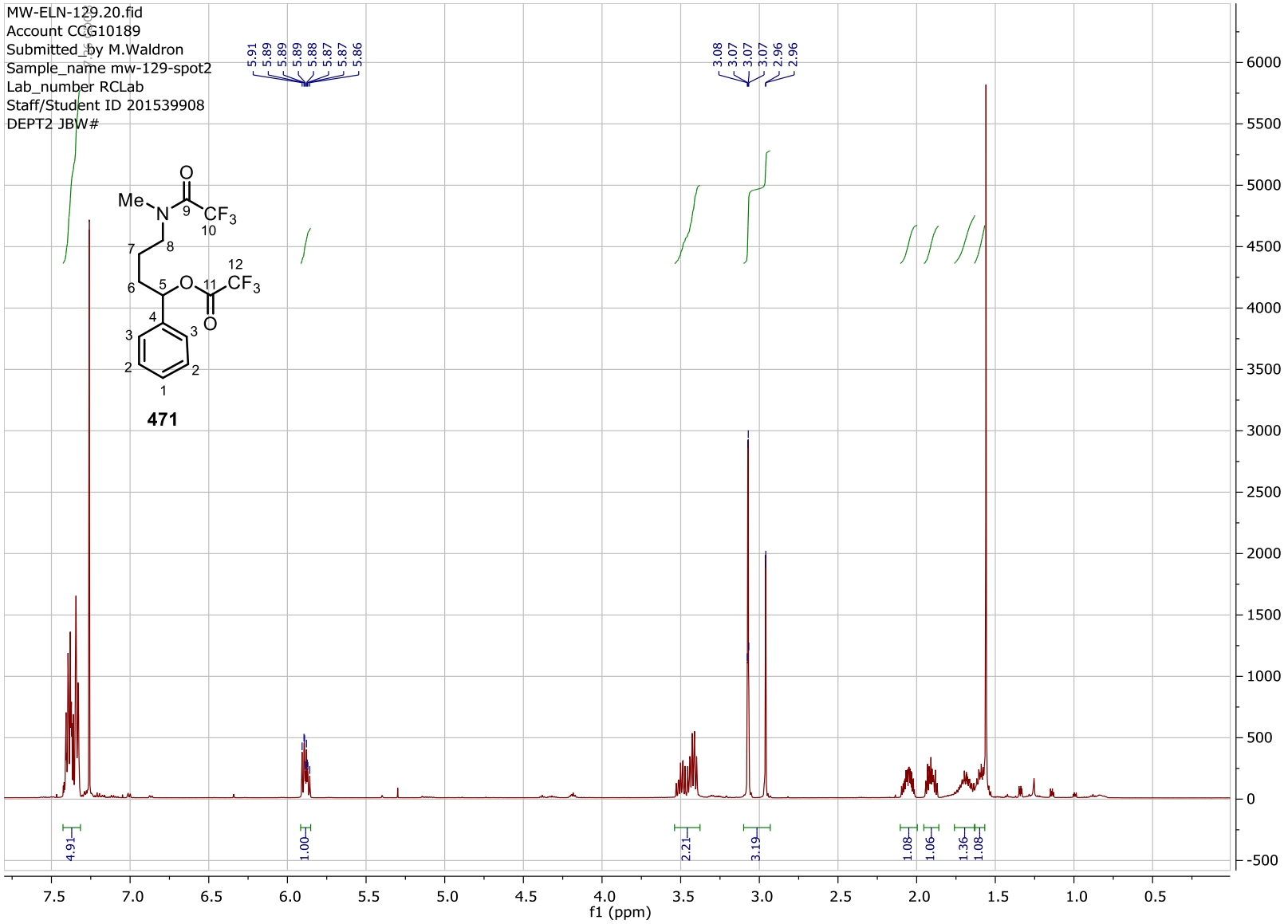
MW-ELN-129.20.fid
Account CCG10189
Submitted_by M.Waldron
Sample_name mw-129-spot2
Lab_number RCLab
Staff/Student ID 201539908
DEPT2 JBW#
5.91
5.89
5.89
5.89
5.88
5.87
5.87
5.86
3.08
3.07
3.07
3.07
2.96
2.96
Me
N
O
9
CF3
10
7
8
6
5
O
11
12
CF3
O
4
3
3
2
2
1
471
4.91
1.00
2.21
3.19
1.08
1.06
1.36
1.08
f1 (ppm)

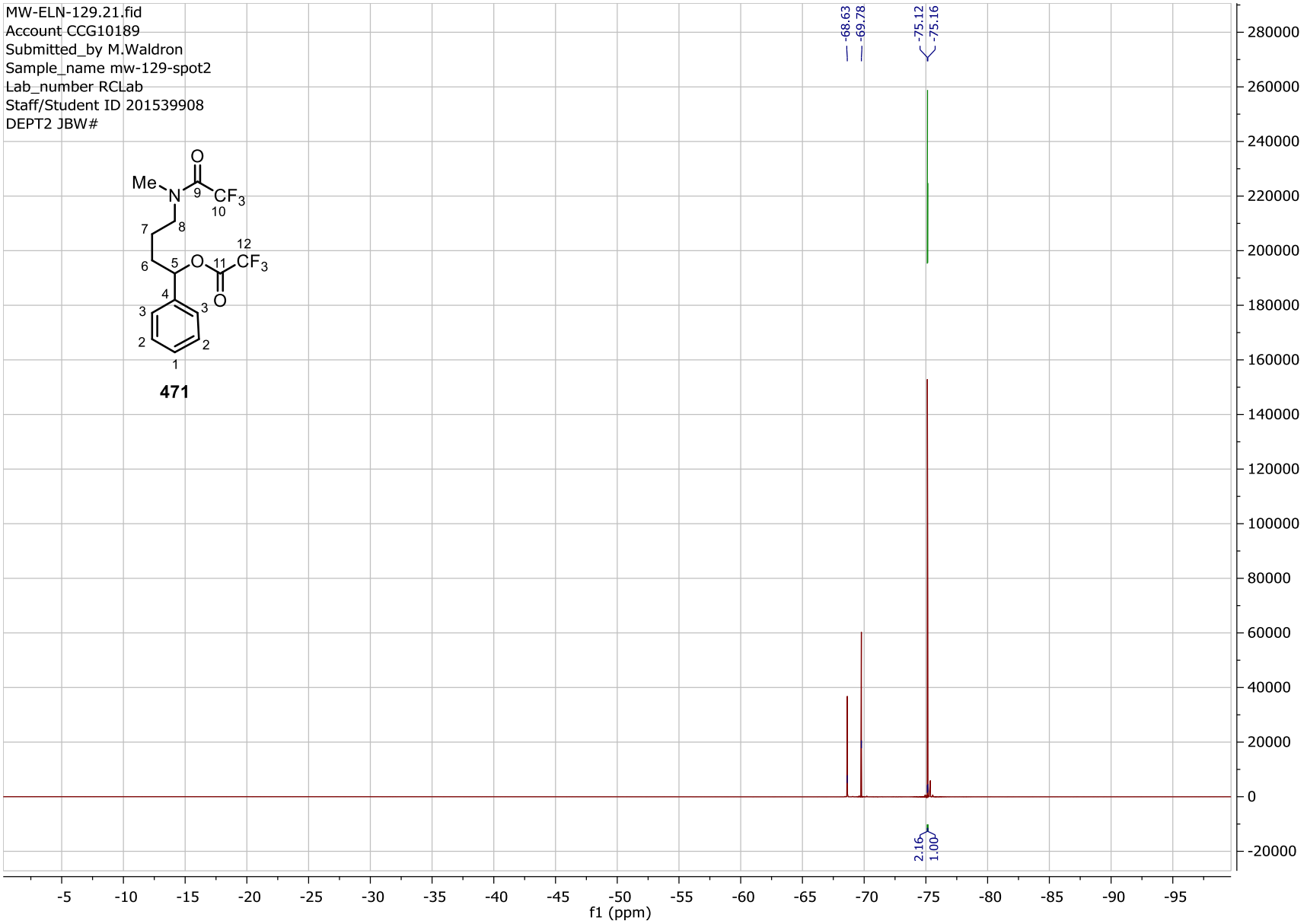
MW-ELN-129.21.fid
Account CCG10189
Submitted_by M.Waldron
Sample_name mw-129-spot2
Lab_number RCLab
Staff/Student ID 201539908
DEPT2 JBW#
Me
N
O
CF3
O
O
CF3
471
-68.63
-69.78
-75.12
-75.16
2.16
1.00
f1 (ppm)

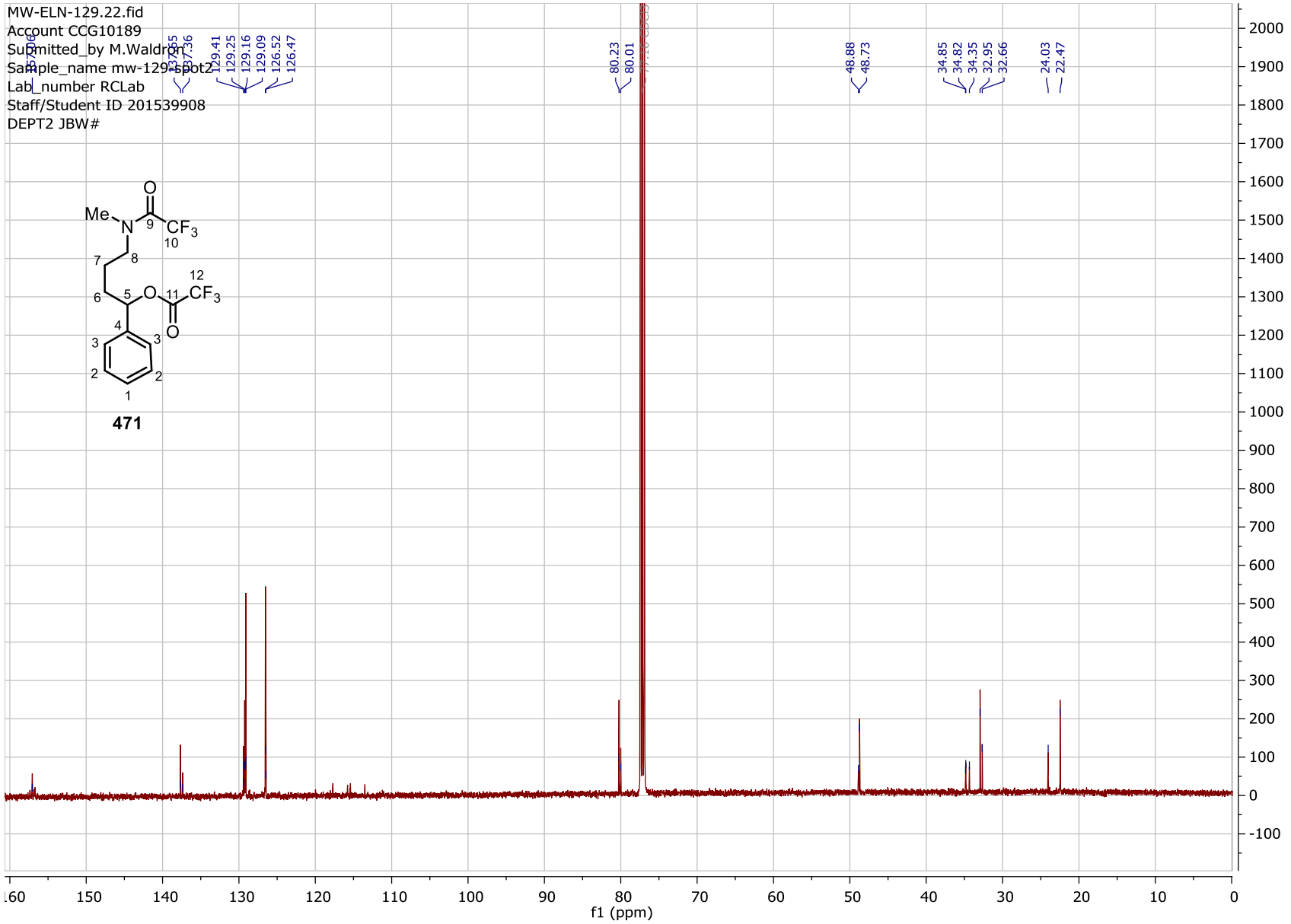
MW-ELN-129.22.fid
Account CCG10189
Submitted_by M.Waldron
Sample_name mw-129-spot2
Lab_number RCLab
Staff/Student ID 201539908
DEPT2 JBW#
129.41
129.25
129.16
129.09
126.52
126.47
80.23
80.01
48.88
48.73
34.85
34.82
34.35
32.95
32.66
24.03
22.47
Me
N
O
CF3
471
f1 (ppm)

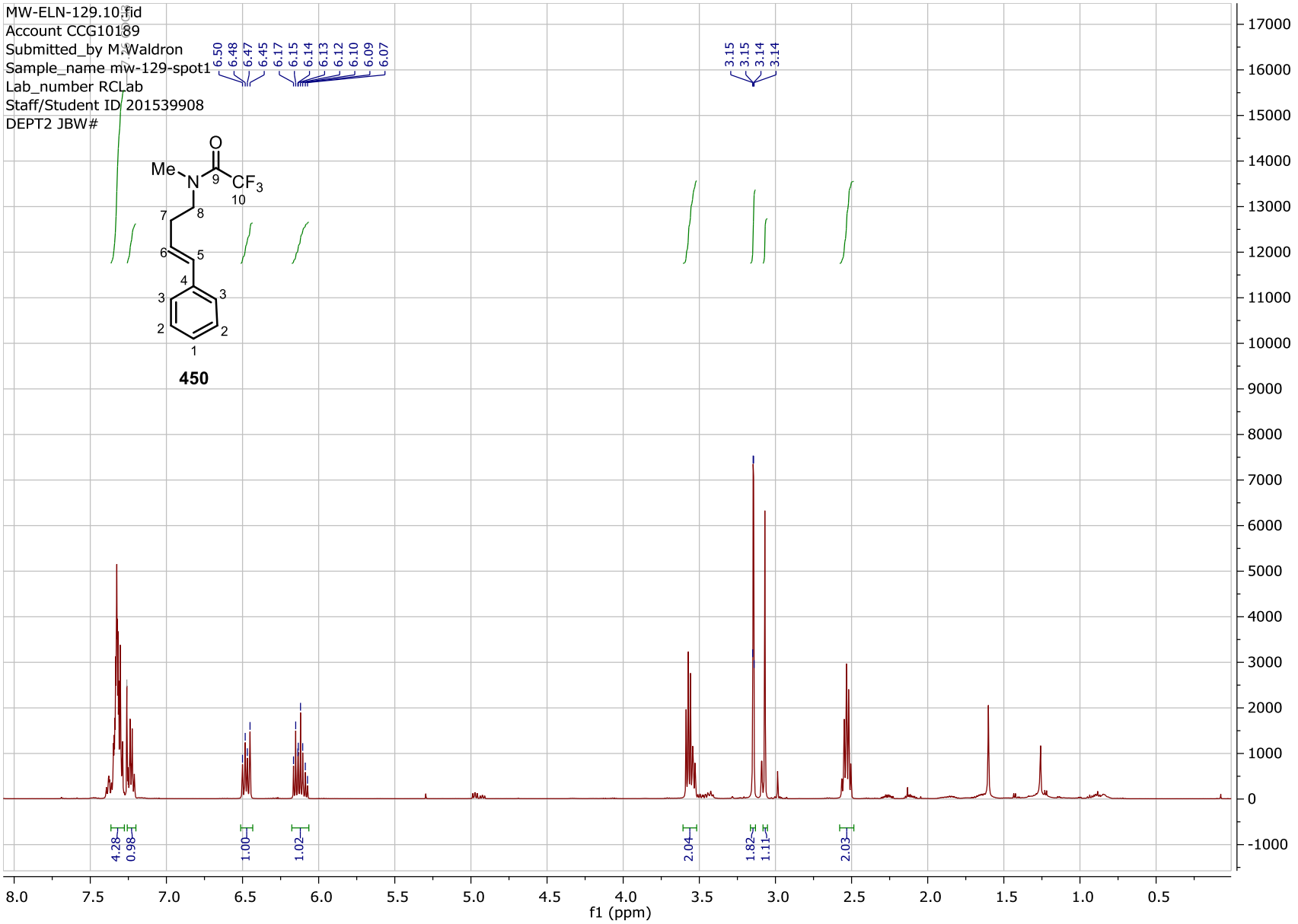
MW-ELN-129.10.fid
Account CCG10189
Submitted_by M.Waldron
Sample_name mw-129-spot1
Lab_number RCLab
Staff/Student ID 201539908
DEPT2 JBW#
6.50
6.48
6.47
6.45
6.17
6.15
6.14
6.13
6.12
6.10
6.09
6.07
3.15
3.15
3.14
3.14
Me
N
O
9
CF3
10
7
8
6
5
4
3
3
2
2
1
450
4.28
0.98
1.00
1.02
2.04
1.82
1.11
2.03
f1 (ppm)

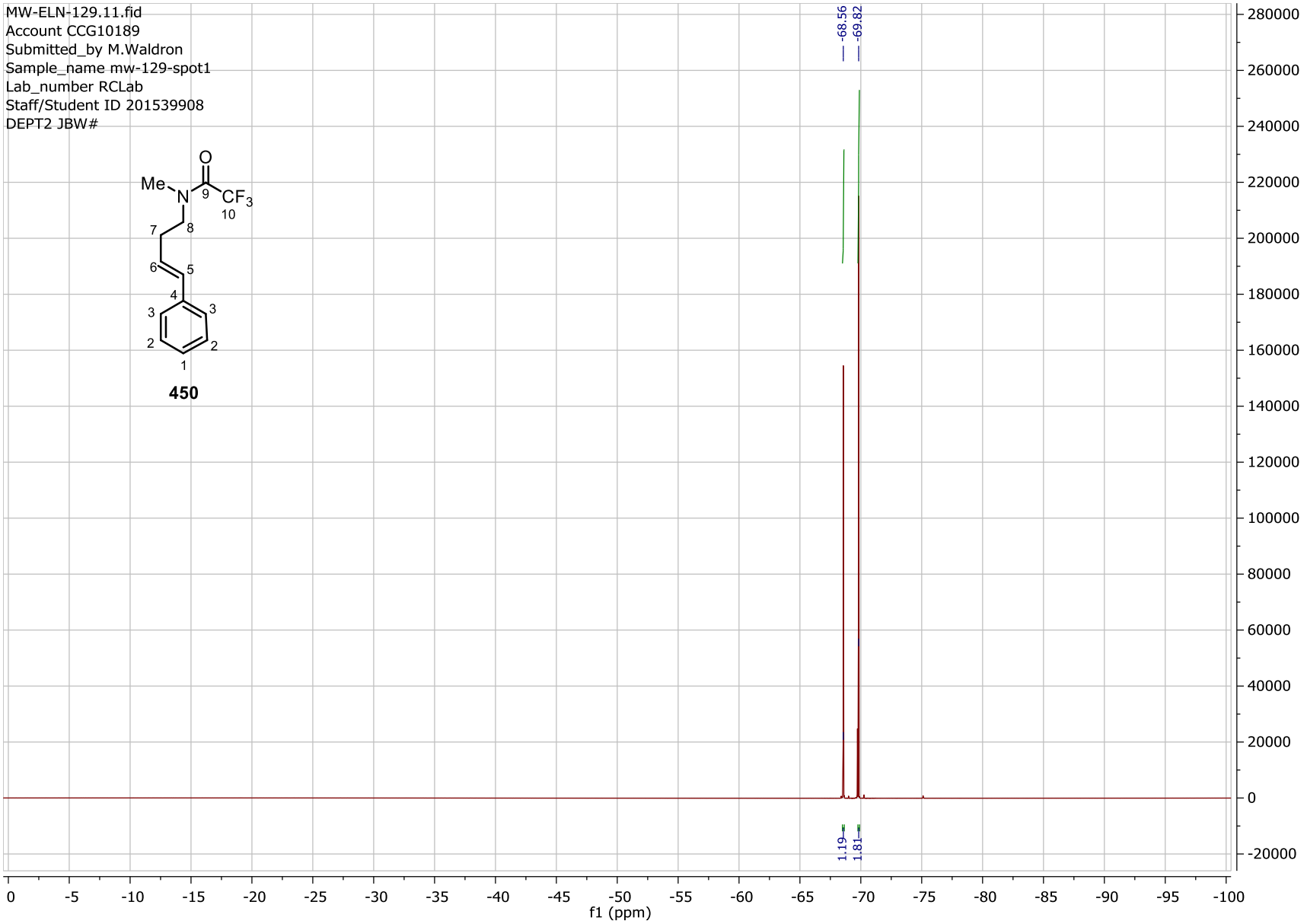
MW-ELN-129.11.fid
Account CCG10189
Submitted_by M.Waldron
Sample_name mw-129-spot1
Lab_number RCLab
Staff/Student ID 201539908
DEPT2 JBW#
Me
N
O
9
CF3
10
7
8
6
5
4
3
2
1
450
-68.56
-69.82
1.19
1.81
f1 (ppm)

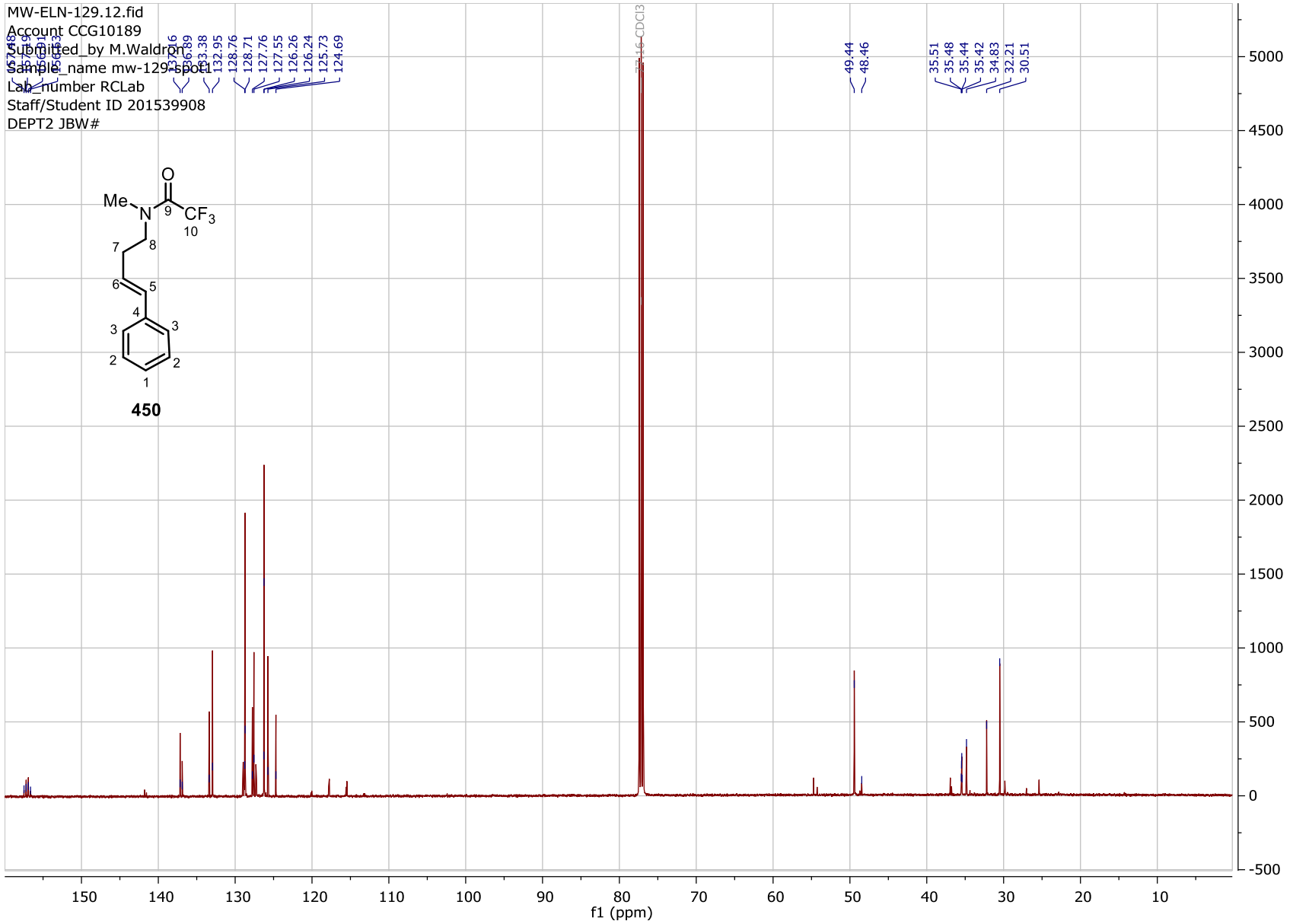
MW-ELN-129.12.fid
Account CCG10189
Submitted_by M.Waldron
Sample_name mw-129-spot1
Lab_number RCLab
Staff/Student ID 201539908
DEPT2 JBW#
77.16 CDCl3
49.44
48.46
35.51
35.48
35.44
35.42
34.83
32.21
30.51
132.95
128.76
128.71
127.76
127.55
126.26
126.24
125.73
124.69
Me
N
O
CF3
450
f1 (ppm)

7.8. Tables of Data

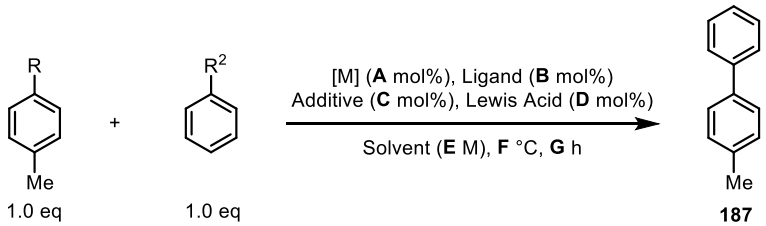

[a]2.0 eq., [b]1.5 eq., [c]General Procedure 1 employed. [d]General Procedure 2 employed (Mesitylene in Flask 1). [e]General Procedure 2 employed (DMF in Flask 1). *Na_2CO_3 (20 mol%) included with SPO pre-mix.

Entry	R	R^2	[M]	A	Ligand	B	Additive	C	Lewis Acid	D	Solvent	E	F	G	187 Yield
1	NMe_2[a]	Bnep	M4	10	180	30	PPh_3	10	$AlMe_3$	100	Mesitylene	0.1	130	68	0%
2	NMe_2[a]	Bnep	M4	10	180	30	-	-	$AlMe_3$	100	Mesitylene	0.1	130	68	0%
3	NMe_2[a]	Bnep	M4	10	180	30	PPh_3	10	$AlMe_3$	100	Mesitylene	0.1	100	68	0%
4	NHMe[a]	Bnep	M4	10	180	30	PPh_3	10	$AlMe_3$	100	Mesitylene	0.1	130	68	0%
5	NH_2[a]	Bnep	M4	10	180	30	PPh_3	10	$AlMe_3$	100	Mesitylene	0.1	130	68	0%
6	NMe_2[a]	Bnep	M4	10	180	30	PPh_3	10	$AlMe_3$	100	Mesitylene	0.1	130	68	12%
7	NMe_2[a]	Bnep	M4	10	180	30	PPh_3	10	-	-	Mesitylene	0.1	130	68	0%
8	NMe_2[a]	Bnep	M4	10	180	30	PPh_3	10	$AlMe_3$	100	Mesitylene	0.1	70	68	0%
9	NMe_2[a]	Bnep	M12	10	180	30	Mg	30	$AlMe_3$	100	THF	0.1	130	41	0%
10	NMe_2[a]	Bnep	M12	10	180	30	Mg	30	-	-	THF	0.1	130	41	0%
11	NMe_2	MgBr[b]	M13	5	186	10	-	-	-	-	THF	0.5	r.t.	17	0%
12	NMe_2	MgBr[b]	M13	5	186	10	-	-	-	-	THF	0.5	70	17	0%
13	NMe_2	MgBr[b]	M13	5	181	10	-	-	-	-	THF	0.5	r.t.	68	0%
14	NHMe	MgBr[b]	M13	5	181	10	-	-	-	-	THF	0.5	r.t.	68	0%
15	NH_2	MgBr[b]	M13	5	181	10	-	-	-	-	THF	0.5	r.t.	68	0%
16	NMe_2	MgBr[b]	M13	5	181	10	-	-	-	-	THF	0.5	70	68	0%
17	NHMe	MgBr[b]	M13	5	181	10	-	-	-	-	THF	0.5	70	68	0%
18	NH_2	MgBr[b]	M13	5	181	10	-	-	-	-	THF	0.5	70	68	0%
19	NMe_2[a]	Bnep	M4	10	180	30	PPh_3	10	$AlMe_3$	100	Mesitylene + H_2O	0.1	130	68	0%
20	NMe_2[a]	Bnep	M12	10	180	30	Mg	30	-	-	THF	0.1	130	68	0%

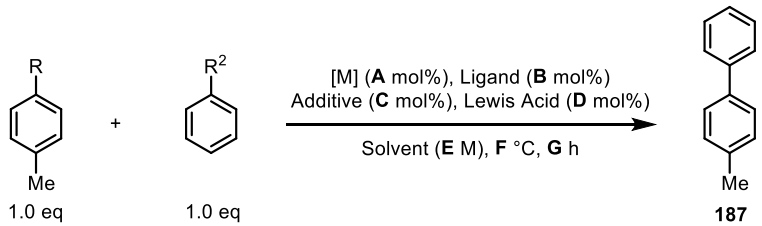

[a]2.0 eq., [b]1.5 eq., [c]General Procedure 1 employed. [d]General Procedure 2 employed (Mesitylene in Flask 1). [e]General Procedure 2 employed (DMF in Flask 1). *Na_2CO_3 (20 mol%) included with SPO pre-mix.

Entry	R	R^2	[M]	A	Ligand	B	Additive	C	Lewis Acid	D	Solvent	E	F	G	187 Yield
21	NMe_2	Bnep	M4	10	180	30	PPh_3	10	$Y(OTf)_3$	100	Mesitylene	0.1	130	65	0%
22	NMe_2	Bnep	M4	10	180	30	PPh_3	10	$FeCl_3$	100	Mesitylene	0.1	130	65	0%
23	NMe_2	Bnep	M4	10	180	30	PPh_3	10	$MgBr_2$	100	Mesitylene	0.1	130	65	0%
24	NMe_2	Bnep	M4	10	180	30	PPh_3	10	-	-	Mesitylene	0.1	130	65	0%
25	NMe_2	Bnep	M4	10	180	30	PPh_3	10	$Y(OTf)_3$	10	Mesitylene	0.1	130	65	0%
26	NMe_2	Bnep	M4	10	180	30	PPh_3	10	$FeCl_3$	10	Mesitylene	0.1	130	65	0%
27	NMe_2	Bnep	M4	10	180	30	PPh_3	10	$MgBr_2$	10	Mesitylene	0.1	130	65	0%
28	OMe	$MgBr^b$	M5	5	181	10	-	-	-	-	THF	0.5	r.t.	17	0%
29	NMe_2	Bnep	M4	10	180	30	PPh_3	10	HBpin	10	Mesitylene	0.1	130	66	0%
30	NMe_2	Bnep	M4	10	180	30	PPh_3	10	HBpin	100	Mesitylene	0.1	130	66	0%
31	NMe_2	Bnep	M4	10	180	30	PPh_3	10	$AlMe_3$	100	Mesitylene	0.1	130	66	17%
32	NMe_2	Bnep	M4	10	180	30	PPh_3	10	$SnCl_4$	10	Mesitylene	0.1	130	66	0%
33	NMe_2	Bnep	M4	10	180	30	PPh_3	10	$SnCl_4$	100	Mesitylene	0.1	130	66	0%
34	OMe	Bnep	M4	10	180	30	PPh_3	10	$AlMe_3$	100	Mesitylene	0.1	130	66	12%
35	OMe	Bnep	M4	10	180	30	PPh_3	10	-	-	Mesitylene	0.1	130	66	0%
36	OMe	Bnep	M4	10	180	30	PPh_3	10	$AlMe_3$	100	THF	0.1	130	66	12%
37	OMe	Bnep	M4	10	180	30	PPh_3	10	-	-	THF	0.1	130	66	0%
38	NMe_2	Bnep	M4	10	180	30	PPh_3	10	$AlMe_3$	30	Mesitylene	0.1	130	16^{c*}	0%
39	NMe_2	Bnep	M4	10	180	30	PPh_3	10	$AlMe_3$	30	Mesitylene	0.1	130	16^c	11%
40	NMe_2	Bnep	M4	10	180	30	-	-	$AlMe_3$	30	Mesitylene	0.1	130	16^{c*}	11%

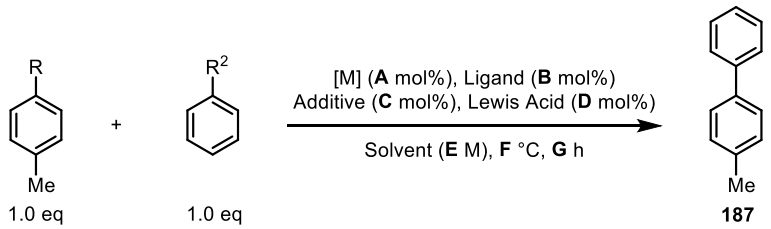

[a]2.0 eq., [b]1.5 eq., [c]General Procedure 1 employed. [d]General Procedure 2 employed (Mesitylene in Flask 1). [e]General Procedure 2 employed (DMF in Flask 1). *Na_2CO_3 (20 mol%) included with SPO pre-mix.

Entry	R	R^2	[M]	A	Ligand	B	Additive	C	Lewis Acid	D	Solvent	E	F	G	187 Yield
41	NMe_2	Bnep	M4	10	180	30	-	-	$AlMe_3$	30	Mesitylene	0.1	130	16[c]	0%
42	NMe_2	Bnep	M4	10	180	30	PPh_3	10	$AlMe_3$	100	Mesitylene	0.1	130	65[d]	11%
43	NMe_2	Bnep	M4	10	180	30	-	-	$AlMe_3$	100	Mesitylene	0.1	130	65[d]*	0%
44	NMe_2	Bnep	M4	10	180	30	PPh_3	10	$AlMe_3$	100	Mesitylene + DMF	0.27	130	18	11%
45	NMe_2	Bnep	M4	10	180	30	-	-	$AlMe_3$	100	Mesitylene + DMF	0.27	130	18	0%
46	NMe_2	Bnep	M4	10	180	30	PPh_3	10	$AlMe_3$	100	Mesitylene + DMF	0.27	130	18	11%
47	NMe_2	Bnep	M4	10	180	30	-	-	$AlMe_3$	100	Mesitylene + DMF	0.27	130	18	0%

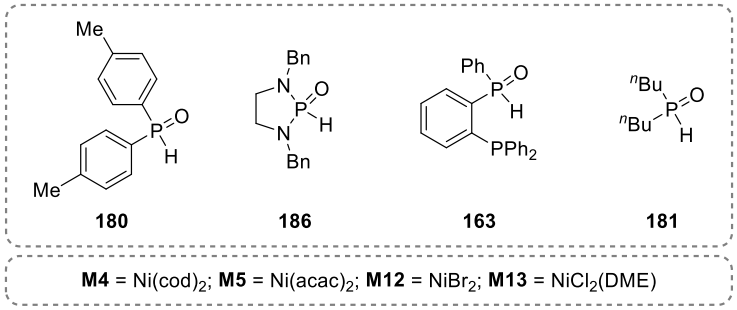

Table SI:2. *SPO ligand cross-coupling optimisation data*

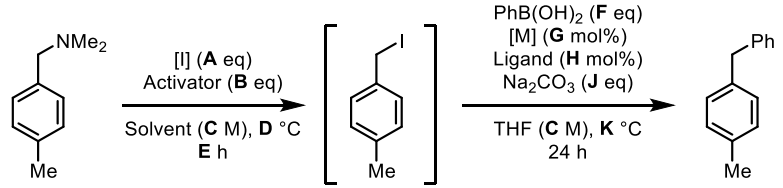

[a] *in situ* ^{1}H NMR yield using 1,4-dinitrobenzene as internal standard; [b] Na_2CO_3 (1.0 eq) added; [c] $NaHCO_3$ (1.0 eq) added; [d] K_2CO_3 (1.0 eq) added; [e] K_3PO_4 (1.0 eq) added; [f] 0.5M solutions of **199** and TFAA added sequentially; [g] $NaHCO_3$; [h] K_2CO_3; [i] K_3PO_4; [j] PhBpin was used; [k] PhBnep was used

Entry	Scale (mmol)	[I]	A	Activator	B	Solvent	C	D	E	237 Yield	F	[M]	G	Ligand	H	J	K	17 Yield
1	0.2	NaI	1.2	MeCOCl	1.0	THF	0.1	r.t.	18	31%[a]	-	-	-	-	-	-	-	-
2	0.2	NaI	1.2	PhCOCl	1.0	THF	0.1	r.t.	18	27%[a]	-	-	-	-	-	-	-	-
3	0.2	NaI	1.2	TFAA	1.0	THF	0.1	r.t.	18	60%[a]	-	-	-	-	-	-	-	-
4	0.2	NaI	1.2	MeCOCl	1.0	Dioxane	0.1	r.t.	18	12%[a]	-	-	-	-	-	-	-	-
5	0.2	NaI	1.2	PhCOCl	1.0	Dioxane	0.1	r.t.	18	3%[a]	-	-	-	-	-	-	-	-
6	0.2	NaI	1.2	TFAA	1.0	Dioxane	0.1	r.t.	18	23%[a]	-	-	-	-	-	-	-	-
7	0.2	NaI	1.2	MeCOCl	1.0	Toluene	0.1	r.t.	18	9%[a]	-	-	-	-	-	-	-	-
8	0.2	NaI	1.2	PhCOCl	1.0	Toluene	0.1	r.t.	18	16%[a]	-	-	-	-	-	-	-	-
9	0.2	NaI	1.2	TFAA	1.0	Toluene	0.1	r.t.	18	7%[a]	-	-	-	-	-	-	-	-
10	0.2	NaI	1.2	MeCOCl	1.0	Hexane	0.1	r.t.	18	29%[a]	-	-	-	-	-	-	-	-
11	0.2	NaI	1.2	PhCOCl	1.0	Hexane	0.1	r.t.	18	34%[a]	-	-	-	-	-	-	-	-
12	0.2	NaI	1.2	TFAA	1.0	Hexane	0.1	r.t.	18	7%[a]	-	-	-	-	-	-	-	-
13	0.2	NaI	1.0	TFAA	1.0	THF	0.1	r.t.	18	29%[a]	-	-	-	-	-	-	-	-
14	0.2	NaI	1.4	TFAA	1.0	THF	0.1	r.t.	18	24%[a]	-	-	-	-	-	-	-	-
15	0.2	NaI	1.6	TFAA	1.0	THF	0.1	r.t.	18	32%[a]	-	-	-	-	-	-	-	-
16	0.2	NaI	1.8	TFAA	1.0	THF	0.1	r.t.	18	25%[a]	-	-	-	-	-	-	-	-
17	0.2	NaI	2.0	TFAA	1.0	THF	0.1	r.t.	18	44%[a]	-	-	-	-	-	-	-	-
18	0.2	NaI	1.2	TFAA	1.0	THF	0.1	r.t.	1	29%[a]	-	-	-	-	-	-	-	-
19	0.2	NaI	1.2	TFAA	1.0	THF	0.1	r.t.	3	40%[a]	-	-	-	-	-	-	-	-
20	0.2	NaI	1.2	TFAA	1.0	THF	0.1	r.t.	5	44%[a]	-	-	-	-	-	-	-	-
21	0.2	NaI	1.2	TFAA	1.0	THF	0.1	r.t.	7	47%[a]	-	-	-	-	-	-	-	-
22	0.2	NaI	1.2	TFAA	1.0	THF	0.1	50	1	48%[a]	-	-	-	-	-	-	-	-
23	0.2	NaI	1.2	TFAA	1.0	THF	0.1	50	3	57%[a]	-	-	-	-	-	-	-	-
24	0.2	NaI	1.2	TFAA	1.0	THF	0.1	50	5	56%[a]	-	-	-	-	-	-	-	-
25	0.2	NaI	1.2	TFAA	1.0	THF	0.1	50	7	63%[a]	-	-	-	-	-	-	-	-

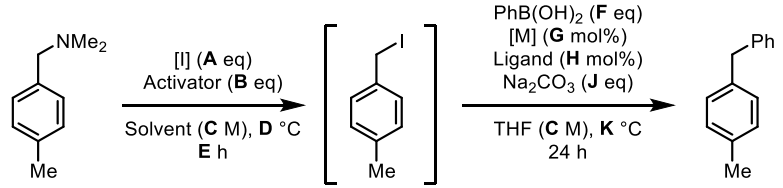

199 **237** **17**

[a] *in situ* ^{1}H NMR yield using 1,4-dinitrobenzene as internal standard; [b] Na_2CO_3 (1.0 eq) added; [c] $NaHCO_3$ (1.0 eq) added; [d] K_2CO_3 (1.0 eq) added; [e] K_3PO_4 (1.0 eq) added; [f] 0.5M solutions of **199** and TFAA added sequentially; [g] $NaHCO_3$; [h] K_2CO_3; [i] K_3PO_4; [j] PhBpin was used; [k] PhBnep was used

Entry	Scale (mmol)	[I]	A	Activator	B	Solvent	C	D	E	237 Yield	F	[M]	G	Ligand	H	J	K	17 Yield
26	0.2	NaI	1.2	TFAA	1.2	THF	0.1	r.t.	18	76%[a]	-	-	-	-	-	-	-	-
27	0.2	NaI	1.2	TFAA	1.5	THF	0.1	r.t.	18	72%[a]	-	-	-	-	-	-	-	-
28	0.2	KI	1.2	TFAA	1.2	THF	0.1	r.t.	18	38%[a]	-	-	-	-	-	-	-	-
29	0.2	LiI	1.2	TFAA	1.2	THF	0.1	r.t.	18	54%[a]	-	-	-	-	-	-	-	-
30	0.2	CsI	1.2	TFAA	1.2	THF	0.1	r.t.	18	6%[a]	-	-	-	-	-	-	-	-
31	0.2	CuI	1.2	TFAA	1.2	THF	0.1	r.t.	18	0%[a]	-	-	-	-	-	-	-	-
32	0.2	TBAI	1.2	TFAA	1.2	THF	0.1	r.t.	18	0%[a]	-	-	-	-	-	-	-	-
33	0.2	TEAI	1.2	TFAA	1.2	THF	0.1	r.t.	18	0%[a]	-	-	-	-	-	-	-	-
34	0.2	ZnI_2	1.2	TFAA	1.2	THF	0.1	r.t.	18	4%[a]	-	-	-	-	-	-	-	-
35	0.1	NaI	1.2	TFAA[b]	1.2	THF	0.1	r.t.	18	62%[a]	-	-	-	-	-	-	-	-
36	0.1	NaI	1.2	TFAA[c]	1.2	THF	0.1	r.t.	18	73%[a]	-	-	-	-	-	-	-	-
37	0.1	NaI	1.2	TFAA[d]	1.2	THF	0.1	r.t.	18	15%[a]	-	-	-	-	-	-	-	-
38	0.1	NaI	1.2	TFAA[e]	1.2	THF	0.1	r.t.	18	37%[a]	-	-	-	-	-	-	-	-
39	0.4	NaI	1.2	TFAA	1.2	THF	0.1	r.t.	18	92%[a,f]	-	-	-	-	-	-	-	-
40	0.4	NaI	1.5	TFAA	1.2	THF	0.1	r.t.	18	84%[a,f]	-	-	-	-	-	-	-	-
41	0.4	NaI	1.2	TFAA	1.2	THF	0.05	r.t.	18	92%[a,f]	-	-	-	-	-	-	-	-
42	0.4	NaI	1.5	TFAA	1.2	THF	0.05	r.t.	18	90%[a,f]	-	-	-	-	-	-	-	-
43	0.2	NaI	1.2	TFAA	1.2	THF	0.1	r.t.	18	-[f]	1.5	M4	10	252	20	3.0	100	17%[a]
44	0.2	NaI	1.2	TFAA	1.2	THF	0.1	r.t.	18	-[f]	1.5	M4	10	483	20	3.0	100	3%[a]
45	0.2	NaI	1.2	TFAA	1.2	THF	0.1	r.t.	18	-[f]	1.5	M4	10	484	20	3.0	100	14%[a]
46	0.2	NaI	1.2	TFAA	1.2	THF	0.1	r.t.	18	-[f]	1.5	M4	10	250	20	3.0	100	0%[a]
47	0.2	NaI	1.2	TFAA	1.2	THF	0.1	r.t.	18	-[f]	1.5	M4	10	485	20	3.0	100	5%[a]
48	0.2	NaI	1.2	TFAA	1.2	THF	0.1	r.t.	18	-[f]	1.5	M4	10	486	20	3.0	100	17%[a]
49	0.2	NaI	1.2	TFAA	1.2	THF	0.1	r.t.	18	-[f]	1.5	M4	10	487	20	3.0	100	5%[a]
50	0.2	NaI	1.2	TFAA	1.2	THF	0.1	r.t.	18	-[f]	1.5	M4	10	488	20	3.0	100	32%[a]

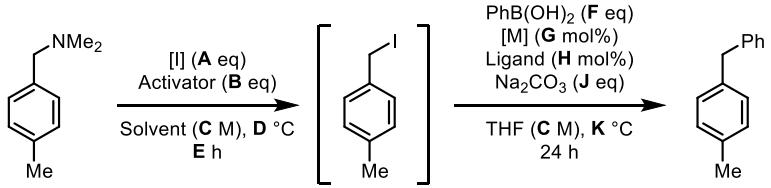

199 **237** **17**

[a] *in situ* ^{1}H NMR yield using 1,4-dinitrobenzene as internal standard; [b] Na_2CO_3 (1.0 eq) added; [c] $NaHCO_3$ (1.0 eq) added; [d] K_2CO_3 (1.0 eq) added; [e] K_3PO_4 (1.0 eq) added; [f] 0.5M solutions of **199** and TFAA added sequentially; [g] $NaHCO_3$; [h] K_2CO_3; [i] K_3PO_4; [j] PhBpin was used; [k] PhBnep was used

Entry	Scale (mmol)	[I]	A	Activator	B	Solvent	C	D	E	237 Yield	F	[M]	G	Ligand	H	J	K	17 Yield
51	0.2	NaI	1.2	TFAA	1.2	THF	0.1	r.t.	18	-[f]	1.5	M4	10	253	20	3.0	100	4%[a]
52	0.2	NaI	1.2	TFAA	1.2	THF	0.1	r.t.	18	-[f]	1.5	M4	10	489	20	3.0	100	54%[a]
53	0.2	NaI	1.2	TFAA	1.2	THF	0.1	r.t.	18	-[f]	1.5	M4	10	254	20	3.0	100	60%
54	0.2	NaI	1.2	TFAA	1.2	THF	0.1	r.t.	18	-[f]	1.5	M4	10	255	20	3.0	100	46%
55	0.2	NaI	1.2	TFAA	1.2	THF	0.1	r.t.	18	-[f]	1.5	M4	10	256	20	3.0	100	57%
56	0.2	NaI	1.2	TFAA	1.2	THF	0.1	r.t.	18	-[f]	1.5	M4	10	257	20	3.0	100	63%
57	0.2	NaI	1.2	TFAA	1.2	THF	0.1	r.t.	18	-[f]	1.5	M4	10	258	20	3.0	100	55%
58	0.2	NaI	1.2	TFAA	1.2	THF	0.1	r.t.	18	-[f]	1.5	M4	10	259	20	3.0	100	59%
59	0.2	NaI	1.2	TFAA	1.2	THF	0.1	r.t.	18	-[f]	1.5	M4	10	260	20	3.0	100	15%
60	0.2	NaI	1.2	TFAA	1.2	THF	0.1	r.t.	18	-[f]	1.5	M4	10	261	20	3.0	100	9%[a]
61	0.2	NaI	1.2	TFAA	1.2	THF	0.1	r.t.	18	-[f]	1.5	M4	10	262	20	3.0	100	67%
62	0.2	NaI	1.2	TFAA	1.2	THF	0.1	r.t.	18	-[f]	1.5	M4	10	263	20	3.0	100	71%
63	0.2	NaI	1.2	TFAA	1.2	THF	0.1	r.t.	18	-[f]	1.5	M4	10	490	20	3.0	100	7%[a]
64	0.2	NaI	1.2	TFAA	1.2	THF	0.1	r.t.	18	-[f]	1.5	M4	10	180	20	3.0	100	24%[a]
65	0.4	NaI	1.2	TFAA	1.2	THF	0.1	r.t.	18	-[f]	1.5	M6	10	262	20	3.0	100	81%
66	0.4	NaI	1.2	TFAA	1.2	THF	0.1	r.t.	18	-[f]	1.5	M6	10	263	20	3.0	100	85%
67	0.4	NaI	1.2	TFAA	1.2	THF	0.1	r.t.	18	-[f]	1.5	M7	10	262	20	3.0	100	75%
68	0.4	NaI	1.2	TFAA	1.2	THF	0.1	r.t.	18	-[f]	1.5	M7	10	263	20	3.0	100	81%
69	0.4	NaI	1.2	TFAA	1.2	THF	0.1	r.t.	18	-[f]	1.5	M8	10	262	20	3.0	100	68%
70	0.4	NaI	1.2	TFAA	1.2	THF	0.1	r.t.	18	-[f]	1.5	M8	10	263	20	3.0	100	76%
71	0.6	NaI	1.2	TFAA	1.2	THF	0.1	r.t.	18	-[f]	1.5	M6	5	262	10	3.0	100	95%
72	0.6	NaI	1.2	TFAA	1.2	THF	0.1	r.t.	18	-[f]	1.5	M6	5	262	5	3.0	100	72%
73	0.6	NaI	1.2	TFAA	1.2	THF	0.1	r.t.	18	-[f]	1.5	M6	2.5	262	5	3.0	100	81%
74	0.6	NaI	1.2	TFAA	1.2	THF	0.1	r.t.	18	-[f]	1.2	M6	5	262	10	3.0	100	79%
75	0.6	NaI	1.2	TFAA	1.2	THF	0.1	r.t.	18	-[f]	1.0	M6	5	262	10	3.0	100	65%

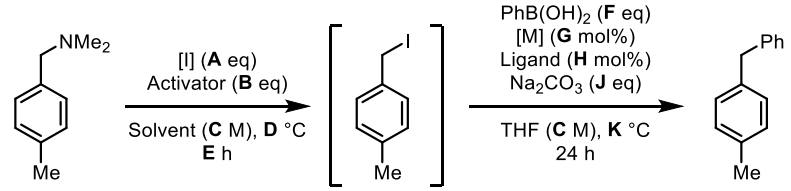

199 **237** **17**

[a]*in situ* ^{1}H NMR yield using 1,4-dinitrobenzene as internal standard; [b]Na_2CO_3 (1.0 eq) added; [c]$NaHCO_3$ (1.0 eq) added; [d]K_2CO_3 (1.0 eq) added; [e]K_3PO_4 (1.0 eq) added; [f]0.5M solutions of **199** and TFAA added sequentially; [g]$NaHCO_3$; [h]K_2CO_3; [i]K_3PO_4; [j]PhBpin was used; [k]PhBnep was used

Entry	Scale (mmol)	[I]	A	Activator	B	Solvent	C	D	E	237 Yield	F	[M]	G	Ligand	H	J	K	17 Yield
76	0.4	NaI	1.2	TFAA	1.2	THF	0.1	r.t.	18	-[f]	1.5	M4	10	255	20	3.0[g]	100	39%
77	0.4	NaI	1.2	TFAA	1.2	THF	0.1	r.t.	18	-[f]	1.5	M4	10	255	20	3.0[h]	100	0%
78	0.4	NaI	1.2	TFAA	1.2	THF	0.1	r.t.	18	-[f]	1.5	M4	10	255	20	3.0[i]	100	0%
79	0.6	NaI	1.2	TFAA	1.2	THF	0.1	r.t.	18	-[f]	1.5	M6	5	262	10	2.0	100	77%
80	0.6	NaI	1.2	TFAA	1.2	THF	0.1	r.t.	18	-[f]	1.5	M6	5	262	10	1.5	100	74%
81	0.6	NaI	1.2	TFAA	1.2	THF	0.1	r.t.	18	-[f]	1.5	M6	5	262	10	1.0	100	76%
82	0.6	NaI	1.2	TFAA	1.2	THF	0.1	r.t.	18	-[f]	1.5	-	-	262	20	3.0	100	0%
83	0.6	NaI	1.2	TFAA	1.2	THF	0.1	r.t.	18	-[f]	1.5	-	-	-	-	3.0	100	0%
84	0.6	NaI	1.2	TFAA	1.2	THF	0.1	r.t.	18	-[f]	1.5	M4	10	-	-	3.0	100	6%
85	0.6	NaI	1.2	TFAA	1.2	THF	0.1	r.t.	18	-[f]	1.5	M4	10	262	20	-	100	0%
86	0.6	NaI	1.2	TFAA	1.2	THF	0.1	r.t.	18	-[f]	1.5	M2	5	262	10	3.0	100	0%
87	0.6	NaI	1.2	TFAA	1.2	THF	0.1	r.t.	18	-[f]	1.5	M14	5	262	10	3.0	100	0%
88	0.6	NaI	1.2	TFAA	1.2	THF	0.1	r.t.	18	-[f]	1.5	M3	5	262	10	3.0	100	0%
89	0.6	NaI	1.2	TFAA	1.2	THF	0.1	r.t.	18	-[f]	1.5[j]	M6	5	262	10	3.0	100	0%
90	0.6	NaI	1.2	TFAA	1.2	THF	0.1	r.t.	18	-[f]	1.5[k]	M6	5	262	10	3.0	100	0%

M2 = $Pd(OAc)_2$; **M3** = $Pd_2(dba)_3$; **M4** = $Ni(acac)_2$; **M6** = Bis(hexafluoroacetylacetonato)nickel(II) hydrate; **M7** = Nickel(II) octanoate hydrate; **M8** = $Ni(THMD)_2$; **M14** = $Pd(PPh_3)_4$

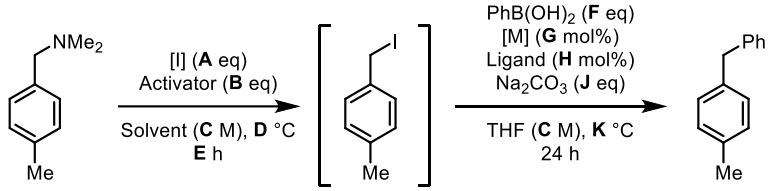

199 **237** **17**

[a] *in situ* ^{1}H NMR yield using 1,4-dinitrobenzene as internal standard; [b] Na_2CO_3 (1.0 eq) added; [c] $NaHCO_3$ (1.0 eq) added; [d] K_2CO_3 (1.0 eq) added; [e] K_3PO_4 (1.0 eq) added; [f] 0.5M solutions of **199** and TFAA added sequentially; [g] $NaHCO_3$; [h] K_2CO_3; [i] K_3PO_4; [j] PhBpin was used; [k] PhBnep was used

Ligands

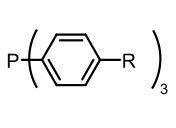

252 R = CF_3
483 R = OMe
484 R = F

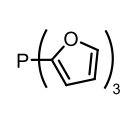

250

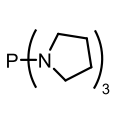

485

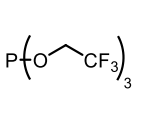

486

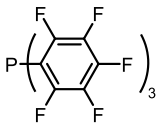

487

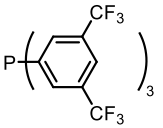

488

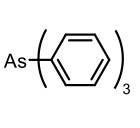

253

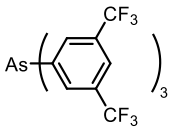

489

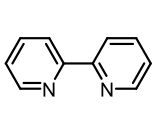

254

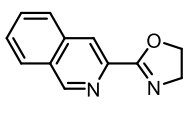

255

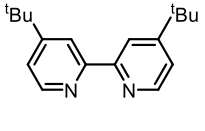

256

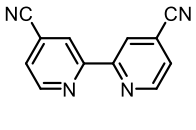

257

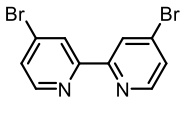

258

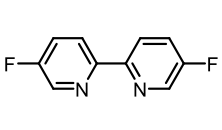

259

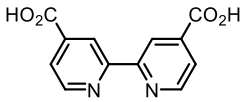

260

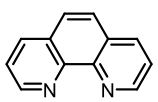

261

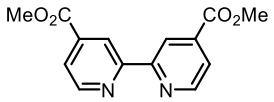

262

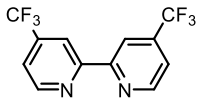

263

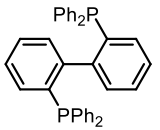

490

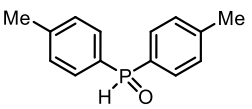

180

Table SI:2. *Optimisation studies into the cross-coupling of α-primary benzylamines*

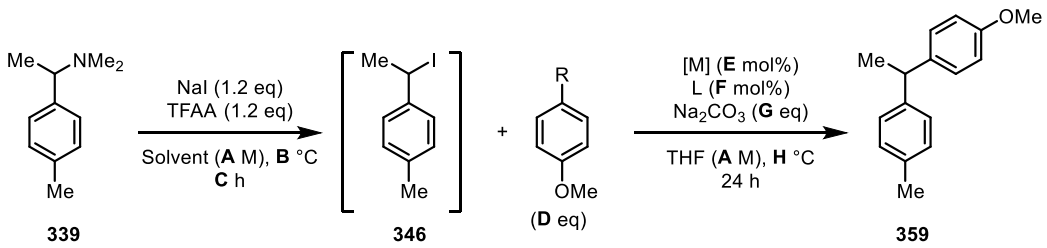

339 **346** **359**

[a] *in situ* ^{1}H NMR yield using 1,4-dinitrobenzene as internal standard; [b] $PhB(OH)_2$ was used; [c] 1 eq $ZnBr_2$ was used; [d] *in situ* GC-MS yield using dodecane as internal standard; [e] Reaction carried out in the dark; [f] No stirring; [g] *in situ* ^{1}H NMR yield using trichloroethylene as internal standard; [h] 2.0 eq NaI; [i] 1.2 eq NaBr; [j] PhBr was used; [k] 2.0 eq Zn and 1.0 eq KF was used.

Entry	Scale (mmol)	A	Solvent	B	C	346 Yield	R	D	[M]	E	L	F	G	H	359 Yield
1	0.6	0.1	THF	r.t.	18	-	$B(OH)_2$[b]	1.5	M6	5	262	10	3	100	21%
2	0.2	0.1	THF	r.t.	18	-	$B(OH)_2$[b]	1.5	M6	5	262	10	3	130	20%[a]
3	0.4	0.1	THF	r.t.	18	-	$B(OH)_2$	1.5	M6	10	262	20	3	100	25%[a]
4	0.4	0.1	THF	r.t.	18	-	$B(OH)_2$	1.5	M6	10	262	20	3	130	19%[a]
5	0.4	0.1	THF	r.t.	18	-	$B(OH)_2$	1.5	M6	10	360	20	3	130	27%[a]
6	0.2	0.1	THF	r.t.	18	-	$B(OH)_2$[b]	1.5	M7	5	262	10	3	100	0%[a]
7	0.2	0.1	THF	r.t.	18	-	$B(OH)_2$[b]	1.5	M8	5	262	10	3	100	9%[a]
8	0.2	0.1	THF	r.t.	18	-	$B(OH)_2$[b]	1.5	M5	5	262	10	3	100	6%[a]
9	0.4	0.1	THF	r.t.	18	-	$B(OH)_2$	1.5	M9	10	262	20	3	100	32%[a]
10	0.4	0.1	THF	r.t.	18	-	$B(OH)_2$	1.5	M9	10	262	20	3	130	25%
11	0.4	0.1	THF	r.t.	18	-	$B(OH)_2$	1.5	M9	10	360	20	3	130	18%[a]
12	0.4	0.1	THF	r.t.	18	-	$B(OH)_2$[b]	1.5	M9	10	360	16	3	130	20%
13	0.4	0.1	THF	r.t.	18	-	$B(OH)_2$[b]	1.5	M9	20	360	32	3	100	30%[a]
14	0.4	0.1	THF	r.t.	18	-	$B(OH)_2$	1.5	M10	10	262	20	3	100	37%[a]
15	0.4	0.1	THF	r.t.	18	-	$B(OH)_2$	1.5	M10	10	360	20	3	100	20%[a]
16	0.4	0.1	THF	r.t.	18	-	$B(OH)_2$	1.5	M10	10	491	20	3	100	0%[a]
17	0.4	0.1	THF	r.t.	18	-	$B(OH)_2$	1.5	M10	10	254	20	3	100	27%[a]
18	0.4	0.1	THF	r.t.	18	-	B(pin)(^{t}Bu)	1.5	M9	20	262	25	-	r.t.	34%
19	0.4	0.1	THF	r.t.	18	-	B(pin)(^{t}Bu)	1.5	M9	20	360	25	-	r.t.	51%
20	0.4	0.1	THF	r.t.	18	-	B(pin)(^{t}Bu)	1.5	M9	20	491	25	-	r.t.	0%[a]

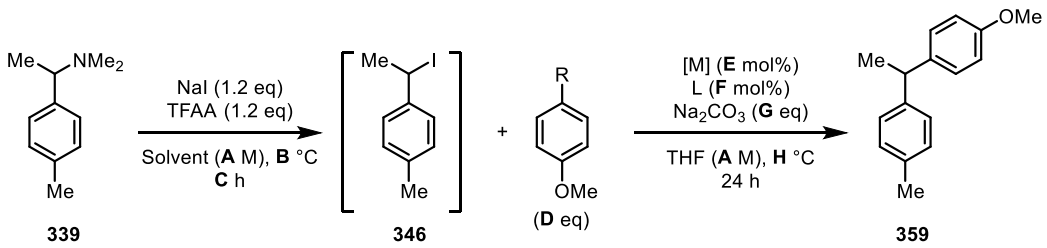

339 **346** **359**

[a] *in situ* ^{1}H NMR yield using 1,4-dinitrobenzene as internal standard; [b] $PhB(OH)_2$ was used; [c] 1 eq $ZnBr_2$ was used; [d] *in situ* GC-MS yield using dodecane as internal standard; [e] Reaction carried out in the dark; [f] No stirring; [g] *in situ* ^{1}H NMR yield using trichloroethylene as internal standard; [h] 2.0 eq NaI; [i] 1.2 eq NaBr; [j] PhBr was used; [k] 2.0 eq Zn and 1.0 eq KF was used.

Entry	Scale (mmol)	A	Solvent	B	C	346 Yield	R	D	[M]	E	L	F	G	H	359 Yield
21	0.4	0.1	THF	r.t.	18	-	B(pin)(^{t}Bu)	1.5	M9	20	255	25	-	r.t.	39%
22	0.4	0.1	THF	r.t.	18	-	B(pin)(^{n}Bu)	1.5	M9	20	262	25	-	r.t.	44%
23	0.4	0.1	THF	r.t.	18	-	B(pin)(^{n}Bu)	1.5	M9	20	360	25	-	r.t.	52%
24	0.4	0.1	THF	r.t.	18	-	B(pin)(^{n}Bu)	1.5	M9	20	255	25	-	r.t.	41%
25	0.4	0.1	THF	r.t.	18	-	B(pin)(^{n}Bu)	1.5	M9	20	262	25	-[c]	r.t.	0%
26	0.4	0.1	THF	r.t.	18	-	B(pin)(^{n}Bu)	1.5	M9	20	360	25	-[c]	r.t.	21%
27	0.4	0.1	THF	r.t.	18	-	B(pin)(^{n}Bu)	1.5	M9	20	255	25	-[c]	r.t.	22%
28	0.4	0.1	THF	r.t.	18	-	B(pin)(^{n}Bu)	1.5	M9	20	-	-	-	r.t.	4%[d]
29	0.4	0.1	THF	r.t.	18	-	B(pin)(^{n}Bu)	1.5	-	-	360	25	-	r.t.	2%[d]
30	0.4	0.1	THF	r.t.	18	-	B(pin)(^{n}Bu)	1.5	-	-	-	-	-	r.t.	2%[d]
31	0.4	0.1	THF	r.t.	18	-	B(pin)(^{n}Bu)	1.5	M10	20	360	25	-	r.t.	62%
32	0.4	0.1	THF	r.t.	18	-	B(pin)(^{n}Bu)	1.5	M6	20	360	25	-	r.t.	26%[d]
33	0.4	0.1	THF	r.t.	18	-	B(pin)(^{n}Bu)	1.5	M5	20	360	25	-	r.t.	19%[d]
34	0.4	0.1	THF	r.t.	18	-	$B(OH)_2$	1.5	M10	20	360	25	-	r.t.	0%
35	0.4	0.1	THF	r.t.	18	-	Bpin	1.5	M10	20	360	25	-	r.t.	0%
36	0.4	0.1	THF	r.t.	18	-	B(pin)(^{n}Bu)	1.5	M10	10	360	20	-	r.t.	63%
37	0.4	0.1	THF	r.t.	18	-	B(pin)(^{n}Bu)	1.5	M10	10	360	12	-	r.t.	65%
38	0.4	0.1	THF	r.t.	18	-	B(pin)(^{n}Bu)	1.5	M10	10	360	5	-	r.t.	15%[d]
39	0.4	0.1	THF	r.t.	18	-	B(pin)(^{n}Bu)	1.5	M10	5	360	10	-	r.t.	60%
40	0.4	0.1	THF	r.t.	18	-	B(pin)(^{n}Bu)	1.5	M10	5	360	6	-	r.t.	41%

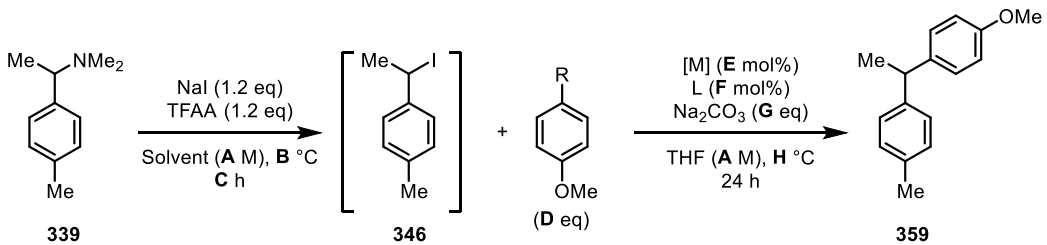

339 **346** **359**

[a] *in situ* ^{1}H NMR yield using 1,4-dinitrobenzene as internal standard; [b] $PhB(OH)_2$ was used; [c] 1 eq $ZnBr_2$ was used; [d] *in situ* GC-MS yield using dodecane as internal standard; [e] Reaction carried out in the dark; [f] No stirring; [g] *in situ* ^{1}H NMR yield using trichloroethylene as internal standard; [h] 2.0 eq NaI; [i] 1.2 eq NaBr; [j] PhBr was used; [k] 2.0 eq Zn and 1.0 eq KF was used.

Entry	Scale (mmol)	A	Solvent	B	C	346 Yield	R	D	[M]	E	L	F	G	H	359 Yield
41	0.4	0.1	THF	r.t.	18	-	B(pin)(^{n}Bu)	1.5	M10	5	360	2.5	-	r.t.	20%[d]
42	0.4	0.1	THF	r.t.	18	-	B(pin)(^{n}Bu)	1.5	M10	2.5	360	5	-	r.t.	37%[d]
43	0.4	0.1	THF	r.t.	18	-	B(pin)(^{n}Bu)	1.5	M10	2.5	360	3	-	r.t.	38%[d]
44	0.6	0.1	THF	r.t.	18	-	B(pin)(^{n}Bu)	1.5	M10	20	360	25	-	r.t.	49%
45	0.6	0.1	THF	r.t.	18	-	B(pin)(^{n}Bu)	1.5	M10	10	360	12	-	r.t.	19%
46	0.6	0.1	THF	r.t.	18	-	B(pin)(^{n}Bu)	1.2	M10	20	360	25	-	r.t.	46%
47	0.6	0.1	THF	r.t.	18	-	B(pin)(^{n}Bu)	1.2	M10	10	360	12	-	r.t.	33%
48	0.6	0.1	THF	r.t.	18	-	B(pin)(^{n}Bu)	1.8	M10	20	360	25	-	r.t.	31%
49	0.6	0.1	THF	r.t.	18	-	B(pin)(^{n}Bu)	1.8	M10	10	360	12	-	r.t.	0%
50	0.4	0.1	THF	r.t.	18	-	B(pin)(^{n}Bu)	1.5	M10	20	360	25	-	r.t.[e]	55%
51	0.4	0.1	THF	r.t.	18	-	B(pin)(^{n}Bu)	1.5	M10	10	360	12	-	r.t.[e]	46%
52	0.4	0.1	THF	r.t.	18	-	B(pin)(^{n}Bu)	1.5	M10	20	360	25	-	40	47%
53	0.4	0.1	THF	r.t.	18	-	B(pin)(^{n}Bu)	1.5	M10	10	360	12	-	40	45%
54	0.4	0.1	THF	r.t.[e]	18	-	B(pin)(^{n}Bu)	1.5	M10	20	360	25	-	r.t.	41%
55	0.4	0.2	THF	r.t.	18	-	B(pin)(^{n}Bu)	1.5	M10	20	360	25	-	r.t.	62%
56	0.4	0.05	THF	r.t.	18	-	B(pin)(^{n}Bu)	1.5	M10	20	360	25	-	r.t.	50%
57	0.4	0.1	THF	0	18	-	B(pin)(^{n}Bu)	1.5	M10	20	360	25	-	r.t.	35%
58	0.4	0.1	THF	0	18	-	B(pin)(^{n}Bu)	1.5	M10	20	360	25	-	0	53%
59	0.4	0.1	THF	r.t.	18	-	B(pin)(^{n}Bu)	1.5	M10	20	360	25	-	0	59%
60	0.4	0.1	THF	r.t.	18	-	B(pin)(^{n}Bu)	1.5	M10	10	360	12	-	0	39%

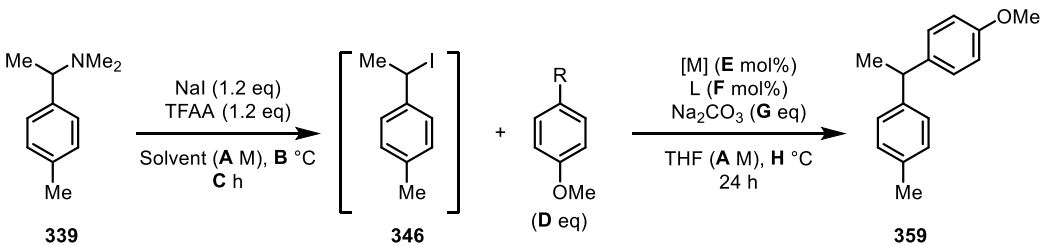

339 **346** **359**

[a] *in situ* ^{1}H NMR yield using 1,4-dinitrobenzene as internal standard; [b] $PhB(OH)_2$ was used; [c] 1 eq $ZnBr_2$ was used; [d] *in situ* GC-MS yield using dodecane as internal standard; [e] Reaction carried out in the dark; [f] No stirring; [g] *in situ* ^{1}H NMR yield using trichloroethylene as internal standard; [h] 2.0 eq NaI; [i] 1.2 eq NaBr; [j] PhBr was used; [k] 2.0 eq Zn and 1.0 eq KF was used.

Entry	Scale (mmol)	A	Solvent	B	C	346 Yield	R	D	[M]	E	L	F	G	H	359 Yield
61	0.4	0.1	Et_2O	r.t.	18	-	B(pin)(^{n}Bu)	1.5	M10	20	360	25	-	0	4%
62	0.4	0.1	2Me-THF	r.t.	18	-	B(pin)(^{n}Bu)	1.5	M10	20	360	25	-	0	35%
63	0.4	0.1	Dioxane	r.t.	18	-	B(pin)(^{n}Bu)	1.5	M10	20	360	25	-	0	14%
64	0.4	0.1	TBME	r.t.	18	-	B(pin)(^{n}Bu)	1.5	M10	20	360	25	-	0	11%
65	0.6	0.1	THF	r.t.	1.5	-	B(pin)(^{n}Bu)	1.5	M10	20	360	25	-	r.t.	50%
66	0.6	0.1	THF	r.t.	5	-	B(pin)(^{n}Bu)	1.5	M10	20	360	25	-	r.t.	57%
67	0.6	0.1	THF	r.t.	8	-	B(pin)(^{n}Bu)	1.5	M10	20	360	25	-	r.t.	46%
68	0.6	0.1	THF	r.t.	18	-	B(pin)(^{n}Bu)	1.5	M10	20	492	25	-	r.t.	25%
69	0.6	0.1	THF	r.t.	18	-	B(pin)(^{n}Bu)	1.5	M10	20	361	25	-	r.t.	44%
70	0.2	0.1	THF[f]	r.t.	18	48%[g]	-	-	-	-	-	-	-	-	-
71	0.2	0.1	THF	r.t.	5	60%[g]	-	-	-	-	-	-	-	-	-
72	0.2	0.2	THF	r.t.	5	55%[g]	-	-	-	-	-	-	-	-	-
73	0.2	0.1	THF[f, h]	r.t.	5	45%[g]	-	-	-	-	-	-	-	-	-
74	0.2	0.1	THF	-10	5	63%[g]	-	-	-	-	-	-	-	-	-
75	0.2	0.1	THF	-10, r.t.	1, 4	51%[g]	-	-	-	-	-	-	-	-	-
76	0.2	0.1	THF	-10, r.t.	1, 17	58%[g]	-	-	-	-	-	-	-	-	-
77	0.2	0.1	MeCN[f]	r.t.	18	13%[g]	-	-	-	-	-	-	-	-	-
78	0.2	0.1	MeCN[f, h]	r.t.	18	13%[g]	-	-	-	-	-	-	-	-	-
79	0.2	0.1	MeCN	r.t.	5	33%[g]	-	-	-	-	-	-	-	-	-
80	0.6	0.1	THF	-10, r.t.	1, 5	-	B(pin)(^{n}Bu)	1.5	M10	20	360	25	-	0, r.t.	50%
81	0.6	0.1	THF	-10	6	-	B(pin)(^{n}Bu)	1.5	M10	20	360	25	-	0, r.t.	48%

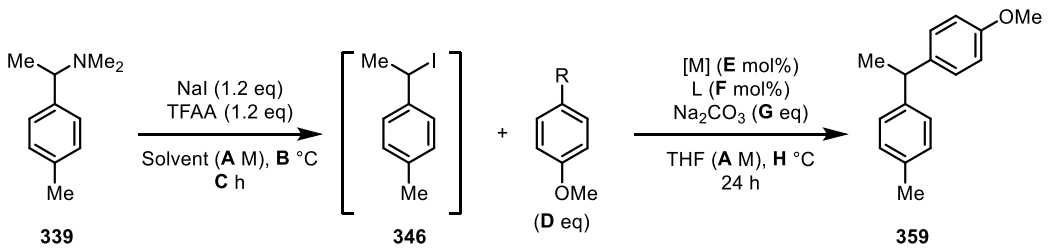

339 **346** **359**

[a] *in situ* ^{1}H NMR yield using 1,4-dinitrobenzene as internal standard; [b] $PhB(OH)_2$ was used; [c] 1 eq $ZnBr_2$ was used; [d] *in situ* GC-MS yield using dodecane as internal standard; [e] Reaction carried out in the dark; [f] No stirring; [g] *in situ* ^{1}H NMR yield using trichloroethylene as internal standard; [h] 2.0 eq NaI; [i] 1.2 eq NaBr; [j] PhBr was used; [k] 2.0 eq Zn and 1.0 eq KF was used.

Entry	Scale (mmol)	A	Solvent	B	C	346 Yield	R	D	[M]	E	L	F	G	H	359 Yield
82	0.6	0.1	THF	-10, r.t.	1, 5	-	B(pin)(^{n}Bu)	1.5	M10	20	360	25	-	0	54%
83	0.6	0.1	THF	-10	6	-	B(pin)(^{n}Bu)	1.5	M10	20	360	25	-	0	51%
84	0.6	0.1	THF	0, r.t.	1, 17	-	B(pin)(^{n}Bu)	1.5	M10	20	360	25	-	0	61%
85	0.6	0.1	THF then DMA	0, r.t.	1, 17	-	Br[j]	1.0	M15	10	410	10	-[k]	r.t.	40%
86	0.6	0.1	THF then DMA	0, r.t.	1, 17	-	Br[j]	2.0	M15	10	410	10	-[k]	r.t.	20%
87	0.6	0.1	THF	0, r.t.	1, 17	-	MgBr	1.3	M16	3	493	3	-	r.t.	20%
88	0.6	0.1	THF[i] then DMA	0, r.t.	1, 17	-	Br[j]	1.0	M15	10	410	10	-[k]	r.t.	0%
89	0.6	0.1	THF[i]	0, r.t.	1, 17	-	B(pin)(^{n}Bu)	1.5	M10	20	360	25	-	0	0%

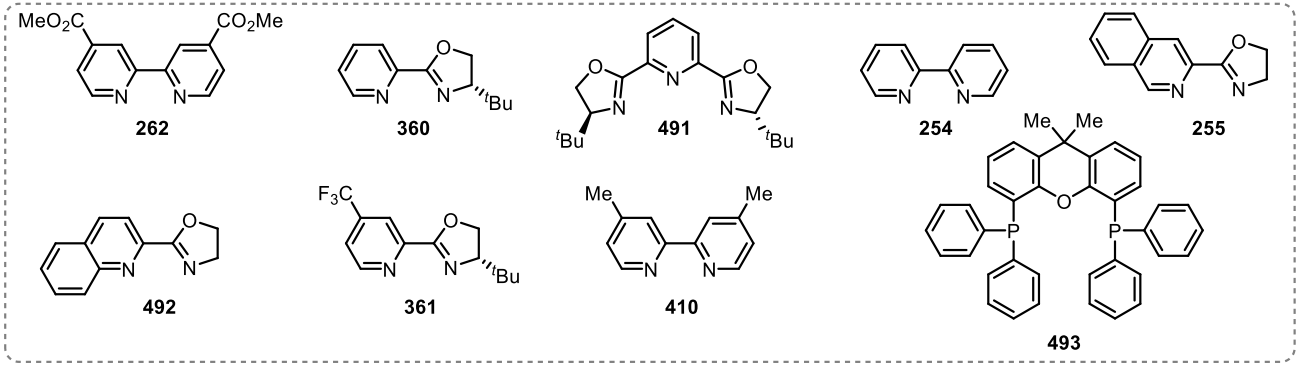

M5 = $Ni(acac)_2$; **M6** = Bis(hexafluoroacetylacetonato)nickel(II) hydrate; **M7** = Nickel(II) octanoate hydrate; **M8** = $Ni(THMD)_2$
M9 = $NiBr_2$(glyme); **M10** = $NiBr_2$(diglyme); **M15** = NiI_2; **M16** = $Pd(MeCN)_2Cl_2$

Table SI:3. *Optimisation studies for the cross-coupling of α-secondary benzylamine* ***339***

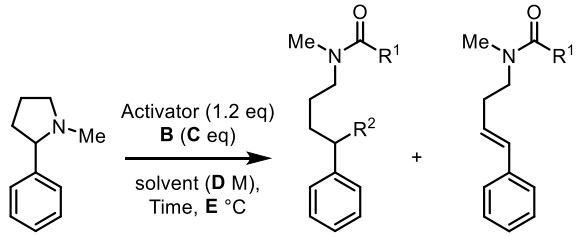

135
A mmol

474 **454**

TFAA = Trifluoroacetic anhydride ($R^1 = CF_3$) ; AcA = Acetic anhydride (R^1 = Me) ; AcCl = Acetyl chloride (R^1 = Me); $^aR^2$ = I; $^bR^2 = OCOCF_3$

Entry	A	Activator	B	C	Solvent	D	Time	E	474 Yield	454 yield	474:454 Ratio
1	0.4	TFAA	NaI	1.2	THF	0.1	1 h, 17 h	0 °C - r.t.	42%[a]	42%	1:1
2	0.3	TFAA	NaI	1.2	THF	0.1	1h	0 °C	36%[a]	36%	1:1
3	0.3	TFAA	NaI	1.2	THF	0.1	4h	0 °C	-	-	1:1
4	0.3	TFAA	NaI	1.2	THF	0.1	7h	0 °C	-	-	0.42:1
5	0.3	TFAA	NaI	2.0	THF	0.1	1h	0 °C	46%[a]	31%	1:0.67
6	0.3	TFAA	NaI	2.5	THF	0.1	1h	0 °C	47%[a]	28%	1:0.6
7	0.3	TFAA	NaI	3.0	THF	0.1	1h	0 °C	42%[a]	24%	1:0.56
8	0.3	TFAA	NaI	2.5	THF	0.06	1h	0 °C	31%[a]	24%	1:0.77
9	0.3	TFAA	NaI	2.5	THF	0.15	1h	0 °C	48%[a]	26%	1:0.54
10	0.3	TFAA	NaI	2.5	THF	0.2	1h	0 °C	46%[a]	22%	1:0.48
11	0.3	TFAA	NaBr	2.5	THF	0.2	1h	0 °C	40%[b]	14%	1:0.34
12	0.3	TFAA	NaBr	1.2	THF	0.1	1h, 17h	0 °C to r.t.	53%[b]	14%	1:0.27
13	0.3	TFAA	NaBr	2.5	THF	0.2	1h, 17h	0 °C to r.t.	61%[b]	17%	1:0.28
14	0.3	TFAA	NaI	2.5	THF	0.2	1h, 17h	0 °C to r.t.	55%[a]	34%	1:0.61
15	0.3	TFAA	NaBr	2.5	Et_2O	0.2	1h, 17h	0 °C to r.t.	66%[b]	17%	1:0.26
16	0.3	TFAA	NaBr	2.5	MeCN	0.2	1h, 17h	0 °C to r.t.	40%[b]	15%	1:0.37
17	0.3	TFAA	NaBr	2.5	Dioxane	0.2	1h, 17h	0 °C to r.t.	0%	0%	-
18	0.3	TFAA	NaBr	2.5	DNBE	0.2	1h, 17h	0 °C to r.t.	44%[b]	19%	1:0.43
19	0.3	TFAA	NaBr	2.5	2-MeTHF	0.2	1h, 17h	0 °C to r.t.	68%[b]	17%	1:0.25
20	0.3	AcA	NaBr	2.5	Et_2O	0.2	1h, 17h	0 °C to r.t.	0%	0%	-

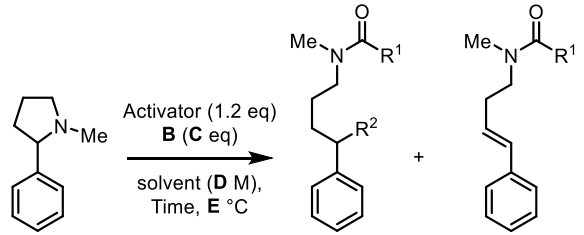

TFAA = Trifluoroacetic anhydride ($R^1 = CF_3$) ; AcA = Acetic anhydride ($R^1 = Me$) ; AcCl = Acetyl chloride ($R^1 = Me$); $^aR^2 = I$; $^bR^2 = OCOCF_3$

Entry	A	Activator	B	C	Solvent	D	Time	E	474 Yield	454 yield	474:454 Ratio
21	0.3	AcA	NaBr	2.5	THF	0.2	1h, 17h	0 °C to r.t.	0%	0%	-
22	0.3	AcA	NaBr	2.5	2-MeTHF	0.2	1h, 17h	0 °C to r.t.	0%	0%	-
23	0.3	TFAA	LiBr	2.5	Et_2O	0.2	1h, 16h	0 °C to r.t.	40%^{b}	17%	1:0.42
24	0.3	TFAA	LiBr	2.5	THF	0.2	1h, 16h	0 °C to r.t.	0%	0%	-
25	0.3	TFAA	LiBr	2.5	2-MeTHF	0.2	1h, 16h	0 °C to r.t.	0%	6%	0:1
26	0.3	TFAA	LiBr	2.5	MeCN	0.2	1h, 17h	0 °C to r.t.	33%^{b}	16%	1:0.48
27	0.3	TFAA	NaI	2.5	MeCN	0.2	1h, 17h	0 °C to r.t.	61%^{a}	40%	1:0.64
28	0.3	AcA	NaI	2.5	THF	0.2	1h, 17h	0 °C to r.t.	33%^{a}	28%	1:0.85
29	0.3	AcCl	NaI	2.5	THF	0.2	1h, 17h	0 °C to r.t.	40%^{a}	33%	1:0.82
30	0.3	AcCl	NaBr	2.5	THF	0.2	1h, 17h	0 °C to r.t.	36%^{b}	8%	1:0.23
31	0.3	TFAA	NaBr	2.5	2-MeTHF	0.2	18 h	50 °C	76%^{b}	23%	1:0.31
32	0.3	AcCl	NaBr	2.5	Et_2O	0.2	1h, 17h	0 °C to r.t.	20%^{b}	8%	1:0.39
33	0.3	AcCl	NaBr	2.5	2-MeTHF	0.2	1h, 17h	0 °C to r.t.	33%^{b}	8%	1:0.24
34	0.3	AcCl	NaBr	2.5	2-MeTHF	0.2	18h	50 °C	95%^{b}	18%	1:0.19
35	0.3	TFAA	NaBr	2.5	2-MeTHF	0.2	18h	40 °C	52%^{b}	18%	1:0.35

Table SI:4. *Full 2-aryl pyrrolidine ring opening optimisation studies*

References

1 N. A. McGrath, M. Brichacek and J. T. Njardarson, *J. Chem. Educ.*, 2010, **87**, 1348–1349.

2 K. Ouyang, W. Hao, W.-X. Zhang and Z. Xi, *Chem. Rev.*, 2015, **115**, 12045–12090.

3 T. Koreeda, T. Kochi and F. Kakiuchi, *J. Am. Chem. Soc.*, 2009, **131**, 7238–7239.

4 D. M. Shacklady-McAtee, K. M. Roberts, C. H. Basch, Y. G. Song and M. P. Watson, *Tetrahedron*, 2014, **70**, 4257–4263.

5 S. J. Blanksby and G. B. Ellison, *Acc. Chem. Res.*, 2003, **36**, 255–263.

6 F. Brotzel, C. C. Ying and H. Mayr, *J. Org. Chem.*, 2007, **72**, 3679–3688.

7 T. Kanzian, T. A. Nigst, A. Maier, S. Pichl and H. Mayr, *Eur. J. Org. Chem.*, 2009, 6379–6385.

8 J. Ammer, M. Baidya, S. Kobayashi and H. Mayr, *J. Phys. Org. Chem.*, 2010, **23**, 1029–1035.

9 J. F. Bower, J. Garcıá-Cárceles and K. A. Bahou, *ACS Catal.*, 2020, **10**, 12738–12759.

10 J. S. Carey, D. Laffan, C. Thomson and M. T. Williams, *Org. Biomol. Chem.*, 2006, **4**, 2337–2347.

11 N. Miyaura, K. Yamada and A. Suzuki, *Tetrahedron Lett.*, 1979, **20**, 3437–3440.

12 W. Guan, J. Liao and M. P. Watson, *Synthesis*, 2018, **50**, 3231–3237.

13 J.-X. Xu, F. Zhao, Y. Yuan and X.-F. Wu, *Org. Lett.*, 2020, **22**, 2756–2760.

14 S. B. Blakey and D. W. C. MacMillan, *J. Am. Chem. Soc.*, 2003, **125**, 6046–6047.

15 US2011293519 (A1), 2011.

16 E. Wenkert, A.-L. Han and C.-J. Jenny, *J. Chem. Soc. Chem. Comm.*, 1988, 975–976.

17 J. T. Reeves, D. R. Fandrick, Z. Tan, J. J. Song, H. Lee, N. K. Yee and C. H. Senanayake, *Org. Lett.*, 2010, **12**, 4388–4391.

18 D.-Y. Wang, M. Kawahata, Z.-K. Yang, K. Miyamoto, S. Komagawa, K. Yamaguchi, C. Wang and M. Uchiyama, *Nat. Commun.*, 2016, **7**, 12937.

19 Z.-K. Yang, D.-Y. Wang, H. Minami, H. Ogawa, T. Ozaki, T. Saito, K. Miyamoto, C. Wang and M. Uchiyama, *Chem. - Eur. J.*, 2016, **22**, 15693–15699.

20 S. Ueno, N. Chatani and F. Kakiuchi, *J. Am. Chem. Soc.*, 2007, **129**, 6098–6099.

21 Q. Zhao, J. Zhang and M. Szostak, *ACS Catal.*, 2019, **9**, 8171–8177.

22 M. R. Islam, J. G. Mahdi and I. D. Bowen, *Drug Safety*, 1997, **17**, 149–165.

23 Z.-B. Zhang, C.-L. Ji, C. Yang, J. Chen, X. Hong and J.-B. Xia, *Org. Lett.*, 2019, **21**, 1226–1231.

24 Z. C. Cao, X. L. Li, Q. Y. Luo, H. Fang and Z. J. Shi, *Org. Lett.*, 2018, **20**, 1995–1998.

25 Z. C. Cao, S. J. Xie, H. Fang and Z. J. Shi, *J. Am. Chem. Soc.*, 2018, **140**, 13575–13579.

26 J. Liao, W. Guan, B. P. Boscoe, J. W. Tucker, J. W. Tomlin, M. R. Garnsey and M. P. Watson, *Org. Lett.*, 2018, **20**, 3030–3033.

27 J. Zhang, A. Bellomo, A. D. Creamer, S. D. Dreher and P. J. Walsh, *J. Am. Chem. Soc.*, 2012, **134**, 13765–13772.

28 Y. Luan and S. E. Schaus, *J. Am. Chem. Soc.*, 2012, **134**, 19965–19968.

29 S. Nave, R. P. Sonawane, T. G. Elford and V. K. Aggarwal, *J. Am. Chem. Soc.*, 2010, **132**, 17096–17098.

30 D.-G. Yu, X. Wang, R.-Y. Zhu, S. Luo, X.-B. Zhang, B.-Q. Wang, L. Wang and Z.-J. Shi, *J. Am. Chem. Soc.*, 2012, **134**, 14638–14641.

31 B. L. H. Taylor, E. C. Swift, J. D. Waetzig and E. R. Jarvo, *J. Am. Chem. Soc.*, 2011, **133**, 389–391.

32 S. Duez, A. K. Steib, S. M. Manolikakes and P. Knochel, *Angew. Chem Int. Ed.*, 2011, **50**, 7686–7690.

33 G. A. Molander and M. D. Elia, *J. Org. Chem.*, 2006, **71**, 9198–9202.

34 P. Maity, D. M. Shacklady-Mcatee, G. P. A. Yap, E. R. Sirianni and M. P. Watson, *J. Am. Chem. Soc.*, 2013, **135**, 280–285.

35 R.-D. He, C.-L. Li, Q.-Q. Pan, P. Guo, X.-Y. Liu and X.-Z. Shu, *J. Am. Chem. Soc.*, 2019, **141**, 12481–12486.

36 S. Xu, Z. Zhang, C. Han, W. Hu, T. Xiao, Y. Yuan and J. Zhao, *J. Org. Chem.*, 2019, **84**, 12192–12197.

37 C. Han, Z. Zhang, S. Xu, K. Wang, K. Chen and J. Zhao, *J. Org. Chem.*, 2019, **84**, 16308–16313.

38 T. Wang, S. Yang, S. Xu, C. Han, G. Guo and J. Zhao, *RSC Adv.*, 2017, **7**, 15805–15808.

39 R. Martin-Montero, V. R. Yatham, H. Yin, J. Davies and R. Martin, *Org. Lett.*, 2019, **21**,

2947–2951.

40 C. H. Basch, J. Liao, J. Xu, J. J. Piane and M. P. Watson, *J. Am. Chem. Soc.*, 2017, **139**, 5313–5316.

41 Y. Li, Z. Wang and X.-F. Wu, *ACS Catal.*, 2018, **8**, 738–741.

42 G. S. Singh, in *Adv. Heterocycl. Chem.*, eds. E. F. V. Scriven and C. A. Ramdsen, 1st edn., 2019, pp. 245–335.

43 G. S. Singh and T. H. Tabane, in *Green Synthetic Approaches for Biologically Relevant Heterocycles*, ed. G. Brahmachari, 2015, pp. 163–184.

44 F. Lovering, J. Bikker and C. Humblet, *J. Med. Chem.*, 2009, **52**, 6752–6756.

45 C. Y. Huang and A. G. Doyle, *J. Am. Chem. Soc.*, 2012, **134**, 9541–9544.

46 C.-Y. Huang and A. G. Doyle, *J. Am. Chem. Soc.*, 2015, **137**, 5638–5641.

47 Y. Takeda, Y. Ikeda, A. Kuroda, S. Tanaka and S. Minakata, *J. Am. Chem. Soc.*, 2014, **136**, 8544–8547.

48 J. G. Estrada, W. L. Williams, S. I. Ting and A. G. Doyle, *J. Am. Chem. Soc.*, 2020, **142**, 8928–8937.

49 D. K. Nielsen, C.-Y. Huang and A. G. Doyle, *J. Am. Chem. Soc.*, 2013, **135**, 13605–13609.

50 M. L. Duda and F. E. Michael, *J. Am. Chem. Soc.*, 2013, **135**, 18347–18349.

51 W. P. Teh and F. E. Michael, *Org. Lett.*, 2017, **19**, 1738–1740.

52 T. J. Steiman, J. Liu, A. Mengiste and A. G. Doyle, *J. Am. Chem. Soc.*, 2020, **142**, 7598–7605.

53 H. Alper and F. Urso, *J. Am. Chem. Soc.*, 1983, **105**, 6737–6738.

54 V. Mahadevan, Y. D. Y. L. Getzler and G. W. Coates, *Angew. Chem. Int. Ed.*, 2002, **41**, 2781–2784.

55 F. Fontana, G. C. Tron, N. Barbero, S. Ferrini, S. P. Thomas and V. K. Aggarwal, *Chem. Commun.*, 2010, **46**, 267–269.

56 F. Fontana, C. C. Chen and V. K. Aggarwal, *Org. Lett.*, 2011, **13**, 3454–3457.

57 Y. Kim, J. Heo, D. Kim, S. Chang and S. Seo, *Nat. Commun.*, 2020, **11**, 4761.

58 J. Van Betsbrugge, W. Van Den Nest, P. Verheyden and D. Tourwé, *Tetrahedron*, 1998, **54**, 1753–1762.

59 T. Honda and F. Ishikawa, *Chem. Commun.*, 1999, **2**, 1065–1066.

60 R. Ito, N. Umezawa and T. Higuchi, *J. Am. Chem. Soc.*, 2005, **127**, 834–835.

61 P. Liu, Y. Liu, E. L.-M. Wong, S. Xiang and C.-M. Che, *Chem. Sci.*, 2011, **2**, 2187–2195.

62 G. Cocquet, C. Ferroud and A. Guy, *Tetrahedron*, 2000, **56**, 2975–2984.

63 A. Christiansen, C. Li, M. Garland, D. Selent, R. Ludwig, A. Spannenberg, W. Baumann, R. Franke and A. Börner, *Eur. J. Org. Chem.*, 2010, 2733–2741.

64 L. Ackermann, *Synthesis*, 2006, **8**, 1557–1571.

65 Y. X. Wang and M. Ye, *Sci. China Chem.*, 2018, **61**, 1004–1013.

66 A. Christiansen, D. Selent, A. Spannenberg, W. Baumann, R. Franke and A. Borner, *Organometallics*, 2010, **29**, 3139–3145.

67 P. A. Donets and N. Cramer, *J. Am. Chem. Soc.*, 2013, **135**, 11772–11775.

68 P. W. N. M. van Leeuwen, I. Cano and Z. Freixa, *ChemCatChem*, 2020, **12**, 3982–3994.

69 A. Gallen, A. Riera, X. Verdaguer and A. Grabulosa, *Catal. Sci. Technol.*, 2019, **9**, 5504–5561.

70 C. H. Wei, C. E. Wu, Y. L. Huang, R. G. Kultyshev and F. E. Hong, *Chem. - Eur. J.*, 2007, **13**, 1583–1593.

71 B. G. Janesko, H. C. Fisher, M. J. Bridle and J. L. Montchamp, *J. Org. Chem.*, 2015, **80**, 10025–10032.

72 F. Hu, B. N. Kumpati and X. Lei, *Tetrahedron Lett.*, 2014, **55**, 7215–7218.

73 T. Achard, L. Giordano, A. Tenaglia, Y. Gimbert and G. Buono, *Organometallics*, 2010, **29**, 3936–3950.

74 B. Stewart, A. Harriman and L. J. Higham, *Organometallics*, 2011, **30**, 5338–5343.

75 D. F. V. Lewis, *Sci. World J.*., 2004, **4**, 1074–1082.

76 R. Cuypers, E. J. R. Sudhölter and H. Zuilhof, *ChemPhysChem*, 2010, **11**, 2230–2240.

77 P. Sutra and A. Igau, *Coordin. Chem. Rev.*, 2016, **308**, 97–116.

78 A. Gallen, S. Orgué, G. Muller, E. C. Escudero-Adán, A. Riera, X. Verdaguer and A. Grabulosa, *Dalton Trans.*, 2018, **47**, 5366–5379.

79 D. Martin, D. Moraleda, T. Achard, L. Giordano and G. Buono, *Chem. - Eur. J.*, 2011, **17**,

12729–12740.

80 Q. S. Liu, D. Y. Wang, Z. J. Yang, Y. X. Luan, J. F. Yang, J. F. Li, Y. G. Pu and M. Ye, *J. Am. Chem. Soc.*, 2017, **139**, 18150–18153.

81 L. V. Graux, M. Giorgi, G. Buono and H. Clavier, *Organometallics*, 2015, **34**, 1864–1871.

82 M. M. Rauhut and H. A. Currier, *J. Org. Chem.*, 1961, **26**, 4626–4628.

83 C. A. Busacca, J. C. Lorenz, N. Grinberg, N. Haddad, M. Hrapchak, B. Latli, H. Lee, P. Sabila, A. Saha, M. Sarvestani, S. Shen, R. Varsolona, X. Wei and C. H. Senanayake, *Org. Lett.*, 2005, **7**, 4277–4280.

84 L. Ackermann, *Israel J. Chem.*, 2010, **50**, 652–663.

85 T. Nemoto, T. Masuda, T. Matsumoto and Y. Hamada, *J. Org. Chem.*, 2005, **70**, 7172–7178.

86 T. Nemoto and Y. Hamada, *Tetrahedron*, 2011, **67**, 667–687.

87 T. Nemoto, L. Jin, H. Nakamura and Y. Hamada, *Tetrahedron Lett.*, 2006, **47**, 6577–6581.

88 T. Nemoto, T. Harada, T. Matsumoto and Y. Hamada, *Tetrahedron Lett.*, 2007, **48**, 6304–6307.

89 H. Landert, F. Spindler, A. Wyss, H. U. Blaser, B. Pugin, Y. Ribourduoille, B. Gschwend, B. Ramalingam and A. Pfaltz, *Angew. Chem. Int. Ed.*, 2010, **49**, 6873–6876.

90 Benoit, P.; Heidi, L.; Bjoern, G.; Andreas, P.; Felix, S. BIDENTATE SECONDARY PHOSPHINE OXIDE CHIRAL LIGANDS FOR USE IN ASYMMETRIC ADDITION REACTIONS. WO2009065783 (A1), 2009.

91 Y. X. Wang, S. L. Qi, Y. X. Luan, X. W. Han, S. Wang, H. Chen and M. Ye, *J. Am. Chem. Soc.*, 2018, **140**, 5360–5364.

92 C. E. Teerlinck and W. J. Bowyer, *J. Org. Chem.*, 1996, **61**, 1059–1064.

93 P. De Medina, L. S. Ingrassia and M. E. Mulliez, *J. Org. Chem.*, 2003, **68**, 8424–8430.

94 M. Yadav and R. Krishnamurthy, *Org. Lett.*, 2019, **21**, 7400–7404.

95 R. Shen, B. Luo, J. Yang, L. Zhang and L. B. Han, *Chem. Commun.*, 2016, **52**, 6451–6454.

96 Q. Chen, J. Zeng, X. Yan, Y. Huang, C. Wen, X. Liu and K. Zhang, *J. Org. Chem.*, 2016, **81**, 10043–10048.

97 C. Zarate, R. Manzano and R. Martin, *J. Am. Chem. Soc.*, 2015, **137**, 6754–6757.

98 L. Mai, N. Boysen, D. Zanders, T. de los Arcos, F. Mitschker, B. Mallick, G. Grundmeier, P.

Awakowicz and A. Devi, *Chem. - Eur. J.*, 2019, **25**, 7489–7500.

99 J. W. Bundens and M. M. Francl, *Organometallics*, 1993, **12**, 1608–1615.

100 C. H. Basch, K. M. Cobb and M. P. Watson, *Org. Lett.*, 2016, **18**, 136–139.

101 G. Dai-ho and P. S. Mariano, *J. Org. Chem.*, 1988, **53**, 5113–5127.

102 H. Fujita, R. Nishikawa, O. Sasamoto, M. Kitamura and M. Kunishima, *J. Org. Chem.*, 2019, **84**, 8380–8391.

103 V. M. Mastranzo, J. L. Olivares Romero, F. Yuste, B. Ortiz, R. Sánchez-Obregón and J. L. García Ruano, *Tetrahedron*, 2012, **68**, 1266–1271.

104 G. A. Molander and S. K. Pack, *Tetrahedron*, 2003, **59**, 10581–10591.

105 D. S. Kashdan, J. A. Schwartz and H. Rapoport, *J. Org. Chem.*, 1982, **47**, 2638–2643.

106 C. R. Nevill and P. L. Fuchs, *Synth. Commun.*, 1990, **20**, 761–772.

107 D. B. Gorbunov, V. V. Ershov and G. A. Nikiforov, *Russ. Chem. Bull.*, 1993, **42**, 481–485.

108 D. B. Gorbunov, V. N. Voznesenskii, V. V. Ershov and G. A. Nikiforov, *Russ. Chem. Bull.*, 1994, **43**, 93–97.

109 F. S. Han, *Chem. Soc. Rev.*, 2013, **42**, 5270–5298.

110 R. B. Grossman, *The Art of Writing Reasonable Organic Reaction Mechanisms: Second Edition*, 2003.

111 R. J. Wakeham, J. E. Taylor, S. D. Bull, J. A. Morris and J. M. J. Williams, *Org. Lett.*, 2013, **15**, 702–705.

112 C. Gardner Swain and C. B. Scott, *J. Am. Chem. Soc.*, 1953, **75**, 141–147.

113 M. G. Voronkov, I. P. Tsyrendorzhieva and V. I. Rakhlin, *Russ. J. Org. Chem+*, 2008, **44**, 481–484.

114 S. Hayat, Atta-Ur-Rahman, K. M. Khan, M. I. Choudhary, G. M. Maharvi, Zia-Ullah and E. Bayer, *Synth. Commun.*, 2003, **33**, 2531–2540.

115 M. E. Greaves, E. L. B. Johnson Humphrey and D. J. Nelson, *Catal. Sci. Technol.*, 2021, **11**, 2980–2996.

116 N. Miyaura and A. Suzuki, *Chem. Rev.*, 1995, **95**, 2457–2483.

117 S. Chowdhury and P. E. Georghiou, *Tetrahedron Lett.*, 1999, **40**, 7599–7603.

118 A. J. J. Lennox and G. C. Lloyd-Jones, *Chem. Soc. Rev.*, 2014, **43**, 412–443.

119 H. Zhang, F. Y. Kwong, Y. Tian and K. S. Chan, *J. Org. Chem.*, 1998, **63**, 6886–6890.

120 C. Amatore and A. Jutand, *Acc. Chem. Res.*, 2000, **33**, 314–321.

121 M. A. Greene, I. M. Yonova, F. J. Williams and E. R. Jarvo, *Org. Lett.*, 2012, **14**, 4293–4296.

122 S. Z. Tasker, E. A. Standley and T. F. Jamison, *Nature*, 2014, **509**, 299–309.

123 Y. Li, Y. Luo, L. Peng, Y. Li, B. Zhao, W. Wang, H. Pang, Y. Deng, R. Bai, Y. Lan and G. Yin, *Nat. Commun.*, 2020, **11**, 417.

124 Y. Yang, Q. Zhou, J. Cai, T. Xue, Y. Liu, Y. Jiang, Y. Su, L. Chung and D. A. Vicic, *Chem. Sci.*, 2019, **10**, 5275–5282.

125 C. Zhao, X. Jia, X. Wang and H. Gong, *J. Am. Chem. Soc.*, 2014, **136**, 17645–17651.

126 N. D. Schley and G. C. Fu, *J. Am. Chem. Soc.*, 2014, **136**, 16588–16593.

127 S. Biswas and D. J. Weix, *J. Am. Chem. Soc.*, 2013, **135**, 16192–16197.

128 X. Hu, *Chem. Sci.*, 2011, **2**, 1867–1886.

129 T. H. Fisher, S. M. Dershem and M. L. Prewitt, *J. Org. Chem.*, 1990, **55**, 1040–1043.

130 K. Muto, J. Yamaguchi, D. G. Musaev and K. Itami, *Nat. Commun.*, 2015, **6**, 7508.

131 B. Wang, H. X. Sun and Z. H. Sun, *European J. Org. Chem.*, 2009, 3688–3692.

132 R. Giovannini, T. Strudemann, A. Devasagayaraj, G. Dussin and P. Knochel, *J. Org. Chem.*, 1999, **64**, 3544–3553.

133 F. S. Wekesa, N. Phadke, C. Jahier, D. B. Cordes and M. Findlater, *Synthesis*, 2014, **46**, 1046–1051.

134 E. C. Calvaresi and P. J. Hergenrother, *Chem. Sci.*, 2013, **4**, 2319–2333.

135 M. B. Li, X. L. Tang and S. K. Tian, *Adv. Synth. Catal.*, 2011, **353**, 1980–1984.

136 F. O. Arp and G. C. Fu, *J. Am. Chem. Soc.*, 2005, **127**, 10482–10483.

137 J. Choi and G. C. Fu, *Science*, 2017, *356*, 152

138 W. Huang, M. Hu, X. Wan and Q. Shen, *Nat. Commun.*, 2019, **10**, 2963.

139 A. López-Pérez, J. Adrio and J. C. Carretero, *Org. Lett.*, 2009, **11**, 5514–5517.

140 W. Huang, X. Wan and Q. Shen, *Angew. Chem.*, 2017, **129**, 12148–12151.

141 J. Caeiro, J. P. Sestelo and L. A. Sarandeses, *Chem. - Eur. J.*, 2008, **14**, 741–746.

142 R. B. Bedford, P. B. Brenner, E. Carter, T. W. Carvell, P. M. Cogswell, T. Gallagher, J. N. Harvey, D. M. Murphy, E. C. Neeve, J. Nunn and D. R. Pye, *Chem. - Eur. J.*, 2014, **20**, 7935–7938.

143 R. J. Procter, J. J. Dunsford, P. J. Rushworth, D. G. Hulcoop, R. A. Layfield and M. J. Ingleson, *Chem. - Eur. J.*, 2017, **23**, 15889–15893.

144 S. Asghar, S. B. Tailor, D. Elorriaga and R. B. Bedford, *Angew. Chem. Int. Ed.*, 2017, **56**, 16367–16370.

145 Y. Kobayashi and R. Mizojiri, *Tetrahedron Lett.*, 1996, **37**, 8531–8534.

146 J. Schmidt, J. Choi, A. T. Liu, M. Slusarczyk and G. C. Fu, *Science*, 2016, **354**, *6317*, 1265–1270.

147 J. Zhou and G. C. Fu, *J. Am. Chem. Soc.*, 2003, **125**, 14726–14727.

148 J. Holz, C. Pfeffer, H. Zuo, D. Beierlein, G. Richter, E. Klemm and R. Peters, *Angew. Chem. Int. Ed.*, 2019, **58**, 10330–10334.

149 R. Sakamoto, T. Inada, S. Selvakumar, S. A. Moteki and K. Maruoka, *Chem. Commun.*, 2016, **52**, 3758–3761.

150 C. C. Tyrol, N. S. Yone, C. F. Gallin and J. A. Byers, *Chem. Commun.*, 2020, **56**, 14661–14664.

151 G. Cheng, B. Xia, Q. Wu and X. Lin, *RSC Adv.*, 2013, **3**, 9820–9828.

152 Q. Zhang, X. Wang, Q. Qian and H. Gong, *Synthesis*, 2016, **48**, 2829–2836.

153 E. P. Gillis, K. J. Eastman, M. D. Hill, D. J. Donnelly and N. A. Meanwell, *J. Med. Chem.*, 2015, **58**, 8315–8359.

154 C. Zhang, Y. Lu, R. Zhao, X. Y. Chen and Z. X. Wang, *Org. Chem. Front.*, 2020, **7**, 3411–3419.

155 M. Su and S. Chu, *J. Am. Chem. Soc.*, 1999, **121**, 1045–1058.

156 J. Davies, D. Janssen-Müller, D. P. Zimin, C. S. Day, T. Yanagi, J. Elfert and R. Martin, *J. Am. Chem. Soc.*, 2021, **143**, 4949–4954.

157 C. H. Xu, J. H. Li, J. N. Xiang and W. Deng, *Org. Lett.*, 2021, **23**, 3696–3700.

158 Y. Toda, R. Matsuda, S. Gomyou and H. Suga, *Org. Biomol. Chem.*, 2019, **17**, 3825–3829.

159 Q. Wu and J. Xu, *Chem. Commun.*, 2022, **58**, 2714–2717.

160 Y. F. Han, Z. H. Gao, C. L. Zhang and S. Ye, *Org. Lett.*, 2020, **22**, 8396–8400.

161 J. Ince, M. Shipman and D. S. Ennis, *Tetrahedron Lett.*, 1997, **38**, 5887–5890.

162 X. E. Hu, *Tetrahedron*, 2004, **60**, 2701–2743.

163 V. G. Nenajdenko, A. S. Karpov and E. S. Balenkova, *Tetrahedron Asymmetry*, 2001, **12**, 2517–2527.

164 S. Kenis, M. D'hooghe, G. Verniest, T. A. Dang Thi, C. Pham The, T. Van Nguyen and N. De Kimpe, *J. Org. Chem.*, 2012, **77**, 5982–5992.

165 S. Seong, H. Lim and S. Han, *Chem*, 2019, **5**, 353–363.

166 N. G. Paciaroni, R. Ratnayake, J. H. Matthews, V. M. Norwood, A. C. Arnold, L. H. Dang, H. Luesch and R. W. Huigens, *Chem. - Eur. J.*, 2017, **23**, 4327–4335.

167 W. S. McCall, T. A. Grillo and D. L. Comins, *Org. Lett.*, 2008, **10**, 3255–3257.

168 G. Glotz, R. Lebl, D. Dallinger and C. O. Kappe, *Angew. Chem. Int. Ed.*, 2017, **56**, 13786–13789.

169 C. Yu, M. A. Shoaib, N. Iqbal, J. S. Kim, H. J. Ha and E. J. Cho, *J. Org. Chem.*, 2017, **82**, 6615–6620.

170 M. C. Warner, G. A. Shevchenko, S. Jouda, K. Bogár and J. E. Bäckvall, *Chem. - Eur. J.*, 2013, **19**, 13859–13864.

171 R. Kuwano and M. Yokogi, *Chem. Commun.*, 2005, 5899–5901.

172 S. Q. Zhang, B. L. H. Taylor, C.-L. Ji, Y. Gao, M. R. Harris, L. E. Hanna, E. R. Jarvo, K. N. Houk and X. Hong, *J. Am. Chem. Soc.*, 2017, **139**, 12994–13005.

173 H. Duan, L. Meng, D. Bao, H. Zhang, Y. Li and A. Lei, *Angew. Chem. Int. Ed.*, 2010, **49**, 6387–6390.

174 H. qing Jing, H. liang Li and J. C. Antilla, *Tetrahedron Lett.*, 2020, **61**, 152401.

175 P. H. Huy and A. M. P. Koskinen, *Org. Lett.*, 2013, **15**, 5178–5181.

176 D. Wei, A. Bruneau-Voisine, D. A. Valyaev, N. Lugan and J. B. Sortais, *Chem. Commun.*, 2018, **54**, 4302–4305.

177 R. Feng, J. Yao, Z. Liang, Z. Liu and Y. Zhang, *J. Org. Chem.*, 2013, **78**, 3688–3696.

178 D. Y. Ong, Z. Yen, A. Yoshii, J. Revillo Imbernon, R. Takita and S. Chiba, *Angew. Chem. Int.*

Ed., 2019, **58**, 4992–4997.

179 C. T. Mbofana, E. Chong, J. Lawniczak and M. S. Sanford, *Org. Lett.*, 2016, **18**, 4258–4261.

180 S. E. Varjosaari, V. Skrypai, P. Suating, J. J. M. Hurley, A. M. De Lio, T. M. Gilbert, M. J. Adler, *Adv. Synth. Catal.*, 2017, **359**, 1872-1878

181 N. Sakai, H. Hori, Y. Yoshida, T. Konakahara and Y. Ogiwara, *Tetrahedron*, 2015, **71**, 4722–4729.

182 S.-E. Park, S. B. Kang, K.-J. Jung, J.-E. Won, S.-G. Lee and Y.-J. Yoon, *Synthesis*, 2009, **5**, 815–823.

183 J. A. Cadge, J. F. Bower and C. A. Russell, *Angew. Chem. Int. Ed.*, 2021, **60**, 24976–24983.

184 B. Lecea, J. M. Aizpurua and C. Palomo, *Tetrahedron*, 1985, **41**, 4657–4665.

185 G. Sun and Z. Wang, *Tetrahedron Lett.*, 2008, **49**, 4929–4932.

186 D. W. Robbins and J. F. Hartwig, *Angew. Chem. Int. Ed.*, 2013, **52**, 933–937.

187 J. Song, Y. Li, W. Sun, C. Yi, H. Wu, H. Wang, K. Ding, K. Xiao and C. Liu, *New J. Chem.*, 2016, **40**, 9030–9033.

188 H. Sterckx, J. De Houwer, C. Mensch, W. Herrebout, K. A. Tehrani and B. U. W. Maes, *Beilstein J. Org. Chem.*, 2016, **12**, 144–153.

189 J. Kim, J. Choi, K. Shin and S. Chang, *J. Am. Chem. Soc.*, 2012, **134**, 2528–2531.

190 H. Ochiai, Y. Uetake, T. Niwa and T. Hosoya, *Angew. Chem. Int. Ed.*, 2017, **56**, 2482–2486.

191 L. Zhang and L. Jiao, *J. Am. Chem. Soc.*, 2019, **141**, 9124–9128.

192 Y. Xu, X. Yang and H. Fang, *J. Org. Chem.*, 2018, **83**, 12831–12837.

193 D. C. Grenz, M. Schmidt, D. Kratzert and B. Esser, *J. Org. Chem.*, 2018, **83**, 656–663.

194 F. Levrat, H. Stoeckli-Evans and N. Engel, *Tetrahedron Asymmetry*, 2002, **13**, 2335–2344.

195 K.-J. Xiao, J.-M. Luo, K.-Y. Ye, Y. Wang and P.-Q. Huang, *Angew. Chem. Int. Ed.*, 2010, **49**, 3037–3040.

196 D. Talwar, N. P. Salguero, C. M. Robertson and J. Xiao, *Chem. - Eur. J.*, 2014, **20**, 245–252.

197 R. Laufer, G. Ng, Y. Liu, N. K. B. Patel, L. G. Edwards, Y. Lang, S. W. Li, M. Feher, D. E. Awrey, G. Leung, I. Beletskaya, O. Plotnikova, J. M. Mason, R. Hodgson, X. Wei, G. Mao, X. Luo, P. Huang, E. Green, R. Kiarash, D. C. C. Lin, M. Harris-Brandts, F. Ban, V. Nadeem, T. W. Mak, G. J. Pan, W. Qiu, N. Y. Chirgadze and H. W. Pauls, *Bioorg.. Med. Chem.*, 2014, **22**,

4968–4997.

198 K. Watanabe, Y. Miyazaki, M. Okubo, B. Zhou, H. Tsuji and M. Kawatsura, *Org. Lett.*, 2018, **20**, 5448–5451.

199 M. Guisán-Ceinos, V. Martín-Heras and M. Tortosa, *J. Am. Chem. Soc.*, 2017, **139**, 8448–8451.

200 J. Albarrán-Velo, I. Lavandera and V. Gotor-Fernández, *ChemBioChem*, 2020, **21**, 200–211.

201 N. J. Adamson, E. Hull and S. J. Malcolmson, *J. Am. Chem. Soc.*, 2017, **139**, 7180–7183.

202 T. Dohi, N. Takenaga, A. Goto, A. Maruyama and Y. Kita, *Org. Lett.*, 2007, **9**, 3129–3132.

203 Y. P. Budiman, A. Jayaraman, A. Friedrich, F. Kerner, U. Radius and T. B. Marder, *J. Am. Chem. Soc.*, 2020, **142**, 6036–6050.

204 H. Xia, G. Wang, D. Zhao and C. Zhu, *Adv. Synth. Catal.*, 2022, **364**, 922–929.

205 S. Y. Lee, A. Villani-Gale and C. C. Eichman, *Org. Lett.*, 2016, **18**, 5034–5037.

206 J. T. Reeves, D. R. Fandrick, Z. Tan, J. J. Song, S. Rodriguez, B. Qu, S. Kim, O. Niemeier, Z. Li, D. Byrne, S. Campbell, A. Chitroda, P. Decroos, T. Fachinger, V. Fuchs, N. C. Gonnella, N. Grinberg, N. Haddad, B. Jäger, H. Lee, J. C. Lorenz, S. Ma, B. A. Narayanan, L. J. Nummy, A. Premasiri, F. Roschangar, M. Sarvestani, S. Shen, E. Spinelli, X. Sun, R. J. Varsolona, N. Yee, M. Brenner and C. H. Senanayake, *J. Org. Chem.*, 2013, **78**, 3616–3635.

207 C. S. Buxton, University of Bristol, 2017.

208 B. Sezen and D. Sames, *J. Am. Chem. Soc.*, 2005, **127**, 5284–5285.

209 R. Ding, H. Chen, Y.-L. Xu, H.-T. Tang, Y.-Y. Chen and Y.-M. Pan, *Adv. Synth. Catal.*, 2019, **361**, 3656–3660.

210 L.-M. Zhao, Q.-Y. Meng, X.-B. Fan, C. Ye, X.-B. Li, B. Chen, V. Ramamurthy, C.-H. Tung and L.-Z. Wu, *Angew. Chem. Int. Ed.*, 2017, **56**, 3020–3024.

211 C.-T. Yang, Z.-Q. Zhang, H. Tajuddin, C.-C. Wu, J. Liang, J.-H. Liu, Y. Fu, M. Czyzewska, P. G. Steel, T. B. Marder, L. Liu, *Angew. Chem. Int. Ed.*, 2012, **51**, 528-532.